

Technical report

TECHNICAL REPORT

CENTER FOR APPLIED AND COASTAL RESEARCH (CACR)
UNIVERSITY OF DELAWARE | NEWARK, DE 19716

Table of Contents

List of Figures	5
List of Tables.....	17
List of Acronyms.....	21
1. Introduction	22
1.1. Background.....	22
1.2. Study Area	22
1.3. Aim and Objectives	24
1.4. Guide to the Report.....	24
2. Methodology Overview.....	24
2.1. Overview of Prediction Approaches	24
2.2. Overview of Simulation Approach	26
2.3. Performance objectives	27
3. Performance metric testing.....	29
3.1. Class I models	29
3.2. Class II models	30
3.2.1. D-Flow FM	30
3.3. Class III models.....	33
4. Model simulation results.....	33
4.1. Calibration Results (Baseline scenarios)	33
5. Model Setup.....	33
5.1. Empirical Models.....	33
5.2. Hydrodynamic modeling (D-Flow FM)	35
5.2.1. Network.....	36
5.2.2. Bathymetry.....	36
5.2.3. Open boundary conditions	39
5.2.4. Meteorological forcing.....	40
5.2.5. Model Characteristics	41
5.3. Wave modeling (SWAN/D-Waves).....	42

5.4.	Wave modeling (FUNWAVE-TVD)	51
5.4.1.	Application of FUNWAVE-TVD modules	51
5.4.2.	FUNWAVE-TVD configuration.....	52
5.5.	Hydrodynamic and Wave Modeling (ADCIRC).....	43
3.5.1	Unstructured Mesh.....	44
3.5.2	Bathymetry	46
3.5.3	Open Boundary Conditions.....	46
3.5.4	Meteorological Forcing.....	47
3.5.5	Model Characteristics.....	48
5.6.	Hydrodynamic and Wave Modeling (NEARCOM)	48
5.6.1.	Selection of wave and circulation modules in NEARCOM	49
5.6.2.	NEARCOM setup	49
5.7.	Performance assessment.....	54
6.	Results.....	60
6.1.	Empirical methods.....	60
6.2.	D-Flow FM	60
6.2.1.	Model Calibration (Base scenarios)	61
6.2.2.	Impacts of Meteorological forcing.....	109
6.2.3.	Impacts of Climate Changes.....	119
6.2.4.	Impacts of Lack of Data (Degradation scenarios)	134
6.3.	SWAN.....	170
6.3.1.	Model Calibration (baseline scenarios)	170
6.4.	NearCoM	178
6.5.	FUNWAVE	305
6.6.	ADCIRC.....	211
6.6.1.	Model Calibration (Base scenarios)	211
6.6.2.	Impacts of Meteorological forcing.....	234
6.6.3.	Impacts of Climate Changes.....	246
6.6.4.	Impacts of Lack of Data (Degradation scenarios)	270

6.7.....	305
7. Discussion	265
7.1. D-Flow FM	265
7.2. SWAN and FUNWAVE.....	266
7.3. ADCIRC.....	266
7.4.....	266
7.5. One-to-One Comparison (D-Flow FM – ADCIRC).....	305
8. Summary and Conclusions.....	306
9. Recommendations and future developments.....	306
10. References.....	307
11. Appendix A (calibration figures)	317
11.1. Hurricane Irene (2011).....	317
11.2. Hurricane Isabel (2003).....	324
11.3. Hurricane Sandy (2012)	333
11.4. Hurricane Michael (2018).....	343
12. Appendix B (Tables)	352
13. Appendix C (Model Results).....	354
13.1. Impacts of Meteorological Forcing.....	354
13.1.1. Pressure Drop.....	354
13.1.2. Radius of Maximum Wind.....	372
13.2. Impacts of Climate Change.....	379
13.2.1. Sea Level Rise.....	379
13.2.2. Increasing Wind Speed.....	390
13.3. Impacts of Lack of Data (Degradation scenarios)	400
13.3.1. Strom Track Shift (Error in Storm Track Prediction)	400
13.3.2. Bathymetry Accuracy.....	400
13.3.3. Bathymetry Resolution	400

List of Figures

Figure 1. Satellite imagery of Norfolk (VA, USA) overlayed by color-coded bathymetry showing the shallow water conditions just offshore with water depths < 10 m. The inset shows the study site location (star marker, for reference between the main figure and inset) relative to the wider USA. The track of Hurricane Irene (2011) is shown as the dash-dot curve in the inset.	23
Figure 2 . Computational network/mesh for the D-Flow FM simulation along the east coast of the US.	36
Figure 3. D-Flow FM bathymetry for the entire domain (upper panel) and a zoom-in on the NSN-Base (Lower panel-blue star).....	38
Figure 4. Comparison between the two employed wind forces, ERA5 (left panel) and HM (right panel), at extreme conditions for hurricane Irene, NSN, US	41
Figure 5. Satellite image showing the model domain (red line) and the observation points used in D-Flow FM, NSN, US.	42
Figure 6. Simulated and measured tidal water level (m) (upper panel) and SA & SSA components (lower panels) during 2011 at Duck, US East Coast.	63
Figure 7. Measured vs Simulated water levels using ERA5 and HM wind forces during hurricane Irene, 2011.	64
Figure 8. Scatter plots of the measured and simulated water levels (m) at Sewells, Duck and Wrightsville using ERA5 (upper panels) and HM (lower panels). Histograms are plotted along the right and upper axes, Irene, 2011, NSN, US.....	65
Figure 9. Summary statistics (RMSE and Baias in meters) of water level prediction using ERA5 and HM at the calibration stations along the US east coast during Hurricane Irene-2011.	66
Figure 10. Flood Duration, Magnitude, and Timing at Sewells Point during Hurricane Irene-2011 (Base-ERA5) at NSN, the US.	68
Figure 11. Flood Duration, Magnitude and Timing at Sewells Point during Hurricane Irene-2011 (Base-HM) at NSN, the US.....	69

Figure 12. Timeseries of the projected average and maximum flood depth (left axis) and flood area (km^2 -right axis) during Hurricane Irene-2011 for ERA5 (upper panel) and HM (lower panel) at NSN, the US	70
Figure 13. Flood map showing the classification of the flood levels at the peak surge during Hurricane Irene-2011 using ERA5 wind forces (left panel) and HM wind forces (right panel) at NSN, the US	71
Figure 14. Flood maps show the classification of the different flood levels (low, medium, high, and extreme) at the peak surge simulation using ERA5 wind forcing during Hurricane Irene-2011 at NSN, the US	71
Figure 15. Satellite image showing NSN (upper panel) and a zoom-in on the projected flooded area under the Base scenarios (lower panel) under the Base-ERA5 and Base-HM scenarios, NSN, the US	73
Figure 16. Pie chart showing the areas, with percentages, for the different flood levels at the peak surge during Hurricane Irene-2011 using ERA5 wind forces (left panel) and HM wind forces (right panel) at NSN, the US	74
Figure 17. Thematic map showing the locations of the flooding during Hurricane Irene based on the STORM anecdotal data. The solid blue line shows the boundary of NSN, and the red triangles represent reported flood location, NSN, the US	74
Figure 18. Measured vs Simulated water levels using ERA5 and HM wind forces during hurricane Isabel, 2003	77
Figure 19. Scatter plots of the measured and simulated water levels (m) at Sewells, Duck and Kiptopeke using ERA5 (upper panels) and HM (lower panels). Histograms are plotted along the right and upper axes, Isabel, 2003, NSN, US.....	78
Figure 20. Wind speed (m/sec) of ERA5 (left panel) and Holland Model (right panel) wind force during the peak surge of Hurricane Isabel 2003. The black dashed line represents the actual path of the hurricane	79
Figure 21. Summary statistics (RMSE and Bias in meters) of water level prediction using ERA5 and HM at the calibration stations along the US east coast during Hurricane Isabel-2003	79
Figure 22. Flood Duration, Magnitude, and Timing at Sewells Point during Hurricane Isabel-2003 (Base-ERA5) at NSN, the US	81

Figure 23. Flood Duration, Magnitude and Timing at Sewells Point during Hurricane Isabel-2003 (Base-HM) at NSN, the US.....	82
Figure 24. Timeseries of the projected average and maximum flood depth (m-left axis) and flood area (km^2 -right axis) during Hurricane Isabel-2003 for ERA5 (upper panel) and HM (lower panel) at NSN, the US	84
Figure 25. Flood map showing the classification of the flood levels at the peak surge during Hurricane Isabel-2003 using ERA5 wind forces (left panel) and HM wind forces (right panel) at NSN, the US	85
Figure 26. Flood maps show the classification of the different flood levels (low, medium, high, and extreme) at the peak surge simulation using ERA5 wind forcing during Hurricane Isabel-2003 at NSN, the US	85
Figure 27. Pie chart showing the areas, with percentages, for the different flood levels at the peak surge during Hurricane Isabel-2003 using ERA5 wind forces (left panel) and HM wind forces (right panel) at NSN, the US.....	86
Figure 28. Measured vs Simulated water levels using ERA5 and HM wind forces during Hurricane Sandy, 2012	88
Figure 29. Scatter plots of the measured and simulated water levels (m) at Sewells, Duck and Kiptopeke using ERA5 (upper panels) and HM (lower panels). Histograms are plotted along the right and upper axes, Sandy, 2012, NSN, US.	89
Figure 30. Summary statistics (RMSE and Bias in meters) of water level prediction using ERA5 and HM at the calibration stations along the US east coast during Hurricane Sandy-2012	90
Figure 31. Wind speed (m/sec) of ERA5 (left panel) and Holland Model (right panel) wind force during the peak surge of Hurricane Sandy 2012. The black dashed line represents the actual path of the hurricane.	91
Figure 32. Flood Duration, Magnitude, and Timing at Sewells Point during Hurricane Sandy-2012 (Base-ERA5) at NSN, the US.....	93
Figure 33. Flood Duration, Magnitude and Timing at Sewells Point during Hurricane Sandy-2012 (Base-HM) at NSN, the US.....	94

Figure 34. Timeseries of the projected average and maximum flood depth (left axis) and flood area (km^2 -right axis) during Hurricane Sandy-2012 for ERA5 (upper panel) and HM (lower panel) at NSN, the US	95
Figure 35. Flood map showing the classification of the flood levels at the peak surge during Hurricane Sandy-2012 using ERA5 wind forces (left panel) and HM wind forces (right panel) at NSN, the US	96
Figure 36. Flood maps show the classification of the different flood levels (low, medium, high, and extreme) at the peak surge simulation using ERA5 wind forcing during Hurricane Sandy-2012 at NSN, the US	96
Figure 37. Pie chart showing the areas, with percentages, for the different flood levels at the peak surge during Hurricane Sandy-2012 using ERA5 wind forces (left panel) and HM wind forces (right panel) at NSN, the US.....	97
Figure 38. Thematic map showing the locations of the flooding during Hurricane Sandy-2012 based on the STORM anecdotal data. The solid blue line shows the boundary of NSN, and the red triangles represent reported flood location, NSN, the US.....	97
Figure 39. Measured vs Simulated water levels using ERA5 and HM wind forces during Hurricane Michael, 2018.....	99
Figure 40. Scatter plots of the measured and simulated water levels (m) at Sewells, Duck and Wrightsville using ERA5 (upper panels) and HM (lower panels). Histograms are plotted along the right and upper axes, Michael, 2018, NSN, US.....	100
Figure 41. Summary statistics (RMSE and Bias in meters) of water level prediction using ERA5 and HM at the calibration stations along the US east coast during Hurricane Michael-2018... ..	101
Figure 42. Wind speed (m/sec) of ERA5 (left panel) and Holland Model (right panel) wind force during the peak surge of Hurricane Michael 2018. The black dashed line represents the actual path of the hurricane (West to East direction).....	102
Figure 43. Flood Duration, Magnitude, and Timing at Sewells Point during Hurricane Michael-2018 (Base-ERA5) at NSN, the US.	104
Figure 44. Flood Duration, Magnitude and Timing at Sewells Point during Hurricane Michael-2018 (Base-HM) at NSN, the US.....	105

Figure 45. Timeseries of the projected average and maximum flood depth (left axis) and flood area (km^2 -right axis) during Hurricane Michael-2018 for ERA5 (upper panel) and HM (lower panel) at NSN, the US	106
Figure 46. Flood map showing the classification of the flood levels at the peak surge during Hurricane Michael-2018 using ERA5 wind forces (left panel) and HM wind forces (right panel) at NSN, the US	107
Figure 47. Flood maps show the classification of the different flood levels (low, medium, high, and extreme) at the peak surge simulation using ERA5 wind forcing during Hurricane Michael-2018 at NSN, the US	107
Figure 48. Pie chart showing the areas, with percentages, for the different flood levels at the peak surge during Hurricane Michael-2018 using ERA5 wind forces (left panel) and HM wind forces (right panel) at NSN, the US	108
Figure 49. Thematic map showing the locations of the flooding during Hurricane Michael-2018 based on the STORM anecdotal data. The solid blue line shows the boundary of NSN, and the red triangles represent reported flood location, NSN, the US	108
Figure 50. Water level time series (m) during the different hurricanes showing the surge magnitude and duration for different surge levels for the base and PD_F0.64 scenarios at Sewells Point, NSN, the US.....	111
Figure 51. Peak surge (m) (left panel) and surge duration (h) of the different surge levels (right panel) for the base and PD_F0.64 scenario for all hurricanes, NSN, the US	111
Figure 52. Average Flood Depth (AFD) & Maximum Flood Depth (MFD) in meters (left panel) and Flood area (km^2) (right panel) of all hurricanes for the Base and PD_F0.64 scenarios, NSN, the US.....	112
Figure 53. Flood maps with the flood levels for the different hurricanes during the peak surge for the PD_F0.64 scenario at NSN, the US.....	113
Figure 54. Flood area classification (Low, Medium, High, and Extreme) in meters of the PD_F0.64 scenarios during hurricane Irene-2011 at NSN base, the US	114
Figure 55. Pie chart of the flood areas, with percentages, of the different flood levels for PD_F0.64 scenario for Hurricane Irene-2011 at NSN, the US	114

Figure 56. Flood area classification (Low, Medium, High, and Extreme) in meters of the PD_F0.64 scenarios during hurricane Isabel-2003 at NSN base, the US.	354
Figure 57. Pie chart of the flood areas, with percentages, of the different flood levels for PD_F0.64 scenario for Hurricane Isabel-2003 at NSN, the US.	355
Figure 58. Flood area classification (Low, Medium, High, and Extreme) in meters of the PD_F0.64 scenarios during hurricane Sandy-2012 at NSN base, the US.	355
Figure 59. Pie chart of the flood areas, with percentages, of the different flood levels for PD_F0.64 scenario for Hurricane Sandy-2012 at NSN, the US.	356
Figure 60. Flood area classification (Low, Medium, High, and Extreme) in meters of the PD_F0.64 scenario during hurricane Michael-2018 at NSN base, the US.	356
Figure 61. Pie chart of the flood areas, with percentages, of the different flood levels for PD_F0.64 scenario for Hurricane Michael-2018 at NSN, the US.	357
Figure 62. Water level time series (m) during the different hurricanes showing the surge magnitude and duration for different surge levels for the base and RMW_F1.25 scenarios at Sewells Point, NSN, the US.	116
Figure 63. Peak surge (m) (left panel) and surge duration (h) of the different surge levels (right panel) for the base and RMW_F1.25 scenario for all hurricanes, NSN, the US.	117
Figure 64. Average Flood Depth (AFD) & Maximum Flood Depth (MFD) in meters (left panel) and Flood area (km ²) (right panel) of all hurricanes for the Base and RMW_F1.25 scenarios, NSN, the US.	117
Figure 65. Flood maps with the flood levels for the different hurricanes during the peak surge for the RMW_F1.25 scenario at NSN, the US.	118
Figure 66. Water level time series (m) during the different hurricanes showing the surge magnitude and duration for different surge levels for the base and SLR_1.3M scenarios at Sewells Point, NSN, the US.	120
Figure 67. Peak surge (m) (left panel) and surge duration (h) of the different surge levels (right panel) for the base and SLR_1.3M scenario for all hurricanes, NSN, the US.	121

Figure 68. Average Flood Depth (AFD) & Maximum Flood Depth (MFD) in meters (left panel) and Flood area (km ²) (right panel) of all hurricanes for the Base and SLR_1.3M scenarios at NSN, the US.....	121
Figure 69. Time series of the projected average and maximum flood depth (left axis) and flood area (km ² -right axis) for all hurricanes for SLR_1.3M scenario at NSN, the US.....	123
Figure 70. Flood maps with the flood levels for the different hurricanes during the peak surge for the SLR_1.3M scenario at NSN, the US.....	124
Figure 71. Flood area classified by level (Low, Medium, High, and Extreme) in meters for the SLR_1.3M scenario during hurricane Irene-2011 at NSN base, the US.....	125
Figure 72. Pie chart of the flood areas, with percentages, of the different flood levels for SLR_1.3M scenario for Hurricane Irene-2011 at NSN, the US.....	125
Figure 73. Water level time series (m) during the different hurricanes showing the surge magnitude and duration for different surge levels for the base and WSF_1.225 scenarios at Sewells Point, NSN, the US.....	127
Figure 74. Water level (m) showing the surge magnitude for the base and WSF_1.225 scenarios during Hurricane Isable (left panel) and Hurricane Sandy (right panel) at Duck and Lewes, DE locations respectively.....	128
Figure 75. Peak surge (m) (left panel) and surge duration (h) of the different surge levels (right panel) for the base and WSF_1.225 scenario for all hurricanes, NSN, the US.....	129
Figure 76. Average Flood Depth (AFD) & Maximum Flood Depth (MFD) in meters (left panel) and Flood area (km ²) (right panel) of all hurricanes for the Base and WSF_1.225 scenarios at NSN, the US.....	130
Figure 77. Time series of the projected average and maximum flood depth (left axis) and flood area (km ² -right axis) for all hurricanes for WSF_1.225 scenario at NSN, the US.....	131
Figure 78. Flood maps with the flood levels for the different hurricanes during the peak surge for the WSF_1.225 scenario at NSN, the US.....	132
Figure 79. Flood area classified by level (Low, Medium, High, and Extreme) in meters for the WSF_1.225 scenario during hurricane Irene-2011 at NSN base, the US.....	133

Figure 80. Pie chart of the flood areas, with percentages, of the different flood levels for WSF_1.225 scenario for Hurricane Irene-2011 at NSN, the US.....	133
Figure 81. Water level time series (m) during the different hurricanes showing the surge magnitude and duration for different surge levels for the base and PD_F0.76 scenarios at Sewells Point, NSN, the US.....	357
Figure 82. Peak surge (m) (left panel) and surge duration (h) of the different surge levels (right panel) for the base and PD_F0.76 scenario for all hurricanes, NSN, the US.	358
Figure 83. Average Flood Depth (AFD) & Maximum Flood Depth (MFD) in meters (left panel) and Flood area (km ²) (right panel) of all hurricanes for the Base and PD_F0.64 scenarios, NSN, the US.	359
Figure 84. Flood maps with the flood levels for the different hurricanes during the peak surge for the PD_F0.76 scenario at NSN, the US.....	360
Figure 85. Flood area classification (Low, Medium, High, and Extreme) in meters of the PD_F0.76 scenarios during hurricane Irene-2011 at NSN base, the US.	361
Figure 86. Pie chart of the flood areas, with percentages, of the different flood levels for PD_F0.76 scenario for Hurricane Irene-2011 at NSN, the US.	361
Figure 87. Flood area classification (Low, Medium, High, and Extreme) in meters of the PD_F0.76 scenarios during hurricane Isabel-2003 at NSN base, the US.	362
Figure 88. Pie chart of the flood areas, with percentages, of the different flood levels for PD_F0.76 scenario for Hurricane Isabel-2003 at NSN, the US.	362
Figure 89. Flood area classification (Low, Medium, High, and Extreme) in meters of the PD_F0.76 scenarios during hurricane Sandy-2012 at NSN base, the US.	363
Figure 90. Pie chart of the flood areas, with percentages, of the different flood levels for PD_F0.76 scenario for Hurricane Sandy-2012 at NSN, the US.	363
Figure 91. Flood area classification (Low, Medium, High, and Extreme) in meters of the PD_F0.76 scenarios during hurricane Michael-2018 at NSN base, the US.	364
Figure 92. Pie chart of the flood areas, with percentages, of the different flood levels for PD_F0.76 scenario for Hurricane Michael-2018 at NSN, the US.	364

Figure 93. Water level time series (m) during the different hurricanes showing the surge magnitude and duration for different surge levels for the base and PD_F0.88 scenarios at Sewells Point, NSN, the US.....	365
Figure 94. Peak surge (m) (left panel) and surge duration (h) of the different surge levels (right panel) for the base and PD_F0.88 scenario for all hurricanes, NSN, the US.	365
Figure 95. Average Flood Depth (AFD) & Maximum Flood Depth (MFD) in meters (left panel) and Flood area (km2) (right panel) of all hurricanes for the Base and PD_F0.88 scenarios, NSN, the US.	366
Figure 96. Flood maps with the flood levels for the different hurricanes during the peak surge for the PD_F0.88 scenario at NSN, the US.	367
Figure 97. Flood area classification (Low, Medium, High, and Extreme) in meters of the PD_F0.88 scenarios during hurricane Irene-2011 at NSN base, the US.	368
Figure 98. Pie chart of the flood areas, with percentages, of the different flood levels for PD_F0.88 scenario for Hurricane Irene-2011 at NSN, the US.	368
Figure 99. Flood area classification (Low, Medium, High, and Extreme) in meters of the PD_F0.88 scenarios during hurricane Isabel-2003 at NSN base, the US.	369
Figure 100. Pie chart of the flood areas, with percentages, of the different flood levels for PD_F0.88 scenario for Hurricane Isabel-2003 at NSN, the US.	369
Figure 101. Flood area classification (Low, Medium, High, and Extreme) in meters of the PD_F0.88 scenarios during hurricane Sandy-2012 at NSN base, the US.	370
Figure 102. Pie chart of the flood areas, with percentages, of the different flood levels for PD_F0.88 scenario for Hurricane Sandy-2012 at NSN, the US.	370
Figure 103. Flood area classification (Low, Medium, High, and Extreme) in meters of the PD_F0.64 scenarios during hurricane Michael-2018 at NSN base, the US.	371
Figure 104. Pie chart of the flood areas, with percentages, of the different flood levels for PD_F0.88 scenario for Hurricane Michael-2018 at NSN, the US.	371
Figure 105. Water level time series (m) during the different hurricanes showing the surge magnitude and duration for different surge levels for the base and RMW_F0.9 scenarios at Sewells Point, NSN, the US.....	372

Figure 106. Peak surge (m) (left panel) and surge duration (h) of the different surge levels (right panel) for the base and RMW_F0.9 scenario for all hurricanes, NSN, the US.	372
Figure 107. Average Flood Depth (AFD) & Maximum Flood Depth (MFD) in meters (left panel) and Flood area (km ²) (right panel) of all hurricanes for the Base and RMW_F0.9 scenarios, NSN, the US.	373
Figure 108. Flood maps with the flood levels for the different hurricanes during the peak surge for the RMW_F0.9 scenario at NSN, the US.	375
Figure 109. Water level time series (m) during the different hurricanes showing the surge magnitude and duration for different surge levels for the base and RMW_F1.1 scenarios at Sewells Point, NSN, the US.	376
Figure 110. Peak surge (m) (left panel) and surge duration (h) of the different surge levels (right panel) for the base and RMW_F1.1 scenario for all hurricanes, NSN, the US.	376
Figure 111. Average Flood Depth (AFD) & Maximum Flood Depth (MFD) in meters (left panel) and Flood area (km ²) (right panel) of all hurricanes for the Base and RMW_F1.1 scenarios, NSN, the US.	377
Figure 112. Flood maps with the flood levels for the different hurricanes during the peak surge for the RMW_F1.1 scenario at NSN, the US.	378
Figure 113. Water level time series (m) during the different hurricanes showing the surge magnitude and duration for different surge levels for the base and SLR_0.4M scenarios at Sewells Point, NSN, the US.	379
Figure 114. Peak surge (m) (left panel) and surge duration (h) of the different surge levels (right panel) for the base and SLR_0.4M scenario for all hurricanes, NSN, the US.	379
Figure 115. Average Flood Depth (AFD) & Maximum Flood Depth (MFD) in meters (left panel) and Flood area (km ²) (right panel) of all hurricanes for the Base and SLR_0.4M scenarios at NSN, the US.	380
Figure 116. Timeseries of the projected average and maximum flood depth (left axis) and flood area (km ² -right axis) for all hurricanes for SLR_0.4M scenario at NSN, the US.	381
Figure 117. Flood maps with the flood levels for the different hurricanes during the peak surge for the SLR_0.4M scenario at NSN, the US.	382

Figure 118. Pie chart of the flood areas, with percentages, of the different flood levels for SLR_0.4M scenarios for all hurricanes at NSN, the US.....	383
Figure 119. Water level time series (m) during the different hurricanes showing the surge magnitude and duration for different surge levels for the base and SLR_0.8M scenarios at Sewells Point, NSN, the US.....	384
Figure 120. Peak surge (m) (left panel) and surge duration (h) of the different surge levels (right panel) for the base and SLR_0.8M scenario for all hurricanes, NSN, the US.	384
Figure 121. Average Flood Depth (AFD) & Maximum Flood Depth (MFD) in meters (left panel) and Flood area (km ²) (right panel) of all hurricanes for the Base and SLR_0.8M scenarios at NSN, the US.	385
Figure 122. Timeseries of the projected average and maximum flood depth (left axis) and flood area (km ² -right axis) for all hurricanes for SLR_0.8M scenario at NSN, the US.	387
Figure 123. Flood maps with the flood levels for the different hurricanes during the peak surge for the SLR_0.8M scenario at NSN, the US.	388
Figure 124. Pie chart of the flood areas, with percentages, of the different flood levels for SLR_0.8M scenarios for all hurricanes at NSN, the US.	389
Figure 125. Water level time series (m) during the different hurricanes showing the surge magnitude and duration for different surge levels for the base and WSF_0.925 scenarios at Sewells Point, NSN, the US.....	390
Figure 126. Peak surge (m) (left panel) and surge duration (h) of the different surge levels (right panel) for the base and WSF_0.925 scenario for all hurricanes, NSN, the US.	390
Figure 127. Average Flood Depth (AFD) & Maximum Flood Depth (MFD) in meters (left panel) and Flood area (km ²) (right panel) of all hurricanes for the Base and WSF_0.925 scenarios at NSN, the US.	391
Figure 128. Timeseries of the projected average and maximum flood depth (left axis) and flood area (km ² -right axis) for all hurricanes for WSF_0.925 scenario at NSN, the US.	393
Figure 129. Flood maps with the flood levels for the different hurricanes during the peak surge for the WSF_0.925 scenario at NSN, the US.	394

Figure 130. Pie chart of the flood areas, with percentages, of the different flood levels for WSF_0.925 scenarios for all hurricanes at NSN, the US.....	394
Figure 131. Water level time series (m) during the different hurricanes showing the surge magnitude and duration for different surge levels for the base and WSF_1.075 scenarios at Sewells Point, NSN, the US.....	395
Figure 132. Peak surge (m) (left panel) and surge duration (h) of the different surge levels (right panel) for the base and WSF_1.075 scenario for all hurricanes, NSN, the US.	395
Figure 133. Average Flood Depth (AFD) & Maximum Flood Depth (MFD) in meters (left panel) and Flood area (km ²) (right panel) of all hurricanes for the Base and WSF_1.075 scenarios at NSN, the US. ..	396
Figure 134. Timeseries of the projected average and maximum flood depth (left axis) and flood area (km ² -right axis) for all hurricanes for WSF_1.075 scenario at NSN, the US.	398
Figure 135. Flood maps with the flood levels for the different hurricanes during the peak surge for the WSF_1.075 scenario at NSN, the US.	399
Figure 136. Pie chart of the flood areas, with percentages, of the different flood levels for WSF_1.075 scenarios for all hurricanes at NSN, the US.	399

List of Tables

Table 1. Degradations applied to the different model simulations.....	27
Table 2. Tidal components with their amplitudes and phases employed in the D-Flow FM simulations, NSN, US.....	39
Table 3. Summary statistics of simulated and measured water levels at the different stations during Hurricane Irene, 2011 using ERA5 and HM wind forces, NSN, US.	65
Table 4. Error statistics (Differences in magnitude (m), timing (h), and duration (h)) of peak surge characteristics at Sewells Point for Hurricane Irene-2011, NSN, US.	67
Table 5. Projected flood area statistics at the peak flood during Hurricane Irene-2011 for the base-ERA5 scenario at NSN, the US.....	75
Table 6. Summary statistics of simulated and measured water levels at the different stations during Hurricane Isabel, 2003 using ERA5 and HM wind forces, NSN, US.	78
Table 7. Error statistics (Differences in magnitude (m), timing (h), and duration (h)) of peak surge characteristics at Sewells Point for Hurricane Isabel-2003, NSN, US.	80
Table 8. Projected flood area statistics at the peak flood during Hurricane Isabel-2003 for the base-ERA5 scenario at NSN, the US	86
Table 9. Summary statistics of simulated and measured water levels at the different stations during Hurricane Sandy, 2012 using ERA5 and HM wind forces, NSN, US.	89
Table 10. Error statistics (Differences in magnitude (m), timing (h), and duration (h)) of peak surge characteristics at Sewells Point for Hurricane Sandy-2012, NSN, US.	95
Table 11. Projected flood area statistics at the peak flood during Hurricane Sandy-2012 for the base-ERA5 scenario at NSN, the US	98
Table 12. Summary statistics of simulated and measured water levels at the different stations during Hurricane Michael, 2018 using ERA5 and HM wind forces, NSN, US.	100
Table 13. Error statistics (Differences in magnitude (m), timing (h), and duration (h)) of peak surge characteristics at Sewells Point for Hurricane Micahel-2018, NSN, US.....	106

Table 14. Projected flood area statistics at the peak flood during Hurricane Michael-2018 for the base-ERA5 scenario at NSN, the US	109
Table 15. Peak surge characteristics (Maximum and Duration) of the worst-case pressure drop scenario (PD_F0.64) and base scenarios for all Hurricanes at Sewells Point, NSN, the US.	112
Table 16. Flood area characteristics of the worst-case pressure drop scenario (PD_F0.64) for all hurricanes at NSN, the US.....	112
Table 17. Peak surge characteristics (Maximum and Duration) of the base and RMW_F1.25 scenarios for all Hurricanes at Sewells Point, NSN, the US.	117
Table 18. Flood area characteristics of the base and RMW_F1.25 scenarios for all hurricanes at NSN, the US.	118
Table 19. Peak surge characteristics (Maximum and Duration) of the base and SLR_1.3M scenarios for all Hurricanes at Sewells Point, NSN, the US.	121
Table 20. Flood area characteristics of the base and SLR_1.3M scenarios for all hurricanes at NSN, the US.	122
Table 21. Peak surge characteristics (Maximum and Duration) of the base and WSF_1.225 scenarios for all Hurricanes at Sewells Point, NSN, the US.	129
Table 22. Flood area characteristics of the base and WSF_1.225 scenarios for all hurricanes at NSN, the US.	130
Table 23. Error statistics of peak surge characteristics for the base scenarios at Sewells Point for all hurricanes, NSN, US.....	110
Table 24. Projected flood area statistics at the peak flood during Hurricane Irene-2011 for the base-HM scenario at NSN, the US.....	352
Table 25. Projected flood area statistics at the peak flood during Hurricane Isabel-2003 for the base-HM scenario at NSN, the US.....	353
Table 26. Projected flood area statistics at the peak flood during Hurricane Sandy-2012 for the base-HM scenario at NSN, the US.....	353
Table 27. Projected flood area statistics at the peak flood during Hurricane Michael-2018 for the base-HM scenario at NSN, the US.....	353

Table 28. Peak surge characteristics (Maximum and Duration) the base and the PD_0.76 scenarios for all Hurricanes at Sewells Point, NSN, the US.....	358
Table 29. Flood area characteristics of the base and the PD_F0.76 for all hurricanes at NSN, the US.....	359
Table 30. Peak surge characteristics (Maximum and Duration) of the worst-case pressure drop scenario (PD_F0.88) and base scenarios for all Hurricanes at Sewells Point, NSN, the US.....	366
Table 31. Flood area characteristics of the worst-case pressure drop scenario (PD_F0.88) for all hurricanes at NSN, the US.....	366
Table 32. Peak surge characteristics (Maximum and Duration) for the base and the RMW_F0.9 scenarios for all Hurricanes at Sewells Point, NSN, the US.....	373
Table 33. Flood area characteristics of the base and the RMW_F0.9 scenarios for all hurricanes at NSN, the US.....	373
Table 34. Peak surge characteristics (Maximum and Duration) the base and the RMW_F1.1 scenarios for all Hurricanes at Sewells Point, NSN, the US.....	376
Table 35. Flood area characteristics of the base and the RMW_F1.1 for all hurricanes at NSN, the US.....	377
Table 36. Peak surge characteristics (Maximum and Duration) of the base and SLR_0.4M scenarios for all Hurricanes at Sewells Point, NSN, the US.....	380
Table 37. Flood area characteristics of the base and SLR_0.4M scenarios for all hurricanes at NSN, the US.....	380
Table 38. Peak surge characteristics (Maximum and Duration) of the base and SLR_0.8M scenarios for all Hurricanes at Sewells Point, NSN, the US.....	385
Table 39. Flood area characteristics of the base and SLR_0.8M scenarios for all hurricanes at NSN, the US.....	385
Table 40. Peak surge characteristics (Maximum and Duration) of the base and WSF_0.925 scenarios for all Hurricanes at Sewells Point, NSN, the US.....	391
Table 41. Flood area characteristics of the base and WSF_0.925 scenarios for all hurricanes at NSN, the US.....	391

Table 42. Peak surge characteristics (Maximum and Duration) of the base and WSF_1.075 scenarios for all Hurricanes at Sewells Point, NSN, the US. 396

Table 43. Flood area characteristics of the base and WSF_1.075 scenarios for all hurricanes at NSN, the US. 396

List of Acronyms

CRM	Coastal Relief Model
CUDEM	Continuously Updated Digital Elevation Model
Delft3D	Deltares 3D hydrodynamic model (Class II)
DEM	Digital Elevation Model
DoD	Department of Defense
ESTCP	Environmental Security Technology Certification Program
ETS	extratropical storms
FM	Flexible Mesh
FUNWAVE	Fully Nonlinear Wave model (Class III)
GEBCO	Generic Bathymetric Chart of the Oceans
HPC	High performance computer
IPCC	Intergovernmental Panel on Climate Change
MSL	Mean Sea Level
NCEI	National Centers for Environmental Information
NHC	National Hurricane Center
NOAA	National Oceanic and Atmospheric Administration
NSN	Naval Station Norfolk
RMW	Radius of Maximum Winds
SLR	Sea Level Rise
SRTM	Shuttle Radar Topography Mission
SWAN	Simulating Waves Nearshore model
TVD	Total Variance Diminishing
TWL	Total Water Level
US	United States
USGS	United States Geological Survey
WGS	World Geodetic Survey
AFD	Average Flood Depth
MFD	Maximum Flood Depth

1. Introduction

1.1. Background

Total water levels (TWL) consist of the mean sea level, tide, storm surge, and wave-induced setup and runup (Figure 1). Although the changes in tidal magnitude are conservative, changes in the non-tidal components are highly affected by the dominant meteorological forcing (e.g. wind and atmospheric pressure) and climate change. Extreme weather events such as hurricanes can impact TWL, while climate change increases the mean sea level.



Figure 1. Schematic showing description of the different components of total water level.

The combined impacts of hurricanes and climate change can lead to an increase in TWL, which can cause severe impacts such as flooding and coastal erosion. Accurate prediction and evaluation of TWL are also needed to predict the impact on military readiness and resilience for coastal facilities, (GAO, 2019; Hall et al., 2016; UOCS, 2016). There are a variety of numerical models available for modeling historical and projected TWL and its associated impacts. Model complexity varies from empirical to full wave resolving. In this demonstration, a combination of hydrodynamic and wave models was used to investigate TWL and its associated flooding at Naval Station Norfolk (NSN), Virginia, USA. Model fidelity and capability for several hurricanes are assessed through comparison to available data and through scenario analysis varying hurricane track (Salehi, 2018), hurricane radius and pressure (Mousavi et al., 2011), hurricane wind field (Camelo et al., 2020; Emanuel, 1987), water level (Sweet et al., 2022), and degradation in forcing and bathymetric data.

1.2. Study Area

Norfolk is located on the south shore of the Chesapeake Bay approximately 30 km west of the Atlantic Ocean in southeastern Virginia (USA), Figure 2. The city has a population of approximately 250,000 people and is home to an active military facility (Naval Station Norfolk).

With most of the elevation within 5 m of mean sea level (MSL), the city is highly vulnerable to the impacts of SLR, nuisance flooding at high tides, and surge during tropical and extratropical storms. For example, in August 2011, during Hurricane Irene, the city experienced significant flooding and damage on the order of USD 12 million. Just offshore of Norfolk, the hurricane brought combined tide and surge levels of up to 1.89 m above MSL, maximum wind speeds of 27 m/s, and significant wave heights of up to 2.62 m.

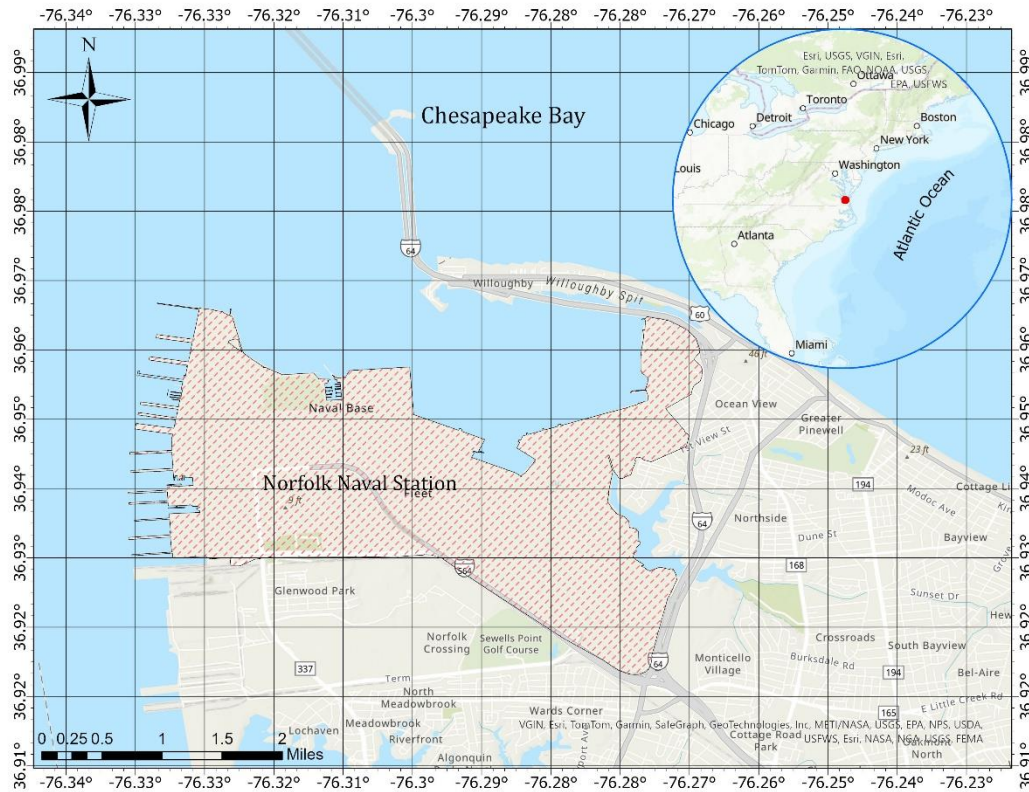


Figure 2. Thematic map showing Naval Station Norfolk (shaded area) with an overview map that shows the study site location (red dot) relative to the wider US east coast.

The area has a mean tidal range of 0.74 m and typically experiences an east-south-easterly wind-wave climate with significant wave heights of 0.4 m and peak periods of 5 s (averaged over data from 2006 to 2021). The Chesapeake Bay-fronting coastline is characterized by average beach and surf zone (wave breaking region) slopes of 1:30 and 1:40, respectively; where the beach is defined as the region $\pm 2\sigma$ around the mean shoreline elevation (setup), σ is the standard deviation of the continuous water level record, and the surf zone is defined as the area between the setup location and the location of wave breaking.

1.3. Aim and Objectives

We aim to enhance military installation readiness and resilience by performing numerous predictive simulations to evaluate the impacts of climate change, hurricane parameters, and the potential lack of accurate data for the prediction of TWL and associated flooding at NSN.

Several objectives were addressed:

- i. Predict the TWL during varied hurricane forcing and quantify the model skill in predicting the timing, magnitude, and duration of the peak surge using available water level station data.
- ii. Identify flooded spatial area as a function of time and flooded depth and compare the results to available anecdotal data.
- iii. Compare the Class III full physics model (FUNWAVE; see Section 2) with the Class II model (D-Flow FM) for the open coast portion of the study to determine the importance of the wave component to TWL. These simulations provide critical information on whether a Class III model is needed to resolve TWL in a geomorphological setting similar to NSN.
- iv. Conduct “degradation simulations” to the base model simulation to quantify prediction error when there is a deficit of information (resolution and/or accuracy). These simulations provide critical information on prediction confidence when input and forcing data are imperfect (always the case in a predictive scenario).
- v. Document time required for model building and computational runtime with associated architecture to quantitatively evaluate the time and effort required to carry out the normal or expert user to implement this work.

1.4. Guide to the Report

The report is organized in a condensed fashion to simplify reading for the Program Manager, reviewers, and other SERDP/ESTCP or military personnel. As such, the main body of the report is streamlined focusing on the performance objectives and results. Details of the study are provided in this appendix.

2. Methodology Overview

2.1. Overview of Prediction Approaches

TWLs were predicted using a suite of simulation models from simple, low-cost empirical to complex, high cost (computation and effort) physics-based (Table 1). The approaches were grouped into three classes: Class I includes empirical approaches that focus on simplified equations for storm surge (Russo, 1998) and runup (Stockdon, et al., 2006). Class II includes (coupled) process-based numerical models, ADCIRC (Dietrich et al., 2011b; Luettich and Westerink, 2004), NearCoM (Shi et al., 2013) and D-flow FM (Deltares, 2023a). The models are

essentially based on the Nonlinear Shallow Water Equations (NSWE) and resolve tides, surges, and statistical wave conditions. The models are dynamically coupled to spectral wave models such as SWAN (e.g. Sebastian et al., 2014). Class III includes dynamical wave models that resolve individual waves, here FUNWAVE-TVD (Shi et al., 2012). Class III models predict the effects of incident sea and swell (SS), IG, and very low frequency (VLF) waves on TWL (Gawehn et al., 2016); processes largely ignored in past efforts.

Table 1. Pros and cons of the models used in the demonstration.

Model	Pros	Cons
Empirical (Class I)	<ul style="list-style-type: none"> • Simple • Inexpensive • Widely adopted 	<ul style="list-style-type: none"> • Poor resolution • Heavily parameterized physics • Limited validation
Delft3D (Class II)	<ul style="list-style-type: none"> • Well-validated for storm waves and surge • Unstructured meshes allow resolution to vary over several orders of magnitude • Computational efficiency allows simulations over 100's of kilometers and timescales of several days 	<ul style="list-style-type: none"> • Model resolution limited to tens of meters at critical infrastructure • Does not resolve wave runup
SWAN+ADCIRC (Class II)	<ul style="list-style-type: none"> • Well-validated for storm waves and surge • Unstructured meshes allow resolution to vary over several orders of magnitude • Parallel efficiency to tens of thousands of computational cores 	<ul style="list-style-type: none"> • Model resolution limited to tens of meters at critical infrastructure • Does not resolve wave runup
NearCom (Class II)	<ul style="list-style-type: none"> • 2DH with 3D dispersive effect 	<ul style="list-style-type: none"> • Analytical solution-based vertical current profile • coupling between wave and

	<ul style="list-style-type: none"> Consider breaking rollers and undertow 	current may be costly in the MPI scheme
FUNWAVE (Class III)	<ul style="list-style-type: none"> Wave-resolving Wave-current interaction IG wave generation 	<ul style="list-style-type: none"> Computationally expensive; limited to domains spanning < 10 km and timescales < 1 hour Shallow water limitation Requires boundary conditions from Class II models

2.2. Overview of Simulation Approach

The demonstration is carried out in three phases.

Phase 1: Numerous simulations were conducted using Class I, II, and III models for Hurricane Irene. These simulations are referred to as base simulations for comparison to subsequent simulations and serve as the output for model calibration/validation. Using the same calibration parameters of Irene, the base simulations for Hurricanes Isabel, Sandy and Michael were established for class II models.

The base simulations were used to investigate the effect of using the parametrized (Holland Model: (Holland, 1980a)) and modeled (ERA5) wind forcing on the accuracy of prediction of the TWL and associated flooding at NSN. The output was calibrated against measured water levels at different locations along the US East Coast and against anecdotal data for flooding.

Phase 2: Hurricane forcing was perturbed to estimate the impacts of changing the meteorological forcing (central pressure drop and the radius of maximum wind) on the model results. In addition, the impacts of climate change in terms of SLR and varying wind speed were evaluated.

Phase 3: A series of degradation scenarios was conducted to evaluate model performance when there is a deficit of accurate data. These degradation scenarios included bathymetry error, model grid resolution, and potential error in the hurricane track. A one-to-one comparison was carried out to evaluate the efficiency of the different models to predict the TWL and its associated impacts on NSN.

Table 2. Degradations applied to the different model simulations.

Parameter	Alteration 1	Alteration 2	Alteration 3
Model bathymetry resolution	Degrade by a factor of 5	Degrade by a factor of 20	Degrade by a factor of 50
Bathymetry accuracy	Add gaussian noise of +/- 0.3 m	Add gaussian noise of +/- 0.5 m	Add gaussian noise of +/- 1 m

2.3. Performance objectives

This demonstration project tests a variety of performance objectives related to TWL-induced flooding at NSN Table 3.

Objective 1: Document the time required to develop the model bathymetry from DEMs and the forcing boundary conditions.

Objective 2: Document the run time and computational architecture used to conduct the various simulations.

Objective 3: Quantify the model skill in predicting the timing of peak surge using available tide station data.

Objective 4: Quantify the model skill in predicting the magnitude of peak surge using available tide station data.

Objective 5: Quantify the model skill in predicting the duration of a particular flooding level using available tide station data.

Objective 6: Quantify flooded spatial area as a function of time and flooded depth and compared the results to available anecdotal data.

Objective 7: Compare the Class III full physics model (FUNWAVE) with the Class II models for the open coast portion of the study to determine the importance of the wave component to TWL. There is no performance metric for this comparison.

Objective 8: Conduct “degradation simulations” to the base model simulation to quantify prediction error when there is a deficit of information (resolution and/or accuracy). There is no performance metric for this comparison. However, these simulations provide critical information on prediction confidence when input and forcing data are imperfect (always the case in a predictive scenario). Objective 9: Model simulation results were provided as layers in a webpage for program manager review.

Table 3. Performance objective for the NSN demonstration study.

Performance Objective	Metric	Data Requirements	Success Criteria
Quantitative Performance Objectives			
1) Model setup	Quantify the time required to generate DEM and boundary conditions	Database supplied bathymetry, wind or storm parameters, waves, offshore water level	< 2 weeks (Class I) < 4 weeks (Class II) < 6 weeks (Class III)
2) Model run time	Quantify the time required to conduct simulation as a function of architecture	Time and computational resources used	< 3 hours (Class I) < 24 hours (Class II) < 30 hours (Class III)
3) Test models' capability in predicting the timing of peak surge	Comparison with available water level data and reference full physics model runs when possible	Water level data from multiple tide stations	± 3 hours of actual timing
4) Test models' capability in predicting the magnitude of peak surge	Comparison with available water level data and reference full physics model runs when possible	Water level data from multiple tide stations	< 20% RMSE; non-wave-driven < 30% RMSE; wave-driven
5) Test models' capability predicting the duration of particular TWL	Comparison with available water level data and reference full physics model runs when possible	Water level data from multiple tide stations	± 3 hours of actual duration
Qualitative Performance Objectives			
6) Test models' capability predicting the spatial extent of flooding for a particular depth and timing	Comparison with available anecdotal data of flooding and reference full physics model runs when possible	Anecdotal data from community reports (note anecdotal data will be incomplete)	Express value in comparing the different model outputs of flooding extent

7) Compare full physics model with Class II models	Importance of the wave component to TWL	Model data from different simulations	Quantification of the importance of the wave component
8) Model degradation simulations	Importance of resolution and accuracy of model inputs and forcing	Model data from different simulations	Quantification of the model output relative to the base simulation with “perfect” inputs
9) Web interface: Ease of use	The ability of technical-level personnel to use/understand the output	Personnel feedback on the interface	Technician-level personnel can select results suitable for the installation

3. Performance metric testing

This study was designed to develop a set of efficient model simulations that can be employed to obtain the most accurate peak surge and associated flood area results. The model performance was evaluated based on the performance metrics, with pre-defined success criteria, Table 3. This section briefly presents an overview of the performance metrics results for the considered baseline simulations for all employed models. More details can be found in the results section.

3.1. Class I models

The Class I models have minimal fidelity in predicting surge and runup and the codes to generate the data are fairly straightforward. The Russo (1998) model takes as input the central pressure deficit, the angle of the hurricane track relative to the shoreline, and the hurricane forward speed. The central pressure deficit data were obtained from NOAA records and the other two parameters were obtained from D-Flow output. The time required for preparation of code in Matlab was less than 3 hours. The subsequent function development could then be used for any parameters in the Russo (1998) formulation. The code runs nearly instantaneously on a 2.1 GHz Intel Xeon Silver 4110 processor with 64 MB of memory.

The Stockdon et al. (2006) model required more effort to generate water level predictions. Data required for the model includes bathymetry to generate a cross-shore profile and offshore wave data. All needed information was provided by D-Flow FM. A Matlab function was generated to select shoreline segments every 100 m along the coast, generate cross-shore profile at that location, quantify the local beach slope, project the profile to a depth of 15 m, and extract the wave height and period. Code development and troubleshooting required roughly 10 hours. Code

execution and plot generation takes less than 1 minute on the same architecture used for the Russo (1998) approach.

The models are generally poor predictors of surge at NSN and the runup calculations are only relevant on Willoughby Spit fronted by a sloping beach as opposed to NSN fronted by civil infrastructure.

3.2. Class II models

3.2.1. D-Flow FM

1. Time required to generate the DEM and the model boundary conditions.

The time required to prepare the model inputs (preprocessing stage) including the bathymetry (DEM) and the boundary conditions are dependent on several factors include, but not limited to, the availability of the appropriate data, the format of the data, the extent of the model domain, the purpose of the model and the experience of the modeler.

This study was conducted with an intel core i9 processor with 24 cores, 3.0 GHz and 64 GB of memory. Considering the large model domain, the model required a massive amount of bathymetry and topography data that needed a significant processing time. In addition, the model was fed by a variety of input forcing including tide, wind and baroclinic water levels. Therefore, the time spent in the preprocessing stage was about 3-4 weeks, which was still within the success criteria of this performance metric.

2. Time required to conduct a simulation as a function of the architecture.

All simulations were run using the same computational architecture. Each simulation was assigned 10 cores and 10-12 GB of memory (average 1 GB/core). The run time varied between 6-14 hours/simulation depending on whether one or more (up to three at maximum) simulations were running simultaneously on the machine. This run time lies within the success criteria of this metric (<24 hours run time).

3. Model capability in predicting the timing of the peak surge.

Evaluating the model performance in predicting the timing, magnitude and duration of the peak surge was conducted at Sewells Point at NSN for all hurricanes (baseline scenarios) using ERA5 and HM wind forces, **Table 4**.

The model was efficiently capable of capturing the correct timing of the peak surge within ± 1 hour of the actual timing (success criteria is < 3 hours) for all hurricanes using ERA5 and HM wind forces.

Table 4. Performance metrics of peak surge prediction for the baseline scenarios at Sewells Point for all hurricanes at NSN.

#	Hurricane/ Wind Forcing	Performance Metrics (Peak Surge)						
		RMSE (m)		Timing (h)	Duration (h)			
		Statistic	Success criteria		Low	Medium	High	
1	Irene	ERA5	0.22	< 0.47	-1.0	-1.0	-2.0	-3.0
2		HM	0.22		0.0	-3.5	-2.0	-1.0
3	Isabel	ERA5	0.15	< 0.42	-1.0	-3.0	-2.0	-1.0
4		HM	0.23		-1.0	-15.0	-4.0	-5.0
5	Sandy	ERA5	0.17	< 0.40	+1.0	-2.0	0.0	0.0
6		HM	0.44		+1.0	-3.0	-28.0	-4.0*
7	Michael	ERA5	0.26	< 0.25	-1.0	-2.0	-2.0*	0.0**
8		HM	0.27		0.0	-3.0	-2.0*	0.0**

4. Model capability in predicting the magnitude of the peak surge.

The model was capable of predicting the peak surge magnitude, **Table 4**, with a RMSE that is less than 10% (success criteria < 20%) of the actual surge magnitude for hurricanes Irene and Isabel using ERA5 and HM wind data. In addition, the model performance during Hurricane Michael can also be considered within the acceptable range with RMSE of 0.26 m - 0.27 m (20.5% - 21.5%), which is 1-2 cm above the success criteria. The lower model performance during Hurricane Michael might be attributed to the approaching angle of the hurricane (coming from land side) and the absence of other processes associated with the hurricane such as the associated precipitation, which was not considered in this study. For Hurricane Sandy, the model satisfied the success criteria with RMSE less than 10% using ERA5 data. However, using HM data, the model performance reduced with a RMSE of 0.44 m (22%). This slight reduction in the model performance was mainly due to the large distance between Hurricane Sandy's track and NSN.

5. Model capability in predicting the duration of a particular TWL.

The model capability of capturing the duration of the peak surge was significantly affected by the underestimation in the peak surge magnitude, which was also affected by different other factors. The peak surge was classified into three levels: low (0.5 m – 1.0 m), medium (1.0 m – 1.5 m) and high level (>1.5 m). observing the medium and high surge levels show that the model was able to predict the duration of these levels with high accuracy (within 0 - 3 hours error margin) using the ERA5 wind data for all hurricanes, **Table 4**. However, using HM wind data, the model performance diminished down to (1 - 5 hours) except for Hurricane Sandy where the significant underestimation in the magnitude prediction resulted in a substantial underestimation in the duration of the medium surge level (-28 hours) and the complete misprediction of the high surge level duration.

6. Model capability in predicting the spatial extent of flooding.

The model was able to efficiently predict the timing and spatial extent of the flood area for all hurricanes. The model outputs were compared to the available anecdotal data obtained from the STORM database where the model shows an excellent agreement between the predicted and the reported anecdotal data. The model was able to predict the spatial extent of the flood area as a function of the flood depth. In addition, the temporal variability of the flood areas was also obtained from the model simulations with associated average and maximum flood depth.

7. Compare the full physics model (class III) to D-Flow FM (class II)

8. Evaluation the sensitivity of the model to the accuracy of model inputs

Sensitivity of the model to the accuracy of the model inputs was evaluated based on three parameters: bathymetry accuracy, bathymetry/mesh resolution, and potential errors in the storm track. Different simulations were conducted, and the results were compared to the baseline scenarios for Hurricane Irene.

Although inaccuracies in the bathymetry/topography accuracy (up to 1.0 m) can have insignificant impact on the prediction of the surge characteristics (magnitude and duration), these inaccuracies can impact on the extent of the flood area where a maximum increase of about 1% was obtained in the predicted flood area under these scenarios. Inaccuracies in the bathymetry/topography less than 0.5 m had no noticeable influence on performance of the model predictions.

A similar pattern was observed while testing the sensitivity of the model to the degradation of the mesh/bathymetry resolution. The mesh resolution was reduced from 15 m for the baseline scenario down to 75 m, 250 m, 500 m and 1000 m. Considering this substantial reduction in the mesh resolution, the impact on the peak surge prediction was negligible. However, the sensitivity of the model performance in flood area prediction to the reduction of the mesh resolution was severe where the predicted flood area increased unrealistically with the resolution degradation up to 51% of NSN area.

The response of the model results to the changes in the hurricane track was substantial. However, the model predictions were highly dependent on the original track and how the track modification affected the distance between the hurricane eye and NSN, where all the data analysis was performed. Generally speaking, the closer the modified track to NSN, the higher the impact on the peak surge and flood area characteristics at the base. However, the intensity of the change, compared to the baseline scenario, was also affected by other factors including the

maximum wind speed, radius of maximum wind (Rmax), angle of approach and the category of the hurricane.

3.2.2. ADCIRC

3.3. Class III models

3.4. Ease of using the web interface

The web interface deliverable date was set for Aug 31, 2024. This qualitative performance objective will be addressed by program managers after the submission of the Demonstration project report.

4. Model simulation results.

4.1. Calibration Results (Baseline scenarios)

5. Model Setup

5.1. Empirical Models

Empirical models for components of TWL are largely data-driven or based on machine learning (e.g. Pearson et al., 2017; Suanez et al., 2016; Tadesse et al., 2020). Empiricism is generally manifested through two components: storm surge and runup. Storm surge is the excess water level due to the wind stress acting over the ocean surface. However, surge magnitudes will also vary based on atmospheric pressure, forward storm speed, angle of shoreline approach, the radius of maximum winds, coastal topography/bathymetry, and funneling into narrow water bodies (e.g. Irish and Resio, 2010; Needham and Keim, 2014; Resio et al., 2009). Simplistic approaches relate the surge, S , as (Russo, 1998)

$$S = PBC, \quad (1)$$

where P is a central pressure factor, B is a bathymetry correction factor, and C is a factor to account for hurricane speed and angle with respect to the shoreline. Use of the Russo model should be restricted to areas in direct vicinity of the storm-landfall location. All three factors have

additional empirical formulations embedded within. Other relations generate surge with respect to some factor multiplied by the square of the wind speed divided by depth (e.g. WMO, 2011) or develop surge hydrographs as a function of time-related to the peak surge elevation at landfall, storm duration, the radius of maximum wind and forward speed (e.g. Xu and Huang, 2014). Only the Russo (1998) empirical approach is used for surge in this demonstration study.

Runup, R , is the summation of wave set up and swash motions. Most empirical relations for runup incorporate the Iribarren Number, ξ , (Iribarren and Nogales, 1949) sometimes referred to as the surf similarity parameter that relates the beach slope to the offshore wave steepness. Hunt (1959) suggested the normalized runup (by wave height) is a function of ξ as

$$\frac{R}{H} = K\xi = K \frac{\beta}{\sqrt{\frac{H}{L}}} \quad (2)$$

where H is wave height, K is a constant, β is the beach slope, and L is the wavelength. The majority of subsequent empirical relations for runup or the 2% runup exceedance, $R_{2\%}$, use the Hunt formula as the root form (e.g. Holman, 1986; Park and Cox, 2016; Stockdon, et al., 2006). It is noted that until recently (Park and Cox, 2016) the Hunt type formulations did not explicitly include beach profile geometry other than beach slope. The (Stockdon et al., 2006) equation for runup exceedance is

$$R_{2\%} = 1.1 \left[0.35\beta(HL)^{0.5} + \frac{(HL\{0.563\beta^2+0.004\})^{0.5}}{2} \right], \quad (3)$$

where the wave height and wavelength are the deep water values, the first term of the equation accounts for wave set up and the second term accounts for swash as the summation of incident and infragravity components.

The Stockdon model is only applicable along shorelines where wave breaking is expected. Thus, application for the demonstration project is along Willoughby Spit rather than NSN where wave breaking is restricted due to limited fetch lengths and bulkhead shorelines. The approach for calculating $R_{2\%}$ is: 1) Obtain offshore wave parameters from D-Flow FM simulations, 2) Start at the east side of Willoughby Spit and identify the shoreline angle with respect to North, 3) Rotate the shoreline angle 90 degrees to obtain a cross-shore orientation, 4) generate Easting and Northing coordinates for a cross-shore transect, 5) Interpolate the bathymetry and topography onto the transect out to a depth of 15 m, 6) Identify the foreshore slope between elevations of -2 m to 2 m, 7) Use the wave parameters and linear wave theory to calculate the wave length, 8) Use the values to calculate $R_{2\%}$, 9) Shift 100 m to the West and re-apply the procedure.

5.2. Hydrodynamic modeling (D-Flow FM)

Delft3D-FM is an open-source flexible integrated modeling suite, that simulates one-dimensional (1D), two-dimensional (2D; in either the horizontal or a vertical plane), and three-dimensional (3D) flow, sediment transport and morphology, waves, water quality, and ecology and is capable of handling the interactions between these processes. The suite is designed for use by domain experts and non-experts alike, which may range from consultants and engineers or contractors to regulators and government officials, all of whom are active in one or more of the stages of the design, implementation, and management cycle. The Delft3D Flexible Mesh Suite (Delft3D FM) is the successor of the structured Delft3D 4 Suite, and it is developed and maintained by Deltares Netherlands as open-source software (www.deltares.nl).

The Delft3D Flexible Mesh Suite is composed of several modules capable of interacting with one another with a mutual interface (D-Flow FM Suite). D-Flow FM is one of these modules. It is a multi-dimensional (1D, 2D, and 3D) hydrodynamic (and transport) simulation module that calculates non-steady flow and transport phenomena resulting from tidal and meteorological forcing on structured and unstructured (flexible), boundary-fitted grids. The term Flexible Mesh refers to the flexible combination of unstructured grids consisting of triangles, quadrangles, pentagons, and hexagons. In 3D simulations, the vertical grid uses the σ coordinate approach as well as a fixed z layers approach, (Deltares, 2023b). D-Flow FM can be used in 2D (depth-averaged) mode, hydrostatic and unsteady form, to solve the continuity and Reynolds-averaged Navier–Stokes equations with an implicit finite volume algorithm under the assumption that vertical length scales are significantly smaller than the horizontal ones, (Lesser et al., 2004)

Delft3D FM allows simulation of the interaction of water, sediment, ecology, and water quality in time and space. The modeling suite is mostly used for the modeling of natural environments like coastal, river, and estuarine areas, but it is equally suitable for more artificial environments like harbors and locks. Delft3D FM consists of several well-tested and validated modules, which are integrated including D-Flow, D-Hydrology, D-Waves, and D-Morphology. In this study, the D-Flow FM and D-Wave modules are used to simulate the interaction between the hurricane-induced wind, waves, currents, and surges. D-Waves is based on the SWAN (Simulating WAves Nearshore) model developed by TU-Delft, the Netherlands. SWAN is a spectral wave action model that can simulate such nearshore dynamics of the waves, (Booij et al., 1999). D-Flow FM has been efficiently used in complex coastal flood modeling applications (Kumbier et al., 2018; Muñoz et al., 2022, 2020; Nederhoff et al., 2021).

5.2.1. Network

The computational network/mesh was created using the D-Flow FM GUI using a spherical coordinate system. The mesh has both rectilinear and triangular components with a resolution that extends from 4 km at the offshore boundary to 1 5m at NSN. The mesh has a spatial extent of about 700 km in the south-north direction and an average of 480 km in the offshore direction, Figure 3. The refinement procedure of the mesh followed the degradation in the bathymetric contours to have high accuracy in the nearshore-shallower waters while maintaining a reasonable computational time.

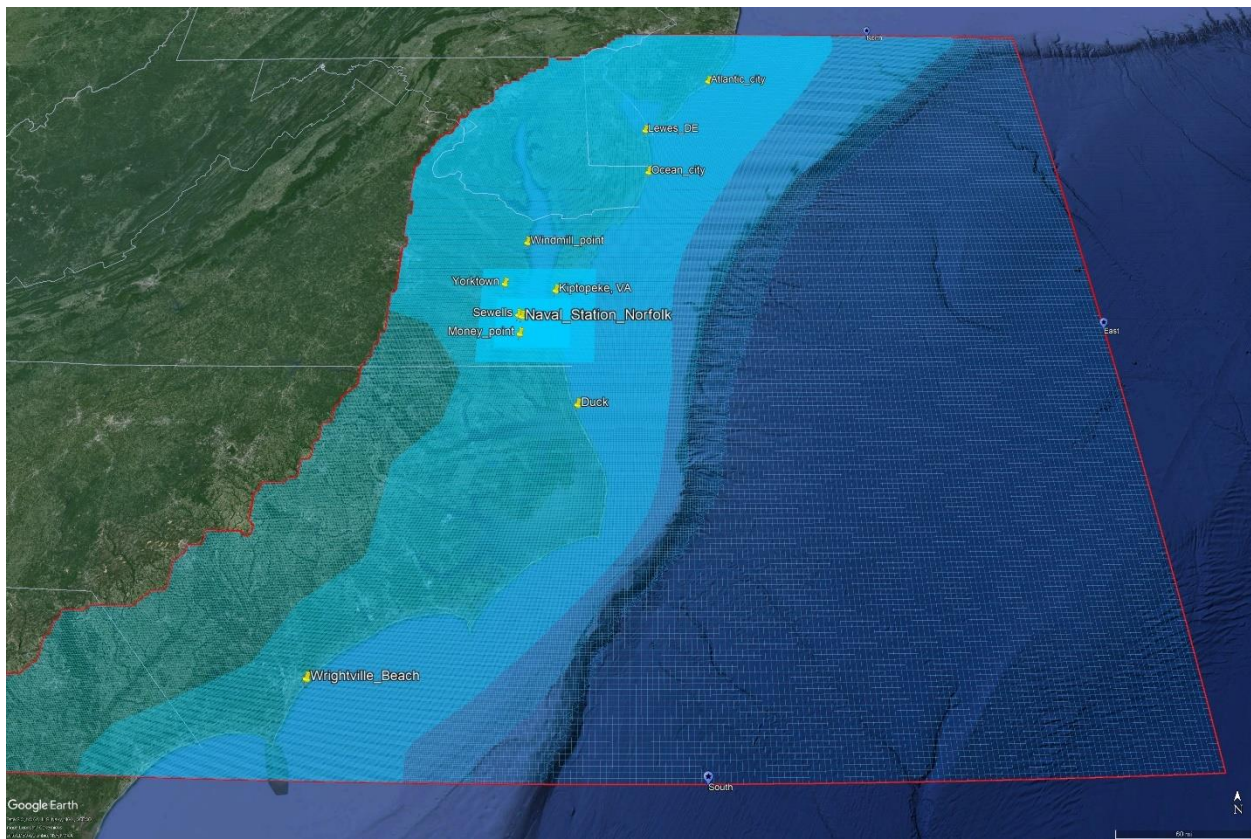


Figure 3 . Computational network/mesh for the D-Flow FM simulation along the east coast of the US.

5.2.2. Bathymetry

Different data sources with different resolutions and accuracies were used to represent the bathymetry and topography of the study area. These data include the Continuously Updated Digital Elevation Model (CUDEM),

<https://coast.noaa.gov/dataviewer/#/lidar/search/where:ID=8483/details/8483>, with a horizontal resolution of 1 m and vertical accuracy of about 0.5 m, National Center for Environmental Information (NCEI) Coastal Relief Model (CRM), <https://www.ncei.noaa.gov/products/coastal-relief-model>, with a horizontal resolution of 90 m and vertical accuracy of about 1m and the General Bathymetric Chart for the Oceans (GEBCO)-v2019, https://www.gebco.net/data_and_products/gridded_bathymetry_data/, which has a horizontal resolution of 450 m with unknown vertical accuracy. All of these data sources were combined and interpolated using the triangulation method using the D-Flow FM Graphical User Interface (GUI). The higher-resolution data were used at the nearshore areas, whereas the lower-resolution data were used at the offshore locations. Figure 4 shows the interpolated bathymetry for the D-Flow FM computational domain.

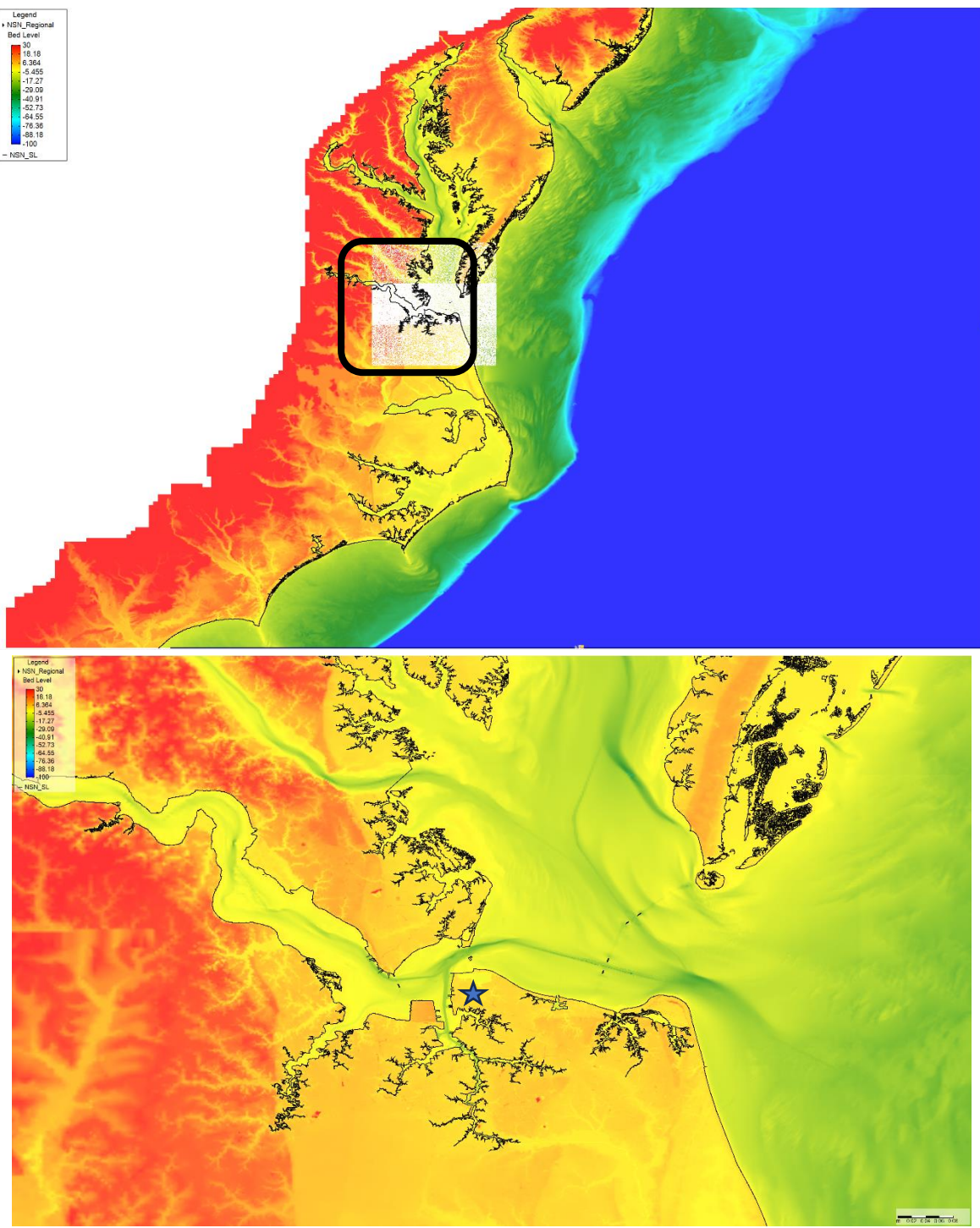


Figure 4. D-Flow FM bathymetry for the entire domain (upper panel) and a zoom-in on NSN (Lower panel-blue star).

5.2.3. Open boundary conditions

The model has three open boundaries, north, east, and south boundaries. The model was forced by two types of data along these boundaries. Tidal forces were employed as astronomical tidal components obtained from the TPXO8 global tidal model using the Delft dashboard toolbox. Two additional components were also added to the tidal forces which are solar annual (SA) and solar semi-annual (SSA). Table 5. shows the used tidal components along with their amplitudes and phases.

In addition to the tidal forces, we tried to mimic the baroclinic changes in the water level using the E.U. Copernicus Marine Environment Monitoring Service (CMEMS). Modeling baroclinic water levels usually requires 3D modeling that considers the vertical layering of the water column to account for the density differences due to changes in temperature and salinity, which should be considered in the model as well, however, in this study we only used 2D depth-averaged model simulations. The CMEMS data are semi-diurnal and referenced to the Geoid model. The data were re-referenced to the mean sea level (MSL) before usage in the simulations.

Table 5. Tidal components with their amplitudes and phases employed in the D-Flow FM simulations, NSN.

#	Component	Amplitude	Phase
1	M2	0.75164	0.55
2	S2	0.12642	18.45
3	N2	0.16137	9.83
4	K2	0.03202	38.66
5	K1	0.10657	189.72
6	O1	0.08139	190.62
7	P1	0.03448	196.86
8	Q1	0.01542	193.27
9	MF	0.00632	341.57
10	MM	0.00224	333.43
11	M4	0.00506	276.47
12	MS4	0.00273	196.77
13	MN4	0.00266	323.98
14	SA	0.02	170
15	SSA	0.02	43.6

5.2.4. Meteorological forcing

Two meteorological forces were used in this study. The entire wind/pressure field can be obtained in a hindcast mode using model-validated wind fields via the European Centre for Medium-Range Weather Forecasts (ECMWF) Re-analysis v5 (ERA5) after the event has occurred. ERA5 also provides predicted wind fields at hourly intervals. The ERA5 is a spatially variable wind field with an average horizontal resolution of 0.25 degrees and a temporal resolution of 1 hour. The data were obtained as a NETCDF format with u (10 m u-component of wind, x-direction) and v (10 m v-component, y-direction) in addition to the atmospheric pressure and spatially variable Charnock coefficient for wind drag, Figure 5.

A second forcing option relies on a parameterized wind field that contains only the hurricane wind field forcing; referred to as the Holland model, (Holland, 2008; Holland, 1980; Holland et al., 2010). Holland model winds can be obtained in real-time or for forecast purposes. The model is easy to implement and perturb. In addition, it can be generated with a resolution as high as the computational domain resolution of the hydrodynamic model if required, Figure 5. The Holland model employs different hurricane characteristics such as the hurricane track, radius of maximum wind, and central pressure drop. The hurricane characteristics were obtained from the National Hurricane Center (NHC).

There are significant differences between both forcings (Table 6) and accurate model calibration should be carried out when using both. We will use and compare the results of both meteorological forcings in this study.

Table 6. Strengths and weaknesses of the ERA5 and Holland model approaches.

	ERA5	Holland Model
Strength	<ul style="list-style-type: none"> • Better representation of complexities of the wind field • Reanalysis products include data assimilation • Accounts for background wind/pressures (those not generated by the storm) <p>Routine predictions available hourly</p>	<ul style="list-style-type: none"> • Definitely available in real-time • Good accuracy relative to cost • Can develop fields at resolution of mesh and model time step • Can perturb inputs
Weakness	<ul style="list-style-type: none"> • Relatively coarse resolution in space (0.25 degrees) and time (hourly) • Difficult to perturb in a physical 	<ul style="list-style-type: none"> • Less accurate than a physics-based model product, no data assimilation

	<p>way, especially the track (due to land masking)</p> <ul style="list-style-type: none"> • Need to adjust wind/pressure field to focus at storm and blend to background meteorology 	
--	---	--

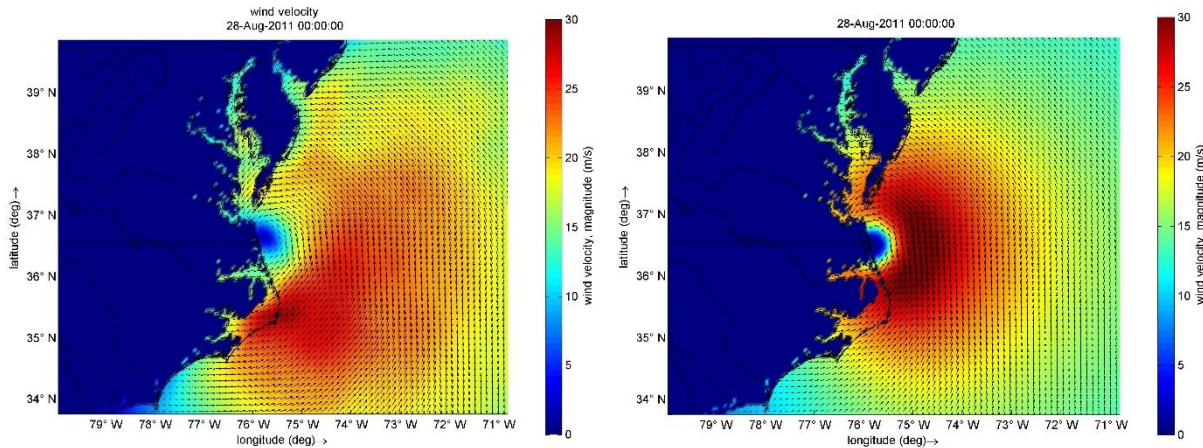


Figure 5. Comparison between the two employed wind forces, ERA5 (left panel) and HM (right panel), at extreme conditions for hurricane Irene, NSN, US

5.2.5. Model Characteristics

The land-sea boundary was obtained from the OpenStreetMap database for the entire eastern US coast, <https://osmdata.openstreetmap.de/data/land-polygons.html>. The model computes the courant criteria at each timestep with an initial value of 0.7. All data were referenced to the MSL and the GMT zone. The model was allowed to run for a few days before the peak surge occurred as a spin-up period. A set of observation points were added to the for the calibration against the measurements. Figure 6 shows the location of the observation points used in the model.

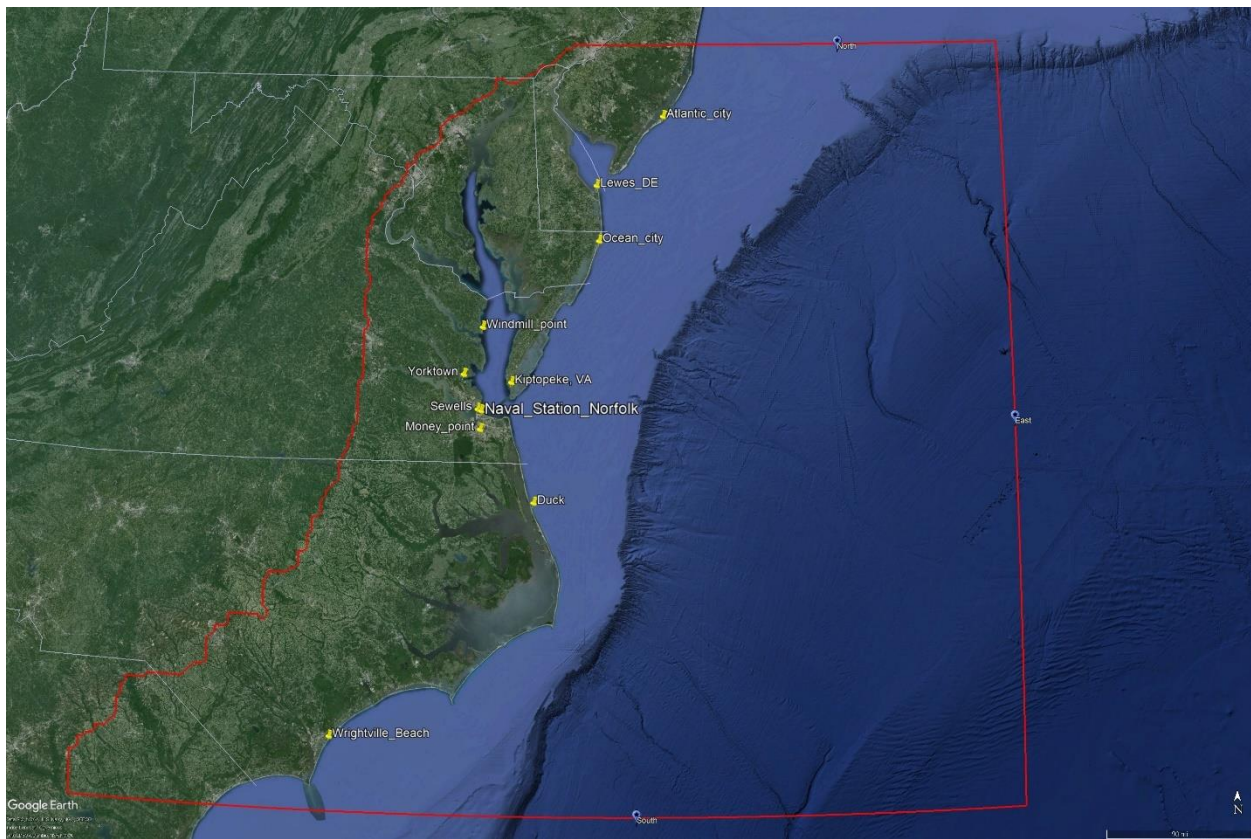


Figure 6. Satellite image showing the model domain (red line) and the observation (calibration) locations used in D-Flow FM, at NSN.

5.3. Wave modeling (SWAN/D-Waves)

D-Waves is based on the third-generation Simulating WAves Nearshore (SWAN) calculation core (Booij et al., 1999). D-Waves computes wave propagation, wave generation by wind, non-linear wave-wave interactions, and dissipation, for a given bottom topography, wind field, water level, and current field in deep, intermediate, and finite depths.

SWAN is a third-generation wave model, developed at Delft University of Technology, that computes random, short-crested wind-generated waves in coastal regions and inland waters, <https://swanmodel.sourceforge.io/download/download.htm>

SWAN is a near-shore spectral wave model that computes wave characteristics due to wind action by solving the wave action equation. SWAN computes the wave statistics, including significant wave height, wave period, and wave direction, iteratively using an implicit time-stepping approach. Wave-current interaction is modeled by coupling SWAN and the circulation model D-Flow. The current-induced Doppler effect is taken into account by incorporating the

current field in SWAN. The wave-induced setups and circulation are computed by D-Flow using the GLM (General Lagrangian Mean)-based radiation stresses, which are calculated in SWAN. Wave radiation stresses and gradients are also calculated.

Three model grids were developed for D-waves computational domain. An overall coarse grid with a resolution of 6 km and a spatial extent a few kilometers larger than the D-flow domain. A 1km grid was nested in the overall grid with a spatial extent of 430 km x 230 km in the alongshore and offshore directions, respectively. A higher resolution grid was nested in the intermediate grid to obtain the best model performance in the surf zone of the area of interest. The high-resolution grid has a 200 m resolution with a spatial extent of 80 km and 30 km alongshore and offshore respectively.

The model was fed by the two meteorological forces used with D-Flow model, ERA5, and HM. In addition, spatially varying time series boundary conditions, obtained from ERA5 database, were used to force the model along the north, east, and southern boundaries. For wave dissipation due to WhiteCapping, the formulation of (van der Westhuysen et al., 2007)was used. Furthermore, a JONSWAP spectrum was used with the peak enhancement factor of 3.3. The model was run in the non-stationary mode with a time step of 1h using the nautical convention.

5.4. Hydrodynamic and Wave Modeling (ADCIRC)

The ADvanced CIRCulation (ADCIRC; Luettich et al. 1992; Westerink et al., 2008) has been developed to simulate coastal circulation due to tides, winds, river flows, and density gradients. ADCIRC solves modified forms of the shallow water equations to predict the water surface elevations and current velocities. It is often applied in the 2D depth-averaged mode, especially for prediction of long ‘waves’ due to tides and storm surge, and it can represent the flooding and drying of overland regions. It has been designed to be highly scalable in high-performance computing (HPC) environments (Tanaka et al., 2011). Due to these modeling choices, ADCIRC has gained prominence for simulations of coastal flooding due to coastal storms like hurricanes, including for real-time forecasts by NOAA and engineering firms.

ADCIRC uses an unstructured, finite-element mesh to represent the complex coastal environment. Triangular finite elements with varying sizes are used to adjust resolution from relatively coarse (10s or 100s of kilometers) in the open ocean to relatively fine (10s of meters) in coastal regions, thus focusing the predictive accuracy where it is most important. Typical domains may include large areas, such as the western North Atlantic Ocean, the Caribbean Sea, and the Gulf of Mexico, in order to represent the offshore development of tides and storm effects, but also include higher resolution in coastal regions. Meshes may focus on a specific coastal region, typically the coastline of a single U.S. state (Bunya et al., 2010; Hope et al., 2013),

but recent studies have used meshes to represent flooding anywhere along the entire U.S. Gulf and Atlantic coasts (Riverside Technology and AECOM, 2015) and worldwide (Pringle et al., 2021).

For real-time forecasts, ADCIRC has been implemented via automated frameworks that: detect when new meteorological forcings are available (either from the NHC or other models), submit and monitor simulations on HPC systems, post-process and visualize the predictions, and communicate the flooding guidance to stakeholders. One widely used framework is the ADCIRC Surge Guidance System (ASGS; Fleming et al., 2008) its predictions are seen by thousands of unique viewers at the Coastal Emergency Risks Assessment (CERA; <https://cera.coastalrisk.live>). Another framework is the ADCIRC Prediction System (APS; <https://www.adcircprediction.org>), which works directly with stakeholders in North Carolina, Florida, and elsewhere.

In this study, ADCIRC was used for predictions of coastal storm effects on water levels at the Naval Station Norfolk. Although ADCIRC can be coupled with spectral wave models (e.g. SWAN; Dietrich et al., 2011), it was used in its stand-alone version in this study due to the sheltered location of NSN (see XXXX). In the following sections, we describe the ADCIRC model implementation for this study.

5.4.1. Unstructured Mesh

To represent storm effects at NSN, an unstructured mesh was developed using OceanMesh2D (Roberts et al., 2019; <https://github.com/CHLNDEV/OceanMesh2D>), which is MATLAB-based and can generate meshes in an automated and reproducible way. We designed the mesh to include a large domain with the western North Atlantic Ocean, the Caribbean Sea, and the Gulf of Mexico, so that tides and atmospheric forcings can be applied offshore and propagate their effects into coastal Virginia. Mesh resolution varies over four levels. In the Caribbean Sea and the Gulf of Mexico, the mesh resolution varies from 20 km offshore to 1 - 2 km along the coast. In the Atlantic Ocean, the mesh resolution varies from 10 km offshore to 500 - 1000 m along the coast. In a region along the U.S. mid-Atlantic coast, the mesh resolution varies from 5 km offshore to 200 - 500 m along the coast. In the region around Norfolk, the mesh resolution varies from 500 m offshore, to 200 m overland, to 20 - 50 m along the coast. Thus, the resolution can vary over three orders of magnitude, but the highest resolution of 20 m is located near NSN. The mesh has about 2.5 million elements and 1.3 million vertices. Figure 7 and Figure 8 shows the mesh's overall domain and a zoom near NSN.

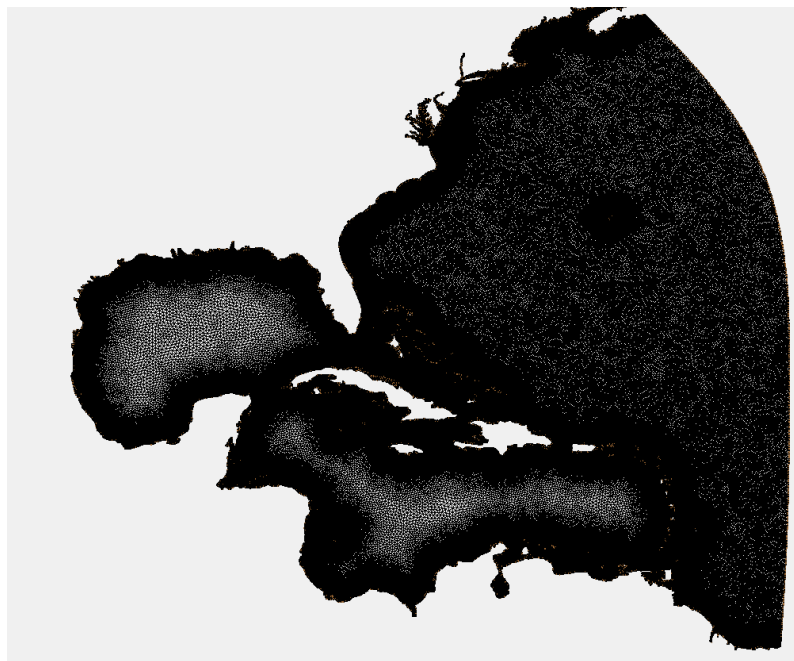


Figure 7. Overall domain showing elements in the Western Atlantic Ocean and Gulf of Mexico.

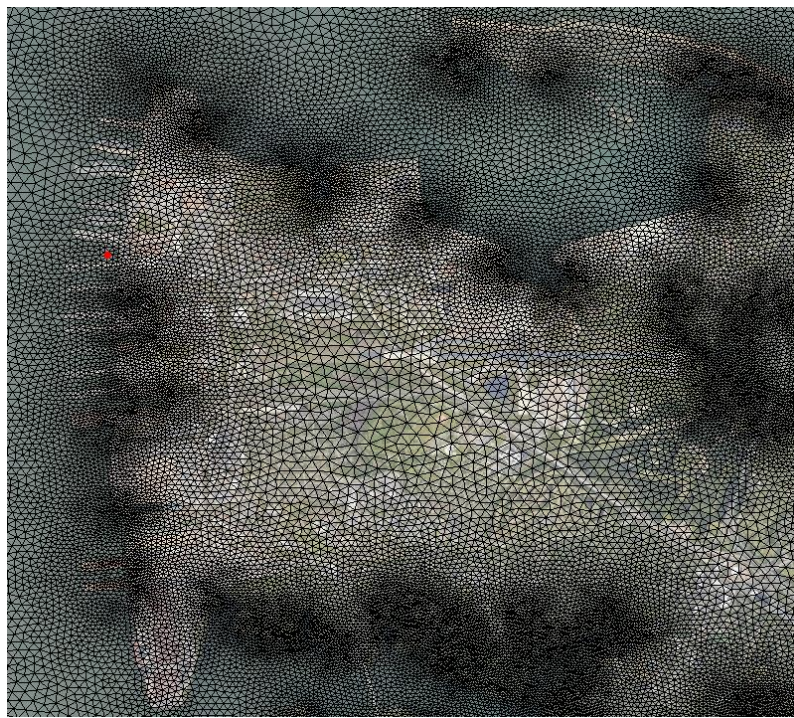


Figure 8. Mesh elements overlaid onto an aerial map of NSN.

5.4.2. Bathymetry

Two datasets at different resolutions were nested together for the accurate representation of the bathymetry and topography of the study area at three resolution and domain extents. These data include CUDEM and the Shuttle Radar Topography Mission (SRTM). The 2018 SRTM data set covers the full domain of the mesh, covering the northwest Atlantic Ocean and Gulf of Mexico at a minimum resolution of 500 m. Zooming into the mid-Atlantic region, specifically Virginia, Maryland and Delaware, the 2014 CUDEM dataset covered this region at minimum resolution at 30 m. At NSN, the 2014 CUDEM dataset covered the Southern Chesapeake Bay and Norfolk region at a minimum resolution of 10 m. Figure 9 shows the full domain and DEM covering NSN.

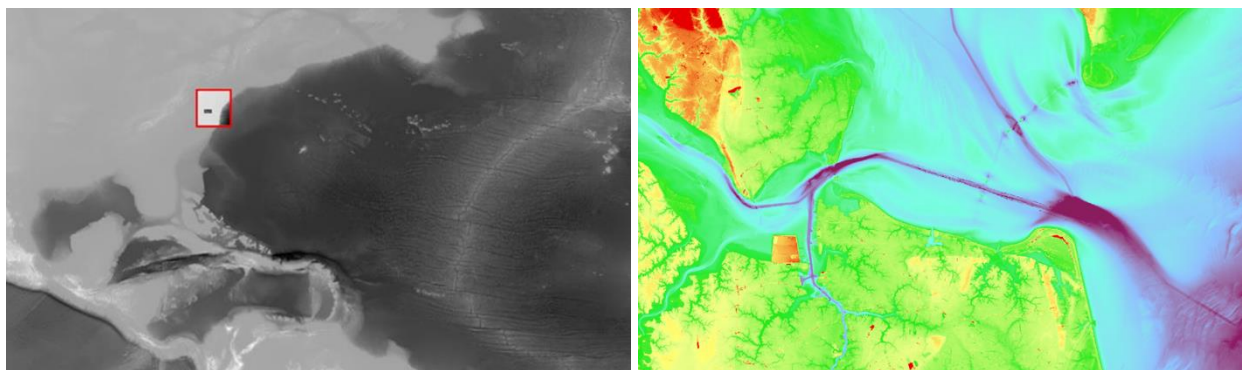


Figure 9. The left panel shows the full extents of the SRTM while the right panel shows the CUDEM used for the Naval Station Norfolk (NSN).

5.4.3. Open Boundary Conditions

Tides are applied at two locations: at the open ocean boundary as a time series of water surface elevations reconstructed from the tidal harmonics, and at every internal vertex as tidal potentials. We use the ‘major 8’ harmonic constituents of Q1, O1, P1, K1, N2, M2, S2, and K2. For each harmonic constituent, location-specific information (e.g. mean amplitude, local epoch) at the boundary vertices is interpolated from the TPXO9 tidal database (Egbert and Erofeeva, 2002; <https://www.tpxo.net/global/tpxo9-atlas>), and time-specific information (e.g. node factor, equilibrium argument) is generated for the period of each storm simulation.

For each simulation, we also adjust the initial water levels with a spatially constant offset to represent the effects of physical processes not predicted by ADCIRC, e.g. baroclinic effects of the Gulf Stream and seasonal warming of the ocean, medium-term (1-2 week) atmospheric events, and relative sea level rise. Each of these processes may cause an increase to the ‘mean’ water levels at NSN that would not be predicted by ADCIRC in a storm-specific simulation, and these increases can be significant – tens of centimeters. For ADCIRC, we increase the water levels at every location in the domain by a spatially constant offset, and then we allow the tides and storm surge to evolve on top of that offset. We computed the offsets by using the NOAA-observed

water levels at Sewells Point, by evaluating the mean of the observed water levels for a period of 7 days immediately before the start of each storm simulation. (The exception was for Hurricane Isabel, where the offsets were computed 11 days before the storm simulation for 7 days to neglect the impact of Henri (2003), which moved offshore and affected water levels at NSN. Table 7 shows the time period and magnitude of the offset for each storm.

Table 7. Summary of offsets for ADCIRC simulations.

Storm	Period to Compute Offset	Offset (m)
Irene	8/17/2011 – 8/24/2011	0.1272
Isabel	9/2/2003 – 9/9/2003	0.1478
Michael	10/1/2018 – 10/7/2018	0.2866
Sandy	10/15/2012 - 10/22/2012	0.1356

5.4.4. Meteorological Forcing

ADCIRC can accept meteorological forcing as surface pressure and wind fields from a variety of sources, ranging from gridded outputs from data assimilation products and full-physics models, to information specified at the vertices as inputs or to be computed during the simulation. In this study, we used the aforementioned Holland model, which has been integrated within ADCIRC and expanded to use the available information in the forecast guidance from the NHC. The Generalized Asymmetric Holland Model (GAHM; Gao, 2018) can use a different radial profile for each storm quadrant, relaxes the assumption about a cyclostrophic balance, and uses two scaling parameters to satisfy $V = V_{max}$ and $dV/dr = 0$ at $r = R_{max}$. GAHM has been shown to reconstruct wind fields that maintain the complexity as specified in the NHC forecasts and compare well to fields from full-physics meteorological models (Dietrich et al., 2018). With time series of only a few parameters, e.g. storm center location and forward speed, central pressure, maximum wind speed and radius, and distances to isotachs in each quadrant, GAHM can reconstruct the surface pressures and wind velocities at every point in the ADCIRC computational domain.

For this study, we used GAHM because it can represent the base and perturbed conditions for each storm simulation. For the base simulation, we used the best-track parameters as released by the NHC. It is important to note that the NHC best-track parameters have become more descriptive over time – for past storms like Isabel, they may not describe the complexity in the quadrants, whereas for recent storms like Michael, they include the full description. Then for each perturbed simulation, we adjusted the parameters in the best-track as input to GAHM. For example, for a perturbation of the maximum wind speeds, we adjusted only that parameter while leaving fixed the other parameters (e.g. radius to maximum winds, central pressure, etc.). Then

GAHM used the perturbed best-track parameters to develop the full fields. Table 8 describes the time period for each storm simulated by GAHM/ADCIRC.

Table 8. Summary of best-track forcing for GAHM/ADCIRC simulations.

Storm	Period of Simulation
Irene	8/24/2011 – 8/30/2011
Isabel	9/14/2003 – 9/20/2003
Michael	10/7/2018 – 10/15/2018
Sandy	10/22/2012 – 10/31/2012

5.4.5. Model Characteristics

ADCIRC simulations used a time step of 1 s and wrote output at an interval of 1 hour. In addition, we used several parameters as spatially varying inputs to the simulations. Bottom friction was represented via Manning's n values, and surface roughness was represented via directional wind reduction factors (which adjust the wind velocity at each vertex based on upwind conditions) and canopy coefficients (which disable the wind velocity at vertices with heavy tree coverage). These parameters were computed from land-use/land-cover datasets from NOAA's Coastal Change Analysis Program (C-CAP; Herold, 2014), with values averaged from the higher-resolution raster to the ADCIRC mesh-scale at each vertex. Other spatially varying inputs are the horizontal eddy viscosity, which was set to 50, and the ADCIRC τ_0 parameter, which used a three-tier scheme with a value of $\tau_0 = 0.005$ in open water, $\tau_0 = 0.02$ in the nearshore, and $\tau_0 = 0.03$ in overland regions.

5.5. Hydrodynamic and Wave Modeling (NEARCOM)

The Nearshore Community Model (NearCoM) is an extensible, user-configurable model system for nearshore wave, circulation and sediment processes developed during the National Oceanographic Partnership Program (NOPP). The model consists of a “backbone”; the master program, handling data input and output as well as internal storage, together with a suite of modules, each of which handles a focused subset of the physical processes being studied. A total of 10 modules exists, developed by a large group of researchers from various institutions. Example modules are: 1) A wave module simulates wave transformation over arbitrary coastal bathymetry and predicts radiation stresses and wave-induced mass fluxes; 2) A circulation module simulates the slowly varying current field driven by waves, wind and buoyancy forcing, and provides information on the bottom boundary layer structure; and 3) A seabed module simulates sediment transport, determines the bedform geometry, parameterizes the bedform effect on bottom friction, and computes morphological evolution resulting from spatial variations in local sediment transport rates.

5.5.1. Selection of wave and circulation modules in NEARCOM

In this demonstration study, we applied the combination of the wave model SWAN and the nearshore circulation model SHORECIRC. The coupled SWAN-SHORECIRC model is also called NearCoM-TVD, which was developed using a hybrid finite-difference finite-volume TVD-type scheme on a generalized curvilinear grid. SWAN and SHORECIRC are tightly coupled using the coupler, MASTER Program in the MPI-based parallel computing framework. SWAN calculates wind waves and provides SHORECIRC with radiation stresses to get wave setup and nearshore circulation. The current effects on waves are computed in SWAN with the current input from SHORECIRC.

The model coupling framework is illustrated in Figure 10. Note that the sediment transport module was not applied in the demonstration.

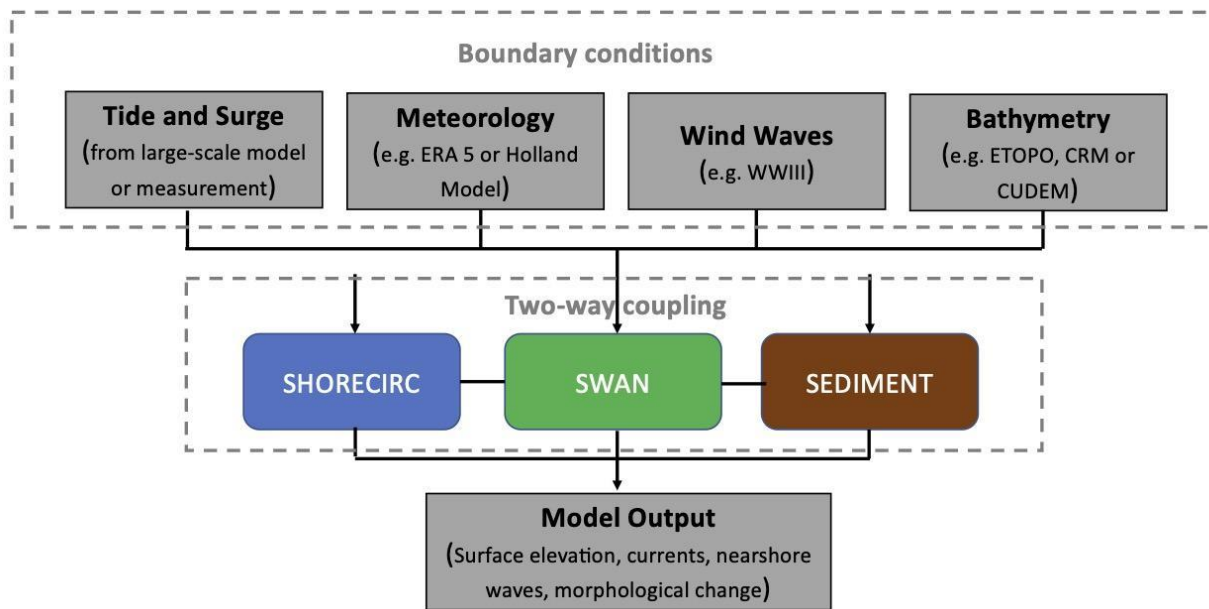


Figure 10. The model coupling framework in NEARCOM-TVD.

5.5.2. NEARCOM setup

Figure 11 shows the generalized curvilinear grid with the fine grid resolution at Naval Station Norfolk. NearCoM addresses the nearshore processes only and thus the computational domain is smaller than that used for D-Flow FM or ADCIRC in a typical tide-surge simulation. The tidal and surge boundary conditions for NearCoM are provided by a large-scale model, such as D-Flow FM or ADCIRC. The data format for the boundary conditions is (time, elevation, <velocity>), where <velocity> represents depth-averaged current velocity components and are optional.

The original Holland model (Holland, 1980) was implemented in NearCoM to model wind/pressure forcing in storm surge simulations. The model also has an optional wind/pressure input which can come from large-scale models. In most NearCoM applications for storm events, the wind/pressure data are provided by a large-scale model, consistent with the boundary conditions from the same large-scale model.

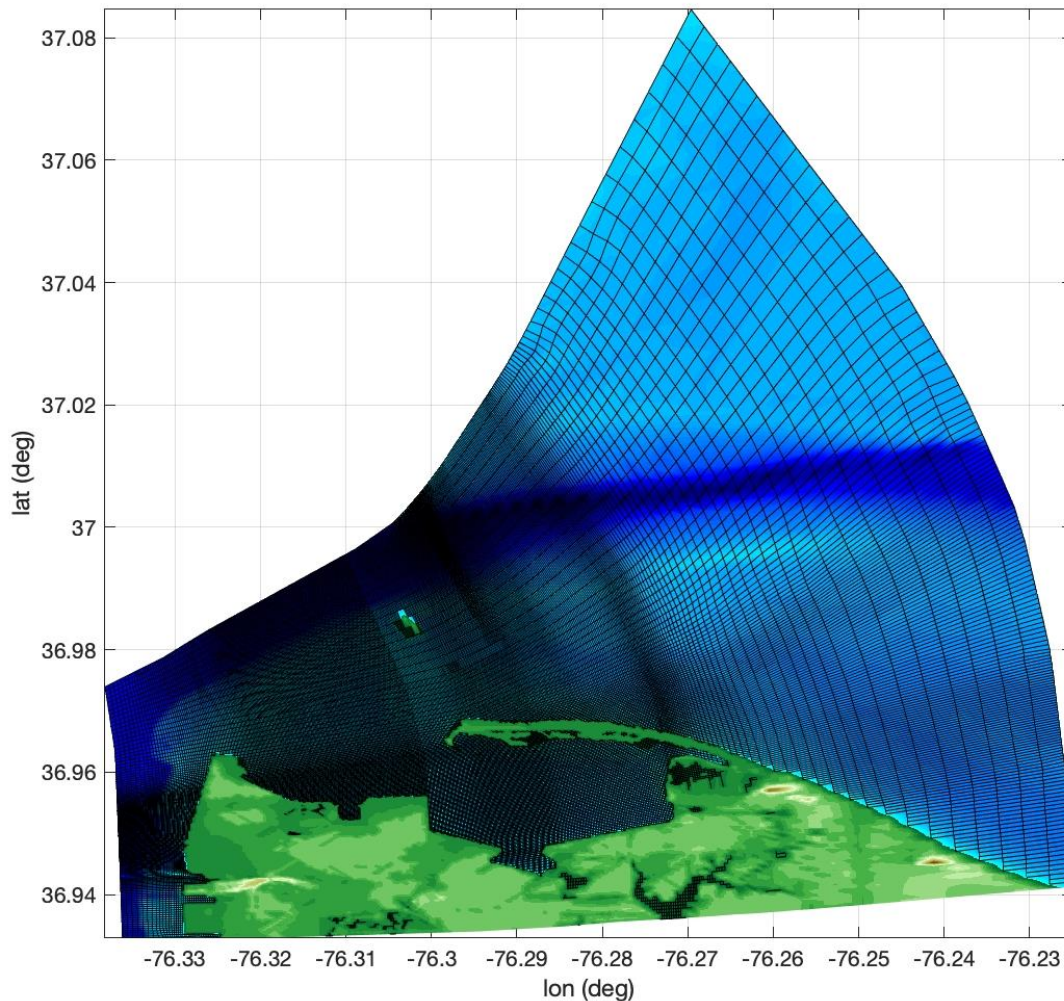


Figure 11. Computational grid of NEARCOM.

5.6. Wave modeling (FUNWAVE-TVD)

FUNWAVE-TVD is the TVD version of the fully nonlinear Boussinesq wave model (FUNWAVE) developed at the University of Delaware (Shi et al., 2012). It is a public domain model maintained by a group of institutions, including the Center for Applied Coastal Research (CACR) at the University of Delaware, Coastal Hydraulics Laboratory, USACE, and the University of Rhode Island. The FUNWAVE model was initially developed by (Kirby et al., 1998) based on (Wei et al., 1995). The development of the TVD version was motivated by a growing demand for phase-resolving modeling of nearshore waves and coastal inundation during storm or tsunami events and predicting sediment transport and short-term morphological processes in a wave-resolving manner.

As a nearshore shallow-to-intermediate water Boussinesq-type numerical wave model, FUNWAVE can resolve many coastal processes. Related to the scopes of this demonstration project, it can predict wave propagation/transformation, refraction, diffraction, reflection, nonlinear shoaling, wave-induced nearshore circulation, nonlinear wave-wave interaction, wave-current interaction, wave breaking, runup and overtopping, IG waves, nearshore sediment transport, and short-term morphological changes. The TVD-type solver particularly has an advantage in resolving wetting and drying processes accurately in modeling storm-induced coastal inundation. FUNWAVE-TVD has been benchmarked for wind wave application in a series of USACE-funded projects, and tsunami application during the National Tsunami Hazard Mitigation Program (NTHMP) which provided the benchmarking standard for judging model acceptance for use in the development of coastal inundation maps and evacuation plans. Source code, documentation, descriptions, and input files for carrying out benchmark tests and various example calculations are available at the FUNWAVE-TVD site (<https://fengyanshi.github.io/build/html/index.html>). In this study, FUNWAVE is used to simulate the contribution of wave runup to coastal flooding under hurricane force.

5.6.1. Application of FUNWAVE-TVD modules

FUNWAVE-TVD consists of several numerical modules for various applications, including Central Module, Tide Module, Meteo. Module, Sediment Transport Module, Precipitation Module, Subgrid Module, Ship-wake Module, Lagrangian Tracking Module, and Bubble and Foam Module. For the application in this study, the model was used to simulate the total water level and coastal inundation by focusing on the effects of wave-resolving processes, such as wave runup, wave overwash and overtopping in a nearshore shallow water domain. The Central Module and Tide Module are the primary modules used in this application. The tides and storm surges were treated as boundary conditions in the model input. The Tide Module was used for the boundary

condition input. Wind forcing is not considered due to the small size of the computational domain.

The numerical experiments showed that the wave-resolving effects occur at the open coast area in the Norfolk computational domain. Therefore, we mainly performed 1D simulations at Willoughby Spit. A 2D simulation was also conducted to illustrate the wave-effects in the entire domain for demonstration.

5.6.2. FUNWAVE-TVD configuration

Figure 12 shows the computational grid in a 2D domain. The model domain spanned 7.4 x 8.7 km, centered at NSN, and was discretized using a constant 1 m x 1 m grid spacing. A high resolution (1 m) topo-bathymetric dataset was obtained for the area using the NOAA Digital Coast: Data Access Viewer to capture the nearshore beach and dune features for accurate wave runup estimates. For 1D simulations, several cross-shore profiles, P1-P6, are selected as shown in the figure. Figure 13 shows the bathymetric profiles in the 1D simulations. Waves and storm tides (tide + surge) are forced at the open boundary. The wave information was obtained from SWAN simulations, and storm tides were from D-Flow simulations.

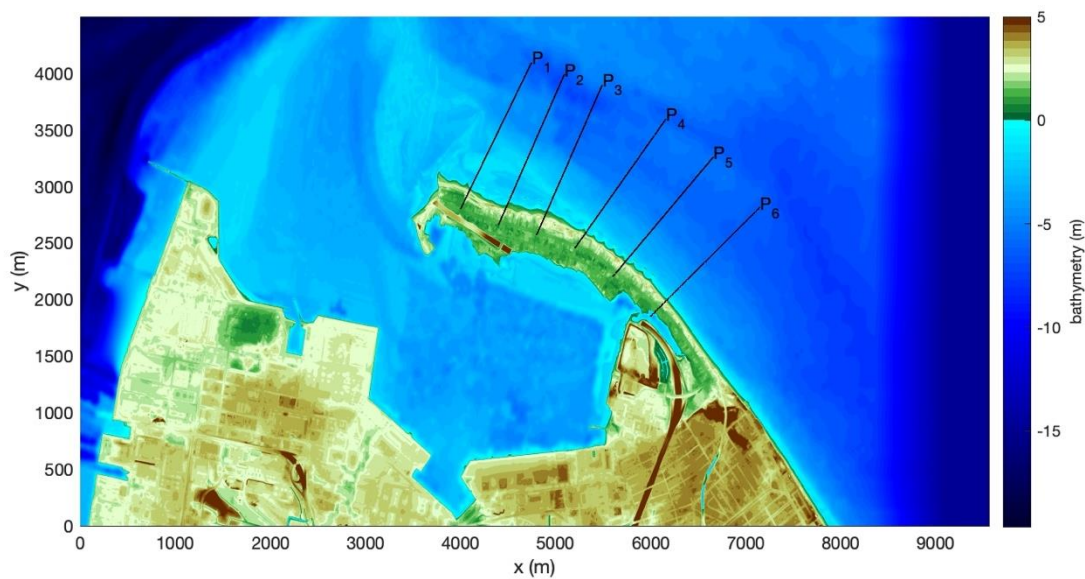


Figure 12. Computational domain for 2D simulations. P1P6 are profiles selected for 1D simulations.

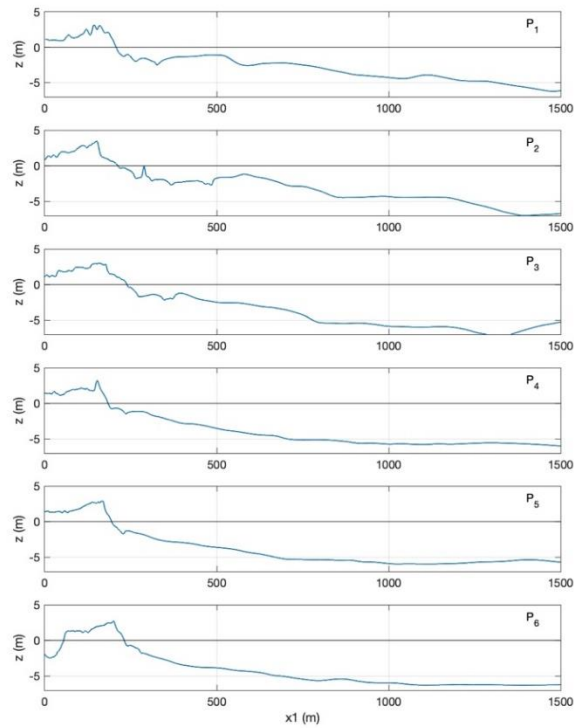


Figure 13. Bathymetric profiles, P1 to P6, for 1D simulations.

5.7. Performance assessment

5.7.1. General Statistical Analyses

Statistically speaking, different error-measuring criteria were used to evaluate the skill of the model in water level prediction. Equations 1 to 8 show the formulae of these metrics.

$$\text{Correlation Coefficient: } R = \frac{\sum_{i=1}^N ((P_i - \bar{P})(M_i - \bar{M}))}{\sqrt{\sum_{i=1}^N (P_i - \bar{P})^2} (\sqrt{\sum_{i=1}^N (M_i - \bar{M})^2})} \quad (1)$$

$$\text{Root Mean Square Error: } RMSE = \sqrt{\frac{1}{N} \sum_{i=1}^N (P_i - M_i)^2} \quad (2)$$

$$\text{Normalized RMSE: } NRMSE = \frac{\sqrt{\frac{1}{N} \sum_{i=1}^N (P_i - M_i)^2}}{(\max(M_i) - \min(M_i))} \quad (3)$$

$$\text{Bias} = \sum_{i=1}^N \frac{1}{N} (P_i - M_i) \quad (4)$$

$$\text{Relative Bias: } RB = \frac{\sum_{i=1}^N (P_i - M_i)}{\sum_{i=1}^N (M_i)} \quad (5)$$

$$\text{Mean Normalized Bias: } MNB = \frac{\sum_{i=1}^N (P_i - M_i)}{\sum_{i=1}^N |P_i|} \quad (6)$$

$$\text{Scatter Index: } SI = \frac{RMSE}{\frac{1}{N} \sum_{i=1}^N M_i} \quad (7)$$

$$\text{Sensitivity Index} = \frac{X_{max} - X_{min}}{X_{max}} \quad (8)$$

Where M_i is the measured value, \bar{M} is the mean value of the measured data, P_i is the predicted value, \bar{P} is the mean value of the predicted data and N is the number of data points. The coefficient of determination (R^2) is the square of the correlation coefficient (R).

Positive or negative relative bias or mean normalized bias indicate over- and under-predictions, respectively, by the model. These parameters enable us to investigate the overall magnitude differences between predictions and observations. The coefficient of determination and corresponding best-fit slope quantify how much the predictions varied from the observations, thereby indicating how well the simulations performed (e.g. a perfect fit would have a slope of unity). The sensitivity of the modeled TWL to the various perturbations Table 2, will also be assessed using a sensitivity index, defined as the relative difference between the minimum and maximum output values, X when a single input variable is changed with the others being constant. Larger sensitivity index values indicate greater parameter influence.

5.7.2. Specific Approaches for Each Objective

Objective 1: Each user will document carefully the personnel time required to prepare a model simulation. These times will be tested against those in the performance matrix using a simple differencing algorithm.

Objective 2: Each user will document carefully the computational run time required to conduct a model simulation. These times will be tested against those in the performance matrix using a simple differencing algorithm.

Objective 3: Data from available stations will be queried for the time of peak surge. Model output interpolated to the station location will also be queried for the time of peak surge. A simple difference algorithm will be used to quantify the skill in predicting peak surge timing. Figure 14.

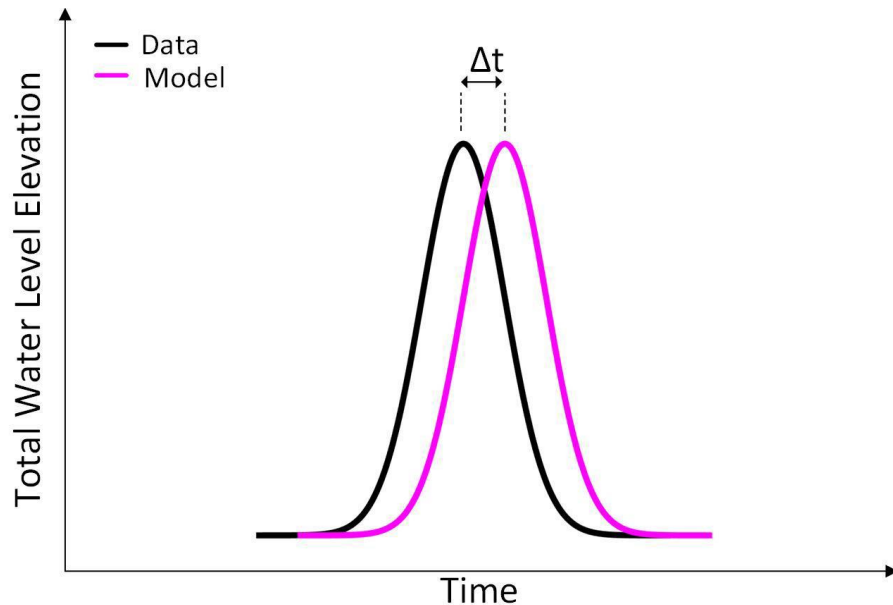


Figure 14. Schematic showing estimate of the timing of model predicted and actual peak surge (Total Water Level Elevation).

Objective 4: Data from available stations will be queried for the magnitude of peak surge. Model output interpolated to the station location will also be queried for the magnitude of peak surge. A simple difference algorithm will be used to quantify the skill in predicting peak surge magnitude, Figure 15.

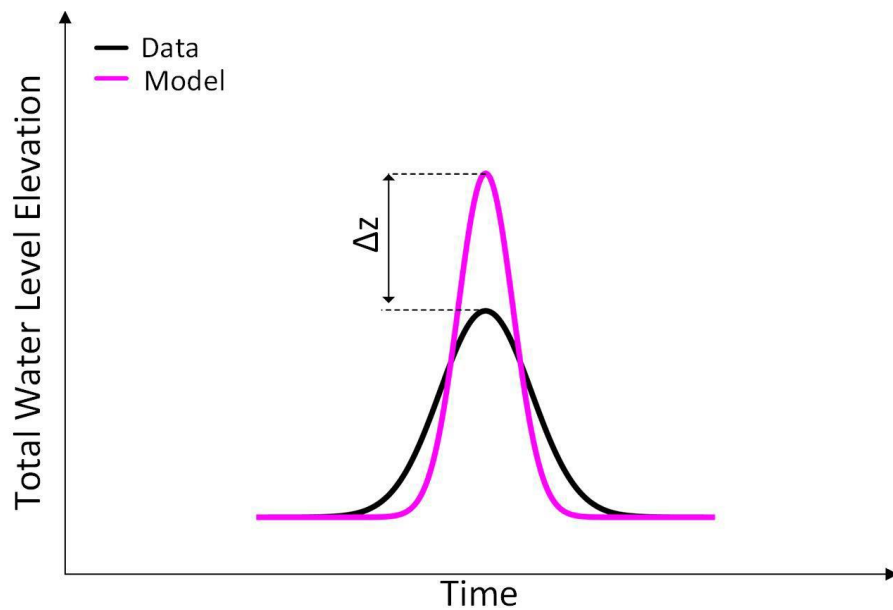


Figure 15. Schematic showing estimate of the maximum amplitude of model predicted and actual peak surge (Total Water Level Elevation).

Objective 5: A range of flooding levels will be selected. Data from available stations will be queried for the start and end time that each flooding level was exceeded. Model output interpolated to the station location will also be queried for the start and end time that each flooding level was exceeded. The difference between start and end time for the data or model output yields the flooding duration at a particular flooding level. A simple difference algorithm will be used to quantify the skill in predicting flooding duration at each flooding level, Figure 16.

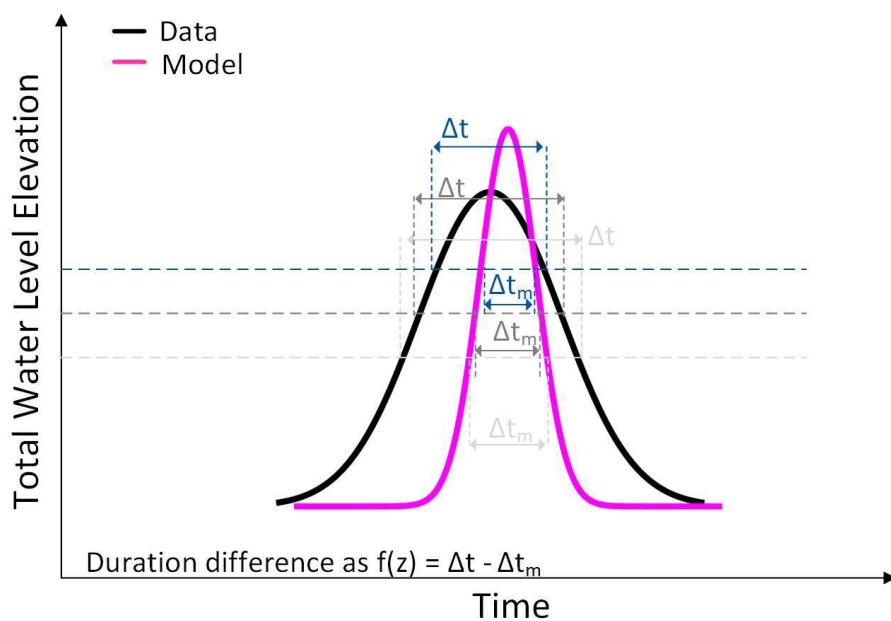


Figure 16. Schematic showing estimate of the duration of model predicted and actual flooding as a function of Total Water Level Elevation cutoff.

Objective 6: We will identify flooded spatial area as a function of time and flooded depth (Figure 17) and compare the results, where possible, to available anecdotal data. The example shown in Figure 17 is meant to provide a description of the approach; here using generic terms such as low, medium, and high with respect to flooding. Actual flood elevations will be determined after conducting the simulation. Subsequently, flooded areas will be quantified for each flood elevation level.

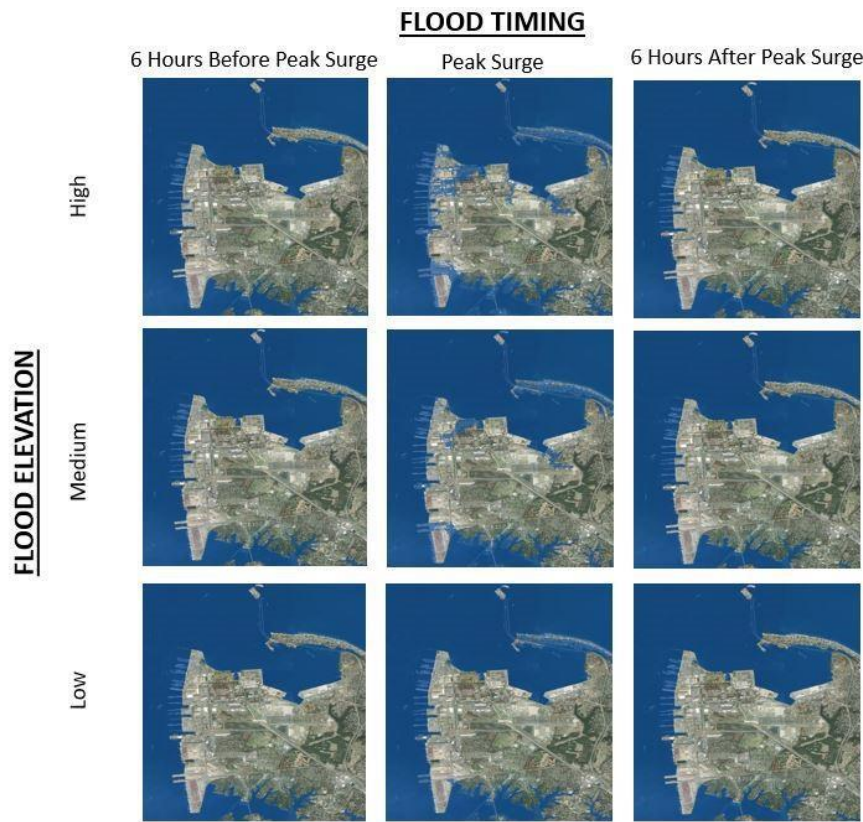


Figure 17. Example maps of inundation area as a function of timing with respect to peak surge.

Objective 7: We will compare the Class III full physics model (FUNWAVE) with the Class II models for the open coast portion of the study to determine the importance of the wave component to TWL. There is no performance metric. However, these simulations provide critical information on whether a Class III model is needed to resolve TWL in a geomorphological setting similar to NSN. This comparison will be carried out by comparing the flood extent predicted using the Class II models (no wave influence) to the flood extent predicted using the Class III model. The contribution of waves to the total flooding, based on the difference in modeled flood extents, can then be expressed as a percentage.

Objective 8: We will conduct “degradation simulations” to the baseline model simulation to quantify prediction error when there is a deficit of information (resolution and/or accuracy). There is no performance metric. However, these simulations provide critical information on prediction confidence when input and forcing data are imperfect (always the case in a predictive scenario). Model to model comparison will be conducted using the relevant parameters.

Objective 9: Model simulation results will be archived in long-term storage systems with hyperlinks provided on a webpage for program manager review. User-interactive graphic views

of model results will be generated using web-friendly interactive mapping techniques, such as the LEAFLET program (Figure 18). Automated programs suitable for multiple computer platforms will be used to transfer data between computational resources and storage systems. The qualitative metric is related to ease of use and ability for technical-level personnel to understand and use the data in a decision-making process.

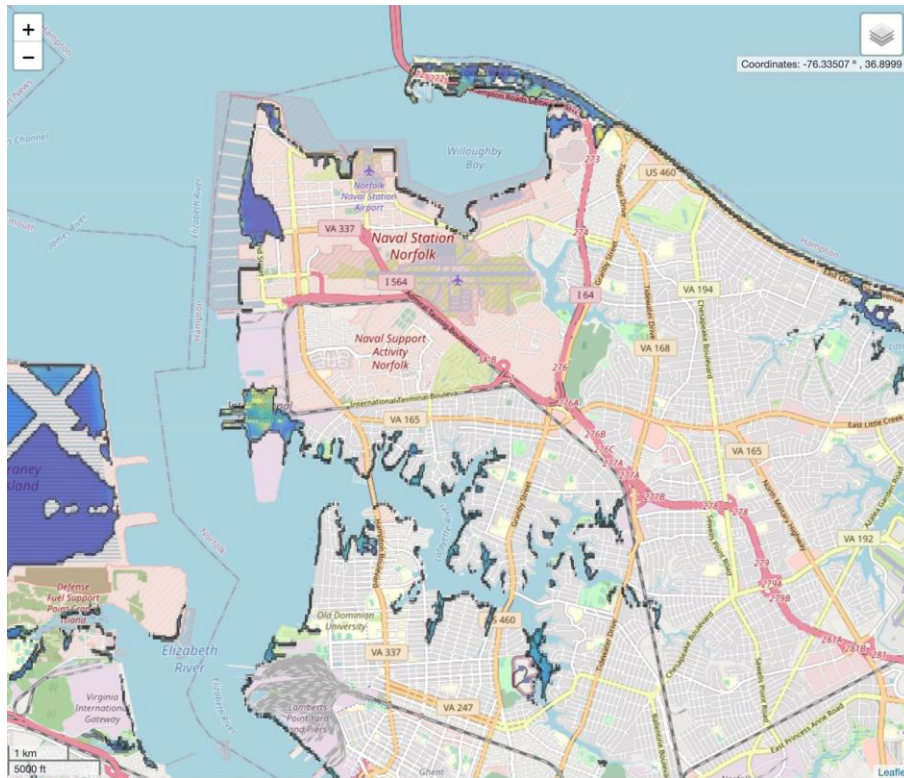


Figure 18. Example snip from the preliminary webpage showing flooded area for a storm event.

6. Results

Results and discussion are divided into a number of sections including the results of using the empirical methods, D-Flow FM, ADCIRC, SWAN, NearCoM, and FUNWAVE models.

6.1. Empirical methods

The (Russo, 1998) model is only applicable for a storm location as it approaches or crosses the shoreline. The Russo model was not applied to Hurricane Sandy because the interaction with the shoreline was too far north of NSN. The empirical model has little fidelity and predicts a surge of 1.22 m, 2.22 m, and 0.29 m for Hurricanes Irene, Isabel, and Michael respectively.

The Stockdon model was applied to all four Hurricanes Figure 19 using output from D-Flow FM. Runup exceedance is shown only for Willoughby Spit where breaking wave driven processes occur. Maximal R2% is roughly 0.9 m with the typical R2% being closer to 0.4 m. There is a weak trend for an increase in R2% to the east along the spit.

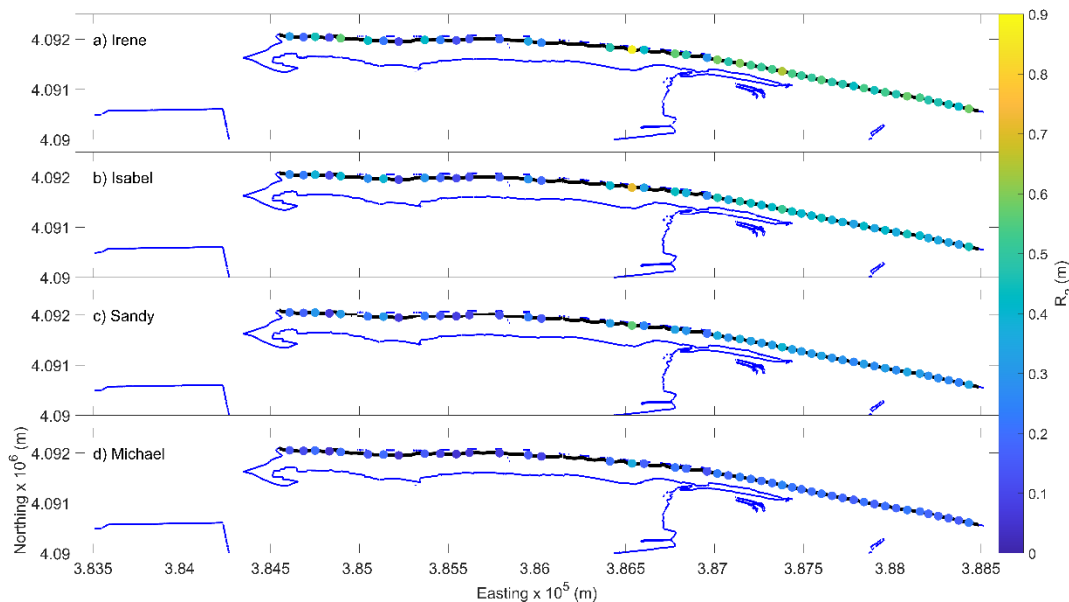


Figure 19. Empirical estimates of R2% from the Stockdon et al. (2006) model for all four hurricanes. Coordinates are shown in UTM for simplicity in calculating distances.

6.2. D-Flow FM

Results and discussion are divided into a number of sections starting with calibration results of the base scenarios followed by the results of manipulating the meteorological forcing, climate change impacts, and degradation scenarios.

6.2.1. Model Calibration (Baseline scenarios)

Calibration for Hurricane Irene was performed at eight stations along the United States East Coast, in the Chesapeake Bay, and in the Delaware Bay, Figure 6. Water level data were obtained at these stations from the NOAA website, <https://www.noaa.gov/>, during the different hurricane times. The data has hourly time intervals and is referenced to the MSL for the later comparison against the model results. The calibration procedure was carried out for Hurricane Irene and the same calibration settings were then used for the rest of the hurricanes (Isabel, Sandy, and Michael), yet the number of calibration stations might be different depending on the availability of the data.

I. Hurricane Irene

Different parameters were used during the calibration procedure of the model including the calibration of the tidal constituents (amplitude and phase) to take all the significant constituents affecting the water level into account. For that purpose, harmonic analysis was performed to separate the tidal water level from the non-tidal water level and the results were compared to the observed data for calibration. The Sun-Annual (SA) and Sun Semi-Annual tidal components were added to the tidal forces along the model boundaries. On the other hand, sensitivity analysis of the bed roughness (Manning coefficient) values was tested to further enhance the model performance. A range (0.01 – 0.03) was used for the sensitivity analysis. The results show that a Manning coefficient of 0.015 gives the best model results. Sensitivity to the network resolution will be evaluated and discussed in a later section.

Figure 20 shows the measured and simulated tidal water level at Duck during 2011 for total tidal level and SA & SSA tidal components. The model shows good performance in modeling tidal water levels with minimum margins of errors. On the other hand, Figure 21 and Figure 22 show an example of the comparison between the measured and simulated water levels, using ERA5 and HM wind forcing, at different locations from the 26th of August 2011 to the 30th of August 2011 (a few days around Hurricane Irene). For calibration figures at all locations, see Appendix A. It can be shown that there is a high agreement between the simulated and measured water levels and the model can efficiently capture the peak surge with high accuracy. This is also evident in the distributions of the measured and simulated water levels which are highly comparable, Figure 22.

It can be observed that the model results have a high correlation/coefficient of determination with the measured data up to 99%. In addition, the RMSE ranges from 0.14 m to 0.29 m, which represents less than 10% of the water level range on average. However, underestimations were also observed along all stations with a bias ranging between -0.09 m and -0.22 m. These

underestimations might be attributed to other factors including fluvial and pluvial impact on the water level, which were not considered in this study. In addition, the wave-induced water level was not included in the calibration procedure as well. It is also worth mentioning that among the 8-calibration locations, some points are located far inside the rivers discharging into the Chesapeake Bay, or located very close to the shoreline where no accurate bathymetry exists. Table 9 and Figure 23 show the error statistics for the simulated water level at the different stations along the east coast of the US during Hurricane Irene using ERA5 and HM wind forces.

Although the error statistics using both ERA5 and HM are relatively comparable with an average RMSE of 0.22 m for both, it can be noted that the model can capture the peak of the storm with high accuracy, especially at Sewells Point, using the HM wind forces. However, this is not the case for all hurricanes as will be discussed in later sections. It appears the accuracy of the HM decreases with increasing the distance from the area of interest to the eye of the storm.

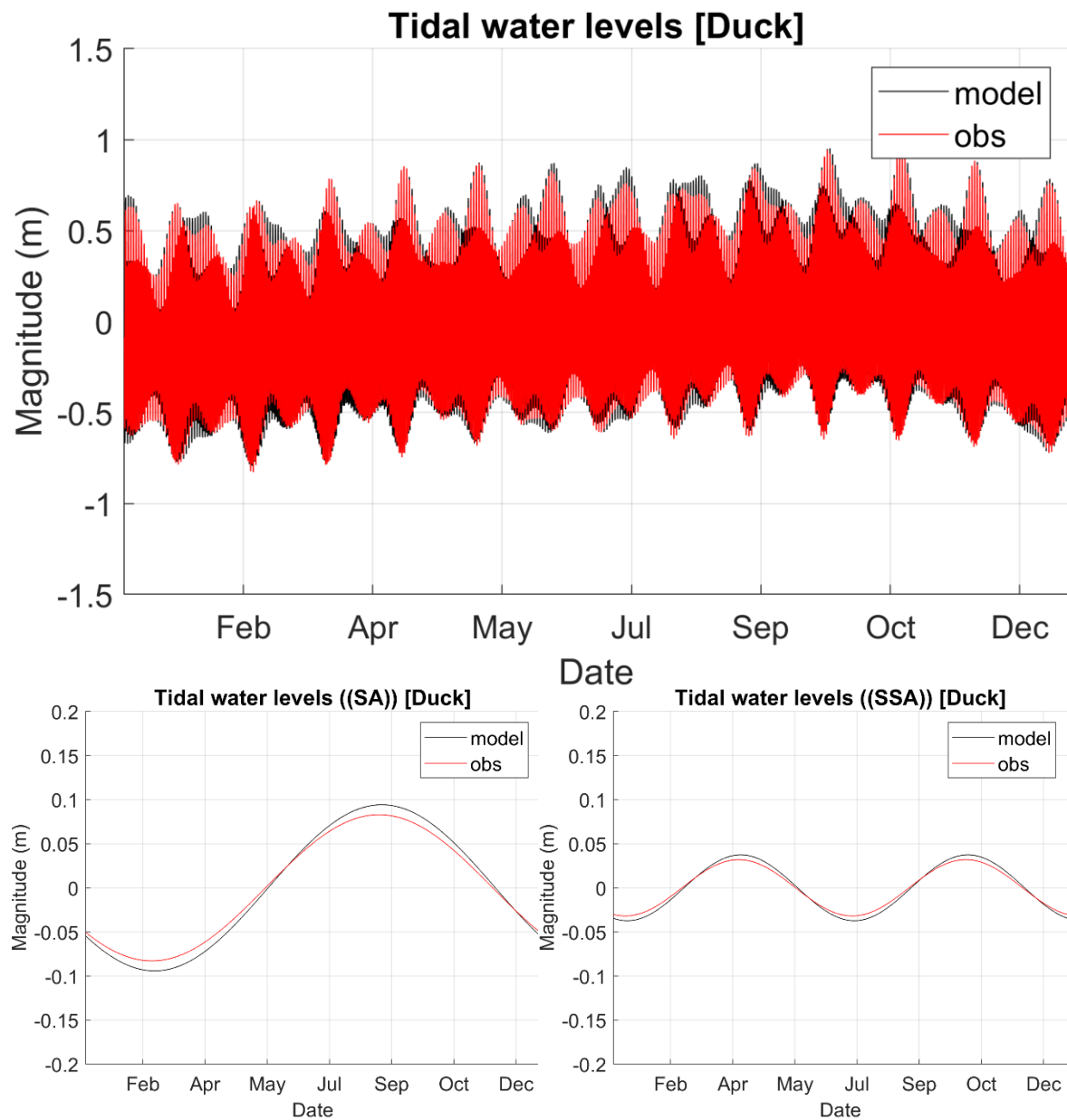


Figure 20. Simulated and measured tidal water level (m) (upper panel) and SA & SSA components (lower panels) during 2011 at Duck, NC.

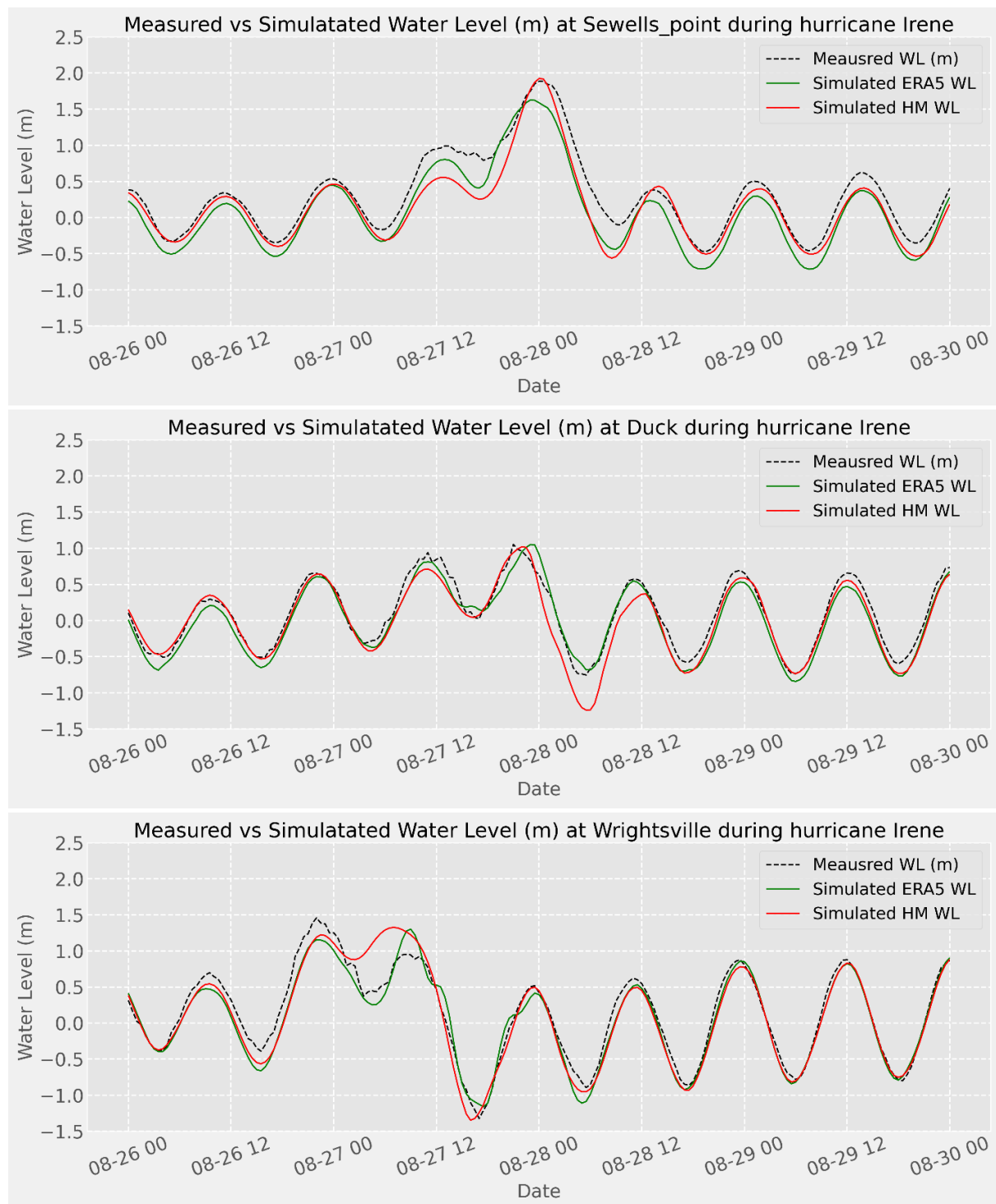


Figure 21. Measured vs Simulated water levels using ERA5 and HM wind forces during hurricane Irene, 2011.

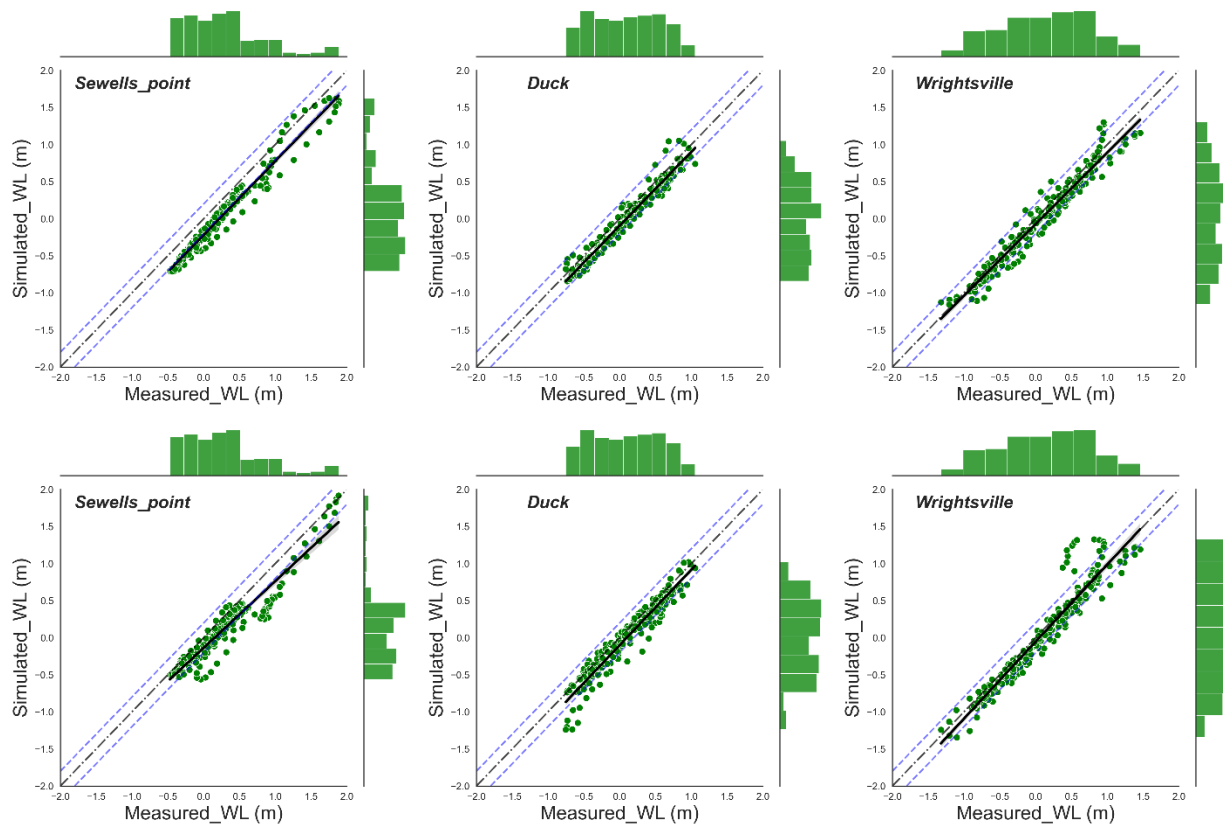


Figure 22. Scatter plots of the measured and simulated water levels (m) at Sewells, Duck and Wrightsville using ERA5 (upper panels) and HM (lower panels). Histograms are plotted along the right and upper axes, Irene, 2011, NSN.

Table 9. Summary statistics of simulated and measured water levels at the different stations during Hurricane Irene, 2011 using ERA5 and HM wind forces, NSN, US.

#	Wind Forces	Location	R	R ²	RMSE	NRMSE	Bias	RB	MNB
1	ERA5	Atlantic_city	0.97	0.94	0.23	0.10	-0.17	-1.18	-0.37
2		Lewes_DE	0.97	0.94	0.26	0.09	-0.20	-1.18	-0.36
3		Yorktown	0.98	0.96	0.25	0.12	-0.22	-0.83	-0.55
4		Kiptopeke	0.99	0.98	0.18	0.09	-0.17	-0.89	-0.45
5		Sewells_point	0.98	0.96	0.24	0.10	-0.22	-0.74	-0.51
6		Money_point	0.96	0.93	0.29	0.11	-0.24	-0.72	-0.51
7		Duck	0.98	0.95	0.14	0.08	-0.09	-1.06	-0.23
8		Wrightsville	0.98	0.95	0.16	0.06	-0.08	-0.62	-0.15

9	HM	Atlantic_city	0.96	0.92	0.24	0.10	-0.17	-1.13	-0.36
10		Lewes_DE	0.97	0.94	0.25	0.08	-0.18	-1.08	-0.37
11		Yorktown	0.95	0.90	0.22	0.11	-0.15	-0.57	-0.43
12		Kiptopeke	0.97	0.94	0.16	0.08	-0.11	-0.56	-0.33
13		Sewells_point	0.95	0.91	0.23	0.10	-0.17	-0.56	-0.43
14		Money_point	0.94	0.89	0.27	0.10	-0.18	-0.55	-0.42
15		Duck	0.96	0.93	0.17	0.09	-0.10	-1.12	-0.24
16		Wrightsville	0.96	0.92	0.20	0.07	-0.05	-0.38	-0.08

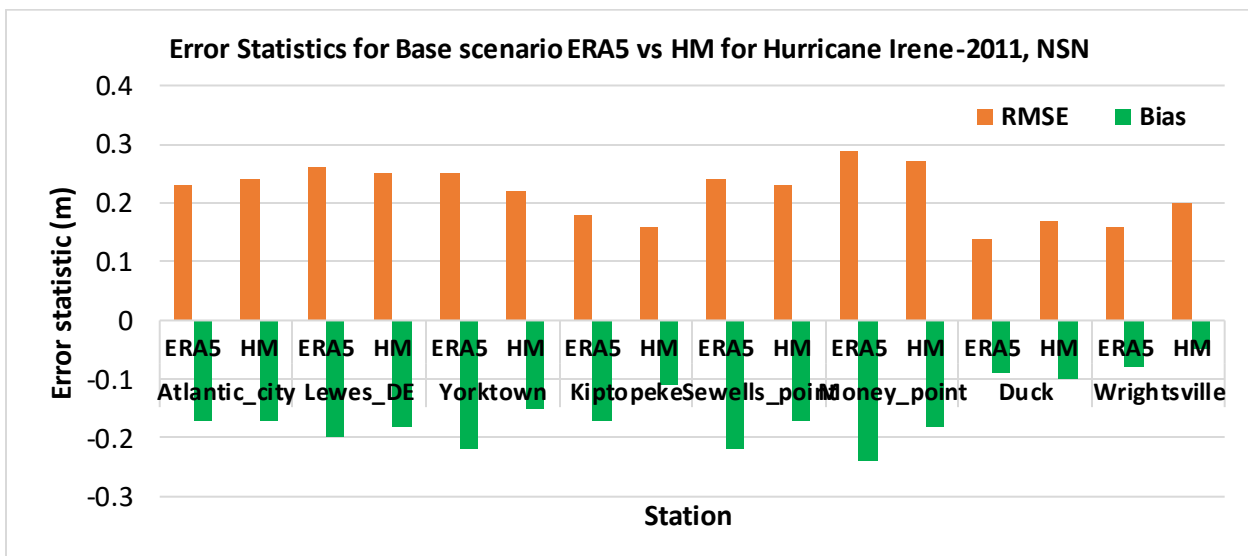


Figure 23. Summary statistics (RMSE and Bias in m) of water level prediction using ERA5 and HM at the calibration stations along the US east coast during Hurricane Irene-2011.

We evaluated the peak surge characteristics based on three criteria, magnitude, duration, and timing. For peak surge magnitude and timing, a simple difference algorithm is applied to assess the skill of the model to predict these criteria. For the peak surge duration on the other hand, we classified the surge into three levels; Low: (0.5 – 1.0 m), Medium: (1.0 – 1.5 m), and High: (>1.5 m). Thereafter, we calculated the duration of each surge level around the peak surge and compared the results to the measured data. All of the calculated statistics were applied to Sewells Point only due to its proximity to the area of interest, Table 10. It is worth noting that model results at Sewells Point do not reflect the best model performance due to its location that can be highly affected by the river discharge, which was not part of this study.

Figure 24 and Figure 25 show the timeseries of predicted and measure water level at Sewells Point, NSN during Hurricane Irene using ERA5 and HM wind forces respectively. The figures show the different surge/flood levels, differences in the peak surge magnitude, the timing of the peak surge, and the duration. Investigating the peak surge characteristics shows that the model can efficiently capture the peak surge during Hurricane Irene at Sewells Point using the HM wind forces with a magnitude difference of about +0.03 m. An underestimation was observed in the peak surge magnitude using the ERA5 wind data, however, still within the acceptable range with an underestimation of -0.28 m. This underestimation might be attributed to the underestimation of the ERA5 wind of the extreme wind speed (storm winds) by 10 - 15% in the Atlantic Ocean, (Campos et al., 2022). This underestimation is manifested when ERA5 and HM wind speeds are compared during the peak of the storm (Figure 5). On the other hand, the timing of the peak surge was captured very well by the model using both wind forces, with almost no delay in the peak surge using HM wind data compared to about an hour delay using ERA5.

Calculating the duration of the surge for the considered levels shows some differences between the measured and simulated water levels. The model generally underestimates the surge duration through all surge levels, partially due to the underestimation in the surge magnitude. However, the maximum underestimation was -3.5 hours for the low-level surge magnitude using HM wind and -3.0 hours for the high-level surge magnitude using ERA5 wind, with less than -1 hour underestimation of the high surge level duration using HM wind forces (Table 10).

Table 10. Error statistics (Differences in magnitude (m), timing (h), and duration (h)) of peak surge characteristics at Sewells Point for Hurricane Irene-2011, NSN.

#	Hurricane/ Wind Forcing		Magnitude (m)	Time (h)	Duration (h)		
					Low	Medium	High
1	Irene	ERA5	-0.25	-1.0	-1.0	-2.0	-3.0
2		HM	+0.04	0.0	-3.5	-2.0	-1.0

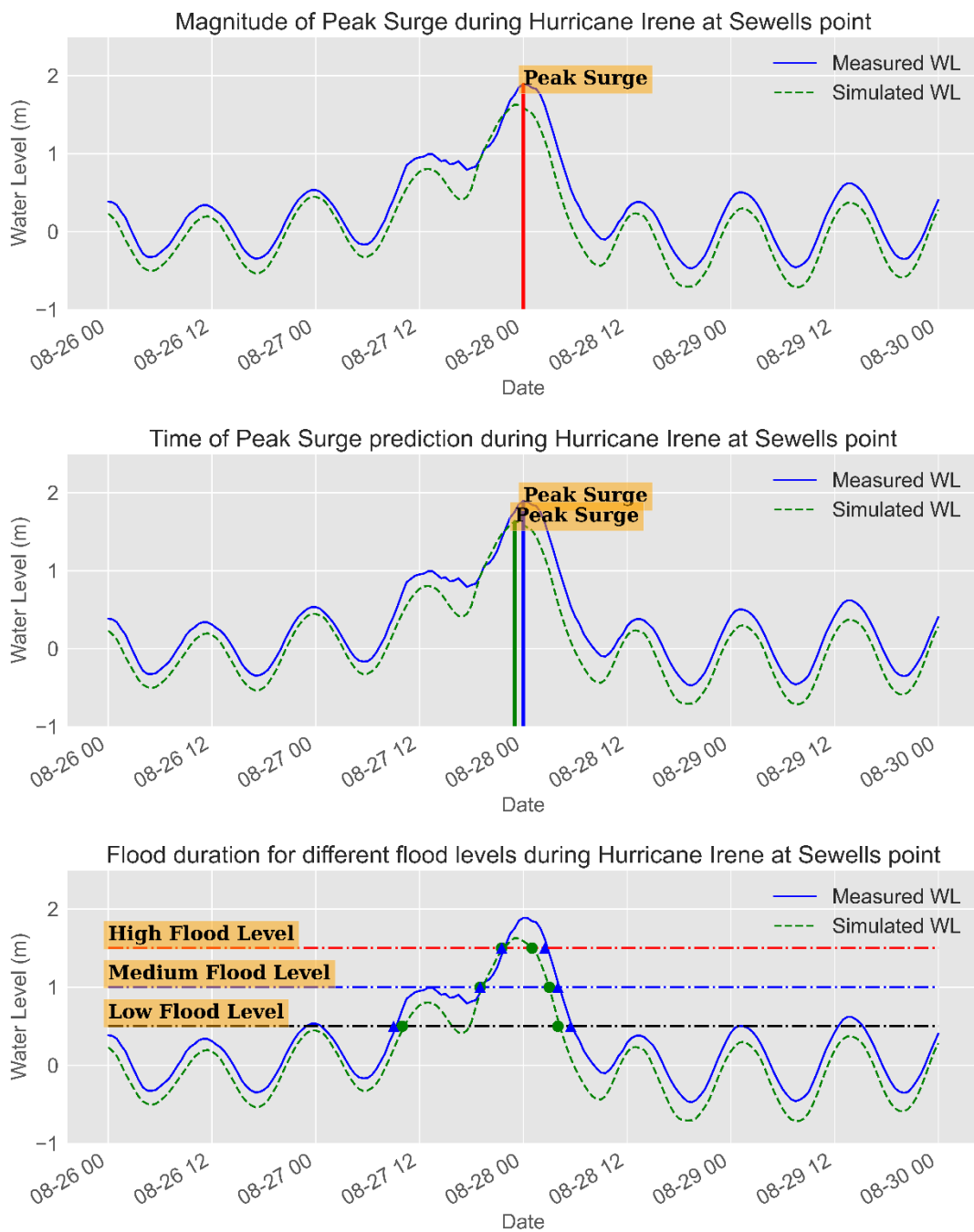


Figure 24. Flood Duration, Magnitude, and Timing at Sewells Point during Hurricane Irene-2011 (Base-ERA5) at NSN.

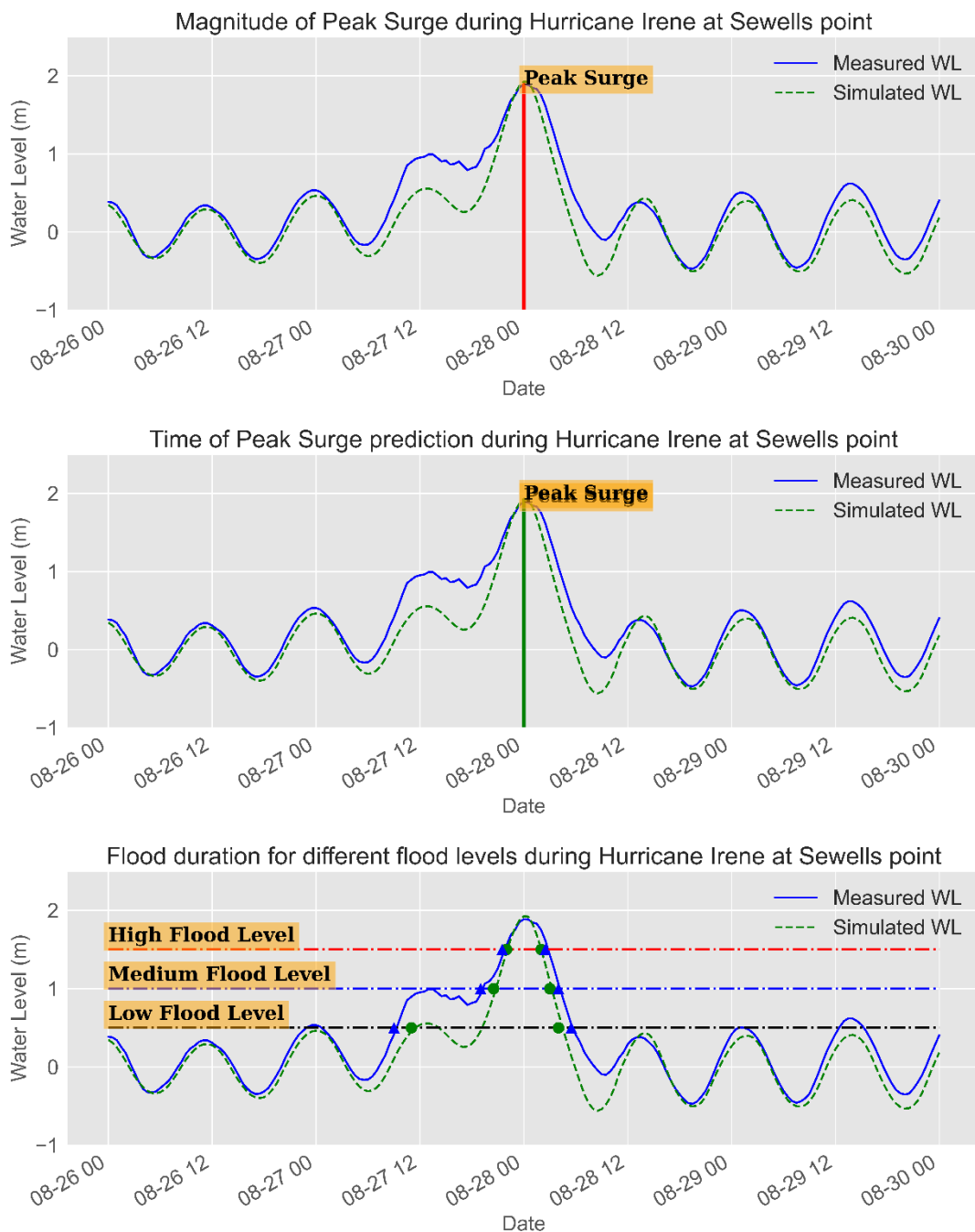


Figure 25. Flood Duration, Magnitude and Timing at Sewells Point during Hurricane Irene-2011 (Base-HM) at NSN.

To investigate the flood areas associated with Hurricane Irene, the projected flood areas, average flood depth, and maximum flood depth were calculated on hourly basis for about 25 hours around the peak surge that occurred on August 28th 00:00. Figure 26 shows the timeseries of the flood areas, average and maximum flood depth at NSN during 25 hours around the peak of Hurricane Irene. In addition, the severity of the flood was evaluated based on the projected flood depth as we classified the flood into four levels; low ($0.1\text{ m} - 0.25\text{ m}$), medium ($0.25\text{ m} - 0.5\text{ m}$), high ($0.5\text{ m} - 1.0\text{ m}$) and extreme ($>1.0\text{ m}$). Based on these levels, a flood map was created for the peak flood (during the peak surge) for NSN using a shapefile delineating the base area. Furthermore, a separate flood map was created for each flood level for more classification of the flood risk at the base. Figure 27 and Figure 28 show the flood maps with the four flood levels for ERA5 and HM simulations at NSN base during the peak surge associated with Hurricane Irene. For more HM flood maps, refer to appendix A.

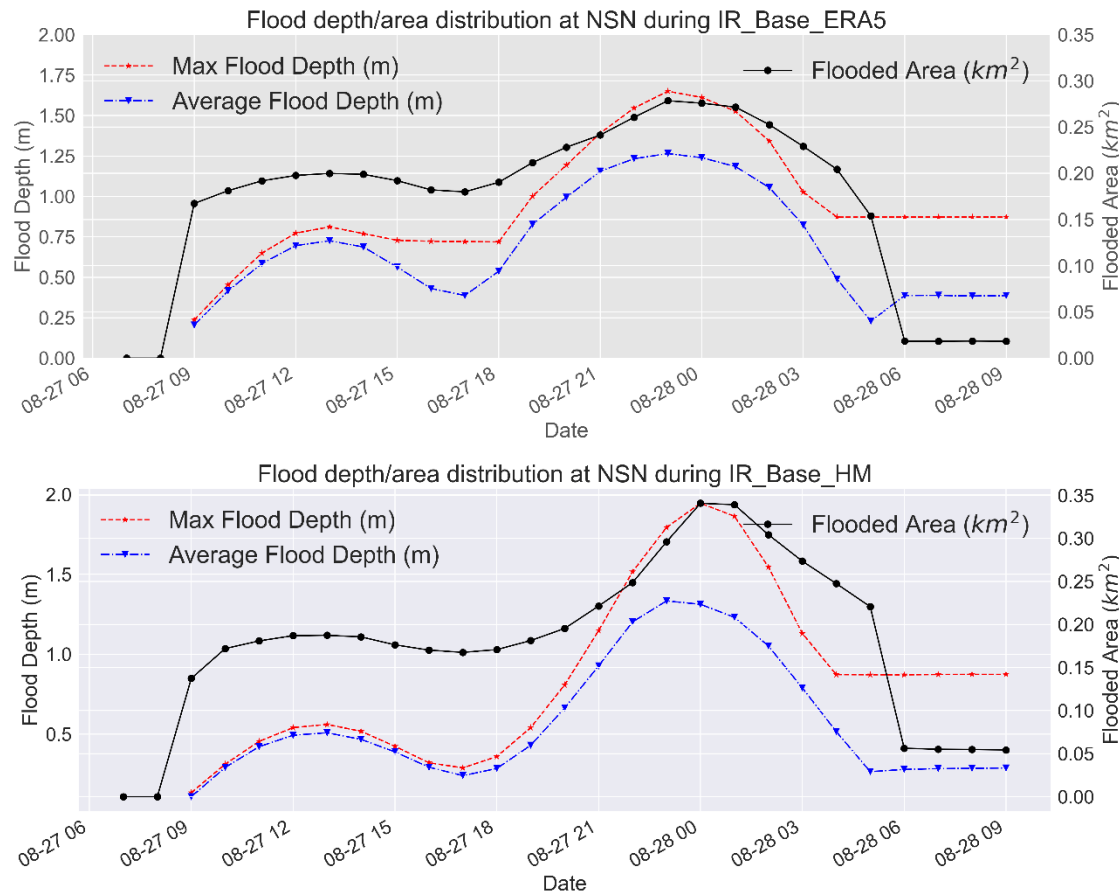


Figure 26. Timeseries of the projected average and maximum flood depth (left axis) and flood area (km^2 -right axis) during Hurricane Irene-2011 for ERA5 (upper panel) and HM (lower panel) at NSN.

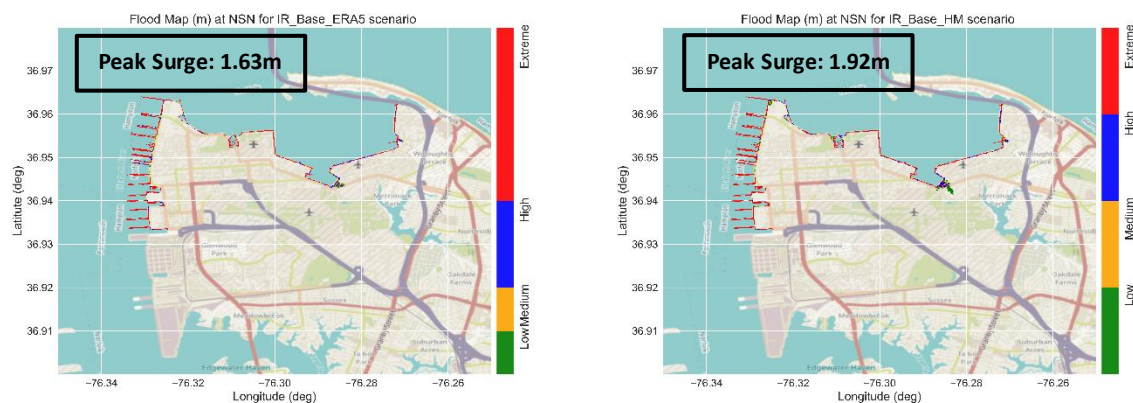


Figure 27. Flood map showing the classification of the flood levels at the peak surge during Hurricane Irene-2011 using ERA5 wind forces (left panel) and HM wind forces (right panel) at NSN.

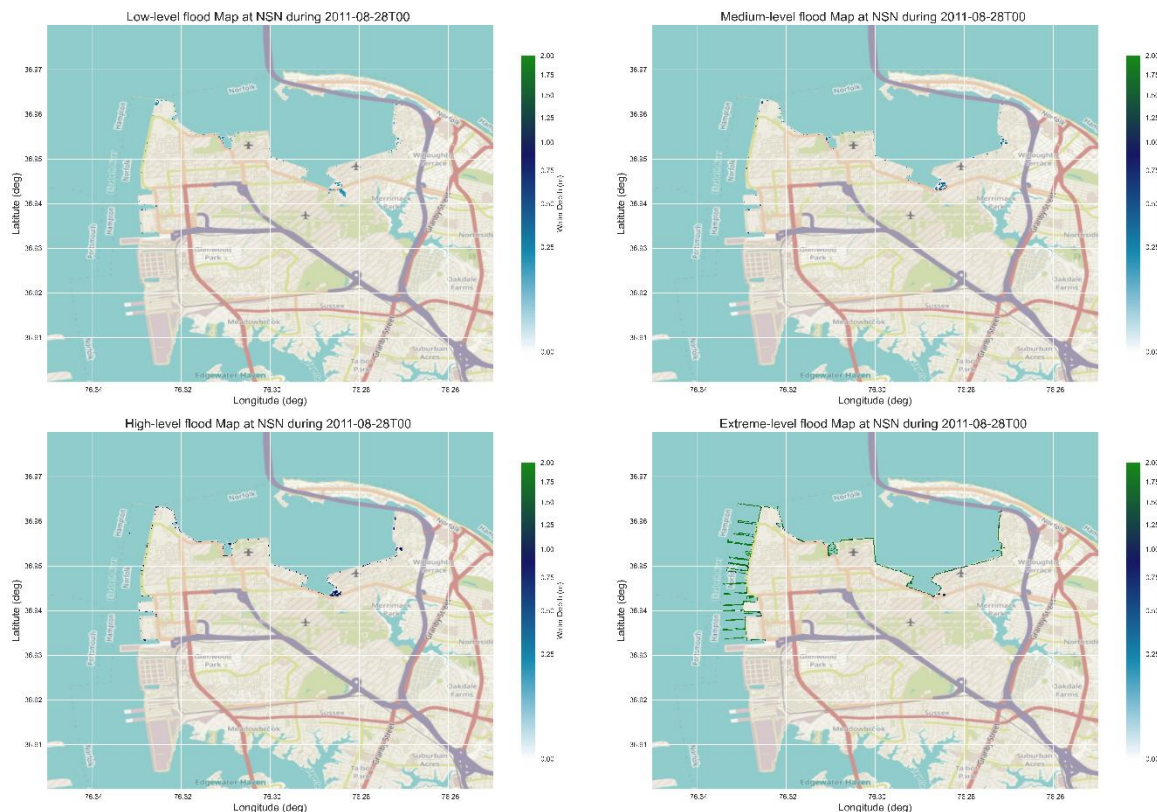


Figure 28. Flood maps show the classification of the different flood levels (low, medium, high, and extreme) at the peak surge simulation using ERA5 wind forcing during Hurricane Irene-2011 at NSN.

Hurricane Irene had a minor impact on NSN in terms of flooding where the maximum detected flood area was 0.34 km^2 (2% of the base area) using HM wind data. However, it should be noticed that most of this flooded area located at the coastal boundaries of the base where the actual performance of the model prediction is highly affected by different factors including the sudden changes in the bed level, the accuracy of the bathymetry (distinguishing wet and dry cells), and the model resolution that should be high enough to capture the small changes in the water depth and hence flood areas. Therefore, it would be more accurate to state that the impact of Hurricane Irene on NSN was minor with about 0.15 km^2 (1% of the base area) or less. In addition, the affected area is located at the northeastern part of the base (Figure 29), where it is fronted by a hard structure that can further protect this area from the high water levels. Due to the lack of information about the structure type and its characteristics, we did not include its impact in the model simulations. Using ERA5 data resulted in lower flood area predictions due to the underestimation of the peak surge. Regardless of the forcing data, the actual flood occurs at NSN when the water level exceeds a certain threshold, 0.75 m.

The classification of the flood areas into flood levels does not reflect valuable information under this scenario since no significant flood was detected. However, for the consistency of the analysis through all scenarios, flood statistics were calculated for the different flood levels (Figure 30). In addition, Table 11 shows the flood statistics for the different flood levels at NSN during the base-ERA5 scenario. Additional statistics for the Base-HM scenario can be found in Appendix B.

The final step of our calibration was to cross-reference model results to the anecdotal data obtained from the System to Track, Organize, Record, and Map (STORM) database, https://data.norfolk.gov/Public-Safety/STORM-System-to-Track-Organize-Record-and-Map/mrv3-rcpc/about_data. STORM system captures data collected by residents and city staff during and after inclement weather events. Figure 31 shows the locations where flood event was reported during Hurricane Irene. It can be noticed that almost no locations were reported to be flooded during the storm except for a single location at southwest of NSN, which might be associated with pluvial flooding (from the heavy rain associated with the storm), which we did not consider in this study. Although these data are only qualitative (anecdotal), it supports the model results and increases our confidence in the model performance at NSN.



Figure 29. Satellite image showing NSN (upper panel) and a zoom-in on the projected flooded area under the Base scenarios (lower panel), NSN.

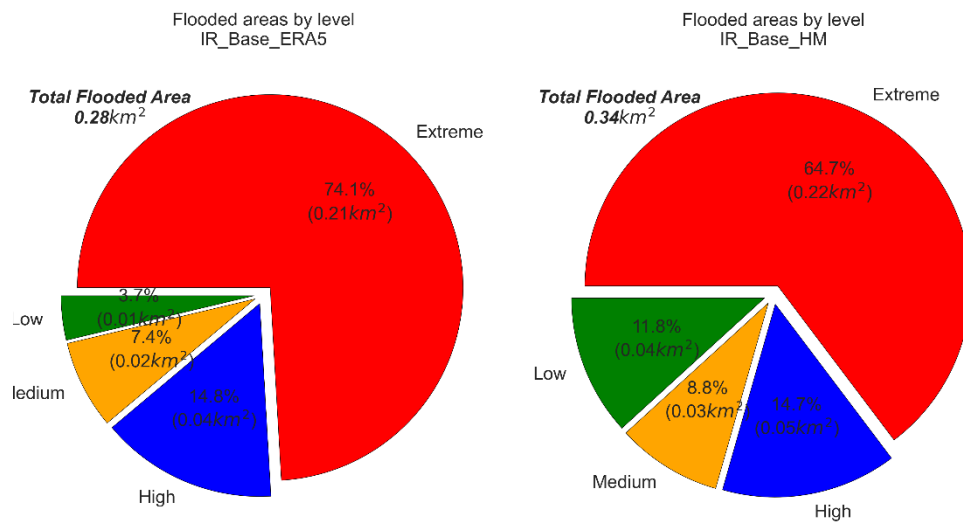


Figure 30. Pie chart showing the areas, with percentages, for the different flood levels at the peak surge during Hurricane Irene-2011 using ERA5 wind forces (left panel) and HM wind forces (right panel) at NSN.

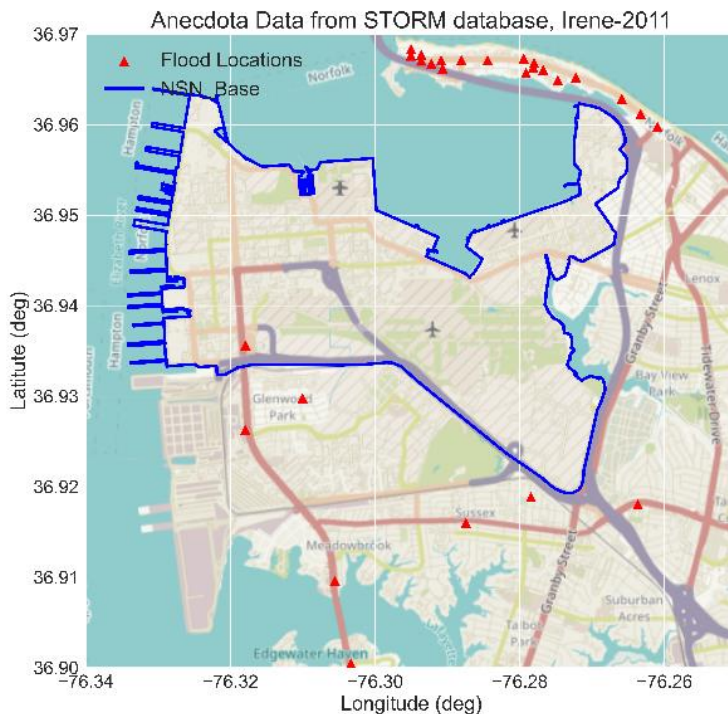


Figure 31. Thematic map showing the locations of the flooding during Hurricane Irene based on the STORM anecdotal data. The solid blue line shows the boundary of NSN, and the red triangles represent reported flood location, NSN.

Table 11. Projected flood area statistics at the peak flood during Hurricane Irene-2011 for the base-ERA5 scenario at NSN, the US

Flood_Level	Average_FD_(m)*	Max_FD_(m)**	Flooded_Area_(km)	Flood %
Low	0.18	0.25	0.01	0.11
Medium	0.37	0.5	0.02	0.17
High	0.73	1	0.04	0.3
Extreme	1.53	1.61	0.2	1.42
No Flood	0	0	13.5	97.97

* Average Flood depth in meters

**Maximum Flood depth in meters

II. Hurricane Isabel

The calibration setting/parameters used for Hurricane Irene were used for Hurricanes Isabel. Two meteorological forcings were also used to force the model, ERA5 and HM. It was observed that the model has a high performance in predicting the water level using ERA5 data and an acceptable performance using HM wind data (Figure 32 and Figure 33). The model was able to capture the peak surge using ERA5 data at almost all locations (Appendix A) with an average RMSE and bias less than 0.15 m and -0.12 m respectively (Table 12). However, the model shows some underestimation in water level prediction, especially around the peak surge, using HM at almost all stations. An average RMSE and bias of about 0.23 m and -0.14 m were observed (Table 12). It is clear that using the modeled meteorological forcing (ERA5) outperforms the parametrized meteorological forcing (HM) in water level prediction for Hurricane Isabel at NSN. This could be explained also by the proximity of the observation point (and the study location) to the eye/the actual path of the storm. Figure 34 shows the wind speed and the hurricane track of Hurricane Isabel during the peak surge at NSN (Sewells Point), while Figure 35 shows some error statistics (RMSE and bias) for water level prediction at seven stations during Hurricane Isabel. The stations are ordered along the x-axis based on their location (north to south). Unlike Hurricane Irene, Hurricane Isabel approached the US east coast at nearly perpendicular to the coast, approximately 200 km south of NSN. The best model performance, using HM data, was observed at Duck , NC, which is the closest station to the eye/track of the hurricane. In addition, the model has a relatively good performance at locations at a large distance from the hurricane eye where the impact of the hurricane itself is minor and most of the water level there is tidal driven, e.g. Atlantic City (Appendix A).

Investigating the peak surge characteristics shows that the model can capture the peak surge during Hurricane Isabel at Sewells Point using the ERA5 wind forces with a magnitude difference of about -0.14 m (Figure 36). However, significant underestimation was observed in the peak

surge magnitude using the HM wind data -0.44 m (Figure 37). On the other hand, the timing of the peak surge was captured well by the model using both wind forces, with less than an hour delay in the peak surge. Calculating the duration of the surge for the considered levels shows good agreement between the measured and simulated water levels using ERA5. The model marginally underestimates the surge duration through all surge levels by -1 h to -3 h, partially due to the minor underestimation in the surge magnitude. However, significant underestimation was observed using HM wind that can reach up to -15 h for the low surge level. Furthermore, the high surge level ($>=1.5$ m) was almost detected by the model using HM data resulting in more than -5 h (more than 60%) underestimation in peak surge duration (Table 13).

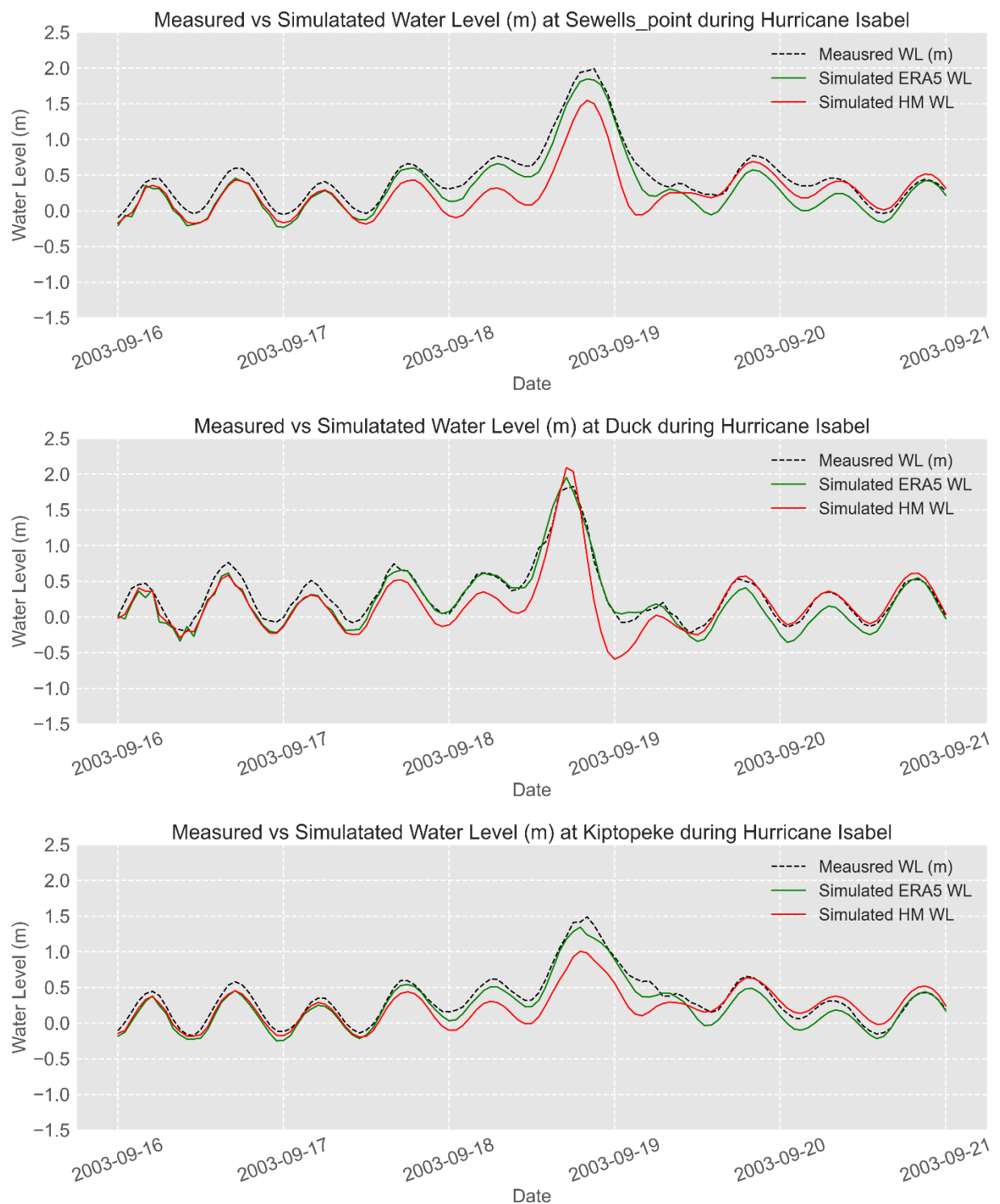


Figure 32. Measured vs simulated water levels using ERA5 and HM wind forces during hurricane Isabel.

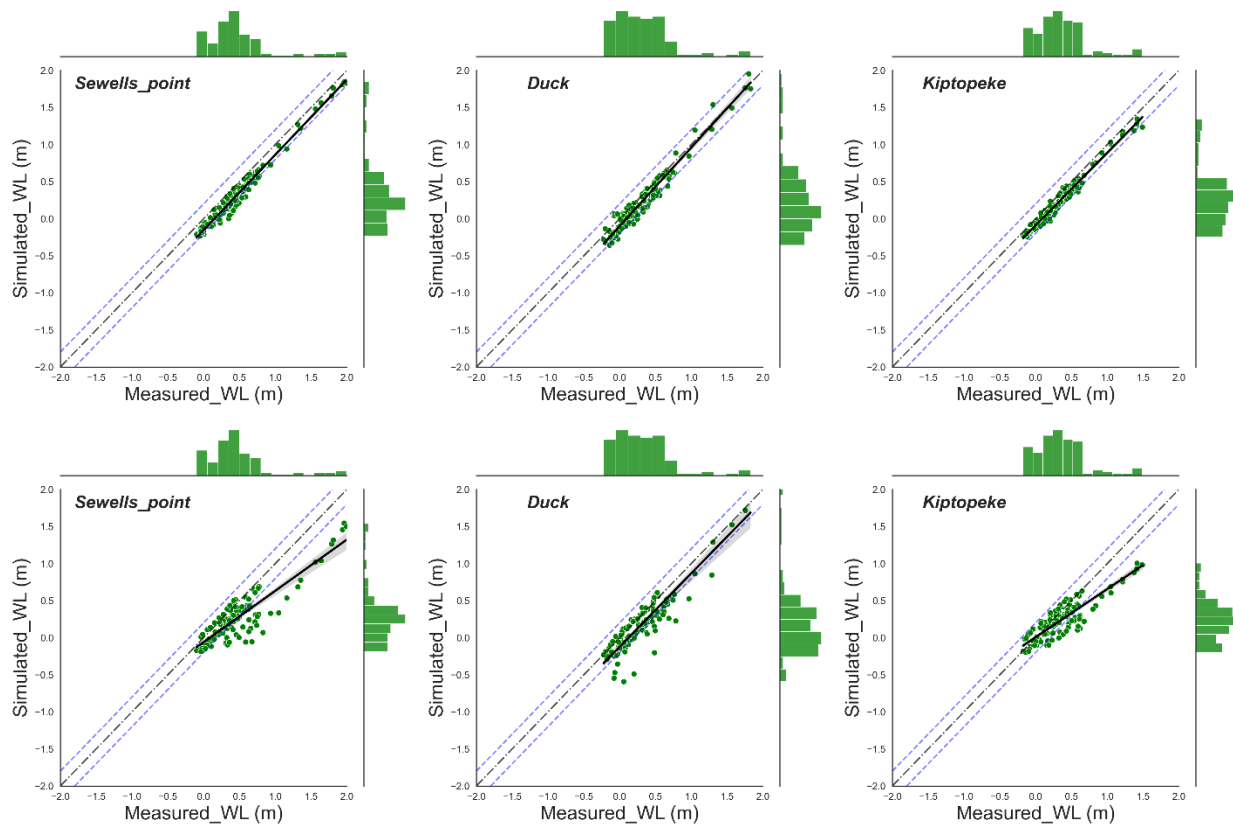


Figure 33. Scatter plots of the measured and simulated water levels (m) at Sewells, Duck and Kiptopeke using ERA5 (upper panels) and HM (lower panels). Histograms are plotted along the right and upper axes, Isabel, NSN.

Table 12. Summary statistics of simulated and measured water levels at the different stations during Hurricane Isabel using ERA5 and HM wind forces, NSN.

#	Location	Wind Forces	R	R ²	RMSE	NRMSE	Bias	RB	MNB
1	Atlantic city	ERA5	0.94	0.89	0.14	0.10	-0.08	-0.36	-0.28
2	Lewes DE		0.96	0.93	0.17	0.10	-0.13	-0.41	-0.35
3	Windmill point		0.98	0.96	0.15	0.17	-0.14	-0.44	-0.66
4	Kiptopeke		0.98	0.97	0.11	0.07	-0.10	-0.28	-0.31
5	Sewells point		0.99	0.97	0.16	0.08	-0.15	-0.31	-0.39
6	Money point		0.98	0.96	0.18	0.08	-0.16	-0.32	-0.41
7	Duck		0.97	0.95	0.13	0.06	-0.08	-0.26	-0.24
8	Atlantic city	HM	0.90	0.82	0.15	0.11	-0.04	-0.19	-0.15
9	Lewes DE		0.88	0.77	0.22	0.14	-0.13	-0.41	-0.40
10	Windmill point		0.89	0.80	0.15	0.16	-0.10	-0.29	-0.40
11	Kiptopeke		0.88	0.77	0.21	0.12	-0.11	-0.33	-0.42

12	Sewells point		0.88	0.78	0.29	0.14	-0.20	-0.43	-0.66
13	Money point		0.78	0.60	0.38	0.17	-0.25	-0.51	-0.82
14	Duck		0.92	0.85	0.21	0.10	-0.13	-0.40	-0.40

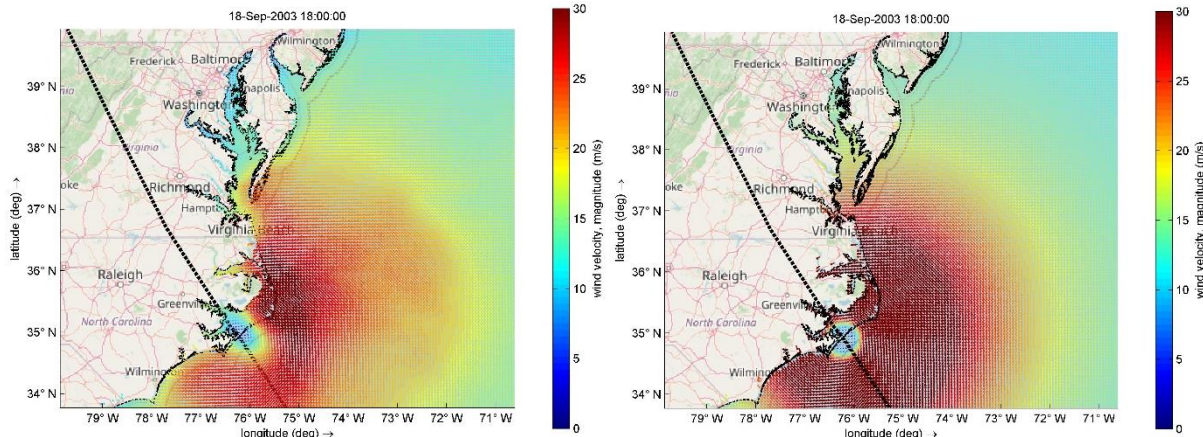


Figure 34. Wind speed (m/sec) of ERA5 (left panel) and Holland Model (right panel) wind force during the peak surge of Hurricane Isabel. The black dashed line represents the actual path of the hurricane.

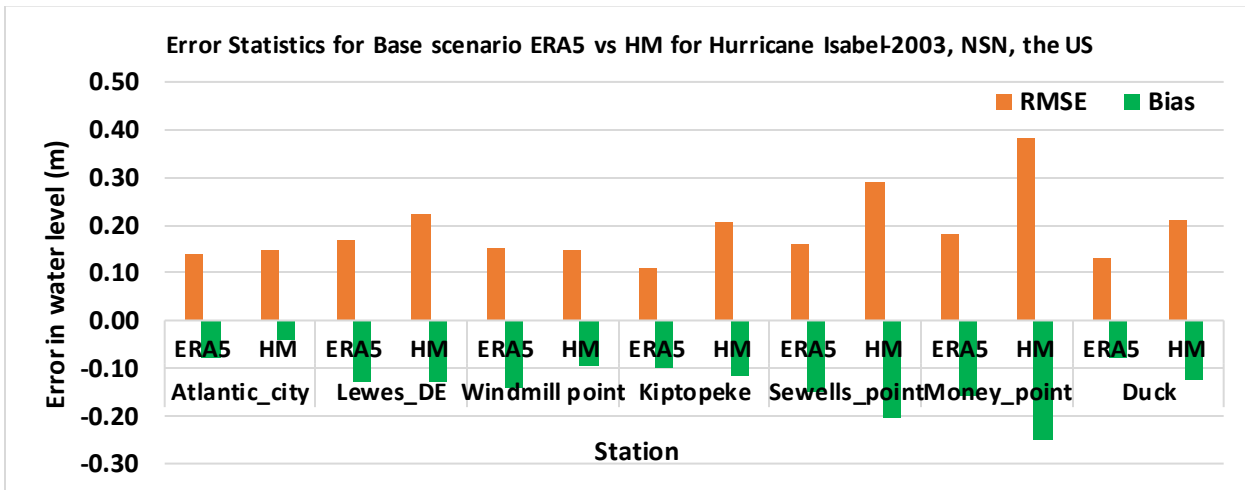


Figure 35. Summary statistics (RMSE and bias in m) of water level prediction using ERA5 and HM at the calibration stations along the US east coast during Hurricane Isabel-2003.

Table 13. Error statistics (Differences in magnitude (m), timing (h), and duration (h)) of peak surge characteristics at Sewells Point for Hurricane Isabel-2003, NSN.

#	Hurricane/ Wind Forcing	Magnitude (m)	Time (h)	Duration (h)			
				Low	Medium	High	
1	Isabel	ERA5	-0.14	-1.0	-3.0	-2.0	-1.0
2		HM	-0.44	-1.0	-15.0	-4.0	-5.0

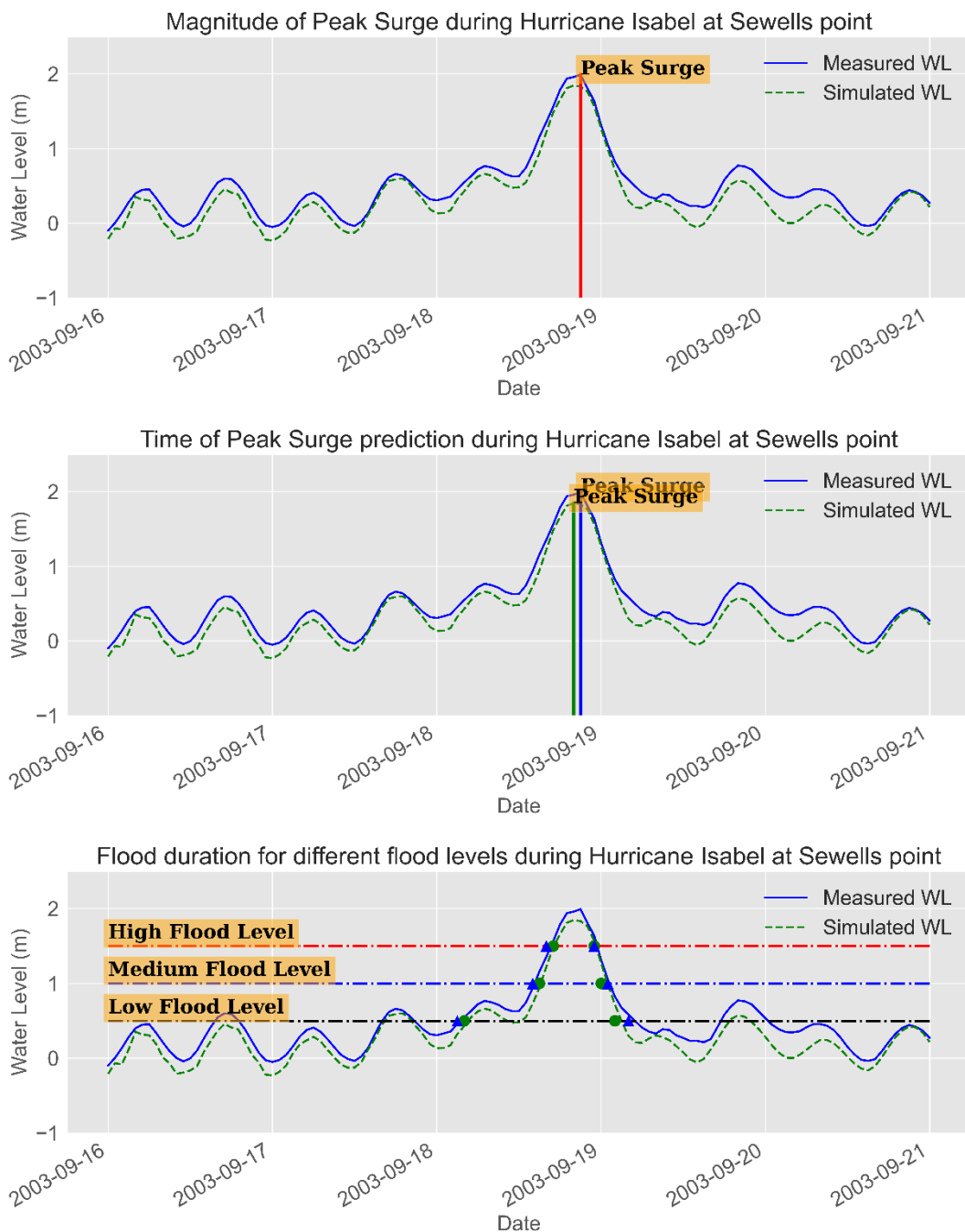


Figure 36. Flood Duration, Magnitude, and Timing at Sewells Point during Hurricane Isabel-2003 (Base-ERA5) at NSN.

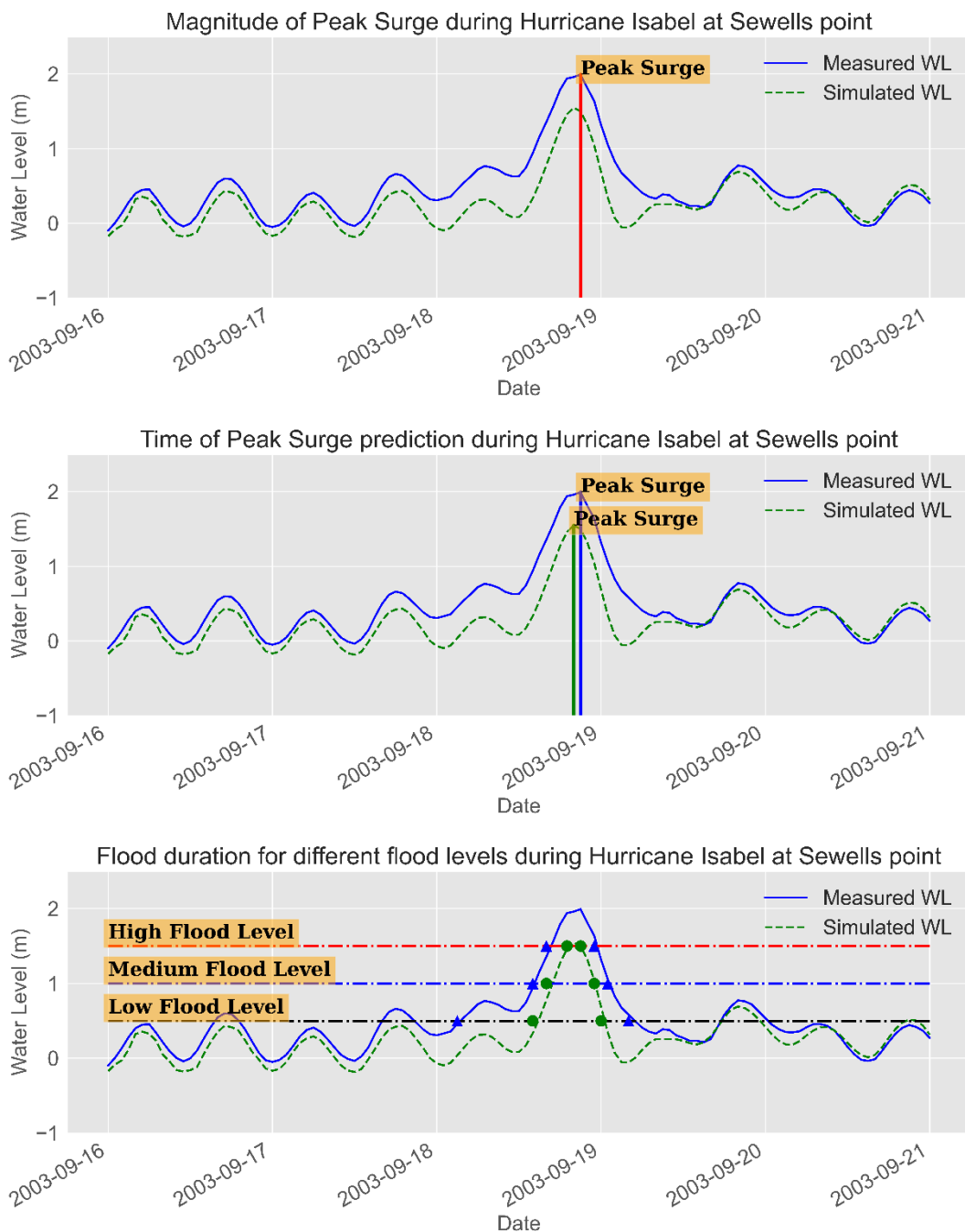


Figure 37. Flood Duration, Magnitude and Timing at Sewells Point during Hurricane Isabel-2003 (Base-HM) at NSN.

Following the same analysis approach we adopted for Hurricane Irene, the flood area statistics were calculated for Hurricane Isabel using both ERA5 and HM model wind forces. Similar to Hurricane Irene, Hurricane Isabel had a minor impact on NSN in terms of flooding where the maximum detected flood area was 0.3 km² (<2% of the base area) using ERA5 winds (Figure 39). This area can be reduced, for the same reasons explained in section 6.2.1 (low accuracy at coastal boundaries, bathymetry and resolution accuracy), to 0.1 km²-0.15 km² (<1% of the base area). In addition, considering the coastal structures protecting the affected area, the flood area could be even less than 1% of the base area (Figure 29). The flooded area has an average flood depth of 1.35 m with a maximum of 1.85 m. Using HM winds results in even more reduction of the predicted flood area (down to 0.24 km²) and flood characteristics, due to the underestimation in the peak surge magnitude and duration in the vicinity of the base.

The classification of the flood areas into flood levels also does not reflect valuable information under this scenario since no significant flood was detected. However, flood statistics were calculated for the different flood levels (Figure 40 and Figure 41). In addition, Table 14 shows the flood statistics for the different flood levels at NSN during the base-ERA5 scenario. Additional statistics for the Base-HM scenario can be found in Appendix B. Unfortunately, there is no additional measured or anecdotal data on the flooding that occurred during Hurricane Isabel at NSN or even the surrounding area.

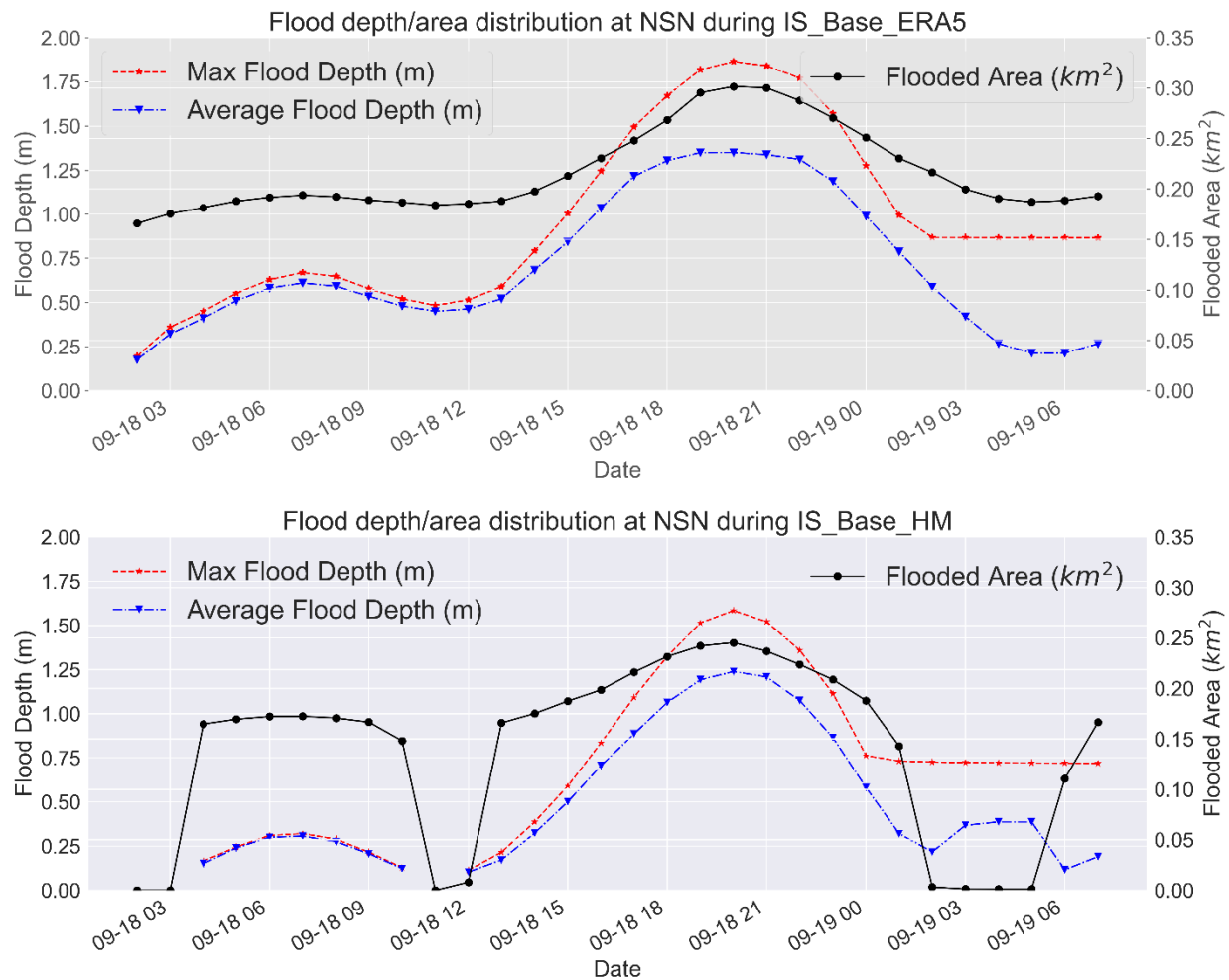


Figure 38. Timeseries of the projected average and maximum flood depth (m-left axis) and flood area (km^2 -right axis) during Hurricane Isabel-2003 for ERA5 (upper panel) and HM (lower panel) at NSN.

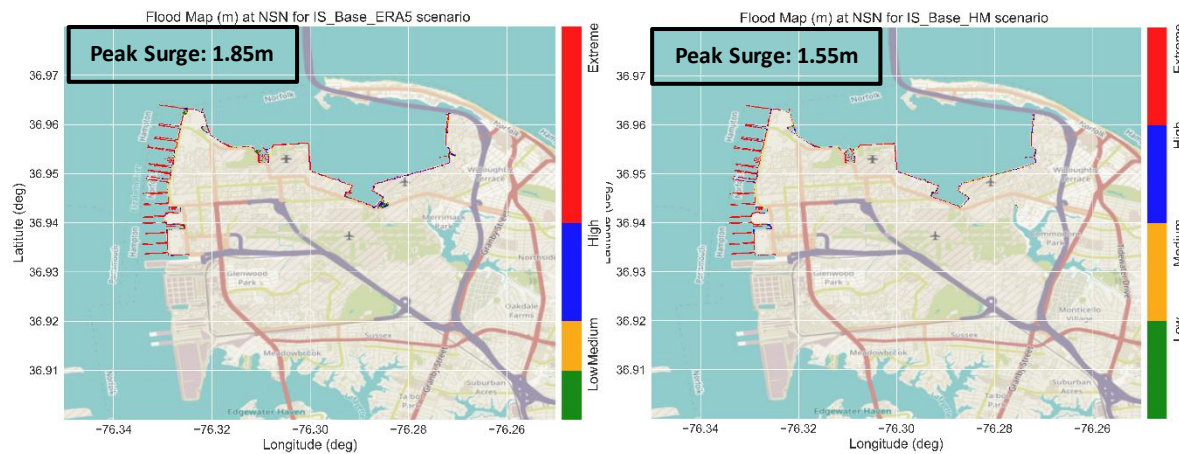


Figure 39. Flood map showing the classification of the flood levels at the peak surge during Hurricane Isabel-2003 using ERA5 wind forces (left panel) and HM wind forces (right panel) at NSN.

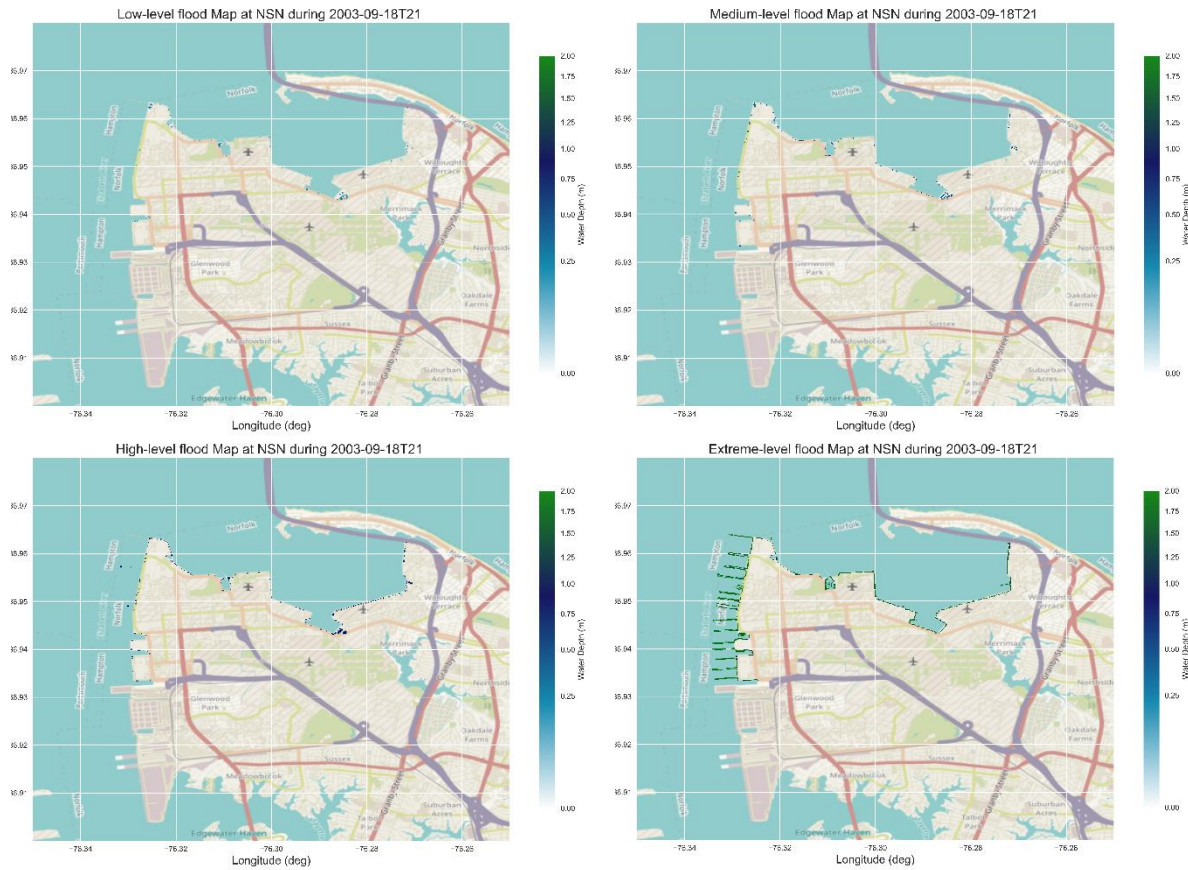


Figure 40. Flood maps show the classification of the different flood levels (low, medium, high, and extreme) at the peak surge simulation using ERA5 wind forcing during Hurricane Isabel-2003 at NSN.

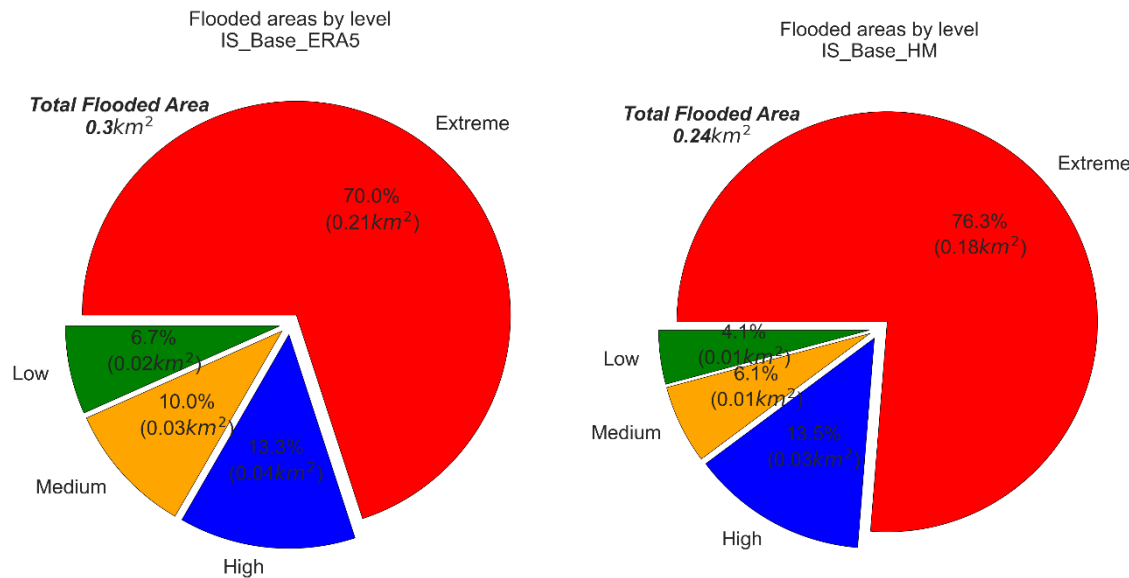


Figure 41. Pie chart showing the areas, with percentages, for the different flood levels at the peak surge during Hurricane Isabel-2003 using ERA5 wind forces (left panel) and HM wind forces (right panel) at NSN.

Table 14. Projected flood area statistics at the peak flood during Hurricane Isabel-2003 for the base-ERA5 scenario at NSN.

Flood_Level	Average_FD (m)*	Max_FD_(m)**	Flooded_Area_(km)	Flood %
Low	0.17	0.25	0.02	0.17
Medium	0.38	0.5	0.03	0.2
High	0.74	0.99	0.04	0.31
Extreme	1.71	1.84	0.21	1.51
No Flood	0	0	13.48	97.82

* Average Flood depth in meters

**Maximum Flood depth in meters

III. Hurricane Sandy

It was observed that the model has a high performance in predicting the water level using ERA5 data and an acceptable performance using HM wind data, Figure 42 and Figure 43. The model was able to efficiently capture the peak surge using ERA5 data at almost all locations, See Appendix A, with an average RMSE and Bias less than 0.17m and -0.10m respectively. However, the model shows significant underestimation in water level prediction using HM at almost all stations. An average RMSE and Bias of about 0.44m and -0.37m were observed, Table 15. For Hurricane Sandy also the modeled meteorological forcing (ERA5) outperforms the parametrized

meteorological forcing (HM) in water level prediction at NSN. Using the HM wind forces, the model has neither been able to predict the normal water level nor the Hurricane-induced water level (peak surge).

Once again this could be explained by the proximity of the study location to the eye/trach of the storm. Figure 44 shows some error statistics (RMSE and Bias) for water level prediction at 9 stations during Hurricane Sandy calibration. The stations are ordered along the x-axis based on their location (north to south) while, Figure 45 shows the wind speed and the hurricane track of Hurricane Sandy during the peak surge at NSN.

Like Hurricane Isabel, Hurricane Sandy approached the US east coast at nearly perpendicular to the coast, but approximately 320km north of NSN which resulted in significant underestimation in water level prediction in the vicinity of the base. However, the best model performance, using HM data, was observed at Atlantic City and Lewes-DE locations, which are the closest stations to the eye/trach of the hurricane. In addition, the model has a relatively good performance, with observed underestimation due to the relative absence of surge, at location at a large distance from the hurricane eye where the impact of the hurricane itself is minor and most of the water level there is tidal driven, e.g. Duck and Wrightsville, see Appendix A.

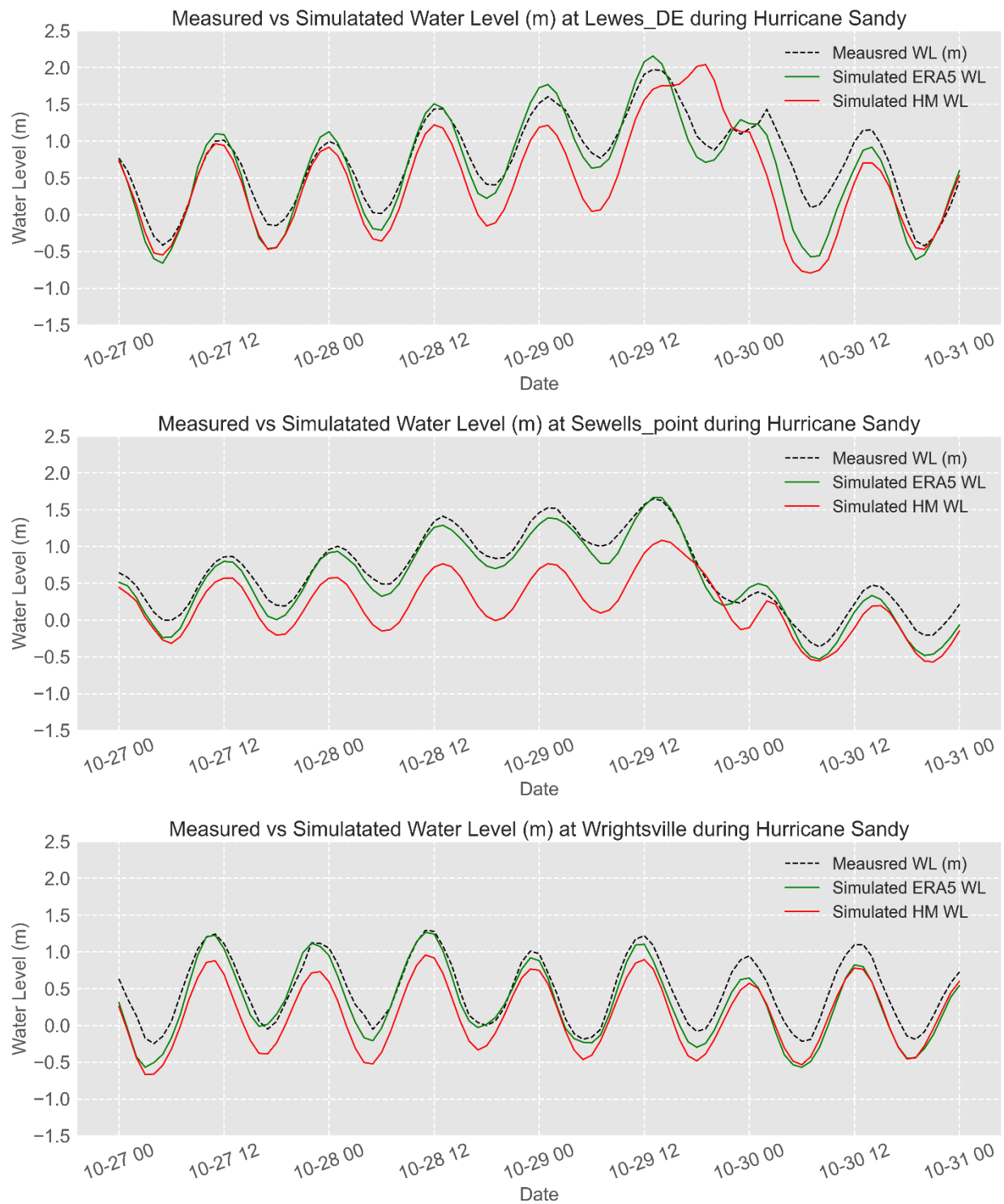


Figure 42. Measured vs Simulated water levels using ERA5 and HM wind forces during Hurricane Sandy, 2012.

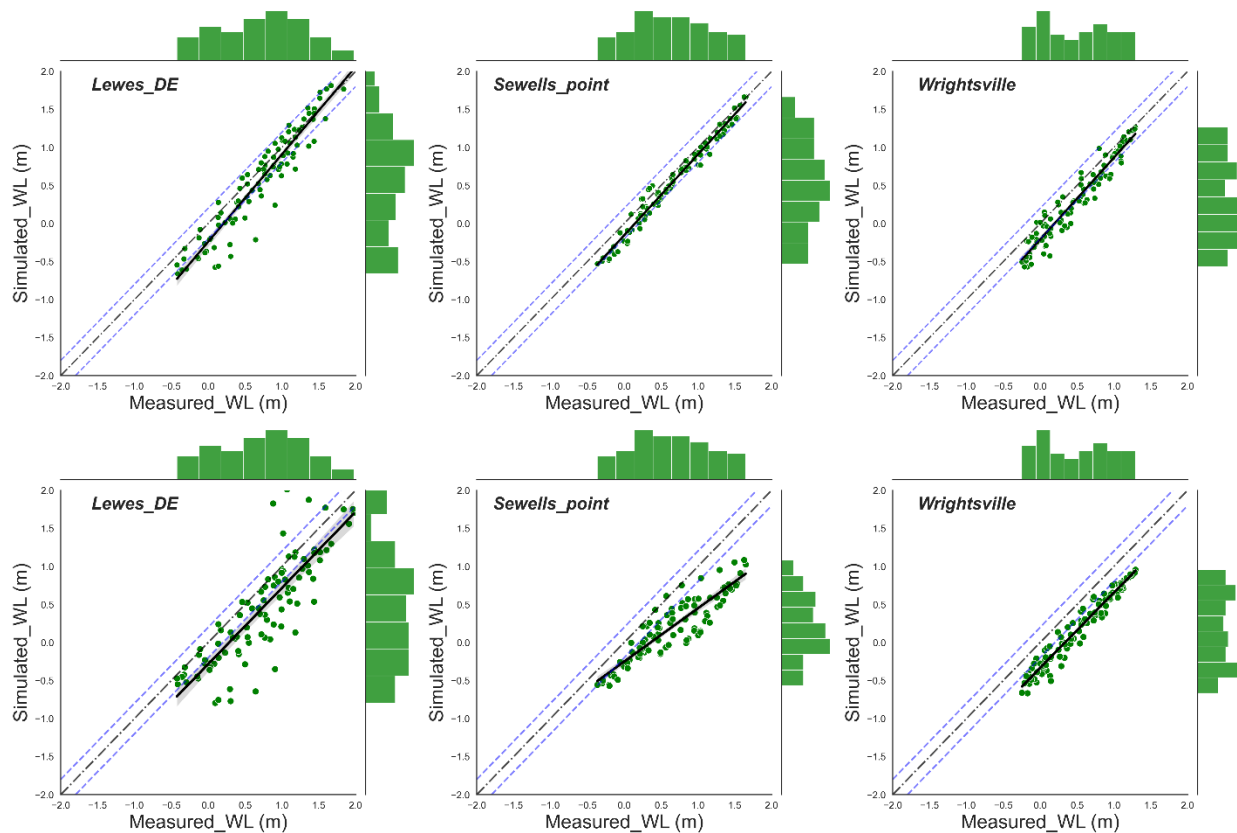


Figure 43. Scatter plots of the measured and simulated water levels (m) at Sewells, Duck and Wrightsville using ERA5 (upper panels) and HM (lower panels). Histograms are plotted along the right and upper axes, Sandy, 2012, NSN, US.

Table 15. Summary statistics of simulated and measured water levels at the different stations during Hurricane Sandy, 2012 using ERA5 and HM wind forces, NSN, US.

#	Location	Wind Forces	R	R ²	RMSE	NRMSE	Bias	RB	MNB
1	Atlantic city	ERA5	0.94	0.89	0.21	0.09	0.00	-0.01	-0.01
2	Lewes DE		0.96	0.91	0.26	0.11	-0.13	-0.18	-0.17
3	Windmill point		0.94	0.89	0.16	0.16	-0.12	-0.21	-0.26
4	Yorktown		0.98	0.96	0.17	0.10	-0.12	-0.20	-0.21
5	Kiptopeke		0.99	0.98	0.13	0.07	-0.07	-0.12	-0.12
6	Sewells point		0.99	0.98	0.15	0.07	-0.12	-0.18	-0.18
7	Money point		0.98	0.97	0.16	0.08	-0.12	-0.19	-0.19
8	Duck		0.99	0.97	0.11	0.06	-0.03	-0.03	-0.03
9	Wrightsville		0.96	0.92	0.22	0.15	-0.17	-0.36	-0.36
10	Atlantic city	HM	0.92	0.85	0.26	0.11	-0.12	-0.19	-0.19
11	Lewes DE		0.83	0.69	0.48	0.20	-0.28	-0.39	-0.43

12	Windmill point		0.77	0.59	0.48	0.46	-0.43	-0.77	-1.52
13	Yorktown		0.93	0.86	0.48	0.28	-0.45	-0.78	-1.41
14	Kiptopeke		0.87	0.76	0.41	0.23	-0.35	-0.60	-0.92
15	Sewells point		0.90	0.80	0.50	0.25	-0.44	-0.69	-1.21
16	Money point		0.86	0.74	0.52	0.24	-0.43	-0.65	-1.04
17	Duck		0.92	0.84	0.50	0.30	-0.47	-0.64	-1.21
18	Wrightsville		0.97	0.95	0.35	0.23	-0.34	-0.71	-0.82

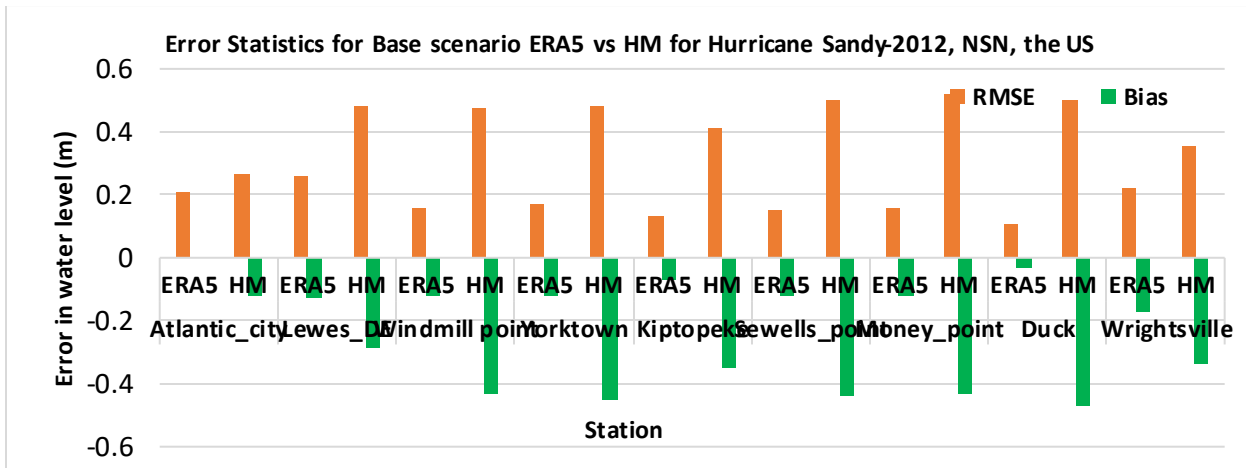


Figure 44. Summary statistics (RMSE and Bias in meters) of water level prediction using ERA5 and HM at the calibration stations along the US east coast during Hurricane Sandy-2012.

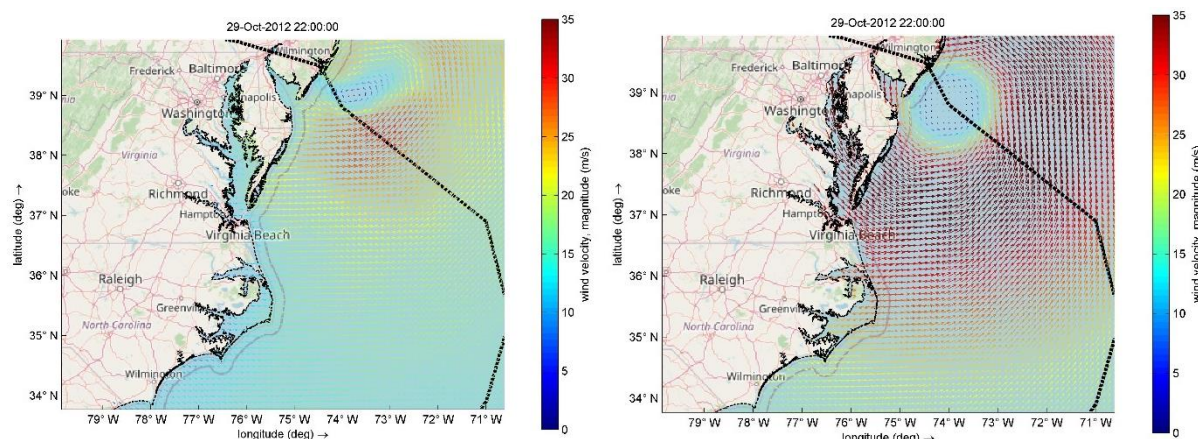


Figure 45. Wind speed (m/sec) of ERA5 (left panel) and Holland Model (right panel) wind force during the peak surge of Hurricane Sandy 2012. The black dashed line represents the actual path of the hurricane.

Investigating the peak surge characteristics shows that the model can efficiently capture the peak surge during Hurricane Sandy at Sewells Point using the ERA5 wind forces with a magnitude difference of about +0.02m, Figure 46. However, significant underestimation was observed in the peak surge magnitude using the HM wind data -0.56m, Figure 47. On the other hand, a small haste (one hour) was detected in the predicted timing of the peak surge by the model using both wind forces. Calculating the duration of the surge for the considered levels shows very good agreement between the measured and simulated water levels using ERA5 forces. The model almost predicts the surge duration with no underestimates/overestimation, except less than -2h in the low level, in the surge duration through all surge levels. However, significant underestimation was observed using HM wind that can reach up to -28h for the medium surge level. Furthermore, the high surge level ($\geq 1.5\text{m}$) was not detected by the model using HM data resulting in more than -4h (100%) underestimation in peak surge duration for this surge level, Table 16.

Following the same analysis approach we adopted for previous hurricanes, the flood area statistics were calculated for Hurricane Sandy using both ERA5 and HM model wind forces. Hurricane Sandy was also found to have a minor impact on NSN in terms of flooding where the maximum detected flood area was 0.28km^2 (<2% of the base area) and 0.23 km^2 using ERA5 and HM winds respectively, Figure 48 and Figure 49. This area can be corrected, for the same reasons explained in section 6.2.1, to 0.04 km^2 - 0.10 km^2 (<0.8% of the base area). In addition, considering

the coastal structures protecting the affected area, Figure 29, the flood area could be even less than 0.5% of the base area.

Flood statistics were calculated for the different flood levels, Figure 50 and Figure 51. In addition, **Table 17** shows the flood statistics for the different flood levels at NSN during the base-ERA5 scenario. Additional statistics for the Base-HM scenario can be found in Appendix B. Figure 52 shows the locations where flood events were reported during Hurricane Sandy 2012, obtained from STORM database. It can be noticed that almost no flood locations were reported during the storm except for a single location at southwest of the base, which might be associated with pluvial flooding (from the heavy rain associated with the storm), which we did not consider in this study. The same location was also reported during Hurricane Irene. This anecdotal data supports the model results and increases our confidence in the model performance at NSN during Hurricane Sandy too.

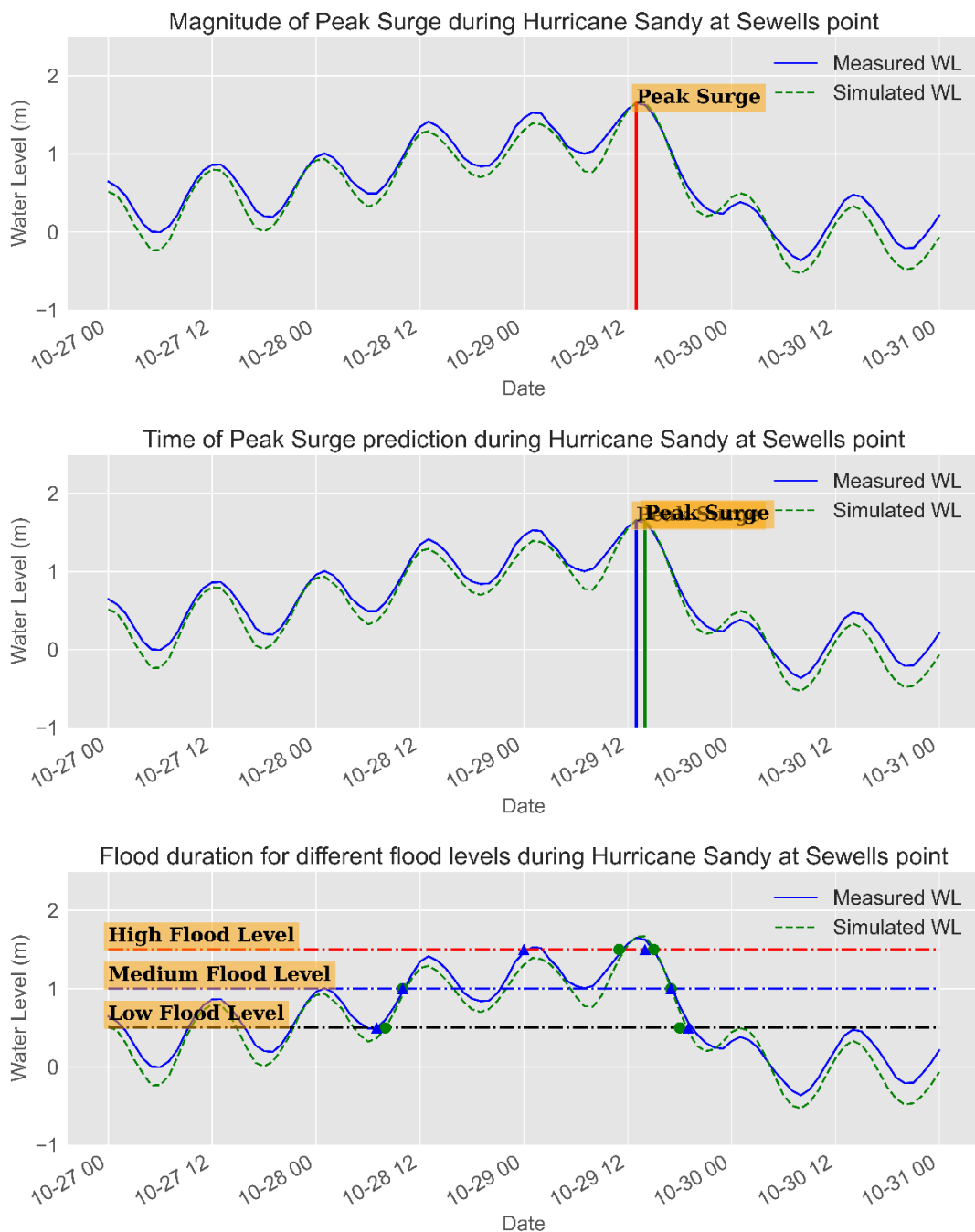


Figure 46. Flood Duration, Magnitude, and Timing at Sewells Point during Hurricane Sandy-2012 (Base-ERA5) at NSN, the US.

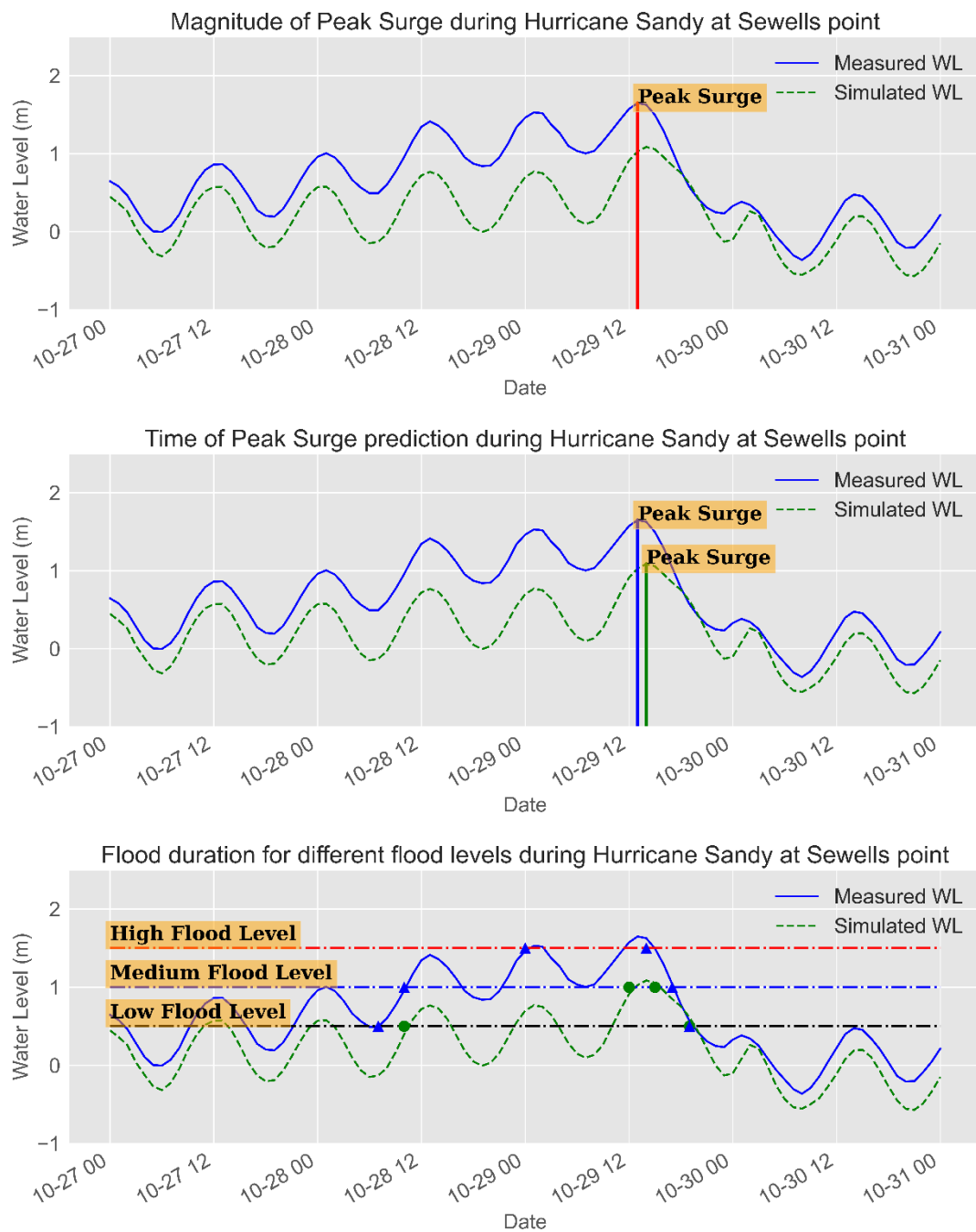


Figure 47. Flood Duration, Magnitude and Timing at Sewells Point during Hurricane Sandy-2012 (Base-HM) at NSN, the US.

Table 16. Error statistics (Differences in magnitude (m), timing (h), and duration (h)) of peak surge characteristics at Sewells Point for Hurricane Sandy-2012, NSN, US.

#	Hurricane/ Wind Forcing	Magnitude (m)	Time (h)	Duration (h)		
				Low	Medium	High
1	Sandy	ERA5	+0.02	+1.0	-2.0	0.0
2		HM	-0.56	+1.0	-3.0	-4.0*

*The High surge level was not detected with HM simulation.

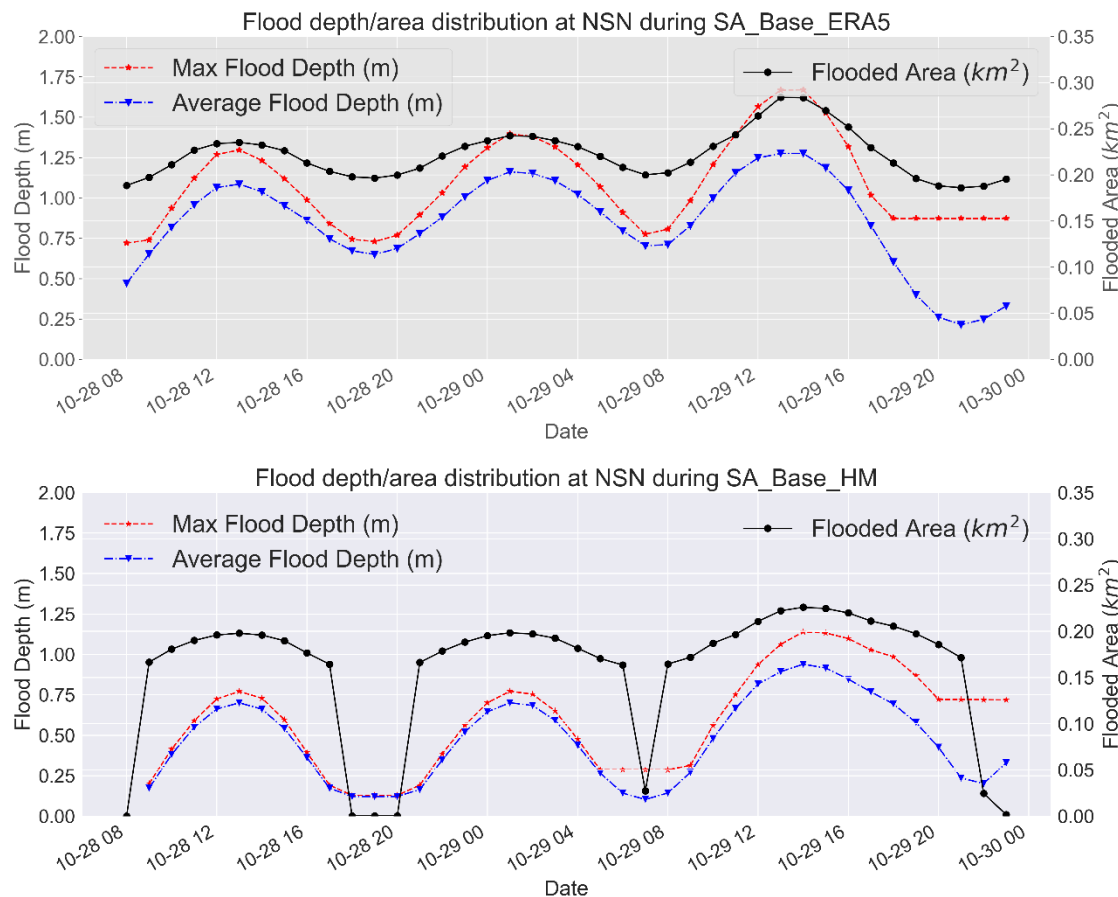


Figure 48. Timeseries of the projected average and maximum flood depth (left axis) and flood area (km^2 -right axis) during Hurricane Sandy-2012 for ERA5 (upper panel) and HM (lower panel) at NSN, the US.

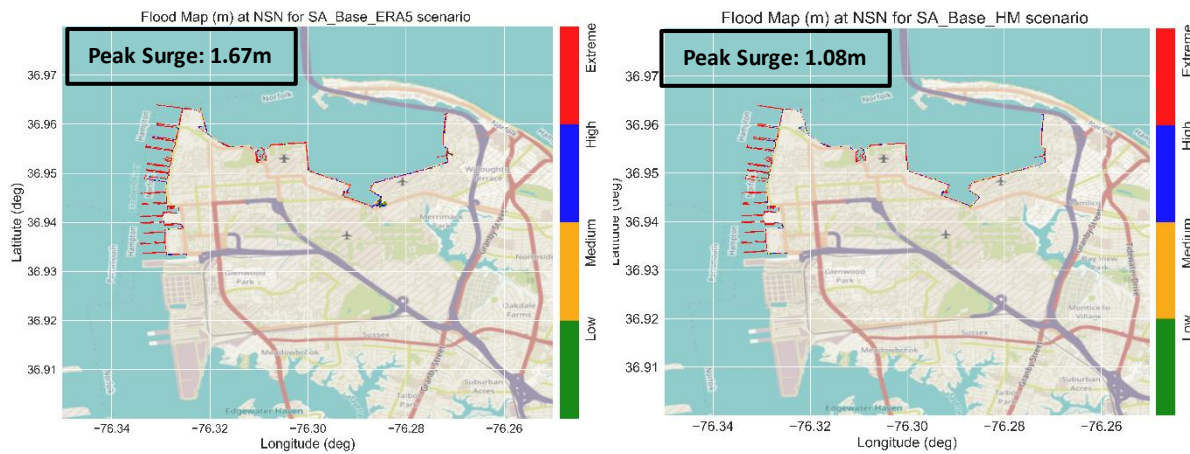


Figure 49. Flood map showing the classification of the flood levels at the peak surge during Hurricane Sandy-2012 using ERA5 wind forces (left panel) and HM wind forces (right panel) at NSN, the US.

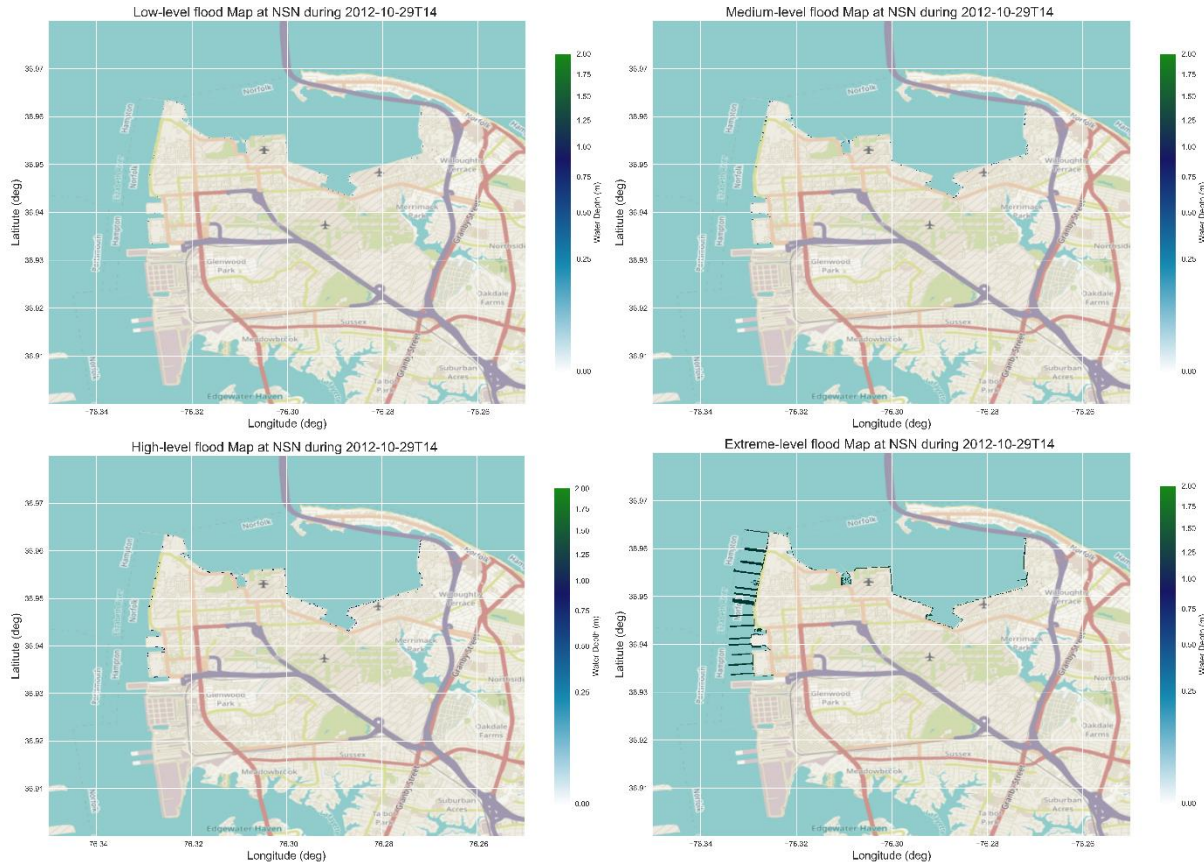


Figure 50. Flood maps show the classification of the different flood levels (low, medium, high, and extreme) at the peak surge simulation using ERA5 wind forcing during Hurricane Sandy-2012 at NSN, the US.

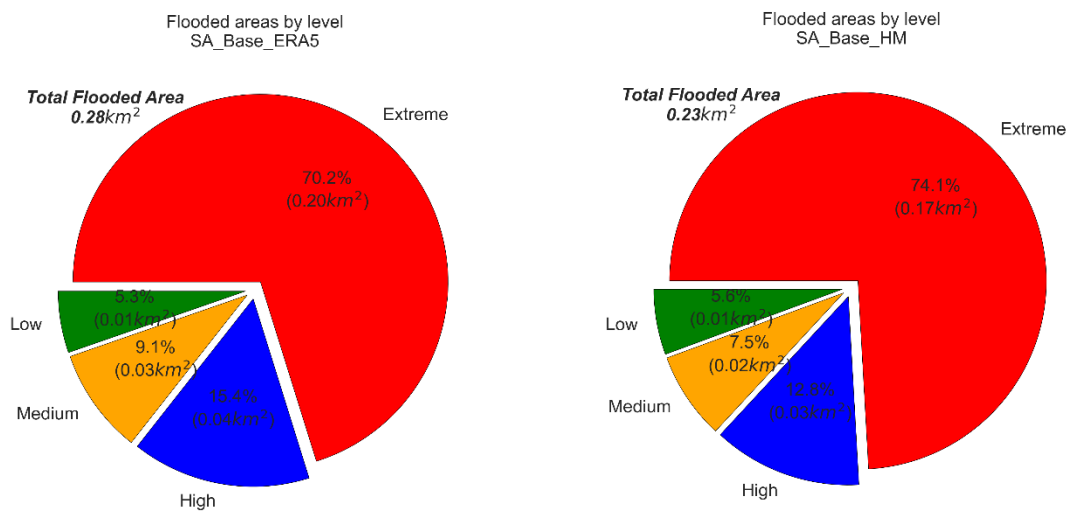


Figure 51. Pie chart showing the areas, with percentages, for the different flood levels at the peak surge during Hurricane Sandy-2012 using ERA5 wind forces (left panel) and HM wind forces (right panel) at NSN, the US.

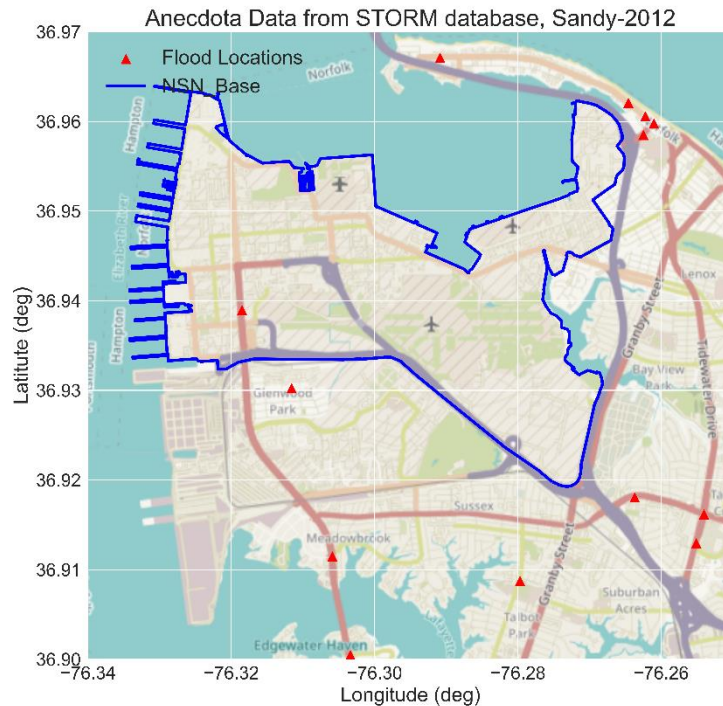


Figure 52. Thematic map showing the locations of the flooding during Hurricane Sandy-2012 based on the STORM anecdotal data. The solid blue line shows the boundary of NSN, and the red triangles represent reported flood location, NSN, the US.

Table 17. Projected flood area statistics at the peak flood during Hurricane Sandy-2012 for the base-ERA5 scenario at NSN, the US

Flood_Level	Average_FD_(m)*	Max_FD_(m)**	Flooded_Area_(km)	Flood %
Low	0.17	0.25	0.02	0.11
Medium	0.38	0.50	0.03	0.19
High	0.75	1.00	0.04	0.32
Extreme	1.59	1.67	0.20	1.45
No Flood	0.00	0.00	13.50	97.97

* Average Flood depth in meters

**Maximum Flood depth in meters

IV. Hurricane Michael

The hurricane approaches the east coast from the west (land side) where the hurricane winds become relatively weak resulting in insignificant increase in the water level with no distinguishable peak surge during the hurricane activity. However, the model performance in predicting the water level using ERA5 and HM data is almost similar and acceptable, Figure 53 and Figure 54, with relative underestimation at most locations. The model was able to simulate the water level with an average RMSE and Bias of 0.27m and -0.23m respectively, Table 18.

Looking at the calibration locations from north to south, Figure 55, reveals no significant changes in model predictive accuracy along the coast except for Atlantic city and Kiptopeke (southeast Chesapeake Bay) locations. The fact that the hurricane is approaching from land direction has made the strong cyclonic winds blow offshore, hence pulling the water away from the coast, with weaker shoreward winds, Figure 56. However, some locations have experienced stronger shoreward winds, e.g. Atlantic City and Kiptopeke, where the model shows relatively better performance.

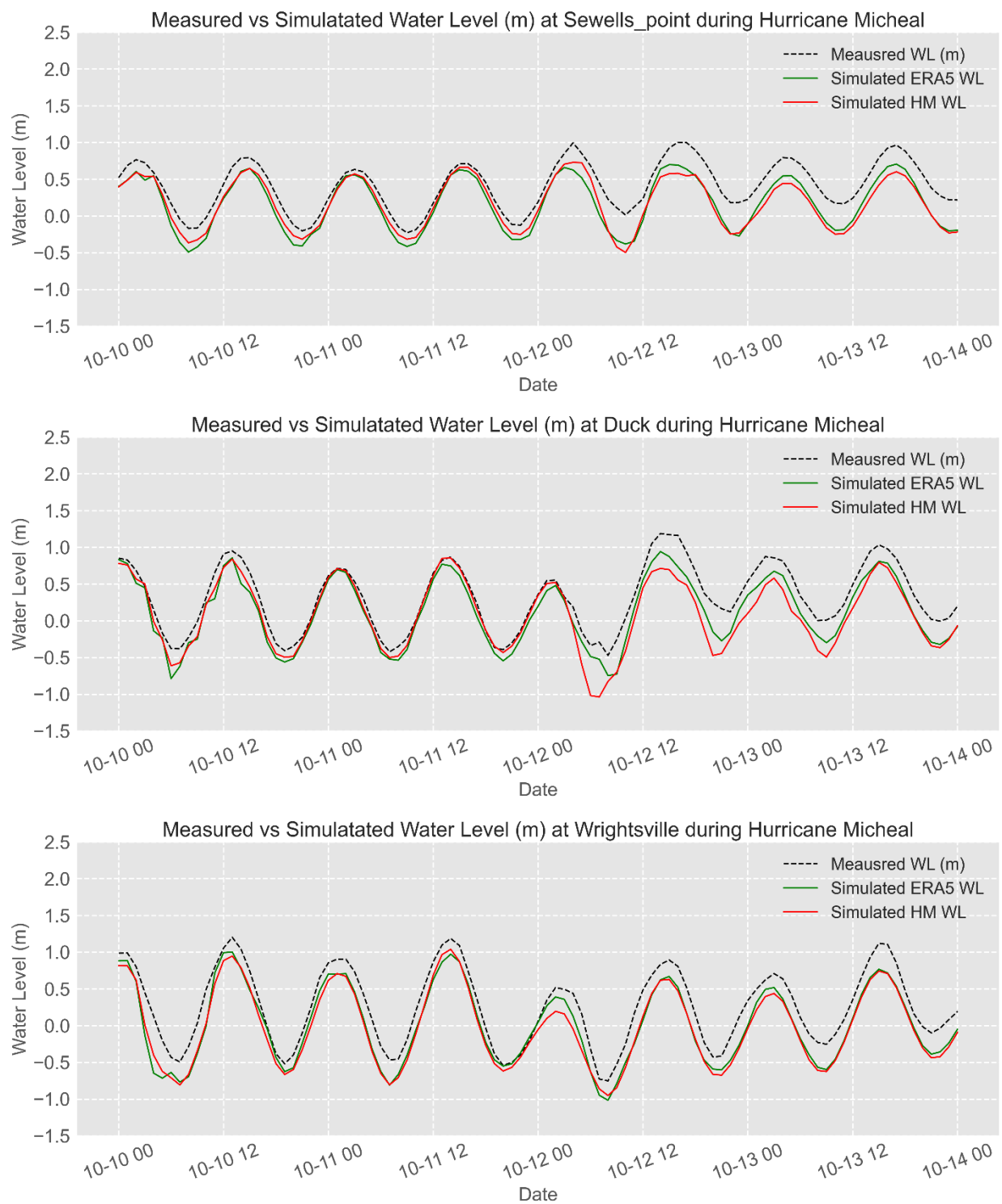


Figure 53. Measured vs Simulated water levels using ERA5 and HM wind forces during Hurricane Michael, 2018.

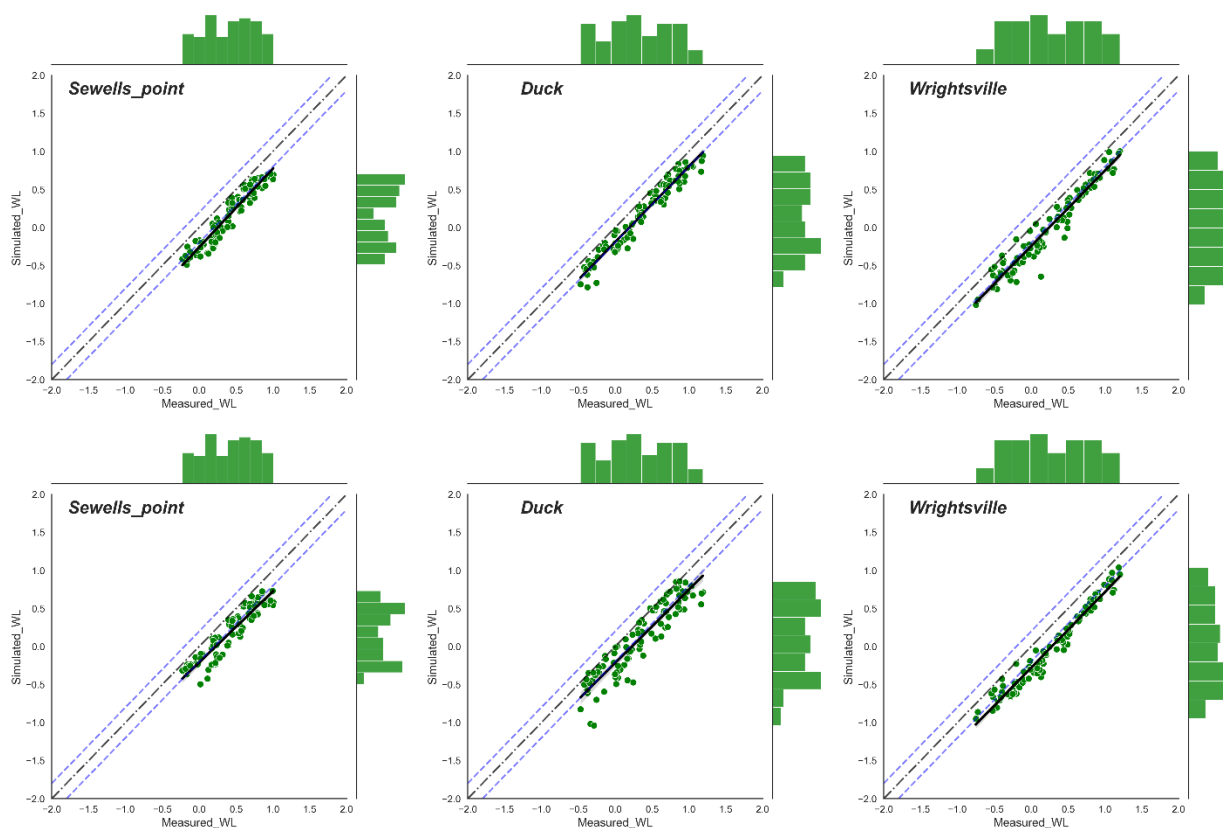


Figure 54. Scatter plots of the measured and simulated water levels (m) at Sewells, Duck and Wrightsville using ERA5 (upper panels) and HM (lower panels). Histograms are plotted along the right and upper axes, Michael, 2018, NSN, US.

Table 18. Summary statistics of simulated and measured water levels at the different stations during Hurricane Michael, 2018 using ERA5 and HM wind forces, NSN, US.

#	Location	Wind Forces	R	R ²	RMSE	NRMSE	Bias	RB	MNB
1	Atlantic city	ERA5	0.97	0.95	0.23	0.11	-0.19	-0.60	-0.41
2	Lewes DE		0.97	0.95	0.28	0.15	-0.23	-0.64	-0.40
3	Yorktown		0.93	0.87	0.28	0.32	-0.27	-0.62	-1.35
4	Kiptopeke		0.95	0.90	0.29	0.27	-0.26	-0.61	-0.79
5	Sewells point		0.97	0.94	0.22	0.17	-0.20	-0.56	-0.56
6	Money point		0.96	0.92	0.27	0.22	-0.25	-0.60	-0.71
7	Duck		0.94	0.88	0.27	0.18	-0.23	-0.57	-0.60
8	Wrightsville		0.98	0.95	0.22	0.13	-0.19	-0.61	-0.47
9	Atlantic city		0.97	0.94	0.28	0.14	-0.24	-0.94	-0.53
10	Lewes DE	HM	0.95	0.91	0.26	0.13	-0.20	-0.63	-0.43
11	Yorktown		0.95	0.90	0.28	0.15	-0.22	-0.63	-0.43

12	Kiptopeke		0.90	0.81	0.27	0.31	-0.25	-0.58	-1.32
13	Sewells point		0.92	0.84	0.28	0.25	-0.25	-0.58	-0.84
14	Money point		0.94	0.89	0.23	0.18	-0.20	-0.54	-0.60
15	Duck		0.92	0.85	0.27	0.22	-0.24	-0.58	-0.72
16	Wrightsville		0.92	0.85	0.27	0.18	-0.22	-0.55	-0.60
17	Atlantic city		0.92	0.85	0.29	0.18	-0.23	-0.72	-0.55
18	Lewes DE		0.98	0.96	0.30	0.15	-0.28	-1.08	-0.61

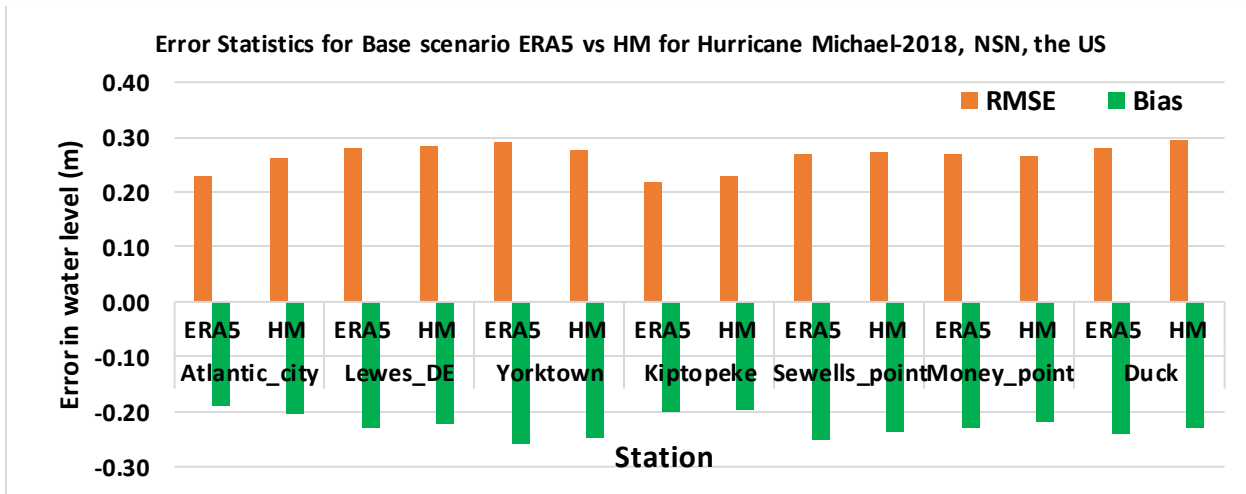


Figure 55. Summary statistics (RMSE and Bias in meters) of water level prediction using ERA5 and HM at the calibration stations along the US east coast during Hurricane Michael-2018.

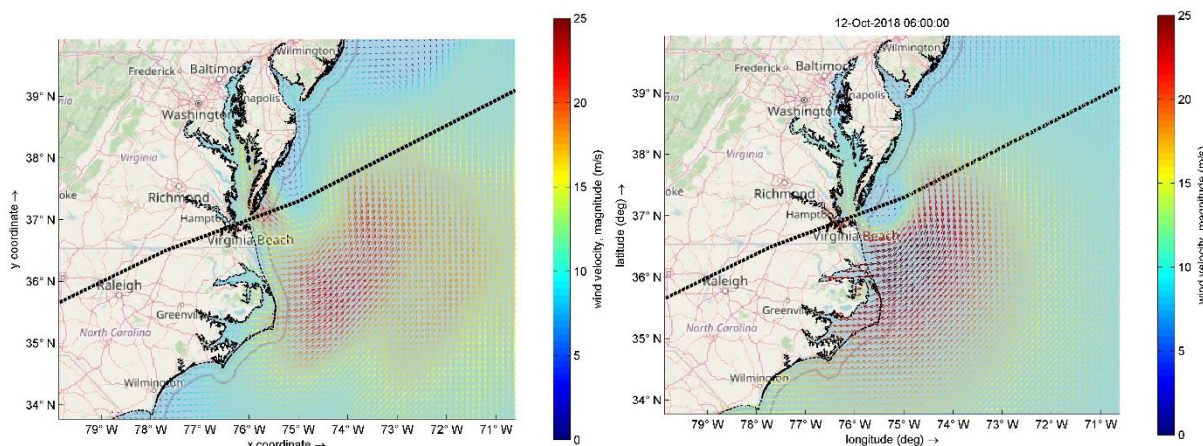


Figure 56. Wind speed (m/sec) of ERA5 (left panel) and Holland Model (right panel) wind force during the peak surge of Hurricane Michael 2018. The black dashed line represents the actual path of the hurricane (West to East direction).

Considering that there is no distinguishable peak surge, the highest peak in the measured data were used for surge characteristic analysis as the peak surge during Hurricane Michael 2018. Investigating the peak surge characteristics at Sewells Point shows that the model underestimates the peak surge magnitude using both ERA5 and HM wind data with a magnitude difference of -0.30m and -0.42m respectively, Figure 57 Figure 58 upper panels. Timing wise, almost no haste or delay was detected in the predicted timing of the peak surge using HM wind forces with only -1h delay using ERA5 data, , Figure 57 and Figure 58 middle panels.

Calculating the duration of the surge for the considered levels was somehow tricky because neither the measured data nor the model has surge magnitude above 1m. Hence, the medium and high surge levels thresholds were not satisfied/detected during Hurricane Micheal. The model results show underestimation in low surge duration by -2h to -3h using ERA5 and HM winds respectively. Beyond this, the model did not detect a 2h medium level surge (1m) using both wind forces, Table 19.

Adopting the same analysis approach previous hurricanes, the flood area statistics were calculated for Hurricane Michael using both ERA5 and HM model wind forces. Hurricane Michael was found to has insignificant impact on NSN in terms of flooding where the maximum detected flood area was 0.2km² (<1.5% of the base area) using ERA5 and HM winds, Figure 59 and Figure 60. The flood maps show almost no flooding inside the base, but only the quays and the shoreline. Therefore, this area can be corrected, for the same reasons explained in section 6.2.1, to almost

zero km² and the results of Hurricane Michael flood areas can be used as a baseline for the flood area correction and analysis using the same model settings.

Although carrying out further analysis for the flood area under hurricane Michael activity is unnecessary, flood statistics were calculated for the different flood levels for the consistency of the analysis approach, Figure 61 and Figure 62. In addition, Table 20 shows the flood statistics for the different flood levels at NSN during the base-ERA5 scenario. Additional statistics for the Base-HM scenario can be found in Appendix B. In addition, Figure 63 shows the locations where flood events were reported during Hurricane Michael 2018, obtained from STORM database. It can be noticed that no flood events/locations were reported during the storm, which supports the model results and increases our confidence in the model performance at NSN throughout the four studied hurricanes.

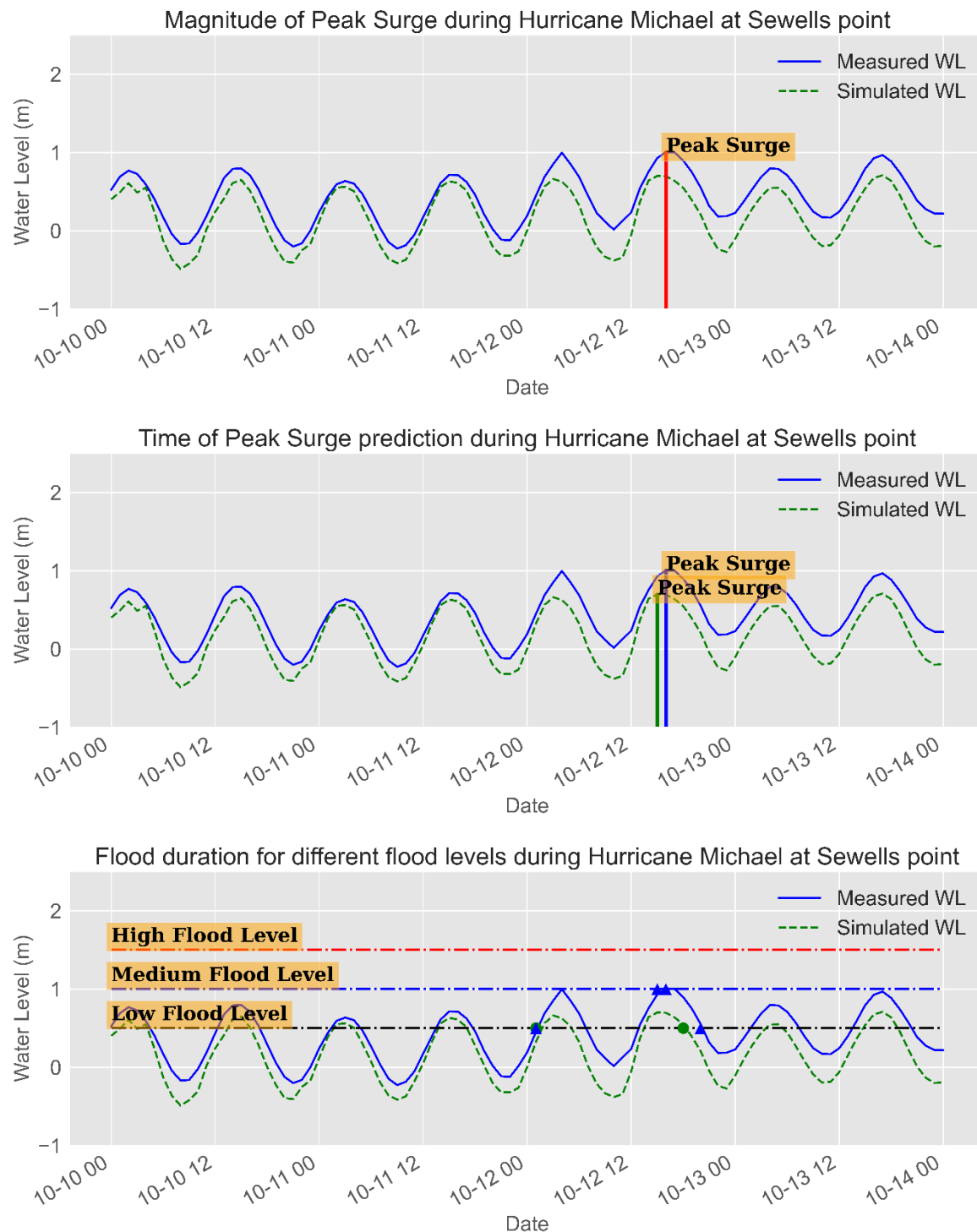


Figure 57. Flood Duration, Magnitude, and Timing at Sewells Point during Hurricane Michael-2018 (Base-ERA5) at NSN, the US.

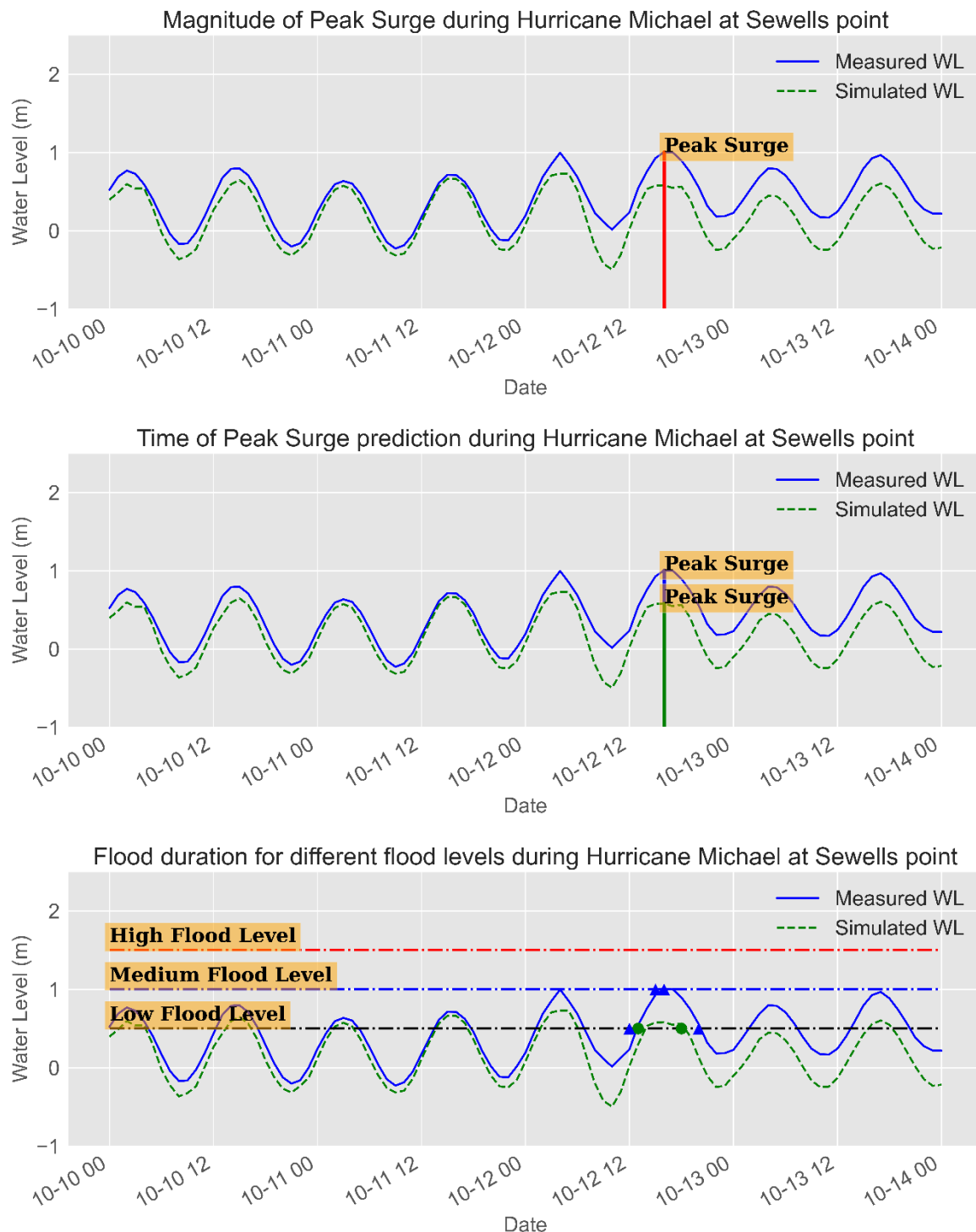


Figure 58. Flood Duration, Magnitude and Timing at Sewells Point during Hurricane Michael-2018 (Base-HM) at NSN, the US

Table 19. Error statistics (Differences in magnitude (m), timing (h), and duration (h)) of peak surge characteristics at Sewells Point for Hurricane Michael-2018, NSN, US.

#	Hurricane/ Wind Forcing	Magnitude (m)	Time (h)	Duration (h)		
				Low	Medium	High
1	Michael	ERA5	-0.30	-1.0	-2.0	-2.0* 0.0**
2		HM	-0.42	0.0	-3.0	-2.0* 0.0**

*The surge level was not detected by the model.

** This surge level was not recorded by the measured data.

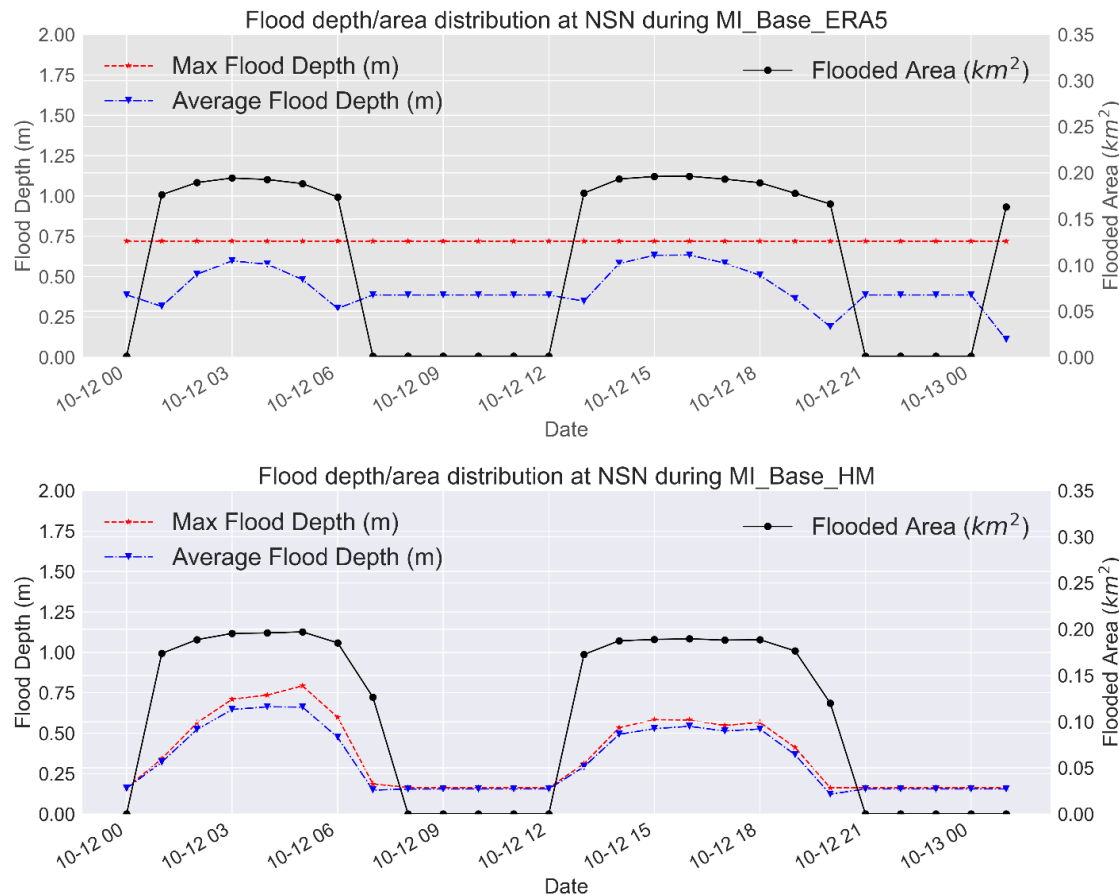


Figure 59. Timeseries of the projected average and maximum flood depth (left axis) and flood area (km^2 -right axis) during Hurricane Michael-2018 for ERA5 (upper panel) and HM (lower panel) at NSN, the US.

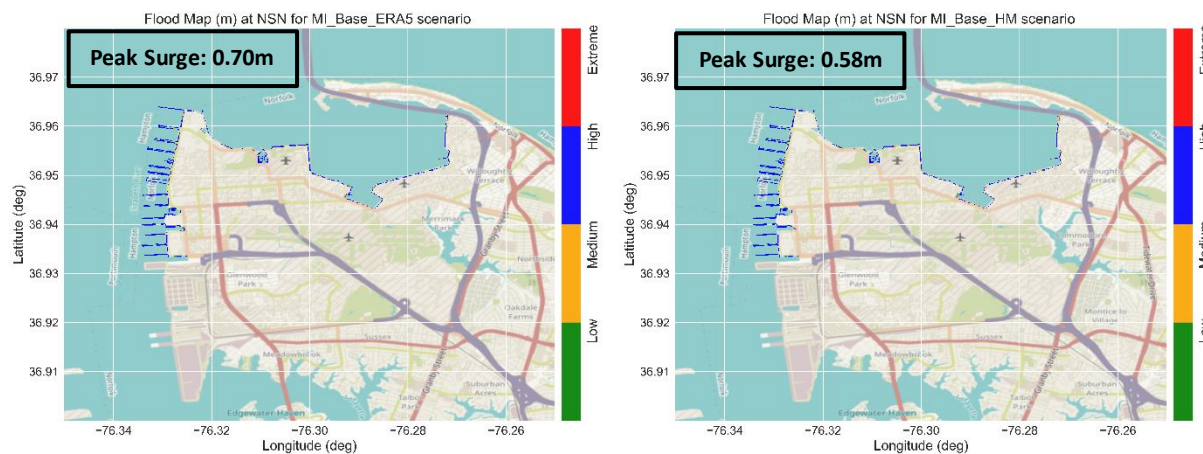


Figure 60. Flood map showing the classification of the flood levels at the peak surge during Hurricane Michael-2018 using ERA5 wind forces (left panel) and HM wind forces (right panel) at NSN, the US.

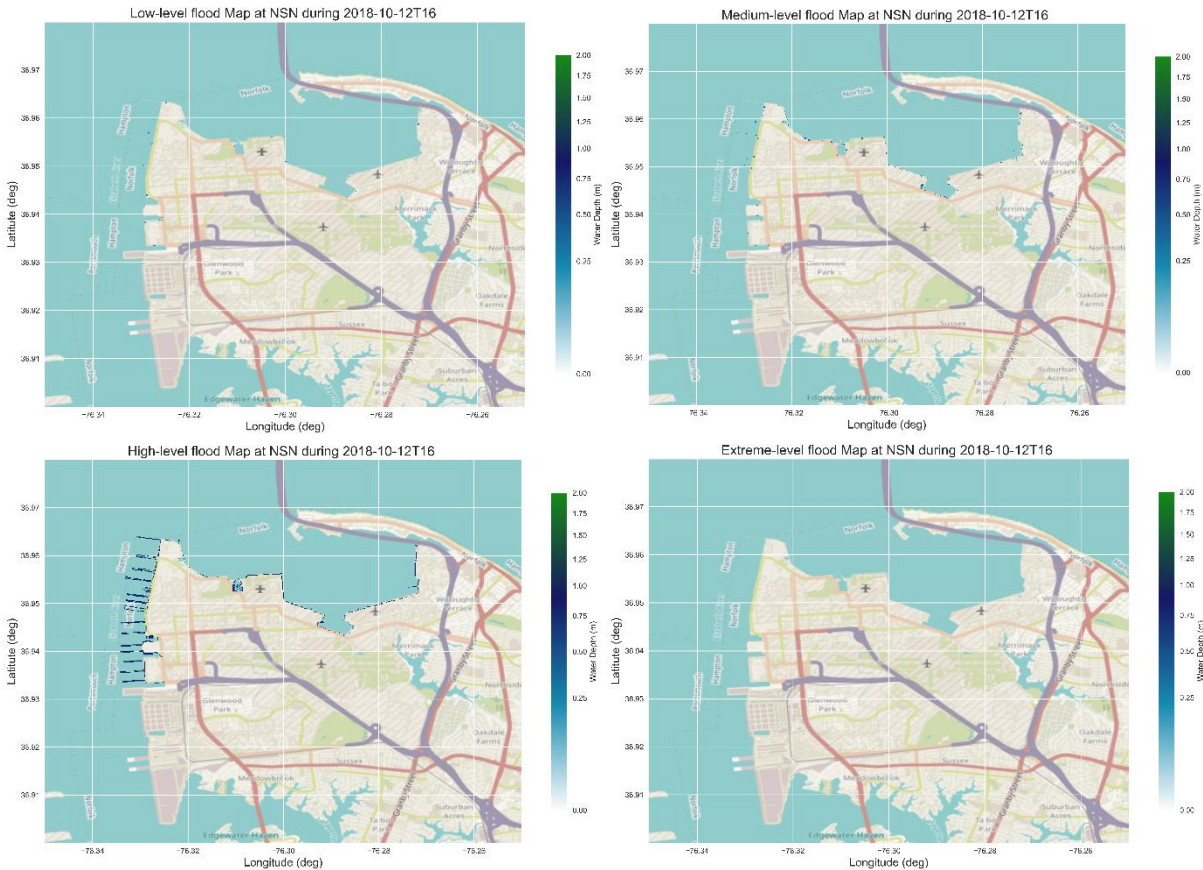


Figure 61. Flood maps show the classification of the different flood levels (low, medium, high, and extreme) at the peak surge simulation using ERA5 wind forcing during Hurricane Michael-2018 at NSN, the US.

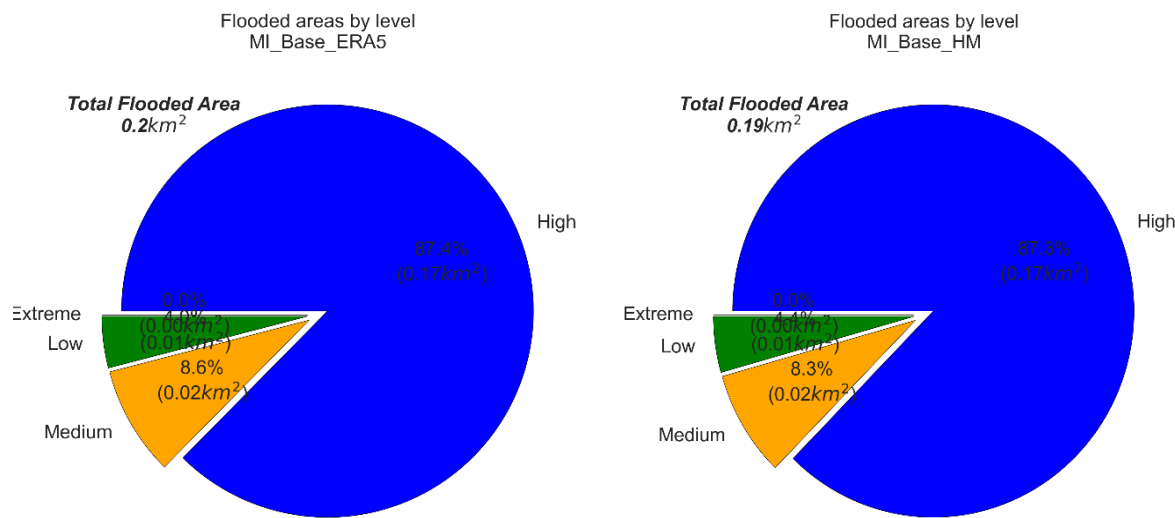


Figure 62. Pie chart showing the areas, with percentages, for the different flood levels at the peak surge during Hurricane Michael-2018 using ERA5 wind forces (left panel) and HM wind forces (right panel) at NSN, the US.

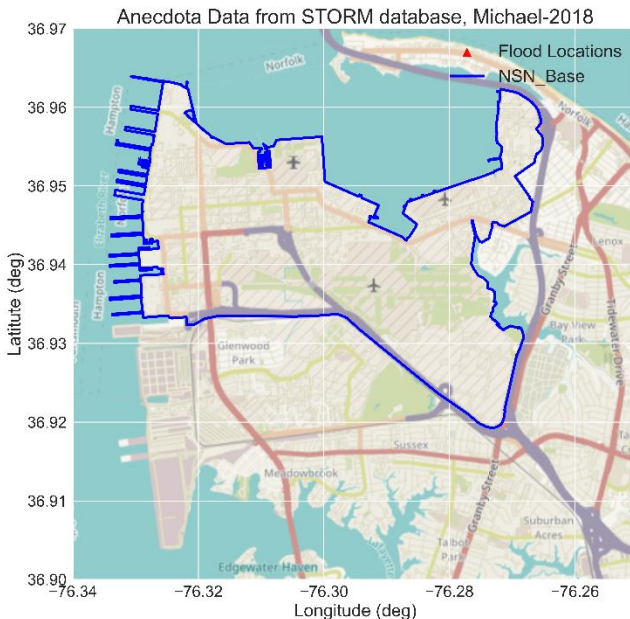


Figure 63. Thematic map showing the locations of the flooding during Hurricane Michael-2018 based on the STORM anecdotal data. The solid blue line shows the boundary of NSN, and the red triangles represent reported flood location, NSN, the US.

Table 20. Projected flood area statistics at the peak flood during Hurricane Michael-2018 for the base-ERA5 scenario at NSN, the US

Flood_Level	AFD_(m)*	MFD_(m)**	Flooded_Area_(km)	Flood %
Low	0.17	0.25	0.01	0.06
Medium	0.38	0.50	0.02	0.12
High	0.68	0.72	0.17	1.25
Extreme	0.00	0.00	0.00	0.00
No Flood	0.00	0.00	13.58	98.55

* Average Flood depth in meters

**Maximum Flood depth in meters

6.2.2. Impacts of Meteorological forcing

Manipulating the hurricane's meteorological forces is crucial for understanding and evaluating the extent of influence of these forces on the severity of the hurricane and its associated impacts on coastal zones. The aim here is to identify and compare the results of the different perturbations in meteorological forces (central pressure drop and radius of maximum wind) of the 4-considered hurricanes on the magnitude, duration, and associated flooding at NSN. This could be crucial for future predictions of hurricane impacts with similar characteristics to the hurricanes in this study.

I. Pressure Drop

Three pressure drop scenarios were considered with an additional drop in the central pressure by 12% (PD_F0.88), 24% (PD_F0.76) and 36% (PD_F0.64) below the recorded central pressure. The surge magnitude and duration for each level were obtained for all scenarios at Sewells Point. In addition, Average Flood Depth (AFD), Maximum Flood Depth (MFD) and projected flood area were calculated for all scenarios. Finally, a flood map was created for each individual scenario with the classification maps of each flood level (low, medium, high, and extreme).

Figure 64 shows the simulated water level at Sewells Point for the base and PD_F.64 scenario for all hurricanes. Reducing the central pressure of the hurricane reflected a marginal increase in the peak surge at Sewells Point with an increase of 3 cm to 10 cm, Table 21. This mild increase in the peak surge reflected an insignificant increase in the surge duration with a maximum increase of 0.5 hour. Figure 65 shows the peak surge magnitude and surge duration for the base and PD_F0.64 scenarios for all hurricanes.

Minor changes were detected in the flood areas along NSN for all PD scenarios compared to the baseline scenarios for all hurricanes. Nevertheless, a minor increase (~0.4 %) in the simulated flood area was detected for Hurricane Irene due to the proximity of the hurricane center (eye) to NSN,

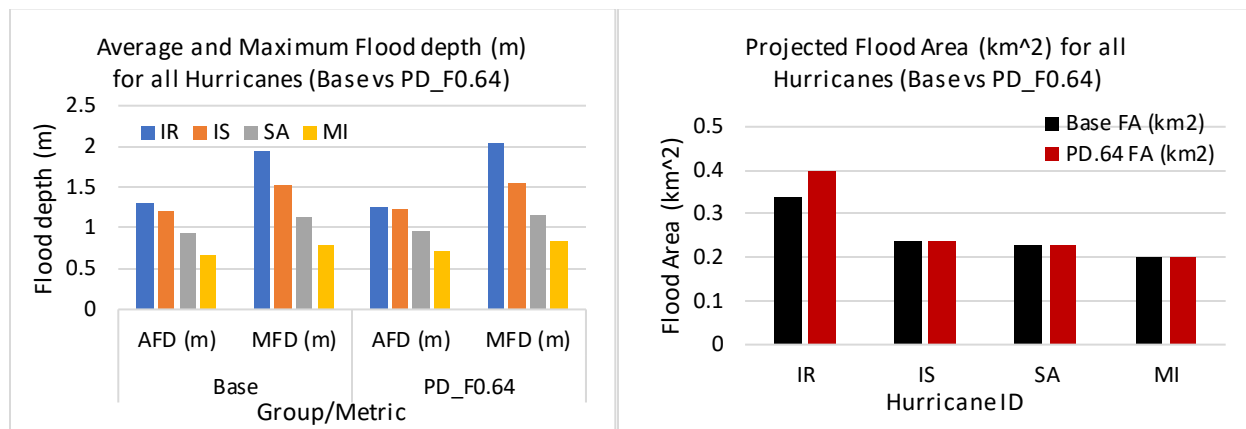


Figure 66 & Table 22.. Otherwise, there is no significant impact of the PD on the flood areas for all hurricanes, Figure 67.

Furthermore, the average and maximum flood depth showed minor response under the PD_F0.64 scenario with a maximum change of 0.1 m. This is also reflected on the flooding areas, where looking at the flood areas by level, Figure 68 to Figure 69, it can be noticed that there are only minor changes in the flood area level compared to the baseline scenario with a dominant high (>0.5m) and extreme (>1.0m) flood levels. For more figures of the PD_F0.64 scenario for all hurricanes, please refer to Appendix C.

Investigating the other two pressure drop scenarios, PD_F0.76 and PD_F0.88 showed lower peak surge and hence duration and flood areas. The impact on the peak surge diminished down to 1 – 3 cm. A maximum impact on the flood area was detected for Hurricane Irene with an increase of 0.2%. Almost no significant impact was detected for the rest of the hurricanes, refer to Appendix C for more figures.

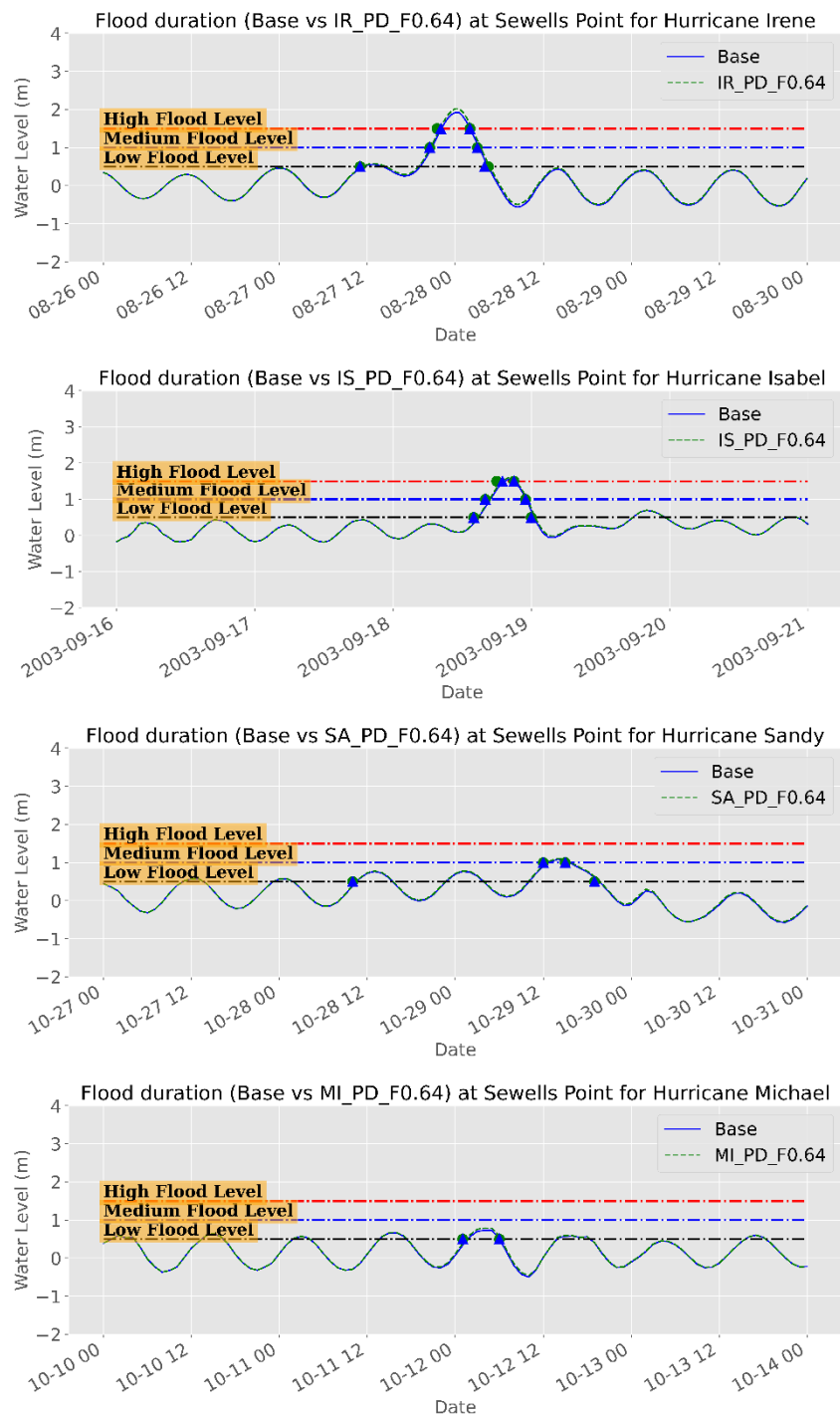


Figure 64. Water level time series (m) during the different hurricanes showing the surge magnitude and duration for different surge levels for the base and PD_F0.64 scenarios at Sewells Point, NSN, the US.

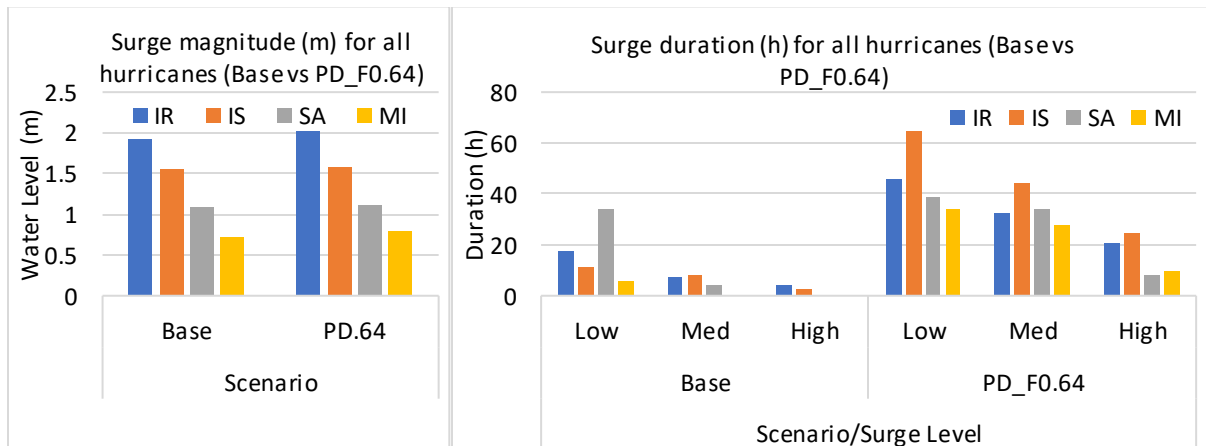


Figure 65. Peak surge (m) (left panel) and surge duration (h) of the different surge levels (right panel) for the base and PD_F0.64 scenario for all hurricanes, NSN, the US.

Table 21. Peak surge characteristics (Maximum and Duration) of the worst-case pressure drop scenario (PD_F0.64) and base scenarios for all Hurricanes at Sewells Point, NSN, the US.

Group	Hurricane ID	Max. Surge (m)		Duration (h)					
		Base	PD_F0.64	Base			PD_F0.64		
				Low	Med	High	Low	Med	High
Meteo. Forcing	IR	1.92	2.02	17.5	7.0	4.5	18	7	5
	IS	1.55	1.59	11.0	8.0	3.0	11	8	4
	SA	1.08	1.11	34.0	4.0	0.0	34	4	0
	MI	0.73	0.79	6.0	0.0	0.0	6	0	0

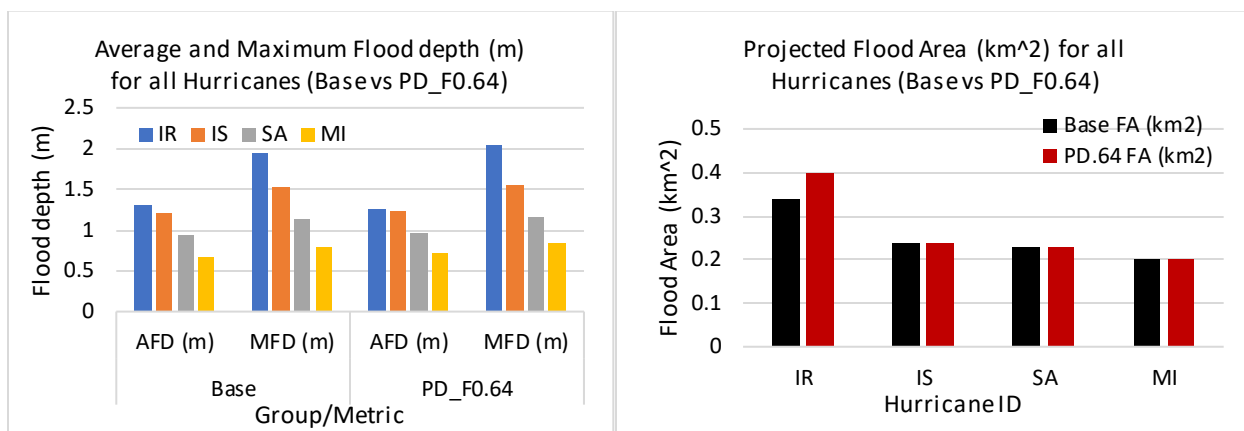


Figure 66. Average Flood Depth (AFD) & Maximum Flood Depth (MFD) in meters (left panel) and Flood area (km^2) (right panel) of all hurricanes for the Base and PD_F0.64 scenarios, NSN, the US.

Table 22. Flood area characteristics of the worst-case pressure drop scenario (PD_F0.64) for all hurricanes at NSN, the US.

Group	Hurricane ID	Base				PD_F0.64			
		Average FD (m)	Max FD (m)	Flood area (km^2)	%	Average FD (m)	Max FD (m)	Flood area (km^2)	%
Meteo. Forcing	IR	1.31	1.94	0.34	2.47	1.25	2.04	0.4	2.9
	IS	1.21	1.52	0.24	1.72	1.24	1.56	0.24	1.7
	SA	0.94	1.14	0.23	1.6	0.96	1.16	0.23	1.7
	MI	0.66	0.79	0.2	1.45	0.71	0.85	0.2	1.5

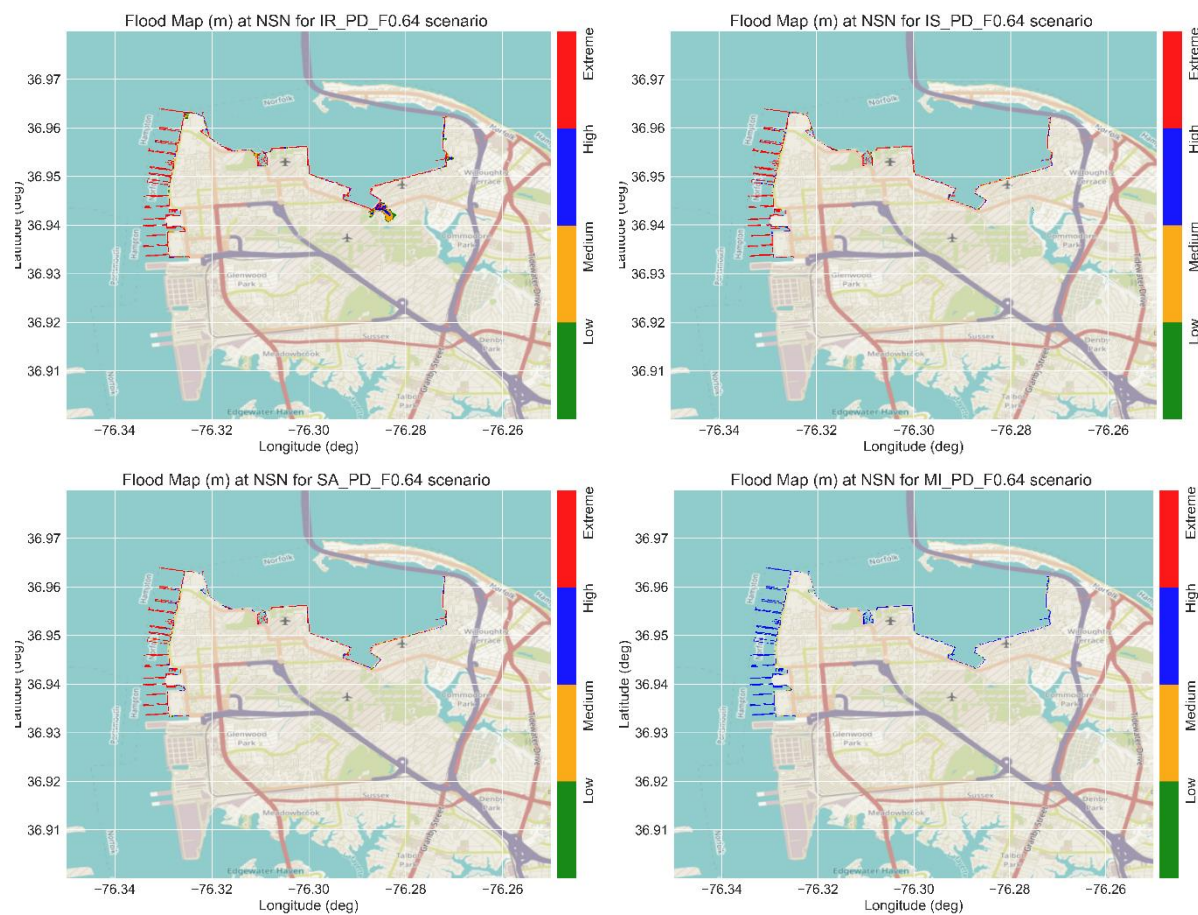


Figure 67. Flood maps with the flood levels for the different hurricanes during the peak surge for the PD_F0.64 scenario at NSN, the US.

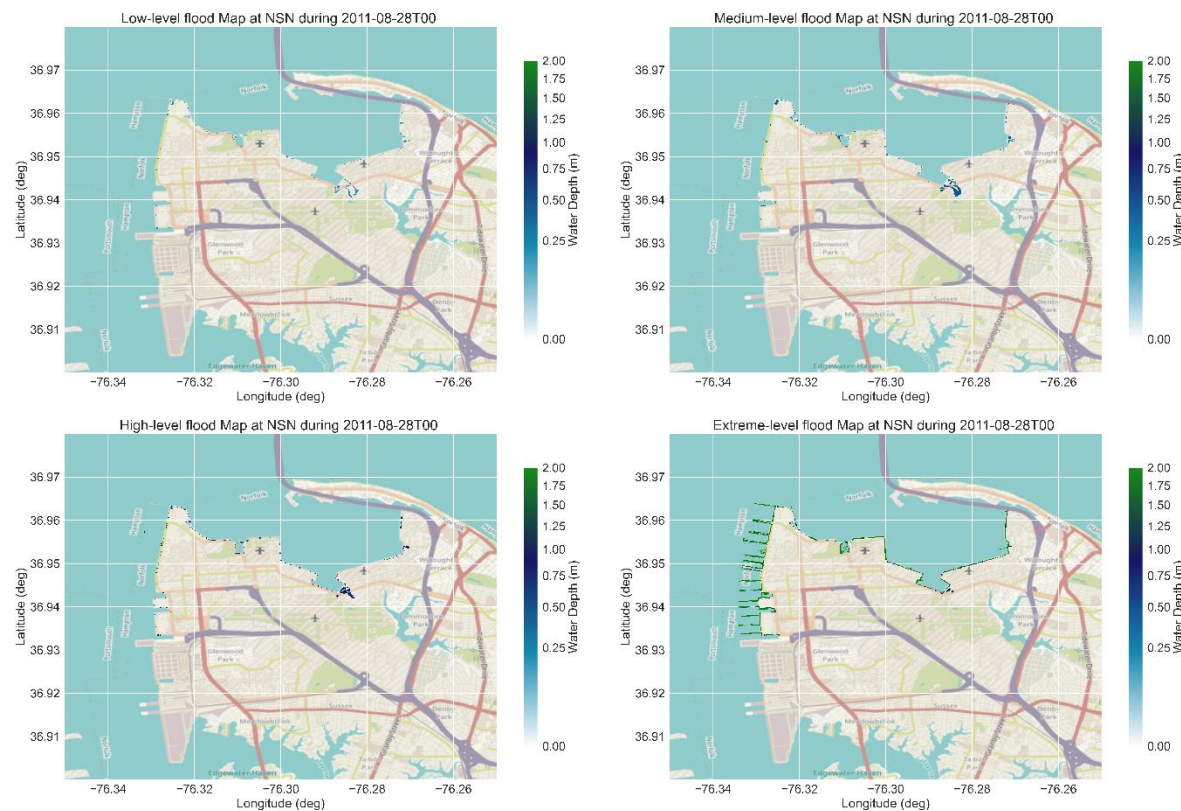


Figure 68. Flood area classification (Low, Medium, High, and Extreme) in meters of the PD_F0.64 scenarios during hurricane Irene-2011 at NSN base, the US.

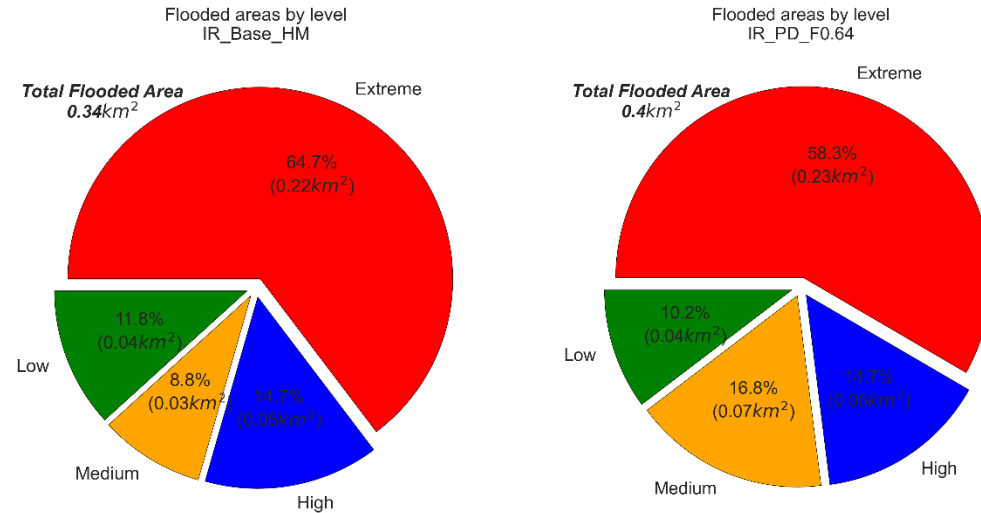


Figure 69. Pie chart of the flood areas, with percentages, of the different flood levels for the baseline (left panel) and PD_F0.64 (right panel) scenarios for Hurricane Irene-2011 at NSN, the US.

II. Radius of Maximum Wind

Three scenarios were considered for the radius of the maximum wind of the hurricane. Reducing the radius by 10%, increasing it by 10% and 25%. Following the same analysis procedure, we evaluated the statistics and characteristics of the peak surge and its associated flood area at NSN.

Figure 70 shows the water level of the base and RMW_F1.25 scenarios for the four hurricanes. More figures are in [Appendix C](#). It can be shown that the impact of changing the radius of the maximum wind is minor for all hurricanes. No significant impact was reported for the peak surge for hurricanes Irene and Michael. While about 15% (+25 cm) and 10% (+10 cm) in the peak surge were detected for hurricanes Isabel and Sandy respectively. These changes in the peak surge reflected marginal changes in the surge duration through all levels where no change was detected for hurricanes Irene and Michael and a marginal change was detected (1-2 hours) for hurricanes Isabel and Sandy, Figure 71 and Table 23. However, it is worth mentioning that increasing the radius of the maximum wind affected the water level around the peak surge. The impact on Hurricane Irene might be more visible compared to the rest of the hurricanes due to the proximity of Sewells Point to the hurricane center.

The same situation was observed for the flood area characteristics. Figure 72 and Table 24 show the characteristics of the flood areas for all hurricanes for the base and the RMW_F1.25 scenarios. It can be shown that the changes in the flood areas are marginal with a maximum flood area less than 3% of NSN area, which might be much lower than this value considering the conditions mentioned in the section 6.2.1. This is also evident in Figure 73, where it can be noticed that the flood areas are insignificant and very comparable to the base situation. Classification of the flood area into the four flood levels reveals no additional valuable information since the changes over the base scenarios are very limited. Investigating the RMW_F0.9 and RMW_F1.1, [appendix C](#) shows even less changes over the base scenarios for all hurricanes.

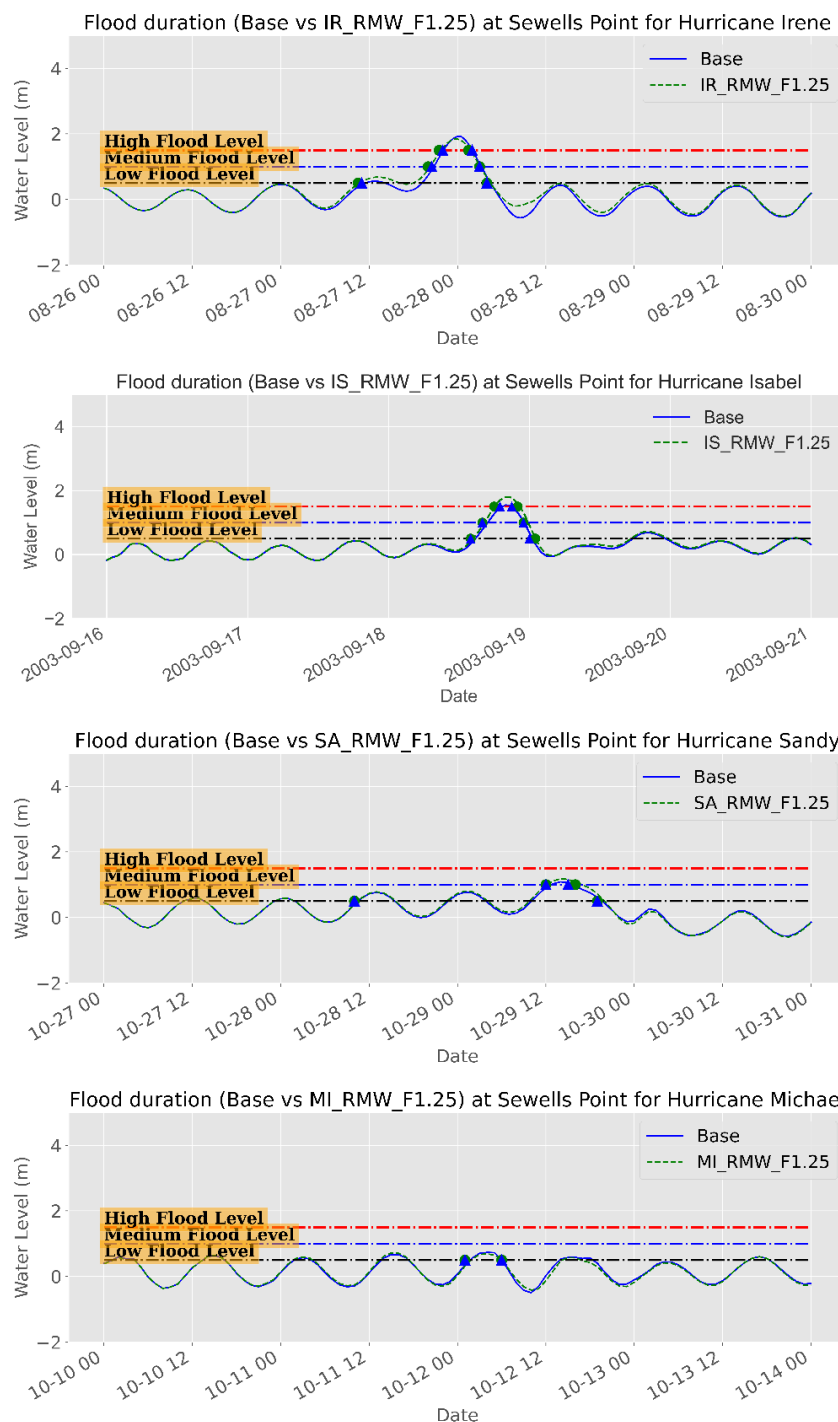


Figure 70. Water level time series (m) during the different hurricanes showing the surge magnitude and duration for different surge levels for the base and RMW_F1.25 scenarios at Sewells Point, NSN, the US.

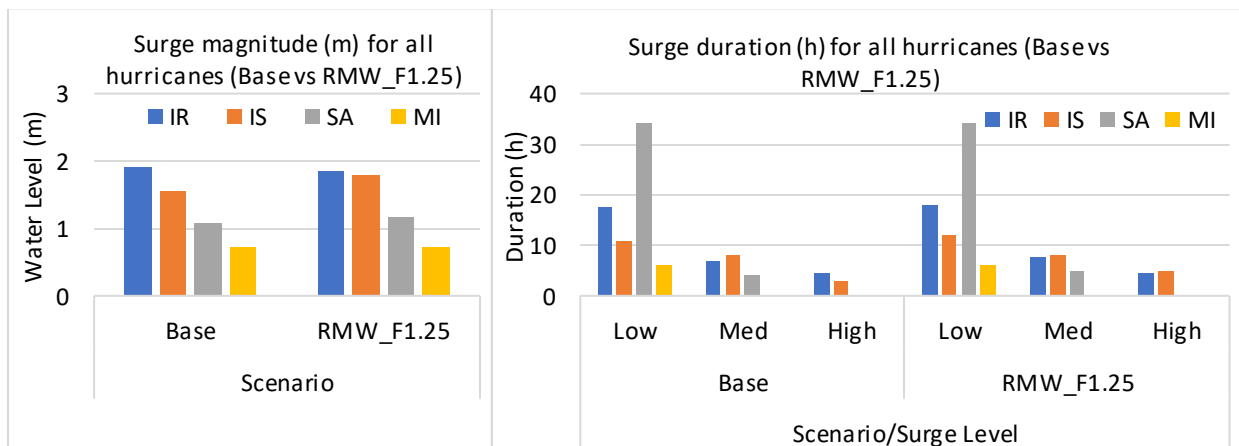


Figure 71. Peak surge (m) (left panel) and surge duration (h) of the different surge levels (right panel) for the base and RMW_F1.25 scenario for all hurricanes, NSN, the US.

Table 23. Peak surge characteristics (Maximum and Duration) of the base and RMW_F1.25 scenarios for all Hurricanes at Sewells Point, NSN, the US.

Group	Hurricane ID	Max. Surge (m)		Duration (h)					
		Base	RMW_F1.25	Base			RMW_F1.25		
				Low	Med	High	Low	Med	High
Meteo. Forcing	IR	1.92	1.84	17.5	7	4.5	18	7.5	4.5
	IS	1.55	1.8	11	8	3	12	8	5
	SA	1.08	1.18	34	4	0	34	5	0
	MI	0.73	0.71	6	0	0	6	0	0

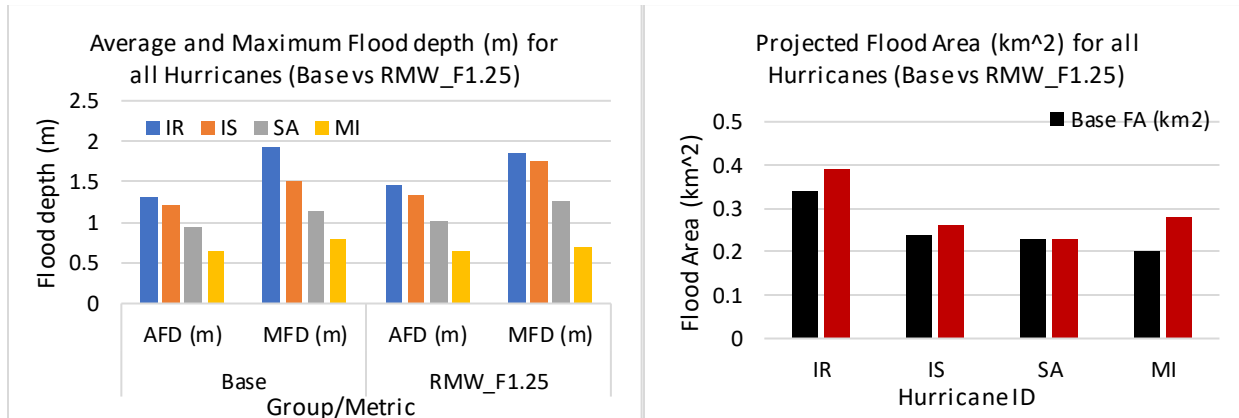


Figure 72. Average Flood Depth (AFD) & Maximum Flood Depth (MFD) in meters (left panel) and Flood area (km²) (right panel) of all hurricanes for the Base and RMW_F1.25 scenarios, NSN, the US.

Table 24. Flood area characteristics of the base and RMW_F1.25 scenarios for all hurricanes at NSN, the US.

Group	Hurricane ID	Base				RMW_F1.25			
		Average FD (m)	Max FD (m)	Flood area (km ²)	%	Average FD (m)	Max FD (m)	Flood area (km ²)	%
Meteo. Forcing	IR	1.31	1.94	0.34	2.47	1.46	1.86	0.39	2.8
	IS	1.21	1.52	0.24	1.72	1.33	1.77	0.26	1.9
	SA	0.94	1.14	0.23	1.6	1.02	1.27	0.23	1.7
	MI	0.66	0.79	0.2	1.45	0.65	0.69	0.28	2.0

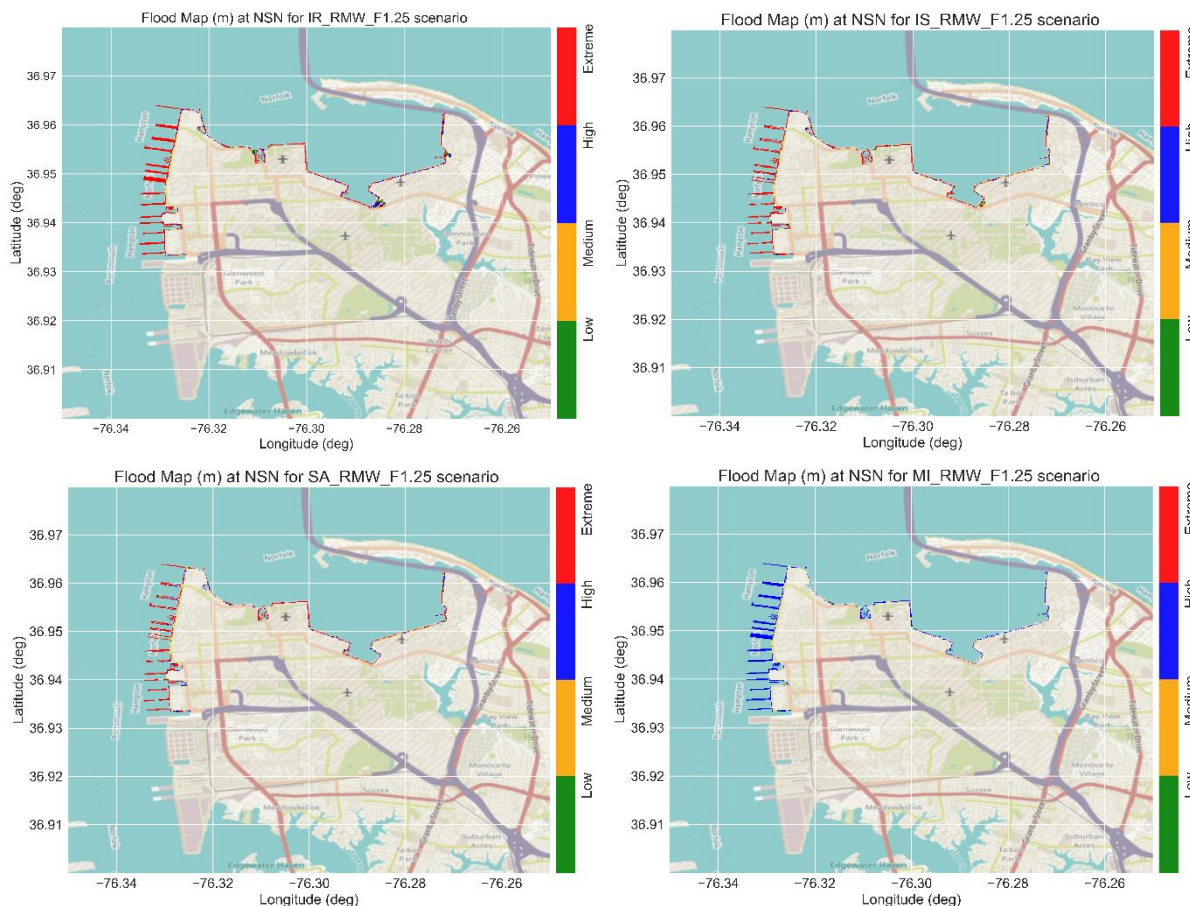


Figure 73. Flood maps with the flood levels for the different hurricanes during the peak surge for the RMW_F1.25 scenario at NSN, the US.

6.2.3. Impacts of Climate Changes

To evaluate the impact of climate change on the coastal flooding at NSN, two scenario groups were considered, the impact of Sea level Rise (SLR) and varying the wind speed. Three scenarios were investigated for each group, SLR_0.4M, SLR_0.8M and SLR_1.3M for SLR group. These scenarios included the projected climate change-induced relative sea level rise (SLR) according to, (Sweet et al., 2022) for Intermediate-Low scenarios for the US East Coast: 0.4m, 0.8m, 1.3m, projected for years 2050, 2100 and 2150 respectively. In addition, the scenarios WSF_0.925, WSF_1.075 and WSF_1.225 were considered for the wind speed group. For more details about the considered scenarios, please refer to the Demonstration plan of this project.

I. Sea Level Rise (SLR)

Three scenarios were considered for SLR scenario group, SLR of 0.4m, 0.8m and 1.3m for years 2050, 2100 and 2150 respectively. Increasing the mean sea level will eventually enhance the peak surge magnitude and duration at all locations. This will clearly reflect on the potential flood areas.

Figure 74 shows the water level for the base and the SLR_1.3M for all hurricanes at Sewells Point. It can be observed that including a SLR of 1.3m enhanced the peak surge for all hurricanes with a maximum and minimum surge of 3.12m and 2.04m for Hurricanes Irene and Michael respectively. Although the increase in the peak surge is not linear with the increase of the mean sea level, the peak surge increased by 1.3m ± 0.1 for hurricanes Irene and Isabel. However, an almost exact increase of 1.3m was observed for hurricanes Sandy and Michael, which might be attributed to the low impact of these hurricanes at Sewells Point where most of the water level is tidal-driven. The water level increased beyond the low and medium surge level for all hurricanes except for Hurricane Irene where the 26h medium surge duration was detected. The high surge level duration increased significantly by 7-39 hours, Figure 75 and Table 25 with the maximum duration for Hurricane Sandy.

On the other hand, the flood area statistics, Figure 76 and Table 26, showed a significant increase in the flood area for all hurricanes under this scenario. The flood area increased from a maximum of 0.34 km² (<2.5% of the base area) up to 5.4 km² (39%) for Hurricane Irene. Lower flood areas were detected for hurricanes Isabel and Sandy (20% and 10.7 respectively) with minimum flood during Hurricane Michael (3.3%). In addition, although the average flood depth showed limited changes with no visible pattern, the maximum flood depth significantly increased for all hurricanes up to more than 3m.

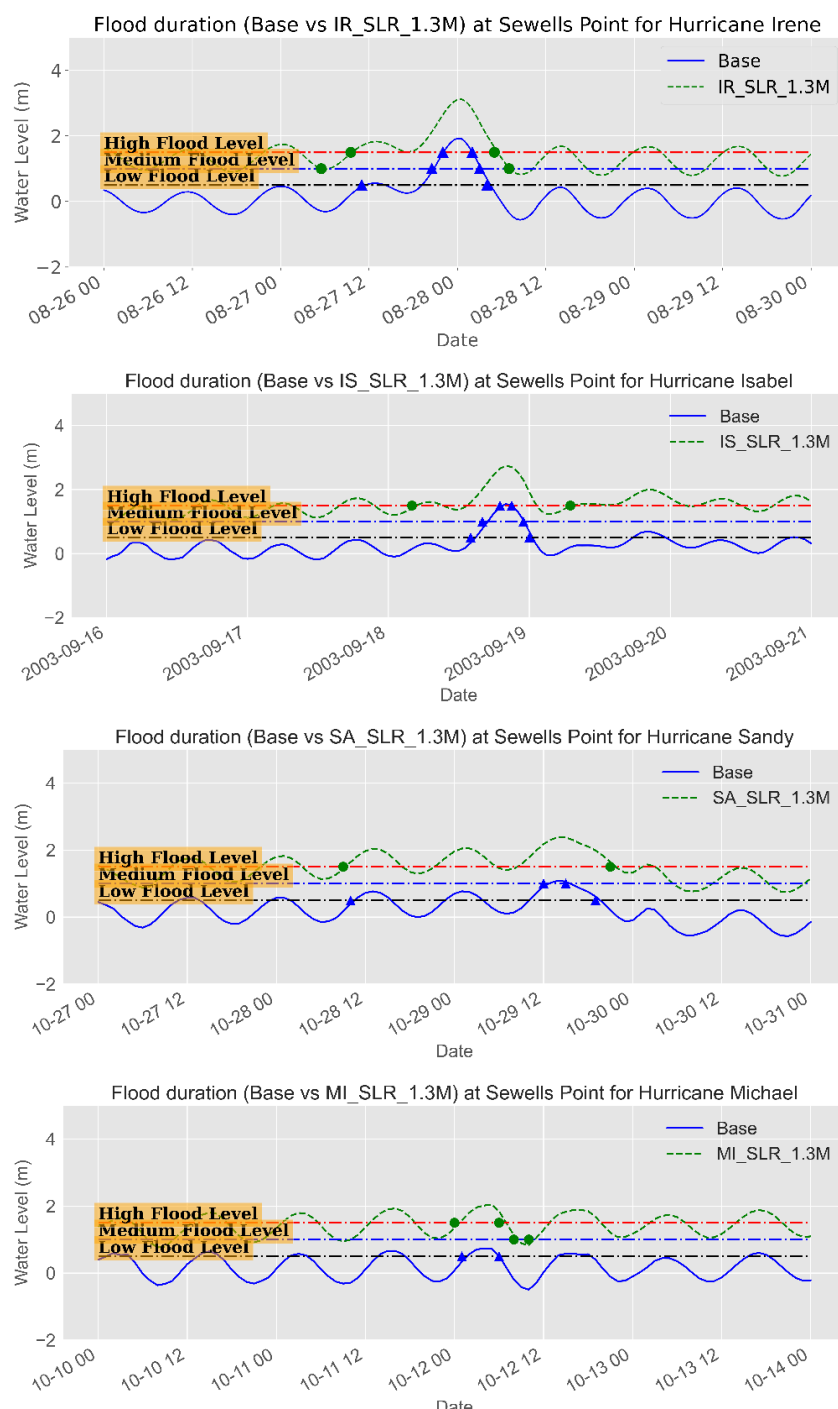


Figure 74. Water level time series (m) during the different hurricanes showing the surge magnitude and duration for different surge levels for the base and SLR_1.3M scenarios at Sewells Point, NSN, the US.

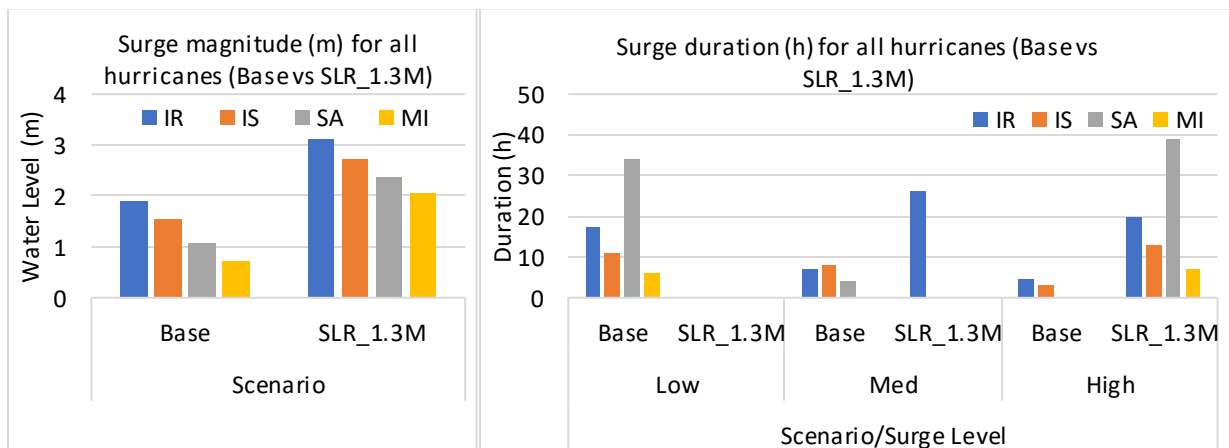


Figure 75. Peak surge (m) (left panel) and surge duration (h) of the different surge levels (right panel) for the base and SLR_1.3M scenario for all hurricanes, NSN, the US.

Table 25. Peak surge characteristics (Maximum and Duration) of the base and SLR_1.3M scenarios for all Hurricanes at Sewells Point, NSN, the US.

Group	Hurricane ID	Max. Surge (m)		Duration (h)					
		Base	SLR_1.3M	Low		Med		High	
				Base	SLR_1.3M	Base	SLR_1.3M	Base	SLR_1.3M
CC*	IR	1.92	3.12	17.5	--	7	26	4.5	20
	IS	1.55	2.74	11	--	8	--	3	13
	SA	1.08	2.38	34	--	4	--	0	39
	MI	0.73	2.04	6	--	0	--	0	7

*Climate Change

--the water level is above this level

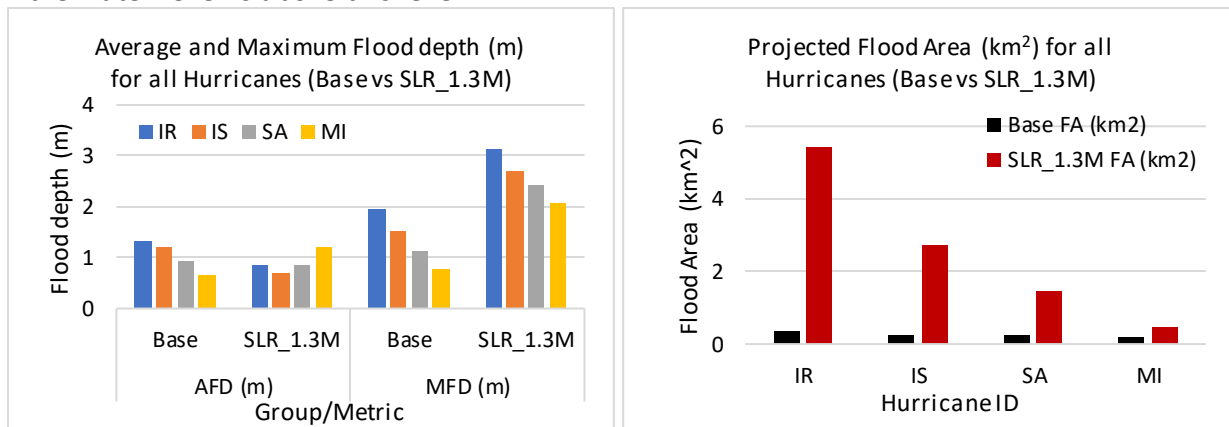


Figure 76. Average Flood Depth (AFD) & Maximum Flood Depth (MFD) in meters (left panel) and Flood area (km²) (right panel) of all hurricanes for the Base and SLR_1.3M scenarios at NSN, the US.

Table 26. Flood area characteristics of the base and SLR_1.3M scenarios for all hurricanes at NSN, the US.

Group	Hurricane ID	Base				SLR_1.3M			
		Average FD (m)	Max FD (m)	Flood area (km ²)	%	Average FD (m)	Max FD (m)	Flood area (km ²)	%
CC	IR	1.31	1.94	0.34	2.47	0.86	3.12	5.41	39.3
	IS	1.21	1.52	0.24	1.72	0.69	2.72	2.74	19.9
	SA	0.94	1.14	0.23	1.6	0.87	2.42	1.47	10.7
	MI	0.66	0.79	0.2	1.45	1.2	2.07	0.45	3.3

The increase in the flood magnitude and duration, especially of the high flood level, also increased the duration of ground flooding. Figure 77 shows the time series of the average and maximum flood depth in meters in addition to the flood area (km²) for all hurricanes for a few hours before and after the peak surge/flood. It can be shown that the flood areas are stable below 0.5 km² till the peak surge where the flood areas increase drastically along with the maximum flood depth. However, even after hours of the peak flood, the flood area and the maximum flood maintain significant values. For instance, observing Hurricane Irene, Figure 77 upper panel, the flood areas remained relatively constant below 0.5 km² till August 27th at 20:00, which is 4 hours before the peak surge, where the flood area increased up to 5.4 km² and then started to decline again. However, the flood areas did not decline down to 0.5 km², but to about 2 km², which means that these areas will be flooded for hours (maybe days) after the peak flood occurs with an average and a maximum water depth of about 0.5 m and 2.5 m respectively.

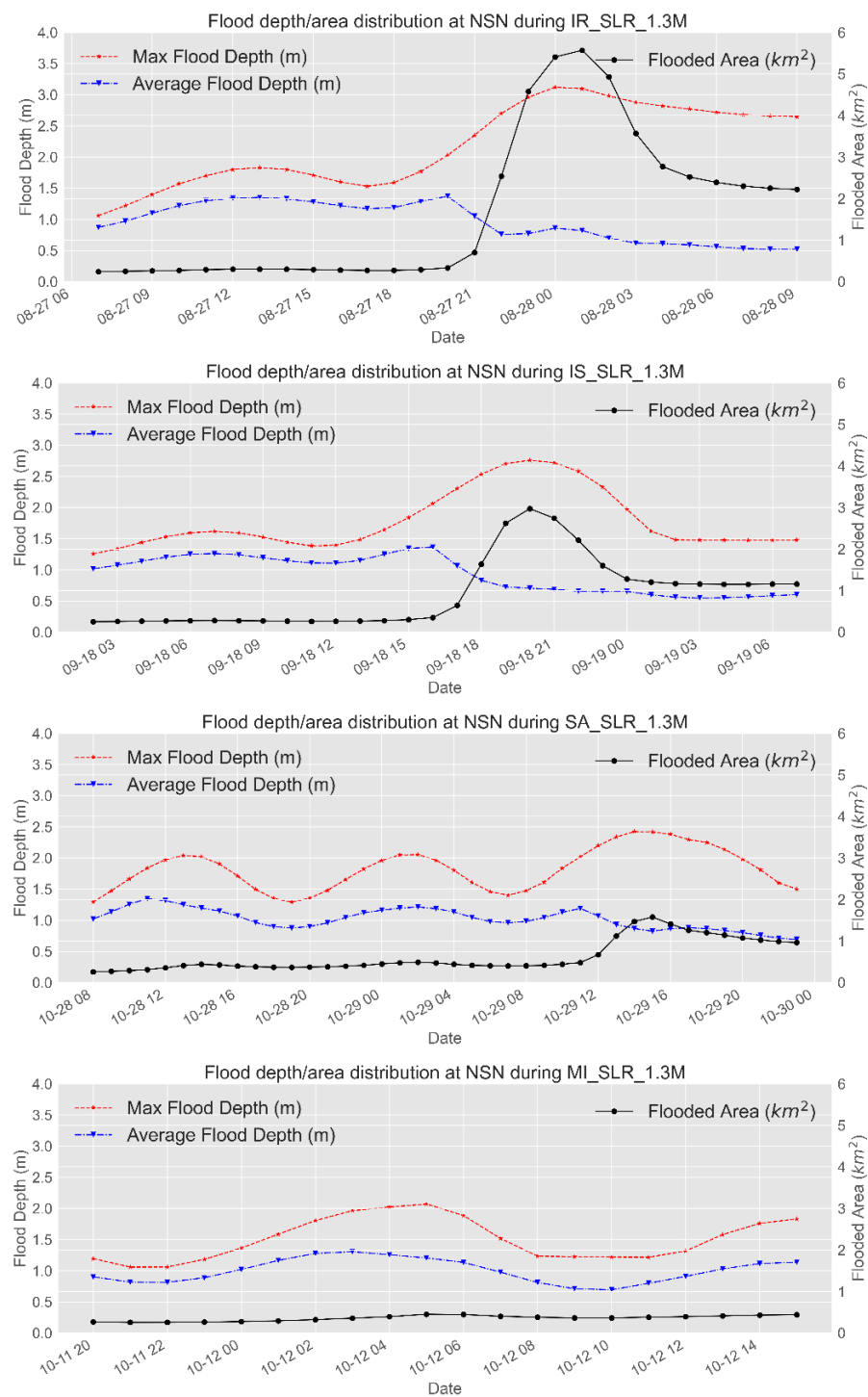


Figure 77. Time series of the projected average and maximum flood depth (left axis) and flood area (km²-right axis) for all hurricanes for SLR_1.3M scenario at NSN, the US.

Investigating the spatial extent of the flood areas revealed that the north and west parts of the base are the most vulnerable areas to flooding, Figure 78. These areas have different flood levels with the extreme flood level (red color) concentrated at two spots. These spots are the vegetation area (golf courses) and the residential area at the northeast with low elevation. Figure 79 shows an example of the classification of the flood areas into the four flood levels for Hurricane Irene during the SLR_1.3m scenario. It can be noticed that most of the flood area lies under the high to extreme flood level (>0.5m above ground level), Figure 80, with most of the extreme level concentrated at the low-elevation green areas.

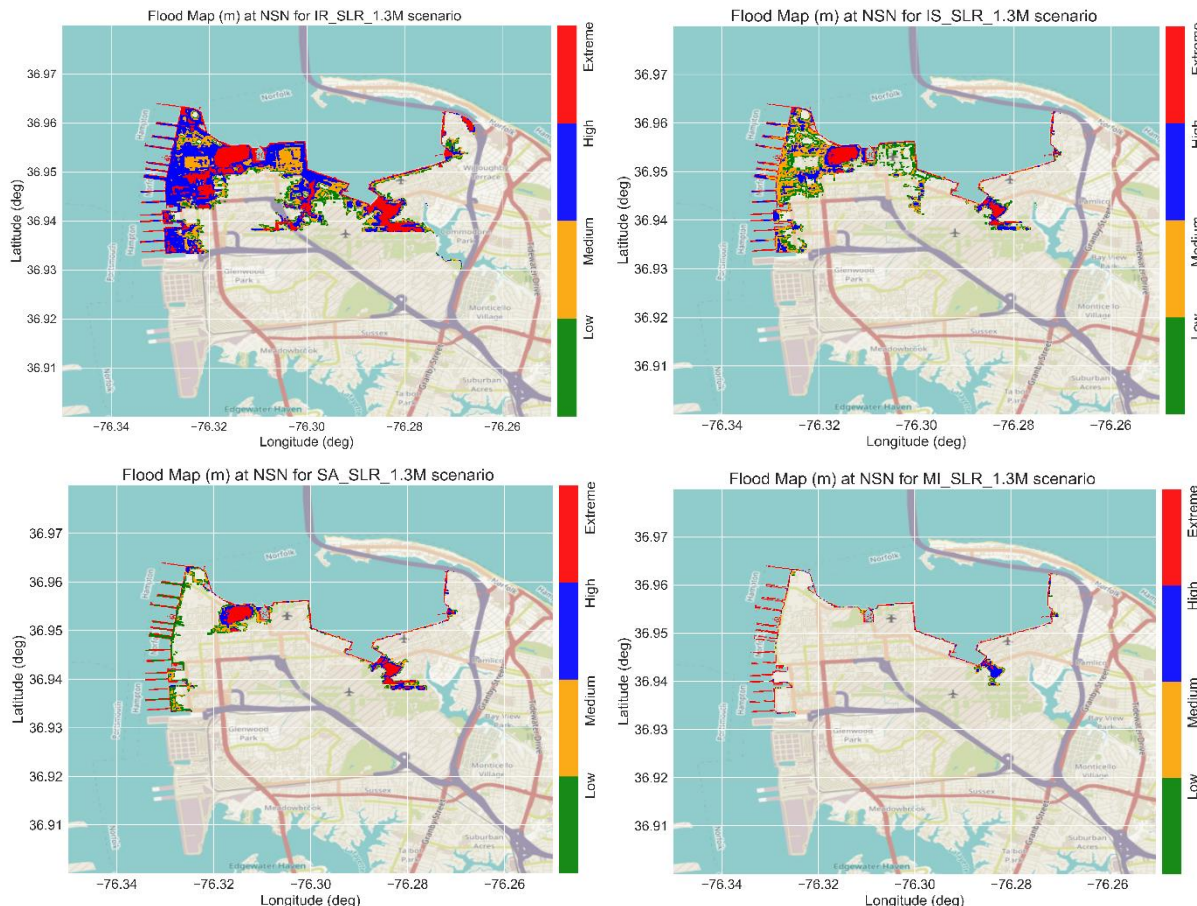


Figure 78. Flood maps with the flood levels for the different hurricanes during the peak surge for the SLR_1.3M scenario at NSN, the US.

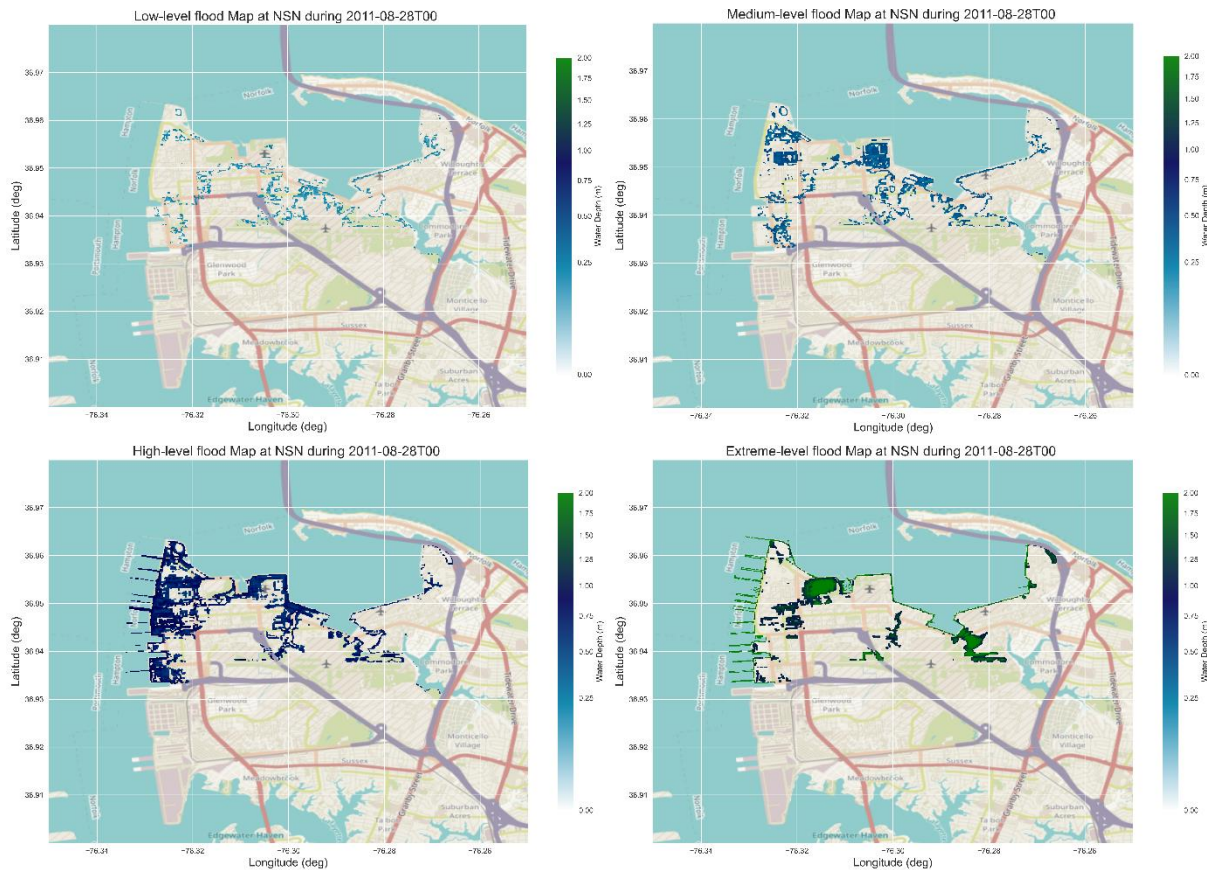


Figure 79. Flood area classified by level (Low, Medium, High, and Extreme) in meters for the SLR_1.3M scenario during hurricane Irene-2011 at NSN base, the US.

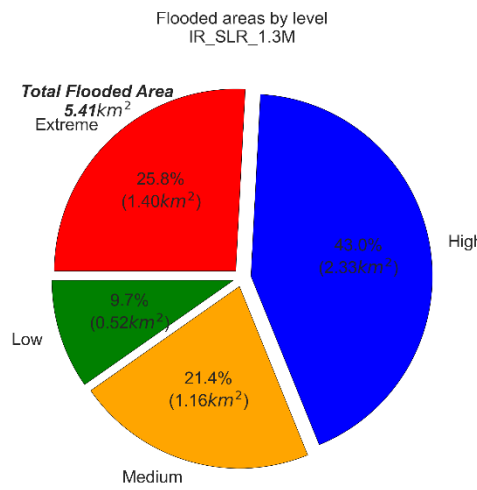


Figure 80. Pie chart of the flood areas, with percentages, of the different flood levels for SLR_1.3M scenario for Hurricane Irene-2011 at NSN, the US.

Considering the SLR_0.4M scenario, the surge magnitude increased by the magnitude of the SLR (0.4m) for all hurricanes with a pronounced increase for Hurricane Michael of about 0.54m. This increase reflects an increase in the surge duration especially for the low surge level with a minor impact on the medium and high levels. The flood area characteristics show some increase in the average and maximum flood depth for all hurricanes with the most pronounced increase during Hurricane Michael. However, this increase did not reflect a significant rise in the spatial extent of the flood area where a significant increase in flood area was detected for Hurricane Irene, 0.9km² (6.5%), with an insignificant increase for all other hurricanes. The most affected areas, with the maximum flood depth, are also located in vegetation areas, see [Appendix C](#).

A similar pattern was detected for SLR_0.8M but with a higher magnitude. A significant increase in surge magnitude and duration was detected for all hurricanes. The high surge level shows a prominent change over the previous scenario where Hurricanes Sandy and Michael showed 8h and 3h high-surge duration respectively compared to zero for the base scenarios. This pattern reflected a significant increase in the average and maximum flood depth but with limited influence on the spatial extent of the flood areas with a maximum change of less than 1%. Although Hurricane Irene showed a decrease in the average flood depth, it showed a significant increase in the flood area from 0.34km² (2.5%) for the base scenario to 2.94km² (21.4%) followed by Hurricane Isabel at 0.72 km² (5.2%). Most of the flood areas are located along the vegetation areas and the western part of the base, see [Appendix C](#).

II. Increasing Wind Speed

Climate change can have a significant impact on enhancing the severity of the hurricane by increasing the intensity of the wind speed. Increasing the hurricane wind speed will eventually enhance the peak surge magnitude and duration which will reflect on the potential flood areas. In the current study, we will consider three scenarios for wind speed change, decreasing the wind speed by 7.5% (WSF_0.925), increasing the wind speed by 7.5% (WSF_1.075), and enhancing the wind speed by 22.5% (WSF_1.225).

Figure 81 shows the water level for the base and the WSF_1.225 for all hurricanes at Sewells Point. It can be observed that enhancing the wind speed resulted in a higher peak surge but not for all hurricanes. Hurricane Irene is the most affected one followed by hurricanes Isabel and Sandy with an almost insignificant impact on Hurricane Michael.

We should note that we are only evaluating the impacts on the surge magnitude at Sewells Point due to its proximity to NSN. However, different results might be obtained at different stations, particularly stations closer to the hurricane's tracks. For instance, a higher impact of enhancing the wind speed is obtained at Duck for Hurricane Isabel or at Delaware Bay for Hurricane Sandy with an increase in surge magnitude of about 0.71m and 0.77m respectively, Figure 82.

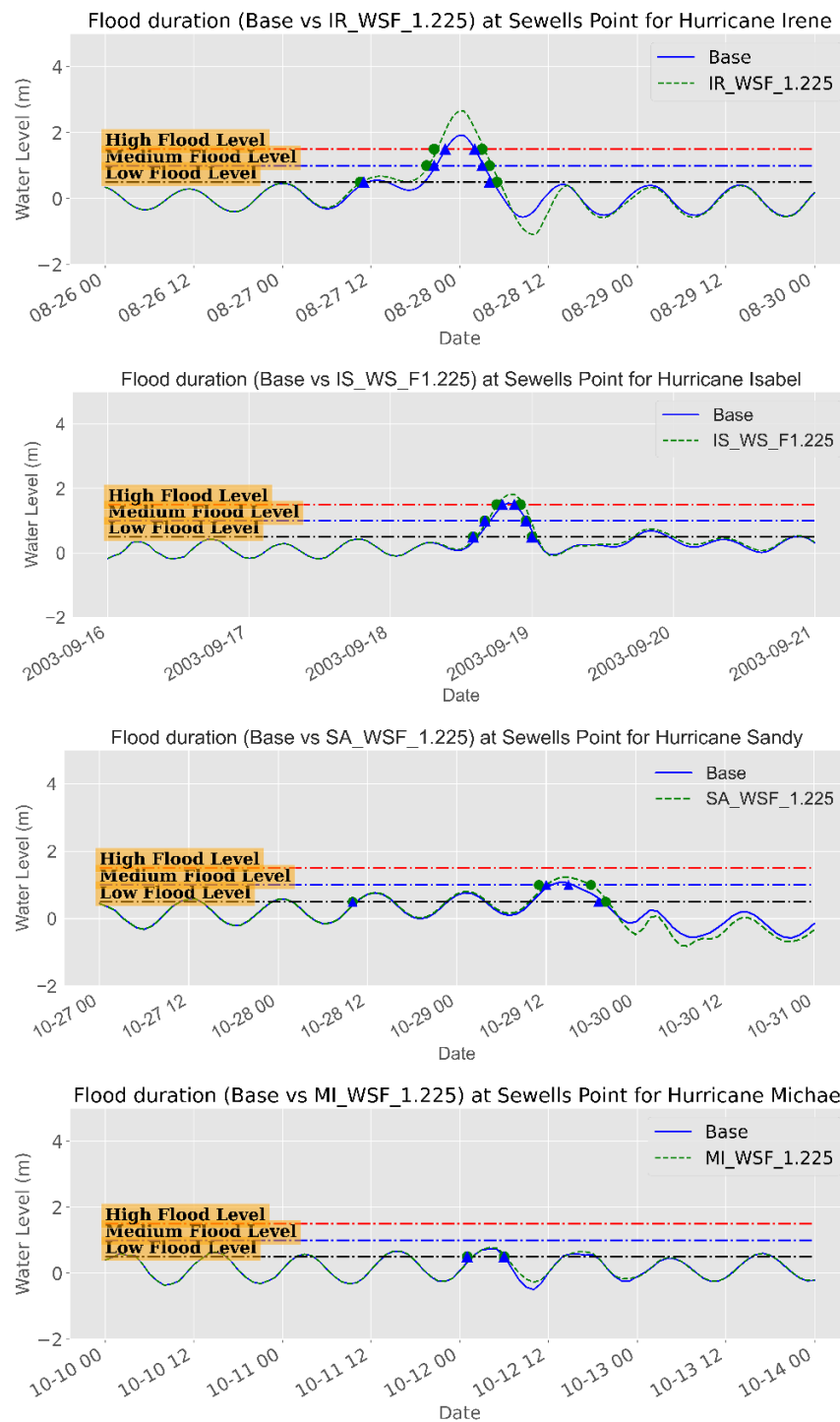


Figure 81. Water level time series (m) during the different hurricanes showing the surge magnitude and duration for different surge levels for the base and WSF_1.225 scenarios at Sewells Point, NSN, the US.

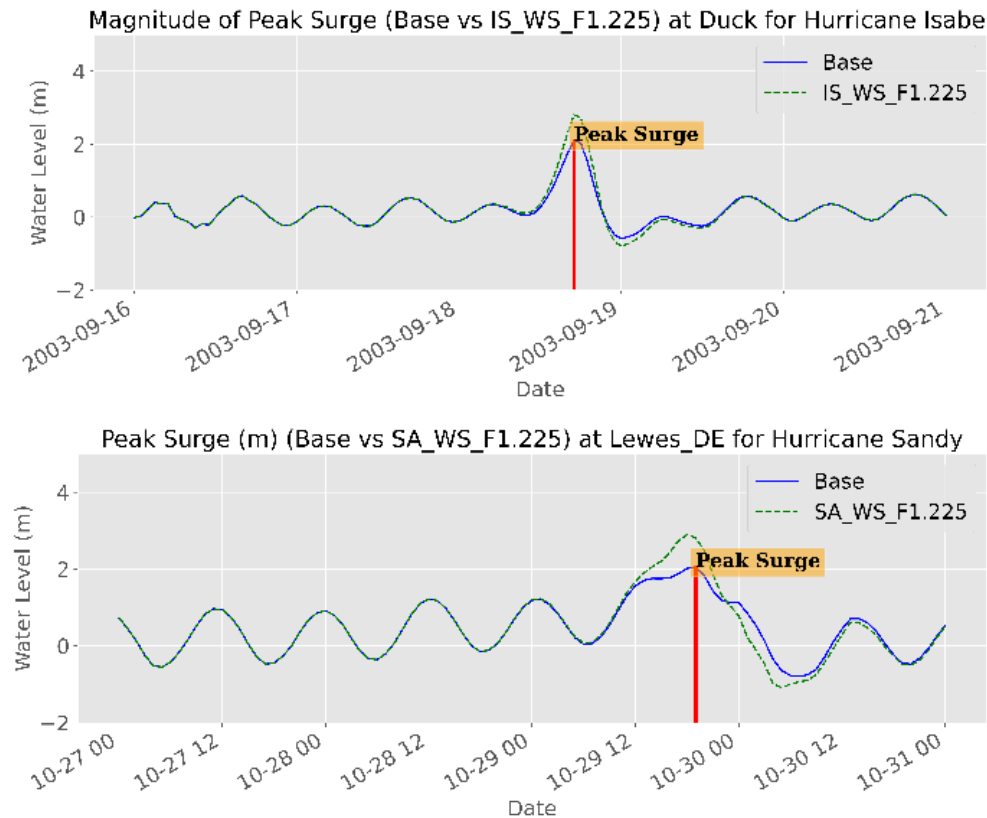


Figure 82. Water level (m) showing the surge magnitude for the base and WSF_1.225 scenarios during Hurricane Isable (left panel) and Hurricane Sandy (right panel) at Duck and Lewes, DE locations respectively.

A maximum surge of 2.66m and 1.82m (1.92m and 1.55m for the base) were observed for hurricanes Irene and Isabel respectively, with a minor increase of 0.15m in surge magnitude for Hurricane Sandy, Figure 83 and Table 27. For the surge duration, limited impact was observed in flood duration for the low surge level. A significant impact was observed for the medium surge level for Hurricane Sandy with an increase of about 4 hours. The high surge level also increased by 2-2.5 hours for hurricanes Irene and Isabel.

On the other hand, the flood area statistics, Figure 84 and Table 28, showed an insignificant increase in the flood area for all hurricanes under this scenario with the exception of Hurricane Irene where the flood areas increased up to 3.15 km² (23%) of NSN area compared to 0.34 km² (2.5%) for the base simulation. In addition, although the average flood depth decreased down to 0.7m, the maximum flood depth significantly increased up to 2.7m. Furthermore, although minor changes in the flood areas were detected for hurricanes Isabel and Sandy, the average and maximum flood depth have significantly increased for both hurricanes. An increase of about

0.12m-0.16m in the average flood depth and an increase of about 0.2m-0.35m in the maximum flood depth were detected for these hurricanes.

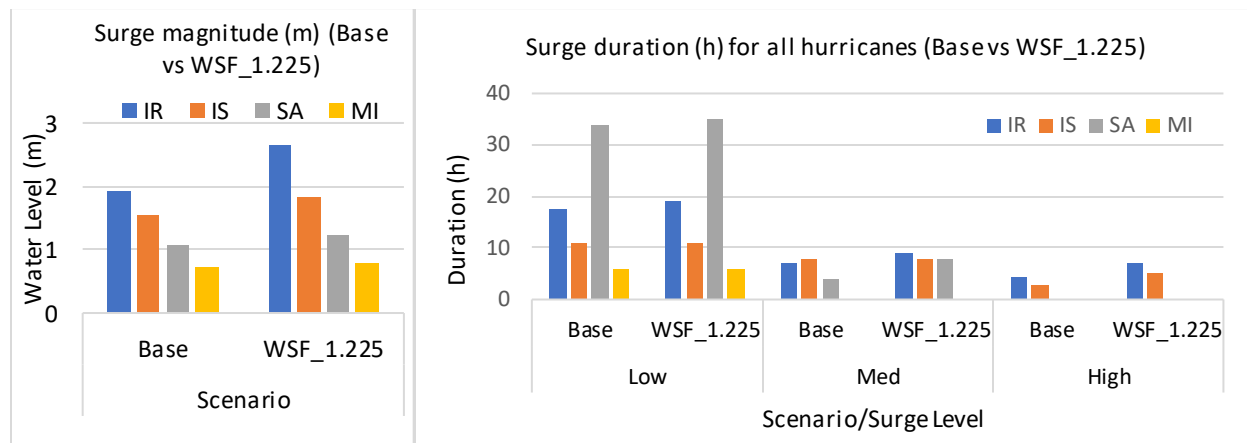


Figure 83. Peak surge (m) (left panel) and surge duration (h) of the different surge levels (right panel) for the base and WSF_1.225 scenario for all hurricanes, NSN, the US.

Table 27. Peak surge characteristics (Maximum and Duration) of the base and WSF_1.225 scenarios for all Hurricanes at Sewells Point, NSN, the US.

Group	Hurricane ID	Max. Surge (m)		Duration (h)					
		Base	WSF_1.225	Base			WSF_1.225		
				Low	Med	High	Low	Med	High
CC*	IR	1.92	2.66	17.5	7	4.5	19	9	7
	IS	1.55	1.82	11	8	3	11	8	5
	SA	1.08	1.23	34	4	0	35	8	--
	MI	0.73	0.78	6	0	0	6	--	--

*Climate Change

--the water level is above this level

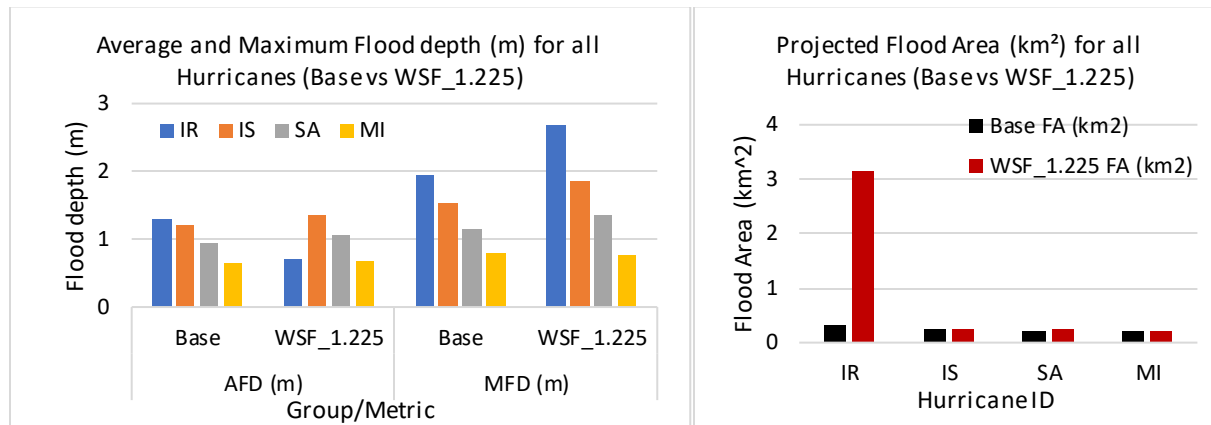


Figure 84. Average Flood Depth (AFD) & Maximum Flood Depth (MFD) in meters (left panel) and Flood area (km^2) (right panel) of all hurricanes for the Base and WSF_1.225 scenarios at NSN, the US.

Table 28. Flood area characteristics of the base and WSF_1.225 scenarios for all hurricanes at NSN, the US.

Group	Hurricane ID	Base				WSF_1.225			
		Average FD (m)	Max FD (m)	Flood area (km^2)	%	Average FD (m)	Max FD (m)	Flood area (km^2)	%
CC	IR	1.31	1.94	0.34	2.47	0.71	2.69	3.15	22.9
	IS	1.21	1.52	0.24	1.72	1.37	1.87	0.26	1.9
	SA	0.94	1.14	0.23	1.6	1.06	1.35	0.24	1.7
	MI	0.66	0.79	0.2	1.45	0.69	0.77	0.2	1.5

The limited increase in the flood magnitude and duration resulted in a limited increase in the duration of ground flooding for all hurricane except for Hurricane Irene where the flood maintained a significant value of 1 km^2 (7.25%) after hours of the peak surge time, Figure 85. These areas might potentially be flooded for hours (maybe days) after the peak flood occurs with an average and a maximum water depth of about 0.5 m and 2.2 m respectively.

Investigating the spatial extent of the flood areas revealed that no significant flood areas were detected for all hurricanes except for Hurricane Irene where significant part of the base were flooded, Figure 86. Considering Hurricane Irene, the golf course and the residential area at the northeast are the most affected areas under this scenario. Most of these areas lies mostly under the extreme flood ($>1 \text{ m}$) category, Figure 87. The high and extreme flood areas represent more than 43% of the total flood area under this scenario, Figure 88.

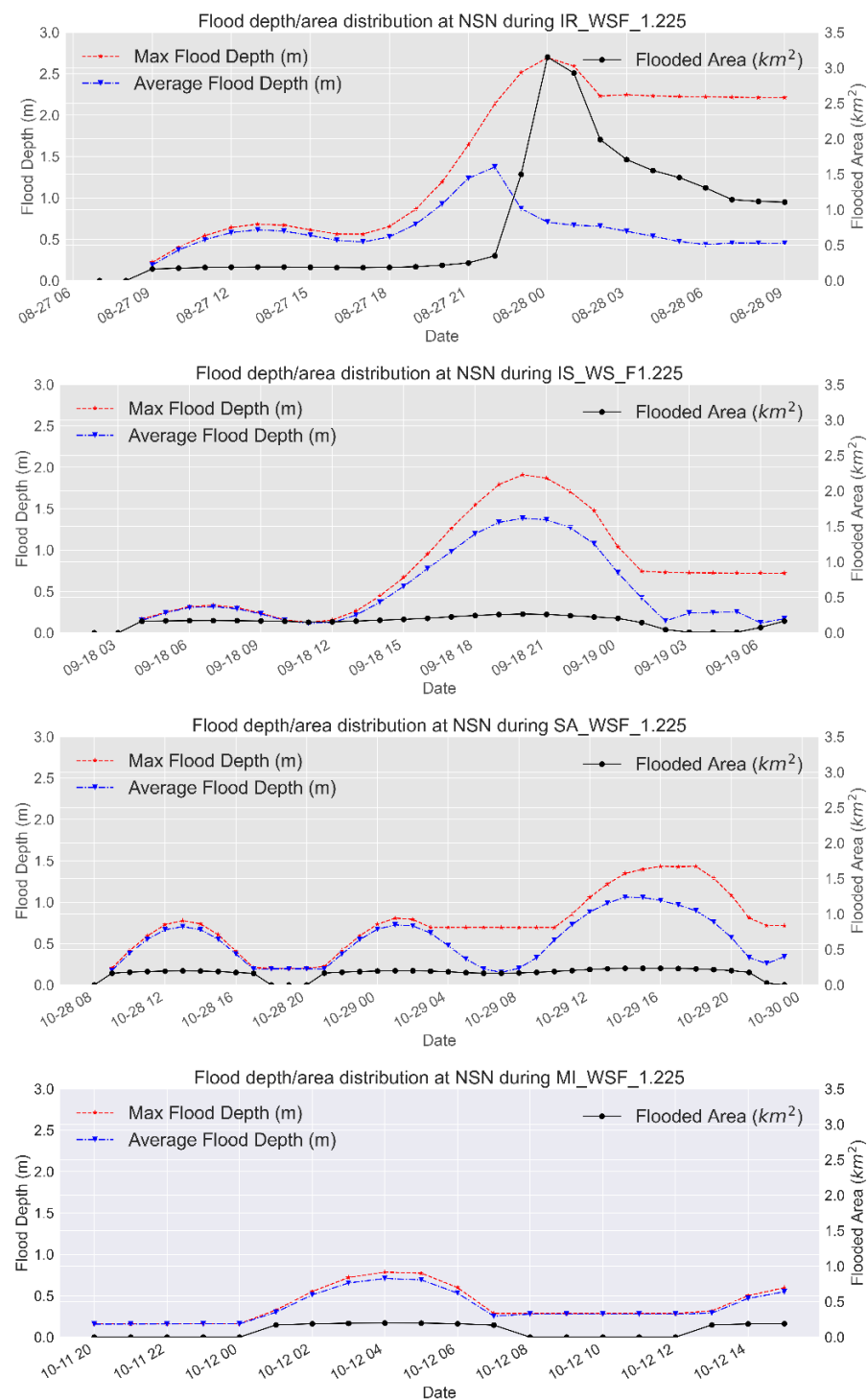


Figure 85. Time series of the projected average and maximum flood depth (left axis) and flood area (km^2 -right axis) for all hurricanes for WSF_1.225 scenario at NSN, the US.

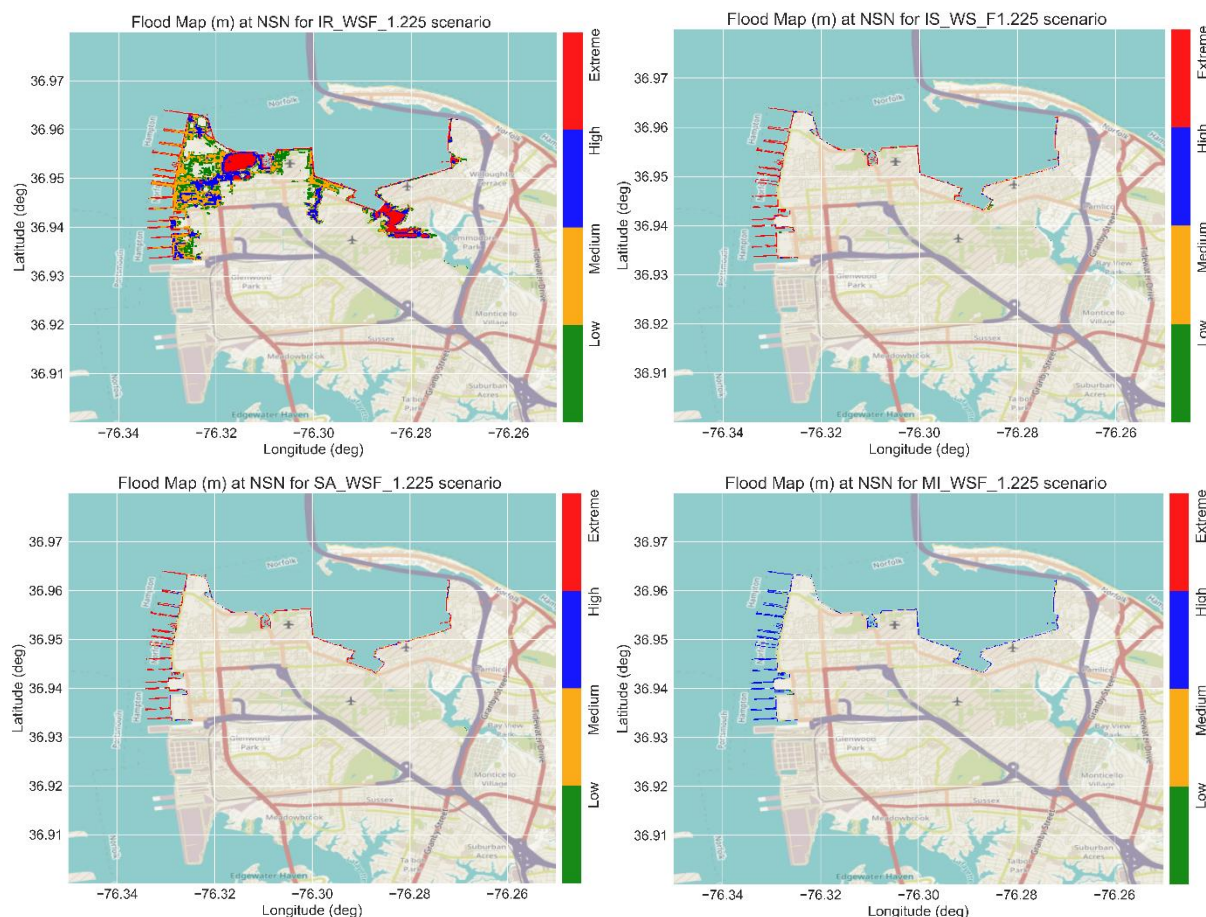


Figure 86. Flood maps with the flood levels for the different hurricanes during the peak surge for the WSF_1.225 scenario at NSN, the US.

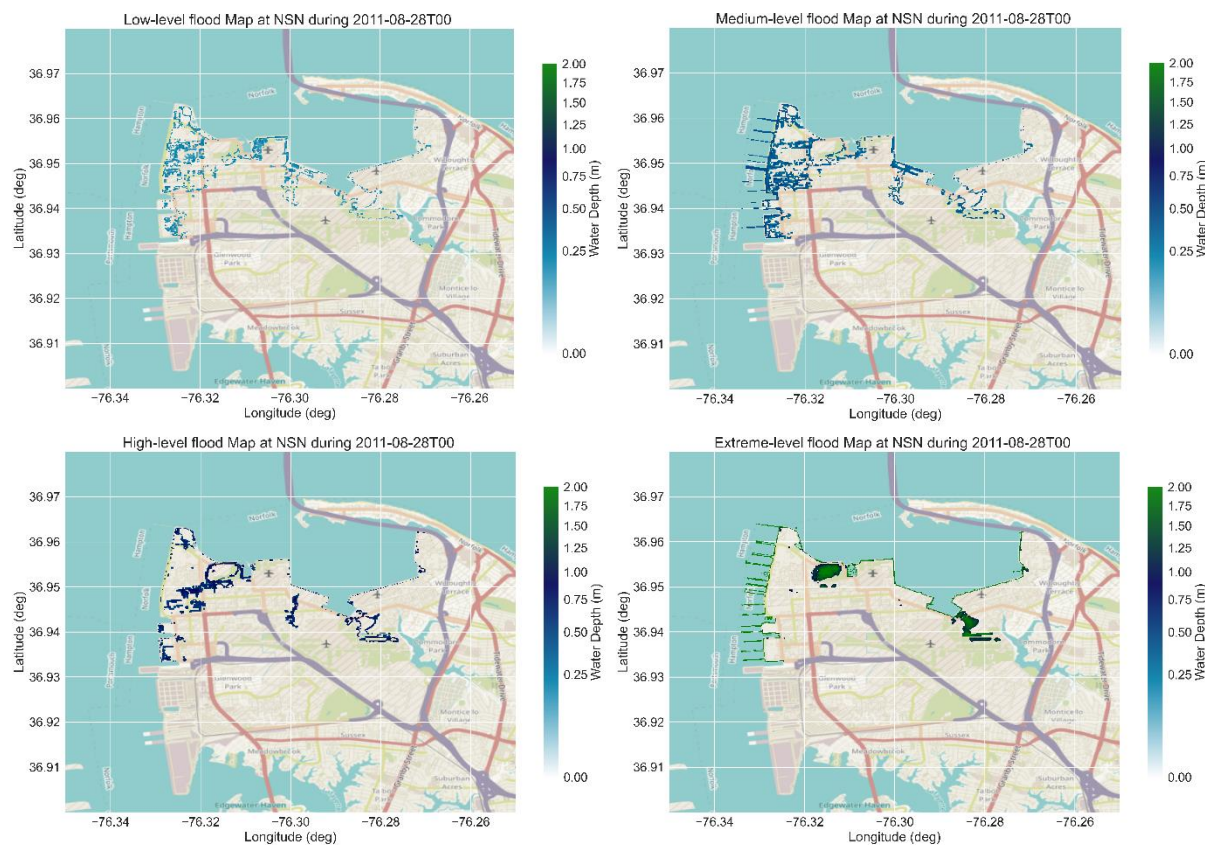


Figure 87. Flood area classified by level (Low, Medium, High, and Extreme) in meters for the WSF_1.225 scenario during hurricane Irene-2011 at NSN base, the US.

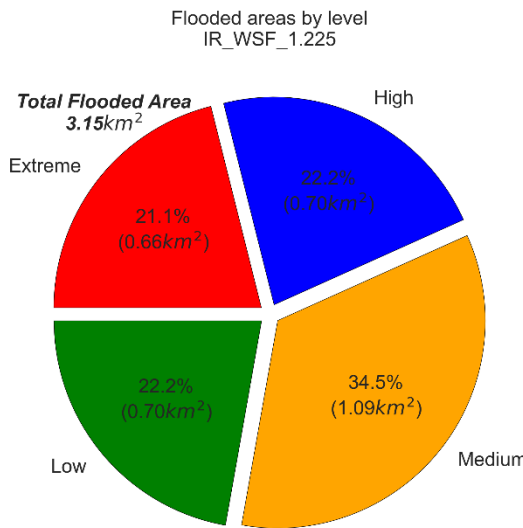


Figure 88. Pie chart of the flood areas, with percentages, of the different flood levels for WSF_1.225 scenario for Hurricane Irene-2011 at NSN, the US.

The impact of decreasing the wind speed by 7.5%, WSF_0.925 scenario, on the surge magnitude is almost insignificant for all hurricanes with a maximum decrease of about 0.11m for Hurricane Irene. This minor change reflects no significant change in the surge duration for all levels. The flood area characteristics show a marginal decrease (3-9 cm) in the average and maximum flood depth for all hurricanes. In addition, these minor changes in the surge characteristics did not reflect a significant change in the spatial extent of the flood area where a maximum decrease in the flood area was detected for Hurricane Irene, -0.04km² (< 0.3%), with an insignificant change for all other hurricanes, see [Appendix C](#).

A similar pattern was detected for WSF_1.075 but with a marginal increase in the surge and flood area characteristics. A limited increase in surge magnitude and duration was detected for hurricanes Irene and Isabel with no significant change for hurricanes Sandy and Michael. The maximum detected increase in surge magnitude was 25cm for Hurricane Irene followed by 11cm for Hurricane Isabel. These changes reflect a minor increase in the surge duration by about 0.5-1 hours. In addition, an increase in the maximum flood depth was also detected for hurricanes Irene and Isabel by about 25cm and 13cm respectively. However, a significant increase in the spatial extent of the flood area was detected for Hurricane Irene only, 0.59 km² (4.3%), with no significant increase for all other hurricanes. About half of this flood area has an extreme flood level with about 20% of it lying under the high flood level. Furthermore, most of the flood areas are located along the vegetation areas and the western part of the base, see [Appendix C](#).

6.2.4. Impacts of Lack of Data (Degradation scenarios)

The lack of accurate representative data has always been a challenge for coastal modelers. One of the most important parameters of hurricanes is the hurricane track. Inaccuracy in the track prediction can lead to underestimation of the hurricane's impact at one place with overestimation at the other. This can lead to catastrophic loss of human lives on one hand and cause significant loss in unnecessary evacuation on the other hand.

Bathymetric and topographic data are widely available from different sources with different resolutions and accuracies. Although some inaccuracies in the bathymetric data can have a minor impact on the total water level prediction, the absence of accurate topographic data can cause overestimation/underestimation of the predicted flood area and hence, affect the reliability of coastal flood predictions.

On the other hand, model resolution (mesh resolution) can significantly impact the model performance. Generally speaking, the model performance is proportional to the mesh resolution, especially for flood prediction simulations. However, with increasing the model resolution the computational timestep becomes significantly lower, to satisfy the corant criteria, which results in a significantly higher computational cost. Therefore, these aspects must be balanced to implement feasible simulations.

The model performance in predicting the water level and the associated flood areas was evaluated under controlled perturbations in the hurricane track, bathymetric accuracy, and bathymetry/mesh resolution. Six scenarios were considered for changing the hurricane track by shifting the original track to the east and the west by 54nm, 96nm, and 138nm for all hurricanes. In addition, three scenarios were studied for bathymetric accuracy by adding a Gaussian noise of 0.3m, 0.5m, and 1.0m to the original bathymetry/topography data. Furthermore, four scenarios were considered to evaluate the sensitivity of the model to the mesh resolution by decreasing the resolution by factor 5, 16, 33, and 66. These factors correspond to a maximum resolution of about 75m, 250m, 500m, and 1000m.

I. Storm Track Shift (Error in Storm Track Prediction)

We will consider six storm track shifts under this scenario group. Three shifts to the east and the west of the original hurricane track by 54nm, 96nm, and 138nm. In addition, we may also shift the track by an angle depending on the original track (angle of approach to the coast). Since each hurricane has its distinctive characteristics, the results of the track shift will be presented for each hurricane separately.

Figure 89 shows the water level for the base and the storm track shift scenarios for Hurricane Irene at Sewells Point. It can be observed that changing the storm track can have a significant impact on the peak surge magnitude and hence the duration of all surge levels. Specifically speaking, shifting the track of Hurricane Irene to the west (left panels of Figure 89) resulted in a drastic decrease in the peak surge. The peak surge diminishes below the low surge level after shifting the track by 96nm to the west. The track of Hurricane Irene can be considered a coast-parallel track, *Figure 90*, which means that shifting the track to the west means that a significant part of the hurricane will be on land resulting in a lower influence of the hurricane on the water level. In addition, a negative surge down to -2 m was observed when shifting the track by 96nm and 138nm to the west where the offshore wind became the more dominant water level driving force. Shifting the track to the east (right panels of Figure 89) also resulted in a declining water level. Although the east shift will move the hurricane further to the ocean, the influence of the hurricane becomes weaker at Sewells Point as the point is now located further away from the hurricane's eye at weaker winds. Nevertheless, the east shift scenarios have higher surge values when compared to the west shift scenarios. A minimum peak surge of 0.71m was observed for the IR_STE_138nm scenario compared to 0.34m for the IR_STW_138nm scenario (1.92m for the baseline scenario). A similar pattern was observed for the surge duration for all levels, *Figure 91* and **Table 29**. No high surge level was detected for all scenarios (zero duration). The medium surge level was detected only for the 54nm scenarios for both directions but with a 30% decrease in the surge duration.

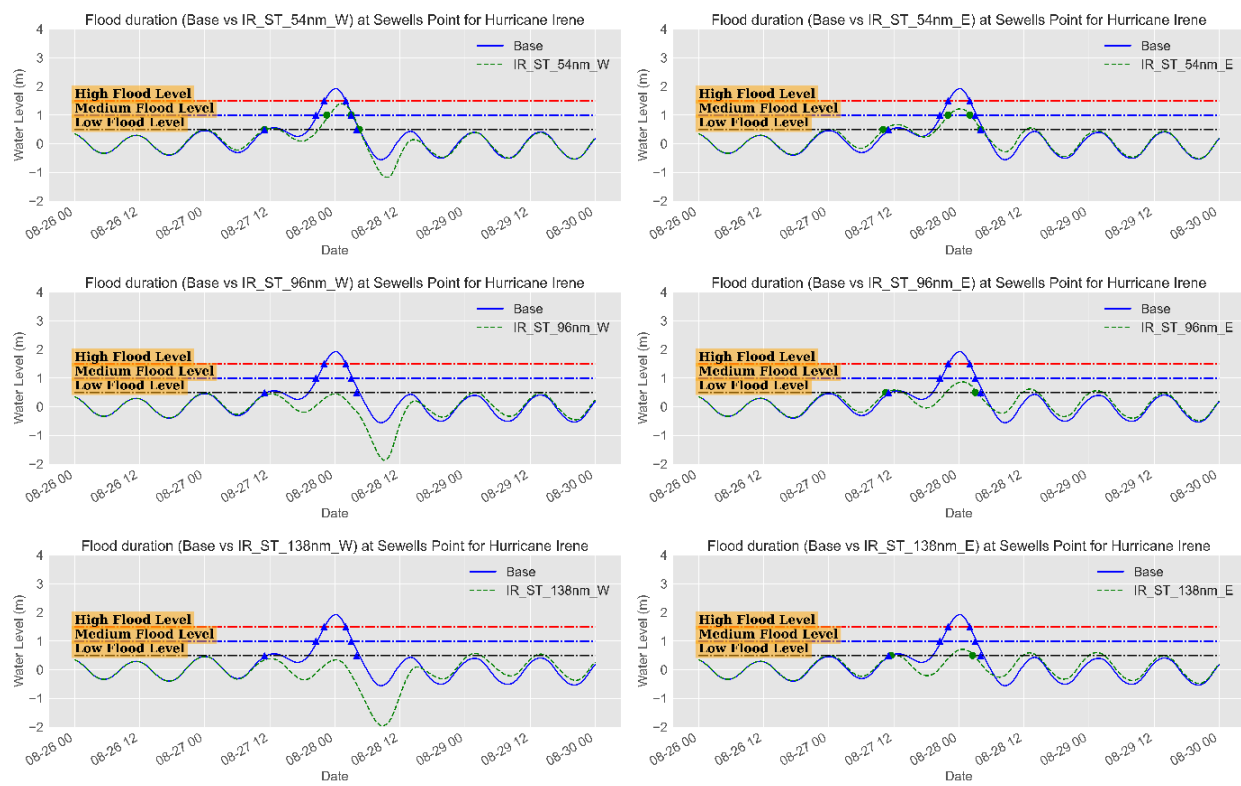


Figure 89. Water level time series (m) during Hurricane Irene showing the surge magnitude and duration for different surge levels for the base and Storm Track Shift scenarios at Sewells Point, NSN, the US.

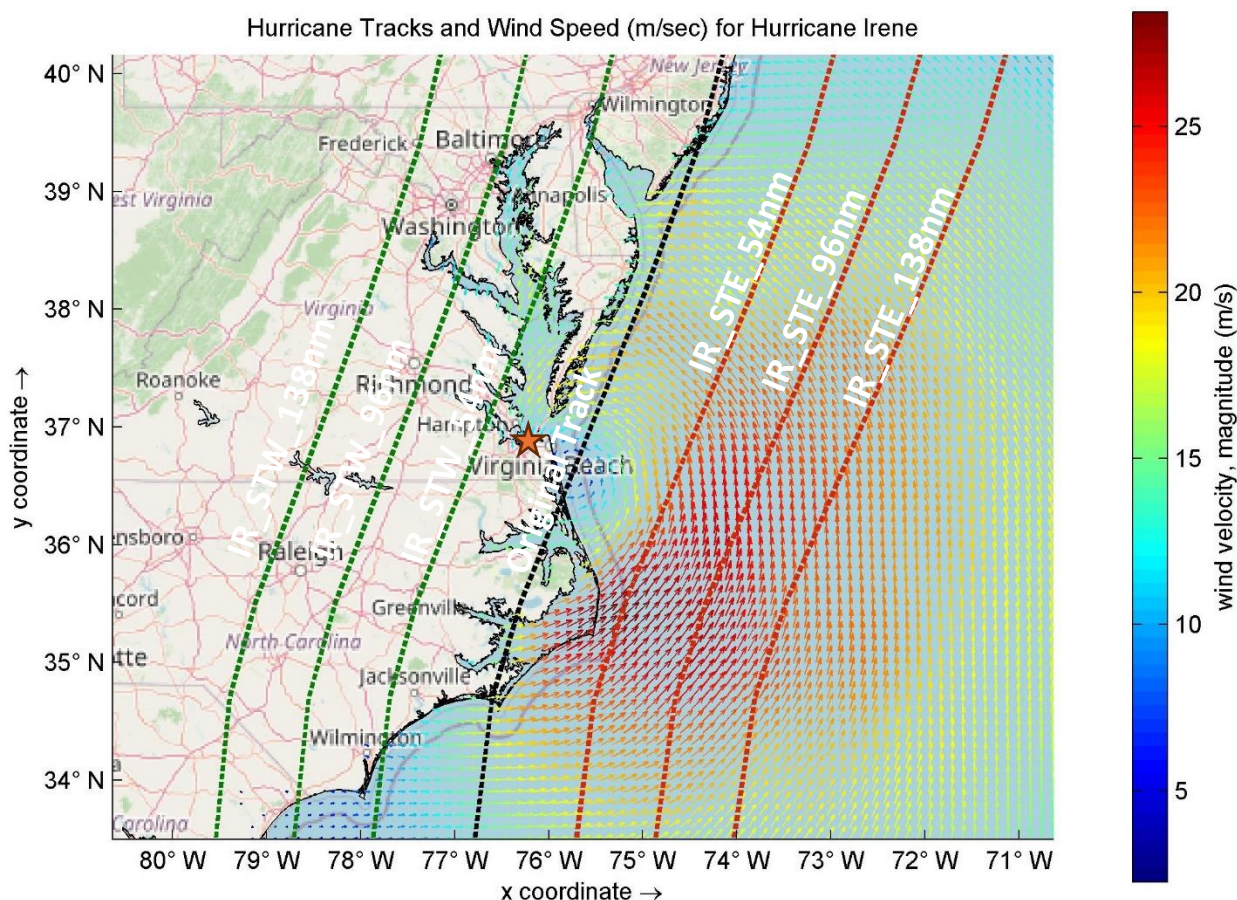


Figure 90. Different hurricane tracks and the wind speed (m/sec) for Hurricane Irene-2011. The orange star is NSN.

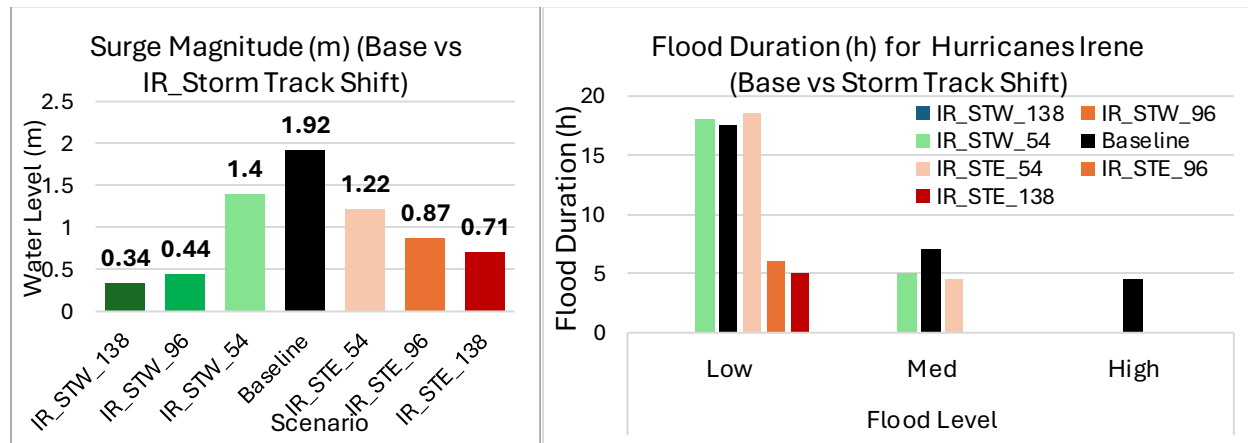


Figure 91. Peak surge (m) (left panel) and surge duration (h) of the different surge levels (right panel) for the base and the storm track shift scenarios for Hurricane Irene at NSN, the US. West shifts and east shifts are in green and red gradients respectively.

Table 29. Peak surge characteristics (Maximum and Duration) of the base and storm track shift scenarios for Hurricane Irene at Sewells Point, NSN, the US.

Group	Scenario	Peak Surge (m)	Flood Level/Duration (h)		
			Low	Med	High
Storm Track Shift (nm)	IR_STW_138	0.34	0	0	0
	IR_STW_96	0.44	0	0	0
	IR_STW_54	1.4	18	5	0
	Baseline	1.92	17.5	7	4.5
	IR_STE_54	1.22	18.5	4.5	0
	IR_STE_96	0.87	6	0	0
	IR_STE_138	0.71	5	0	0

On the other hand, the flood area statistics, Figure 92 and Table 30, showed a decrease in the flood area for all simulations compared to the baseline simulation under this scenario group. The flood area has decreased from 0.34 km² (<2.5% of the base area) down to 0.24 km² (1.7%) and 0.28 km² (2%) for the west and east track shifts respectively for Hurricane Irene. In addition, the average and maximum flood depths have also diminished down to 0.32 m and 0.39 m respectively for the west shift simulations and 0.65 m and 0.69 m respectively for the east shift simulations.

The reduction in the flood magnitude and duration, especially of the high and medium flood levels, has also reduced the duration of ground flooding. Figure 93 shows the time series of the average and maximum flood depth in meters and the flood area (km²) for Hurricane Irene for a few hours before and after the peak surge/flood. It can be shown that there is no pronounced peak for the flood areas or average and maximum flood depth for track shifts of 96nm and 138nm in both directions. However, a small peak for AFD and MFD was detected for 54nm simulations with an average of 1.1 m and 1.25 m respectively for both directions.

Investigating the spatial extent of the flood areas revealed no significant flooding for Hurricane Irene storm track shift scenarios, Figure 94. The impact of track shift for Hurricane Irene flooding was generally lower than the baseline scenario. This means that the original Irene track can be considered the worst-case scenario for this hurricane.

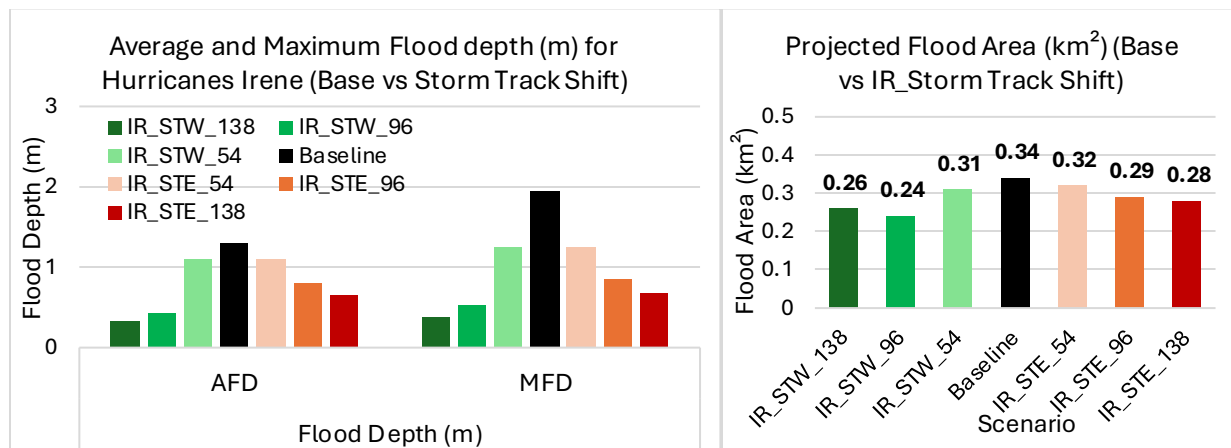


Figure 92. Average Flood Depth (AFD) & Maximum Flood Depth (MFD) in meters (left panel) and Flood area (km^2) (right panel) of Hurricane Irene for the Base and storm track shift scenarios at NSN, the US. West shifts and east shifts are in green and red gradients respectively.

Table 30. Flood area characteristics of the base and storm track shift scenarios for Hurricane Irene at NSN, the US.

Group	Scenario	Flood Depth (m)		FA (km^2)	FA (%)
		AFD	MFD		
Storm Track Shift (nm)	IR_STW_138	0.32	0.39	0.26	1.89
	IR_STW_96	0.42	0.52	0.24	1.74
	IR_STW_54	1.09	1.26	0.31	2.25
	Baseline	1.31	1.94	0.34	2.47
	IR_STE_54	1.1	1.24	0.32	2.32
	IR_STE_96	0.8	0.86	0.29	2.11
	IR_STE_138	0.65	0.69	0.28	2.03

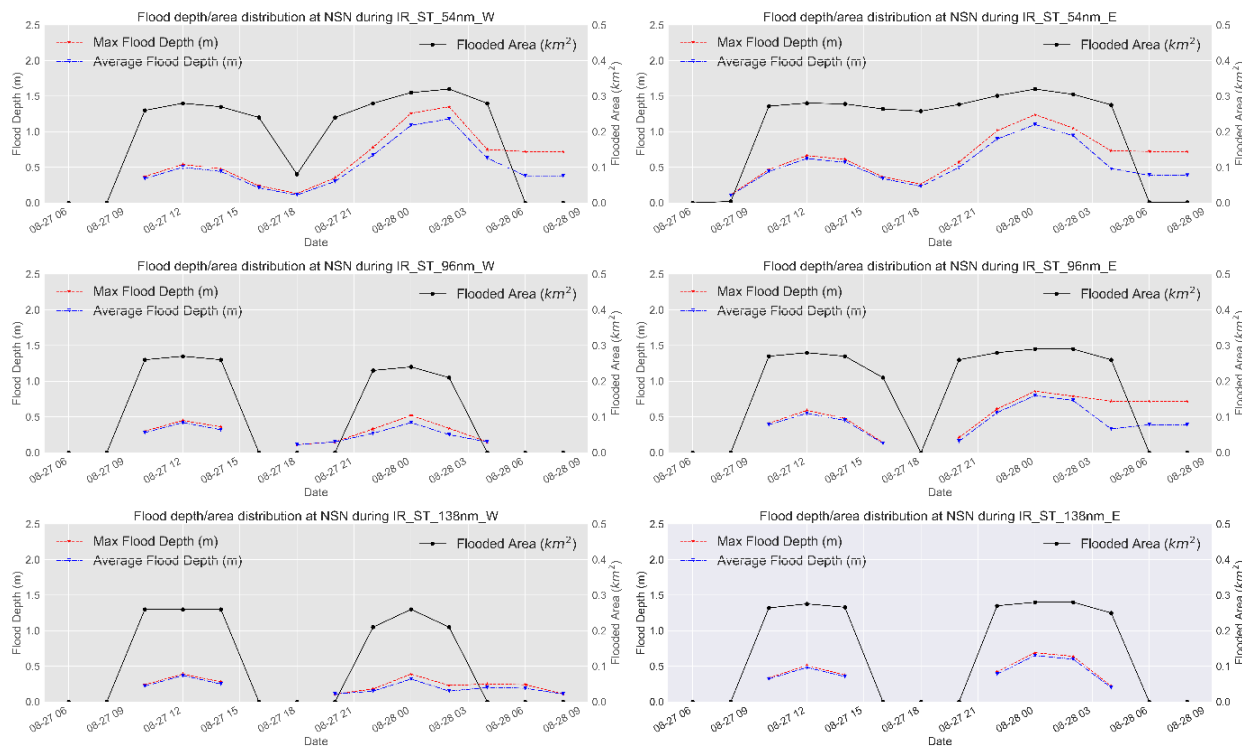


Figure 93. Time series of the projected average and maximum flood depth (left axis) and flood area (km^2 -right axis) for Hurricane Irene for storm track shift scenarios at NSN, the US.

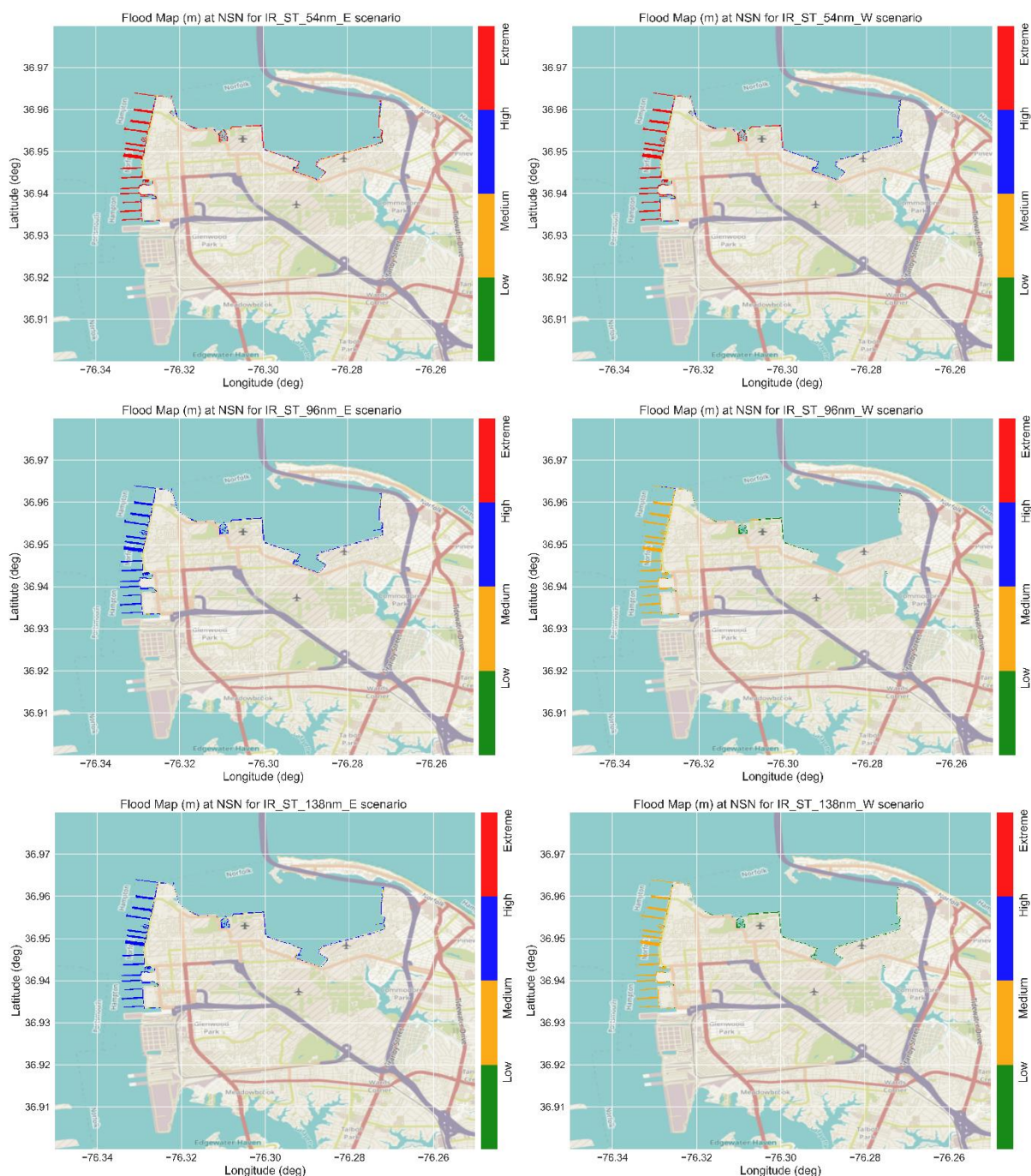


Figure 94. Flood maps with the flood levels for Hurricane Irene during the peak surge for the storm track shift scenarios at NSN, the US. West shifts (left panels) and East shifts (right panels).

Hurricane Isabel has a different track compared to Hurricane Irene. Isabel approaches the US East coast at an angle of 325 degrees with North where it makes landfall near Drum Inlet on the Outer Banks of North Carolina, Figure 95. Shifting the track of Hurricane Isabel to the eastward or westward directions will not have a meaningful impact on the original track. Therefore, we shifted Hurricane Isabel's track by 54nm, 96nm, and 138nm but with a 45-degree angle, i.e. in a perpendicular direction to the original track.

Figure 96 shows the water level for the base and the storm track shift scenarios for Hurricane Isabel at Sewells Point. Shifting Isabel's track to the west (left panels of Figure 96) resulted in a drastic decrease in the peak surge at Sewells Point. The peak surge diminishes almost to the low surge level (0.5m) after shifting the track by 96nm to the west.

Hurricane Isabel passed approximately 65nm west of NSN (hence, Sewells Point), therefore, shifting the track to the west will displace the hurricane further away from NSN resulting in a lower surge magnitude, duration, and hence, diminished associated flood. On the other hand, shifting Isabel's track to the east will result in a higher surge magnitude, duration, and associated flooding. This pattern can be observed in Figure 97 and Table 31. It can be noticed that shifting Hurricane Isabel to the west resulted in a significant decrease in the surge magnitude down to 0.58 m while shifting the hurricane to the east resulted in a significant increase in the surge magnitude up to 3.2 m for the IS_STE_54nm scenario (compared to 1.55m for the baseline). This pattern is also reflected in the surge duration where a significant increase was detected for IS_STE_54nm and IS_STE_96nm scenarios up to 5 hours. Shifting the track further to the east (IS_STE_138nm) yields very close results to the baseline scenario since the hurricane is shifted more than 70 nm east to NSN.

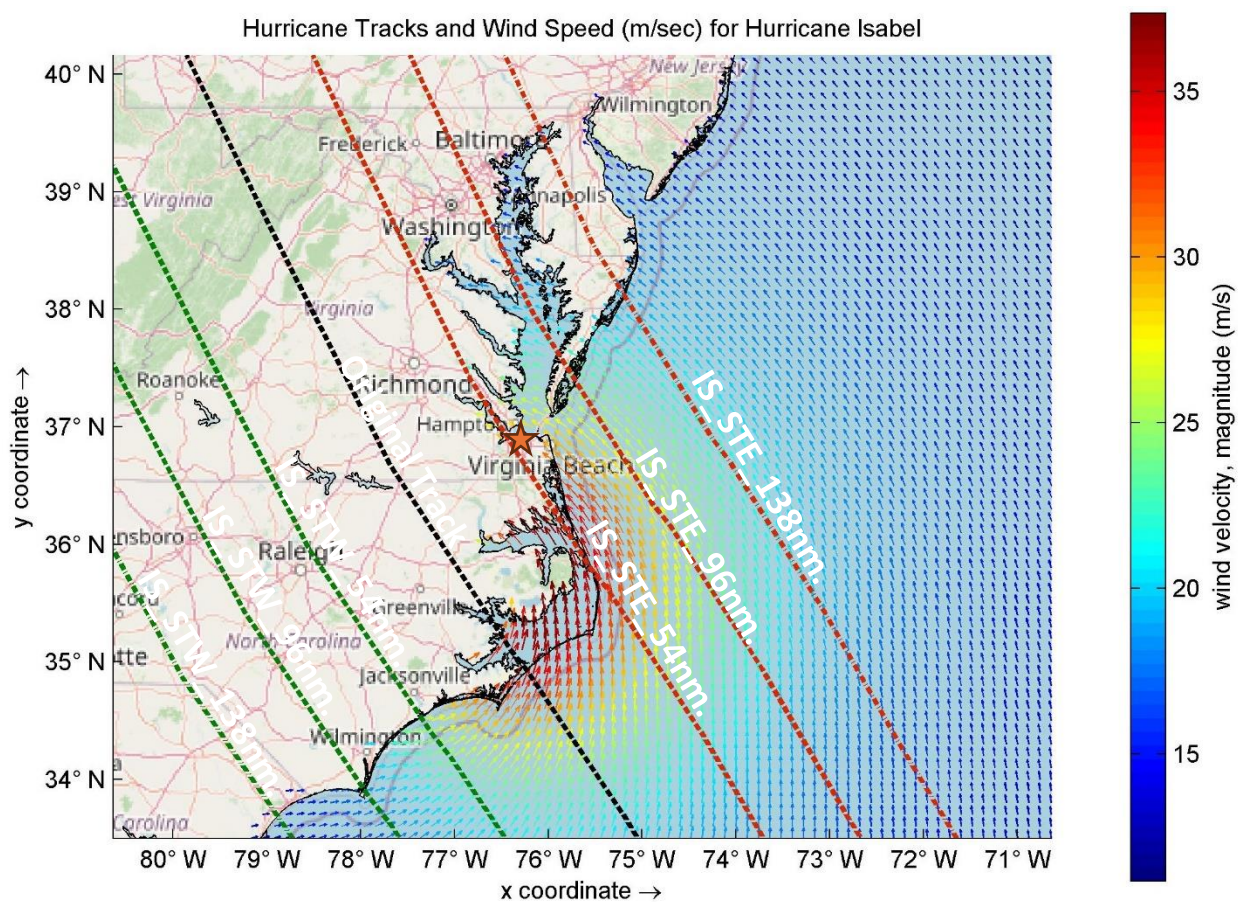


Figure 95. Different hurricane tracks and the wind speed (m/sec) for Hurricane Isabel-2003. The orange star is NSN.

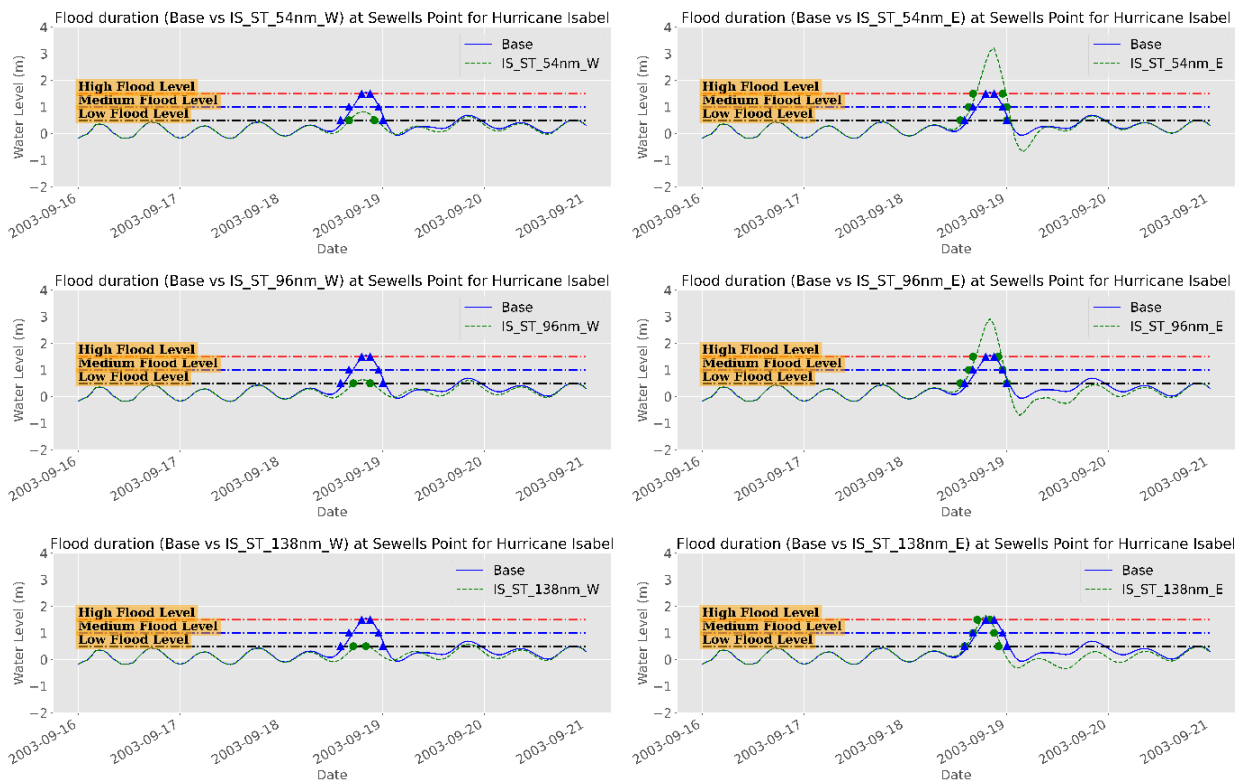


Figure 96. Water level time series (m) during Hurricane Isabel showing the surge magnitude and duration for different surge levels for the base and Storm Track Shift scenarios at Sewells Point, NSN, the US.

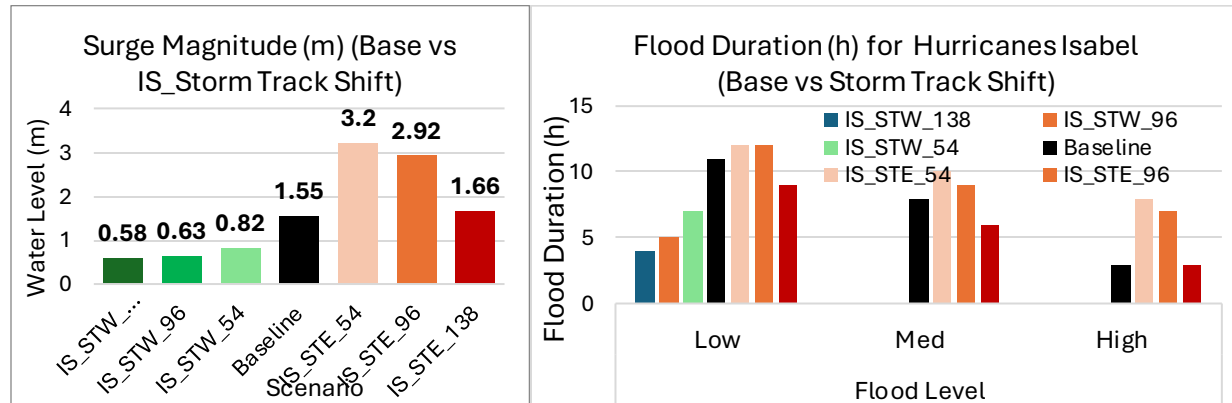


Figure 97. Peak surge (m) (left panel) and surge duration (h) of the different surge levels (right panel) for the base and the storm track shift scenarios for Hurricane Isabel at NSN, the US. West shifts and east shifts are in green and red gradients respectively.

Table 31. Peak surge characteristics (Maximum and Duration) of the base and storm track shift scenarios for Hurricane Isabel at Sewells Point, NSN, the US.

Group	Scenario	Peak Surge (m)	Flood Level/Duration (h)		
			Low	Med	High
Storm Track Shift (nm)	IS_STW_138	0.58	4	--	--
	IS_STW_96	0.63	5	--	--
	IS_STW_54	0.82	7	--	--
	Baseline	1.55	11	8	3
	IS_STE_54	3.2	12	10	8
	IS_STE_96	2.92	12	9	7
	IS_STE_138	1.66	9	6	3

On the other hand, the flood area statistics, Figure 98 and Table 32, showed a decrease in the flood area for all simulations shifted to the west and a drastic increase for all simulations shifted to the east. The flood area decreased from 0.24 km² (<1.7% of the base area) down to 0.18 km² (1.3%) for the west track shifts while about 6 km² and 5.2 km² were detected to be flooded under the IS_STE_54nm and IS_STE_96nm scenarios respectively. In addition, the average and maximum flood depths have also diminished down to 0.5 m for the west shift simulations and increased up to 0.85 m and 3.25 m respectively for the east shift simulations.

The west shift of Hurricane Isabel's track has almost no influence on the flood areas and the duration of the ground flooding. The results are highly comparable to the baseline scenario. On the other hand, the dramatic increase in the surge statistics associated with the east shift simulations significantly affected the characteristics of the ground flooding, Figure 99. Large areas (up to 2 km²) maintain flooding for hours (or days) with an average and maximum flood depth of about 0.5m and 2.5 m respectively. The spatial extent of the flood areas, Figure 100, shows the significant flooding associated with the east shift of Hurricane Isabel scenarios where the northern and western parts of NSN are the most affected areas. The vegetation areas have the extreme flood level (>1m).

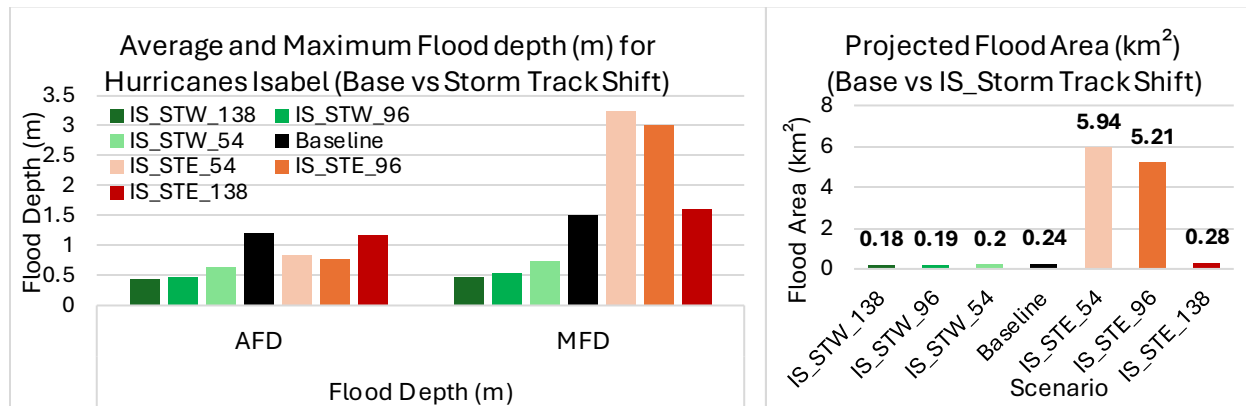


Figure 98. Average Flood Depth (AFD) & Maximum Flood Depth (MFD) in meters (left panel) and Flood area (km^2) (right panel) of Hurricane Isabel for the Base and storm track shift scenarios at NSN, the US. West shifts and east shifts are in green and red gradients respectively.

Table 32. Flood area characteristics of the base and storm track shift scenarios for Hurricane Isabel at NSN, the US.

Group	Scenario	Flood Depth (m)		FA (km^2)	FA (%)
		AFD	MFD		
Storm Track Shift (nm)	IS_STW_138	0.44	0.47	0.18	1.31
	IS_STW_96	0.49	0.54	0.19	1.38
	IS_STW_54	0.64	0.75	0.2	1.45
	Baseline	1.21	1.52	0.24	1.74
	IS_STE_54	0.84	3.25	5.94	43.14
	IS_STE_96	0.77	3.02	5.21	37.84
	IS_STE_138	1.19	1.61	0.28	2.03

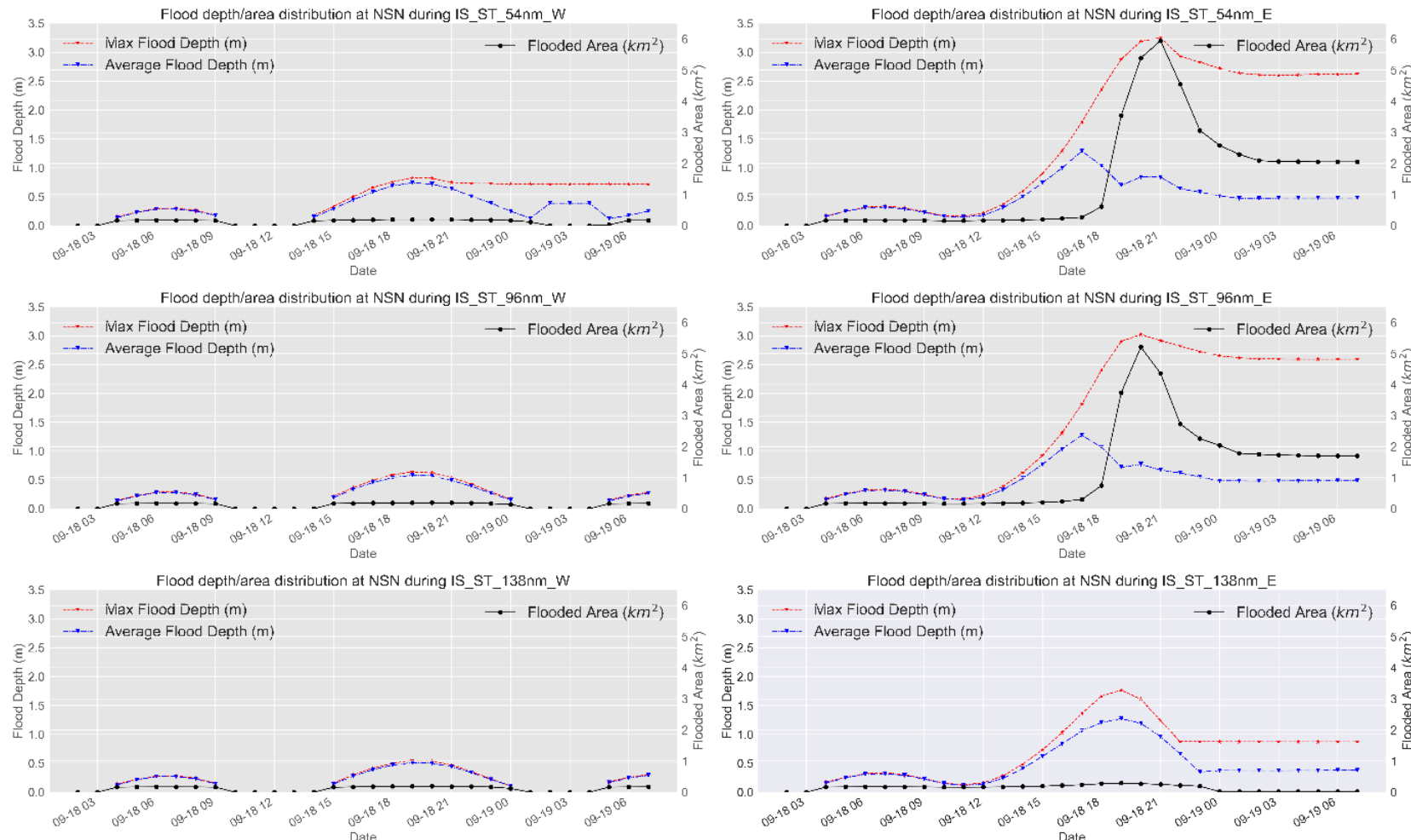


Figure 99. Time series of the projected average and maximum flood depth (left axis) and flood area (km²-right axis) for Hurricane Isabel for storm track shift scenarios at NSN, the US.

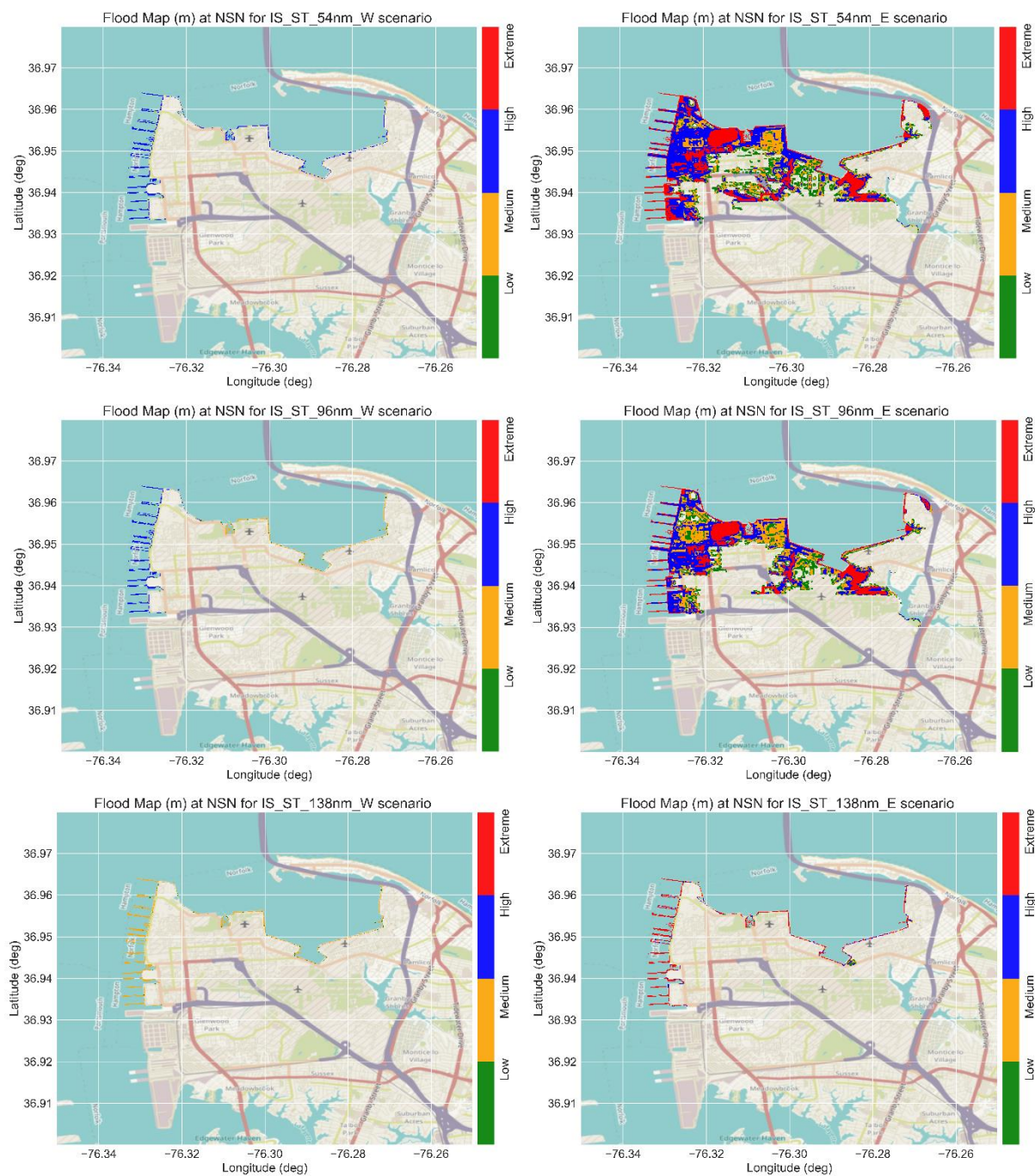


Figure 100. Flood maps with the flood levels for Hurricane Isabel during the peak surge for the storm track shift scenarios at NSN, the US. West shifts (left panels) and East shifts (right panels).

Hurricane Sandy approached the US East coast at an angle of 330 degrees with the North where it made landfall as a post-tropical cyclone near Brigantine, New Jersey, approximately 175nm north of NSN base, Figure 101. The hurricane track was shifted by 138nm to the east and west directions, however, even with the 138nm west shift, the Hurricane Sandy track was still about 70nm away from NSN. This means that only the SA_STW_138nm scenario might have a significant impact on the flooding at NSN. However, it should be mentioned that the impact on Delaware Bay might be quite enormous.

Figure 102 shows the water level for the base and the storm track shift scenarios for Hurricane Sandy at Sewells Point. Shifting Sand's track to the west (left panels of Figure 102) resulted in a significant impact on the peak surge characteristics at Sewells Point. The peak surge increased from about 1.08 m for the baseline scenario up to 2.45 m for the SA_STW_138nm scenario. High surge magnitude was also detected for the SA_STW_96nm and SA_STW_54nm scenarios with 1.4 m and 1.82 m respectively. However, due to the existence of the hurricane tens of nautical miles north of Sewells Point (NSN base), the region is caught in the offshore wind force of the hurricane pushing water away from the coastline and causing an enormous negative surge reaching down to -3.2 m. High negative surge values were also detected for the SA_STW_96nm and SA_STW_54nm of about 2.65 m and 1.1 m respectively. These high negative surge values might have adverse impacts on the navigational activities in this area. The impact of the west track shifts is evident also in the surge duration results where a significant increase was detected in the surge duration for medium and high surge levels with a minor impact on the low surge level, Figure 103 and Table 33. Shifting Hurricane Sandy's track to the east shows a slight decrease in the hurricane's impact on NSN. The hurricane shifts further away from NSN with each scenario causing a minor decrease in the surge characteristics at Sewells Point.

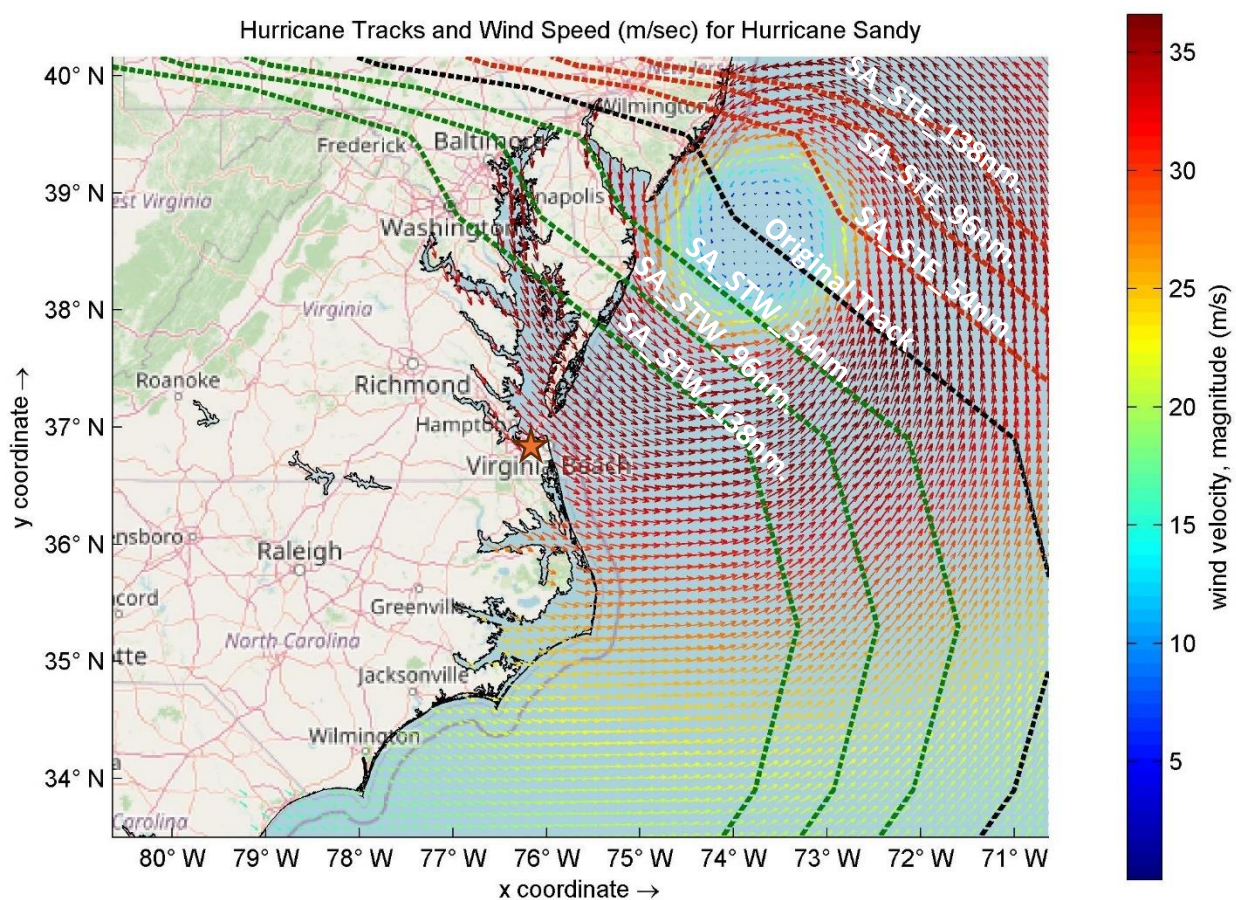


Figure 101. Different hurricane tracks and the wind speed (m/sec) for Hurricane Sandy 2012. The orange star is NSN.

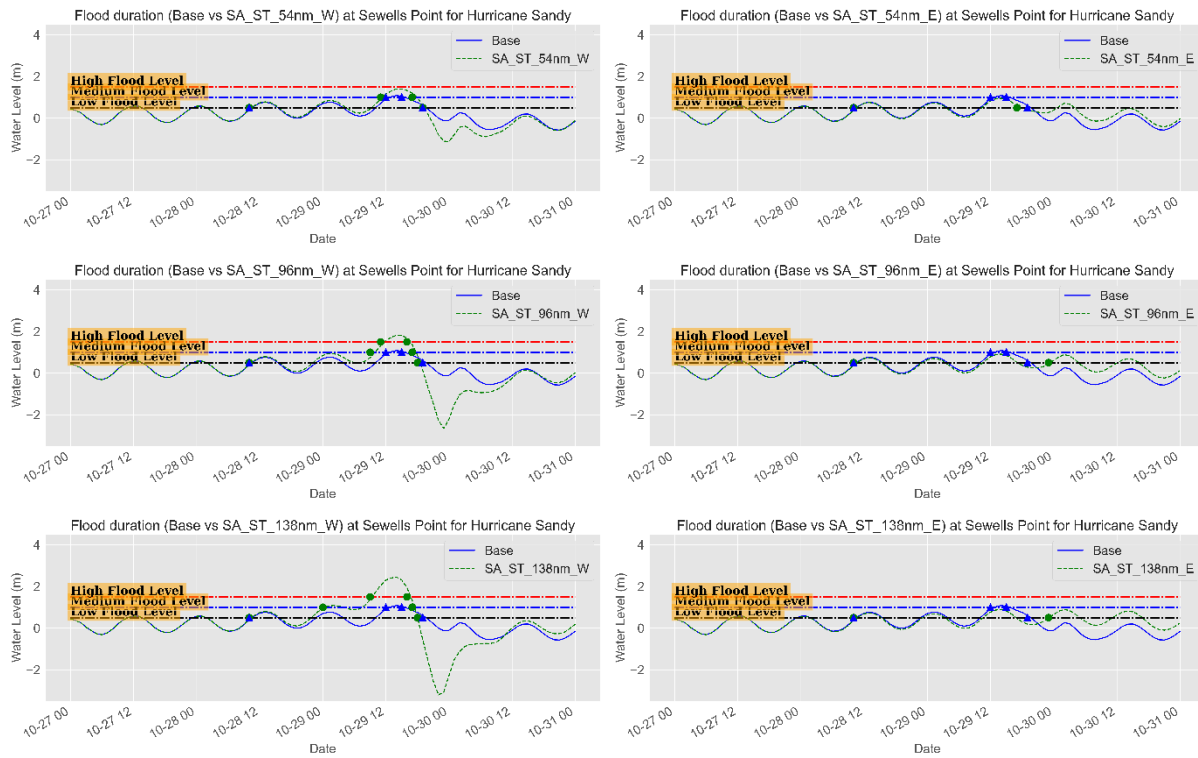


Figure 102. Water level time series (m) during Hurricane Sandy showing the surge magnitude and duration for different surge levels for the base and Storm Track Shift scenarios at Sewells Point, NSN, the US.

The same pattern was also observed in the flood area statistics, Figure 104 and Table 34, where a substantial increase in the flood area for all simulations shifted to the west and a slight decrease for all simulations shifted to the east. The flood area increased from 0.23 km^2 ($<1.7\%$ of the base area) up to 3.37 km^2 (24.5%) for the west track shifts while about maintained 0.21 km^2 for the east track shift scenarios. In addition, the maximum flood depth also increased substantially from 1.1m for the baseline scenario up to 2.8 m for the SA_STW_138nm scenario. The east track shift simulations maintained average and maximum flood depths of 0.8 m and 0.9 m respectively.

The influence on the duration of the ground flooding was also observed for the west shift scenarios. However, the most pronounced impacts were detected for the SA_STW_138nm where about 1.2 km^2 (8.7%) of the base area was susceptible to flooding even after hours from the peak surge. in addition, this area maintains average and maximum flood depth of about 0.5 m and 2.2 m respectively. For the east shift scenarios, no detectable impact was observed on the duration of the ground flooding compared to the baseline scenario, Figure 105.

The spatial extent of the flood areas, Figure 106, shows the significant flooding associated with the west shift SA_STW_96nm and SA_STW_138nm scenarios where the vegetation areas located

at the northern parts of NSN along with some other areas at the west and north parts of the base are the most affected. Most of the affected areas have low to medium flood levels except for the vegetation areas where they have an extreme flood level (>1m).

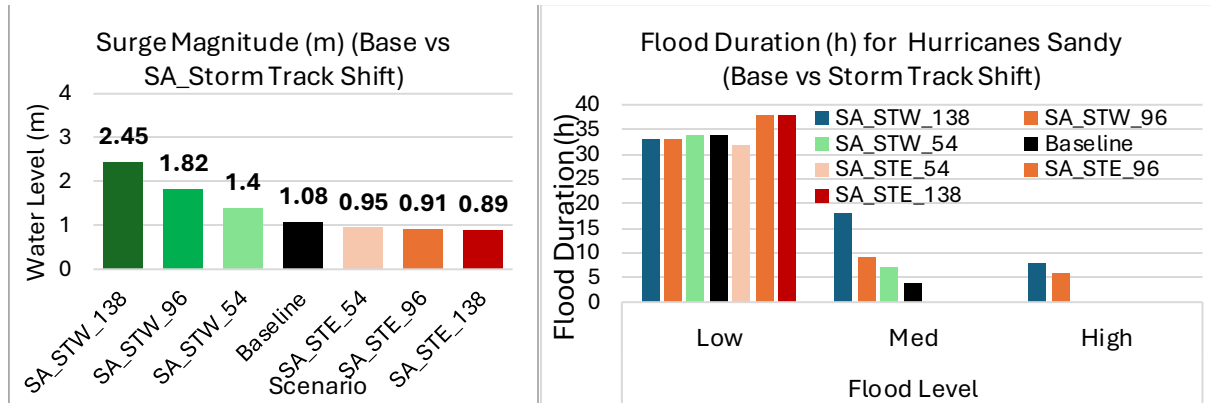


Figure 103. Peak surge (m) (left panel) and surge duration (h) of the different surge levels (right panel) for the base and the storm track shift scenarios for Hurricane Sandy at NSN, the US. West shifts and east shifts are in green and red gradients respectively.

Table 33. Peak surge characteristics (Maximum and Duration) of the base and storm track shift scenarios for Hurricane Isabel at Sewells Point, NSN, the US.

Group	Scenario	Peak Surge (m)	Flood Level/Duration (h)		
			Low	Med	High
Storm Track Shift (nm)	SA_STW_138	2.45	33	18	8
	SA_STW_96	1.82	33	9	6
	SA_STW_54	1.4	34	7	--
	Baseline	1.08	34	4	0
	SA_STE_54	0.95	32	--	--
	SA_STE_96	0.91	38	--	--
	SA_STE_138	0.89	38	--	--

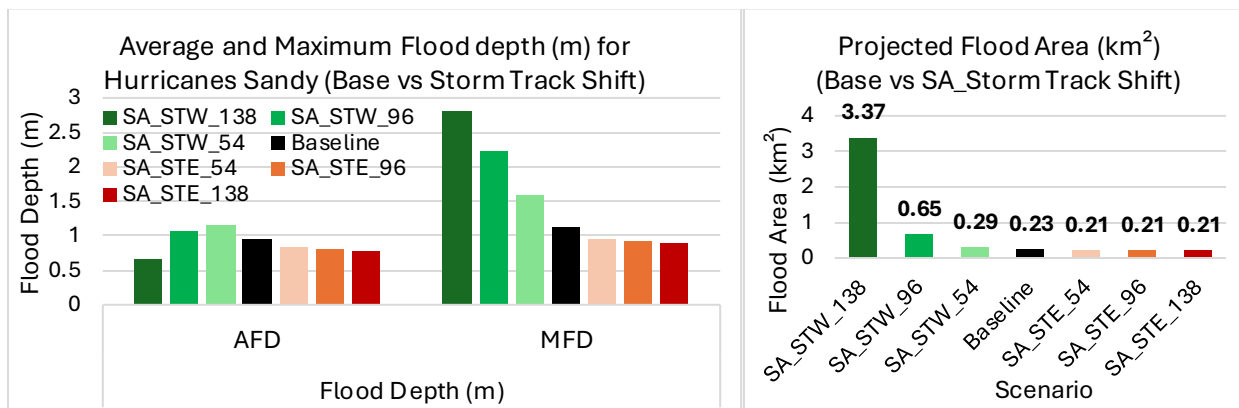


Figure 104. Average Flood Depth (AFD) & Maximum Flood Depth (MFD) in meters (left panel) and Flood area (km^2) (right panel) of Hurricane Sandy for the Base and storm track shift scenarios at NSN, the US. West shifts and east shifts are in green and red gradients respectively.

Table 34. Flood area characteristics of the base and storm track shift scenarios for Hurricane Sandy at NSN, the US.

Group	Scenario	Flood Depth (m)		FA (km^2)	FA (%)
		AFD	MFD		
Storm Track Shift (nm)	SA_STW_138	0.67	2.82	3.37	24.47
	SA_STW_96	1.09	2.22	0.65	3.56
	SA_STW_54	1.15	1.59	0.29	2.11
	Baseline	0.94	1.14	0.23	1.67
	SA_STE_54	0.85	0.96	0.21	1.53
	SA_STE_96	0.81	0.92	0.21	1.53
	SA_STE_138	0.79	0.89	0.21	1.53

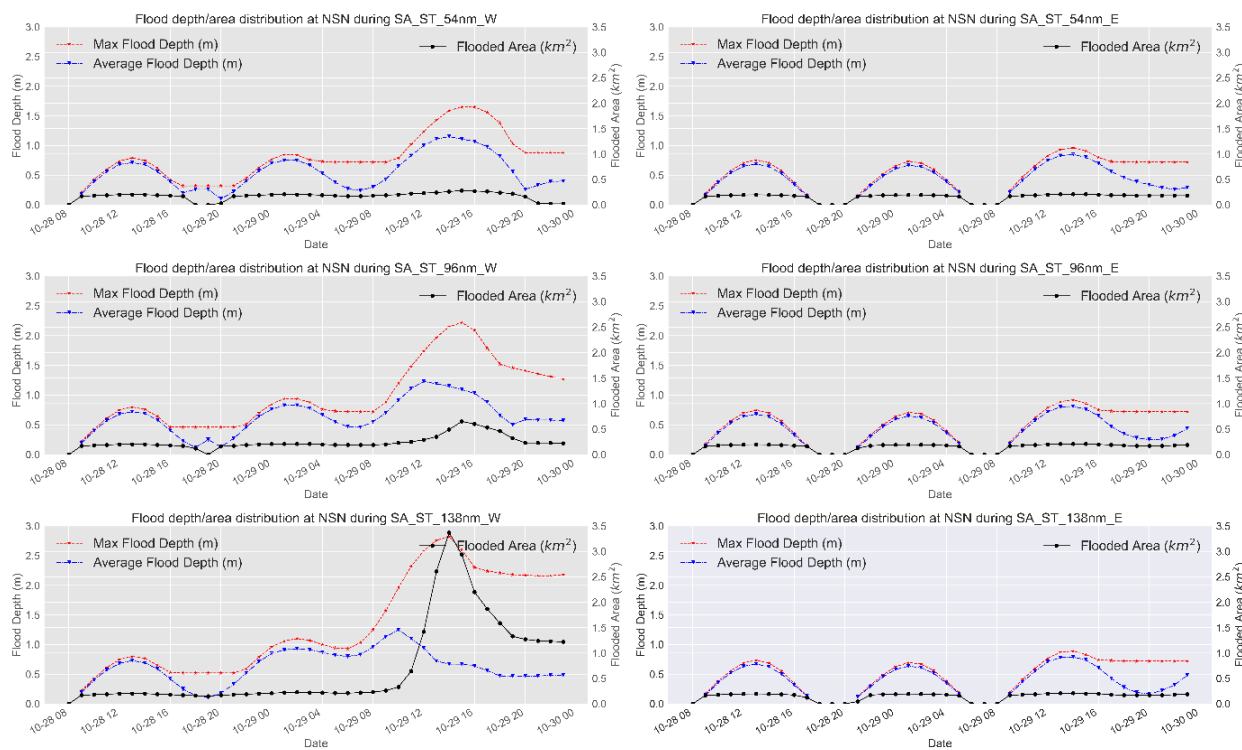


Figure 105. Time series of the projected average and maximum flood depth (left axis) and flood area (km^2 -right axis) for Hurricane Sandy for storm track shift scenarios at NSN, the US.

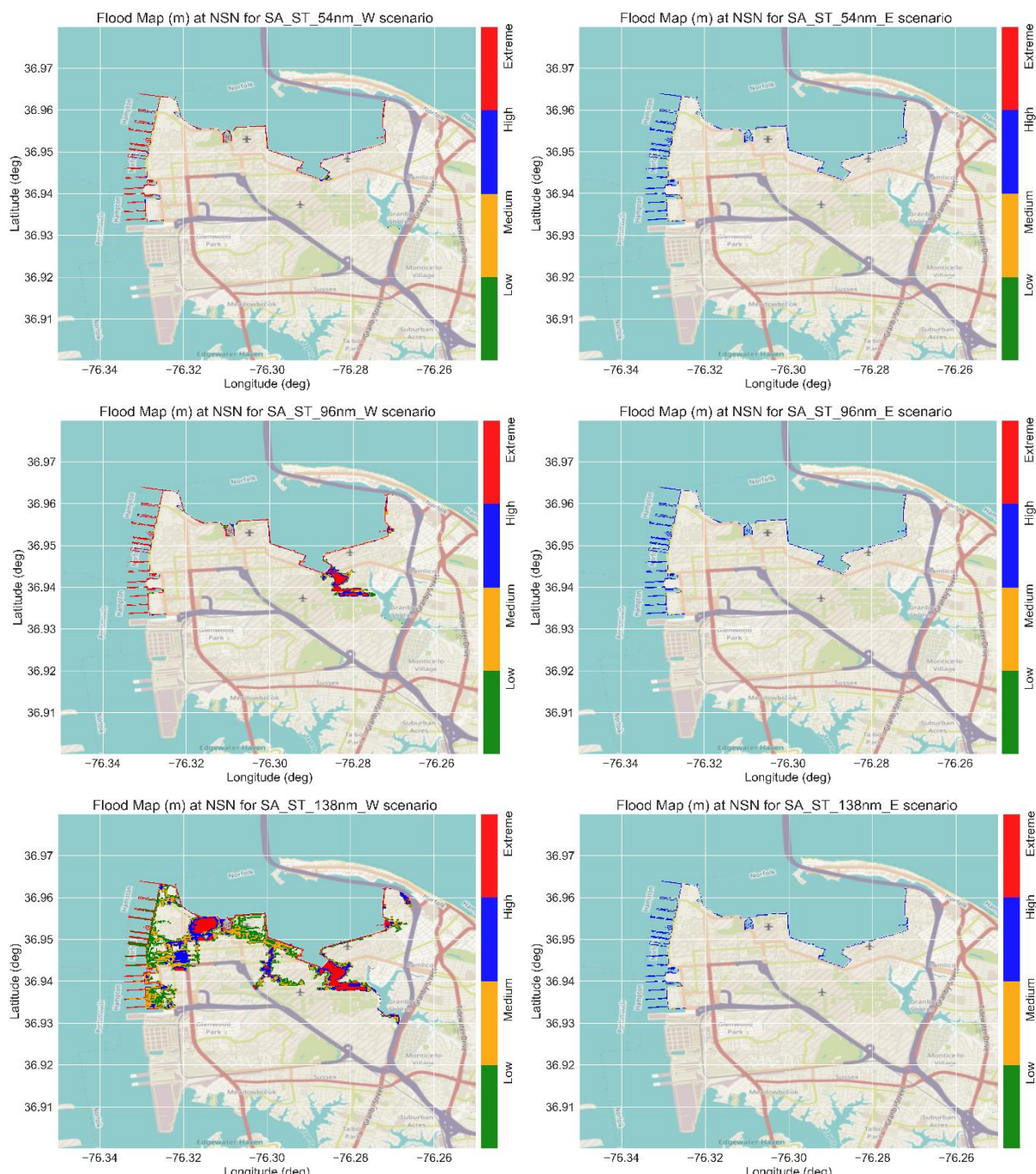


Figure 106. Flood maps with the flood levels for Hurricane Sandy during the peak surge for the storm track shift scenarios at NSN, the US. West shifts (left panels) and East shifts (right panels).

Hurricane Michael on the other hand approached the US East coast at an angle of 30 degrees and it made its landfall near Mexico Beach and Tyndall Air Force Base, Florida, producing devastating winds and storm surge near the coast, and rain and wind inland. However, we have considered Hurricane Michael in this study because it also continued its track till it reached Norfolk from the land side with an approximate angle of 70 degrees, Figure 107. Although Micheal was a category five hurricane (on the Saffir-Simpson Hurricane Wind Scale) that had a catastrophic impact on the US south coast where it made its landfall, it continued its path to the east coast passing through Norfolk, Virginia as an Extratropical cyclone with wind speed 60-65 kt at 0600 UTC on 12 October 2018.

Figure 108 shows the water level for the base and the storm track shift scenarios for Hurricane Michael at Sewells Point. Shifting Hurricane Michael's track to the west (left panels of Figure 108) or to the east (right panels of Figure 108) results in a minor impact on the peak surge characteristics at Sewells Point. The simulated surge did not exceed the low surge level for all simulations. A limited increase in the peak surge magnitude was detected for the east shift simulations with a maximum surge of 0.96m for the MI_STE_96nm compared to 0.73 m for the baseline simulation. The peak surge diminished to some extent for the west shift simulations down to 0.51 m for the MI_STW_96nm simulation, Figure 109. In addition, a minor shift in the peak surge timing (1-2 hours) and hence, associated maximum flooding, was detected for the west and east simulations. No significant influence on the surge duration was detected for all simulations except the increase in the low surge level for the MI_STE_138nm scenario where the duration increased up to 16 hours compared to 6 hours for the baseline scenario. No surge was detected higher than the low level, hence no durations were detected (zero) for the medium and high surge levels, Figure 109 and Table 35.

The same pattern was also observed in the flood area statistics, Figure 110 and **Table 36**, where no significant changes in the flood area were observed for all scenarios with about ± 0.02 change beyond the baseline simulation. However, a minor increase in the average and maximum flood depth was detected for the east shift simulations by about 0.2 m, while a minor decrease was observed for the west shift simulation by the same magnitude.

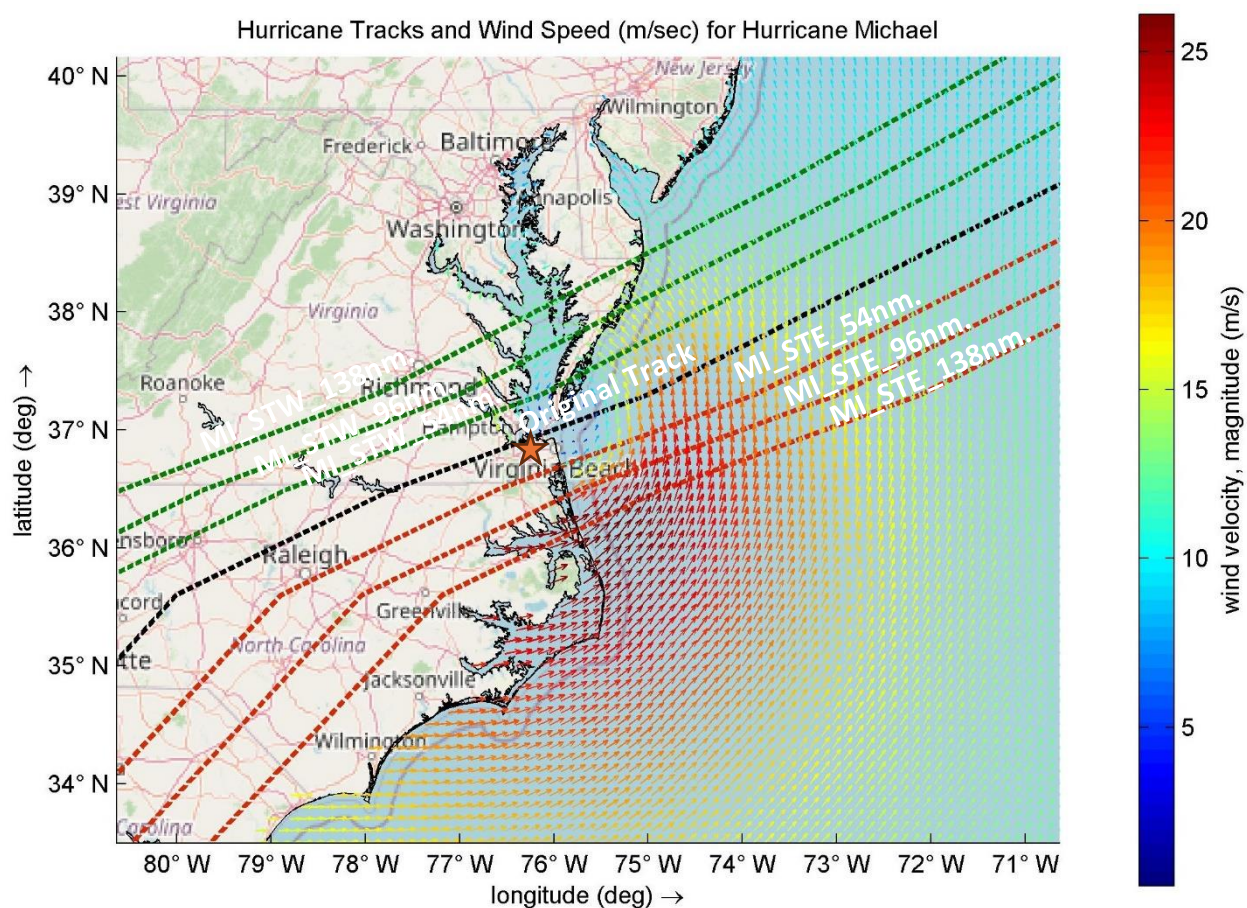


Figure 107. Different hurricane tracks and the wind speed (m/sec) for Hurricane Michael 2018. The orange star is NSN.

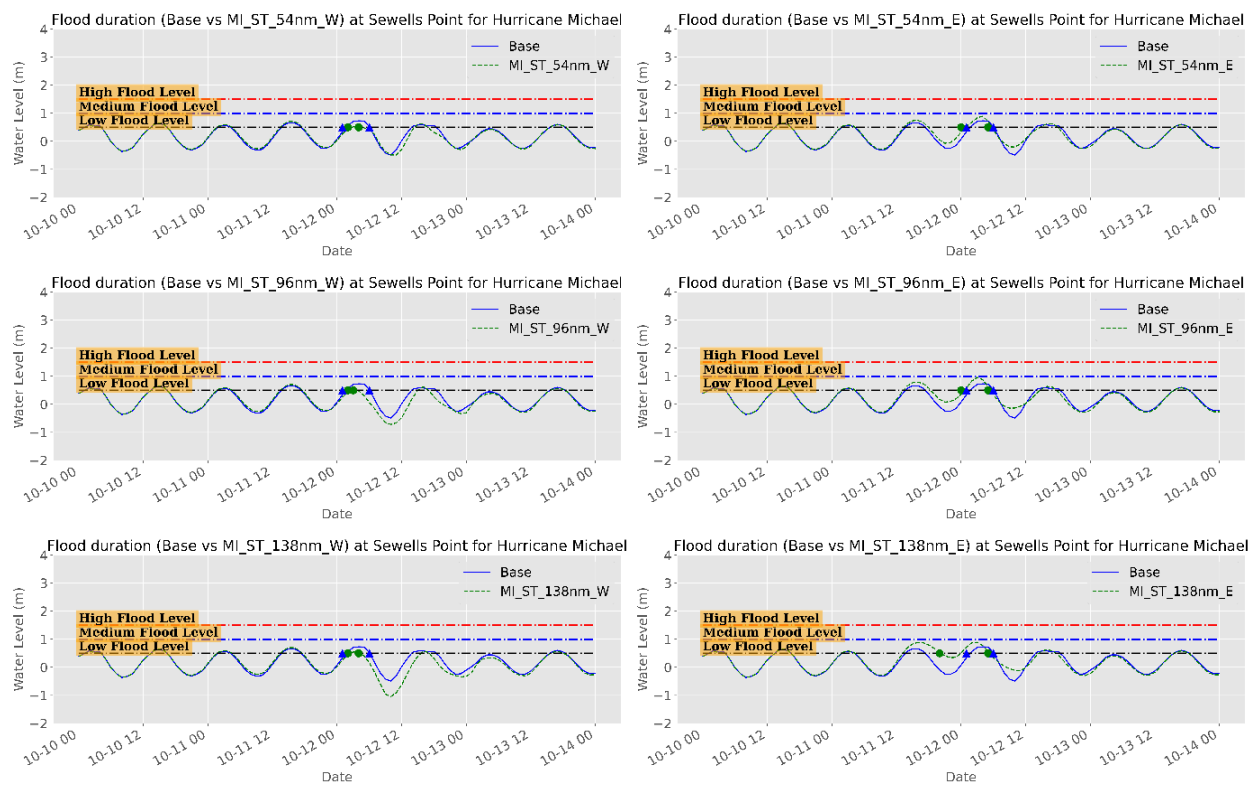


Figure 108. Water level time series (m) during Hurricane Michael showing the surge magnitude and duration for different surge levels for the base and Storm Track Shift scenarios at Sewells Point, NSN, the US.

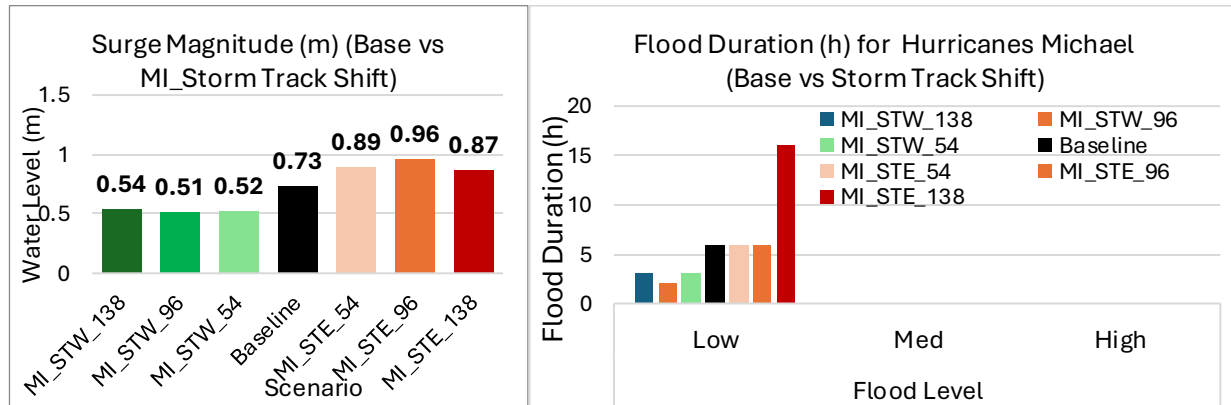


Figure 109. Peak surge (m) (left panel) and surge duration (h) of the different surge levels (right panel) for the base and the storm track shift scenarios for Hurricane Michael at NSN, the US. West shifts and east shifts are in green and red gradients respectively.

Table 35. Peak surge characteristics (Maximum and Duration) of the base and storm track shift scenarios for Hurricane Michael at Sewells Point, NSN, the US.

Group	Scenario	Peak Surge (m)	Flood Level/Duration (h)		
			Low	Med	High
Storm Track Shift (nm)	MI_STW_138	0.54	3	--	--
	MI_STW_96	0.51	2	--	--
	MI_STW_54	0.52	3	--	--
	Baseline	0.73	6	0	0
	MI_STE_54	0.89	6	--	--
	MI_STE_96	0.96	6	--	--
	MI_STE_138	0.57	16	--	--

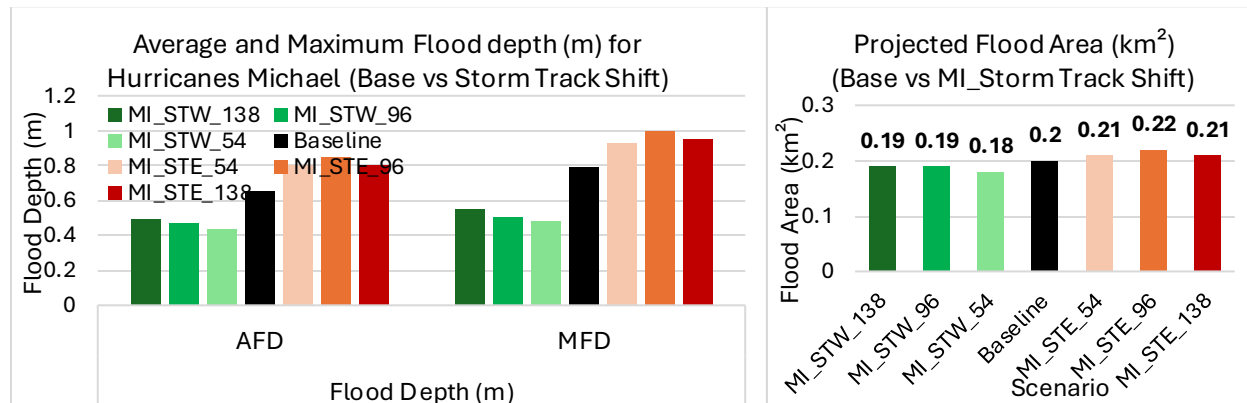


Figure 110. Average Flood Depth (AFD) & Maximum Flood Depth (MFD) in meters (left panel) and Flood area (km^2) (right panel) of Hurricane Michael for the Base and storm track shift scenarios at NSN, the US. West shifts and east shifts are in green and red gradients respectively.

Table 36. Flood area characteristics of the base and storm track shift scenarios for Hurricane Michael at NSN, the US.

Group	Scenario	Flood Depth (m)		FA (km^2)	FA (%)
		AFD	MFD		
Storm Track Shift (nm)	MI_STW_138	0.5	0.55	0.19	1.38
	MI_STW_96	0.47	0.51	0.19	1.38
	MI_STW_54	0.44	0.48	0.18	1.31
	Baseline	0.66	0.79	0.20	1.45
	MI_STE_54	0.8	0.93	0.21	1.53
	MI_STE_96	0.85	1.00	0.22	1.60
	MI_STE_138	0.8	0.95	0.21	1.53

The influence on the duration of the ground flooding was also minor for all scenarios. However, the most pronounced impacts were detected for the east shift simulation where the flooded areas maintained an average and maximum flood depth of about 0.4 m and 0.7 m respectively, Figure 111. The spatial extent of the flood areas, Figure 112, shows that there is no significant flooding associated with the west and east shifts of Hurricane Michael's track. Only small areas were detected around the land-sea boundary where the model accuracy is relatively low. It is worth noting that the flooded area is very small for all scenarios and lies within the range of the marginal error of the model prediction. This means, as mentioned in previous sections, that there is almost no flood area associated with Hurricane Michael at NSN.

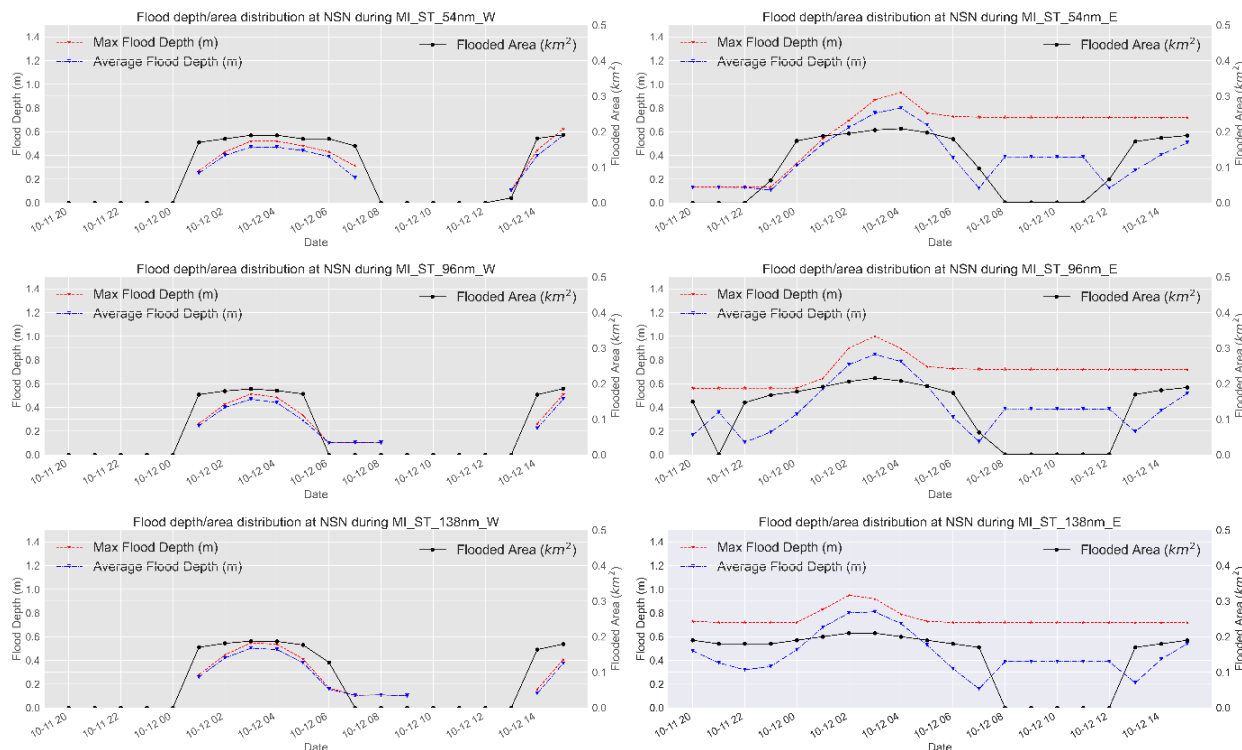


Figure 111. Time series of the projected average and maximum flood depth (left axis) and flood area (km^2 -right axis) for Hurricane Michael for storm track shift scenarios at NSN, the US.

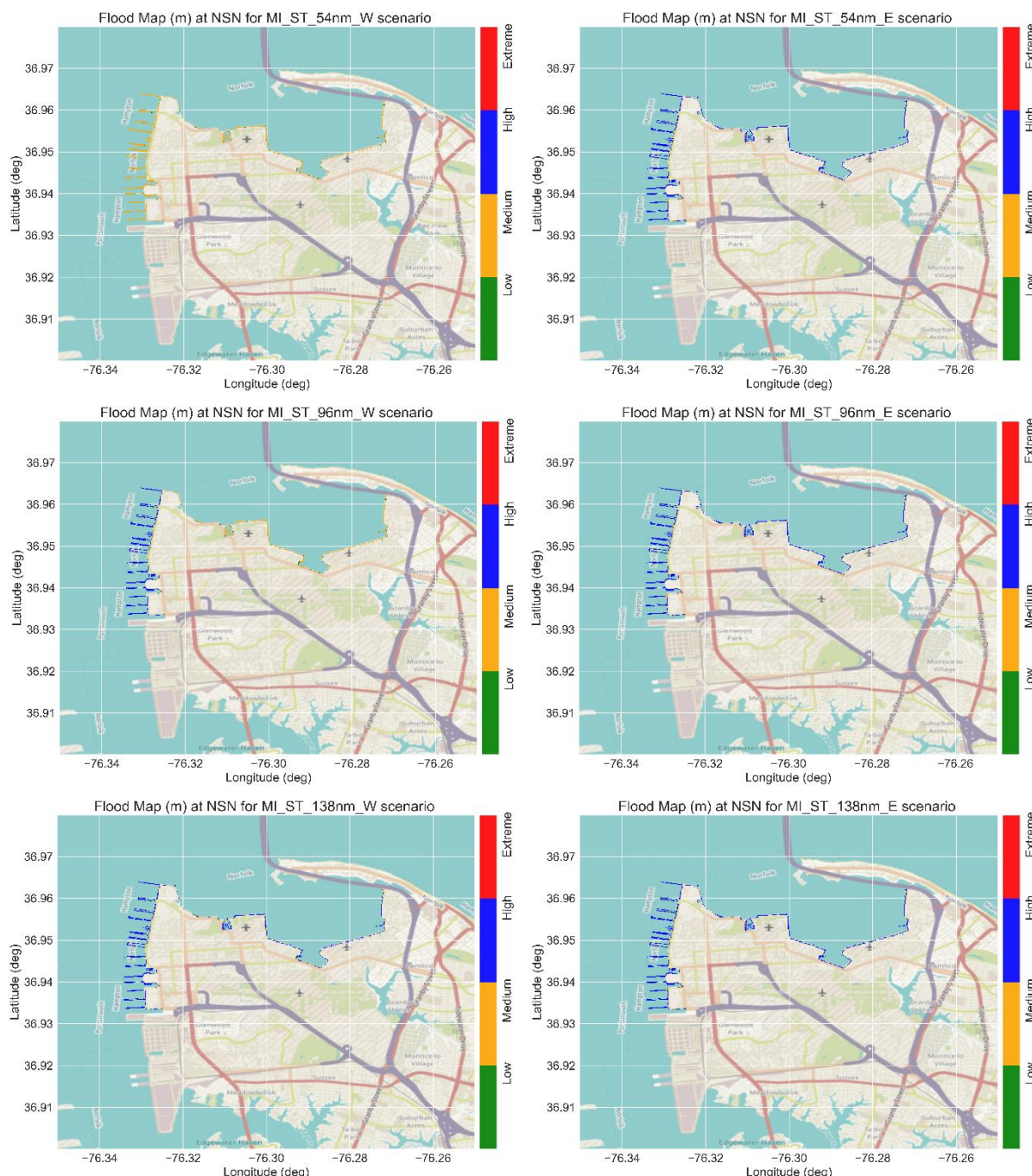


Figure 112. Flood maps with the flood levels for Hurricane Michael during the peak surge for the storm track shift scenarios at NSN, the US. West shifts (left panels) and East shifts (right panels).

II. Bathymetry Accuracy

We will consider three scenarios for bathymetry accuracy for Hurricane Irene only by adding a Gaussian noise of 0.3m (IR_Bathy_Acc_GN_0.3m), 0.5m (IR_Bathy_Acc_GN_0.5m), and 1.0m (IR_Bathy_Acc_GN_1.0m). The model performance will be evaluated in terms of peak surge and flood area characteristics.

Figure 113 shows the water level for the base and the bathymetry accuracy scenarios for Hurricane Irene at Sewells Point. It can be observed that minor inaccuracies in the bathymetric data (up to 1 m in the current study) have no impact on the prediction of the water level and the peak surge. No significant change was observed in the peak surge characteristics (magnitude or duration) at Sewells Point for the three scenarios.

On the other hand, a minor increase in the flood area was observed for all scenarios, Figure 114 and Table 37. Although no changes were observed in the peak surge magnitude and duration, an increase in the predicted flood areas was observed with a significant increase for the Bathy_Acc_GN_1.0m scenario. The predicted flood area increased from 0.34 km² (2.47%) for the base scenario to about 0.48 km² (3.5%) for the Bathy_Acc_GN_1.0m scenario. No detectable change was reported for the average and maximum flood depth for all scenarios. In addition, investigating the flood characteristics with time, Figure 115, showed no change compared to the baseline scenario except for the Bathy_Acc_GN_1.0m scenario where the flood area maintained a slightly higher value of 0.2 km² (1.4%) a few hours after the peak surge. Finally, the spatial extent of the flood areas showed that the extent of the flood area is concentrated in the residential area located in the northeastern part of the base, Figure 116. Most of these areas lie mostly under the extreme flood (>1 m) category (50% to 65% of the total flood area), Figure 117.

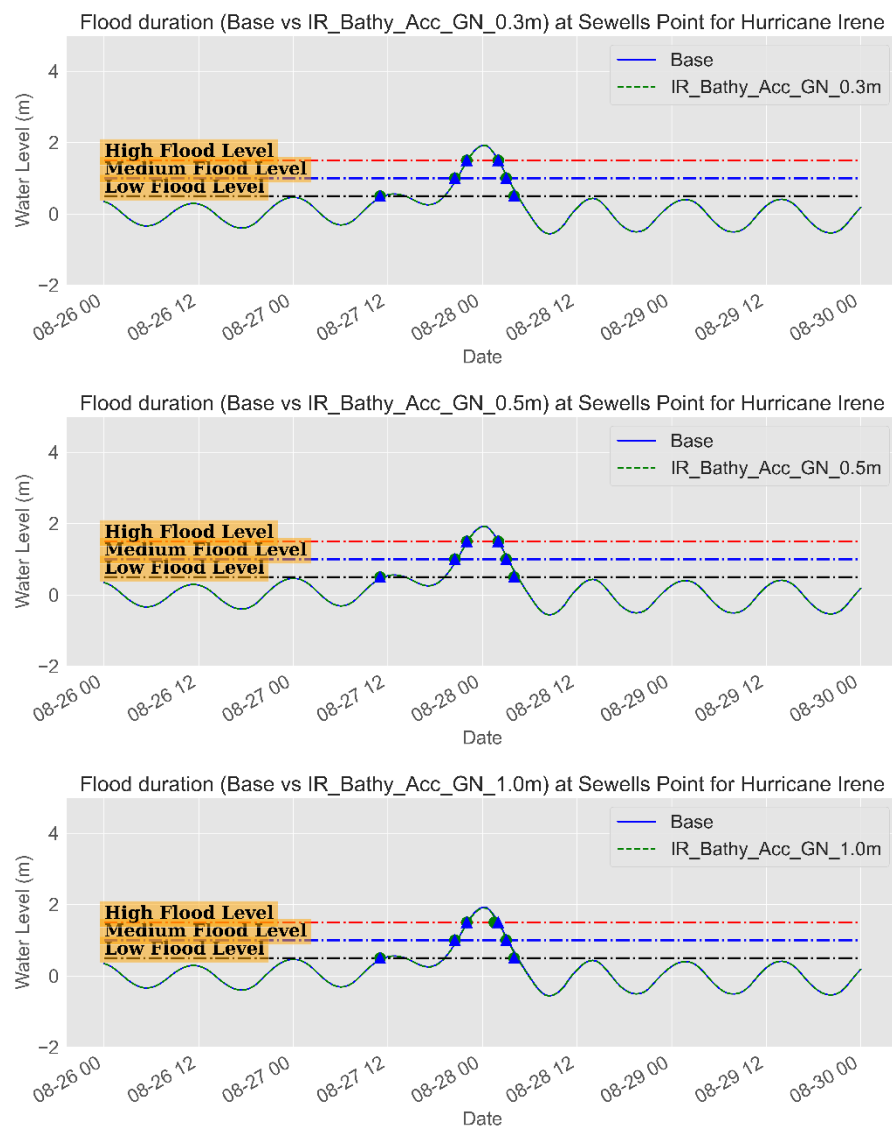


Figure 113. Water level time series (m) during Hurricane Irene showing the surge magnitude and duration for different surge levels for the base and Bathymetry Accuracy scenarios at Sewells Point, NSN, the US.

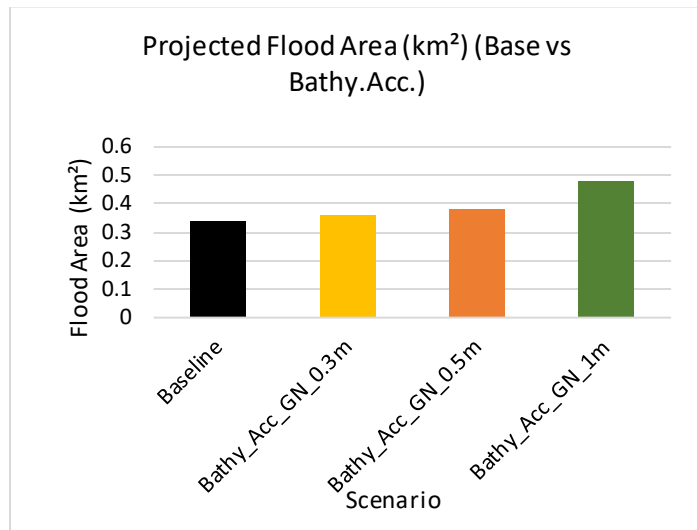


Figure 114. Flood area (km^2) of the Base and Bathymetry Accuracy scenarios at NSN, the US

Table 37. Flood area characteristics of the base and bathymetry accuracy scenarios at NSN, the US.

Group	Scenario	AFD (m)	MFD (m)	Flood area (km^2)	Flood (%)
Deg. Sc.	Base	1.31	1.94	0.34	2.47
	Bathy_Acc_GN_0.3m	1.27	1.94	0.36	2.6
	Bathy_Acc_GN_0.5m	1.23	1.94	0.38	2.8
	Bathy_Acc_GN_1m	1.1	1.93	0.48	3.5

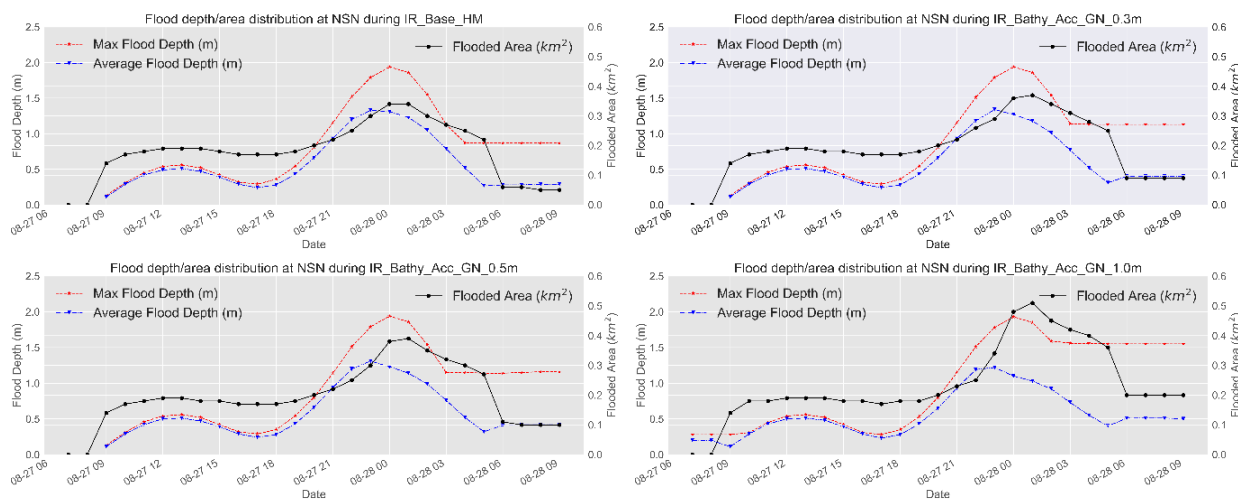


Figure 115. Time series of the projected average and maximum flood depth (left axis) and flood area (km^2 -right axis) for Hurricane Irene for the base and Bathymetry accuracy scenarios at NSN, the US.

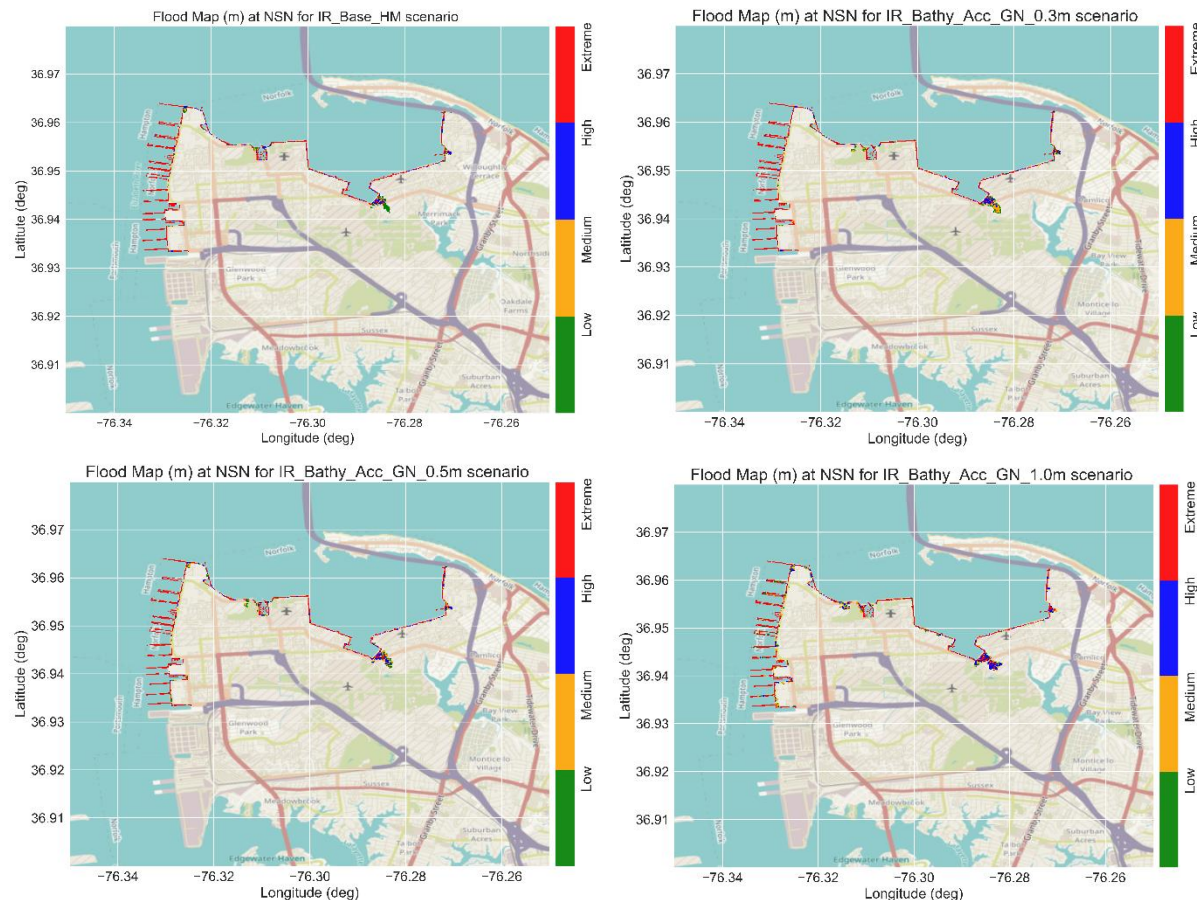


Figure 116. Flood maps with the flood levels for Hurricane Irene during the peak surge for the base and bathymetry accuracy scenarios at NSN, the US.

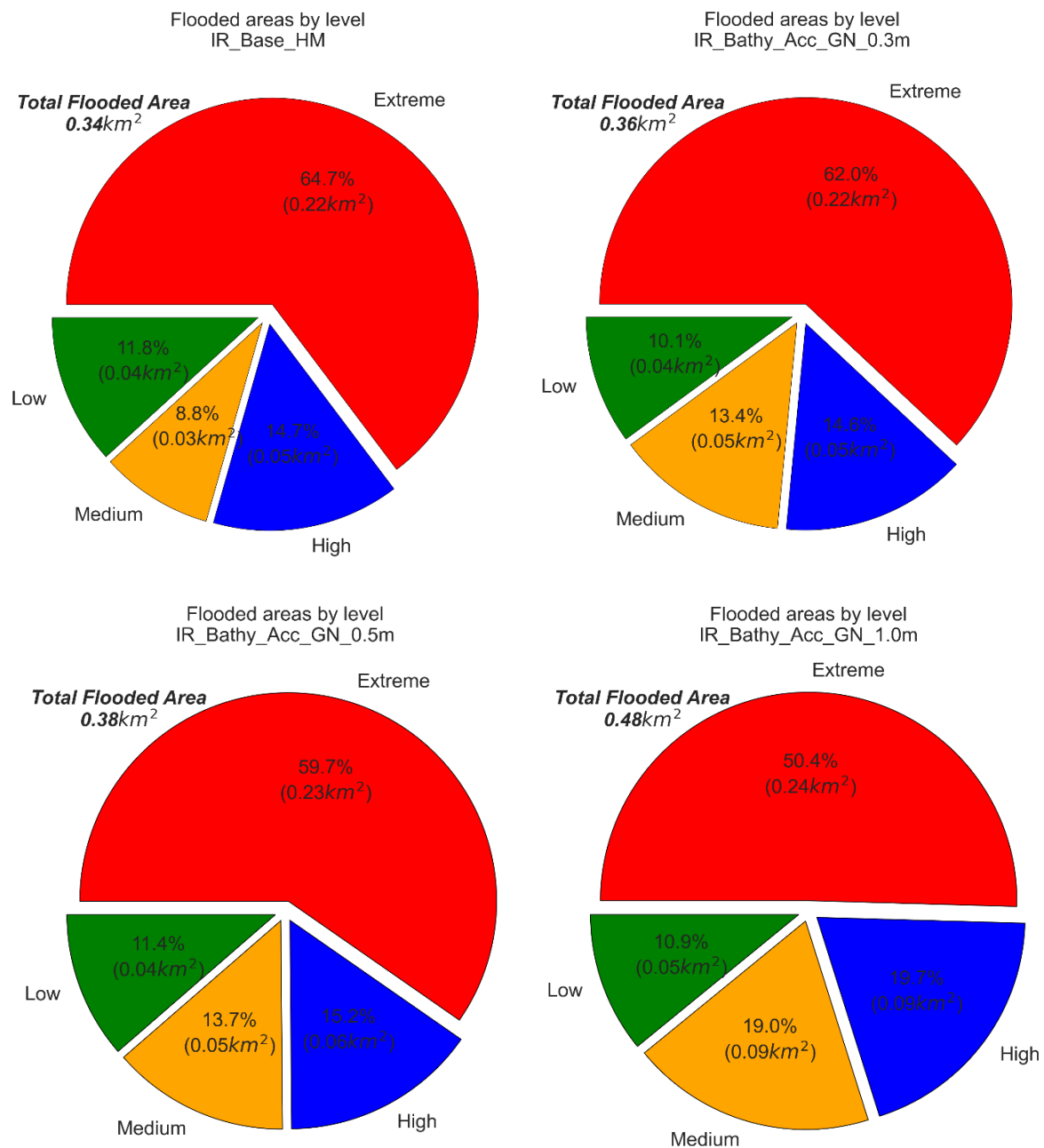


Figure 117. Pie chart of the flood areas, with percentages, of the different flood levels for the base and bathymetry accuracy scenario for Hurricane Irene-2011 at NSN, the US.

III. Bathymetry Resolution

We will consider four scenarios for bathymetry/mesh resolution for Hurricane Irene only by decreasing the resolution of the baseline simulation by a factor of 5 (IR_Bathy_Res_F05), 16 (IR_Bathy_Res_F16), 33 (IR_Bathy_Res_F33), and 66 (IR_Bathy_Res_F66). The model performance will be evaluated regarding peak surge and flood area characteristics.

Figure 118 shows the water level for the base and the bathymetry resolution scenarios for Hurricane Irene at Sewells Point. Although the model resolution was reduced drastically from 15m down to 1000m, the sensitivity to this resolution degradation was minor, and the model performance in terms of water level and peak surge prediction is still relatively accurate. A maximum change in the peak surge was about -5 cm for the Bathy_Res_F66 scenario, which is still acceptable even with this low-resolution mesh. No changes were observed for the water level prediction for the other scenarios.

On the other hand, although no changes were observed in the peak surge magnitude and duration, the influence of resolution degradation on flood area characteristics is enormous. The lower resolution reflected an inaccurate topographic representation of the base in terms of elevation and spatial representations. This resulted in an unrealistic increase in the predicted flood areas for all scenarios, Figure 119 and Table 38.

An increase in the average flood depth and the predicted flood areas was observed for all scenarios. The flood depth increased from 1.3 m for the base scenario up to 1.85 m. The predicted flood area increased from 0.34 km² (2.47%) for the base scenario to about 7 km² (51%) for the Bathy_Res_F66 scenario. No detectable change was reported for the maximum flood depth for all scenarios. In addition, investigating the flood characteristics with time, Figure 120, showed an unrealistic increase in the flood area that diminished again to almost zero a few hours after the peak surge. This pattern is obvious for F16, F33, and F66 scenarios. It can also be observed in the spatial extent of the flood areas where the extent of the flood area is dominated by the pixelized nature of the mesh rather than the actual topography, Figure 121.

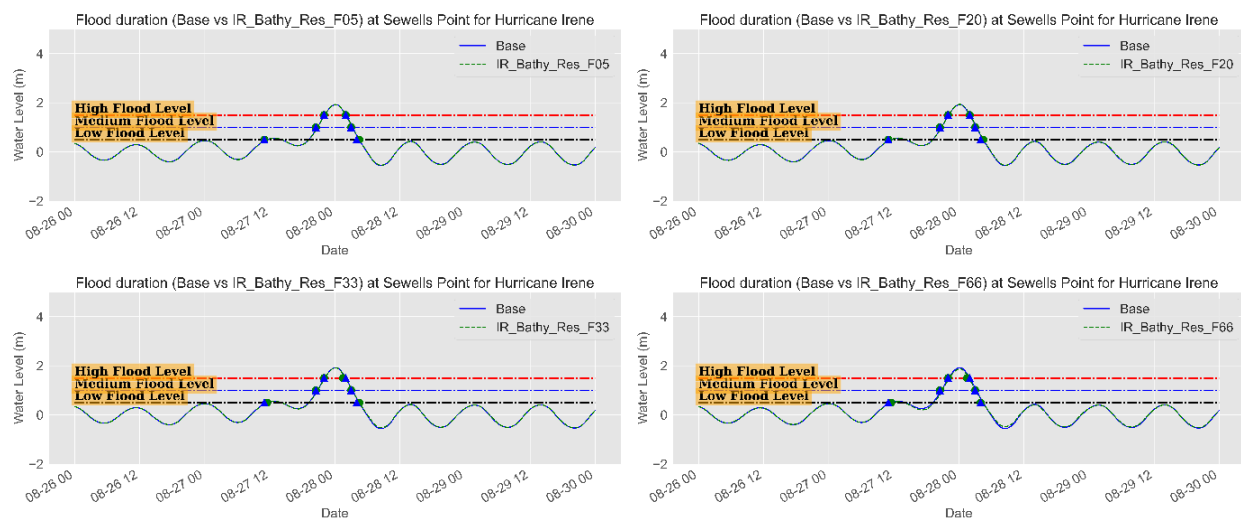


Figure 118. Water level time series (m) during Hurricane Irene showing the surge magnitude and duration for different surge levels for the base and Bathymetry Resolution scenarios at Sewells Point, NSN, the US.

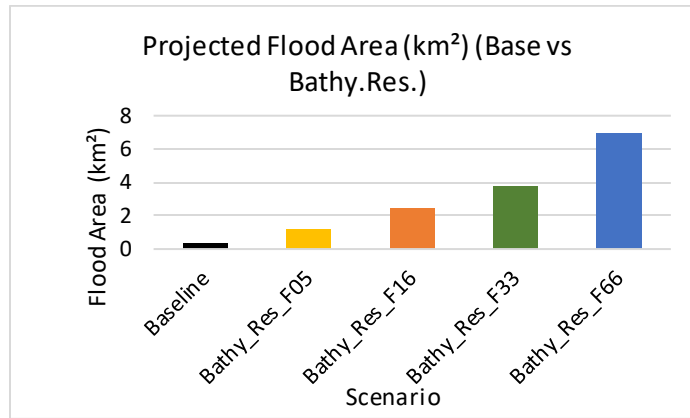


Figure 119. Flood area (km²) of the Base and Bathymetry Resolution scenarios at NSN, the US

Table 38. Flood area characteristics of the base and bathymetry Resolution scenarios at NSN, the US.

Group	Scenario	AFD (m)	MFD (m)	Flood area (km ²)	Flood (%)
Deg. Sc.	Base	1.31	1.94	0.34	2.47
	Bathy_Res_F05	1.23	1.96	1.18	8.6
	Bathy_Res_F16	1.67	1.96	2.43	17.6
	Bathy_Res_F33	1.85	1.94	3.77	27.4
	Bathy_Res_F66	1.83	1.89	6.99	50.8

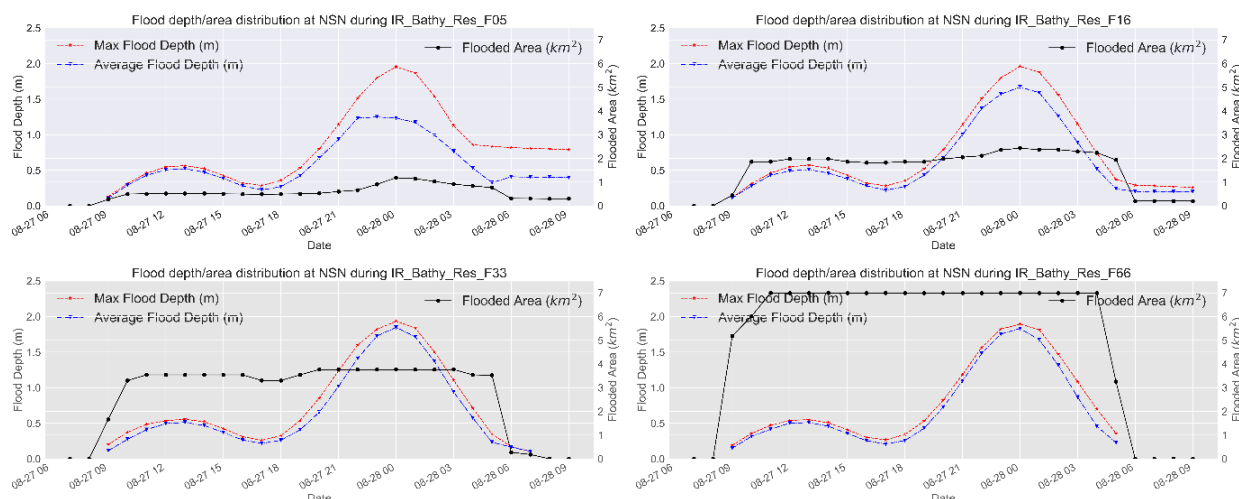


Figure 120. Time series of the projected average and maximum flood depth (left axis) and flood area (km²-right axis) for Hurricane Irene for the Bathymetry Resolution scenarios at NSN, the US.

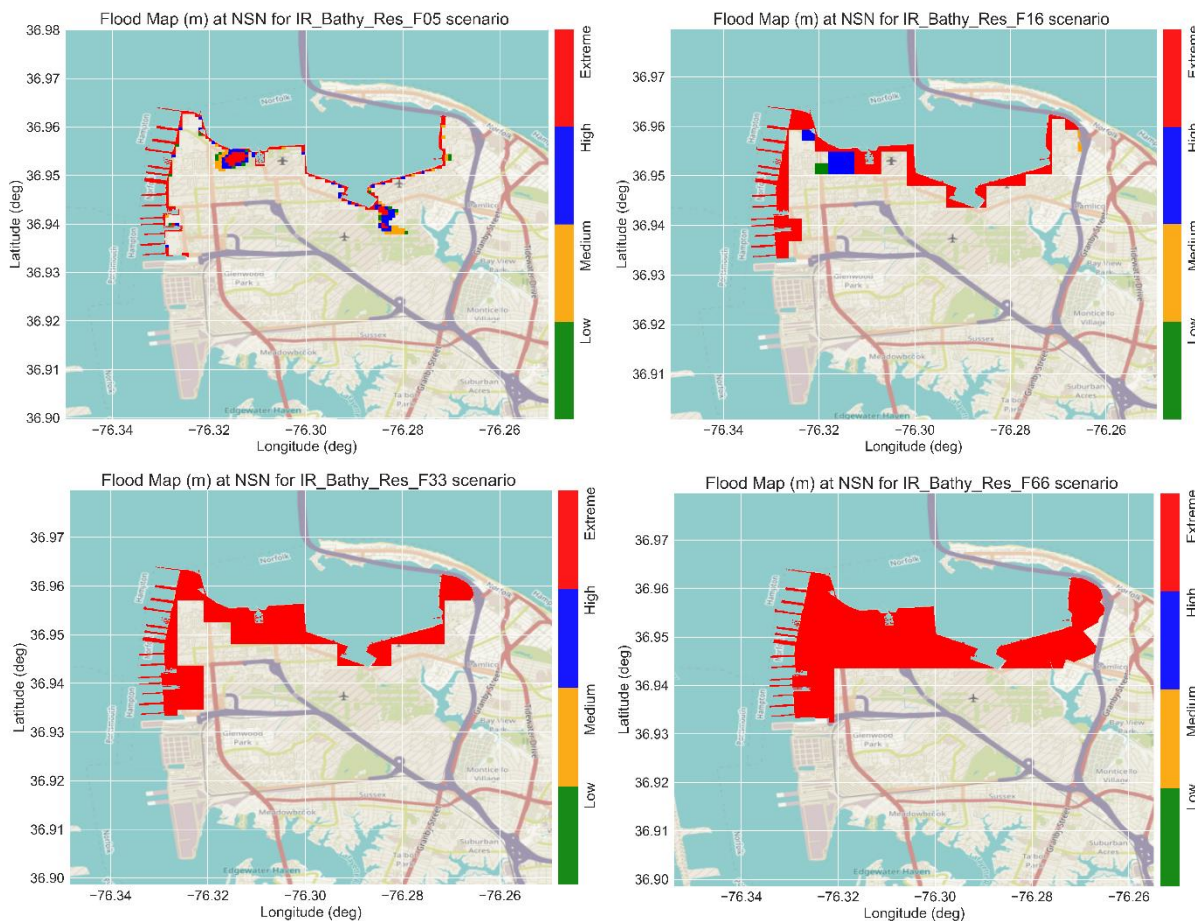


Figure 121. Flood maps with the flood levels for Hurricane Irene during the peak surge for the bathymetry Resolution scenarios at NSN, the US.

6.3. SWAN

6.3.1. Model Calibration (baseline scenarios)

I. Hurricane Irene

Model calibration was carried out at several locations, Figure 122, by comparing the measured Significant Wave Height (SWH) with the simulated wave heights. The calibration procedure was done for both wind forces and all hurricanes, based on Hurricane Irene calibration settings.

Figure 123 and Figure 124 show the time series and the scatter plot of the measured and simulated SWH at the different stations during August 2011 (Hurricane Irene). It can be shown that there is a high agreement between the simulated and measured SWH at all stations. However, an overestimation was detected during the peak of the storm at Virginia Beach. Statistically speaking, the model shows a good performance with a high correlation coefficient and RMSE up to 98% and 0.23m respectively with an average bias of a few centimeters, Table 39.

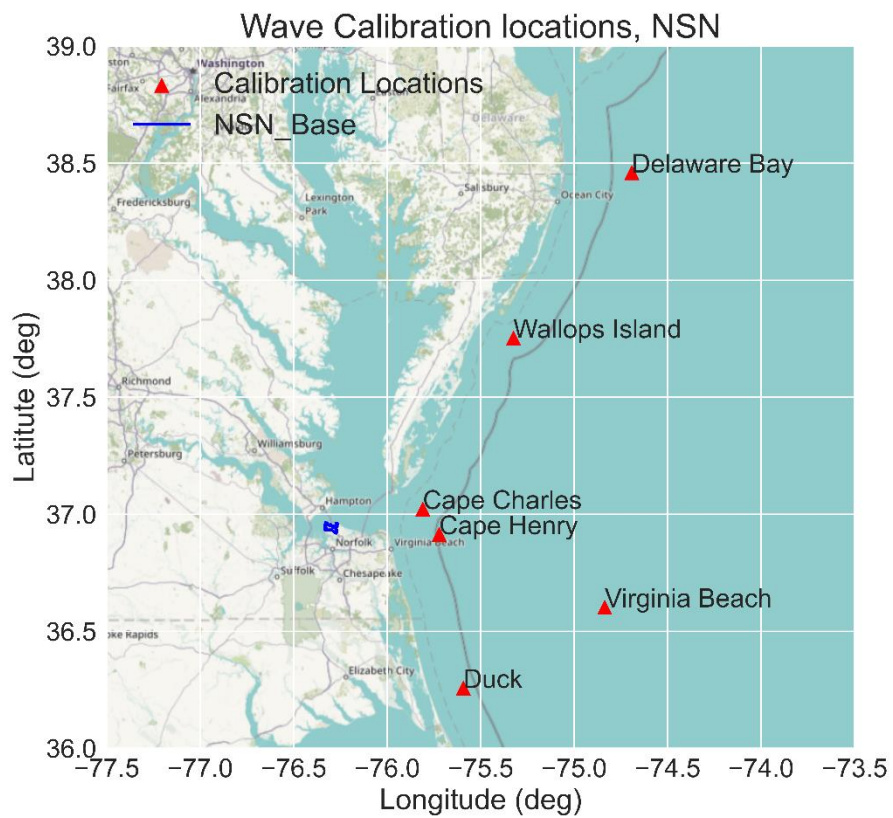


Figure 122. Thematic map showing the wave calibration locations along the US east coast during all hurricanes.

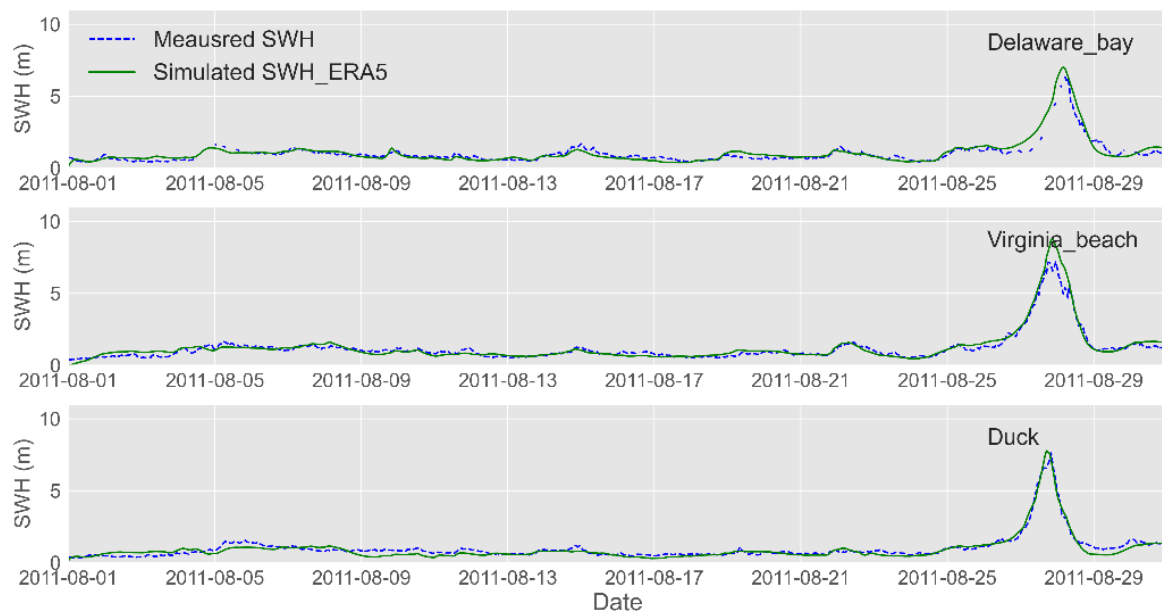


Figure 123. Time series of the measured and simulated SWH (m) at Delaware Bay, Virginia Beach, and Duck during August 2011 (Hurricane Irene).

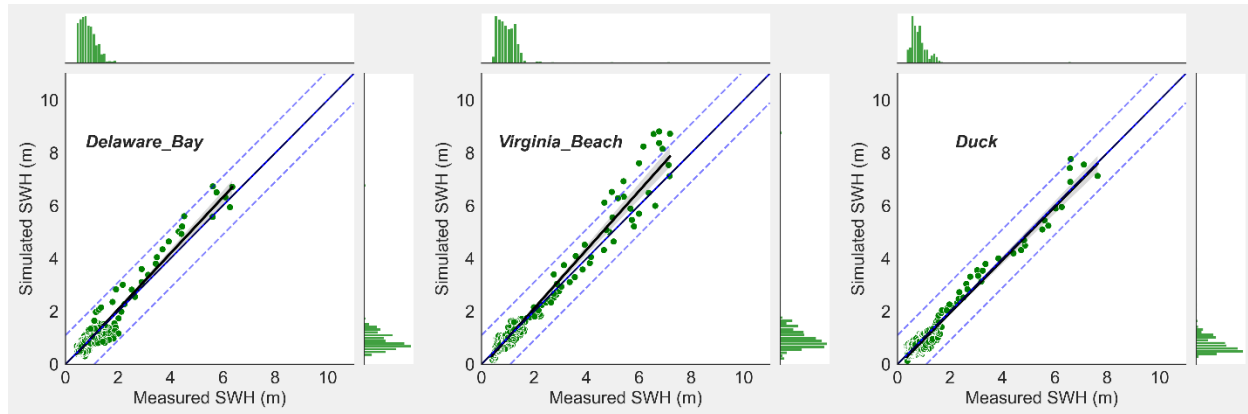


Figure 124. Scatter plot showing the measured vs simulated SWH (m) at Delaware Bay, Virginia Beach, and Duck during August 2011 (Hurricane Irene). Histograms are plotted along the upper and right axes.

Table 39. Error statistics of the D-waves model calibration at the different stations during Hurricane Irene 2011, US East Coast.

R	R ²	RMSE	NRMSE	Bias	RB	MNB	SI
---	----------------	------	-------	------	----	-----	----

Duck	0.97	0.94	0.23	0.03	-0.08	-0.08	-0.09	0.23
Delaware Bay	0.95	0.91	0.27	0.05	0.03	0.03	0.03	0.27
Virginia Beach	0.98	0.96	0.29	0.04	0.05	0.04	0.04	0.24

However, significant variations were observed in the predicted SWH using ERA5 and HM winds. The model has a high tendency to overestimate the peak wave height using HM wind forces compared to ERA5 winds, Figure 125 and Figure 126. This resulted in a more accurate prediction of the SWH (during the storm) using ERA5 with an average RMSE and Bias of 0.46m and 0.10m respectively, compared to 0.91m and 0.48m respectively for the HM simulation, Table 40. Nevertheless, model results using both wind forces are still within the acceptable range except for Virginia Beach where the model overestimates the SWH by more than 3m using the HM wind forces. This overestimation might be attributed to the inaccurate representation of the bathymetry at this offshore deep-water location.

The same pattern can be observed in the spatial distribution of the SWH along the US East Coast, Figure 127, where it can be observed that, compared to the ERA5 results, the model significantly overestimates the SWH using HM pushing higher waves towards the east coast, *Figure 127* (middle panels). However, most of these waves rapidly dissipate as they approach the Chesapeake Bay such that a maximum wave height of less than 1m was predicted at NSN (Sewells Point), with higher waves up to 2m, along the Willoughby Spit, *Figure 127* (lower panels).

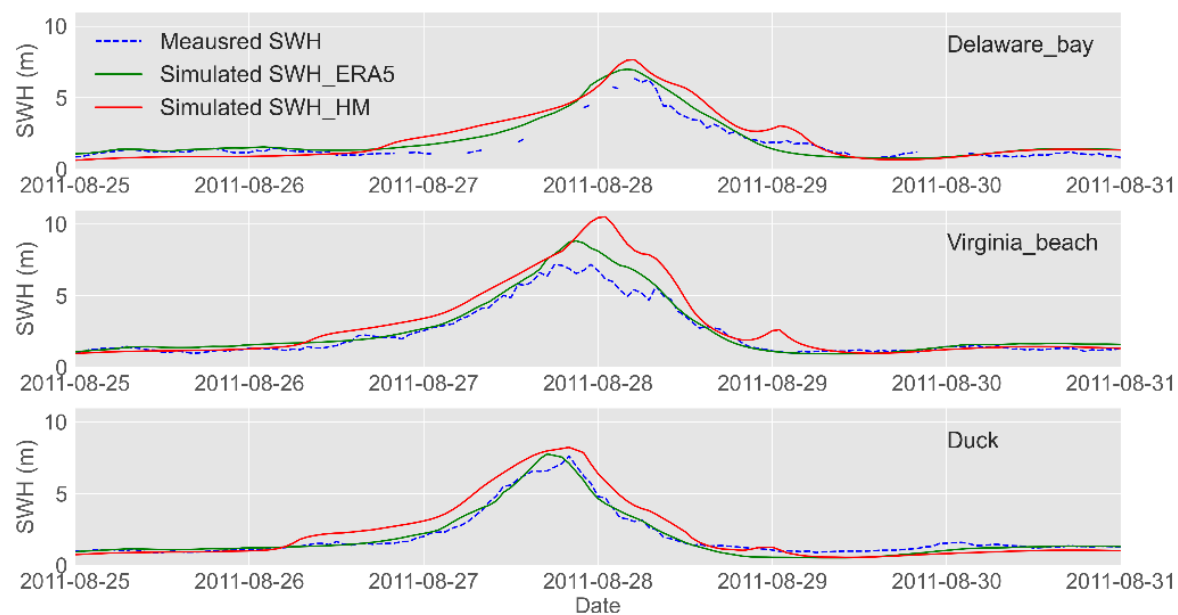
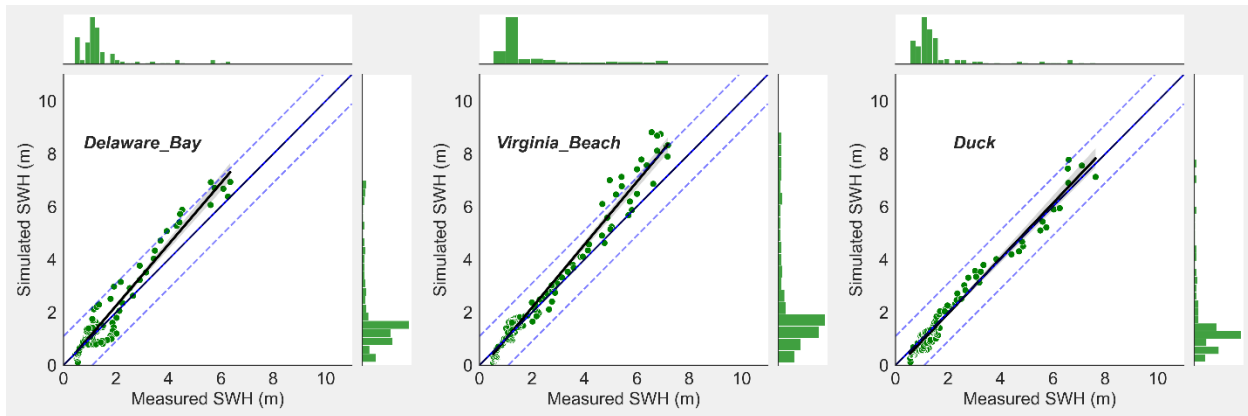


Figure 125. Time series of the measured and simulated SWH using ERA5 (green) and HM (red) wind data during Hurricane Irene 2011, US East Coast.



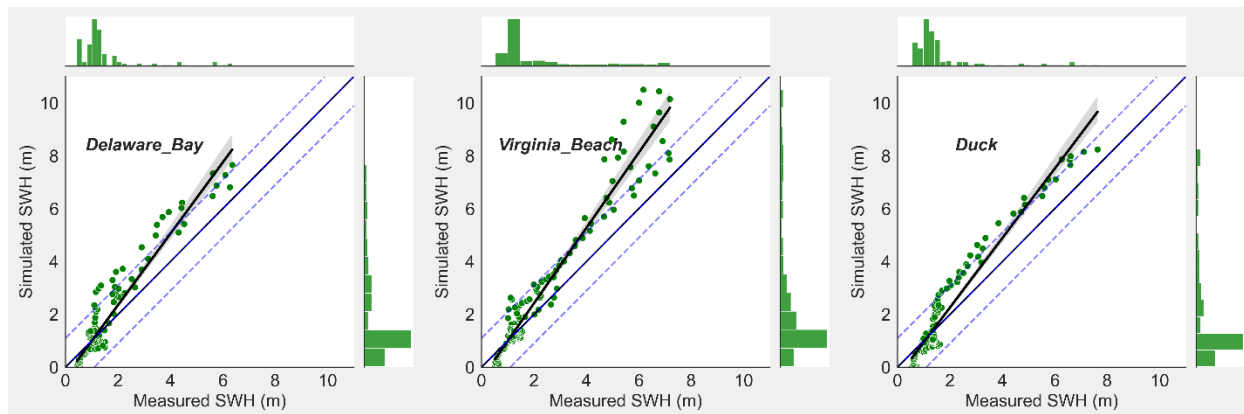


Figure 126. Scatter plots of the measured and simulated SWH (m) using ERA5 (upper panels) and HM (lower panels) during Hurricane Irene 2011, US East Coast.

Table 40. Error statistics of the simulated SWH (m) using ERA5 and HM during Hurricane Irene 2011, US East Coast.

Hurricane		R	RMSE	Bias
IR	ERA5_1M*	0.97	0.27	0.01
	ERA5	0.97	0.46	0.10
	HM	0.96	0.91	0.48

*1M: One-month simulation

Although the storm introduced relatively high-energy waves approaching the Chesapeake Bay from the ESE direction, the surf zone of NSN seems to be dominated by a lower energy wave approaching from the N-NE direction (from the Chesapeake Bay).

Therefore, a comparison between the baseline scenarios and all the implemented scenarios, in terms of wave heights, was made at four points around the Willoughby Spit and NSN, Figure 128 and Figure 129. It can be noticed that the predicted SWH using HM is relatively higher than the predicted values using ERA5 at all locations. In addition, different peaks were observed which might be associated with the typical change in the wind direction as the storm passes through. These peaks are more pronounced in the HM simulations.

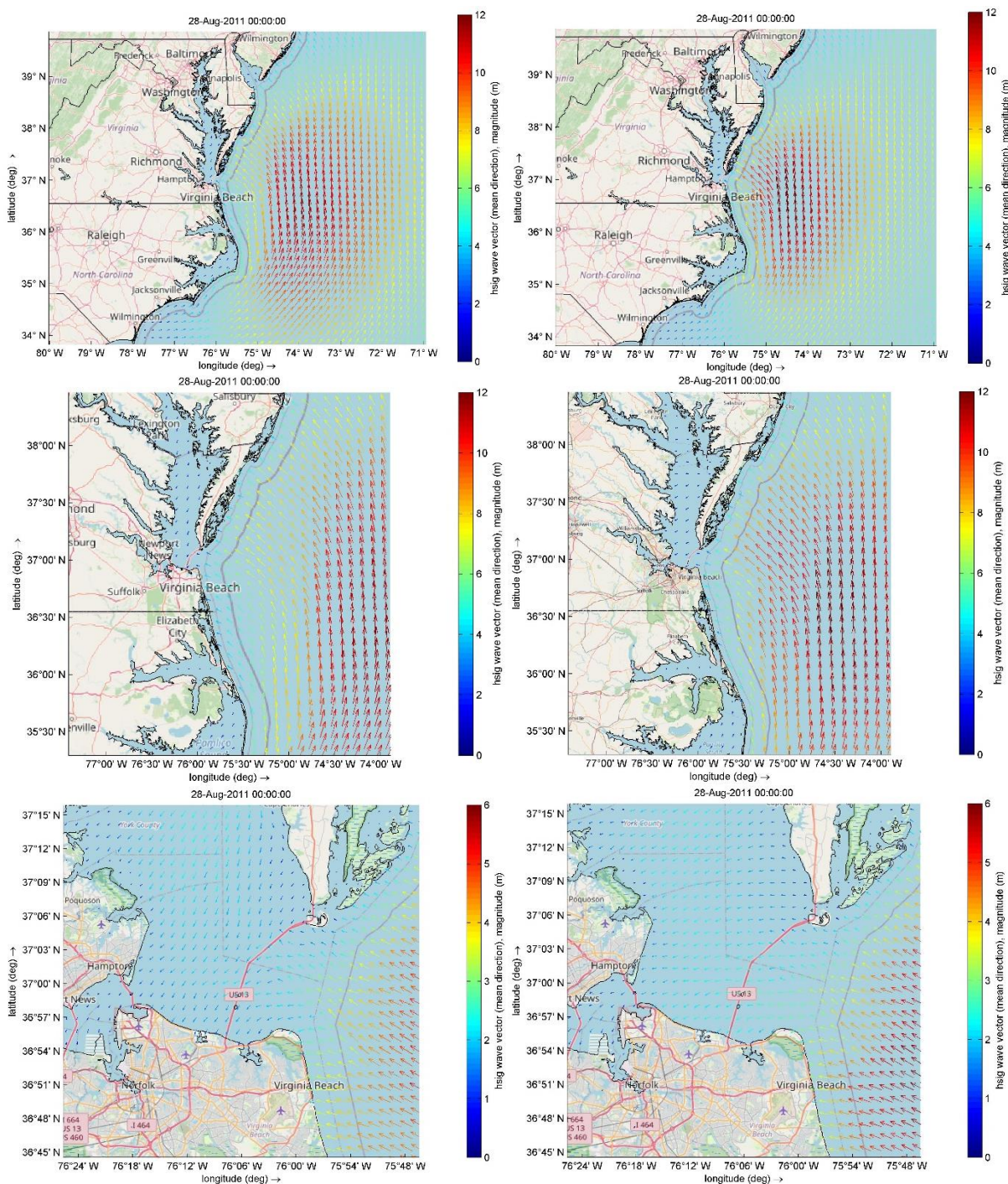


Figure 127. Spatial distribution of the SWH (m) and wave direction (degree) using ERA5 (left panels) and HM (right panels) winds during Hurricane Irene along the different D-Waves domains, coarse domain (upper panels), intermediate domain (middle panels) and high-resolution domain (lower panels), the US east coast.

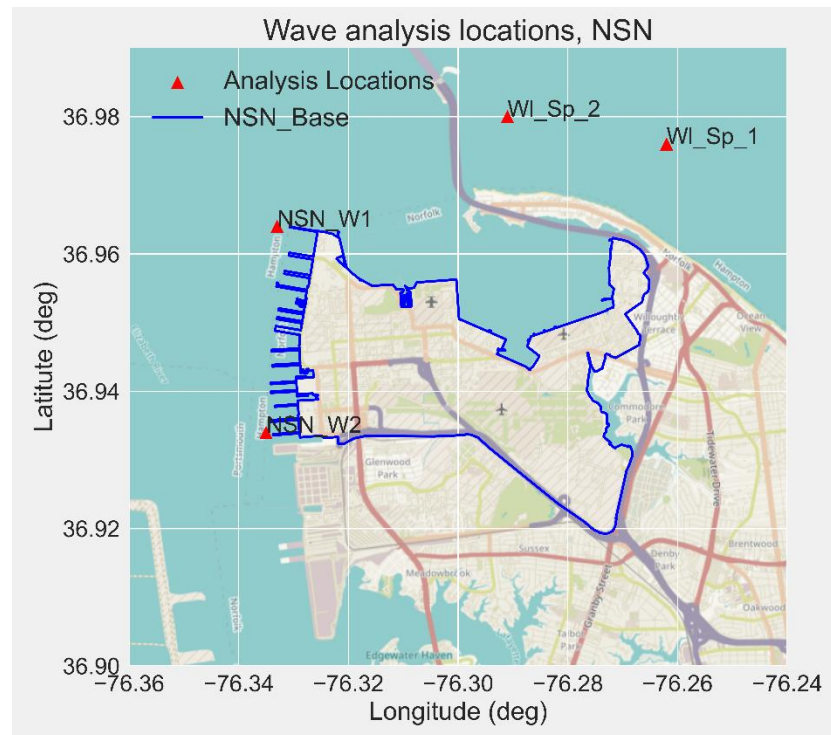


Figure 128. Thematic map showing the locations where the wave analysis was carried out at NSN, the US.

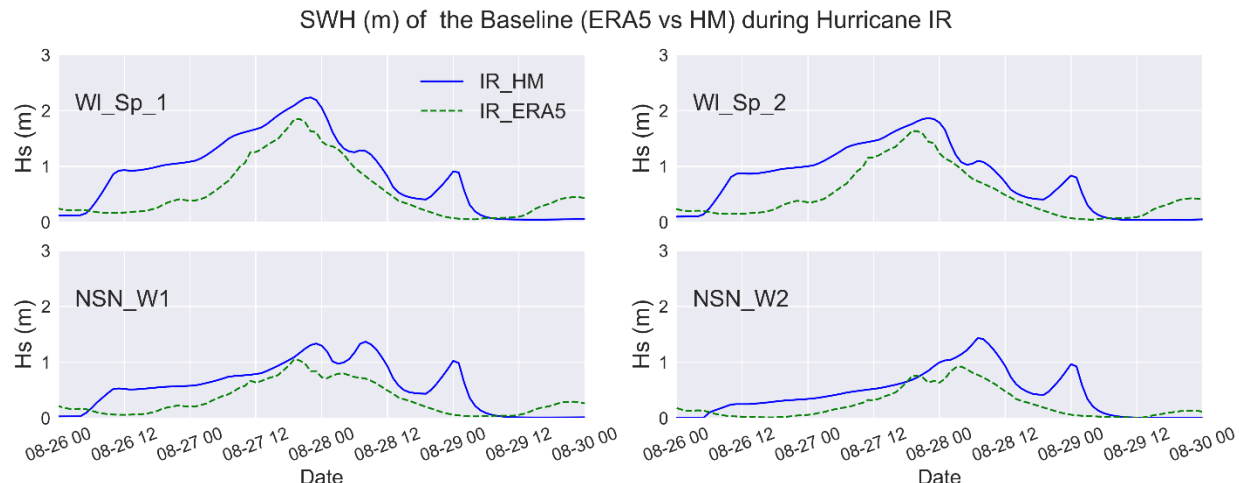


Figure 129. Significant wave height (H_s) (m) using ERA5 and HM at the four points along the Willoughby Spit and NSN base during Hurricane Irene 2011, the US East Coast.

II. Hurricane Isabel

Due to the lack of measurements, the calibration of Hurricane Isabel was performed at the Delaware Bay buoy only. Figure 130 and Figure 131 show the time series and the scatter plot of

the measured and simulated SWH at Delaware Bay station during September 2003 (Hurricane Isabel). It can be shown that there is a high agreement between the simulated and measured SWH with some overestimation during the peak of the storm. The results have a high correlation coefficient and RMSE up to 94% and 0.37m respectively, Table 41. Although the RMSE is a bit higher than that obtained for Hurricane Irene, it is still within the acceptable range (< 20%).

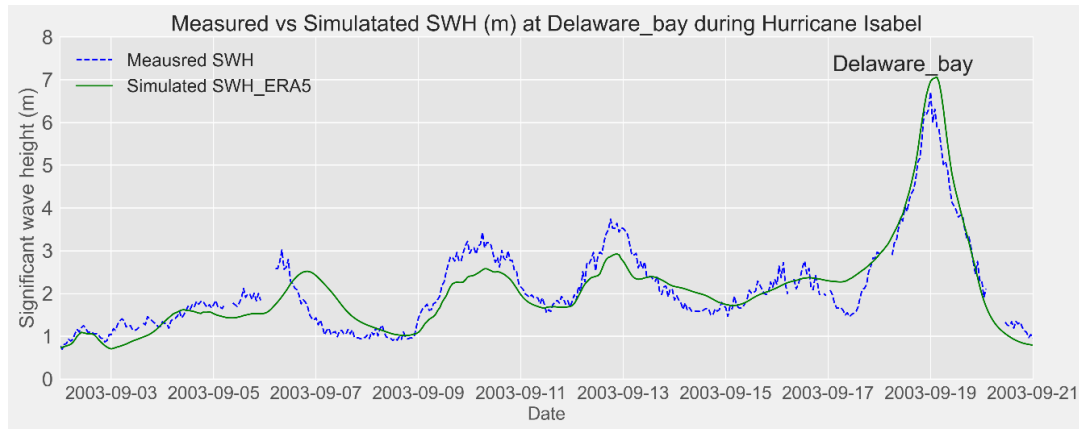


Figure 130. Time series of the measured and simulated SWH (m) at Delaware Bay during September 2003 (Hurricane Isabel).

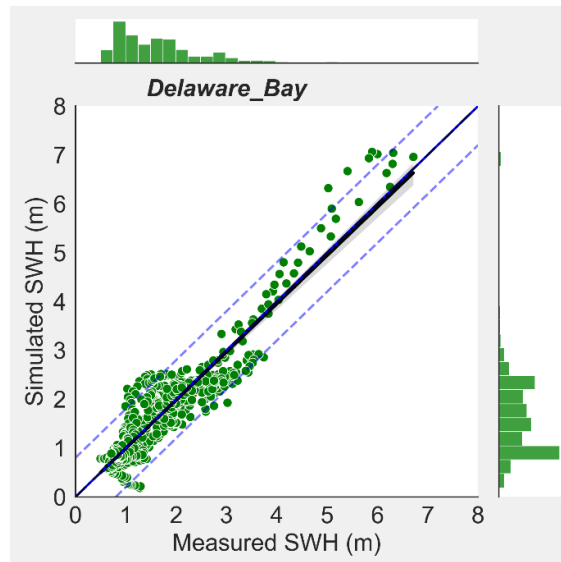


Figure 131. Scatter plot showing the measured vs simulated SWH (m) at Delaware Bay. Histograms are plotted along the upper and right axes.

Table 41. Error statistics of the D-waves model calibration at the Delaware Bay

Station	R	R ²	RMSE	NRMSE	Bias	RB	MNB	SI
Delaware Bay	0.94	0.88	0.37	0.06	0.01	0	0	0.21

Minor variations though were detected in the predicted SWH during Hurricane Isabel using ERA5 and HM winds, however, the model overestimated the peak wave height using both wind forces, Figure 132 and Figure 133 with an average RMSE and Bias of 0.49m and 0.21m respectively.

The same pattern can be observed in the spatial distribution of the SWH along the US East Coast, Figure 134, where comparable results were obtained using both wind forces data with relatively high wave heights approaching the area from the east with a magnitude of >6m. The waves still rapidly dissipate as they approach the Chesapeake Bay such that a maximum wave height of 1m was predicted at NSN (Sewells Point), with slightly higher waves, up to 2-2.5m, along Willoughby Spit. In addition, the storm-induced waves approaching the Chesapeake Bay from the E-ESE sector dominate the surf zone of NSN, Figure 134 (lower panels). No distinguishable peaks were observed in addition to the main peak of the storm for Hurricane Isabel, Figure 135. This might be attributed to the difference between Hurricane Isabel and Hurricane Irene tracks. Hurricane Isabel passed 220km south of NSN, hence the base experienced the impact of the onshore wind only without any significant impact of the offshore directed winds.

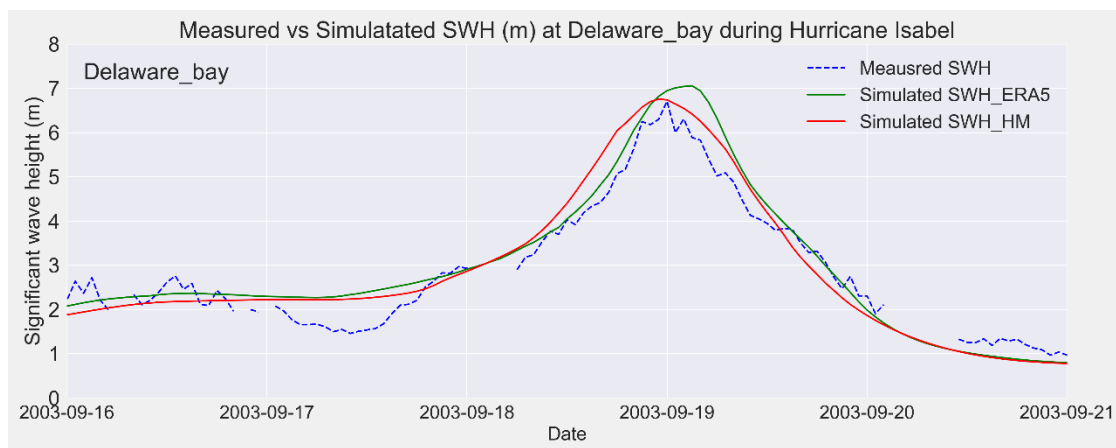


Figure 132. Time series of the measured and simulated SWH using ERA5 (green) and HM (red) wind data during Hurricane Isabel 2003, US East Coast.

Table 42. Error statistics of the simulated SWH (m) using ERA5 and HM during Hurricane Isabel 2003, US east coast.

Hurricane	R	RMSE	Bias
IS	ERA5 1M	0.94	0.37
	ERA5	0.96	0.50
	HM	0.98	0.49

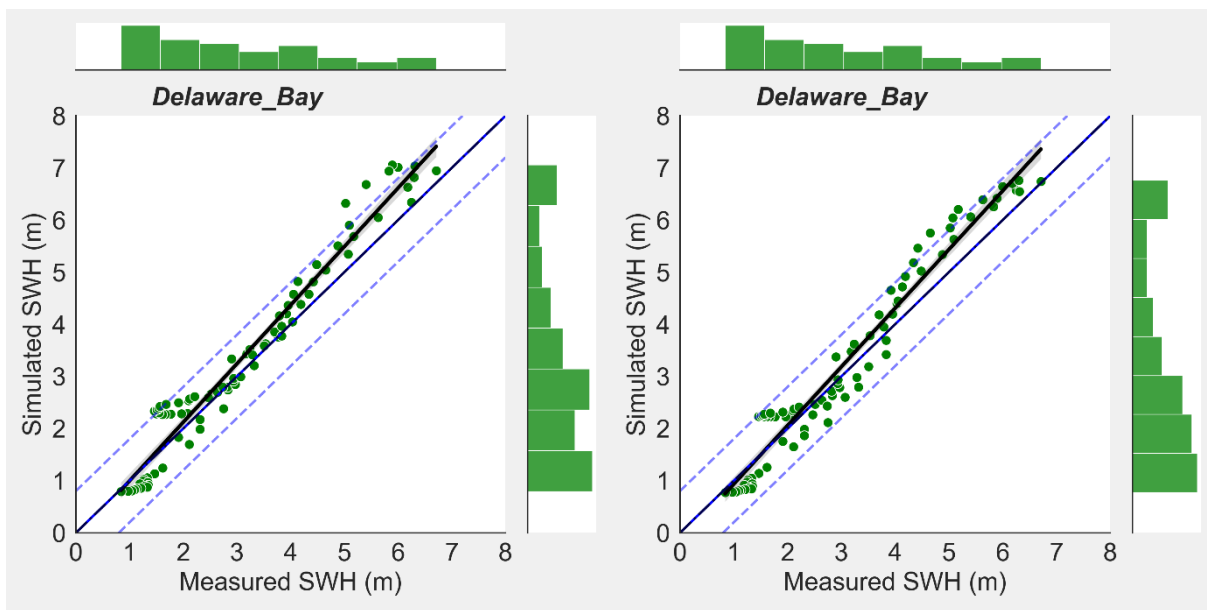


Figure 133. Scatter plots of the measured and simulated SWH (m) using ERA5 (left panel) and HM (right panel) during Hurricane Isabel 2003, US East Coast.

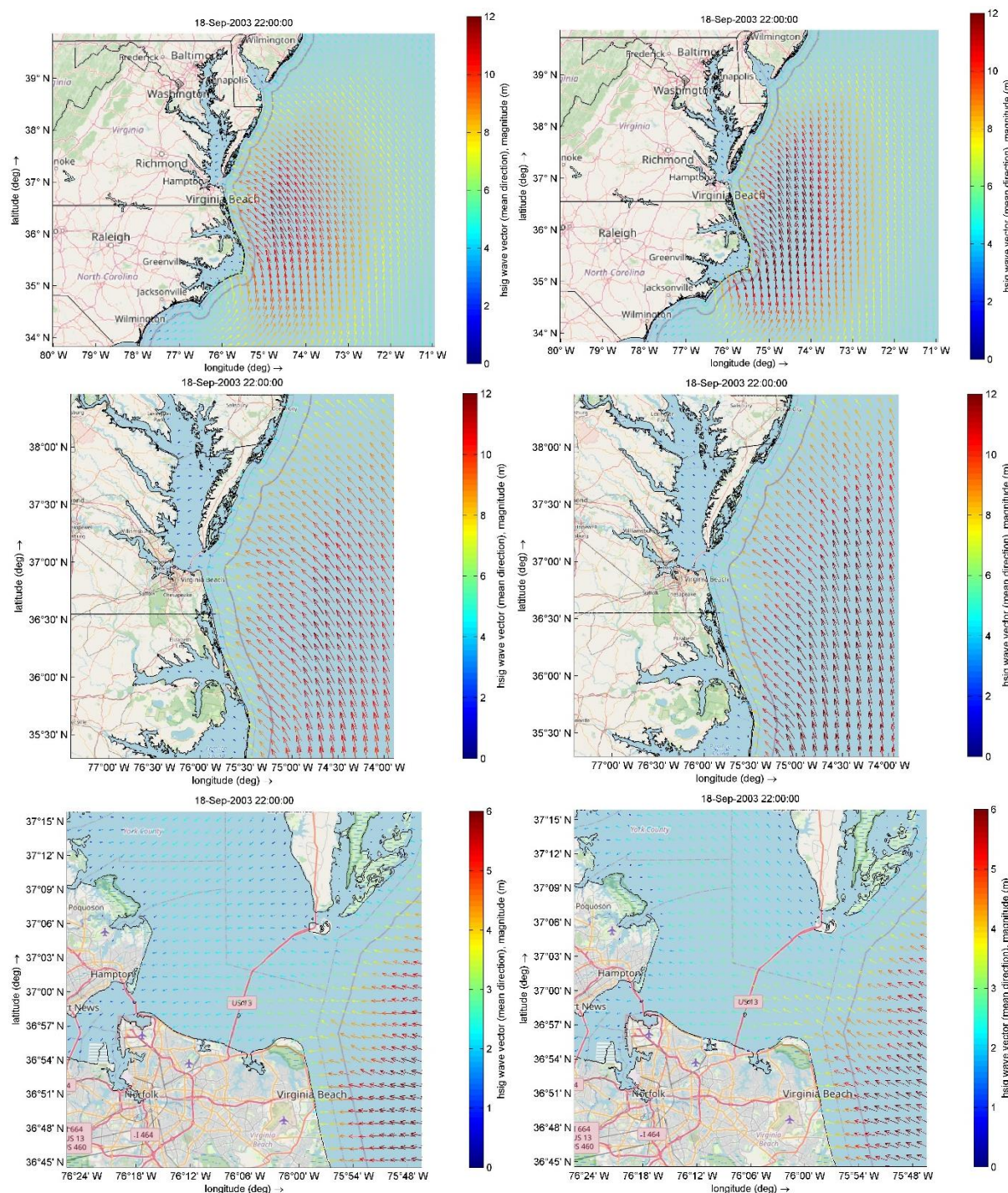


Figure 134. Spatial distribution of the SWH (m) and wave direction (degree) using ERA5 (left panels) and HM (right panels) winds during Hurricane Isabel along the different D-Waves domains, coarse domain (upper panels), intermediate domain (middle panels) and high-resolution domain (lower panels), the US east coast.

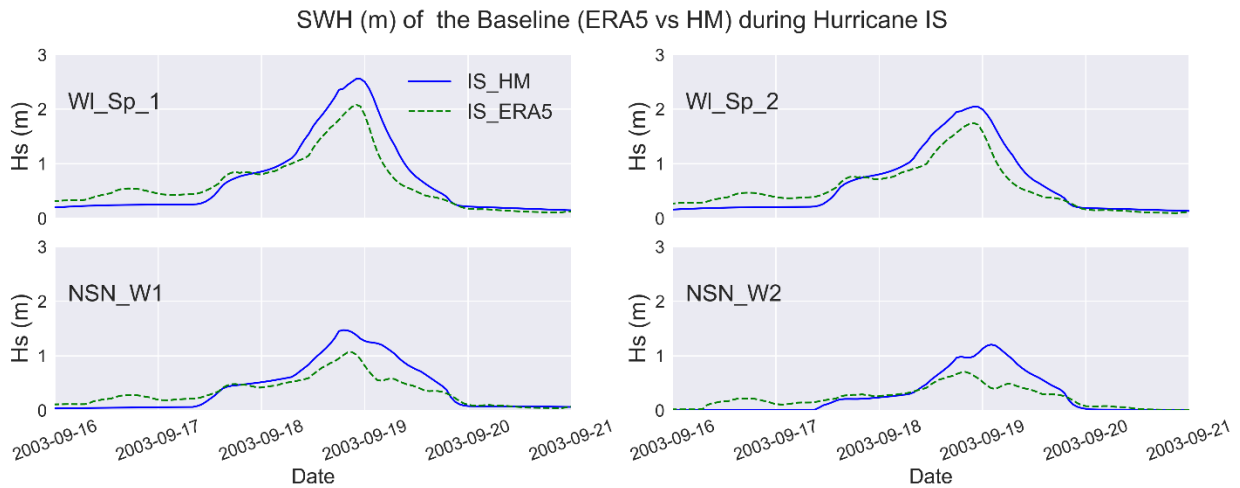


Figure 135. Significant wave height (H_s) (m) using ERA5 and Hm at the four points along the Willoughby Spit and NSN base during Hurricane Isabel 2003, the US east coast.

III. Hurricane Sandy

The calibration of Hurricane Sandy was performed at three locations, Delaware Bay, Cape Henry, and Cape Charles. Figure 136 and Figure 137 shows the time series and the scatter plot of the measured and simulated SWH at all stations during October 2012 (Hurricane Sandy). The model shows a high performance in predicting significant wave heights at all locations with some underestimation during the peak of the storm at the Delaware Bay location. The results have a high correlation coefficient and RMSE up to 98% and 0.25m respectively with an average bias of -0.11m, Table 43. Although the RMSE is a bit higher than that obtained for Hurricane Irene, it is still within the acceptable range (< 20%).

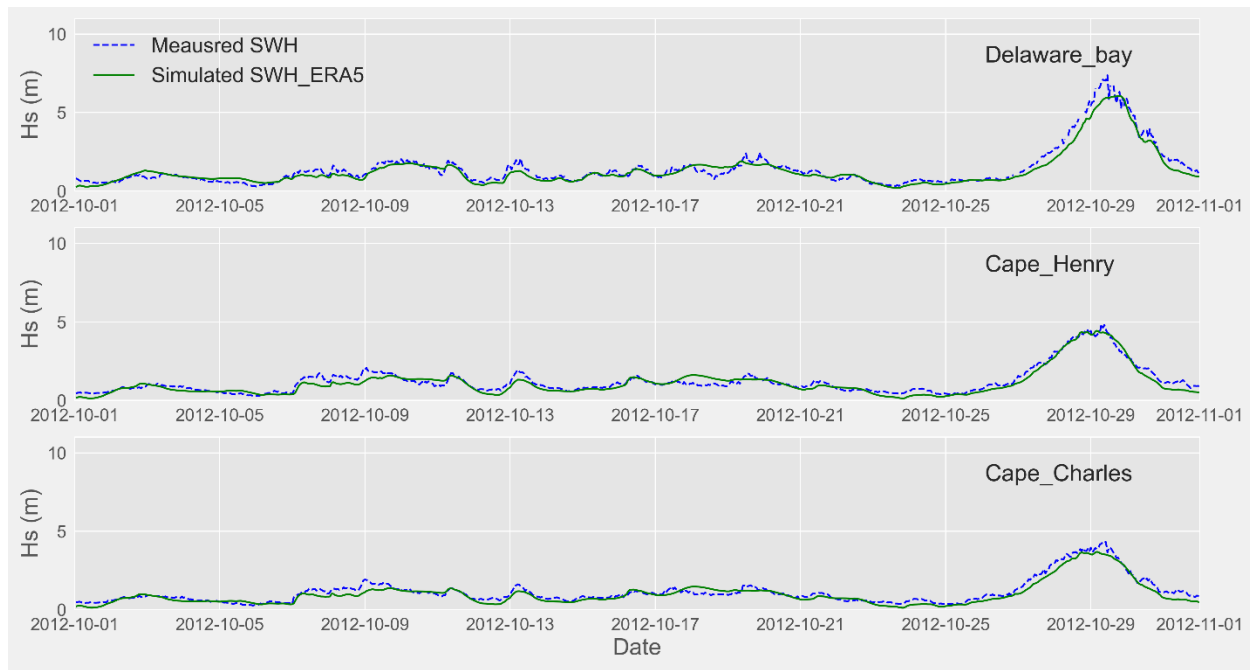


Figure 136. Time series of the measured and simulated SWH (m) at Delaware Bay, Cape Henry, and Cape Charles during October 2012 (Hurricane Sandy).

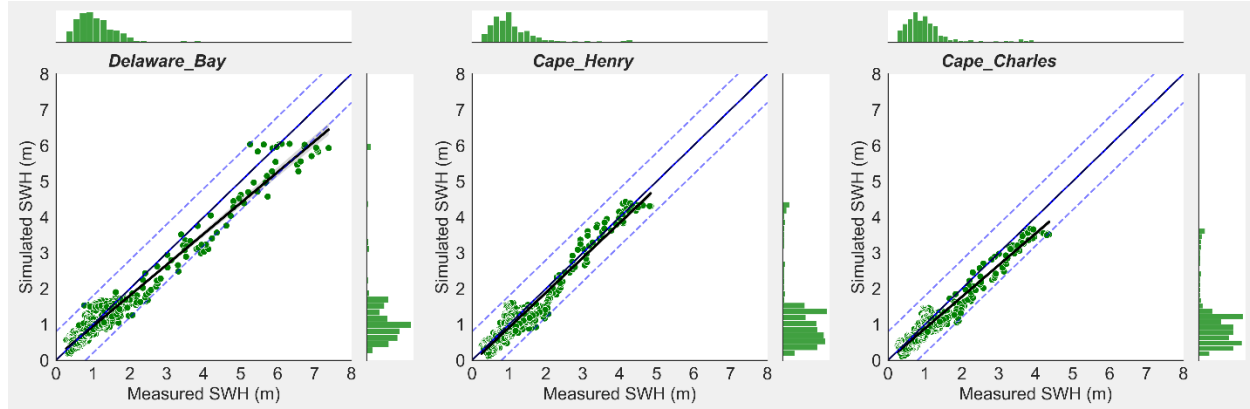


Figure 137. Scatter plot showing the measured vs simulated SWH (m) at Delaware Bay, Cape Henry, and Cape Charles. Histograms are plotted along the upper and right axes.

Table 43. Error statistics of the D-waves model calibration at the different stations.

	R	R^2	RMSE	NRMSE	Bias	RB	MNB	SI
Delaware Bay	0.98	0.95	0.32	0.04	-0.12	-0.08	-0.09	0.22
Cape Henry	0.96	0.93	0.26	0.06	-0.1	-0.08	-0.09	0.21
Cape Charles	0.97	0.93	0.25	0.06	-0.13	-0.12	-0.13	0.22

Comparing the model results using ERA5 and HM wind data during Hurricane Sandy showed significant variation between both wind forces. Although the model marginally underestimated the SWH using ERA5 data, a significant overestimation was observed in SWH at or near the measured peak with underestimation everywhere else using HM wind data, Figure 138 and Figure 139. This resulted in a relatively large RMSE and bias of 0.91m and -0.39 with a lower correlation of 90% using HM data, Table 44.

Observing the spatial distribution of the SWH, Figure 140, showed significantly higher SWH using HM compared to ERA5 data with relatively lower wave heights approaching the area from the east with a magnitude of 4m. The waves still rapidly dissipate as they approach Chesapeake Bay such that a maximum wave height of less than 0.7m was predicted at NSN, with slightly higher waves, up to 1m, along Willoughby Spit using ERA5 data. The waves approaching from the Chesapeake Bay from the N-E sector seem to dominate the area of NSN, Figure 140 (lower panels). However, higher values were obtained using HM data with SWH up to 2.25m in the vicinity of NSN, Figure 141. These waves are associated with the NW winds of Hurricane Sandy as it made its landfall 320km north of the study area. These winds blow over Chesapeake Bay generating relatively high wave heights, higher than that generated offshore by the storm, along NSN.

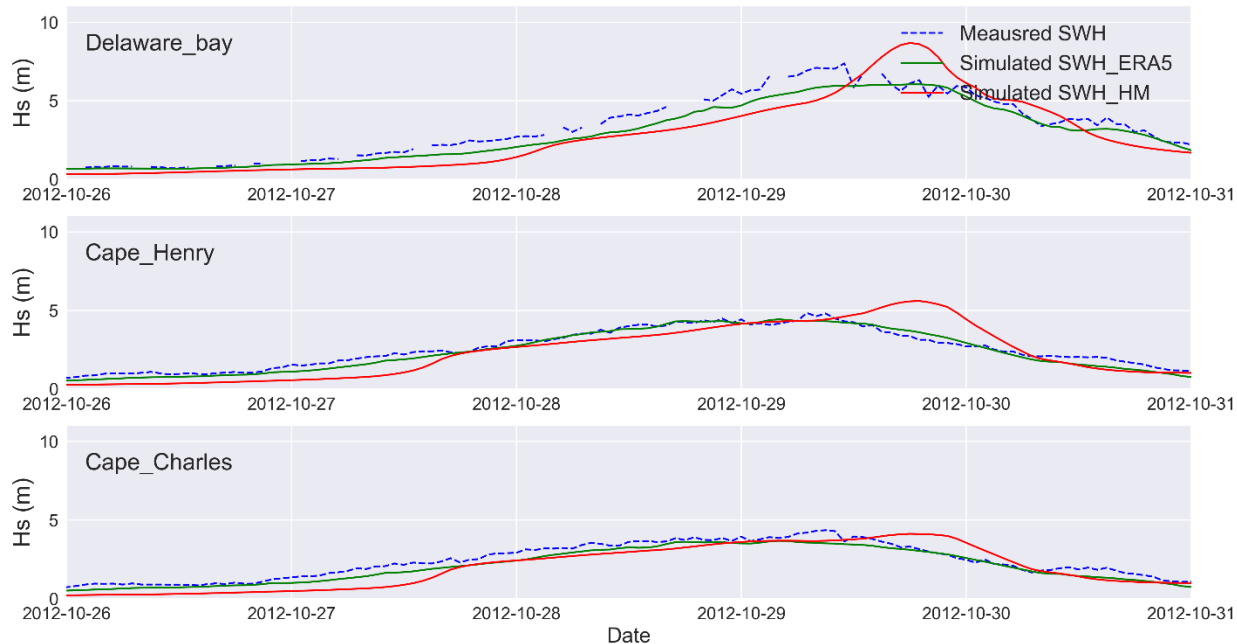


Figure 138. Time series of the measured and simulated SWH using ERA5 (green) and HM (red) wind data during Hurricane Sandy 2012, US East Coast.

Table 44. Error statistics of the simulated SWH (m) using ERA5 and HM during Hurricane Sandy 2012, US East Coast.

Hurricane		R	RMSE	Bias
SA	ERA5_1M	0.97	0.28	-0.12
	ERA5	0.98	0.41	-0.30
	HM	0.90	0.91	-0.39

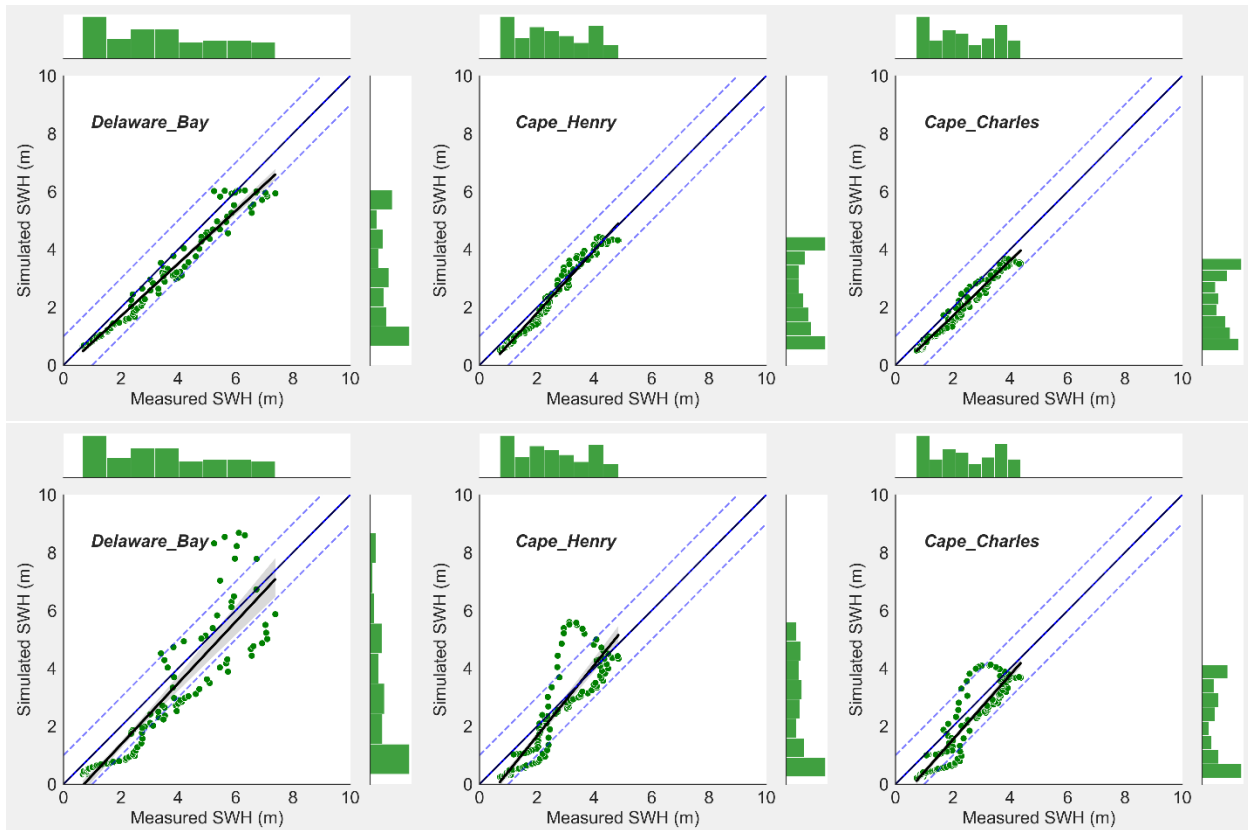


Figure 139. Scatter plots of the measured and simulated SWH (m) using ERA5 (upper panels) and HM (lower panels) during Hurricane Sandy 2012, US East Coast.

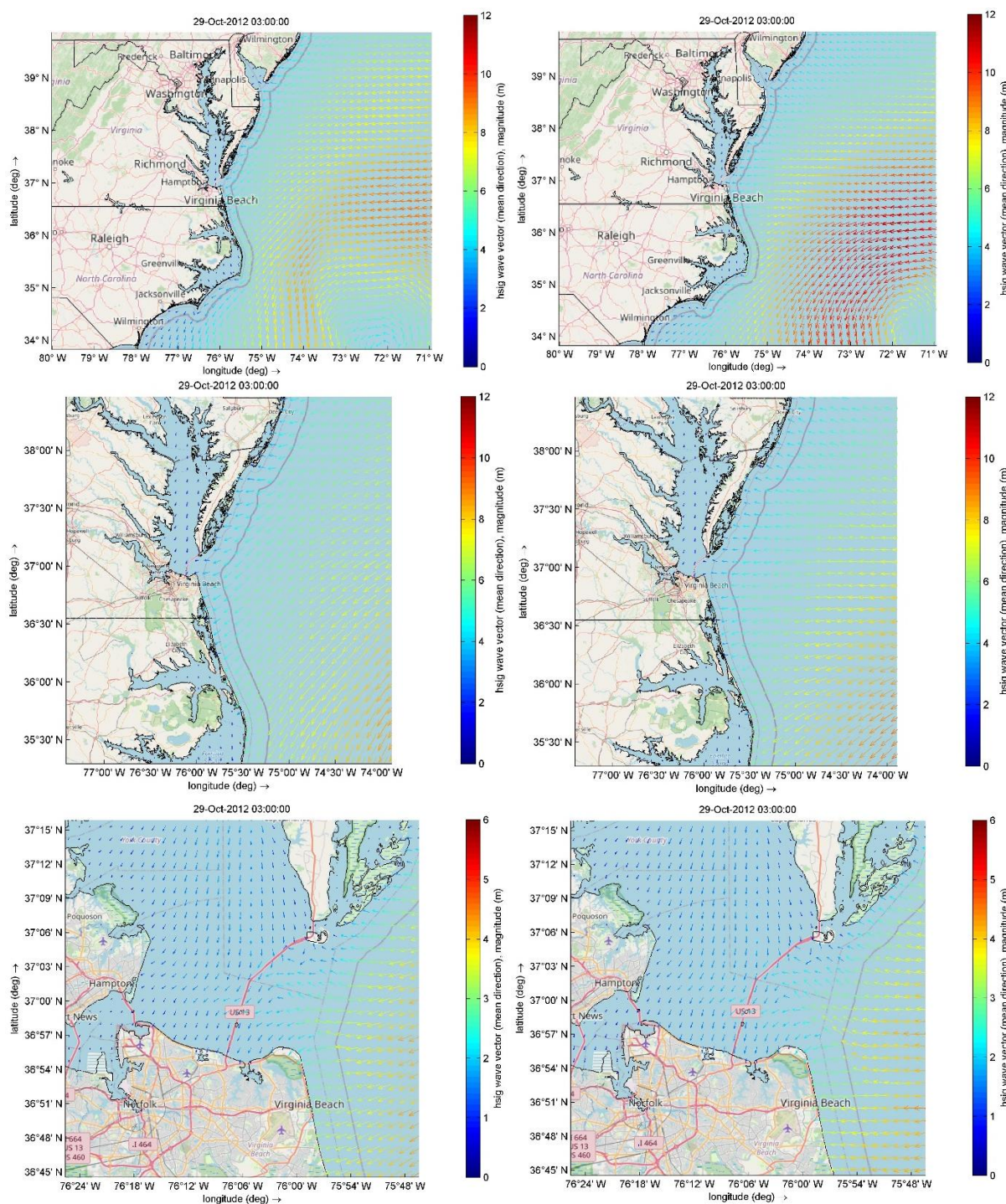


Figure 140. Spatial distribution of the SWH (m) and wave direction (degree) using ERA5 (left panels) and HM (right panels) winds during Hurricane Sandy along the different D-Waves domains, coarse domain (upper panels), intermediate domain (middle panels) and high-resolution domain (lower panels), the US east coast.

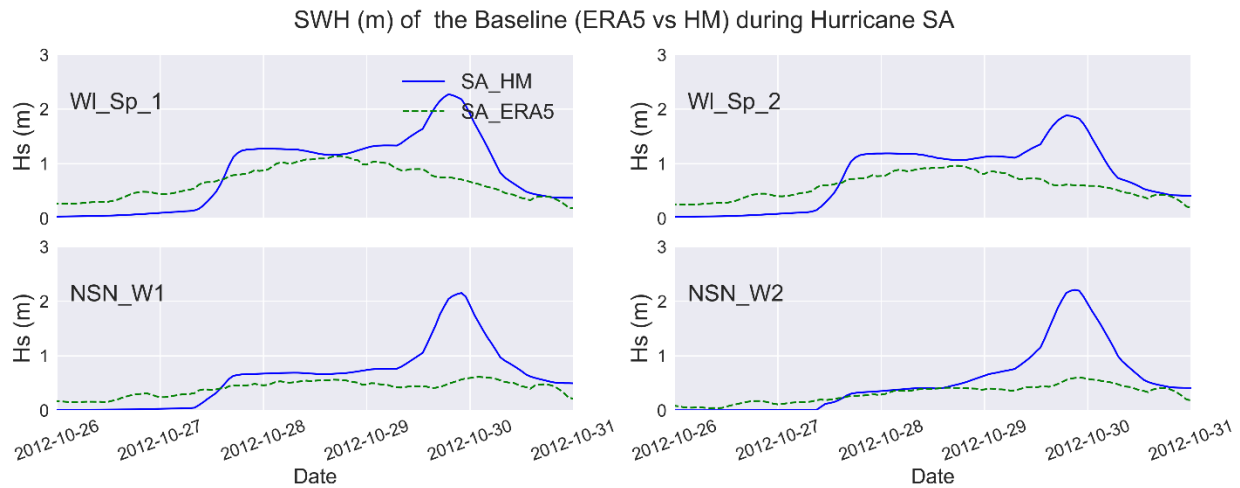


Figure 141. Significant wave height (H_s) (m) using ERA5 and HM at the four points along the Willoughby Spit and NSN base during Hurricane Sandy 2012, the US East Coast.

IV. Hurricane Michael

The calibration of Hurricane Michael was performed at four locations, Delaware Bay, Duck, Cape Henry, and Wallops Island. Figure 142 and Figure 143 show the time series and the scatter plot of the measured and simulated SWH at all stations during October 2018 (Hurricane Michael). The model shows a good performance in predicting significant wave heights at all locations with some underestimation. The results have a correlation coefficient of 79% - 93% with an average RMSE and bias of 0.3m and -0.14m respectively, Table 45. These results are still within the acceptable range (< 20%).

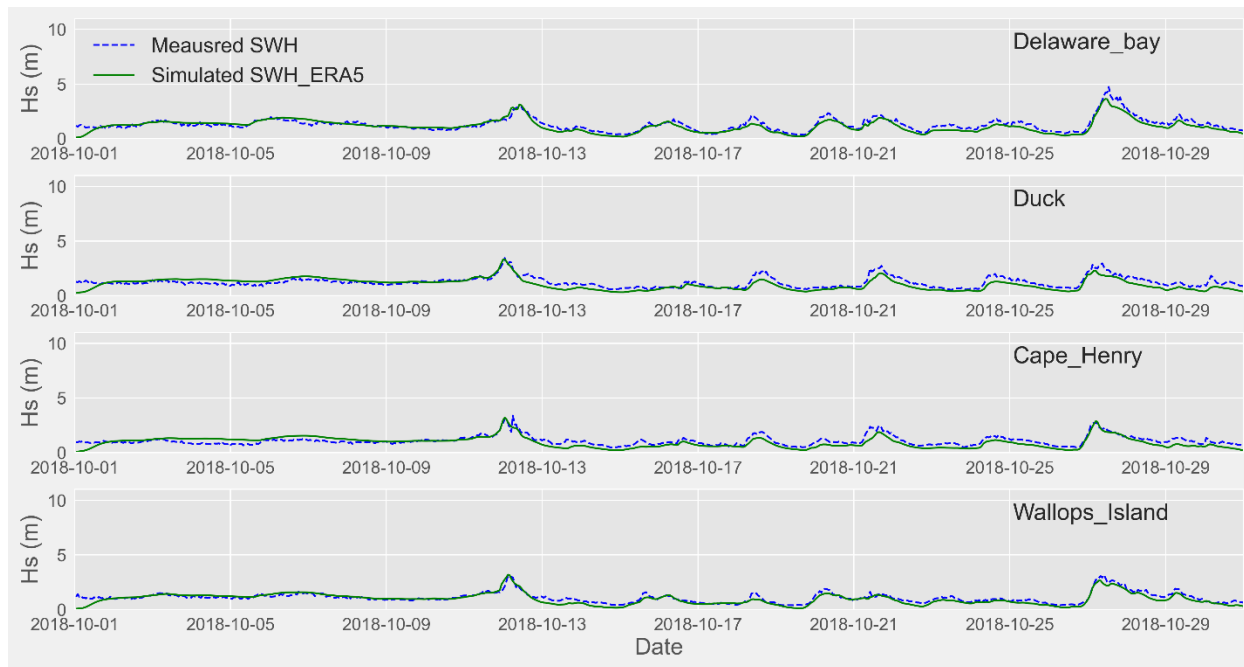


Figure 142. Time series of the measured and simulated SWH (m) at Delaware Bay, Duck, Cape Henry, and Wallops Island during October 2018 (Hurricane Michael).

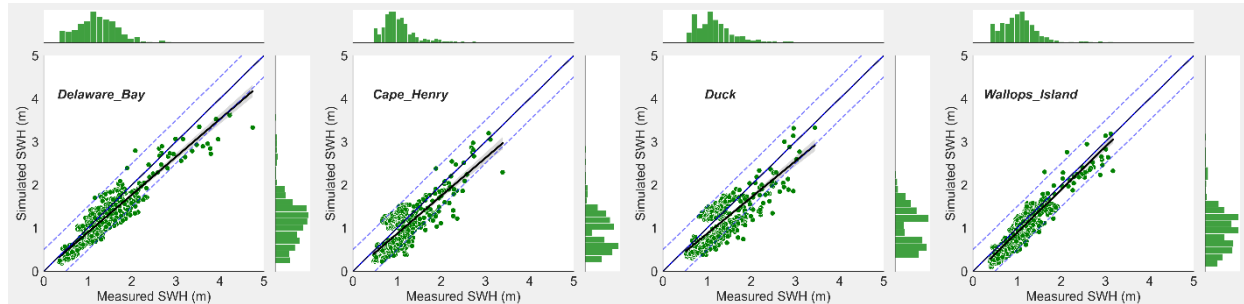


Figure 143. Scatter plot showing the measured vs simulated SWH (m) at Delaware Bay, Virginia Beach, and Duck. Histograms are plotted along the upper and right axes.

Table 45. Error statistics of the D-waves model calibration at the different stations during Hurricane Michael 2018, US East Coast.

Station	R	R2	RMSE	NRMSE	Bias	RB	MNB	SI
Delaware Bay	0.92	0.84	0.29	0.06	-0.15	-0.11	-0.13	0.22
Cape Henry	0.79	0.63	0.34	0.12	-0.15	-0.14	-0.16	0.31
Duck	0.8	0.64	0.36	0.12	-0.17	-0.14	-0.17	0.29
Wallops Island	0.93	0.86	0.22	0.08	-0.11	-0.1	-0.11	0.2

Comparing the model results using ERA5 and HM wind data during Hurricane Michael showed that the model marginally underestimated the SWH using ERA5 data. A significant overestimation was observed in SWH around the peak with underestimation away from the peak ($H_s < 1.5$) using HM wind data at all locations, Figure 144 and Figure 145. This resulted in a relatively large RMSE of 0.39m but with -0.04m bias due to the equivalence of the underestimation and overestimation in the SWH, Table 46.

Observing the spatial distribution of the SWH, Figure 146, showed significantly higher SWH using HM compared to ERA5 data with relatively lower wave heights approaching the area from the east with a magnitude of 3-4m. The waves still rapidly dissipate as they approach the Chesapeake Bay such that a maximum wave height of less than 0.5m was predicted at NSN, with slightly higher waves, up to 0.7m, along Willoughby Spit using ERA5 data. However, higher values were obtained using HM data with SWH up to 1.35m in the vicinity of NSN, Figure 147. These higher waves were also associated with the NW wind blowing along the Chesapeake Bay as the hurricane passed through NSN offshore.



Figure 144. Time series of the measured and simulated SWH using ERA5 (green) and HM (red) wind data during Hurricane Michael 2018, US East Coast.

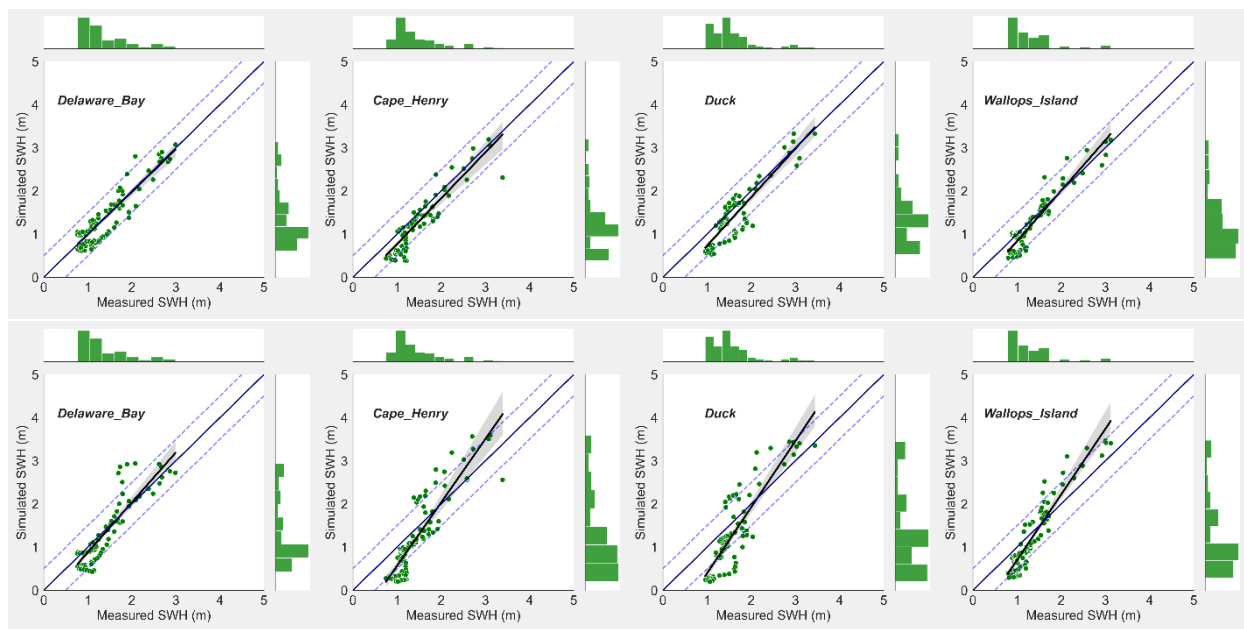


Figure 145. Scatter plots of the measured and simulated SWH (m) using ERA5 (upper panels) and HM (lower panels) during Hurricane Michael 2018, US East Coast.

Table 46. Error statistics of the simulated SWH (m) using ERA5 and HM during Hurricane Michael 2018, US east coast

Hurricane	R	RMSE	Bias
MI	ERA5_1M	0.86	0.30
	ERA5	0.92	-0.14
	HM	0.89	-0.04

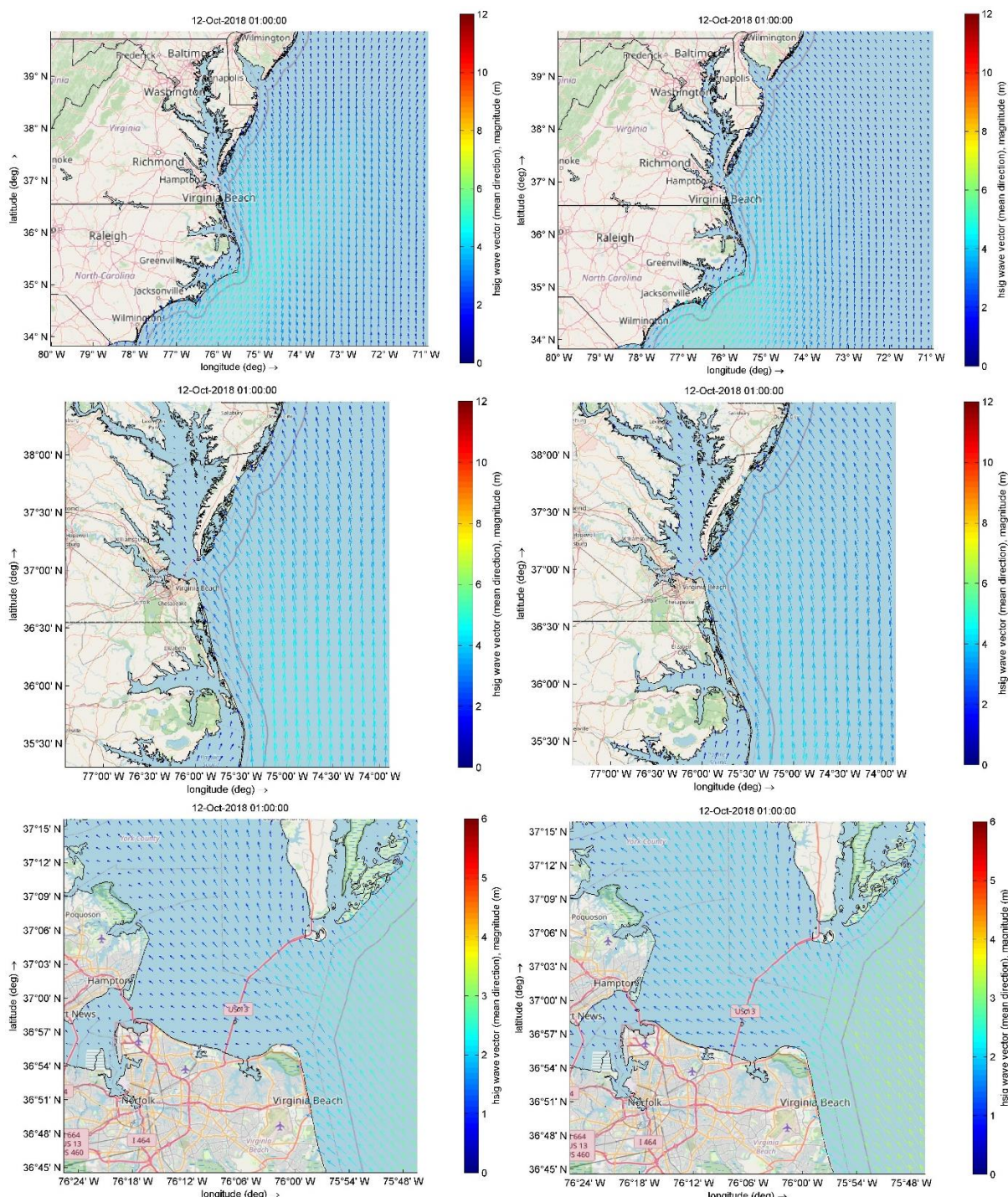


Figure 146. Spatial distribution of the SWH (m) and wave direction (degree) using ERA5 (left panels) and HM (right panels) winds during Hurricane Michael along the different D-Waves domains, coarse domain (upper panels), intermediate domain (middle panels) and high-resolution domain (lower panels), the US east coast.

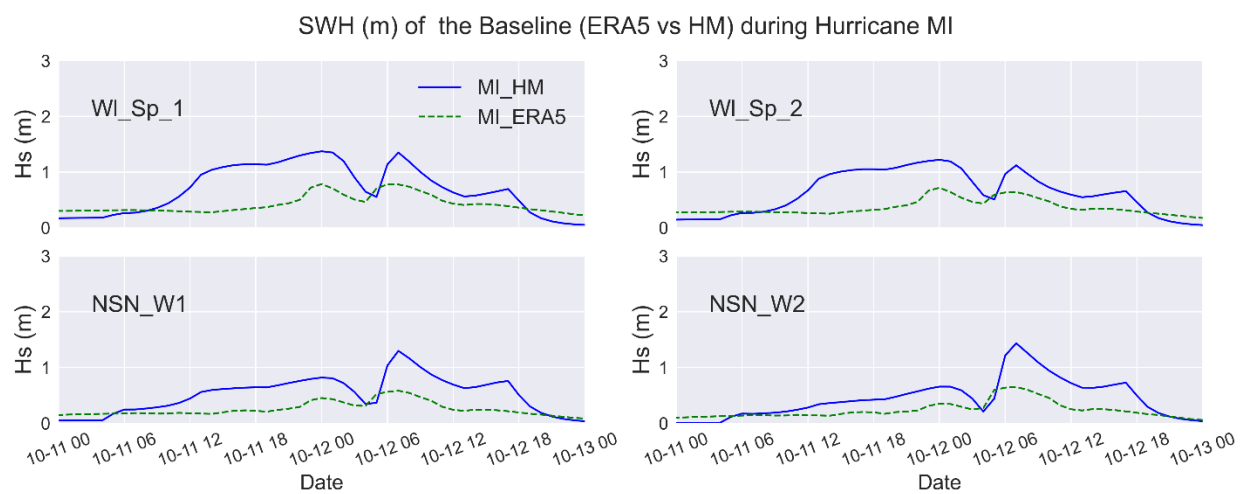


Figure 147. Significant wave height (H_s) (m) using ERA5 and HM at the four points along the Willoughby Spit and NSN base during Hurricane Michael 2018, the US East Coast.

6.3.2. Impacts of Meteorological Forces

i. Pressure Drop

Changing the central pressure of the hurricane showed an insignificant influence on the predicted wave height for all hurricanes at all stations, Figure 148. The contribution of the pressure gradient force showed a minor contribution compared to the surface wind stress, which is the dominant factor for wave growth.

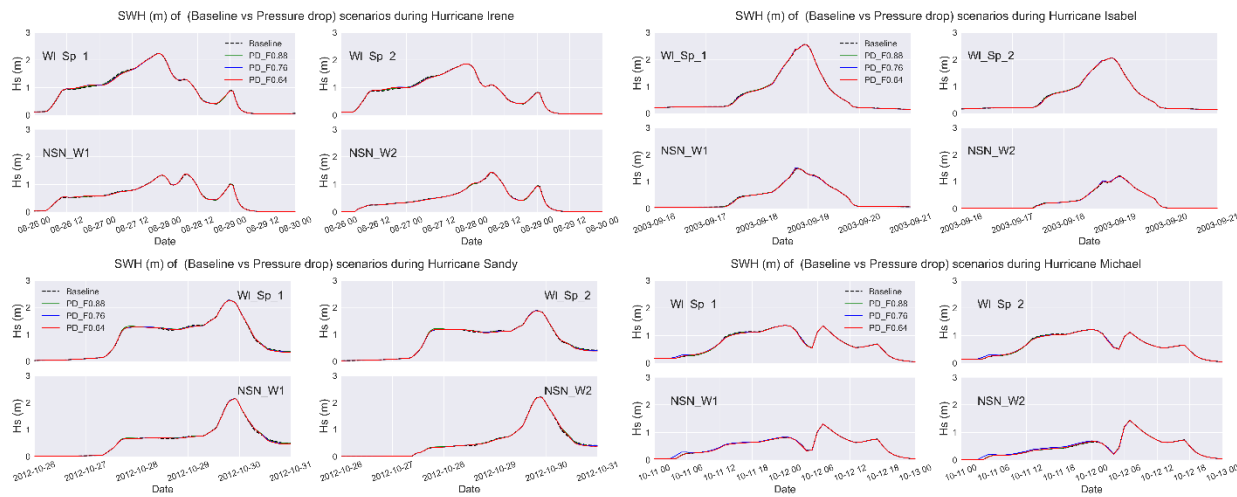


Figure 148. Significant wave height (H_s) (m) at the four points along the Willoughby Spit and NSN for Baseline and PD scenarios for all hurricanes, at NSN, the US.

During Hurricane Irene and Isabel, the maximum waves (peaks in Figure 148) are dominated by the waves approaching NSN from the offshore direction, Figure 149 panels A&B. Hurricane Sandy, however, affected the waves approaching the base from Chesapeake Bay, Figure 149 panel C, which is mainly attributed to the N-NW wind associated with the hurricane as it approaches the land. Hurricane Michael showed no dominant wave pattern, where offshore and Chesapeake Bay waves had almost equal significance, Figure 149 panel D.

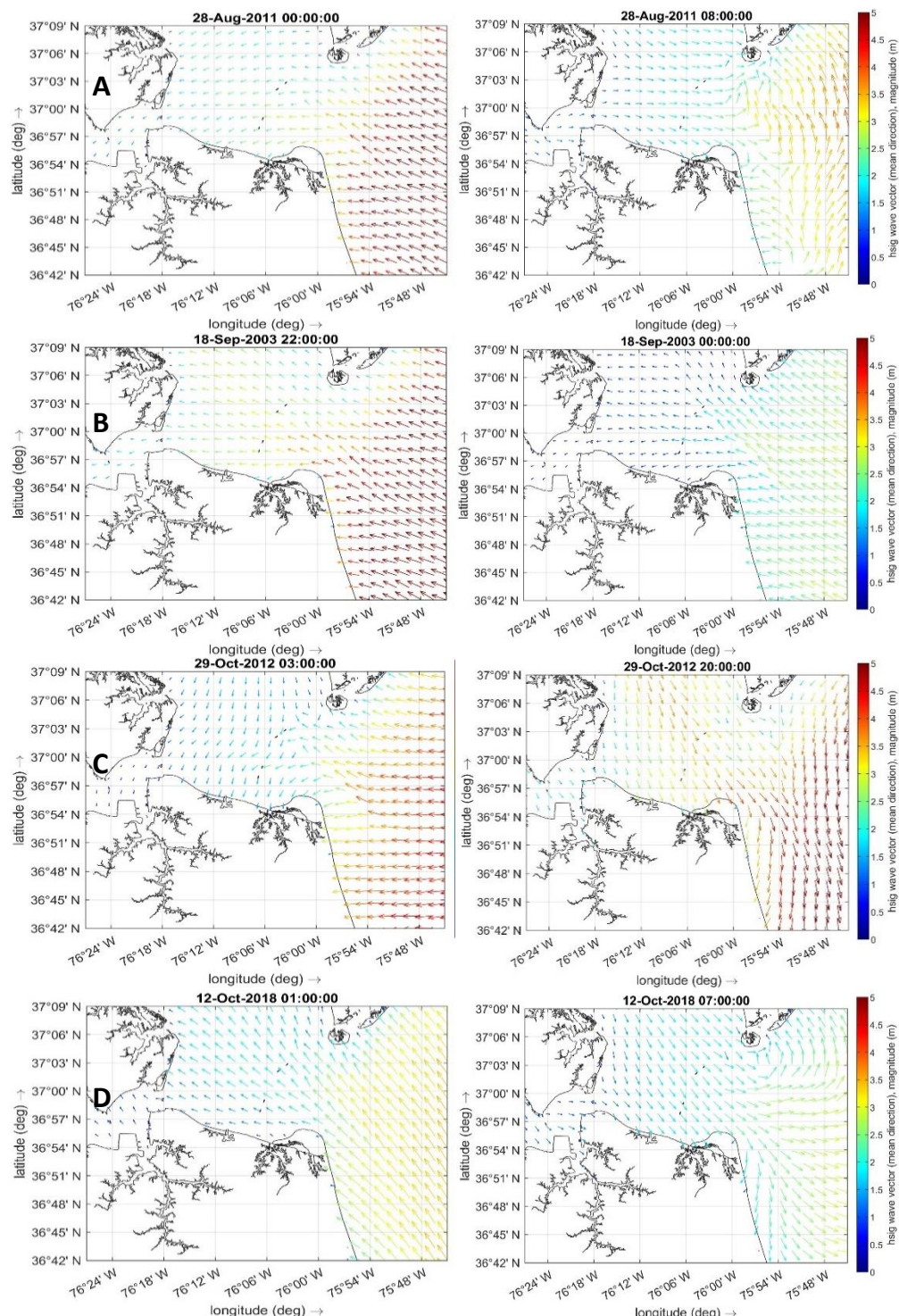


Figure 149. SWH (m) with the different dominant offshore (left panels) and Chesapeake Bay (right panels) wave directions for hurricanes A) Irene, B) Isabel, C) Sandy, and D) Michael for the PD_F0.64 scenario, at NSN base, the US.

ii. Radius of maximum wind.

The impact of changing the RMW on the predicted SWH was found to be minor for all hurricanes except Hurricane Michael where the wave height along the Willoughby Spit showed a significant response to the changes in the RMW with an SWH up to 1.8m for MI_RMW_F1.1 scenario (compared to 1.3m for the baseline), Figure 151 and Figure 152.

Changing the RMW might displace the area of interest within a higher or lower wind region, depending on the hurricane track and the original RMW. Therefore, changing the RMW might enhance the wave growth in some situations, but might also diminish their growth in other situations. For instance, increasing Hurricane Michael's RMW by 10% resulted in a higher wind speed (up to 20m/sec), compared to 12m/sec for the baseline, approaching NSN from the SE, Figure 150. These winds enhanced the wave growth resulting in higher waves along Willoughby Spit, Figure 151.

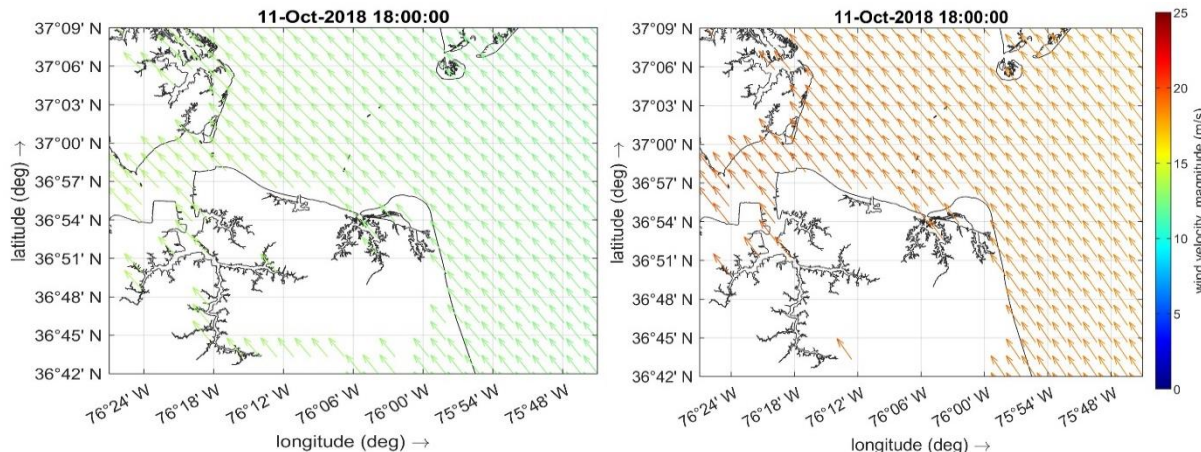


Figure 150. Wind speed (m/sec) with direction (nautical convention) for the baseline (left panel) and MI_RMW_F1.1 (right panel), Hurricane Michael, at NSN, the US.

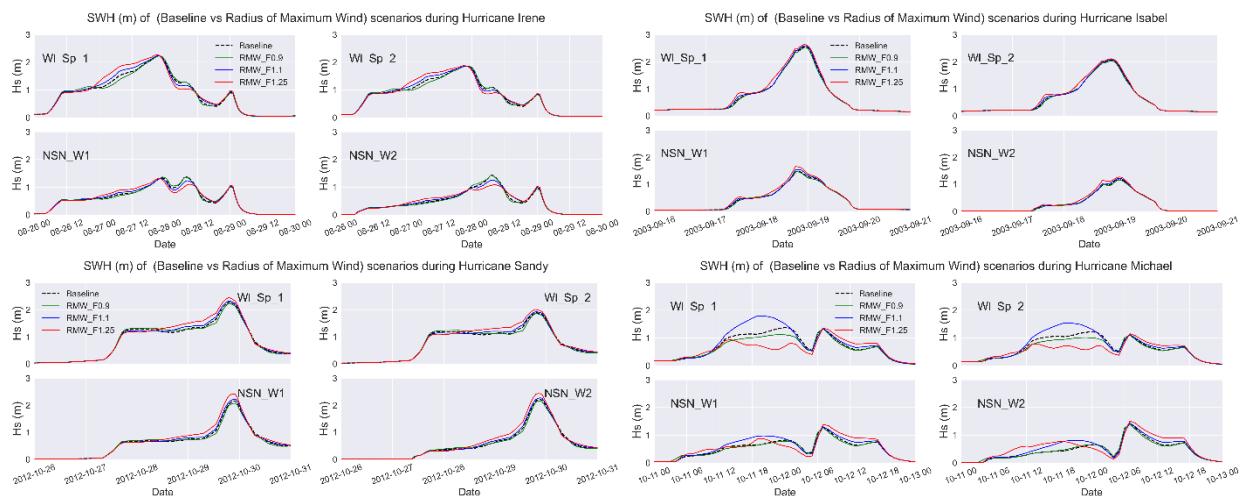


Figure 151. Significant wave height (H_s) (m) at the four points along the Willoughby Spit and NSN for Baseline and RMW scenarios for all hurricanes, at NSN, the US.

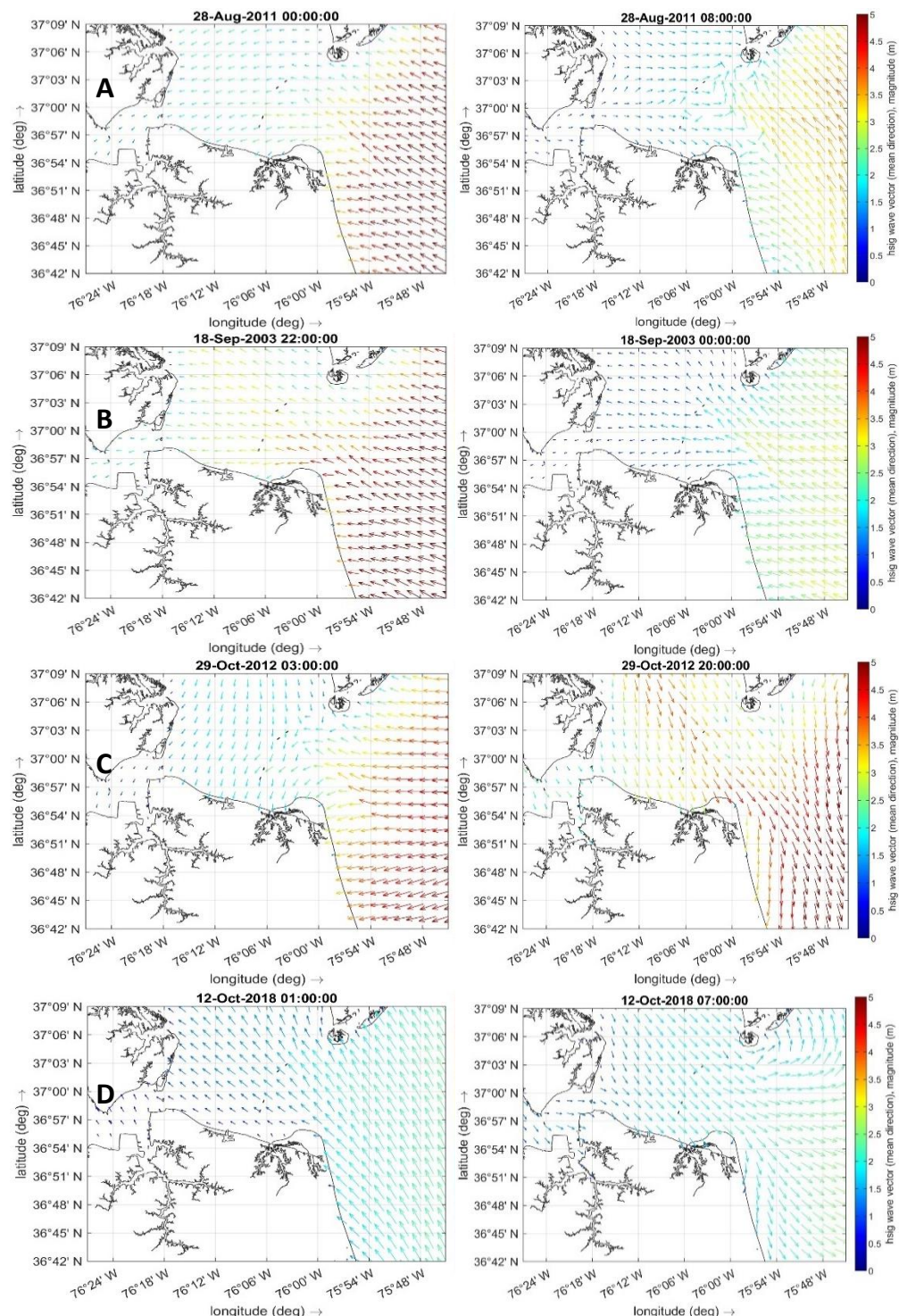


Figure 152. SWH (m) with the different dominant offshore (left panels) and Chesapeake Bay (right panels) wave directions for hurricanes A) Irene, B) Isabel, C) Sandy, and D) Michael for the RMW_F1.25 scenario, at NSN base, the US.

6.3.3. Impacts of Climate Change

i. Sea Level Rise (SLR)

The predicted wave height was found to be increasing with increasing the mean water level during the peak of the storm. However, the most pronounced impact was detected along the Willoughby Spit (WL_Sp_1 and WL_Sp_2) where the area is relatively shallow and SLR will increase to water depth, diminish the wave dissipation due to bottom friction, and reduce the wave breaking, Figure 153. Therefore, the maximum impact was detected for the SLR_1.3M scenario and decreased with the decrease in the SLR value. In addition, the maximum SWH increase was observed for Hurricane Isabel followed by Hurricane Irene. Hurricane Michael showed almost no impacts of SLR on the wave height at NSN. However, the magnitude of the predicted increase was relatively minor and ranged from 0.1m up to 0.4m for all SLR scenarios. Minor impact of SLR was observed along the western boundary of the base (NSN_W1 and NSN_W2) where the water depth is relatively deep due to the navigational activities in this area. No changes were detected in the wave pattern compared to the baseline, Figure 154.

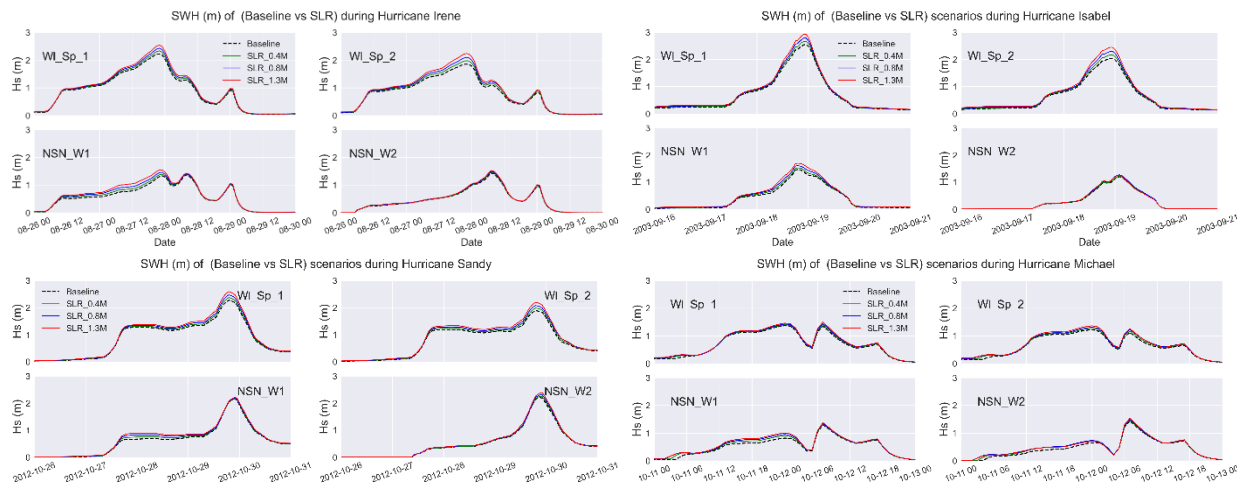


Figure 153. Significant wave height (Hs) (m) at the four points along the Willoughby Spit and NSN for Baseline and SLR scenarios for all hurricanes, at NSN, the US.

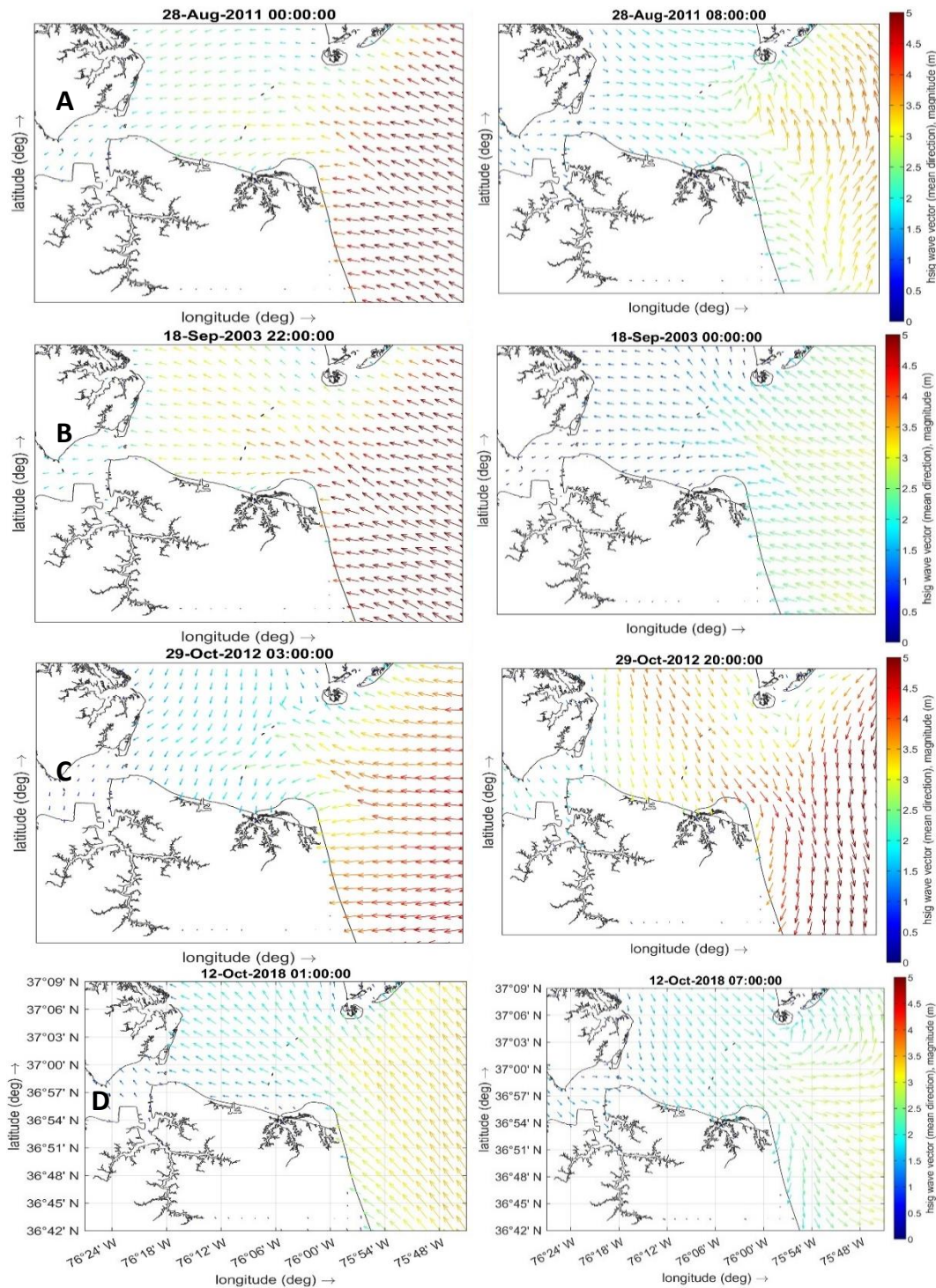


Figure 154. SWH (m) with the different dominant offshore (left panels) and Chesapeake Bay (right panels) wave directions for hurricanes A) Irene, B) Isabel, C) Sandy, and D) Michael for the SLR_1.3m scenario, at NSN base, the US.

ii. Wind Speed group.

Increasing the wind speed resulted in higher waves, because of higher wind stress, except for Hurricane Michael where wave height diminished along the western boundary of the base during the MI_WSF_1.225 scenario. The maximum increase was detected along the western boundary of the base (NSN_W1 and NSN_W2) dominated by the waves approaching from the Chesapeake Bay, and to some extent from James River, Figure 155 and Figure 156, with about 50% and 30% increases up to 2.1m (IR_WSF_1.225) and 2.78m (SA_WSF_1.225) compared to 1.4m and 2.15m for the baseline scenarios respectively. On the other hand, reducing the wind speed (e.g. IR_WSF_0.9) resulted in a minor reduction in the predicted wave height at all locations, as expected.

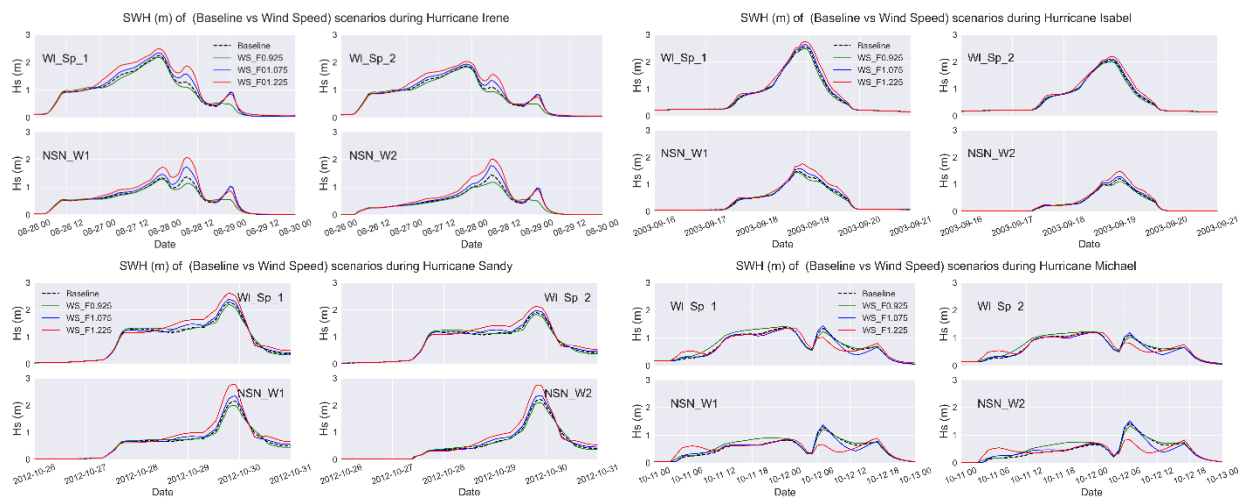


Figure 155. Significant wave height (H_s) (m) at the four points along the Willoughby Spit and NSN for Baseline and WS scenarios at NSN base, the US.

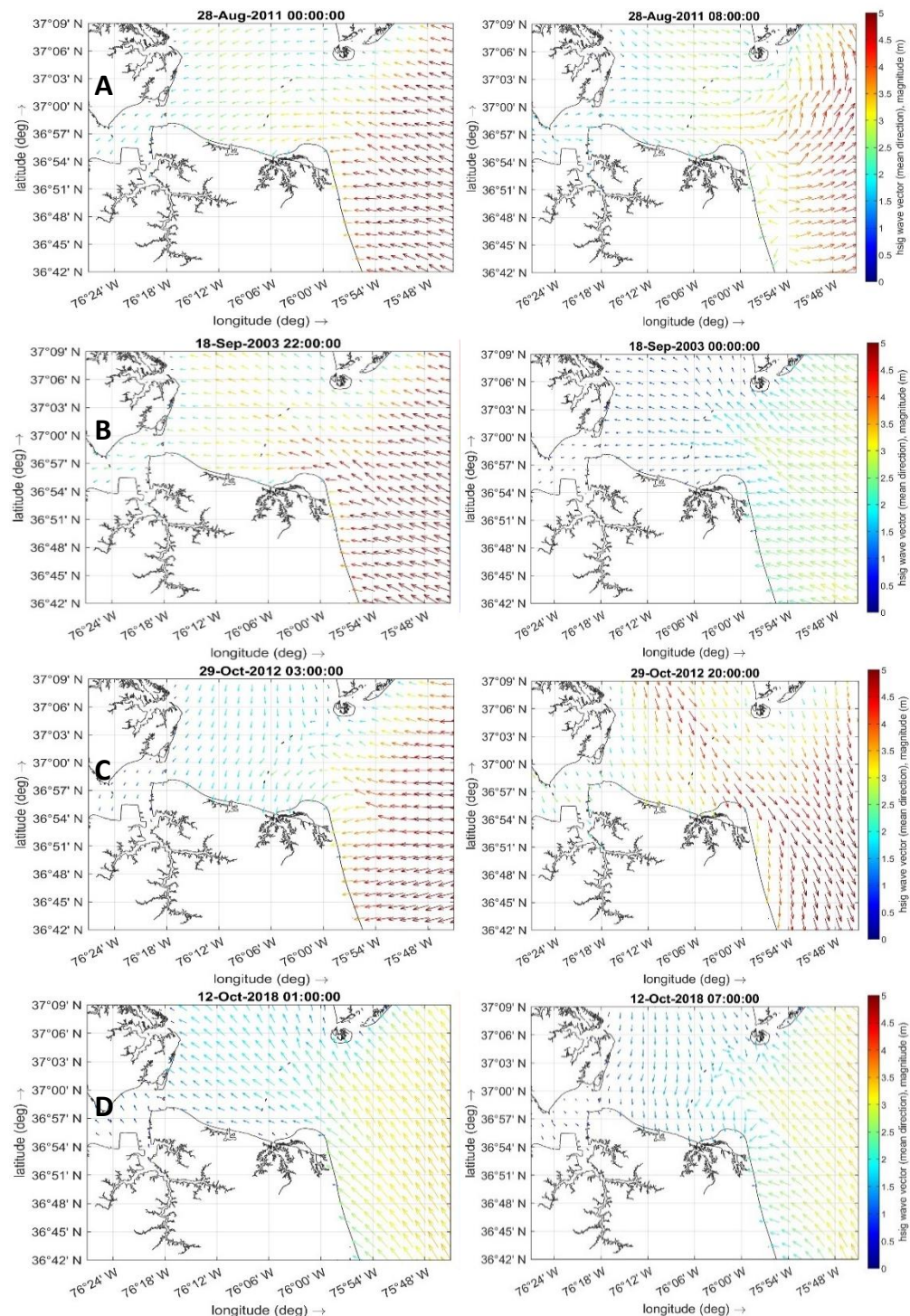


Figure 156. SWH (m) with the different dominant offshore (left panels) and Chesapeake Bay (right panels) wave directions for hurricanes A) Irene, B) Isabel, C) Sandy, and D) Michael for the WSF_1.225 scenario, at NSN base, the US.

6.3.4. Impacts of lack of data (Degradation scenarios)

The predicted SWH showed a high sensitivity to the changes in the hurricane track. However, the response of all hurricanes was not the same due to the differences in the original hurricane tracks and angle of approach.

Shifting Hurricane Irene's track to the east displaced the hurricane further offshore away from the coast. This resulted in a weaker impact of the hurricane on the coastal area that caused a significant diminishing of the predicted SWH at all analysis locations, with a maximum of 0.55m along the western boundary of NSN (NSN_W1) for IR_STE_138nm scenario compared to 1.37m for the baseline scenario, Figure 157 and Figure 158 (middle panels). On the other hand, shifting Irene's track to the west displaced the area of interest in the strong onshore winds of the hurricane. Therefore, an offshore dominant wave direction was detected for these scenarios, with a maximum SWH of 2.5m for the IR_STW_54nm compared to 2.2m for the baseline, with the almost absence of waves approaching from the Chesapeake Bay, Figure 157. However, shifting the track further to the west (IR_STW_138nm) resulted in a lower predicted SWH due to the displacement of the hurricane on land with a lower impact on the ocean surface, Figure 157 and Figure 158 (lower panels).

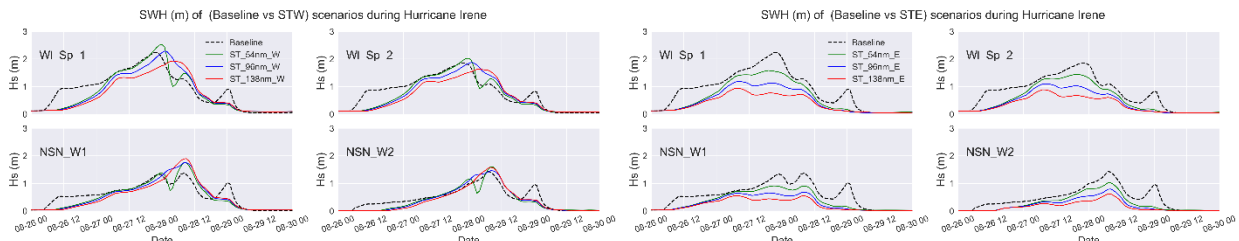


Figure 157. Significant wave height (H_s) (m) at the four points along the Willoughby Spit and NSN for Baseline and storm track shift scenarios for Hurricane Irene at NSN, the US.

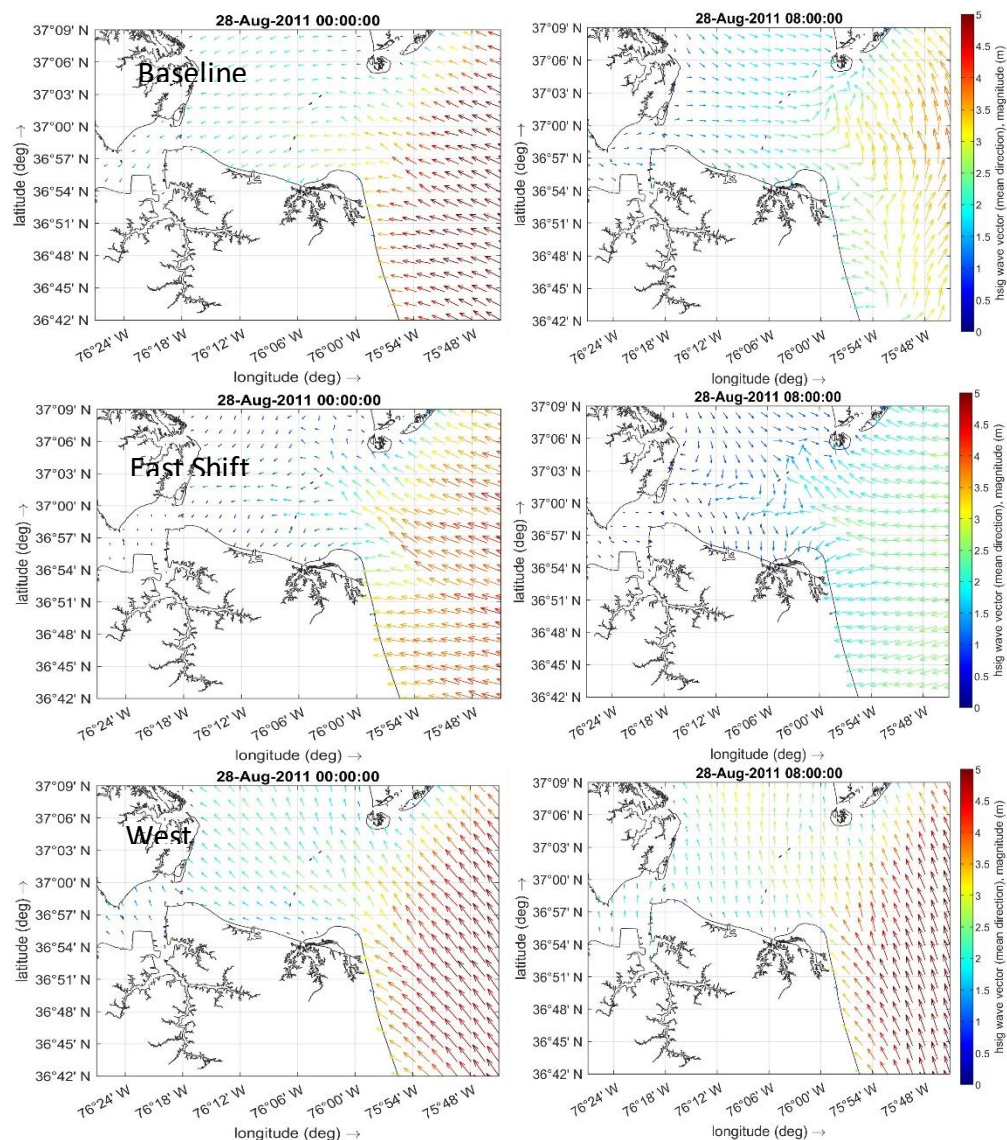


Figure 158. Example of SWH (m) with the different dominant wave directions during the baseline (upper panels) and IR_ST_138nm scenarios, east shifts (middle panels) and west shifts (lower panels), for hurricane Irene at NSN, the US.

Shifting Hurricane Isabel's track to the east displaced the hurricane further offshore closer to the NSN area. This resulted not only in enhancing the growth of waves approaching from the offshore direction but also the waves coming from the Chesapeake Bay. However, the most pronounced impact was detected along the western boundary of the base (NSN_W1 and NSN_W2) with a maximum SWH of 2.05m compared to 1.47m for the baseline (NSN_W1- IS_STE_54nm), Figure 159 and Figure 160 (middle panels). Shifting Isabel further to the east resulted in a lower predicted SWH at all stations. On the other hand, the west shift of Hurricane Isabel displaced the hurricane further away from the NSN region causing consistently lower predicted SWH with each west shift. In addition, the region was found to be still dominated by the offshore wave component with the complete absence of the Chesapeake Bay waves, Figure 159 and Figure 160 (lower panels).

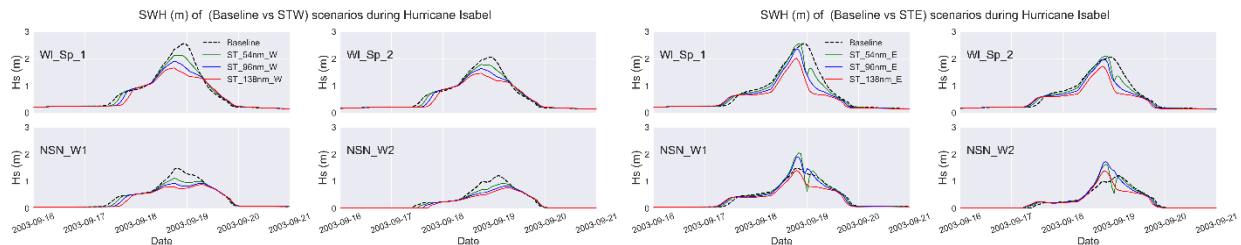


Figure 159. Significant wave height (H_s) (m) at the four points along the Willoughby Spit and NSN for Baseline and storm track shift scenarios for Hurricane Isabel at NSN, the US.

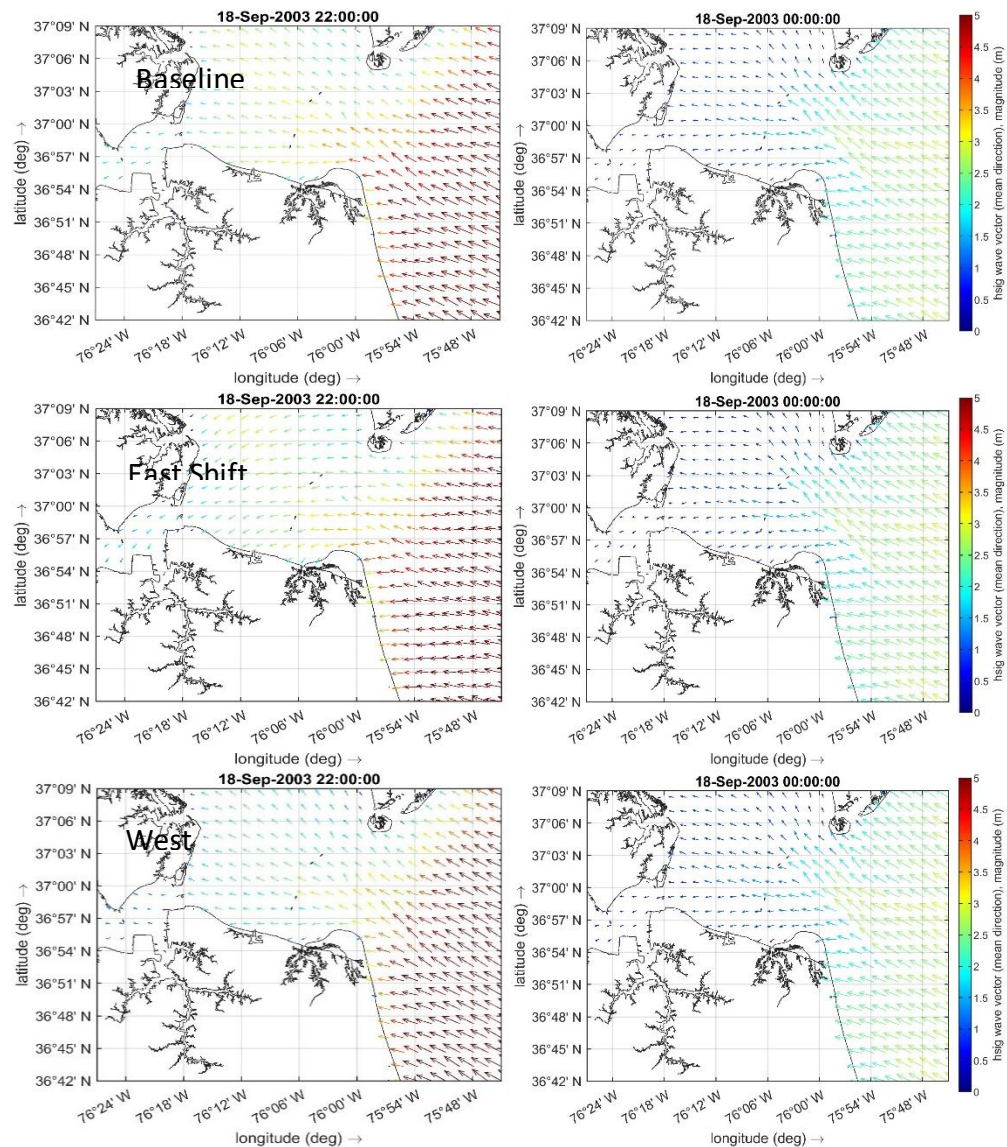


Figure 160. Example of SWH (m) with the different dominant wave directions during the baseline (upper panels) and IS_ST_54nm scenarios, east shifts (middle panels) and west shifts (lower panels), for hurricane Isabel at NSN, the US.

Hurricane Sandy made its landfall 320km north of NSN, hence, shifting Hurricane Sandy's track to the east displaced the hurricane further away from the NSN area. This resulted in a weaker component of offshore and Chesapeake Bay waves with lower SWH approaching the base from all directions with each shift at all locations, Figure 161 and Figure 162 (middle panels).

On the other hand, shifting Hurricane Sandy to the west significantly enhanced the wind field (by displacement of the hurricane closer to the base) and hence the generation and growth of the wind-waves approaching the base from all directions. However, the most pronounced impact was detected along the western boundary of the base (NSN_W1) with relatively higher waves, up to 2.94m, associated partly with the wind/waves approaching the base from the Chesapeake Bay and partly with the wind/waves approaching from James River, Figure 161 and Figure 162 (lower panels). Generally speaking, the NSN region becomes dominated by offshore-directed winds associated with the hurricane cyclonic winds for this set of scenarios (west shifts). Therefore, the contribution of the offshore waves is relatively weak at the NSN compared to the waves approaching from the Chesapeake Bay and James River.

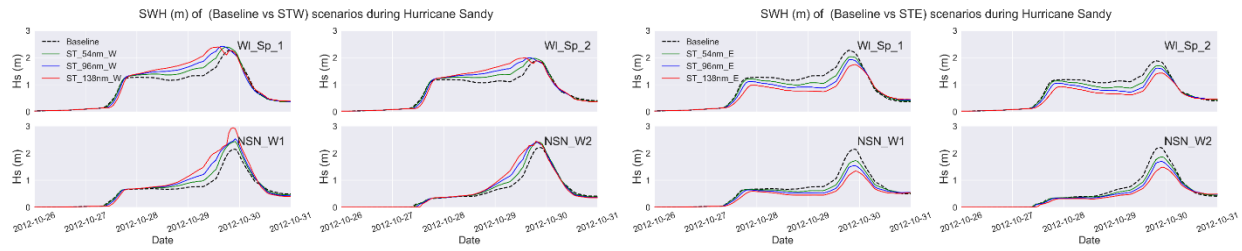


Figure 161. Significant wave height (H_s) (m) at the four points along the Willoughby Spit and NSN for Baseline and storm track shift scenarios for Hurricane Sandy at NSN, the US.

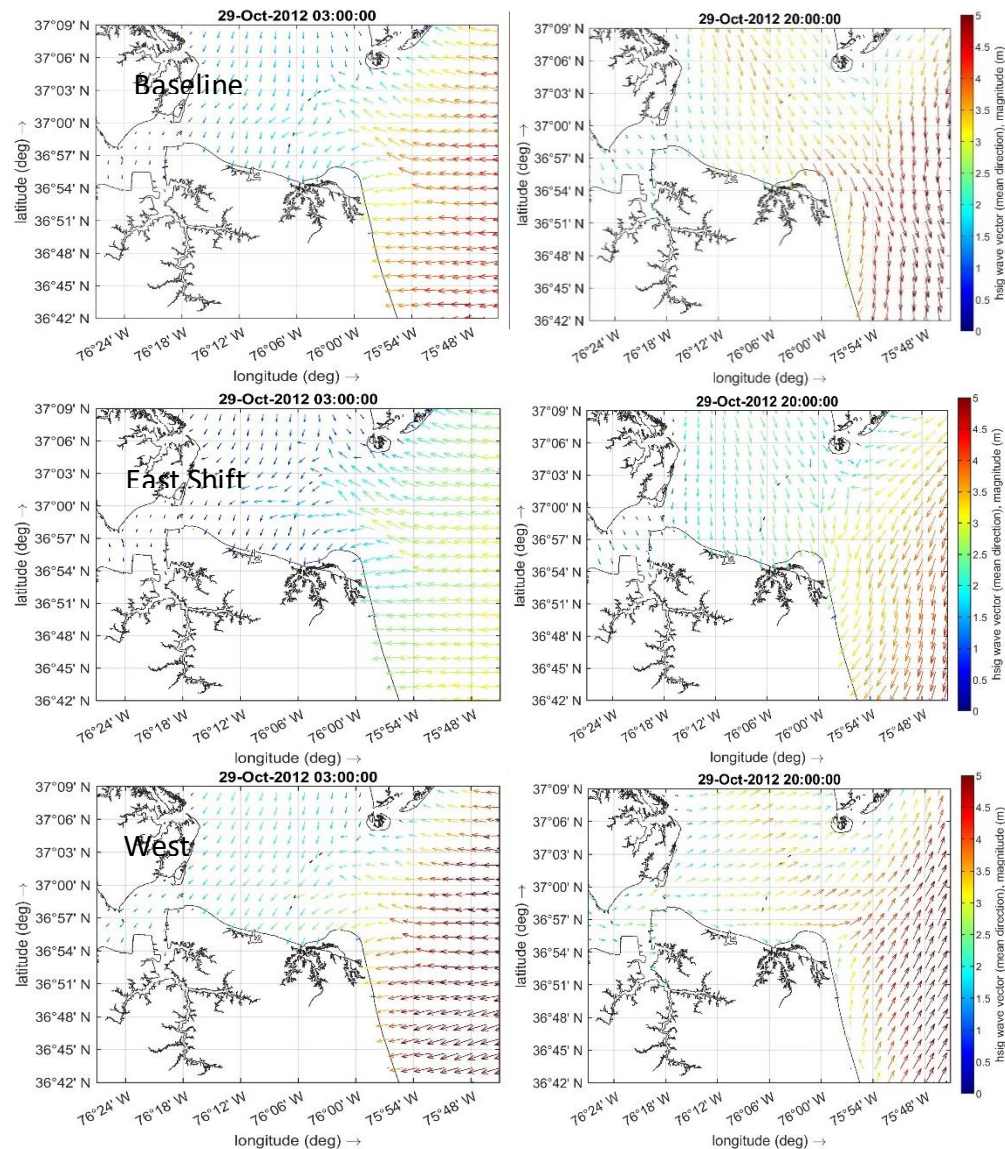


Figure 162. Example of SWH (m) with the different dominant wave directions during the baseline (upper panels) and SA_ST_138nm scenarios, east shifts (middle panels) and west shifts (lower panels), for Hurricane Sandy at NSN, the US.

The original track of Hurricane Michael almost passed through NSN in the west-east direction. Shifting Hurricane Michael's track to the east resulted in significantly higher offshore approaching waves that increased the SWH along the Willoughby Spit up to 2.2m (WL_Sp_1- MI_STE_138nm) compared to 1.37m for the baseline, with limited influence on the western boundary of the Base. In addition, a slight increase in the SWH for waves coming from Chesapeake Bay was also detected along the spit. However, minor decrease

was detected along the western boundary of the base for waves coming from this direction, Figure 163 and Figure 164 (middle panels).

On the other hand, shifting Michael's track to the west resulted in diminishing the influence of the hurricane on the ocean surface. The offshore waves were diminished in height down to 0.55m along the Willoughby Spit (MI_STW_138nm). However, a marginal increase in the predicted SWH was detected for the waves approaching the western boundary of the base. This might be attributed to the offshore (SW) winds associated with the hurricane that enhanced the wave growth in this area, Figure 163 and Figure 164 (lower panels).

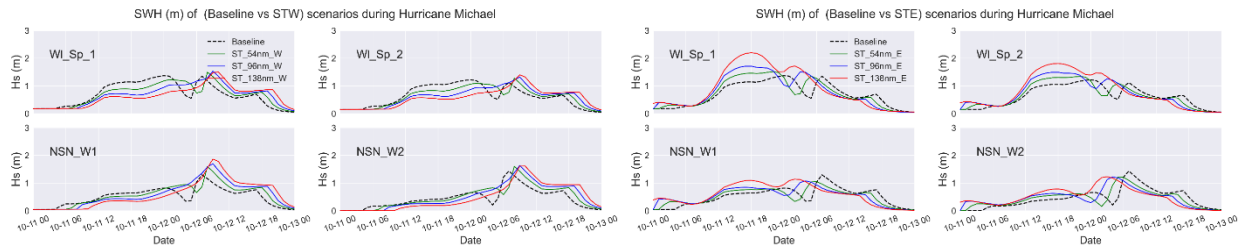


Figure 163. Significant wave height (H_s) (m) at the four points along the Willoughby Spit and NSN for Baseline and storm track shift scenarios for Hurricane Michael at NSN, the US.

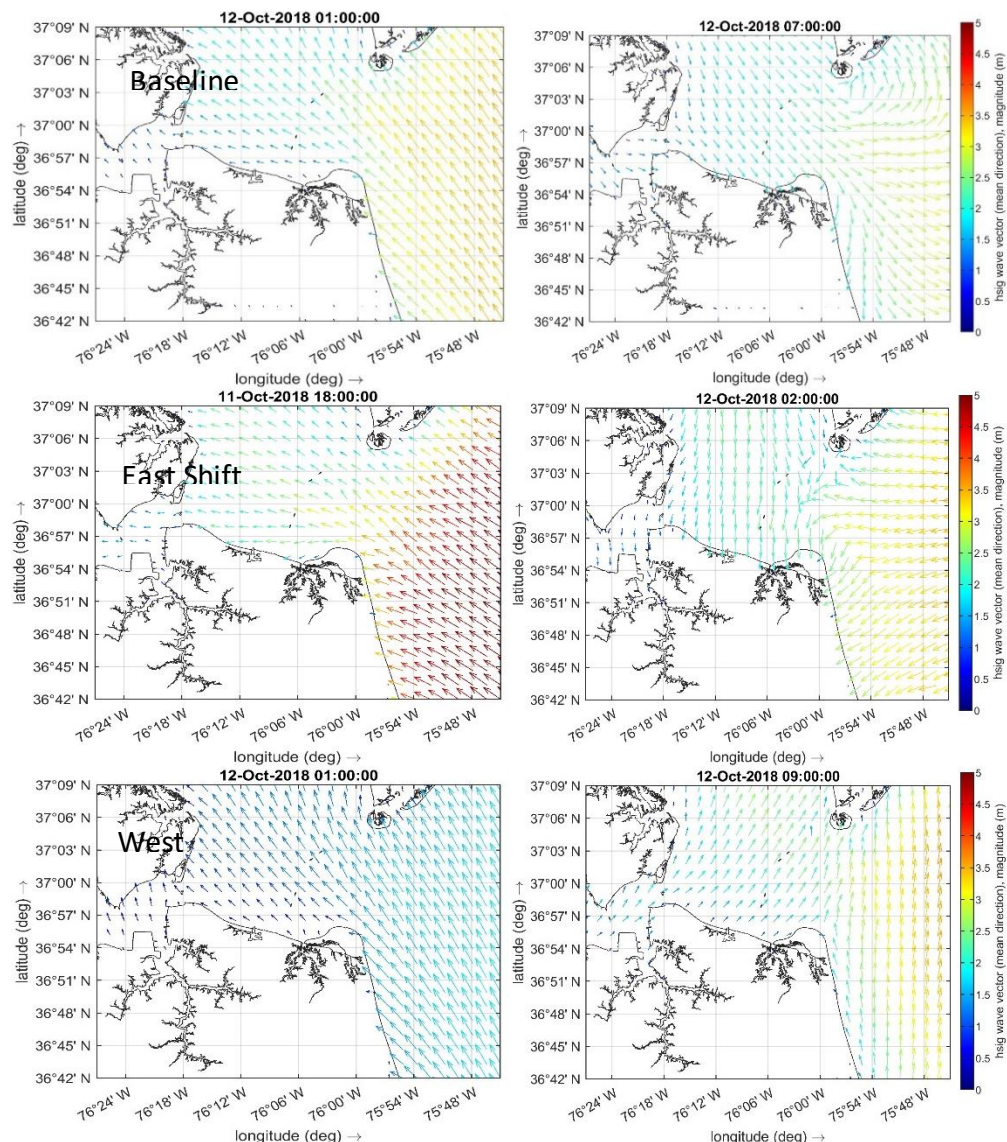


Figure 164. Example of SWH (m) with the different dominant wave directions during the baseline (upper panels) and MI_ST_138nm scenarios, east shifts (middle panels) and west shifts (lower panels), for hurricane Michael at NSN, the US.

Minor inaccuracies in the used bathymetry (up to 1m) showed almost no influence on the prediction accuracy of the wave characteristics, even within shallow areas (down to 6-7m), Figure 165. However, it should be noted that the maximum predicted waves approaching the NSN location are below 3m. Higher waves might show a more significant response to the changes/inaccuracies in the used bathymetry.

On the other hand, reducing the mesh resolution reflected a drastic change in the predicted wave characteristics. Even with resolution reduction by a factor of 5 (1km), a noticeable reduction in the predicted SWH was detected at all analysis locations, Figure 165. In addition, more reduction in the mesh resolution resulted in a complete misrepresentation of the nearshore bathymetry such that no waves were predicted at three locations, with significant overestimation at the fourth location. Reducing the mesh resolution to such an extent might lead to unpredictable results in the nearshore area. However, it can still be feasible to use such resolution for offshore wave prediction, with offshore (deep water) calibration.

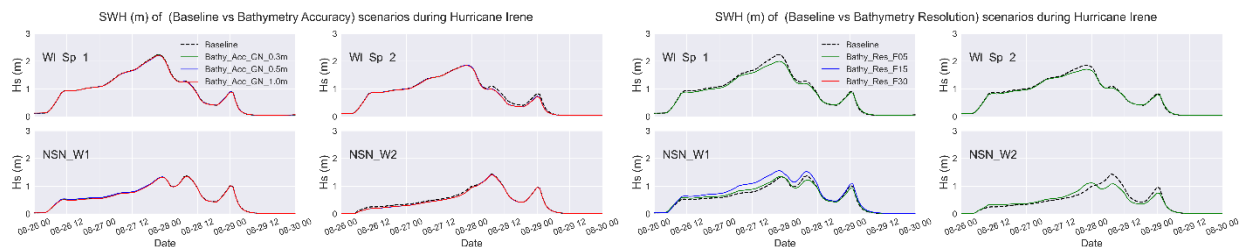


Figure 165. Significant wave height (H_s) (m) at the four points along the Willoughby Spit and NSN for Baseline, Bathymetry Accuracy (left panels), and Bathymetry Resolutions (right panels) scenarios for Hurricane Irene at NSN, the US.

6.4. ADCIRC

Results and discussion are divided into subsubsections, starting with calibration results of the base scenarios, followed by the results for scenarios of meteorological forcing, climate change, and model input degradation.

6.4.1. Model Calibration (Base Scenarios)

Calibration for the base storm scenarios was computed using the offsets for tides shown in Table 7. The offsets were applied to the storm simulations and used for computation in the total water levels modeled by ADCIRC. Observed water levels were obtained from the NOAA tide gauge at Sewell's Point during the respective times for each hurricane simulation. The observed data has hourly time intervals and is referenced to the mean sea level (MSL) for the later comparison against the model results.

I. Hurricane Irene (2011)

ADCIRC predictions for Irene show comparable results to the observed water levels at the NOAA tide gauge at Sewell's Point. The predicted peak water level is higher by about 30 cm above the observed peak, and the results show an overestimation prior to the storm and an underestimation after the storm passes. These discrepancies in the results are summarized in

Table 47 with the statistics for the ‘base’ storm simulation. Modeled results show good performance, because the correlation coefficient (R) is very close to 1 and the root mean square error is 0.21, which is considered acceptable for storm surge simulations that do not include wave data.

The storm duration was computed at 3 different levels and summarized in Table 48. This table also shows the error statistics for the differences in magnitude and timing of the peak storm surge between the modeled and observed data.

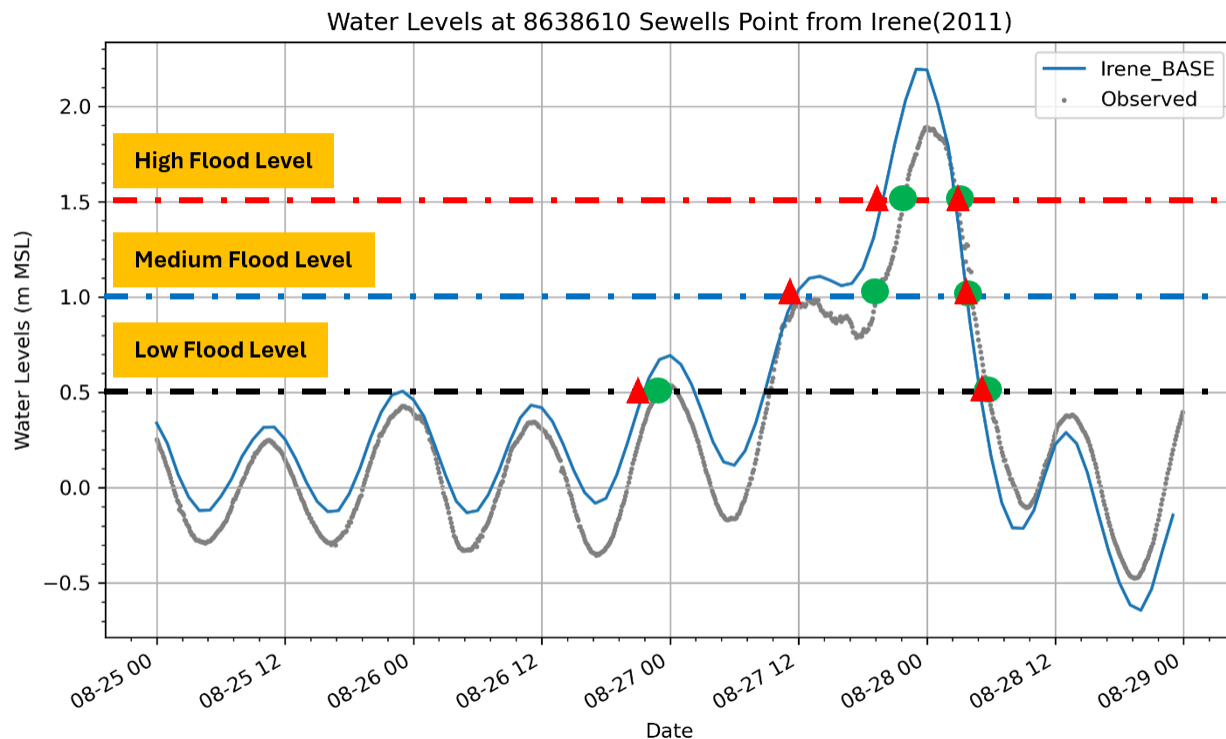


Figure 166 shows a plot of the water levels at Sewell’s Point during Irene showing the observed and simulated water levels during the storm. The plot shows the modeled results being consistent with the observed data with a slight overestimation during the tides and peak of the storm. The observed peak was seen as 1.89 m while the modeled was 2.20 m. It also shows an early peak of 1 hour in the modeled compared to the observed data.

The values for the storm duration were computed from the differences between the modeled and observed water levels at the different flood levels.

Water Levels at 8638610 Sewells Point from Irene(2011)

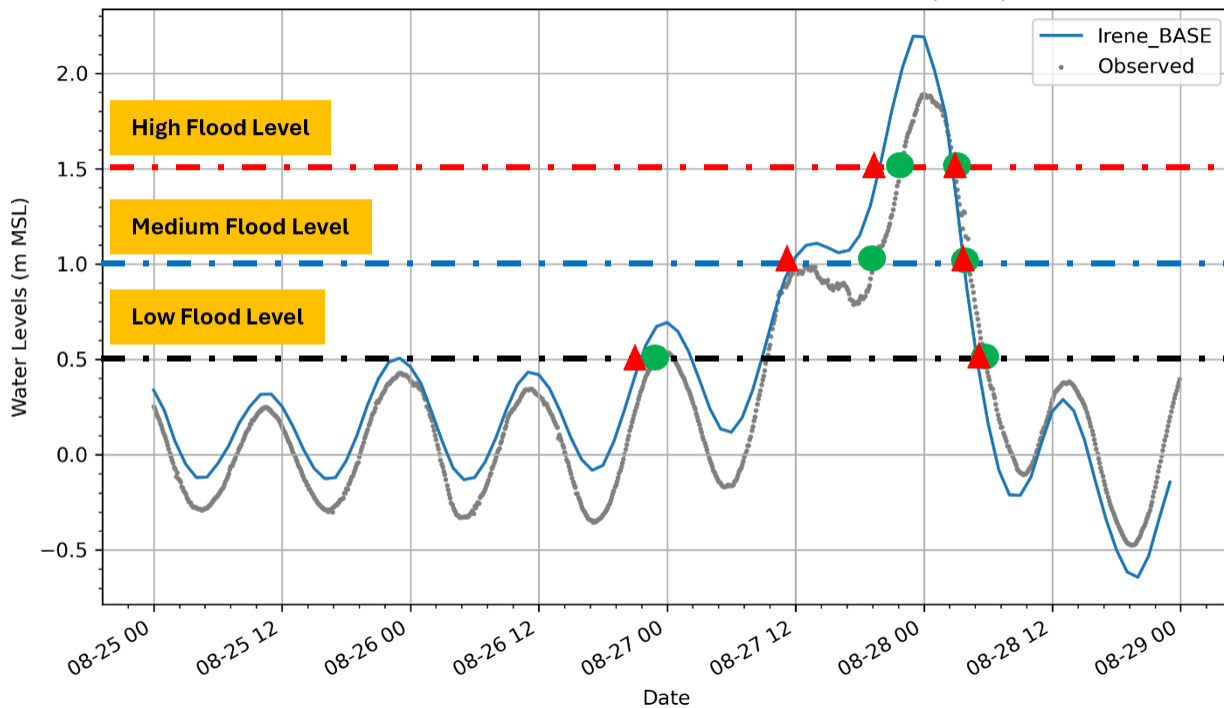


Figure 166 shows the timing differences at the low, medium, and high flood levels.

While the flood levels were assessed at Sewell's Point, which was used for validation against the flooded depths over Naval Station Norfolk. To investigate the flooding associated with Irene, the average and maximum flood depths were calculated on hourly basis for 24 hours around the peak surge that occurred on 28 August 2011 0000 UTC. Figure 167 shows the timeseries of the average and maximum flood depth at the NSN. The maximum flood depth was about 2.2 m, while the average flood depths ranged between about 0.5 to 0.75 m.

In addition, the severity of the flood was evaluated based on the projected flood depth as we classified the flood into four levels: low (0.1 m to 0.25 m), medium (0.25 m to 0.5 m), high (0.5 m to 1.0 m) and extreme (greater than 1.0 m). Based on these levels, a flood map was created for the peak flood (during the peak surge) for the NSN using a shapefile delineating the base area. Furthermore, a separate flood map was created for each individual flood level for more classification of the flood risk at the base. Figure 168 show the flood maps with the four flood levels for simulations at NSN base during the peak surge associated with Irene.

Table 47. ADCIRC/GAHM base scenario of Irene; error statistics for predicted water levels, relative to observations at Sewell's Point.

Wind Input	Location	R	R ²	RMSE	NRMSE	Bias	RB	MNB	SI
GAHM	Sewell's Point	0.96	0.89	0.21	0.09	0.09	33.75	-0.34	0.08

Table 48. ADCIRC/GAHM base scenario of Irene; error statistics as differences in magnitude (m), timing (h), and duration (h) of peak surge characteristics.

Wind Input		Magnitude (m)	Timing (h)	Duration (h)		
				Low	Medium	High
Irene	GAHM	+0.31	-0.9	+0.3	+6.1	+0.9

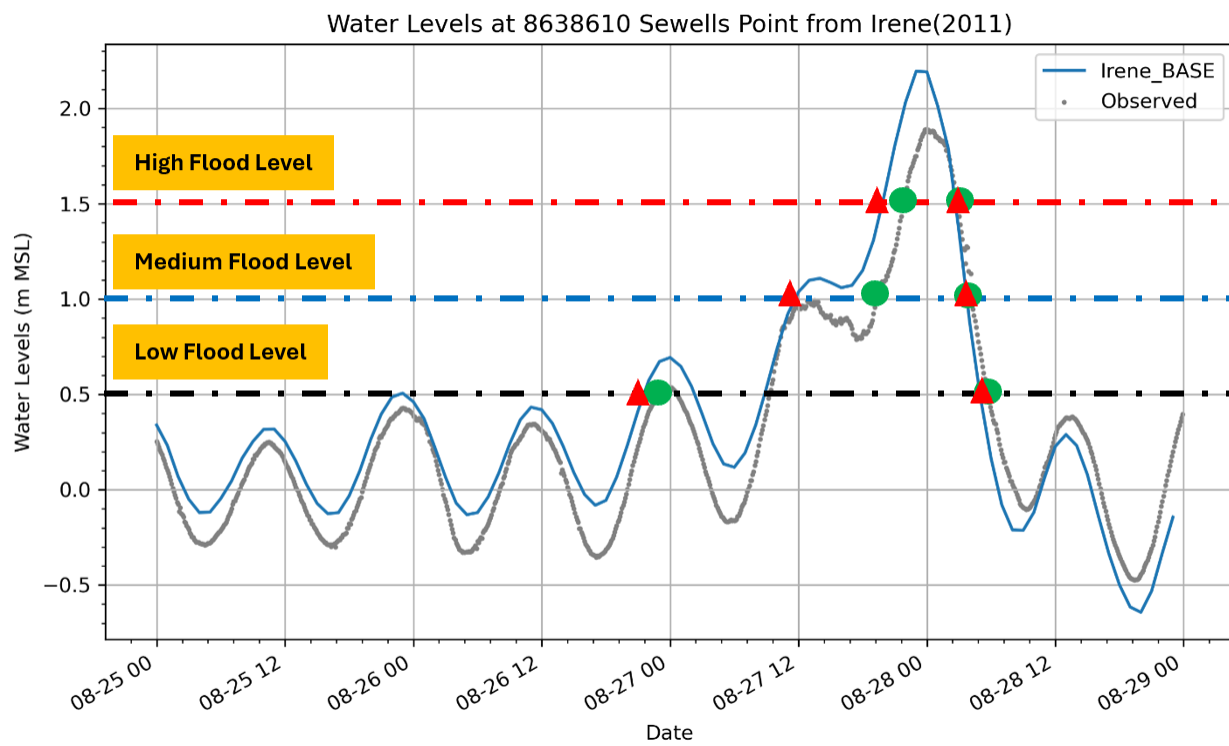


Figure 166. ADCIRC/GAHM base scenario of Irene; time series of the observed and predicted water levels at Sewell's Point, with indicators for the flood level classes.

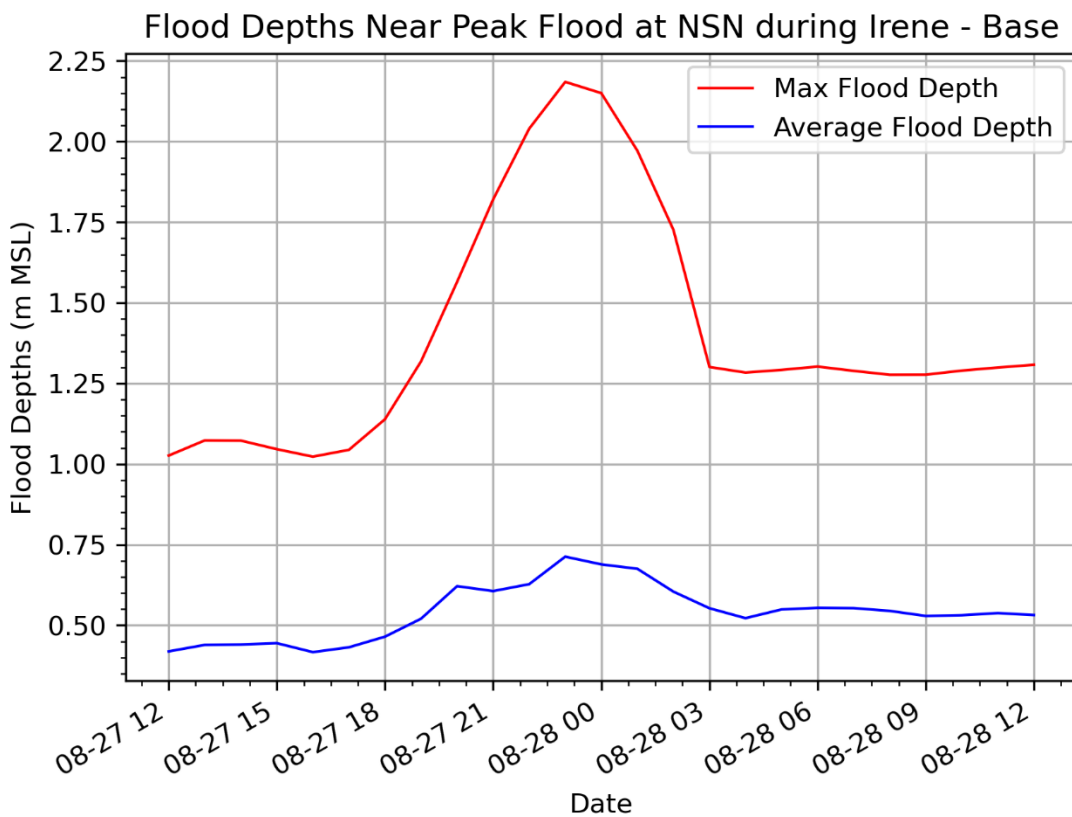


Figure 167. ADCIRC/GAHM base scenario of Irene; time series of the average and maximum flood depths (m MSL).

Hurricane Irene(2011) - Base Scenario

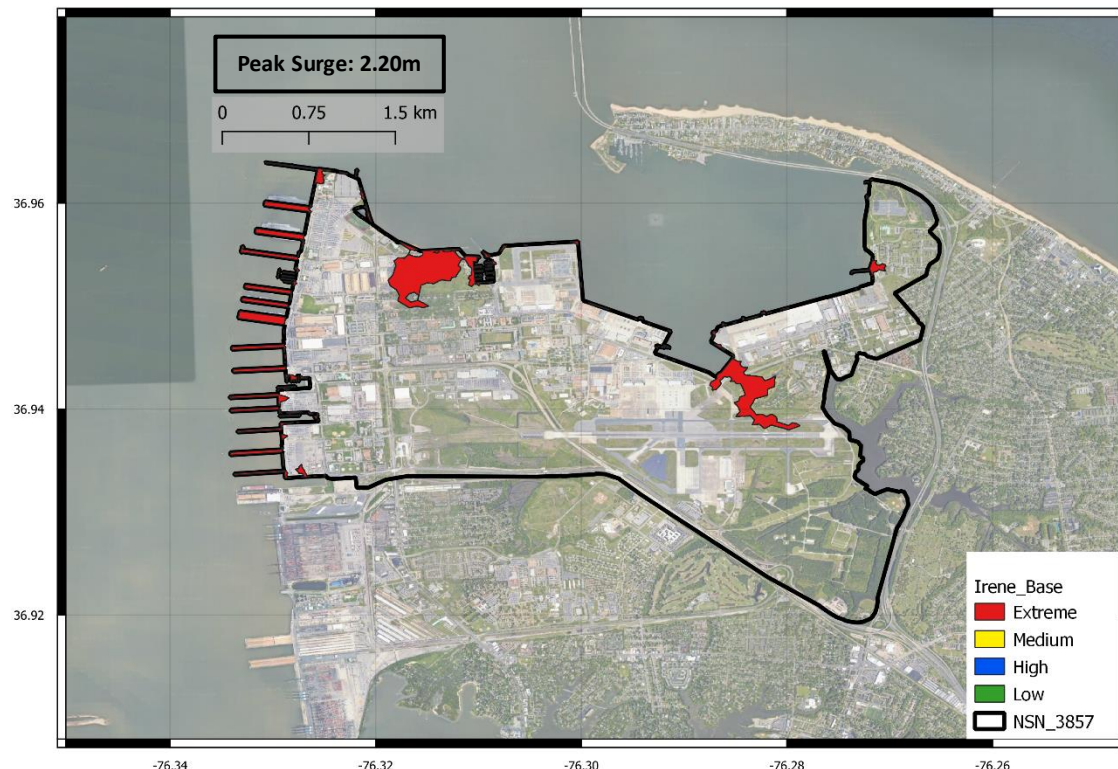


Figure 168. ADCIRC/GAHM base scenario of Irene; flood map showing the classification of the flood levels at the peak surge.

II. Hurricane Isabel (2003)

Isabel was a shore-perpendicular storm that made landfall in the Outer Banks of North Carolina and moved inland. Although its worst impacts were farther south, it did cause an increase in water levels near NSN. Its counterclockwise winds pushed waters into the southern part of Chesapeake Bay, and the water levels had an observed peak value of about 2 m MSL.

Table 49 summarizes the ADCIRC model performance in predicting the water levels during Isabel. Predicted and observed water levels are compared at the NOAA tide gauge at Sewell's Point. The overall performance is good, with an RMSE = 0.24 m, and a zero Bias. However, much of that good performance is in the tide predictions in the days preceding the storm. During the storm, ADCIRC overpredicts the effects of Isabel on the water levels, as shown in Figure 169.

The storm duration was computed at 3 different levels and summarized in Table 50. This table also shows the error statistics for the differences in magnitude and timing of the peak storm surge between the modeled and observed data.

Although several factors may contribute to this overprediction, the significant factor is the wind input to ADCIRC. The parametric GAHM (based on Holland 1980) is limited for Isabel, for two reasons: the storm's distance from NSN, and the relative lack of information in the NHC best-track file for this storm. The storm distance is important – parametric models like GAHM can reproduce the wind fields due to the hurricane, but they do not represent any other meteorological features like background winds or atmospheric fronts. GAHM can provide good results at locations close to the storm, where the hurricane winds are dominant, but its performance can deteriorate farther from the storm, where the hurricane winds are combined with other winds. For Isabel, because the storm tracked farther from NSN, the winds from GAHM are not as good a representation of the storm.

Another limiter is the relative lack of information in the NHC best-track file for this storm. The NHC provides information about storm parameters, like the eye location, maximum wind speed, radius to maximum winds, and central pressure. For recent storms, the NHC has expanded the best-track file to include information for multiple isotachs in each quadrant, i.e. it describes not just the shape of the inner storm, but also the shape at outer radii. These extra information/parameters can be extremely helpful for parametric models to reproduce the full shape of the storm. However, for older storms like Isabel, this extra information is not available. Thus, the storm shape may not be reproduced as well by GAHM, with the result that the winds and water levels are overpredicted at distant locations like NSN.

Figure 170 shows the average and maximum flood depths for Isabel in the NSN, and Figure 171 shows the classified flood extents for Isabel in the NSN. The maximum flood depth was about 2.80 m and the average flood depths had a peak of about 0.42 m. Due to the overprediction of the peak water levels, there is also an overprediction of the peak flood extents. A significant portion of the northwest portion of the NSN is flooded at 'extreme' levels.

Table 49. ADCIRC/GAHM base scenario of Isabel; error statistics for predicted water levels, relative to observations at Sewell's Point.

Wind	Location	R	R ²	RMSE	NRMSE	Bias	RB	MNB	SI
GAHM	Sewell's Point	0.96	0.77	0.24	0.11	-0.00	-0.83	-0.01	0.22

Table 50. ADCIRC/GAHM base scenario of Isabel; error statistics as differences in magnitude (m), timing (h), and duration (h) of peak surge characteristics at Sewell's Point.

Wind Input		Magnitude (m)	Timing (h)	Duration (h)		
				Low	Medium	High
Isabel	GAHM	+0.85	-1.0	-20.8	+0.1	+1.2

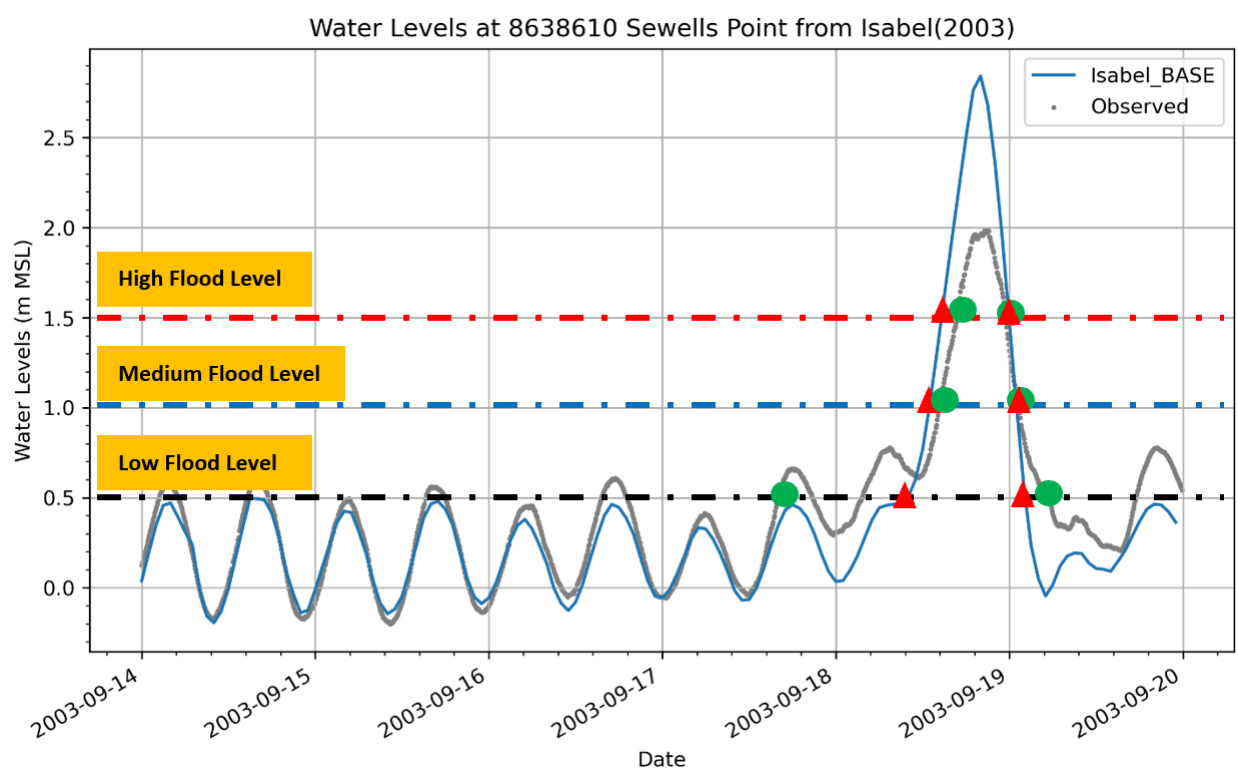


Figure 169. ADCIRC/GAHM base scenario of Isabel; time series of the observed and predicted water levels at Sewell's Point, with indicators for the flood level classes.

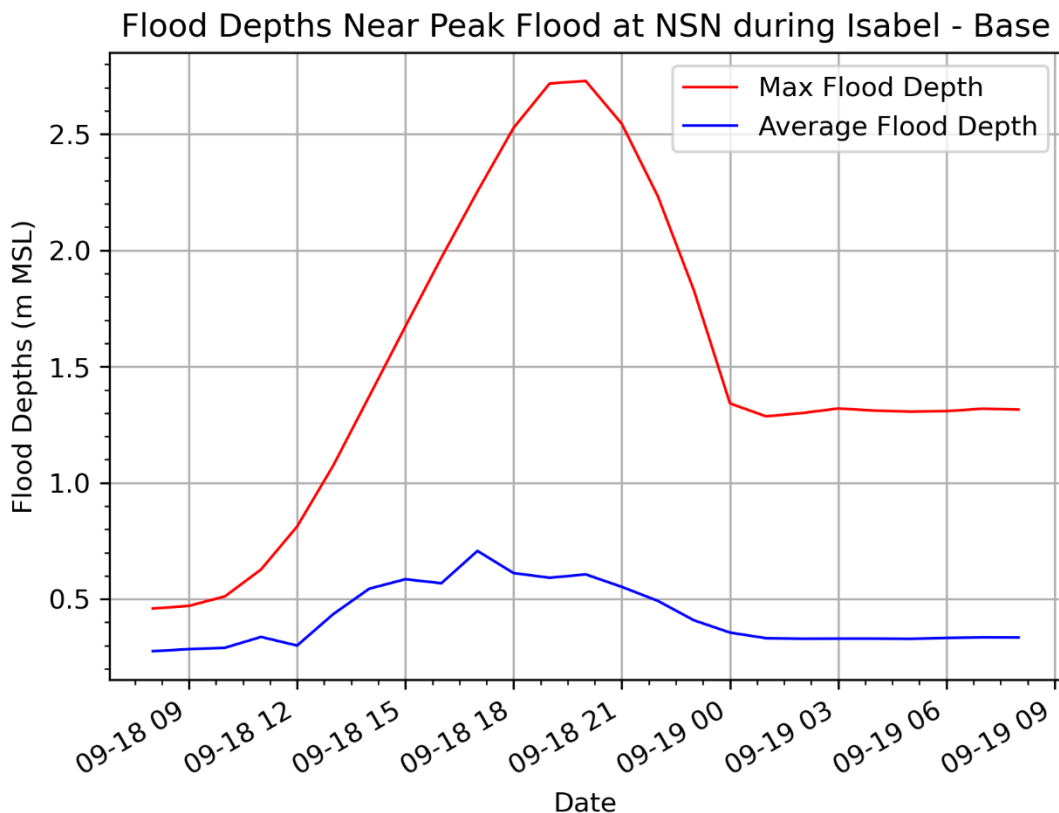


Figure 170. ADCIRC/GAHM base scenario of Isabel; time series of the average and maximum flood depths (m MSL).

Hurricane Isabel(2003) - Base Scenario

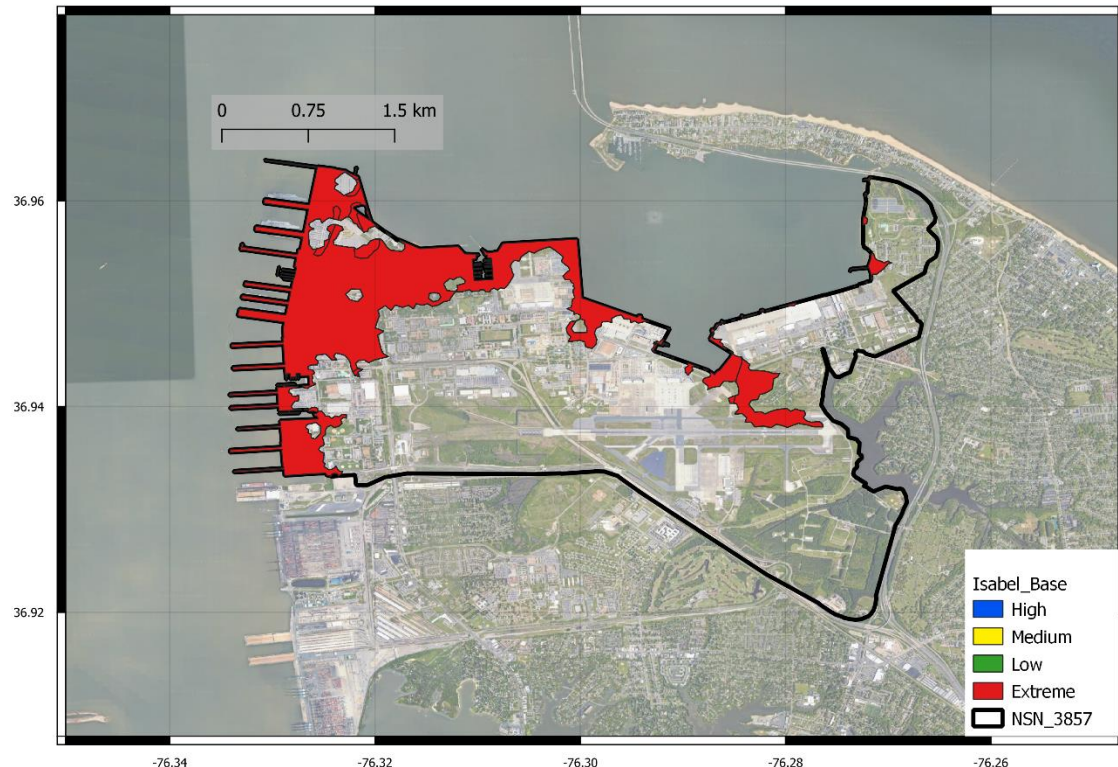


Figure 171. ADCIRC/GAHM base scenario of Isabel; flood map showing the classification of the flood levels at the peak surge.

III. Hurricane Sandy (2012)

Sandy stayed offshore and moved northward on a shore-parallel track, before turning to make landfall in New Jersey. Because it stayed offshore of Virginia, its effects were less pronounced at NSN. Water levels were elevated during several tidal cycles, with a peak water level of about 1.6 m MSL observed at the NOAA tide gauge at Sewell's Point.

Table 51 summarizes the ADCIRC model performance in its predictions of the water levels during Sandy. Error statistics are computed via comparisons of predicted and observed water levels at the NOAA tide gauge at Sewell's Point. ADCIRC performs well in an overall sense, with an RMSE = 0.24 m and a Bias = -0.09 m, which are similar with previous studies.

The storm duration was computed at 3 different levels and summarized in Table 52. This table also shows the error statistics for the differences in magnitude and timing of the peak storm surge between the modeled and observed data.

Figure 172 shows the ADCIRC-predicted and NOAA-observed water levels at the tide gauge at Sewell's Point. The observations show a rise in the water levels during three successive tidal cycles as the storm moved offshore, with a peak water level of about 1.6 m. ADCIRC underpredicts this rise in water levels – it does show an increase as the storm moved offshore, but its peak water level is about 1.2 m.

Again, several factors may contribute to this underprediction, but the controlling factor is the wind input. As noted above, GAHM performs best at locations close to the storm track, where the local wind fields are dominated by the hurricane winds. At locations farther from the storm track, such as NSN during Sandy, the wind fields may be less accurate. This inaccuracy in the wind predictions can then lead to inaccuracies in the water-level predictions.

Figure 173 shows time series of the average and maximum flood depths during Sandy, and Figure 174 shows the classified flood extents for Sandy, as computed by ADCIRC. The maximum flood depth was about 1.2 m, and the average flood depths had a peak of about 0.5 m. Flooding was localized to the piers on the west side of NSN, with no flooding predicted within the base itself.

Table 51. ADCIRC/GAHM base scenario of Sandy; error statistics for predicted water levels, relative to observations at Sewell's Point.

Wind	Location	R	R ²	RMSE	NRMSE	Bias	RB	MNB	SI
GAHM	Sewell's Point	0.94	0.77	0.24	0.12	-0.09	-21.73	-0.22	0.27

Table 52. ADCIRC/GAHM base scenario of Sandy; error statistics as differences in magnitude (m), timing (h), and duration (h) of peak surge characteristics at Sewell's Point.

Wind Input		Magnitude (m)	Timing (hr)	Duration		
				Low	Medium	High
Isabel	GAHM	- 0.5	0.7	-18.8	-3.9	-14.8

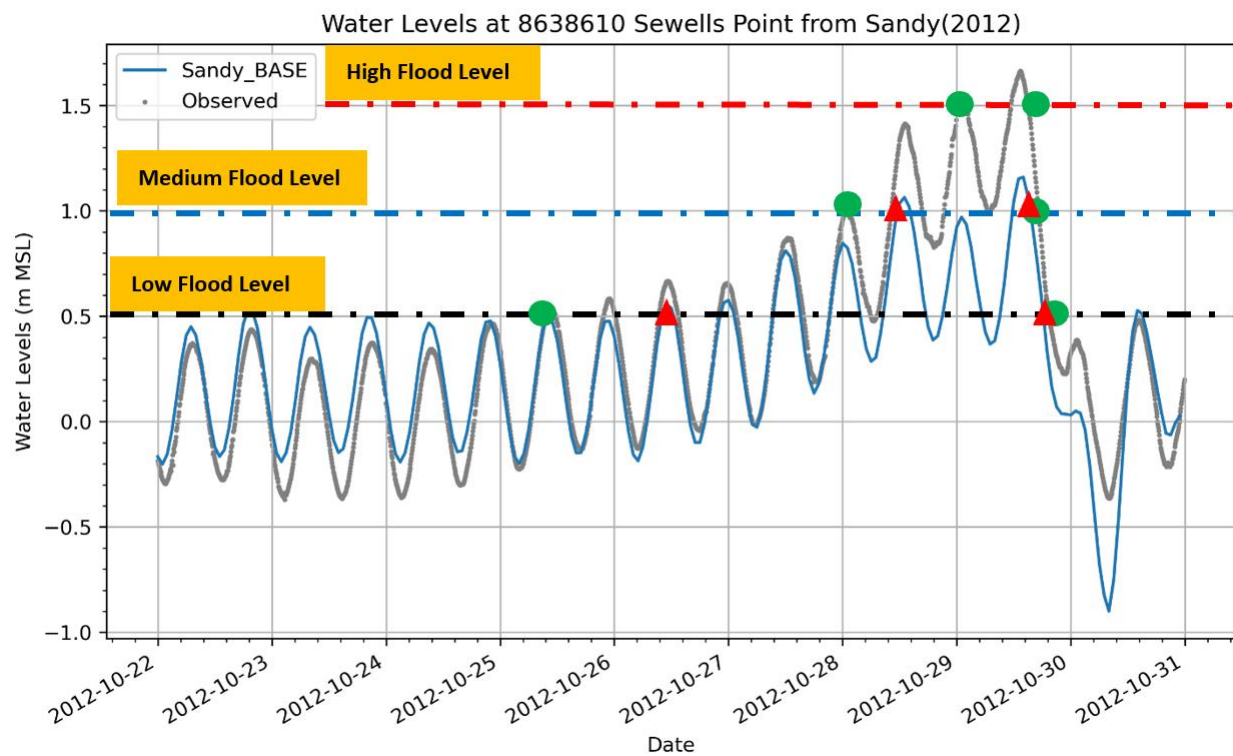


Figure 172. ADCIRC/GAHM base scenario of Sandy; time series of the observed and predicted water levels at Sewell's Point, with indicators for the flood level classes.

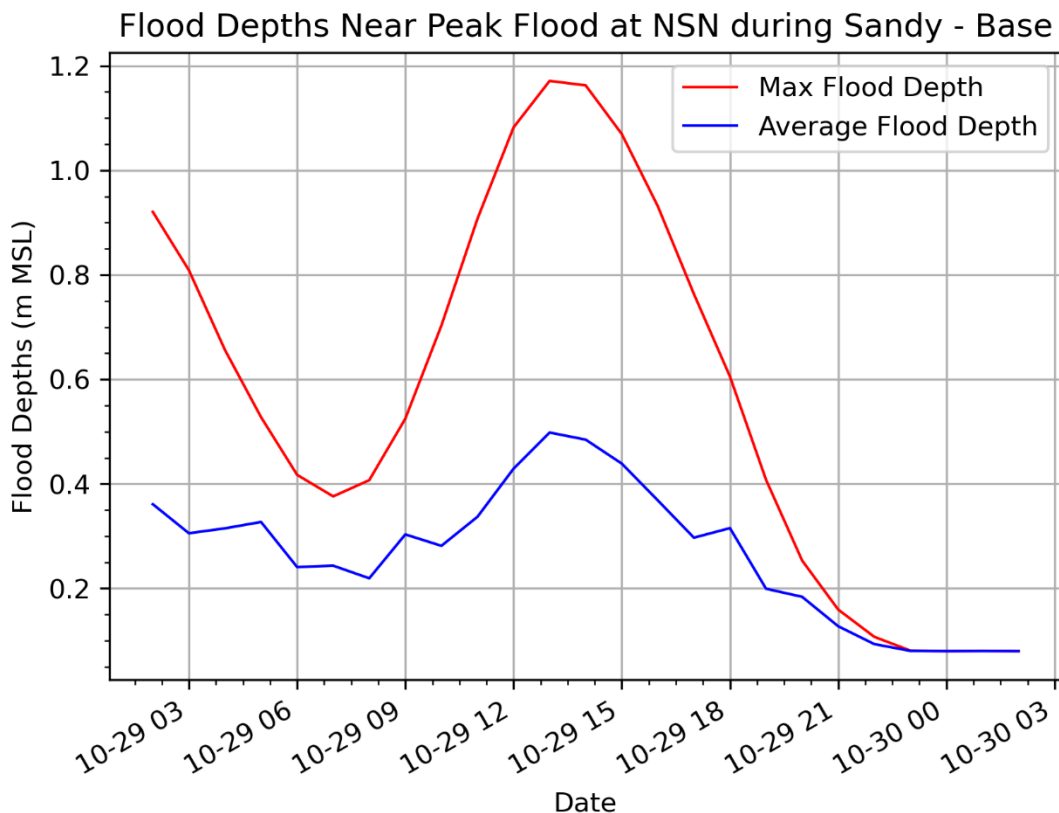


Figure 173. ADCIRC/GAHM base scenario of Sandy; time series of the average and maximum flood depths (m MSL).

Hurricane Sandy- Base Scenario

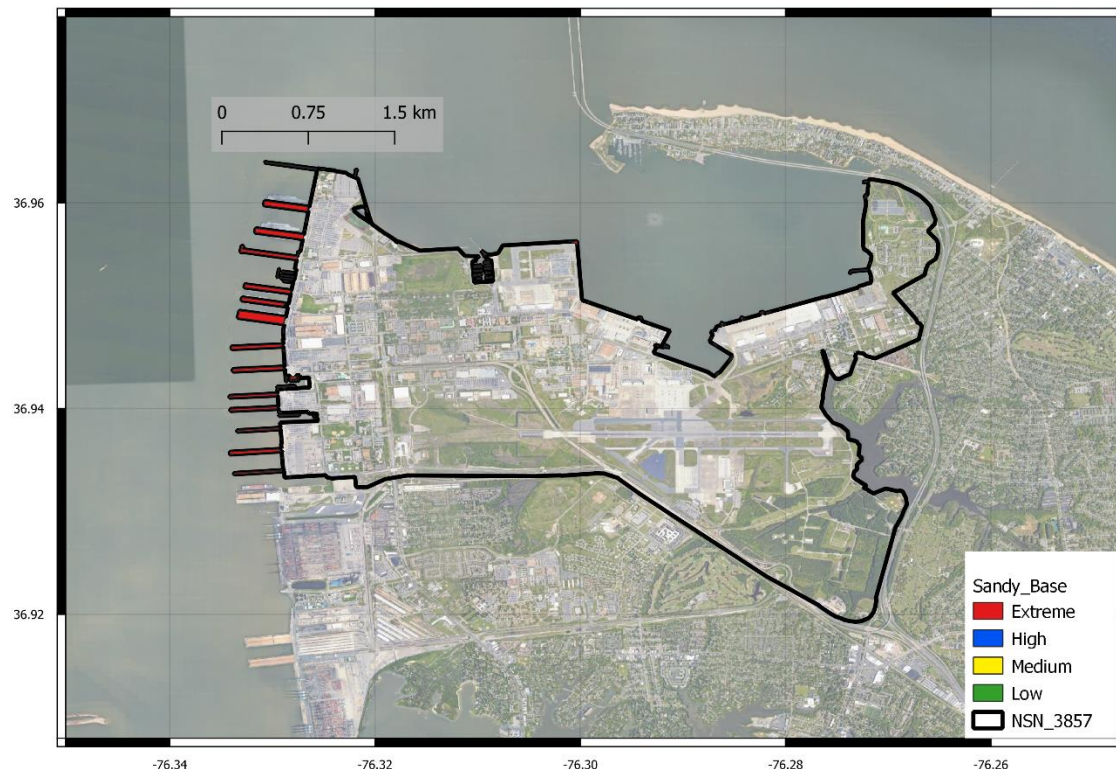


Figure 174. ADCIRC/GAHM base scenario of Sandy; flood map showing the classification of the flood levels at the peak surge.

IV. *Hurricane Michael (2018)*

Michael formed in the Gulf of Mexico, moved quickly northward, and made landfall in the Florida panhandle. It was a category-5 storm at landfall, and thus its waves and water levels were devastating to coastal communities in the northern Gulf, especially the cities of Mexico Beach and Panama City. However, its effects were minimal at NSN due to its long path overland. The storm tracked northward over the southeast United States, passing over parts of Florida, Georgia, South Carolina, North Carolina, Virginia, and Maryland, before moving offshore of Delaware and into the Atlantic Ocean. Thus, the storm moved close to NSN, but only after it had weakened overland for more than a day.

Table 53 summarizes the ADCIRC model performance in predicting water levels during Michael at the NOAA tide gauge at Sewell's Point. Performance is quantified by comparing ADCIRC predictions with NOAA observations. The ADCIRC model performance is excellent, with an RMSE = 0.12 m and a Bias = -0.05 m. These quantitative results are confirmed qualitatively via the time series comparison in **Error! Reference source not found..**

The storm duration was computed at 3 different levels and summarized in Table 54. This table also shows the error statistics for the differences in magnitude and timing of the peak storm surge between the modeled and observed data.

At Sewell's Point, the water levels were observed to peak at about 1 m (MSL), or only about 10 to 20 cm above their normal tidal range. In Figure 175, the effects of Michael are seen as an increase in the water levels for about four tidal cycles as the storm passed the NSN. ADCIRC does not predict this increase in water levels, with its peak values of about 0.8 m within the normal tidal range.

Again, this underprediction may be caused by several factors, but the critical factor is the wind input. As a parametric model, GAHM can reproduce the hurricane wind fields when they are smooth and well-described by a few parameters (e.g. maximum wind speeds, radius to maximum winds, and central pressure). However, for storms like Michael, which weakened and lost its shape as it tracked for more than a day over the southeast United States, parametric models like GAHM will struggle to reproduce the complexities of the wind fields. For Michael, this poor performance of the wind inputs then leads to an underprediction of the water levels during the storm.

Figure 176 shows time series of the maximum and average flood depths during Michael, and Figure 177 shows the classified flood extents during Michael at the NSN. The maximum flood depth was about 0.8 m, and the average flood depths were between 0.2 to 0.3 m. Flooding is minimal, with only 'high' flood levels at the piers on the west edge of the NSN, and no flooding predicted within the base itself.

Table 53. ADCIRC/GAHM base scenario of Michael; error statistics for predicted water levels, relative to observations at Sewell's Point.

Wind	Location	R	R ²	RMSE	NRMSE	Bias	RB	MNB	SI
GAHM	Sewell's Point	0.91	0.81	0.15	0.12	-0.05	-14.34	-0.14	0.08

Table 54. ADCIRC/GAHM base scenario of Michael; error statistics as differences in magnitude (m), timing (h), and duration (h) of peak surge characteristics at Sewell's Point.

Wind Input		Magnitude (m)	Timing (h)	Duration (h)		
				Low	Medium	High
Michael	GAHM	- 0 .17	0.9	0.0	-13.3	0.0

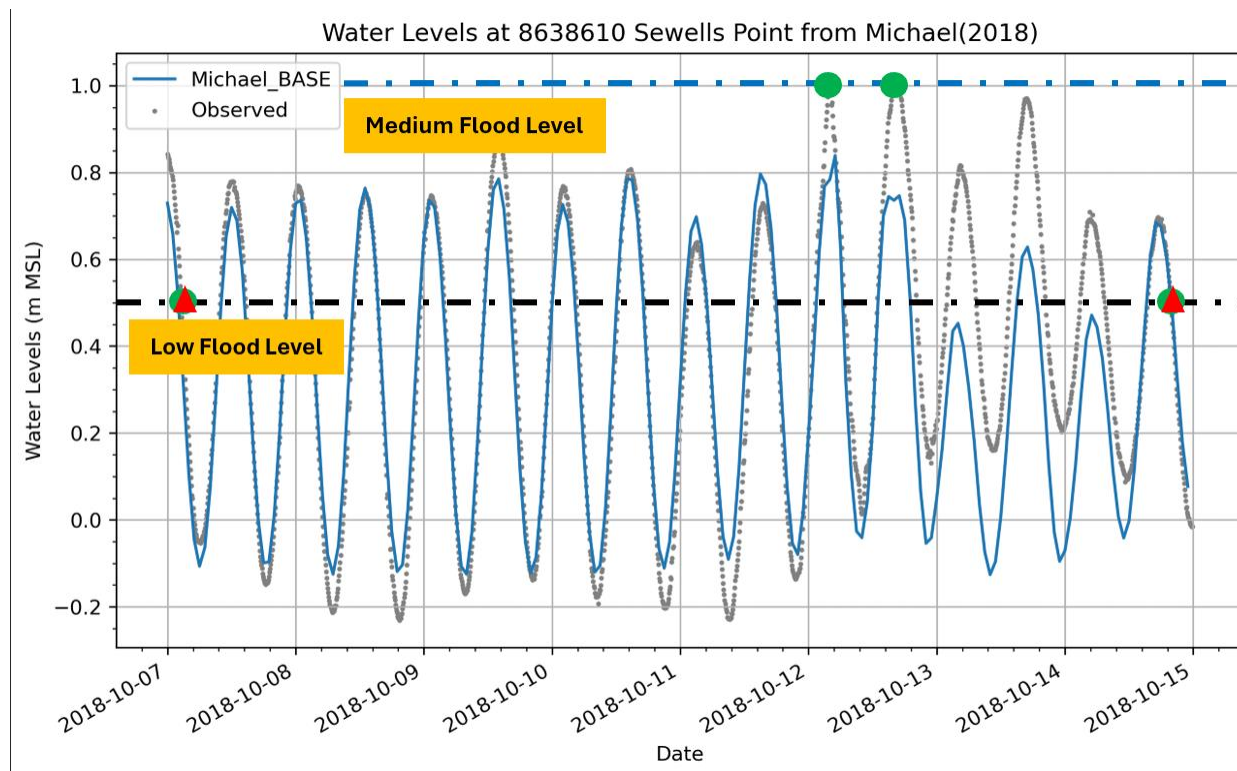


Figure 175. ADCIRC/GAHM base scenario of Michael; time series of the observed and predicted water levels at Sewell's Point, with indicators for the flood level classes.

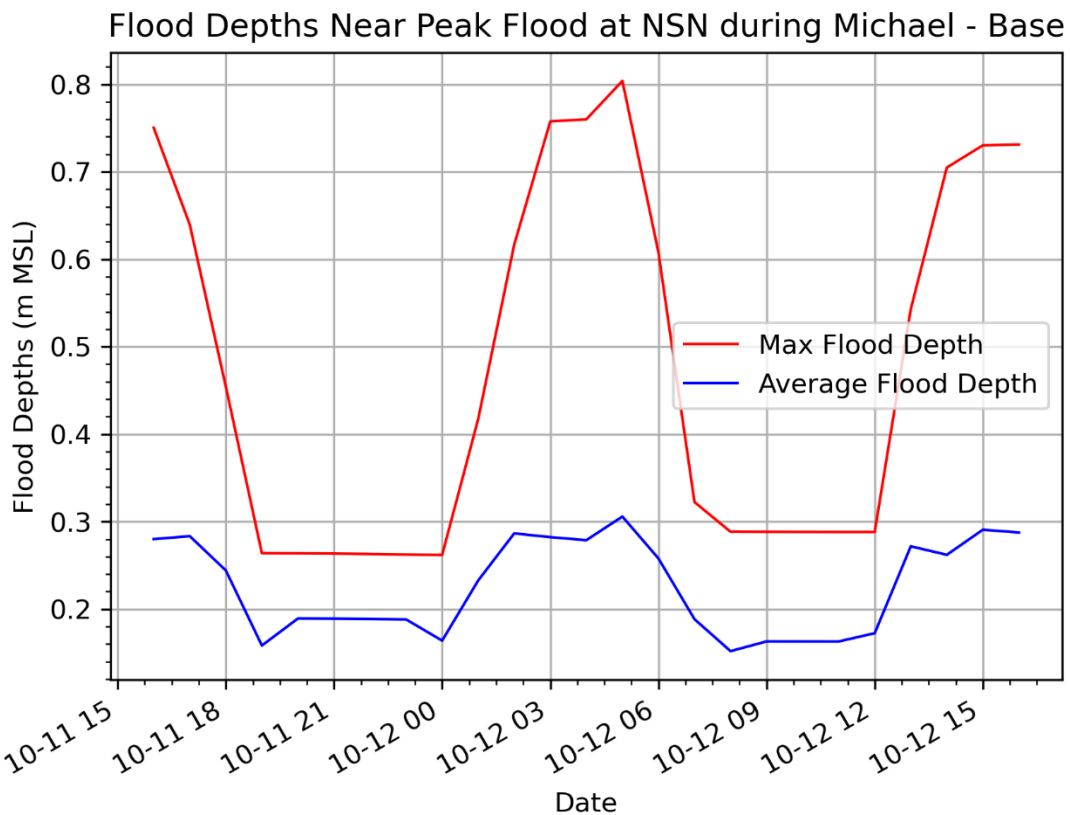


Figure 176. ADCIRC/GAHM base scenario of Michael; time series of the average and maximum flood depths (m MSL).

Hurricane Michael (2018) - Base Scenario

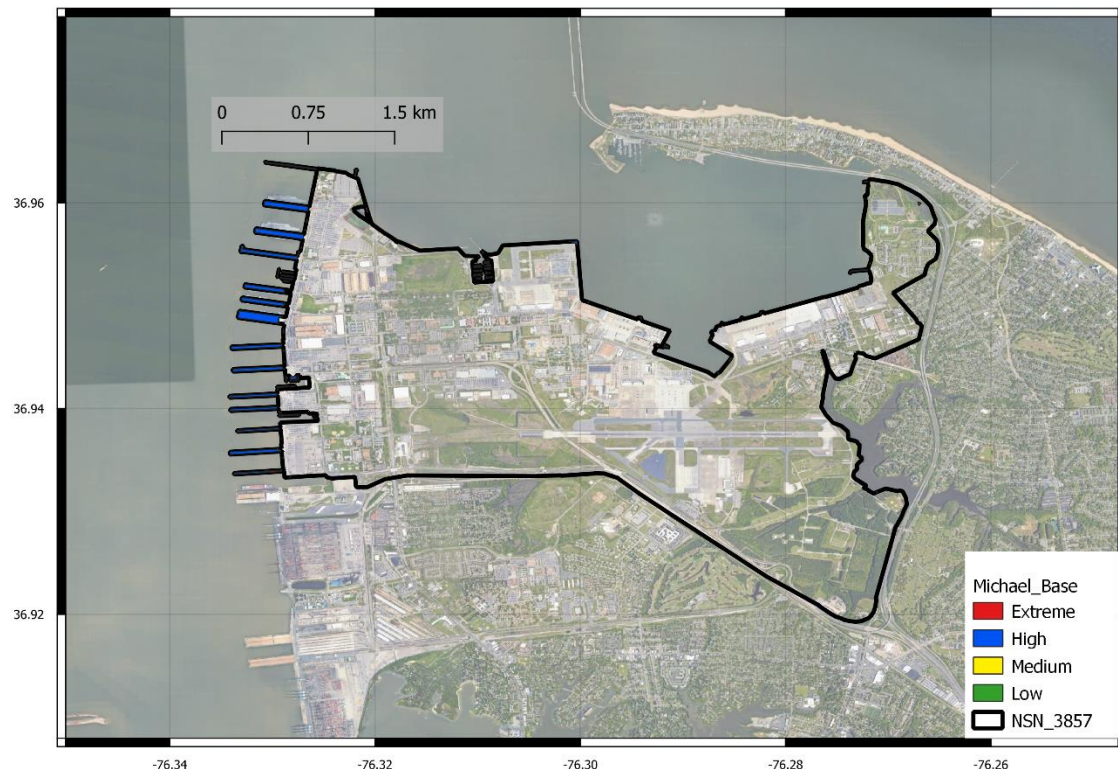


Figure 177. ADCIRC/GAHM base scenario of Michael; flood map showing the classification of the flood levels at the peak surge.

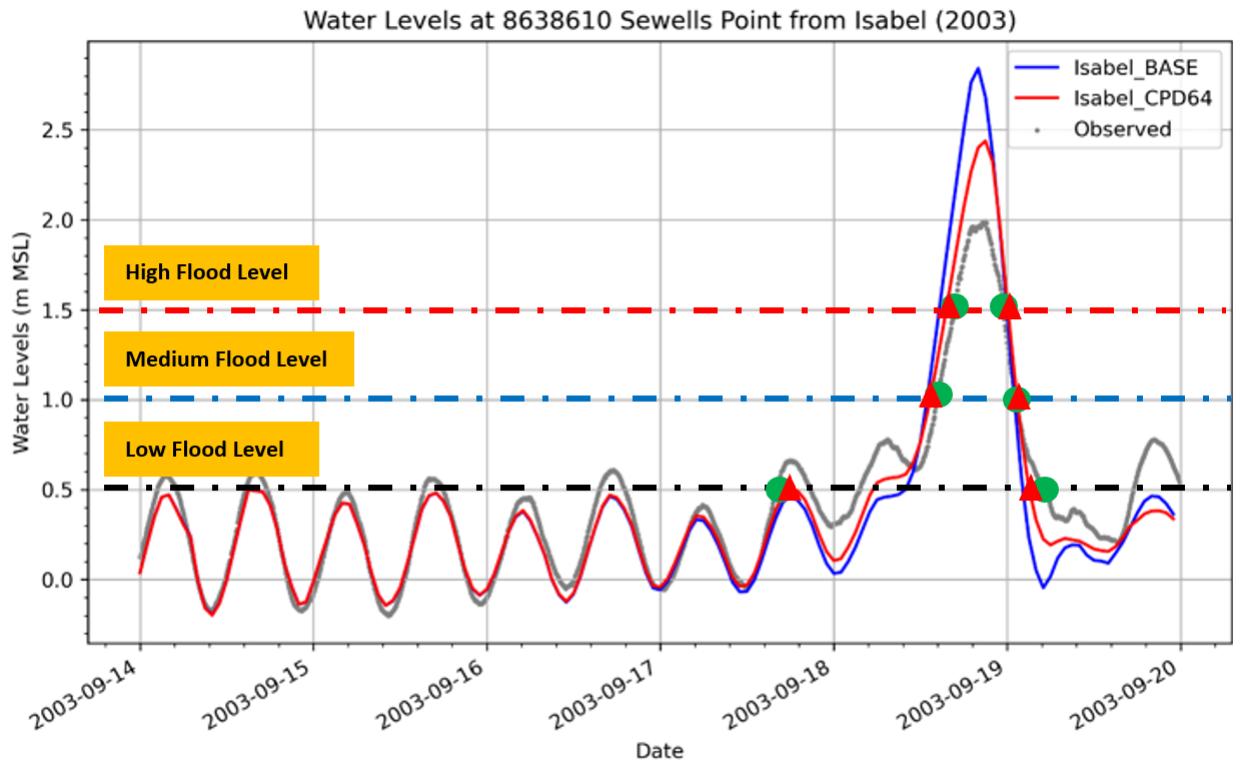
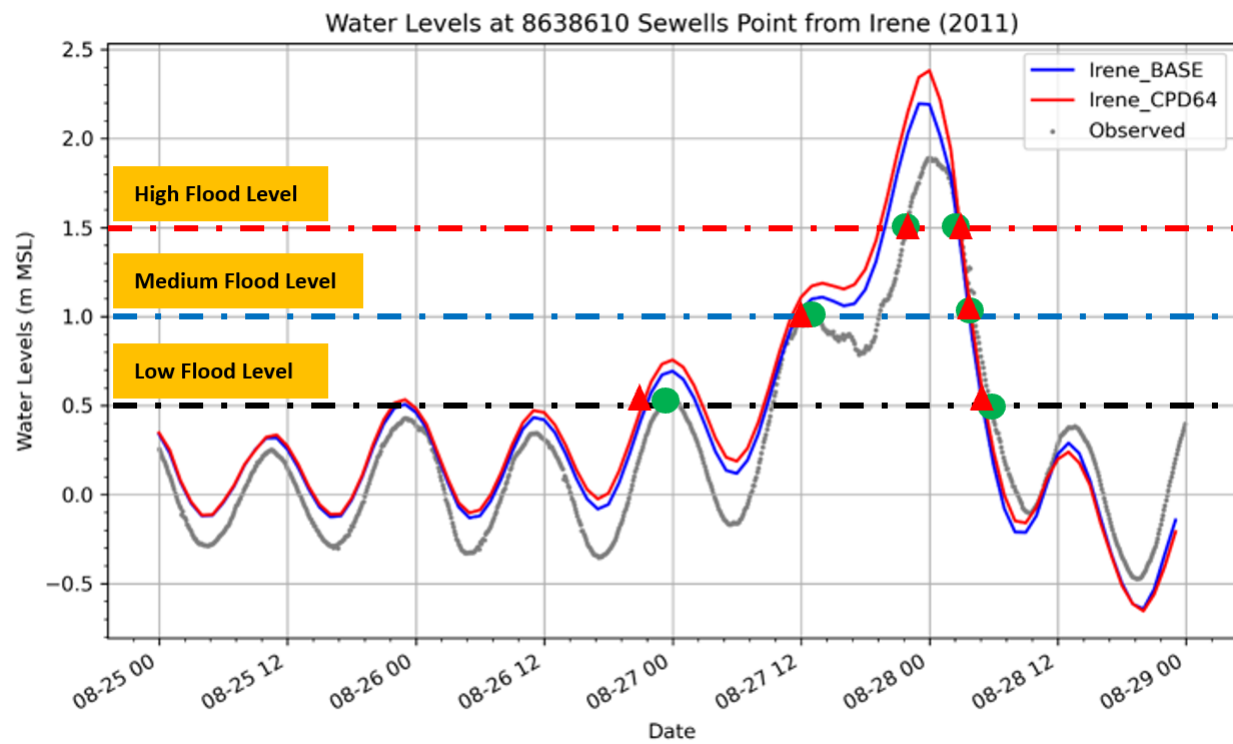
6.4.2. Impacts of Meteorological forcing

In this and the following subsubsections, we investigate the effects of storm parameter uncertainties (central pressure, storm size) on the predicted total water levels. These parameters would be uncertain as an active storm moves toward and threatens the coast, and thus it is crucial to understand the influence of these uncertainties on the hazard at NSN. The aim here is to identify and compare the results of the different perturbations in storm parameters (central pressure deficit, radius of maximum wind) of the four hurricanes on the magnitude, duration, and associated flooding at NSN. This could be crucial for future predictions of hurricane impacts with similar characteristics to the hurricanes in this study.

I. Central Pressure Deficit

Three pressure scenarios were considered with an additional drop in the central pressure deficit by 12% (PD_F0.88), 24% (PD_F0.76) and 36% (PD_F0.64) below the recorded central pressure deficit. The surge magnitude and duration for each level were obtained for all scenarios at Sewell's Point. In addition, average flood depth (AFD), maximum flood depth (MFD), and projected flood area were calculated for all scenarios. Finally, a flood map was created for each individual scenario with the classifications of each flood level (low, medium, high, and extreme). For all results in this subsubsubsection, we show only the PD_F0.64 scenario, which was the largest perturbation to the central pressure deficit, and thus it caused the largest change in the predicted water levels.

Write-up to be added when results are ready.



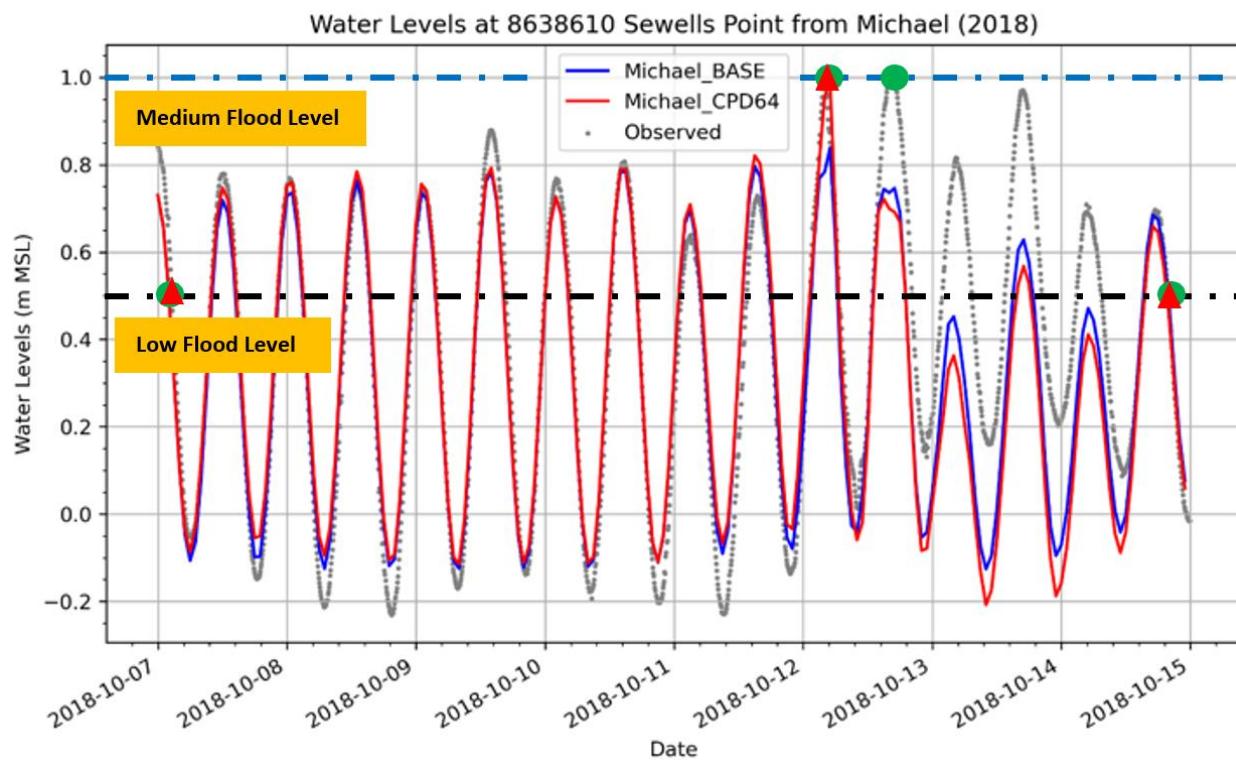


Table 55. ADCIRC/GAHM base and pressure deficit (PD_F0.64) scenarios for all storms; peak water levels (m) and surge durations (hr) at Sewell's Point.

Hurricane	Peak			Duration					
	Base	PD_F0.64	Base			PD_F0.64			
			Low	Med	High	Low	Med	High	
Irene	2.20	2.38	31	15	6	31	15	6	
Isabel	2.84	2.44	16	11	8	33	11	8	
Sandy	1.16	XX	87	27	0	87	29	0	
Michael	0.84	0.99	187	13	0	187	0	0	

Table 56. ADCIRC/GAHM base and pressure deficit (PD_F0.64) scenarios for all storms; average and maximum flood depths (m) and flooded areas (km^2) at the NSN.

Hurricane	Base				PD_F0.64			
	Average	Max	Area	%	Average	Max	Area	%
Irene	0.54	2.19	1.04	4.77	0.50	2.35	1.90	8.75
Isabel	0.42	2.80	4.43	20.40	0.48	2.34	1.53	7.05
Sandy	0.27	1.17	0.31	1.43				
Michael	0.23	0.80	0.30	1.37	0.24	0.99	0.31	1.43

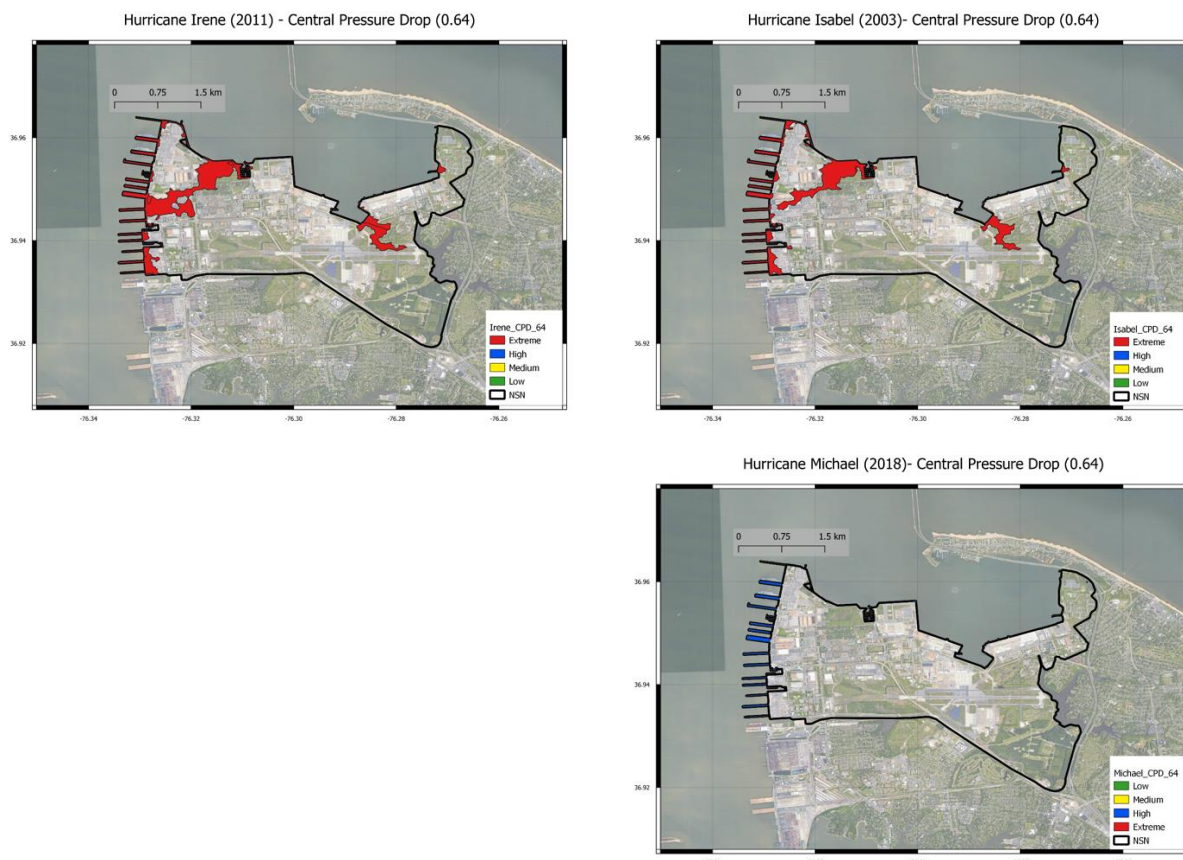
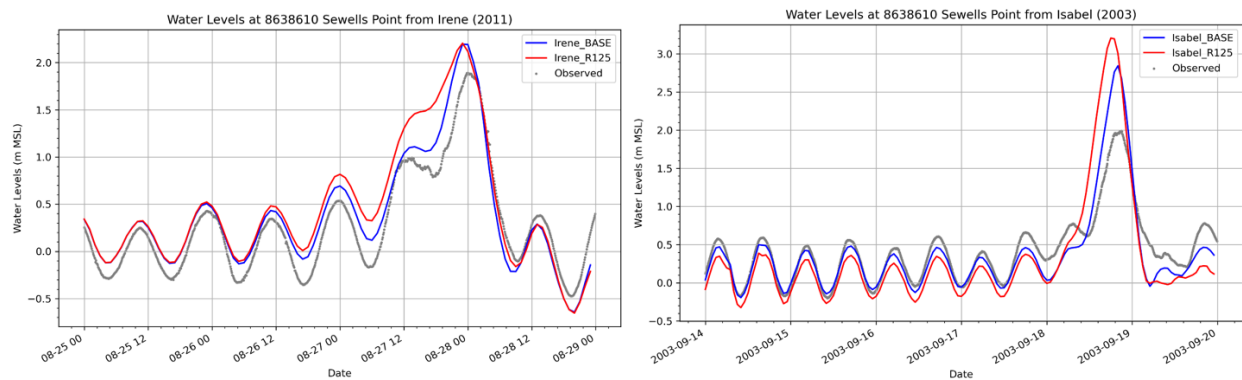


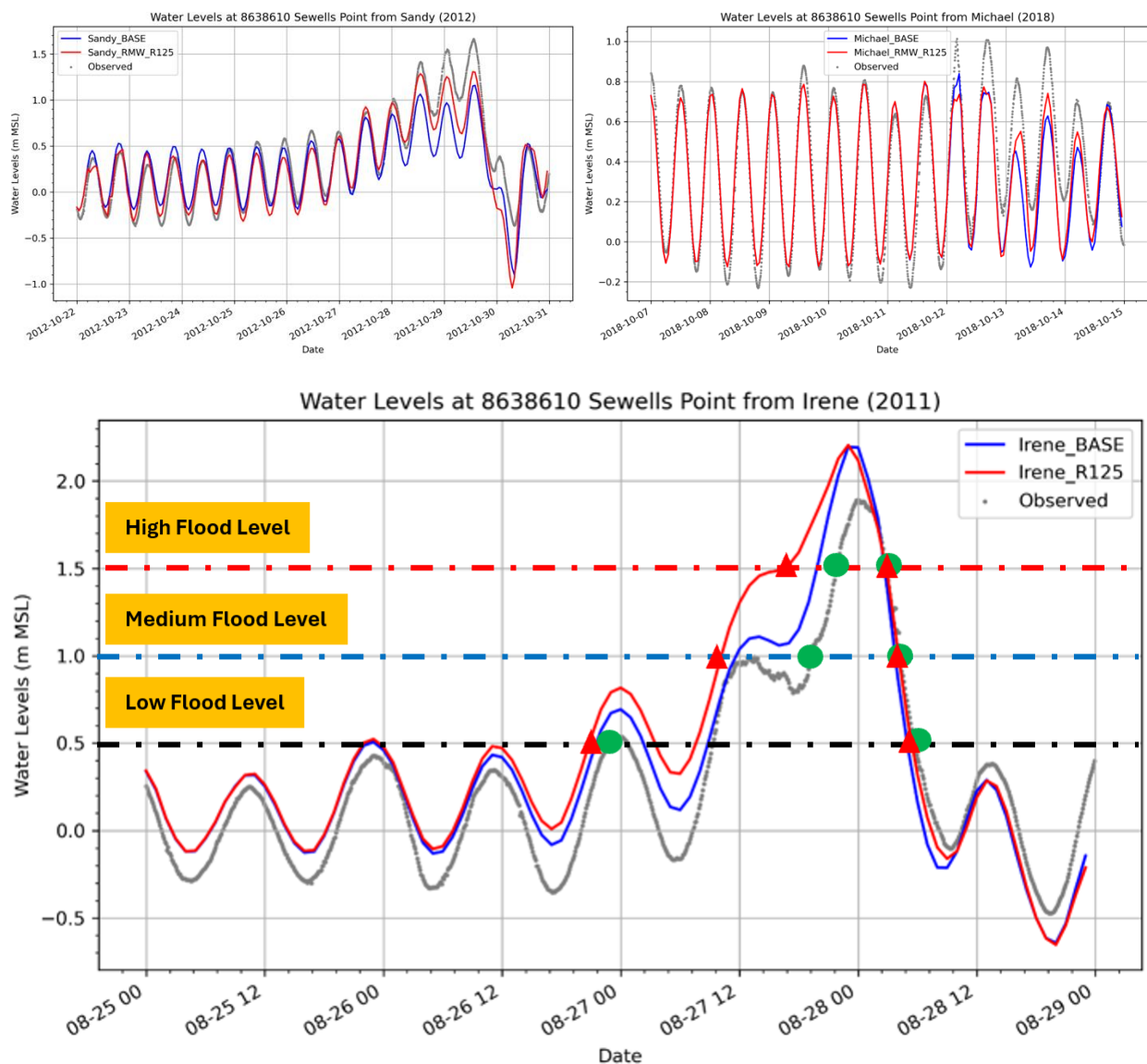
Figure 178. ADCIRC/GAHM pressure deficit (PD_F0.64) scenario for all four storms; flood maps showing the classification of the flood levels at the peak surge.

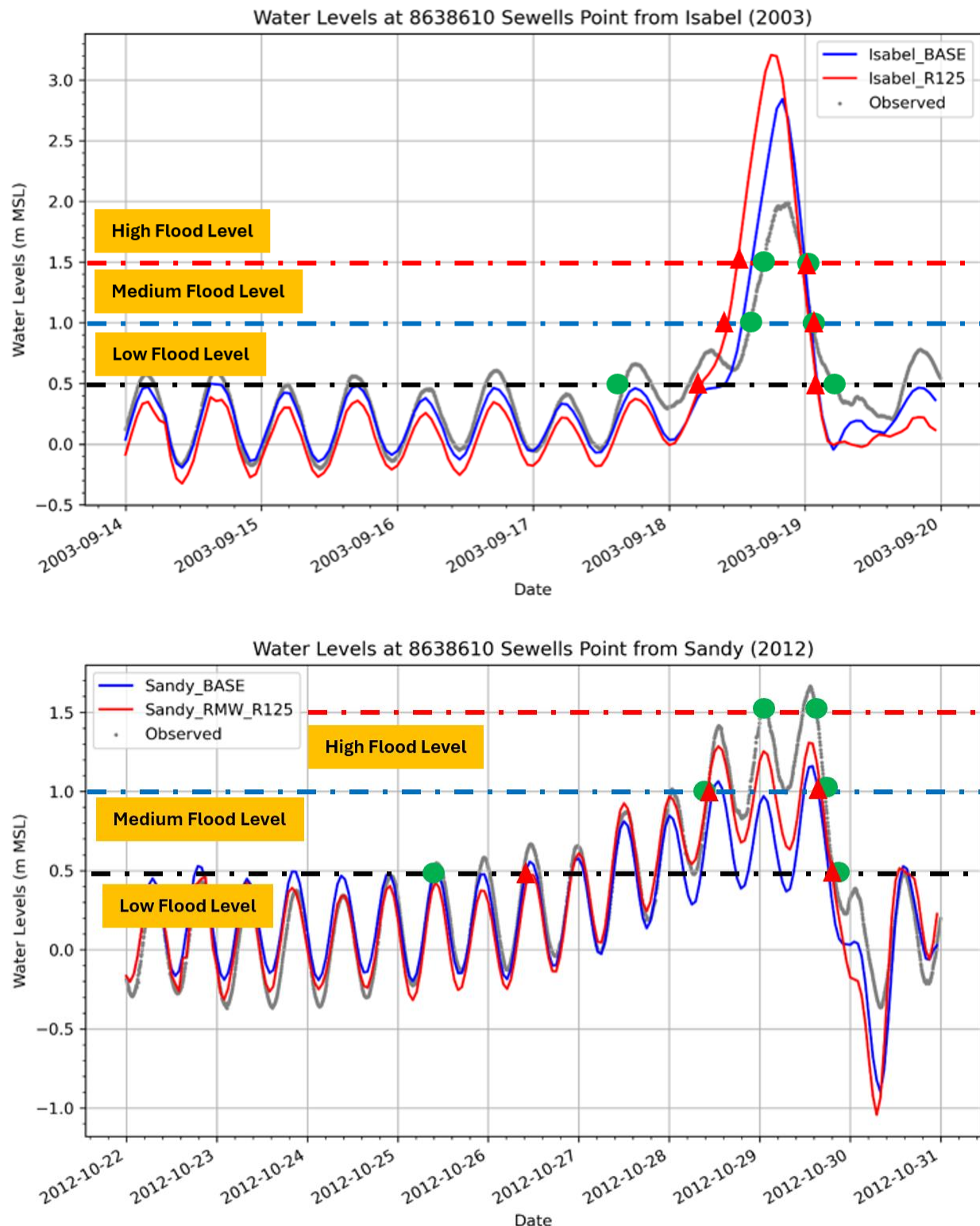
II. Radius of Maximum Wind

Three scenarios were considered for the radius of the maximum wind of the hurricane. Reducing the radius by 10% (RMW_F0.9), increasing it by 10% (RMW_F1.1) and 25% (RMW_F1.25). Following the same analysis procedure, we evaluated the statistics and characteristics of the peak surge and its associated flood area at the NSN.

Write-up to be added when results are ready.







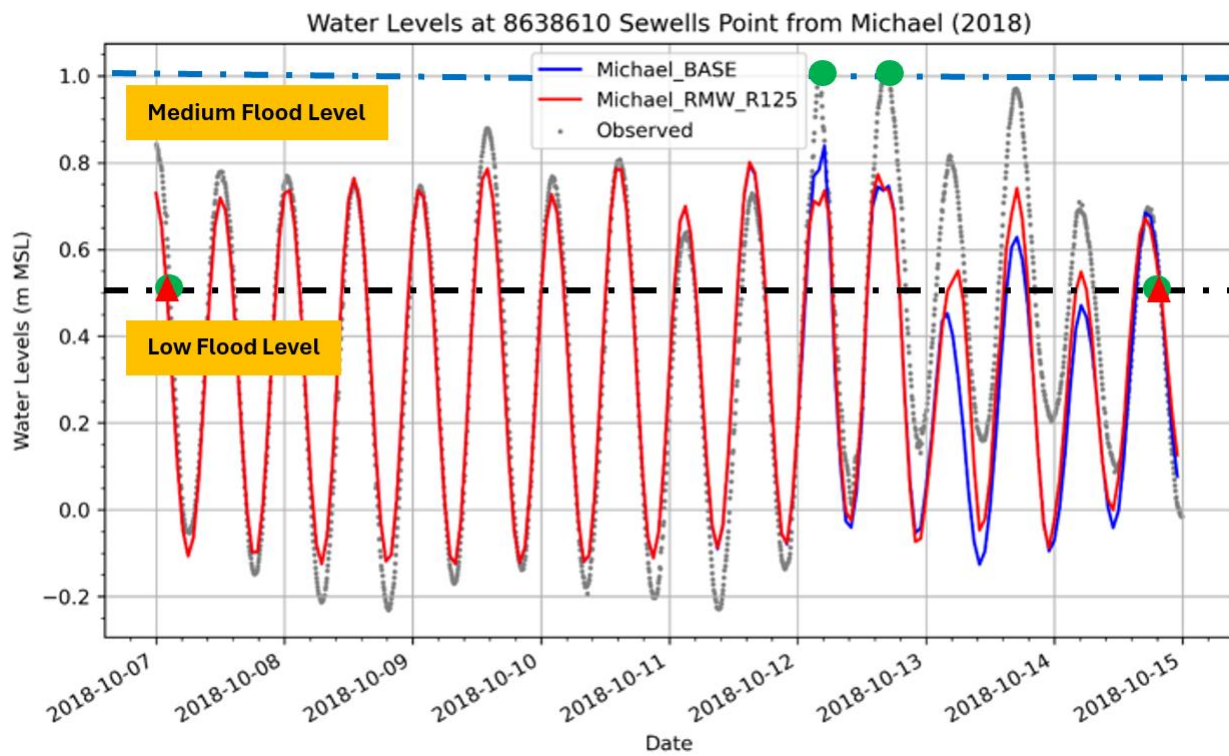


Figure 179. ADCIRC/GAHM storm size (RMW_F1.25) scenario for all storms; time series of observed and predicted water levels (m MSL) at Sewell's Point.

Table 57. ADCIRC/GAHM base and storm size (RMW_F1.25) scenarios for all storms; peak water levels (m MSL) and surge durations (hr) at Sewell's Point.

Hurricane	Peak			Duration					
	Base	RMW_F1.25	Base			RMW_F1.25			
			Low	Med	High	Low	Med	High	
Irene	2.20	2.21	31	15	6	32	17	9	
Isabel	2.84	3.21	16	11	8	20	13	10	
Sandy	1.16	1.31	87	27	0	87	29	0	
Michael	0.84	0.80	187	0	0	187	0	0	

Table 58. ADCIRC/GAHM base and storm size (RMW_F1.25) scenarios for all storms; average and maximum flood depths (m) and flooded areas (km^2) at the NSN.

Hurricane	Base				RMW_F1.25			
	Average	Max	Area	%	Average	Max	Area	%
Irene	0.54	2.19	1.04	4.77	0.59	2.16	1.00	4.59
Isabel	0.42	2.80	4.43	20.40	0.53	3.12	7.10	32.71
Sandy	0.27	1.17	0.31	1.43	0.32	1.34	0.32	1.46
Michael	0.23	0.80	0.30	1.37	0.23	0.76	0.29	1.33

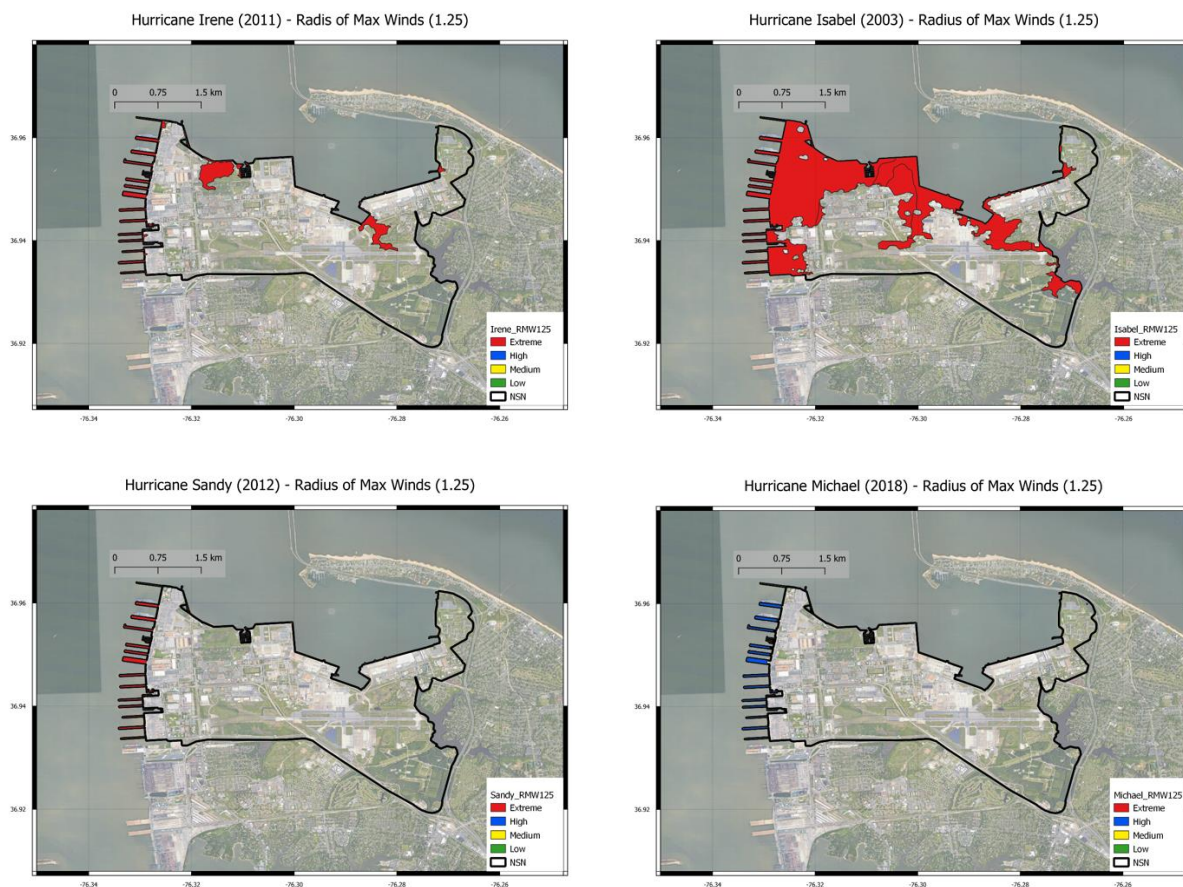


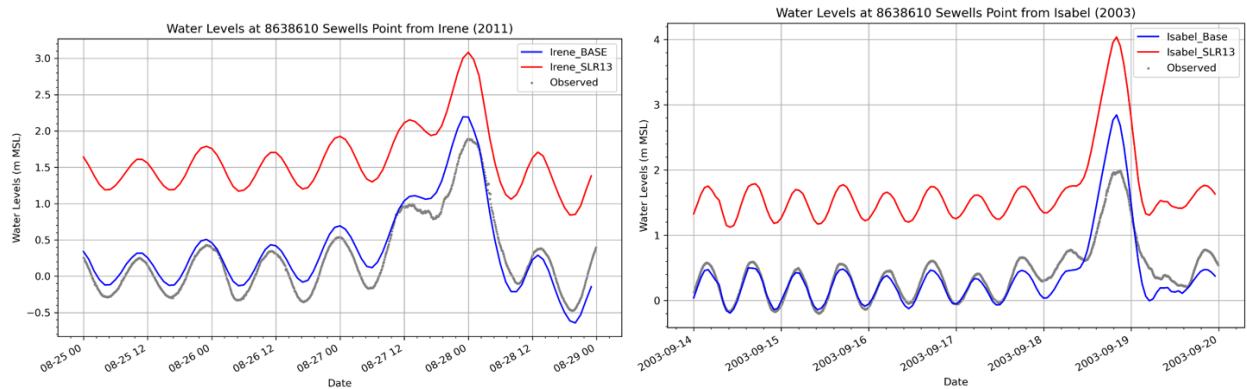
Figure 180. ADCIRC/GAHM storm size (RMW_F1.25) scenario for all four storms; flood maps showing the classification of the flood levels at the peak surge.

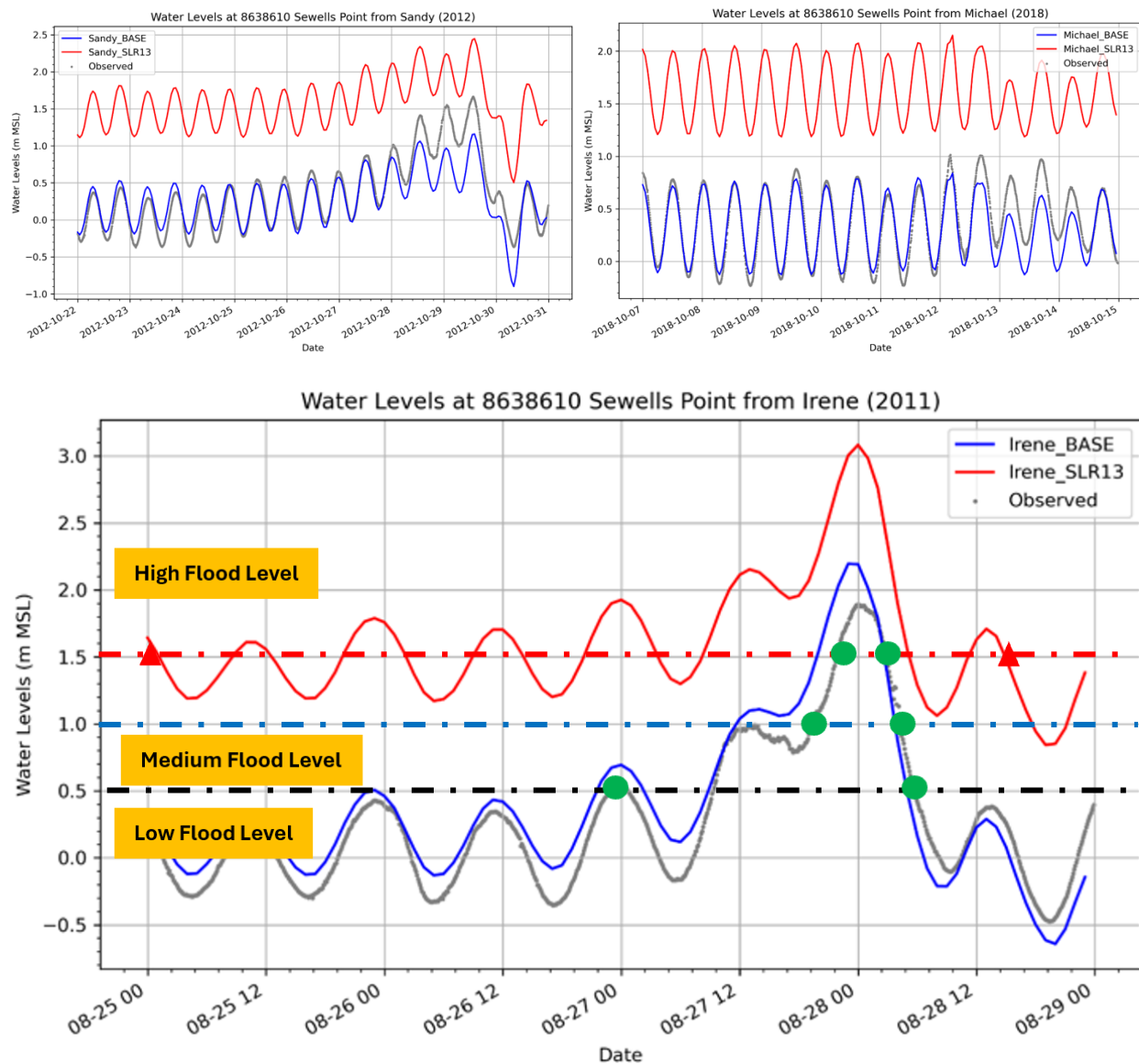
6.4.3. Impacts of Climate Changes

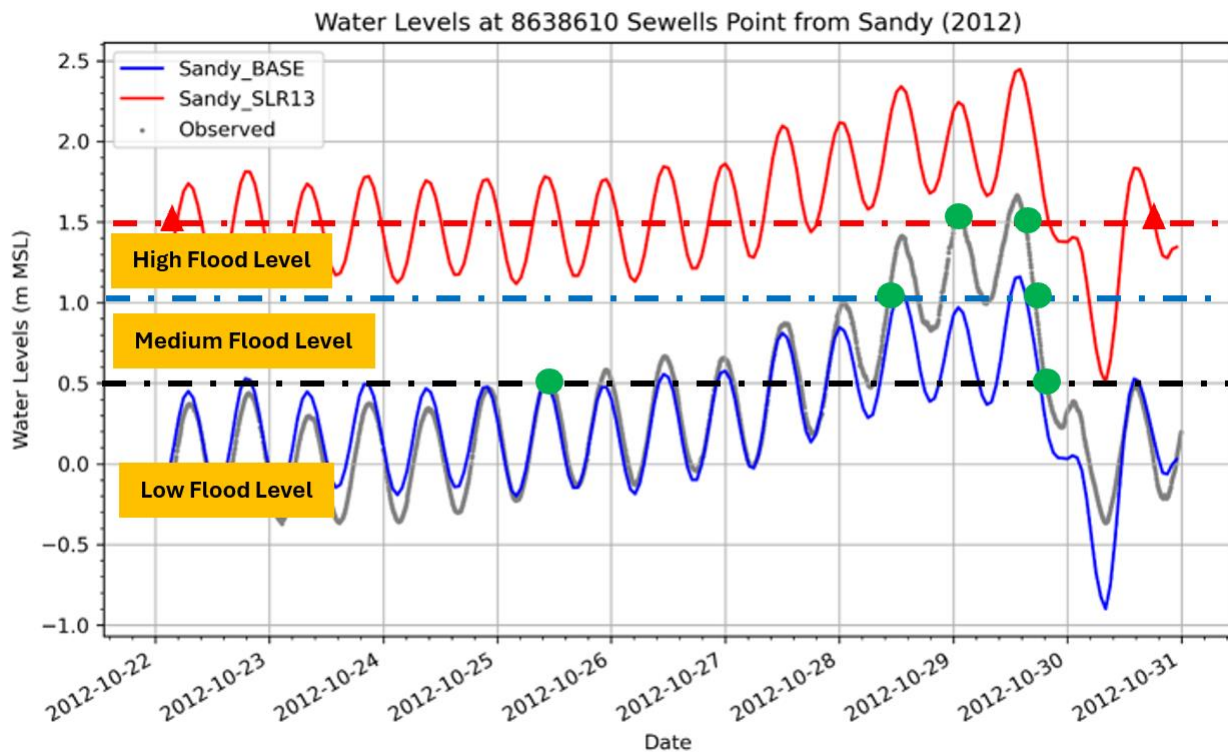
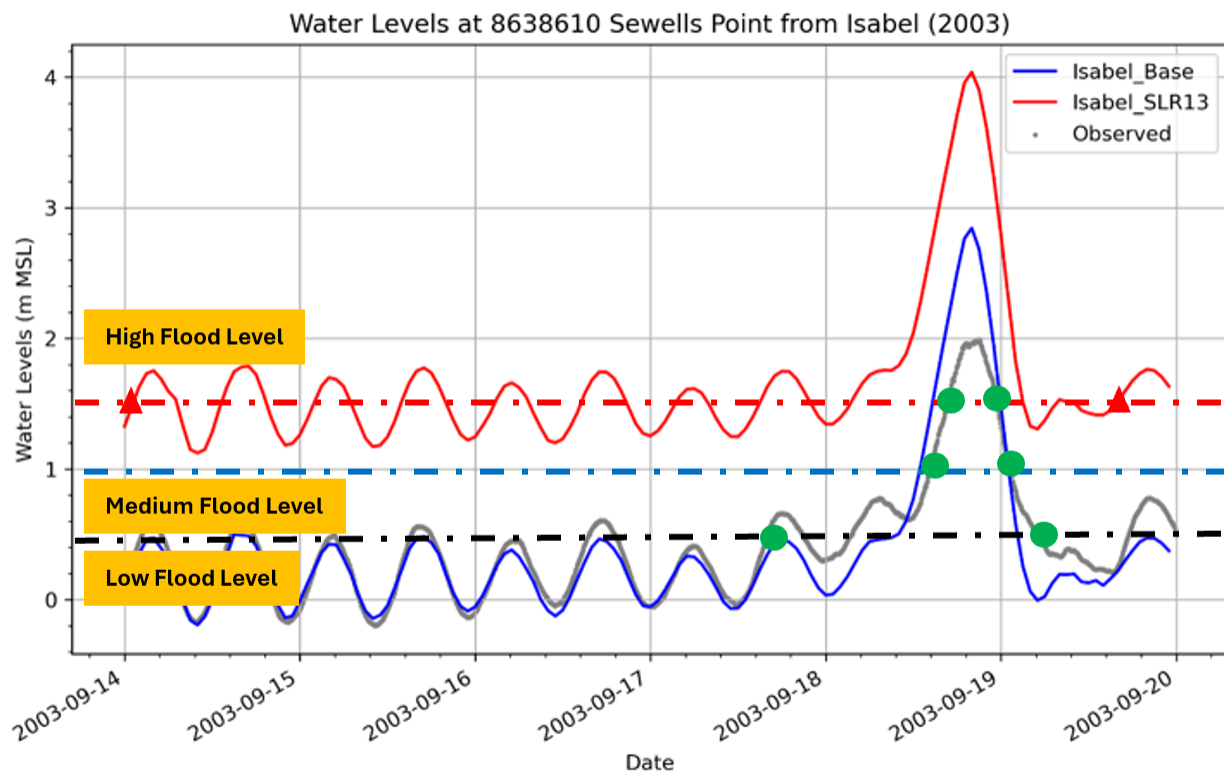
To evaluate the impact of climate change on the coastal flooding at NSN, two scenario groups were considered, the impact of Sea level Rise (SLR) and varying the wind speed. Three scenarios were investigated for each group, SLR_0.4M, SLR_0.8M and SLR_1.3M for SLR group. These scenarios included the projected climate change-induced relative sea level rise (SLR) according to, (Sweet et al., 2022) for Intermediate-Low scenarios for the US East Coast: 0.4m, 0.8m, 1.3m, projected for years 2050, 2100 and 2150 respectively. In addition, the scenarios WSF_0.925, WSF_1.075 and WSF_1.225 were considered for the wind speed group. For more details about the considered scenarios, please refer to the Demonstration plan of this project.

I. Sea Level Rise (SLR)

Three scenarios were considered for SLR scenario group, SLR of 0.4 m, 0.8 m and 1.3 m for years 2050, 2100 and 2150 respectively. Increasing the mean sea level will eventually enhance the peak surge magnitude and duration at all locations. This will clearly reflect on the potential flood areas.







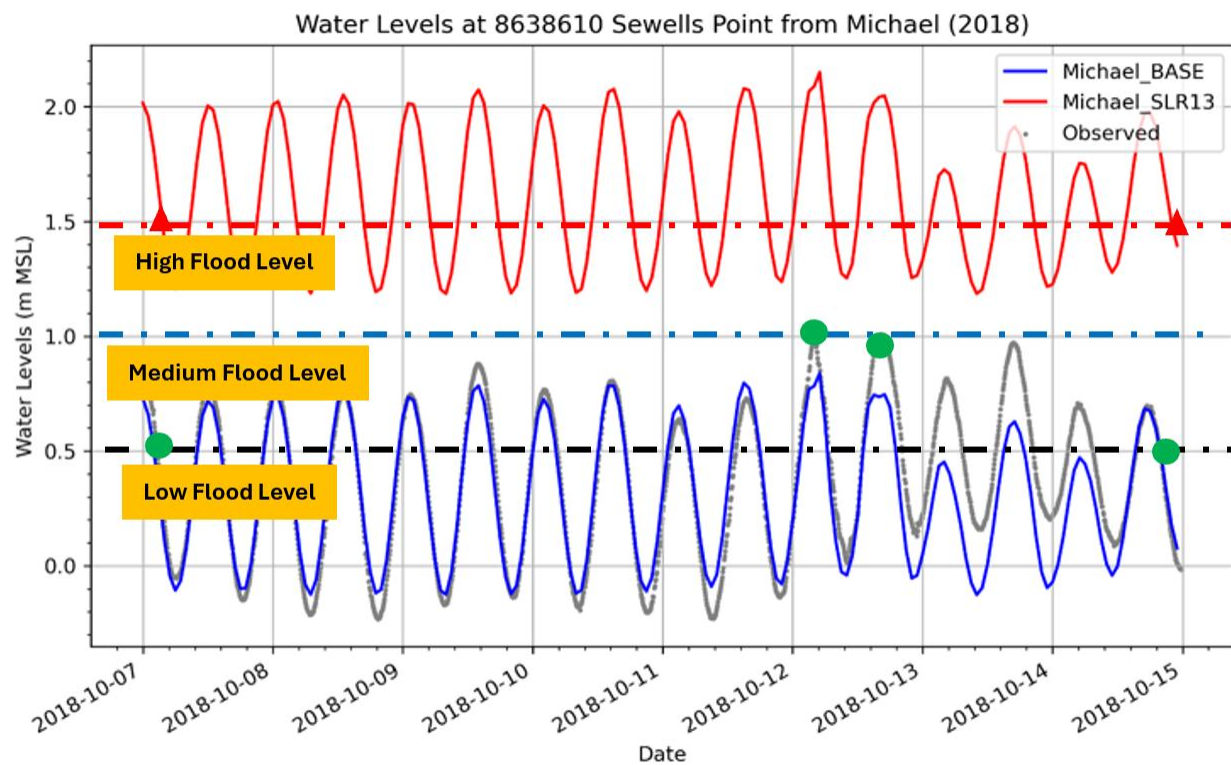


Figure 181. ADCIRC/GAHM sea level rise (SLR_1.3M) scenario for all storms; time series of observed and predicted water levels (m MSL) at Sewell's Point.

Figure 182. Water level time series (m) during the different hurricanes showing the surge magnitude and duration for different surge levels for the base and SLR_1.3M scenarios at Sewells Point, NSN, the US.

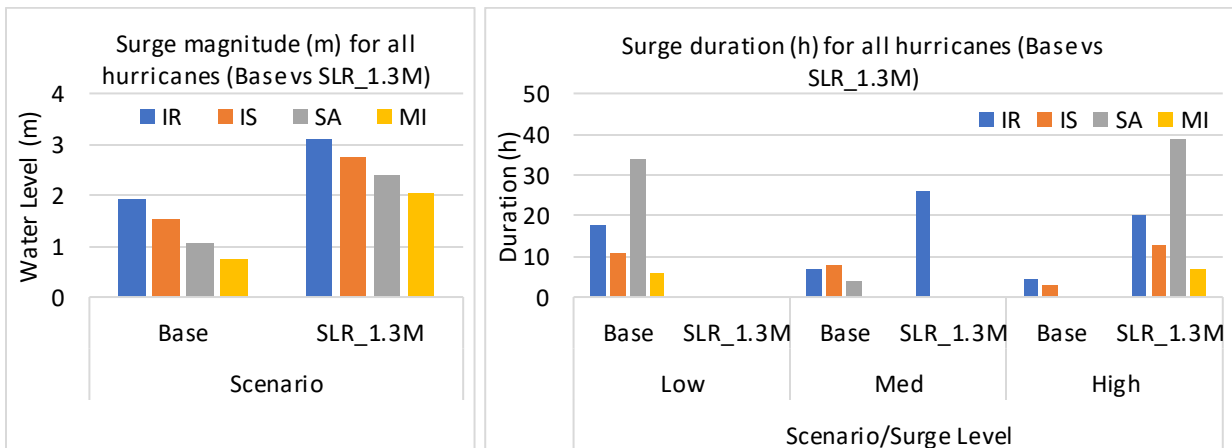


Figure 183. Peak surge (m) (left panel) and surge duration (h) of the different surge levels (right panel) for the base and SLR_1.3M scenario for all hurricanes, NSN, the US.

Table 59. Peak surge characteristics (Maximum and Duration) of the base and SLR_1.3M scenarios for all Hurricanes at Sewells Point, NSN, the US.

Group	Hurricane ID	Max. Surge (m)		Duration (h)					
		Base	SLR_1.3M	Low		Med		High	
				Base	SLR_1.3M	Base	SLR_1.3M	Base	SLR_1.3M
CC*	IR	1.92	3.12	17.5	--	7	26	4.5	20
	IS	1.55	2.74	11	--	8	--	3	13
	SA	1.08	2.38	34	--	4	--	0	39
	MI	0.73	2.04	6	--	0	--	0	7

*Climate Change

--the water level is above this level

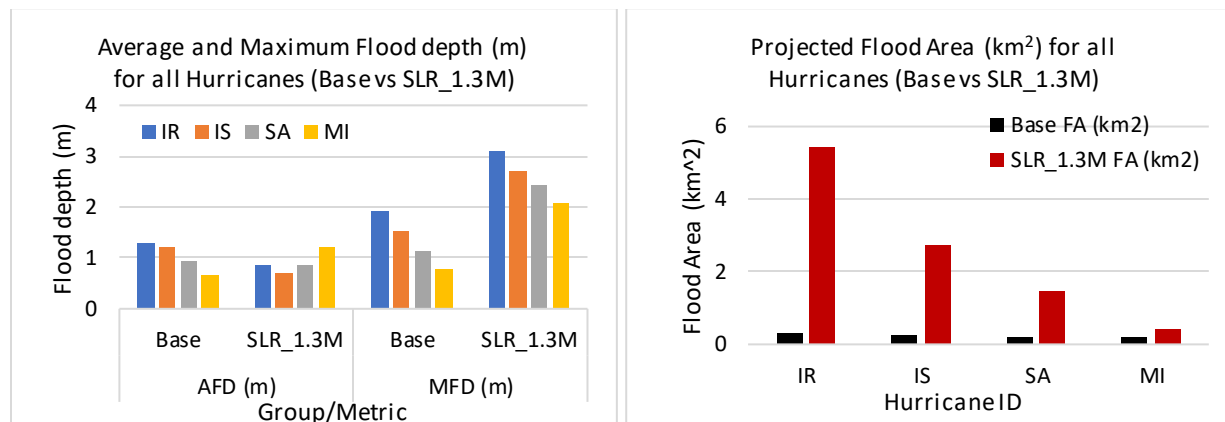
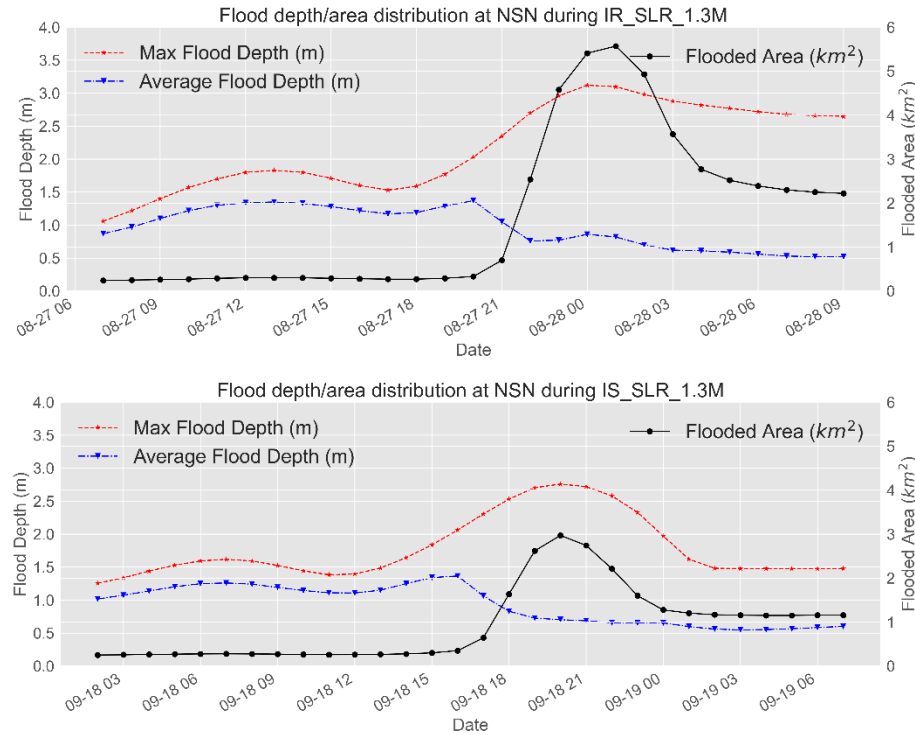


Figure 184. Average Flood Depth (AFD) & Maximum Flood Depth (MFD) in meters (left panel) and Flood area (km^2) (right panel) of all hurricanes for the Base and SLR_1.3M scenarios at NSN, the US.

Table 60. Flood area characteristics of the base and SLR_1.3M scenarios for all hurricanes at NSN, the US.

Group	Hurricane ID	Base				SLR_1.3M			
		Average FD (m)	Max FD (m)	Flood area (km^2)	%	Average FD (m)	Max FD (m)	Flood area (km^2)	%
CC	IR	1.31	1.94	0.34	2.47	0.86	3.12	5.41	39.3
	IS	1.21	1.52	0.24	1.72	0.69	2.72	2.74	19.9
	SA	0.94	1.14	0.23	1.6	0.87	2.42	1.47	10.7
	MI	0.66	0.79	0.2	1.45	1.2	2.07	0.45	3.3

The increase in the flood magnitude and duration, especially of the high flood level, has also increased the duration of ground flooding. Figure 77 shows the time series of the average and maximum flood depth in meters in addition to the flood area (km^2) for all hurricanes for a few hours before and after the peak surge/flood. It can be shown that the flood areas are stable below 0.5 km^2 till the peak surge where the flood areas increase drastically along with the maximum flood depth. However, even after hours of the peak flood, the flood area and the maximum flood maintain significant values. For instance, observing Hurricane Irene, Figure 77 upper panel, the flood areas remained relatively constant below 0.5 km^2 till August 27th at 20:00, which is 4 hours before the peak surge, where the flood area increased up to 5.4 km^2 and then started to decline again. However, the flood areas did not decline down to 0.5 km^2 , but to about 2 km^2 , which means that these areas will be flooded for hours (maybe days) after the peak flood occurs with an average and a maximum water depth of about 0.5 m and 2.5 m respectively.



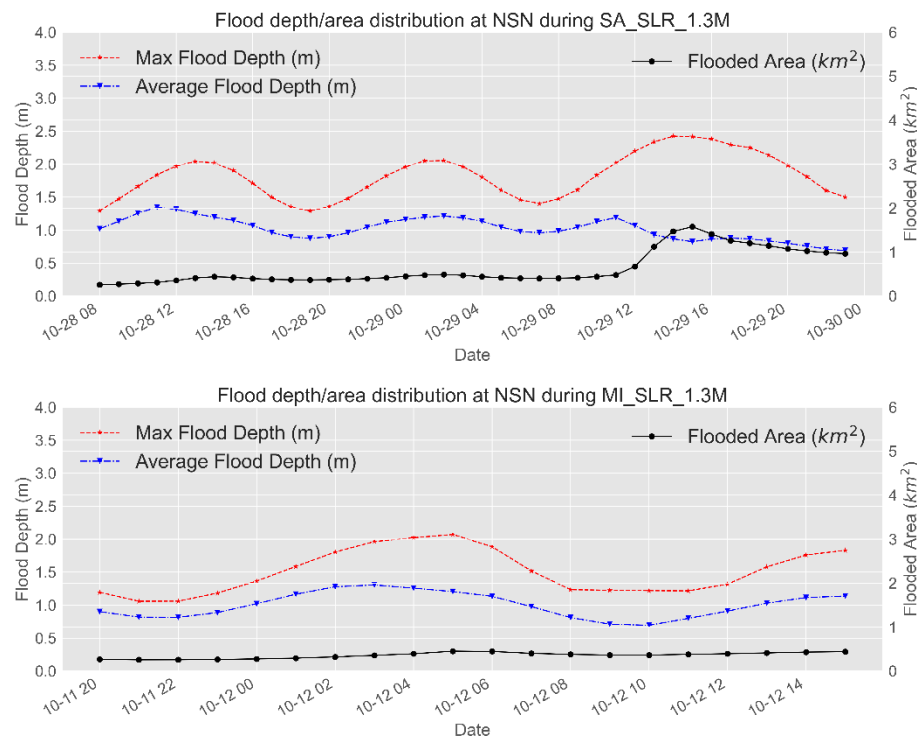


Figure 185. Time series of the projected average and maximum flood depth (left axis) and flood area (km^2 -right axis) for all hurricanes for SLR_1.3M scenario at NSN, the US.

Investigating the spatial extent of the flood areas revealed that the north and west parts of the base are the most vulnerable areas to flooding, Figure 78. These areas have different flood levels with the extreme flood level (red color) concentrated at two spots. These spots are the vegetation area (golf courses) and the residential area at the northeast with low elevation. Figure 79 shows an example of the classification of the flood areas into the four flood levels for Hurricane Irene during the SLR_1.3m scenario. It can be noticed that most of the flood area lies under the high to extreme flood level (>0.5m above ground level), Figure 80, with most of the extreme level concentrated at the low-elevation green areas.

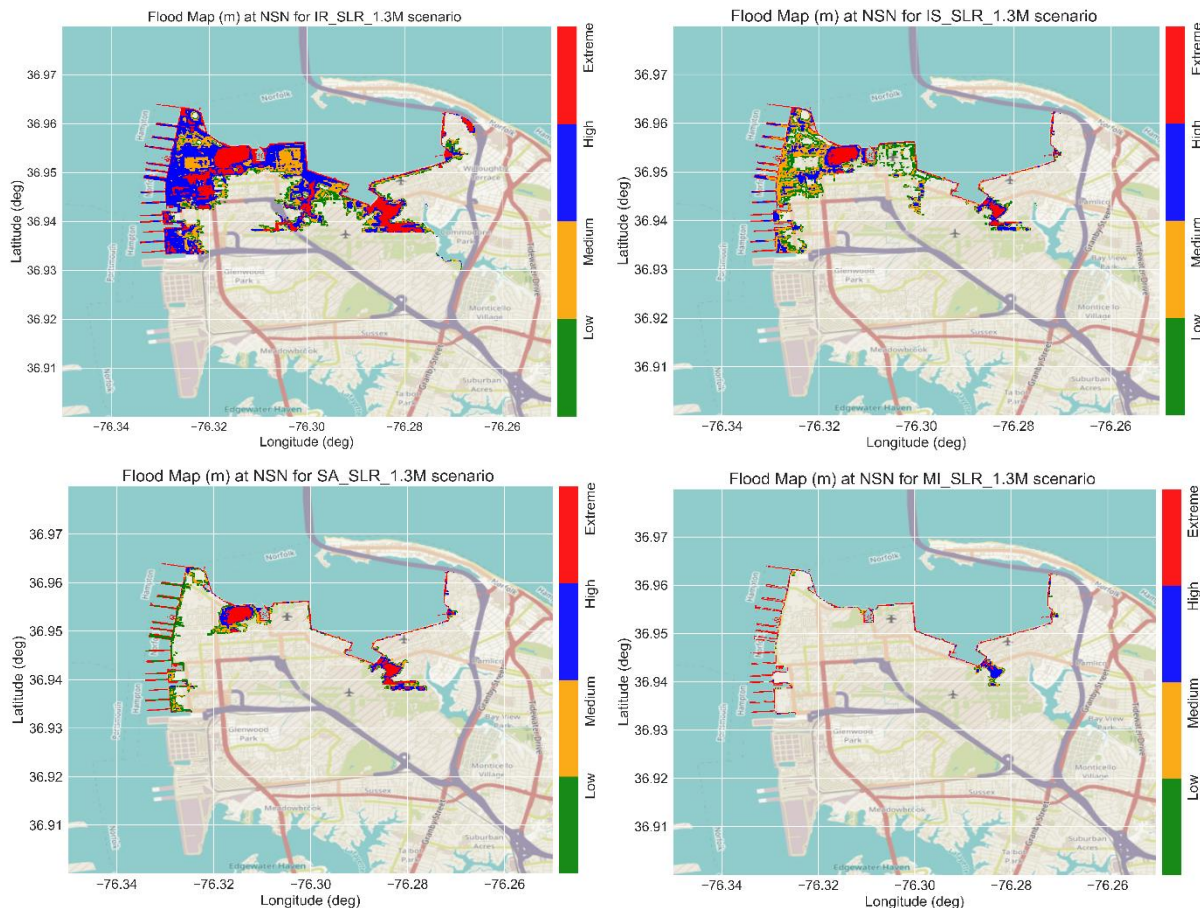
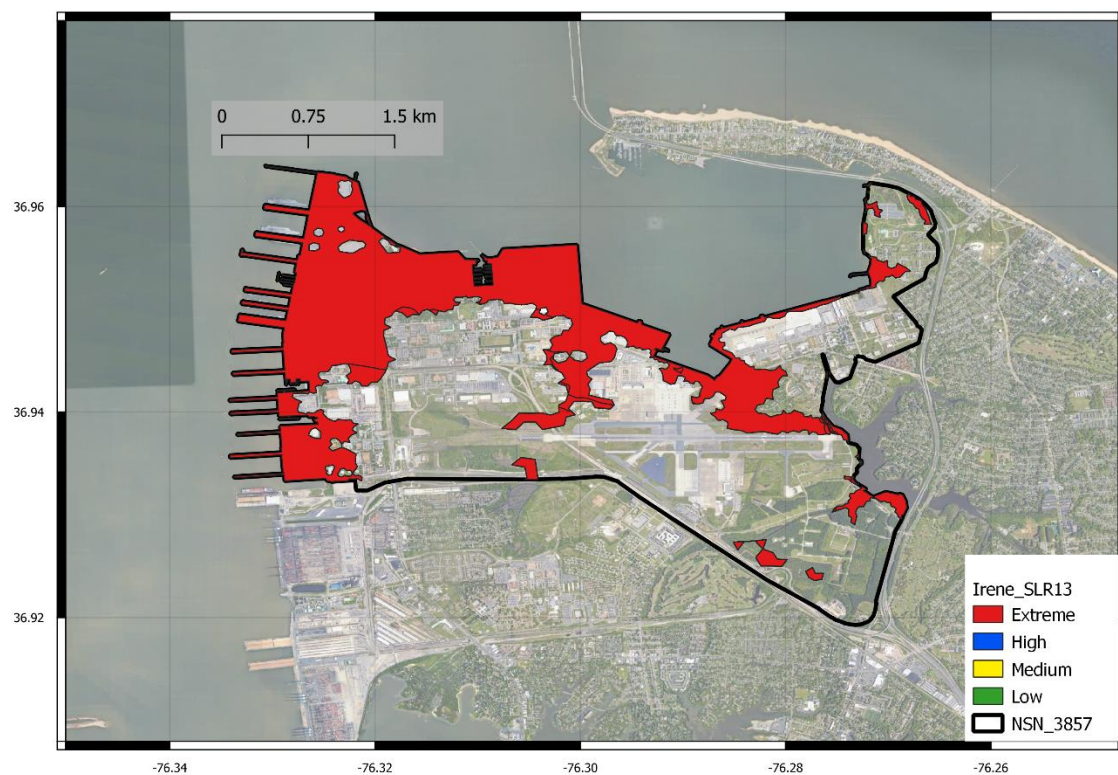
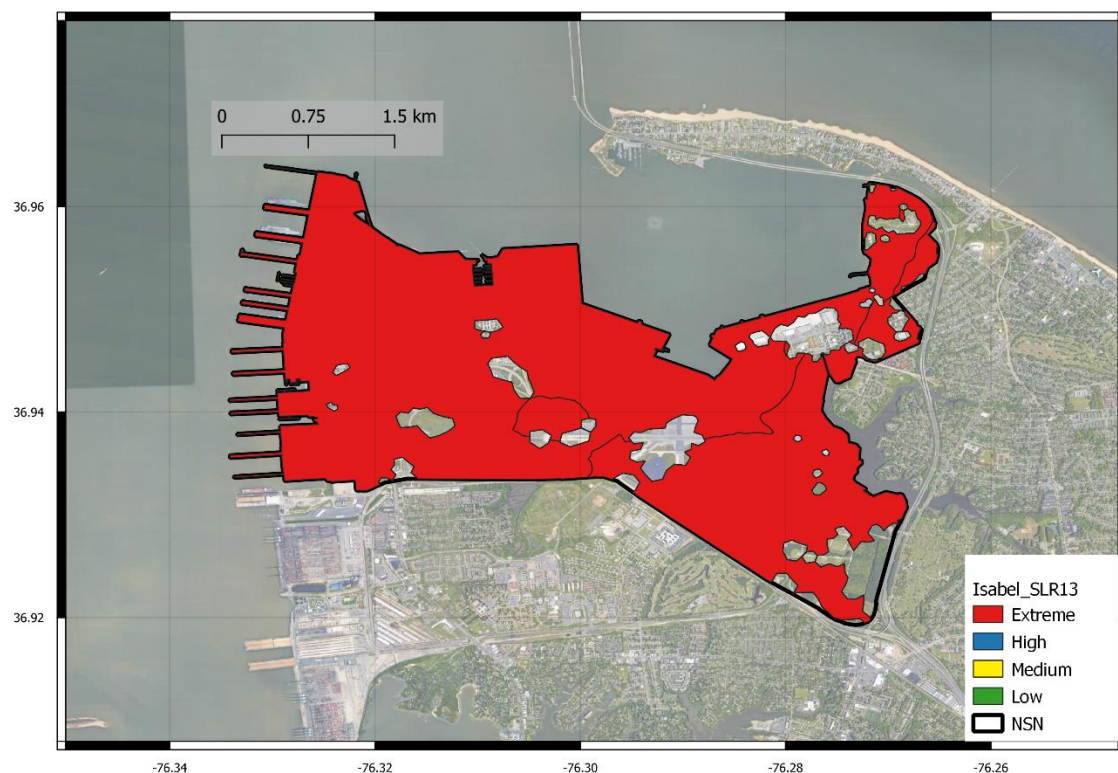


Figure 186. Flood maps with the flood levels for the different hurricanes during the peak surge for the SLR_1.3M scenario at NSN, the US.

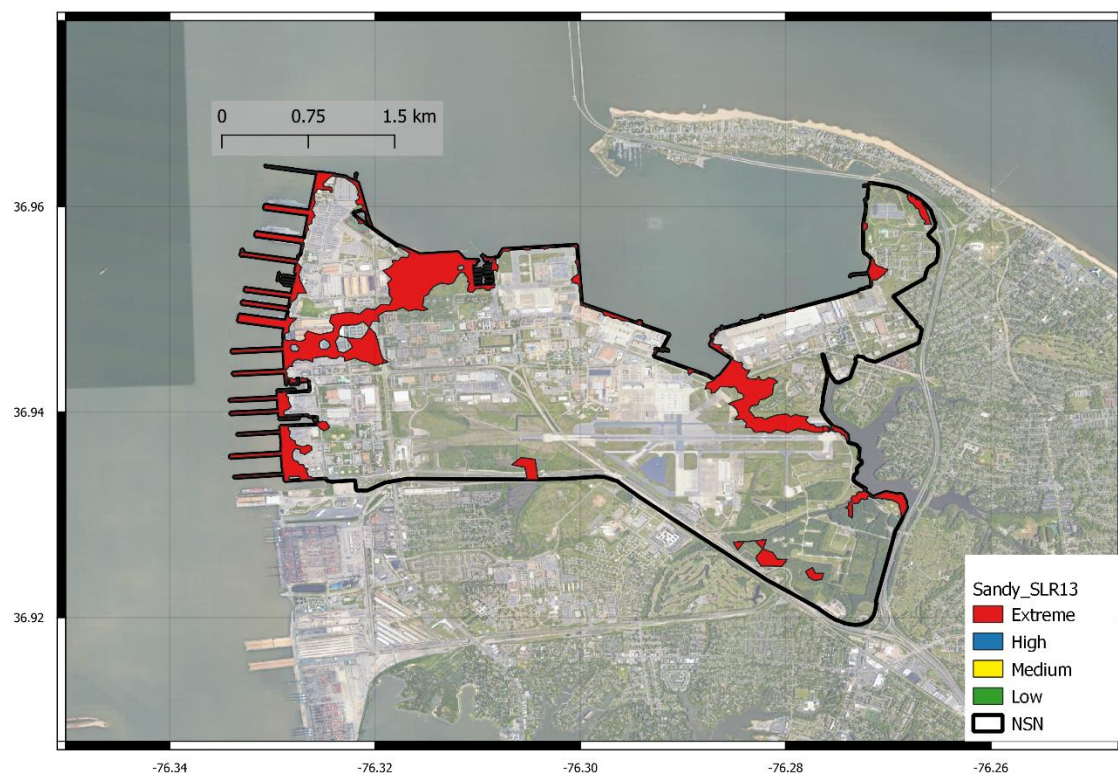
Hurricane Irene (2011) - Sea Level Rise (1.3)



Hurricane Isabel (2003) - Sea Level Rise (1.3)



Hurricane Sandy (2012) - Sea Level Rise (1.3)



Hurricane Michael (2018) - Sea Level Rise (1.3)

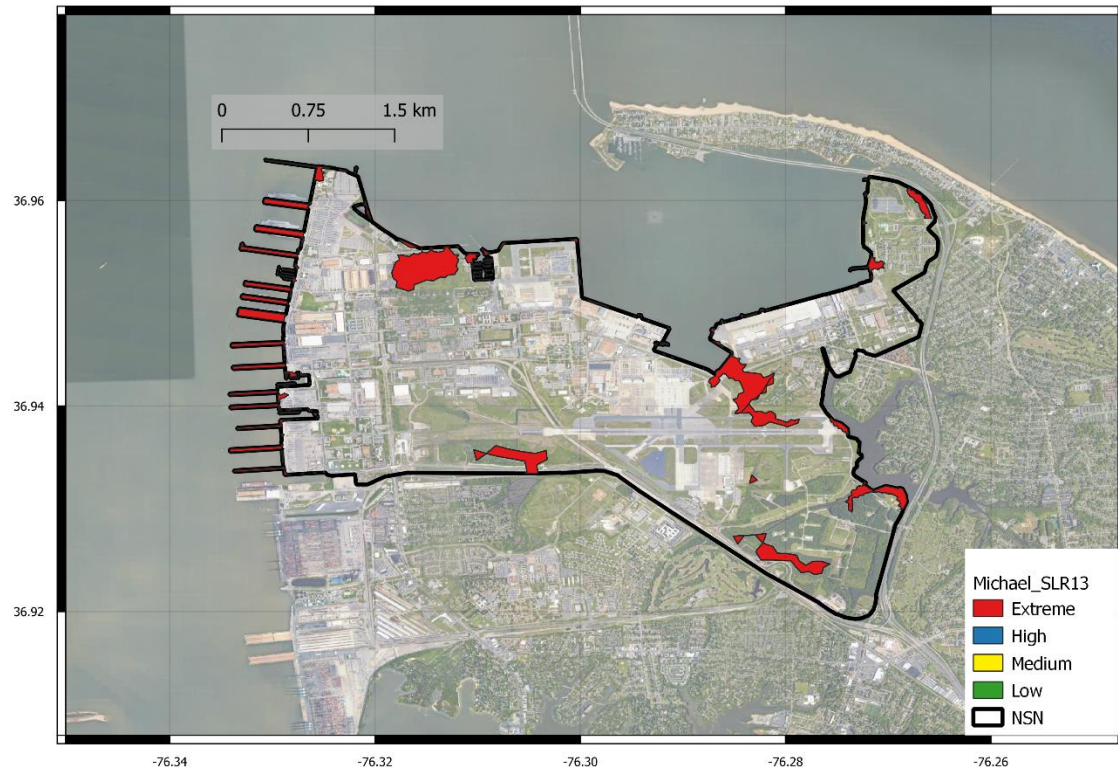


Figure 187. Flood area classified by level (Low, Medium, High, and Extreme) in meters for the SLR_1.3M scenario during hurricane Irene-2011 at NSN base, the US.

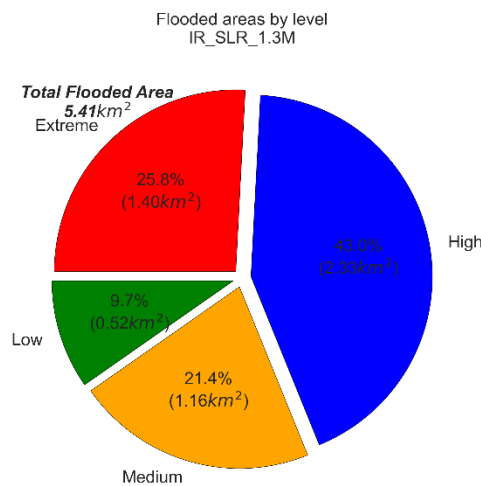


Figure 188. Pie chart of the flood areas, with percentages, of the different flood levels for SLR_1.3M scenario for Hurricane Irene-2011 at NSN, the US.

Considering the SLR_0.4M scenario, the surge magnitude has increased by the magnitude of the SLR (0.4m) for all hurricanes with a pronounced increase for Hurricane Michael of about 0.54m. This increase reflects an increase in the surge duration especially for the low surge level with a minor impact on the medium and high levels. The flood area characteristics show some increase in the average and maximum flood depth for all hurricanes with the most pronounced increase during Hurricane Michael. However, this increase did not reflect a significant rise in the spatial extent of the flood area where a significant increase in flood area was detected for Hurricane Irene, 0.9km² (6.5%), with an insignificant increase for all other hurricanes. The most affected areas, with the maximum flood depth, are also located in vegetation areas, see Appendix C.

A similar pattern was detected for SLR_0.8M but with a higher magnitude. A significant increase in surge magnitude and duration was detected for all hurricanes. The high surge level shows a prominent change over the previous scenario where Hurricanes Sandy and Michael showed 8h and 3h high-surge duration respectively compared to zero for the base scenarios. This pattern reflected a significant increase in the average and maximum flood depth but with limited influence on the spatial extent of the flood areas with a maximum change of less than 1%. Although Hurricane Irene showed a decrease in the average flood depth, it showed a significant increase in the flood area from 0.34km² (2.5%) for the base scenario to 2.94km² (21.4%) followed by Hurricane Isabel at 0.72 km² (5.2%). Most of the flood areas are located along the vegetation areas and the western part of the base, see Appendix C.

II. Increasing Wind Speed

Climate change can have a significant impact on enhancing the severity of the hurricane by increasing the intensity of the wind speed. Increasing the hurricane wind speed will eventually enhance the peak surge magnitude and duration which will reflect on the potential flood areas. In the current study, we will consider three scenarios for wind speed change, decreasing the wind speed by 7.5% (WSF_0.925), increasing the wind speed by 7.5% (WSF_1.075), and enhancing the wind speed by 22.5% (WSF_1.225).

Write-up to be added when results are ready.

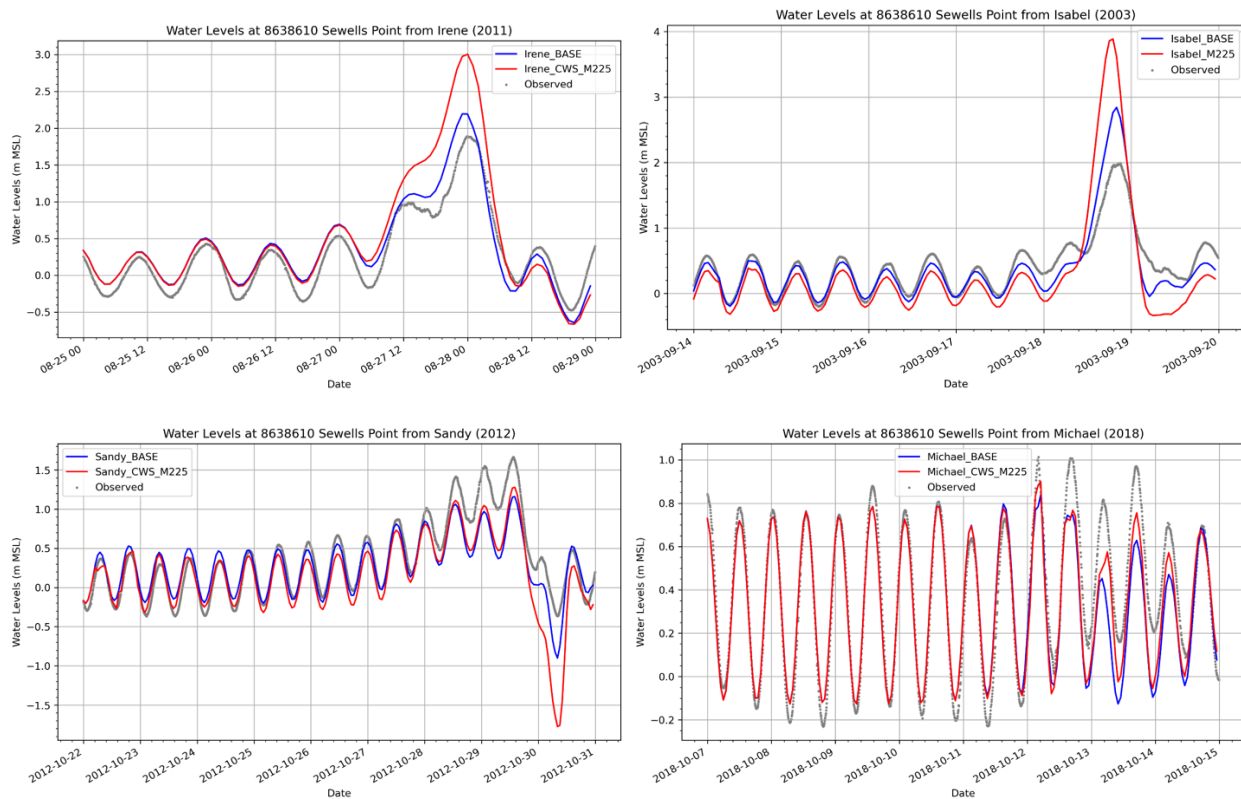


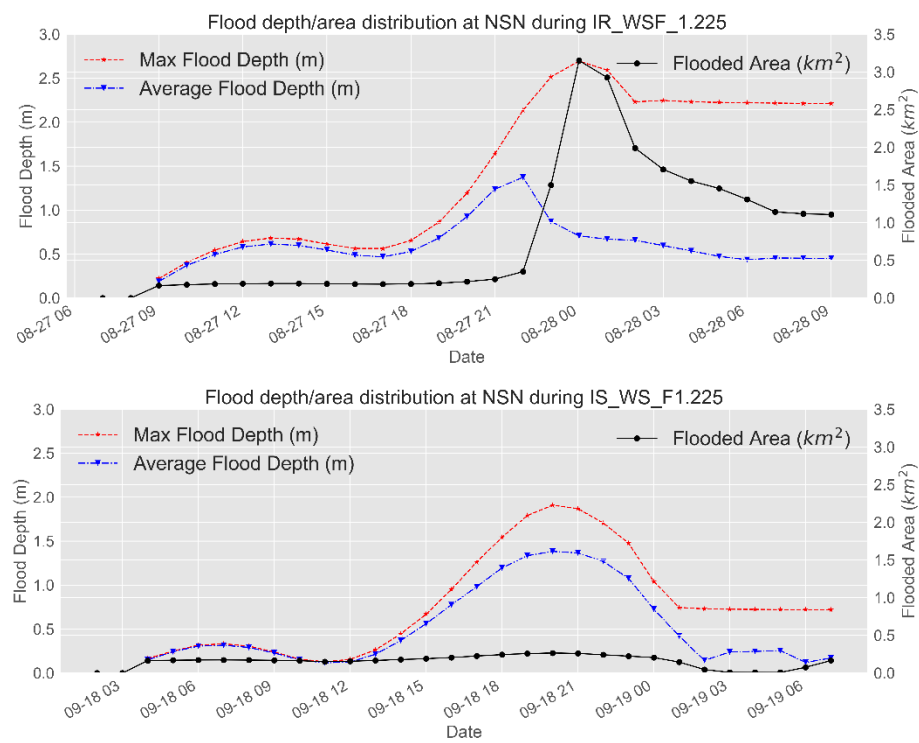
Figure 189. ADCIRC/GAHM base and wind speed (WSF_1.225) scenarios for all storms; time series of observed and predicted water levels (m MSL) at Sewell's Point.

Table 61. ADCIRC/GAHM base and wind speed (WSF_1.225) scenarios for all storms; peak water levels (m MSL) and surge durations (hr) at Sewell's Point.

Hurricane	Max. Surge (m)			Duration (hr)					
	Base	WSF_1.225		Base			WSF_1.225		
				Low	Med	High	Low	Med	High
Irene	2.20	3.01	53	15	6	32	17	13	
Isabel	2.84	3.89	16	11	8	16	13	10	
Sandy	1.16	1.31	87	27	0	56	28	0	
Michael	0.84	0.80	187	0	0	187	0	0	

Table 62. ADCIRC/GAHM base and storm size (WSF_1.225) scenarios for all storms; average and maximum flood depths (m) and flooded areas (km^2) at the NSN.

Hurricane	Base				WSF_F1.225			
	Average	Max	Area	%	Average	Max	Area	%
Irene	0.54	2.19		4.77	0.50	2.98		34.08
Isabel	0.42	2.80		20.40	0.64	3.80		80.97
Sandy	0.27	1.17		1.43	0.30	1.31		1.46
Michael	0.23	0.80		1.37	0.22	0.95		1.34



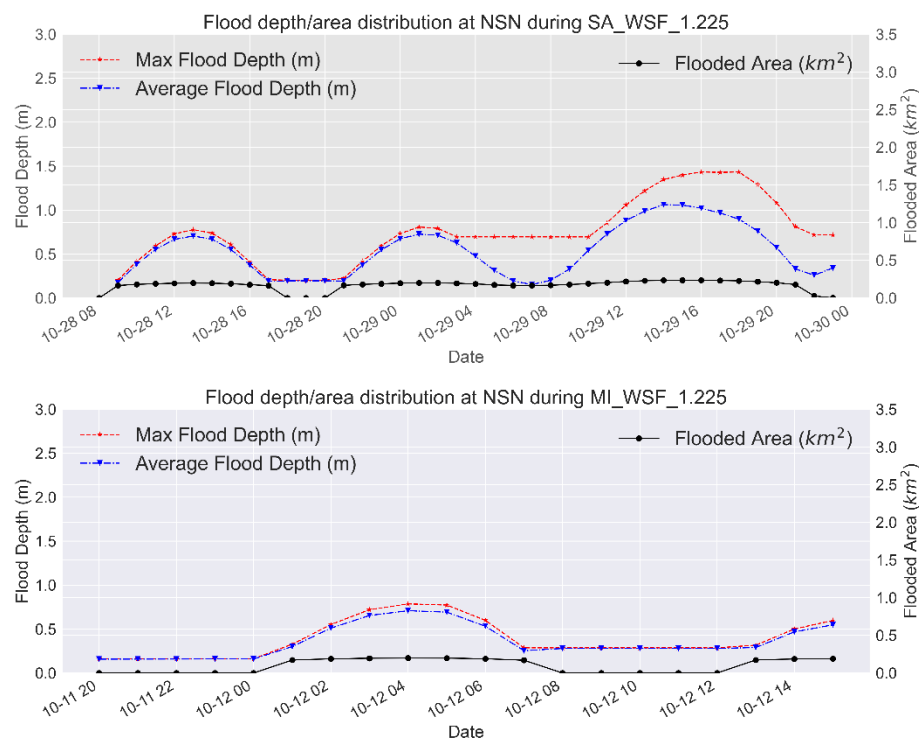


Figure 190. Time series of the projected average and maximum flood depth (left axis) and flood area (km^2 -right axis) for all hurricanes for WSF_1.225 scenario at NSN, the US. **PLACEHOLDER**

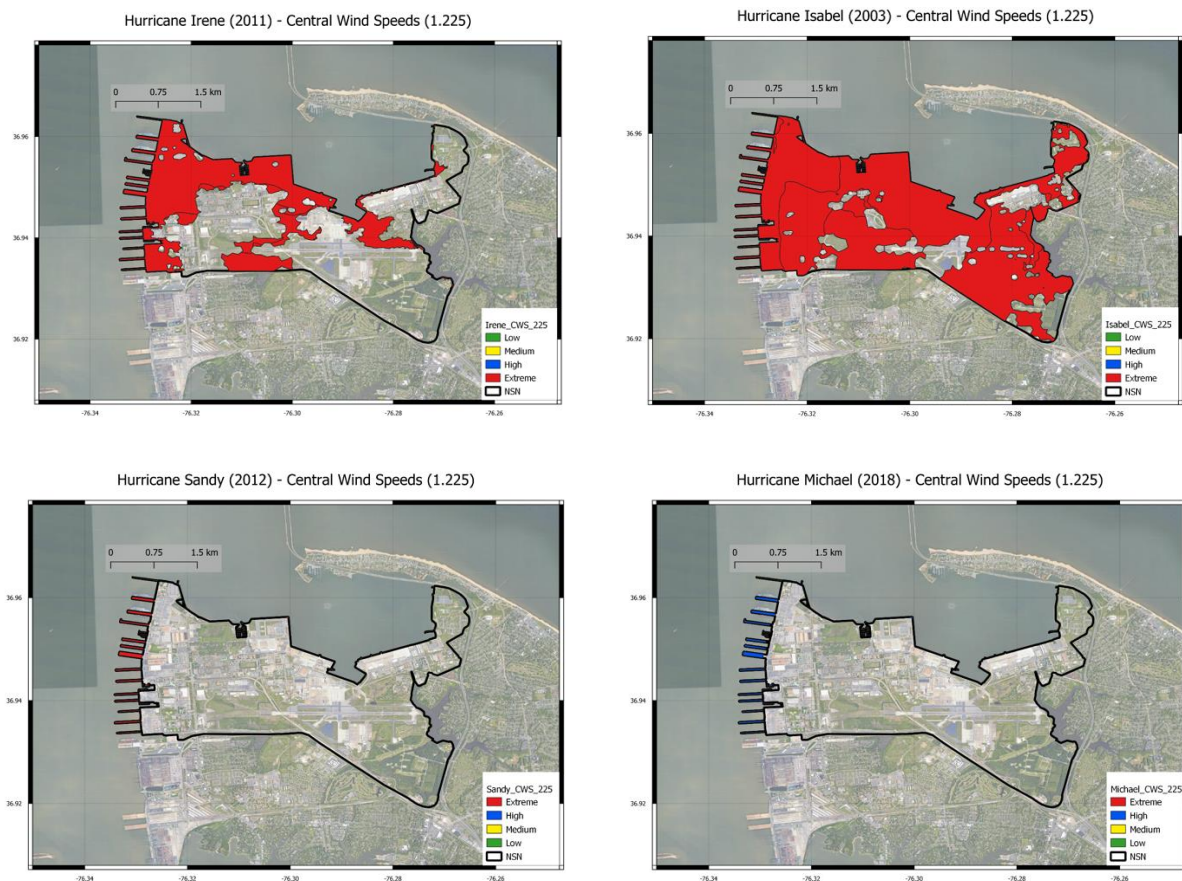


Figure 191. ADCIRC/GAHM wind speed (WSF_F1.225) scenario for all four storms; flood maps showing the classification of the flood levels at the peak surge .

6.4.4. Impacts of Lack of Data (Degradation scenarios)

The lack of accurate representative data has always challenged coastal modelers. One of the most important parameters of hurricanes is the hurricane track. Inaccuracy in the track prediction can lead to underestimation of the hurricane's impact at one place with overestimation at the other. This can lead to catastrophic loss of human lives on one hand and cause significant loss in unnecessary evacuation on the other hand.

Bathymetric and topographic data are widely available from different sources with different resolutions and accuracies. Although some inaccuracies in the bathymetric data can have a minor impact on the total water level prediction, the absence of accurate topographic data can cause overestimation/underestimation of the predicted flood area and hence, affect the reliability of coastal flood predictions.

On the other hand, model resolution (mesh resolution) can significantly impact the model performance. Generally speaking, the model performance is proportional to the mesh resolution, especially for flood prediction simulations. However, with increasing the model resolution the computational timestep becomes significantly lower, to satisfy the corant criteria, which results in a significantly higher computational cost. Therefore, these aspects must be balanced to implement feasible simulations.

The model performance in predicting the water level and the associated flood areas was evaluated under controlled perturbations in the hurricane track, bathymetric accuracy, and bathymetry/mesh resolution. Six scenarios were considered for changing the hurricane track by shifting the original track to the east and the west by 54 nm, 96 nm, and 138 nm for all hurricanes. In addition, three scenarios were studied for bathymetric accuracy by adding a Gaussian noise of 0.3 m, 0.5 m, and 1.0 m to the original bathymetry/topography data. Furthermore, four scenarios were considered to evaluate the sensitivity of the model to the mesh resolution by decreasing the resolution by factor 5, 16, 33, and 66. These factors correspond to a maximum resolution of about 75 m, 250 m, 500 m, and 1000 m.

IV. *Strom Track Shift (Error in Storm Track Prediction)*

We will consider six storm track shifts under this scenario group. Three shifts to the east and the west of the original hurricane track by 54 nm, 96 nm, and 138 nm. In addition, we may also shift the track by an angle depending on the original track (angle of approach to the coast). Since each hurricane has its distinctive characteristics, the results of the track shift will be presented for each hurricane separately.

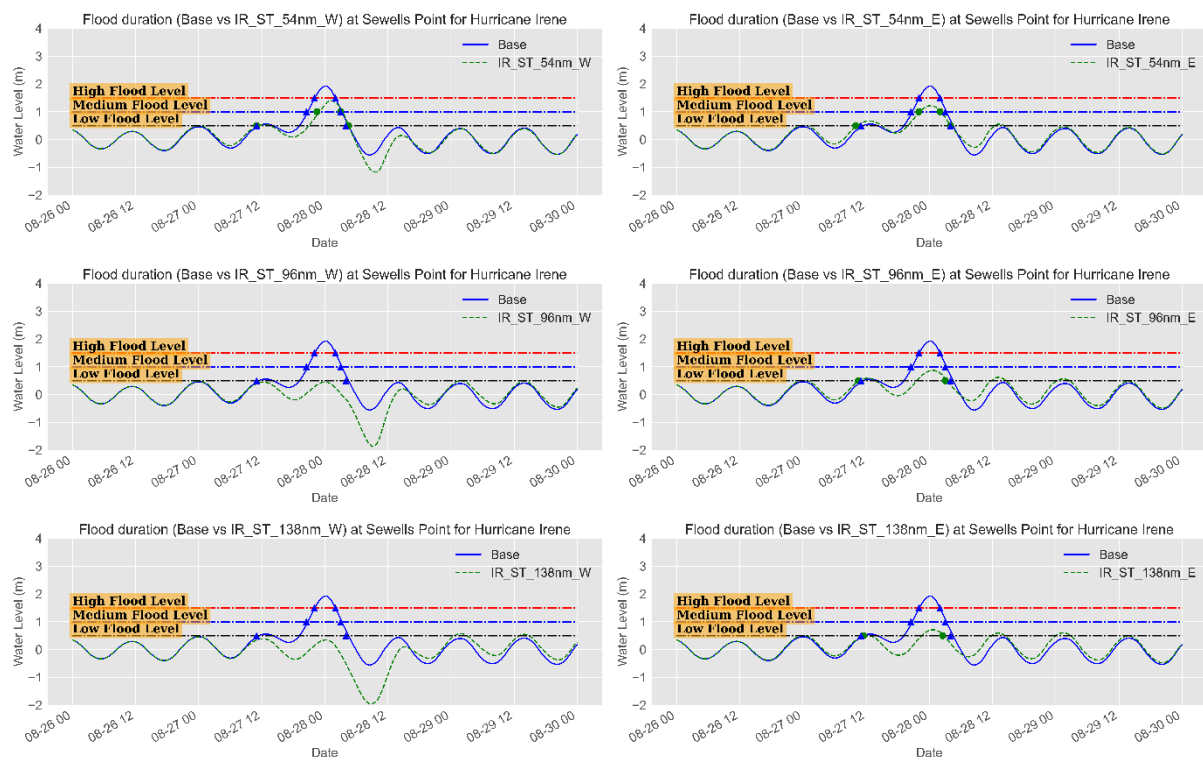


Figure 192. Water level time series (m) during Hurricane Irene showing the surge magnitude and duration for different surge levels for the base and Storm Track Shift scenarios at Sewells Point, NSN, the US.
PLACEHOLDER

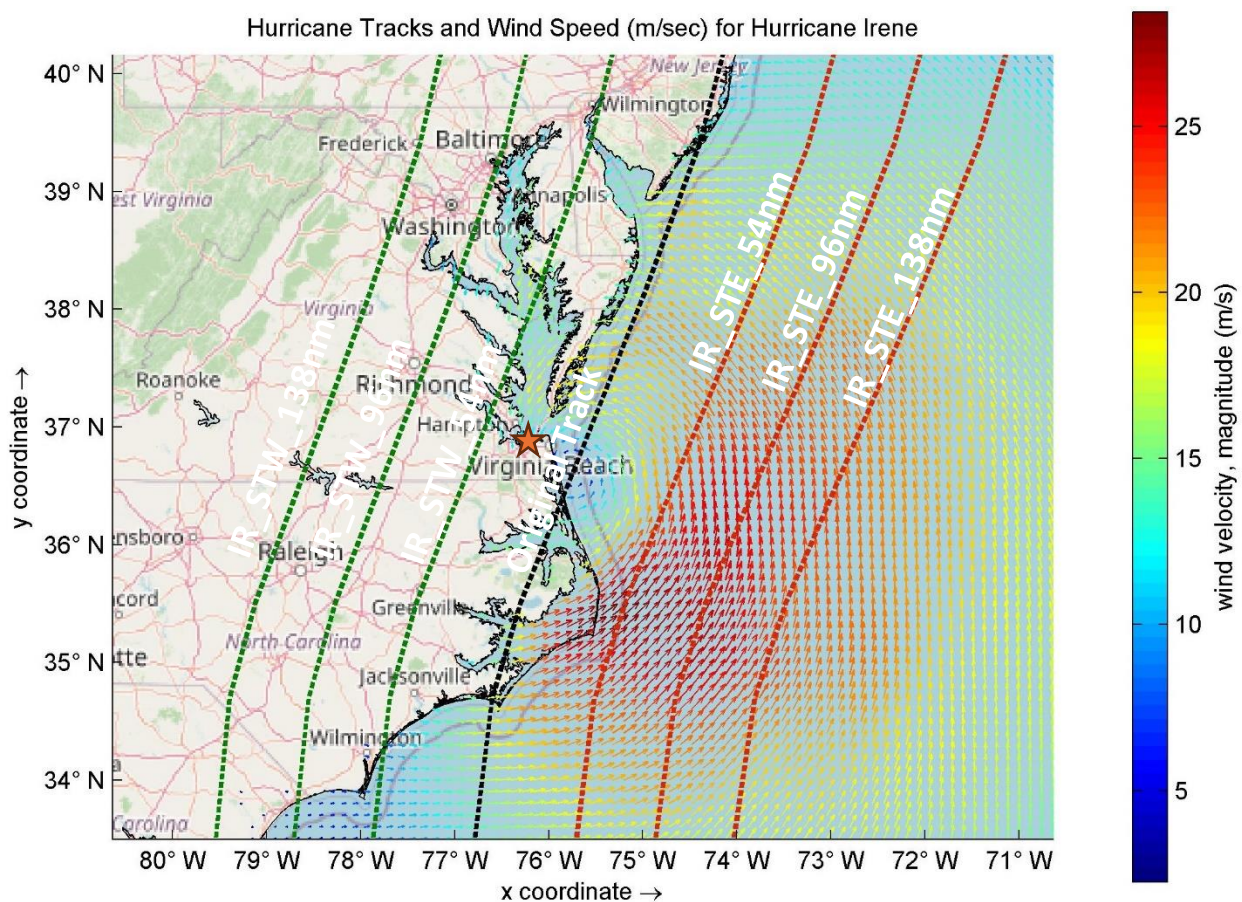


Figure 193. Different hurricane tracks and the wind speed (m/sec) for Hurricane Irene-2011. The orange star is NSN.

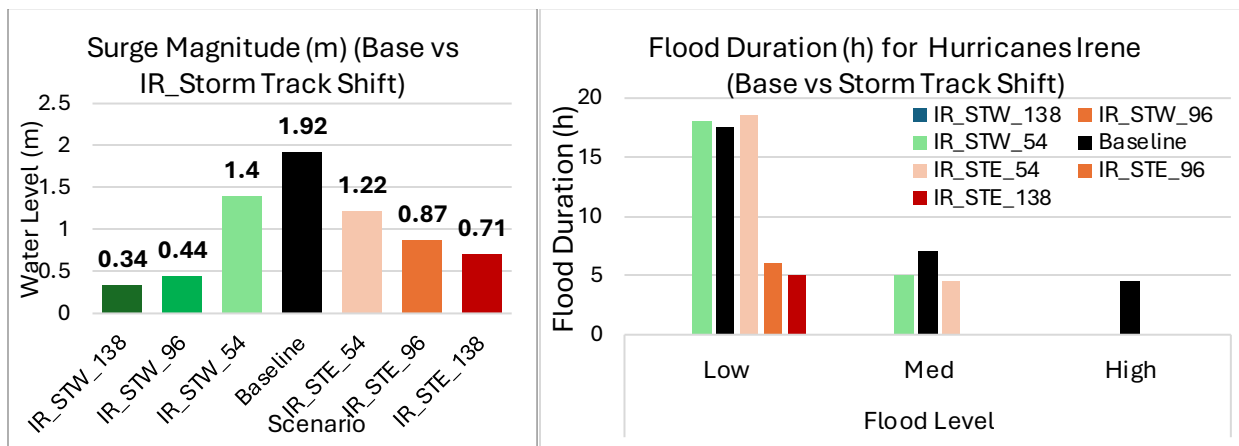


Figure 194. Peak surge (m) (left panel) and surge duration (h) of the different surge levels (right panel) for the base and the storm track shift scenarios for Hurricane Irene at NSN, the US. West shifts and east shifts are in green and red gradients respectively.

Table 63. Peak surge characteristics (Maximum and Duration) of the base and storm track shift scenarios for Hurricane Irene at Sewells Point, NSN, the US.

Group	Scenario	Peak Surge (m)	Flood Level/Duration (h)		
			Low	Med	High
Storm Track Shift (nm)	IR_STW_138	0.34	0	0	0
	IR_STW_96	0.44	0	0	0
	IR_STW_54	1.4	18	5	0
	Baseline	1.92	17.5	7	4.5
	IR_STE_54	1.22	18.5	4.5	0
	IR_STE_96	0.87	6	0	0
	IR_STE_138	0.71	5	0	0

On the other hand, the flood area statistics, Figure 92 and Table 30, showed a decrease in the flood area for all simulations compared to the baseline simulation under this scenario group. The flood area has decreased from 0.34 km^2 ($<2.5\%$ of the base area) down to 0.24 km^2 (1.7%) and 0.28 km^2 (2%) for the west and east track shifts respectively for Hurricane Irene. In addition, the average and maximum flood depths have also diminished down to 0.32 m and 0.39 m respectively for the west shift simulations and 0.65 m and 0.69 m respectively for the east shift simulations.

The reduction in the flood magnitude and duration, especially of the high and medium flood levels, has also reduced the duration of ground flooding. Figure 93 shows the time series of the average and maximum flood depth in meters and the flood area (km^2) for Hurricane Irene for a few hours before and after the peak surge/flood. It can be shown that there is no

pronounced peak for the flood areas or average and maximum flood depth for track shifts of 96nm and 138nm in both directions. However, a small peak for AFD and MFD was detected for 54nm simulations with an average of 1.1 m and 1.25 m respectively for both directions.

Investigating the spatial extent of the flood areas revealed no significant flooding for Hurricane Irene storm track shift scenarios, Figure 94. The impact of track shift for Hurricane Irene flooding was generally lower than the baseline scenario. This means that the original Irene track can be considered the worst-case scenario for this hurricane.

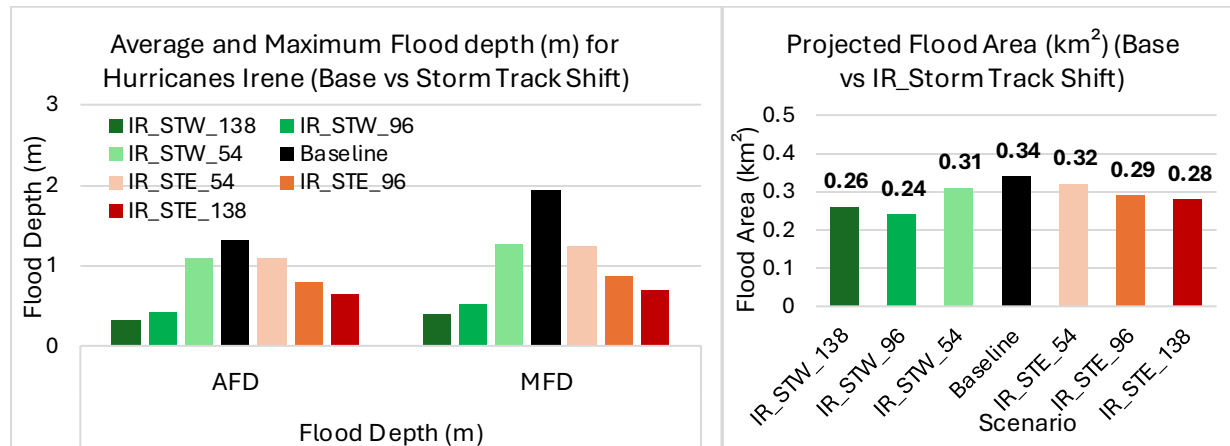


Figure 195. Average Flood Depth (AFD) & Maximum Flood Depth (MFD) in meters (left panel) and Flood area (km^2) (right panel) of Hurricane Irene for the Base and storm track shift scenarios at NSN, the US. West shifts and east shifts are in green and red gradients respectively.

Table 64. Flood area characteristics of the base and storm track shift scenarios for Hurricane Irene at NSN, the US.

Group	Scenario	Flood Depth (m)		FA (km^2)	FA (%)
		AFD	MFD		
Storm Track Shift (nm)	IR_STW_138	0.32	0.39	0.26	1.89
	IR_STW_96	0.42	0.52	0.24	1.74
	IR_STW_54	1.09	1.26	0.31	2.25
	Baseline	1.31	1.94	0.34	2.47
	IR_STE_54	1.1	1.24	0.32	2.32
	IR_STE_96	0.8	0.86	0.29	2.11
	IR_STE_138	0.65	0.69	0.28	2.03

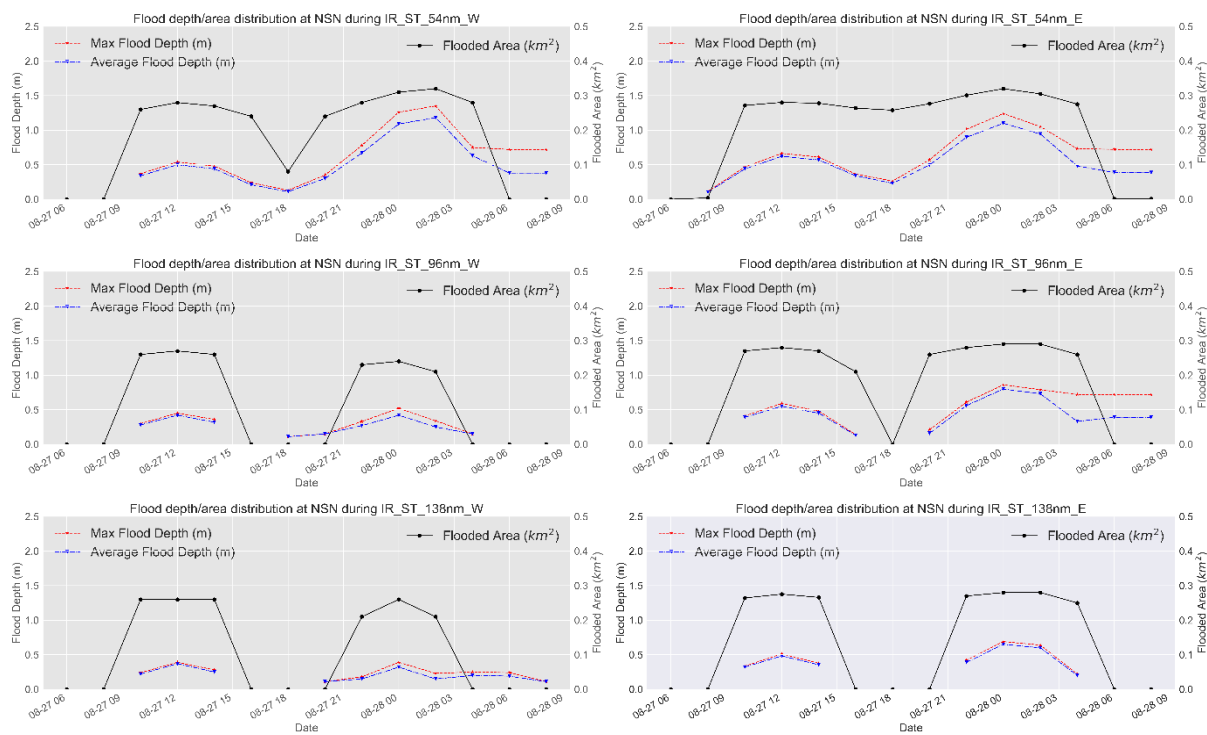


Figure 196. Time series of the projected average and maximum flood depth (left axis) and flood area (km^2 -right axis) for Hurricane Irene for storm track shift scenarios at NSN, the US.

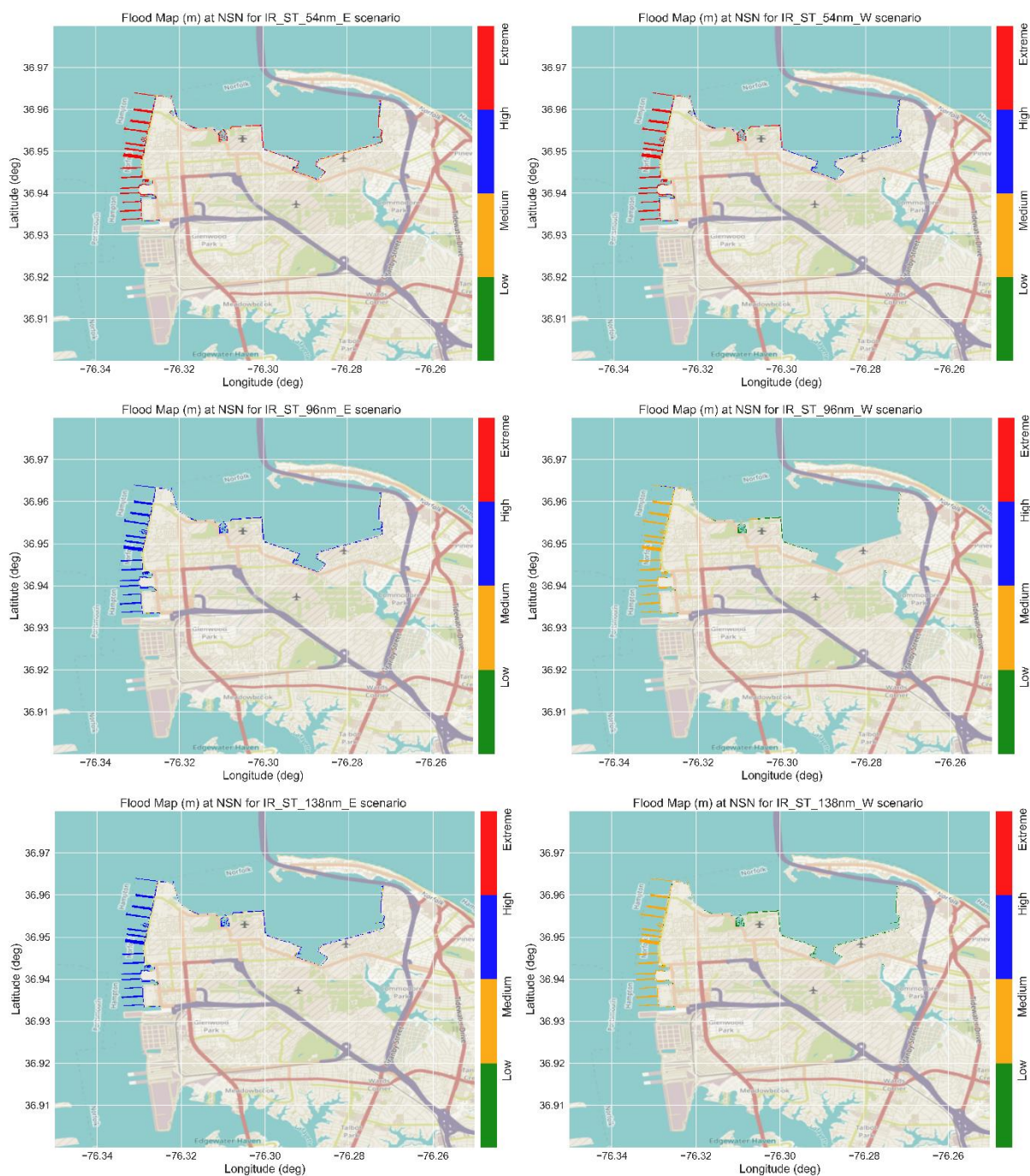


Figure 197. Flood maps with the flood levels for Hurricane Irene during the peak surge for the storm track shift scenarios at NSN, the US. West shifts (left panels) and East shifts (right panels).

Hurricane Isabel has a different track compared to Hurricane Irene. Isabel approaches the US East coast at an angle of 325 degrees with North where it makes landfall near Drum Inlet on the Outer Banks of North Carolina, Figure 95. Shifting the track of Hurricane Isabel to the eastward or westward directions will not have a meaningful impact on the original track. Therefore, we shifted Hurricane Isabel's track by 54nm, 96nm, and 138nm but with a 45-degree angle, i.e. in a perpendicular direction to the original track.

Figure 96 shows the water level for the base and the storm track shift scenarios for Hurricane Isabel at Sewells Point. Shifting Isabel's track to the west (left panels of Figure 96) has resulted in a drastic decrease in the peak surge at Sewells Point. The peak surge diminishes almost to the low surge level (0.5m) after shifting the track by 96nm to the west.

Hurricane Isabel passed approximately 65nm west of NSN (hence, Sewells Point), therefore, shifting the track to the west will displace the hurricane further away from NSN resulting in a lower surge magnitude, duration, and hence, diminished associated flood. On the other hand, shifting Isabel's track to the east will result in a higher surge magnitude, duration, and associated flooding. This pattern can be observed in Figure 97 and **Table 31**. It can be noticed that shifting Hurricane Isabel to the west has resulted in a significant decrease in the surge magnitude down to 0.58 m while shifting the hurricane to the east resulted in a significant increase in the surge magnitude up to 3.2 m for the IS_STE_54nm scenario (compared to 1.55m for the baseline). This pattern is also reflected in the surge duration where a significant increase was detected for IS_STE_54nm and IS_STE_96nm scenarios up to 5 hours. Shifting the track further to the east (IS_STE_138nm) yields very close results to the baseline scenario since the hurricane is shifted more than 70 nm east to NSN.

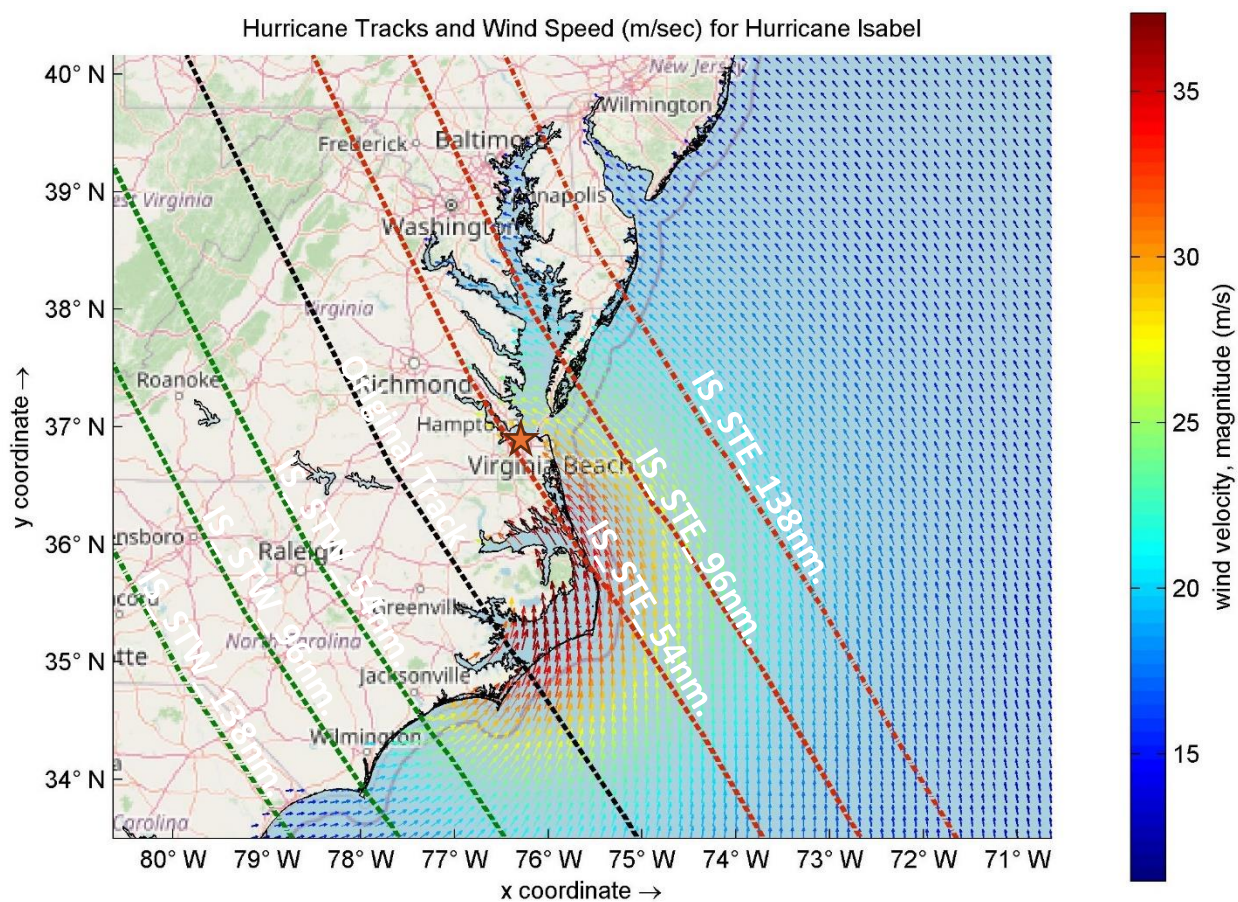


Figure 198. Different hurricane tracks and the wind speed (m/sec) for Hurricane Isabel-2003. The orange star is NSN.

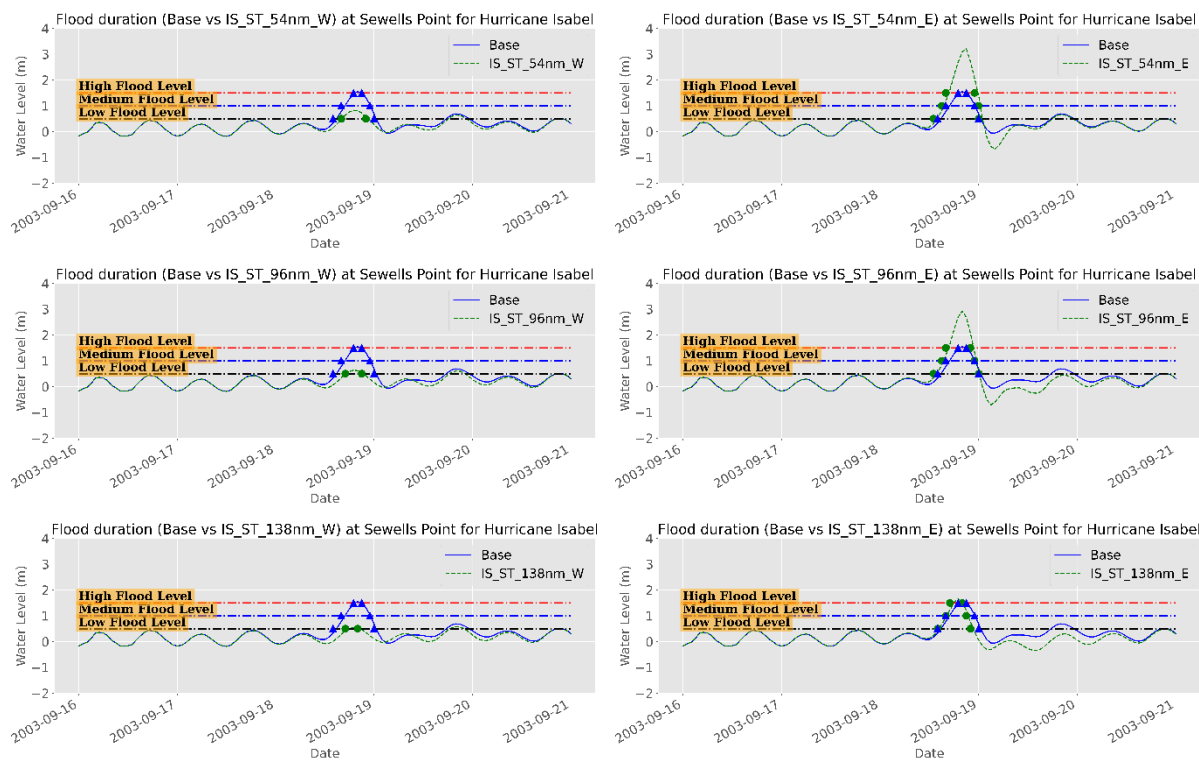


Figure 199. Water level time series (m) during Hurricane Isabel showing the surge magnitude and duration for different surge levels for the base and Storm Track Shift scenarios at Sewells Point, NSN, the US.

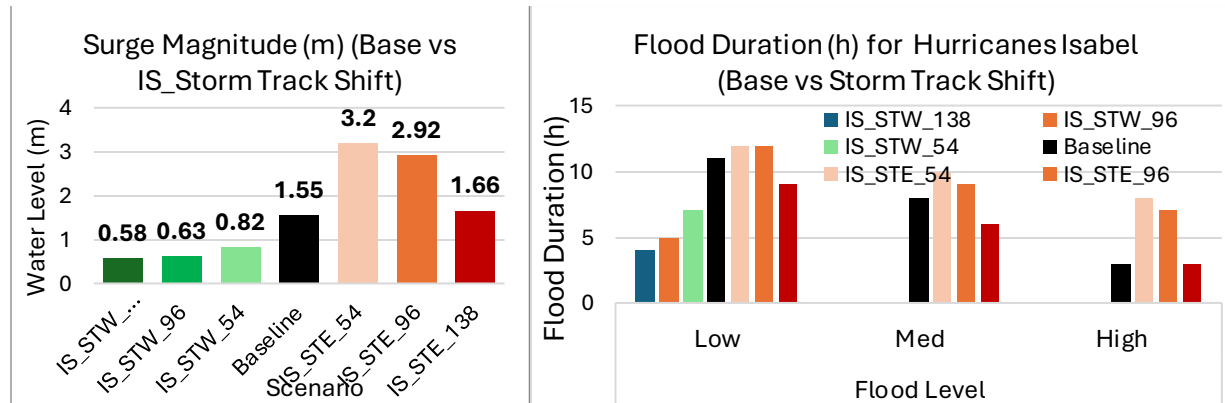


Figure 200. Peak surge (m) (left panel) and surge duration (h) of the different surge levels (right panel) for the base and the storm track shift scenarios for Hurricane Isabel at NSN, the US. West shifts and east shifts are in green and red gradients respectively.

Table 65. Peak surge characteristics (Maximum and Duration) of the base and storm track shift scenarios for Hurricane Isabel at Sewells Point, NSN, the US.

Group	Scenario	Peak Surge (m)	Flood Level/Duration (h)		
			Low	Med	High
Storm Track Shift (nm)	IS_STW_138	0.58	4	--	--
	IS_STW_96	0.63	5	--	--
	IS_STW_54	0.82	7	--	--
	Baseline	1.55	11	8	3
	IS_STE_54	3.2	12	10	8
	IS_STE_96	2.92	12	9	7
	IS_STE_138	1.66	9	6	3

On the other hand, the flood area statistics, Figure 98 and **Table 32**, showed a decrease in the flood area for all simulations shifted to the west and a drastic increase for all simulations shifted to the east. The flood area has decreased from 0.24 km^2 ($<1.7\%$ of the base area) down to 0.18 km^2 (1.3%) for the west track shifts while about 6 km^2 and 5.2 km^2 were detected to be flooded under the IS_STE_54nm and IS_STE_96nm scenarios respectively. In addition, the average and maximum flood depths have also diminished down to 0.5 m for the west shift simulations and increased up to 0.85 m and 3.25 m respectively for the east shift simulations.

The west shift of Hurricane Isabel's track has almost no influence on the flood areas and the duration of the ground flooding. The results are highly comparable to the baseline scenario. On the other hand, the dramatic increase in the surge statistics associated with the east shift simulations has significantly affected the characteristics of the ground flooding, Figure 99. Large areas (up to 2 km^2) maintain flooding for hours (or days) with an average and maximum flood depth of about 0.5m and 2.5 m respectively. The spatial extent of the flood areas, Figure 100, shows the significant flooding associated with the east shift of Hurricane Isabel scenarios where the northern and western parts of NSN are the most affected areas. The vegetation areas have the extreme flood level ($>1\text{m}$).

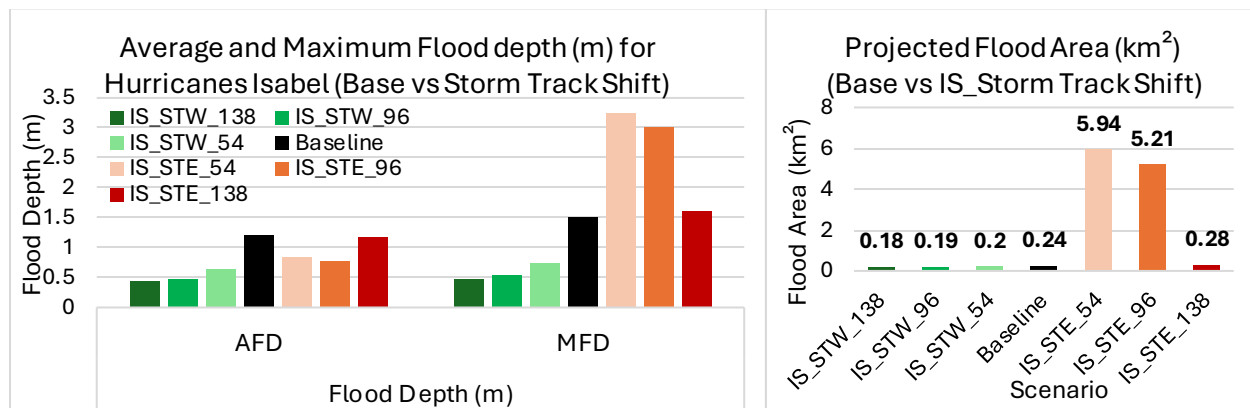


Figure 201. Average Flood Depth (AFD) & Maximum Flood Depth (MFD) in meters (left panel) and Flood area (km^2) (right panel) of Hurricane Isabel for the Base and storm track shift scenarios at NSN, the US. West shifts and east shifts are in green and red gradients respectively.

Table 66. Flood area characteristics of the base and storm track shift scenarios for Hurricane Isabel at NSN, the US.

Group	Scenario	Flood Depth (m)		FA (km^2)	FA (%)
		AFD	MFD		
Storm Track Shift (nm)	IS_STW_138	0.44	0.47	0.18	1.31
	IS_STW_96	0.49	0.54	0.19	1.38
	IS_STW_54	0.64	0.75	0.2	1.45
	Baseline	1.21	1.52	0.24	1.74
	IS_STE_54	0.84	3.25	5.94	43.14
	IS_STE_96	0.77	3.02	5.21	37.84
	IS_STE_138	1.19	1.61	0.28	2.03

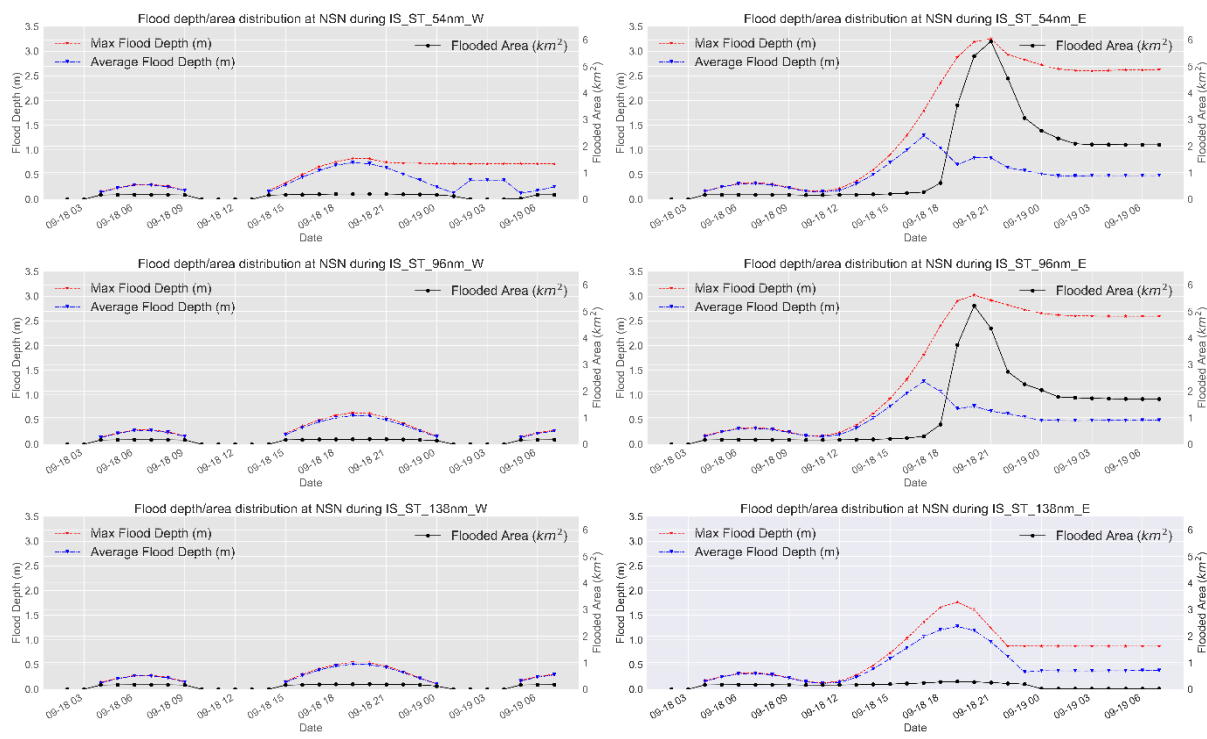


Figure 202. Time series of the projected average and maximum flood depth (left axis) and flood area (km²-right axis) for Hurricane Isabel for storm track shift scenarios at NSN, the US.

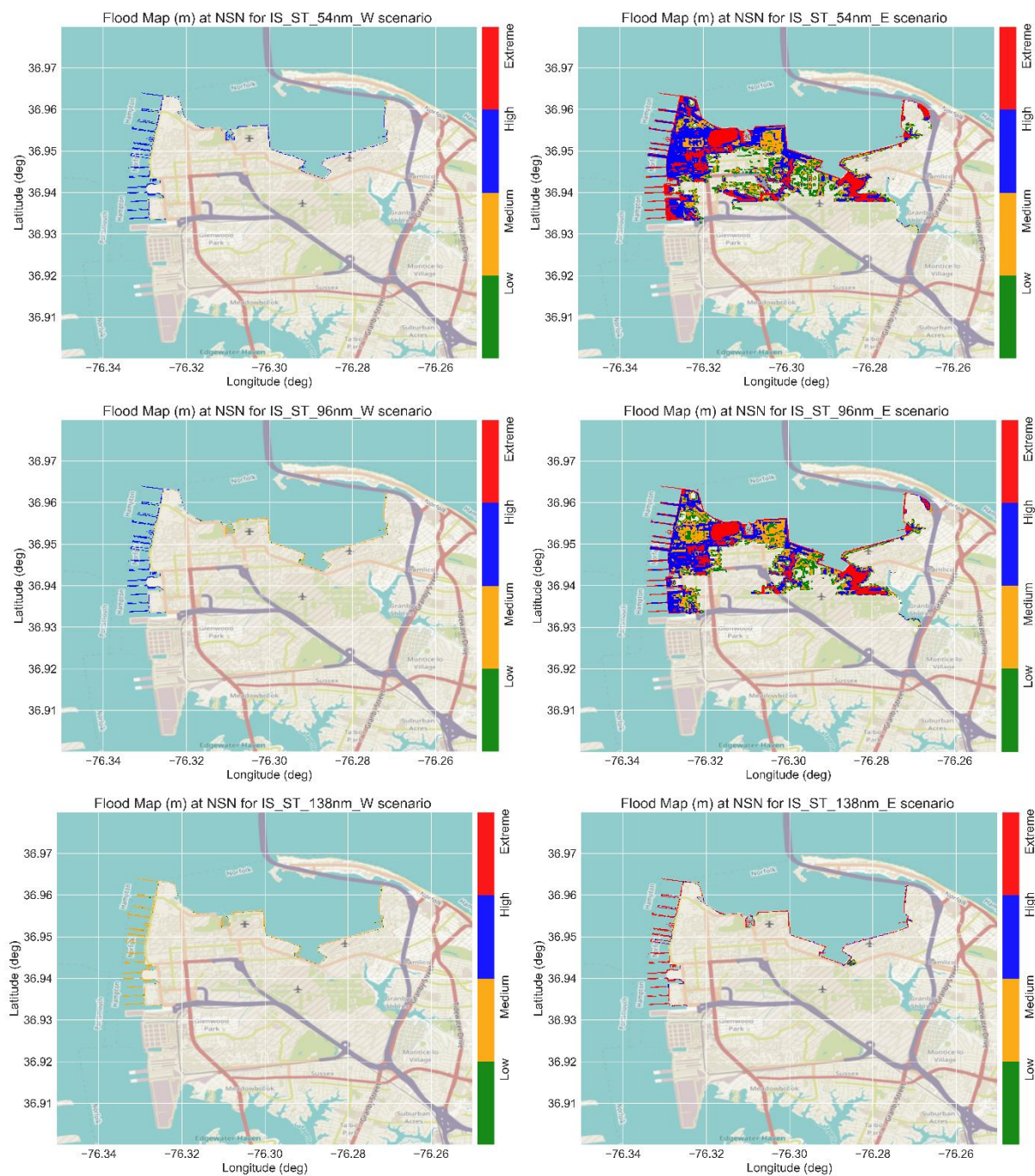


Figure 203. Flood maps with the flood levels for Hurricane Isabel during the peak surge for the storm track shift scenarios at NSN, the US. West shifts (left panels) and East shifts (right panels).

Hurricane Sandy approached the US East coast at an angle of 330 degrees with the North where it made landfall as a post-tropical cyclone near Brigantine, New Jersey, approximately 175nm north of NSN base, Figure 101. The hurricane track was shifted by 138nm to the east and west directions, however, even with the 138nm west shift, the Hurricane Sandy track was still about 70nm away from NSN. This means that only the SA_STW_138nm scenario might have a significant impact on the flooding at NSN. However, it should be mentioned that the impact on Delaware Bay might be quite enormous.

Figure 102 shows the water level for the base and the storm track shift scenarios for Hurricane Sandy at Sewells Point. Shifting Sand's track to the west (left panels of Figure 102) has resulted in a significant impact on the peak surge characteristics at Sewells Point. The peak surge increased from about 1.08 m for the baseline scenario up to 2.45 m for the SA_STW_138nm scenario. High surge magnitude was also detected for the SA_STW_96nm and SA_STW_54nm scenarios with 1.4 m and 1.82 m respectively. However, due to the existence of the hurricane tens of nautical miles north of Sewells Point (NSN base), the region is caught in the offshore wind force of the hurricane pushing water away from the coastline and causing an enormous negative surge reaching down to -3.2 m. High negative surge values were also detected for the SA_STW_96nm and SA_STW_54nm of about 2.65 m and 1.1 m respectively. These high negative surge values might have adverse impacts on the navigational activities in this area. The impact of the west track shifts is evident also in the surge duration results where a significant increase was detected in the surge duration for medium and high surge levels with a minor impact on the low surge level, Figure 103 and **Table 33**. Shifting Hurricane Sandy's track to the east shows a slight decrease in the hurricane's impact on NSN. The hurricane shifts further away from NSN with each scenario causing a minor decrease in the surge characteristics at Sewells Point.

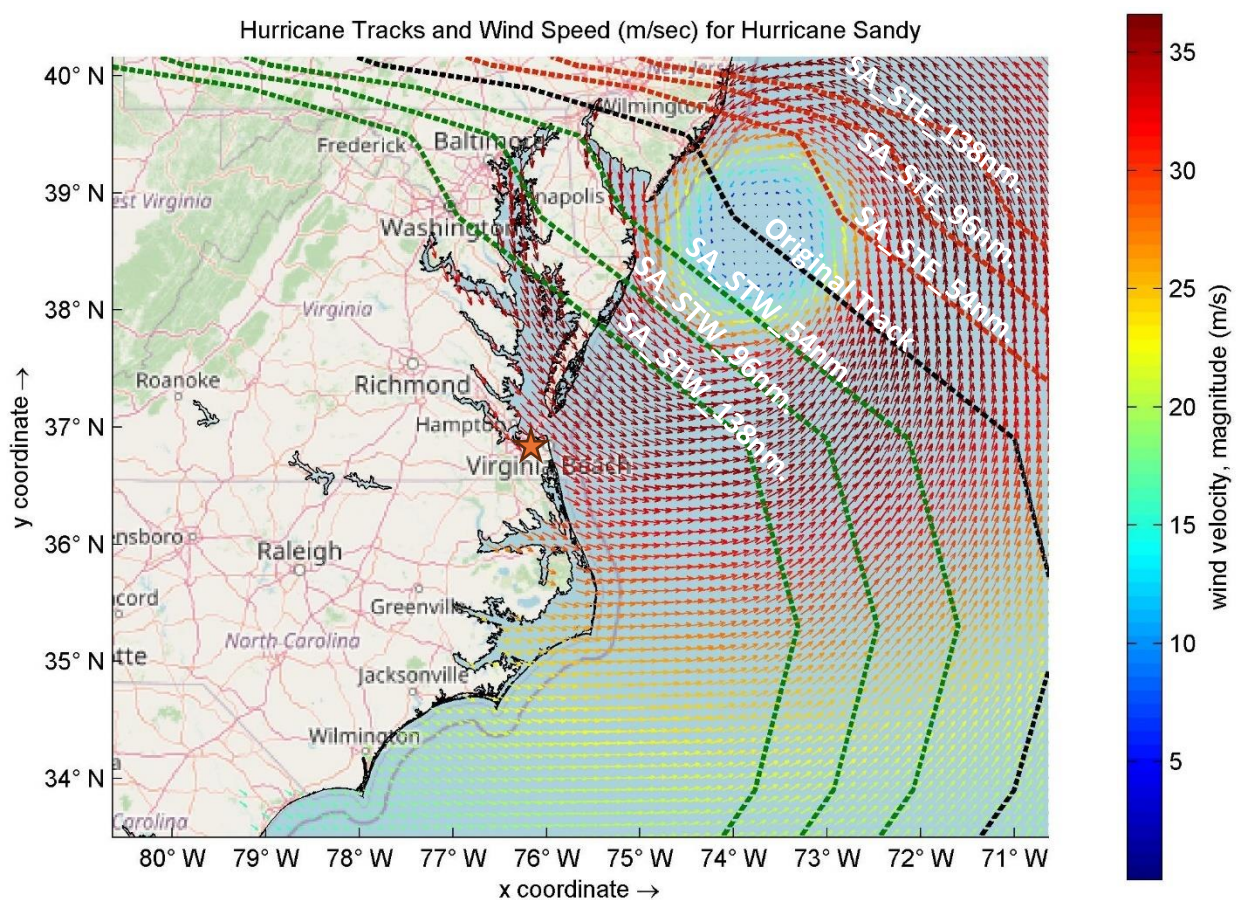


Figure 204. Different hurricane tracks and the wind speed (m/sec) for Hurricane Sandy 2012. The orange star is NSN.

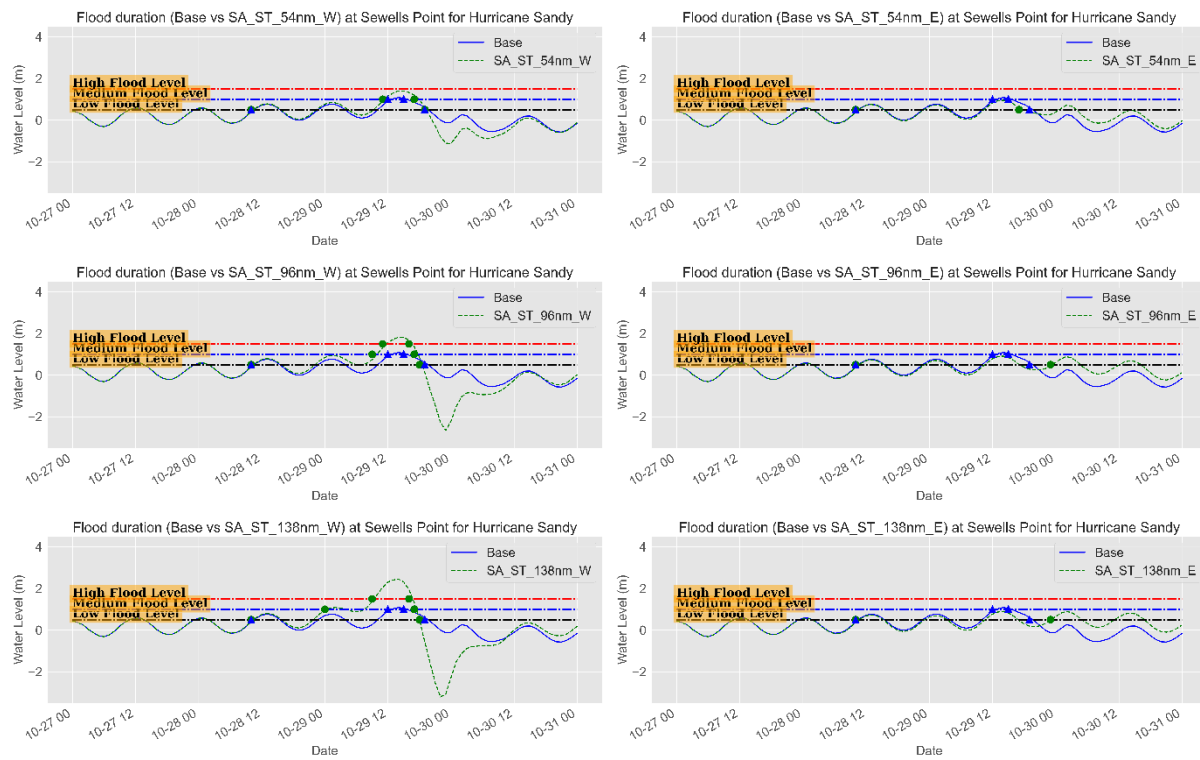


Figure 205. Water level time series (m) during Hurricane Sandy showing the surge magnitude and duration for different surge levels for the base and Storm Track Shift scenarios at Sewells Point, NSN, the US.

The same pattern was also observed in the flood area statistics, Figure 104 and **Table 34**, where a substantial increase in the flood area for all simulations shifted to the west and a slight decrease for all simulations shifted to the east. The flood area has increased from 0.23 km^2 ($<1.7\%$ of the base area) up to 3.37 km^2 (24.5%) for the west track shifts while about maintained 0.21 km^2 for the east track shift scenarios. In addition, the maximum flood depth has also increased substantially from 1.1m for the baseline scenario up to 2.8 m for the SA_STW_138nm scenario. The east track shift simulations maintained average and maximum flood depths of 0.8 m and 0.9 m respectively.

The influence on the duration of the ground flooding was also observed for the west shift scenarios. However, the most pronounced impacts were detected for the SA_STW_138nm where about 1.2 km^2 (8.7%) of the base area was susceptible to flooding even after hours from the peak surge. in addition, this area maintains average and maximum flood depth of about 0.5 m and 2.2 m respectively. For the east shift scenarios, no detectable impact was observed on the duration of the ground flooding compared to the baseline scenario, Figure 105.

The spatial extent of the flood areas, Figure 106, shows the significant flooding associated with the west shift SA_STW_96nm and SA_STW_138nm scenarios where the vegetation areas located at the northern parts of NSN along with some other areas at the west and north parts of the base are the most affected. Most of the affected areas have low to medium flood levels except for the vegetation areas where they have an extreme flood level (>1m).

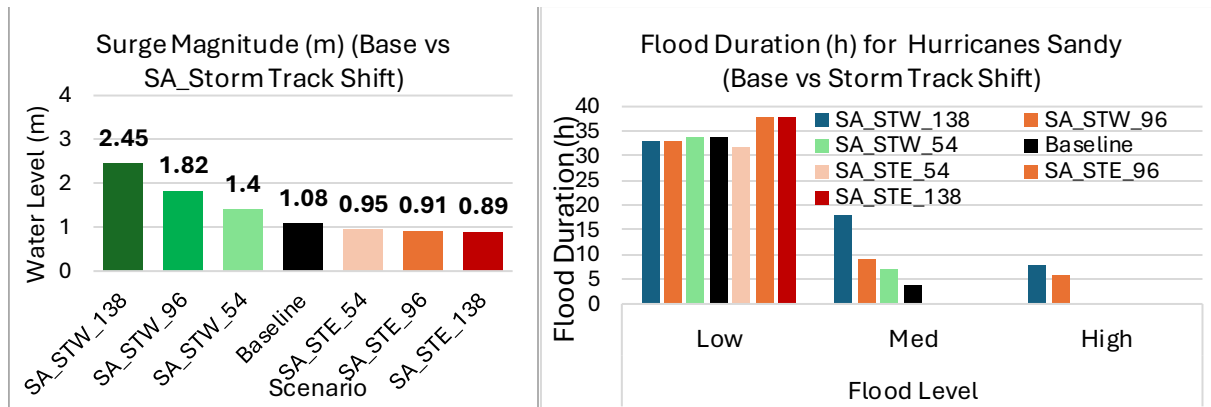


Figure 206. Peak surge (m) (left panel) and surge duration (h) of the different surge levels (right panel) for the base and the storm track shift scenarios for Hurricane Sandy at NSN, the US. West shifts and east shifts are in green and red gradients respectively.

Table 67. Peak surge characteristics (Maximum and Duration) of the base and storm track shift scenarios for Hurricane Isabel at Sewells Point, NSN, the US.

Group	Scenario	Peak Surge (m)	Flood Level/Duration (h)		
			Low	Med	High
Storm Track Shift (nm)	SA_STW_138	2.45	33	18	8
	SA_STW_96	1.82	33	9	6
	SA_STW_54	1.4	34	7	--
	Baseline	1.08	34	4	0
	SA_STE_54	0.95	32	--	--
	SA_STE_96	0.91	38	--	--
	SA_STE_138	0.89	38	--	--

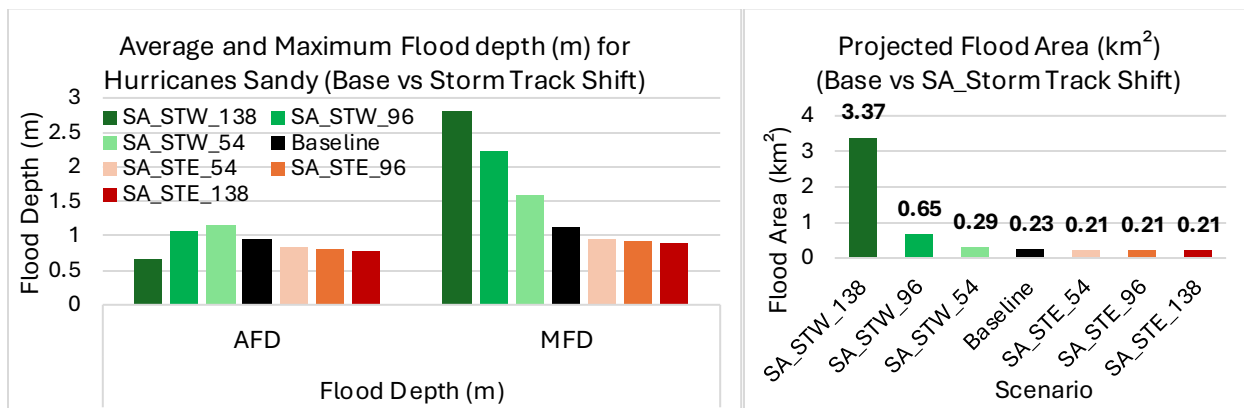


Figure 207. Average Flood Depth (AFD) & Maximum Flood Depth (MFD) in meters (left panel) and Flood area (km^2) (right panel) of Hurricane Sandy for the Base and storm track shift scenarios at NSN, the US. West shifts and east shifts are in green and red gradients respectively.

Table 68. Flood area characteristics of the base and storm track shift scenarios for Hurricane Sandy at NSN, the US.

Group	Scenario	Flood Depth (m)		FA (km^2)	FA (%)
		AFD	MFD		
Storm Track Shift (nm)	SA_STW_138	0.67	2.82	3.37	24.47
	SA_STW_96	1.09	2.22	0.65	3.56
	SA_STW_54	1.15	1.59	0.29	2.11
	Baseline	0.94	1.14	0.23	1.67
	SA_STE_54	0.85	0.96	0.21	1.53
	SA_STE_96	0.81	0.92	0.21	1.53
	SA_STE_138	0.79	0.89	0.21	1.53

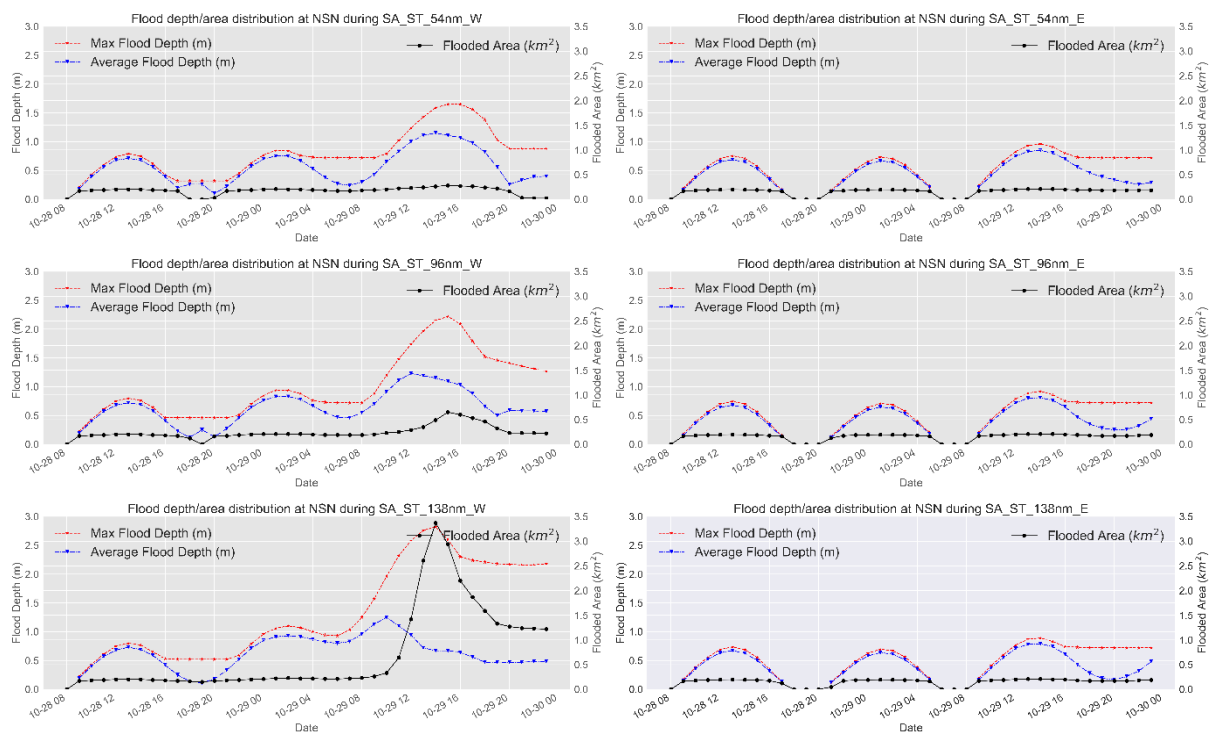


Figure 208. Time series of the projected average and maximum flood depth (left axis) and flood area (km^2 -right axis) for Hurricane Sandy for storm track shift scenarios at NSN, the US.

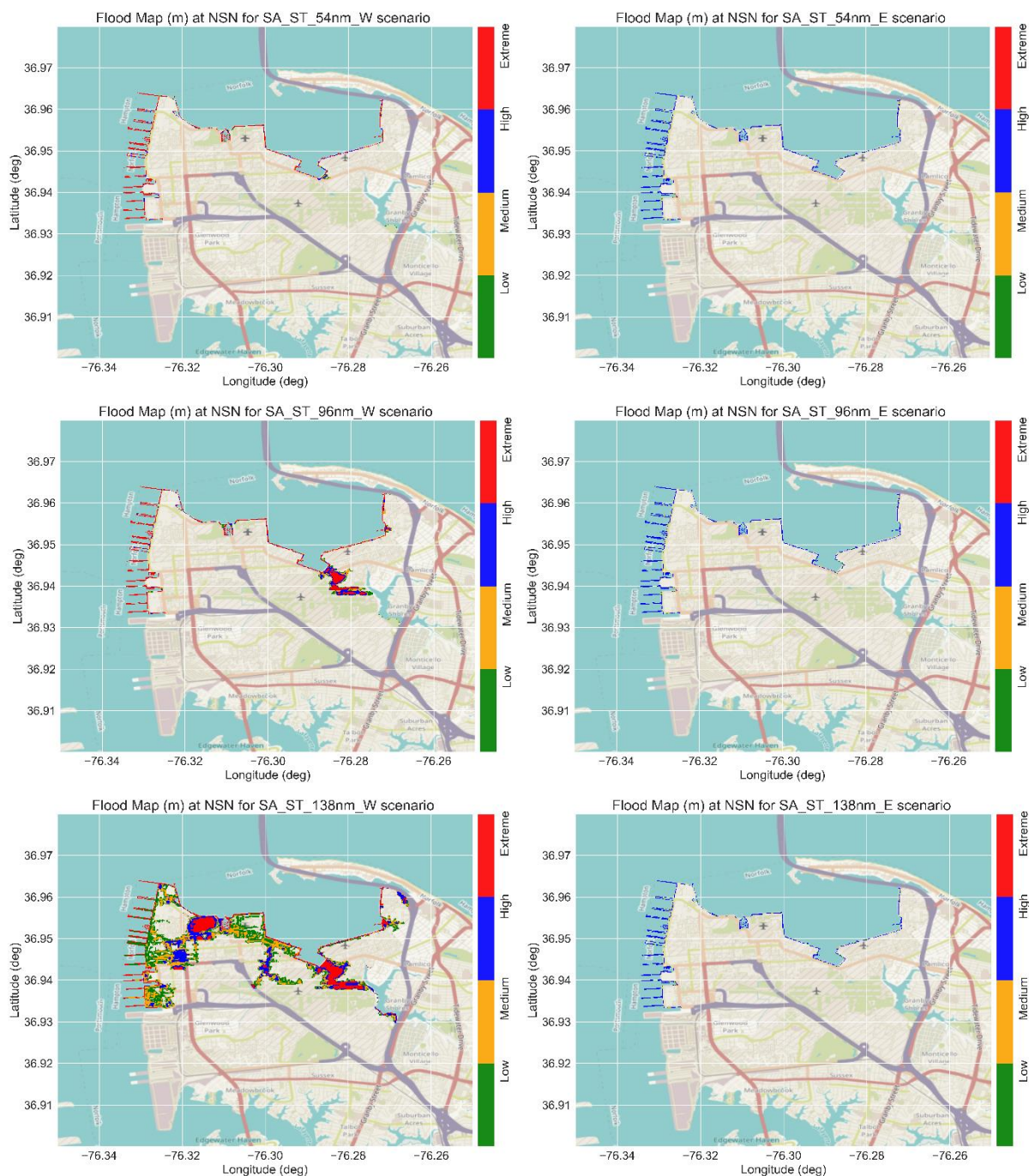


Figure 209. Flood maps with the flood levels for Hurricane Sandy during the peak surge for the storm track shift scenarios at NSN, the US. West shifts (left panels) and East shifts (right panels).

Hurricane Michael on the other hand approached the US East coast at an angle of 30 degrees and it made its landfall near Mexico Beach and Tyndall Air Force Base, Florida, producing devastating winds and storm surge near the coast, and rain and wind inland. However, we have considered Hurricane Michael in this study because it also continued its track till it reached Norfolk from the land side with an approximate angle of 70 degrees, Figure 107. Although Micheal was a category five hurricane (on the Saffir-Simpson Hurricane Wind Scale) that had a catastrophic impact on the US south coast where it made its landfall, it continued its path to the east coast passing through Norfolk, Virginia as an Extratropical cyclone with wind speed 60-65 kt at 0600 UTC on 12 October 2018.

Figure 108 shows the water level for the base and the storm track shift scenarios for Hurricane Michael at Sewells Point. Shifting Hurricane Michael's track to the west (left panels of Figure 108) or to the east (right panels of Figure 108) results in a minor impact on the peak surge characteristics at Sewells Point. The simulated surge did not exceed the low surge level for all simulations. A limited increase in the peak surge magnitude was detected for the east shift simulations with a maximum surge of 0.96m for the MI_STE_96nm compared to 0.73 m for the baseline simulation. The peak surge diminished to some extent for the west shift simulations down to 0.51 m for the MI_STW_96nm simulation, Figure 109. In addition, a minor shift in the peak surge timing (1-2 hours) and hence, associated maximum flooding, was detected for the west and east simulations. No significant influence on the surge duration was detected for all simulations except the increase in the low surge level for the MI_STE_138nm scenario where the duration increased up to 16 hours compared to 6 hours for the baseline scenario. No surge was detected higher than the low level, hence no durations were detected (zero) for the medium and high surge levels, Figure 109 and **Table 35**.

The same pattern was also observed in the flood area statistics, Figure 110 and **Table 36**, where no significant changes in the flood area were observed for all scenarios with about ± 0.02 change beyond the baseline simulation. However, a minor increase in the average and maximum flood depth was detected for the east shift simulations by about 0.2 m, while a minor decrease was observed for the west shift simulation by the same magnitude.

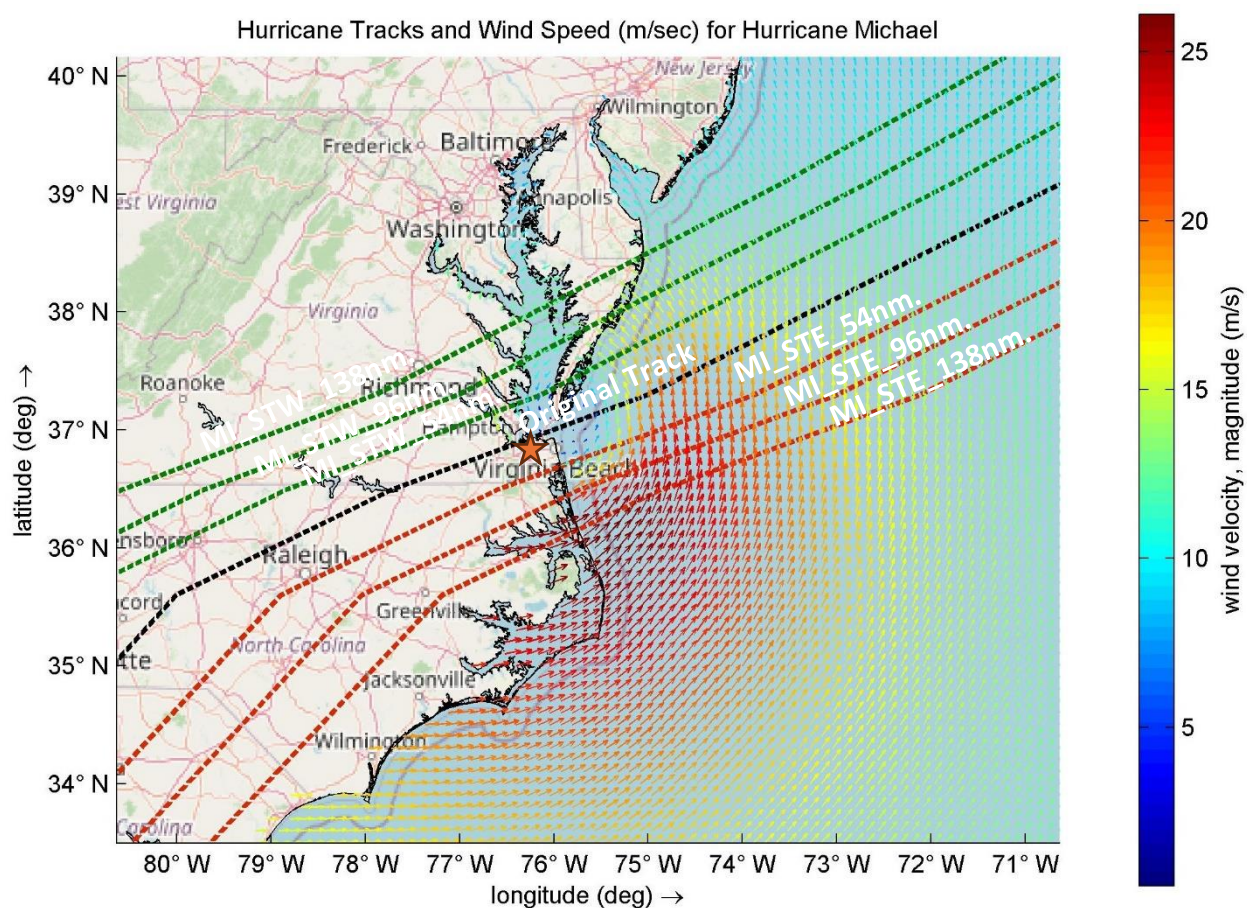


Figure 210. Different hurricane tracks and the wind speed (m/sec) for Hurricane Michael 2018. The orange star is NSN.

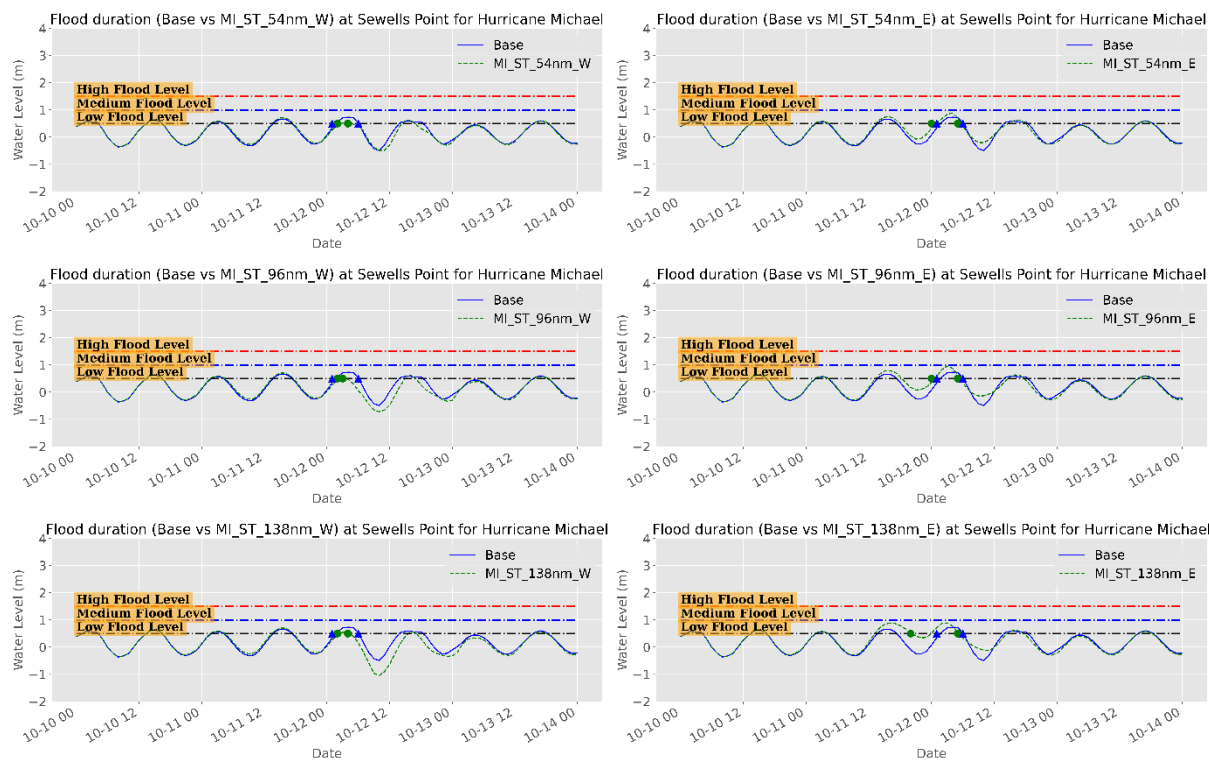


Figure 211. Water level time series (m) during Hurricane Michael showing the surge magnitude and duration for different surge levels for the base and Storm Track Shift scenarios at Sewells Point, NSN, the US.

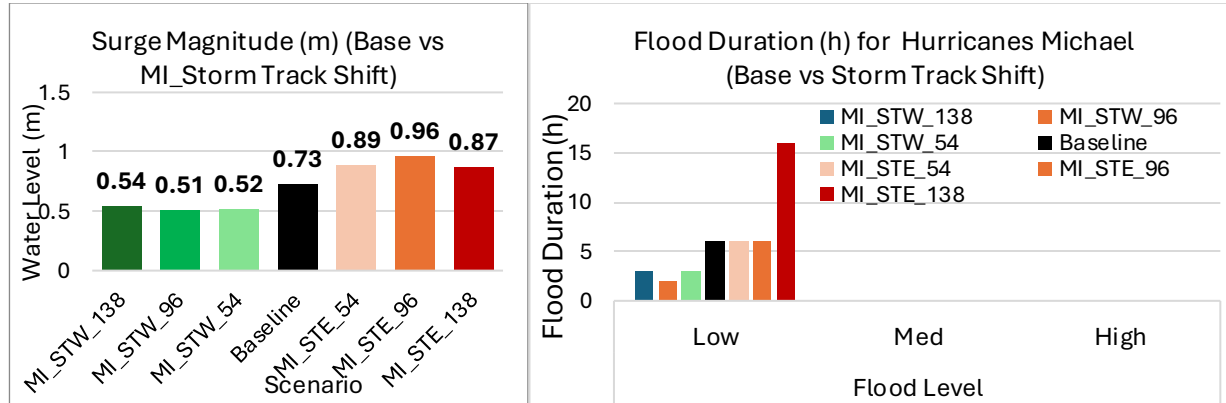


Figure 212. Peak surge (m) (left panel) and surge duration (h) of the different surge levels (right panel) for the base and the storm track shift scenarios for Hurricane Michael at NSN, the US. West shifts and east shifts are in green and red gradients respectively.

Table 69. Peak surge characteristics (Maximum and Duration) of the base and storm track shift scenarios for Hurricane Michael at Sewells Point, NSN, the US.

Group	Scenario	Peak Surge (m)	Flood Level/Duration (h)		
			Low	Med	High
Storm Track Shift (nm)	MI_STW_138	0.54	3	--	--
	MI_STW_96	0.51	2	--	--
	MI_STW_54	0.52	3	--	--
	Baseline	0.73	6	0	0
	MI_STE_54	0.89	6	--	--
	MI_STE_96	0.96	6	--	--
	MI_STE_138	0.57	16	--	--

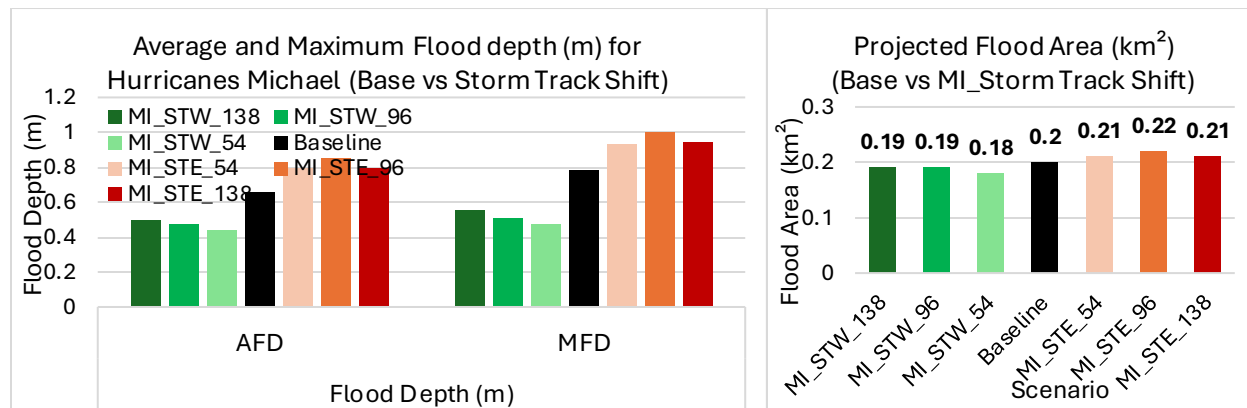


Figure 213. Average Flood Depth (AFD) & Maximum Flood Depth (MFD) in meters (left panel) and Flood area (km^2) (right panel) of Hurricane Michael for the Base and storm track shift scenarios at NSN, the US. West shifts and east shifts are in green and red gradients respectively.

Table 70. Flood area characteristics of the base and storm track shift scenarios for Hurricane Michael at NSN, the US.

Group	Scenario	Flood Depth (m)		FA (km^2)	FA (%)
		AFD	MFD		
Storm Track Shift (nm)	MI_STW_138	0.5	0.55	0.19	1.38
	MI_STW_96	0.47	0.51	0.19	1.38
	MI_STW_54	0.44	0.48	0.18	1.31
	Baseline	0.66	0.79	0.2	1.45
	MI_STE_54	0.8	0.93	0.21	1.53
	MI_STE_96	0.85	1	0.22	1.6
	MI_STE_138	0.8	0.95	0.21	1.53

The influence on the duration of the ground flooding was also minor for all scenarios. However, the most pronounced impacts were detected for the east shift simulation where the flooded areas maintained an average and maximum flood depth of about 0.4 m and 0.7 m respectively, Figure 111. The spatial extent of the flood areas, Figure 112, shows that there is no significant flooding associated with the west and east shifts of Hurricane Michael's track. Only small areas were detected around the land-sea boundary where the model accuracy is relatively low. It is worth noting that the flooded area is very small for all scenarios and lies within the range of the marginal error of the model prediction. This means, as mentioned in previous sections, that there is almost no flood area associated with Hurricane Michael at NSN.

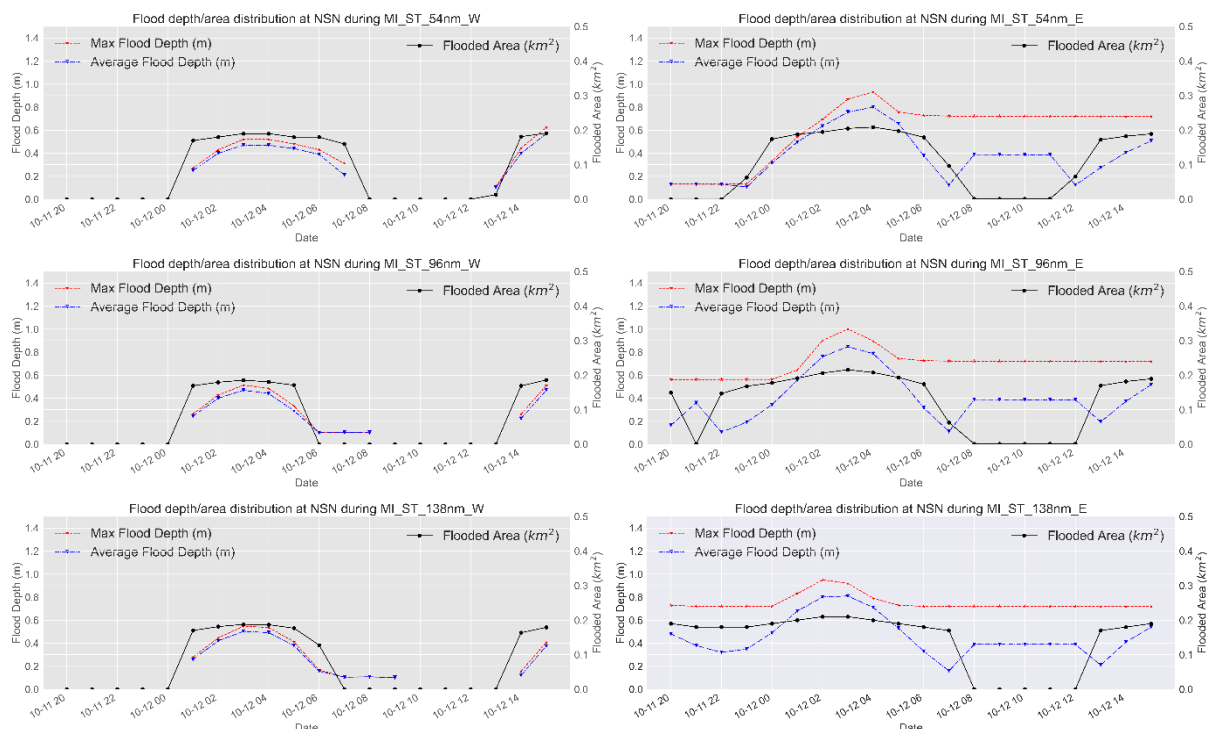


Figure 214. Time series of the projected average and maximum flood depth (left axis) and flood area (km^2 -right axis) for Hurricane Michael for storm track shift scenarios at NSN, the US.

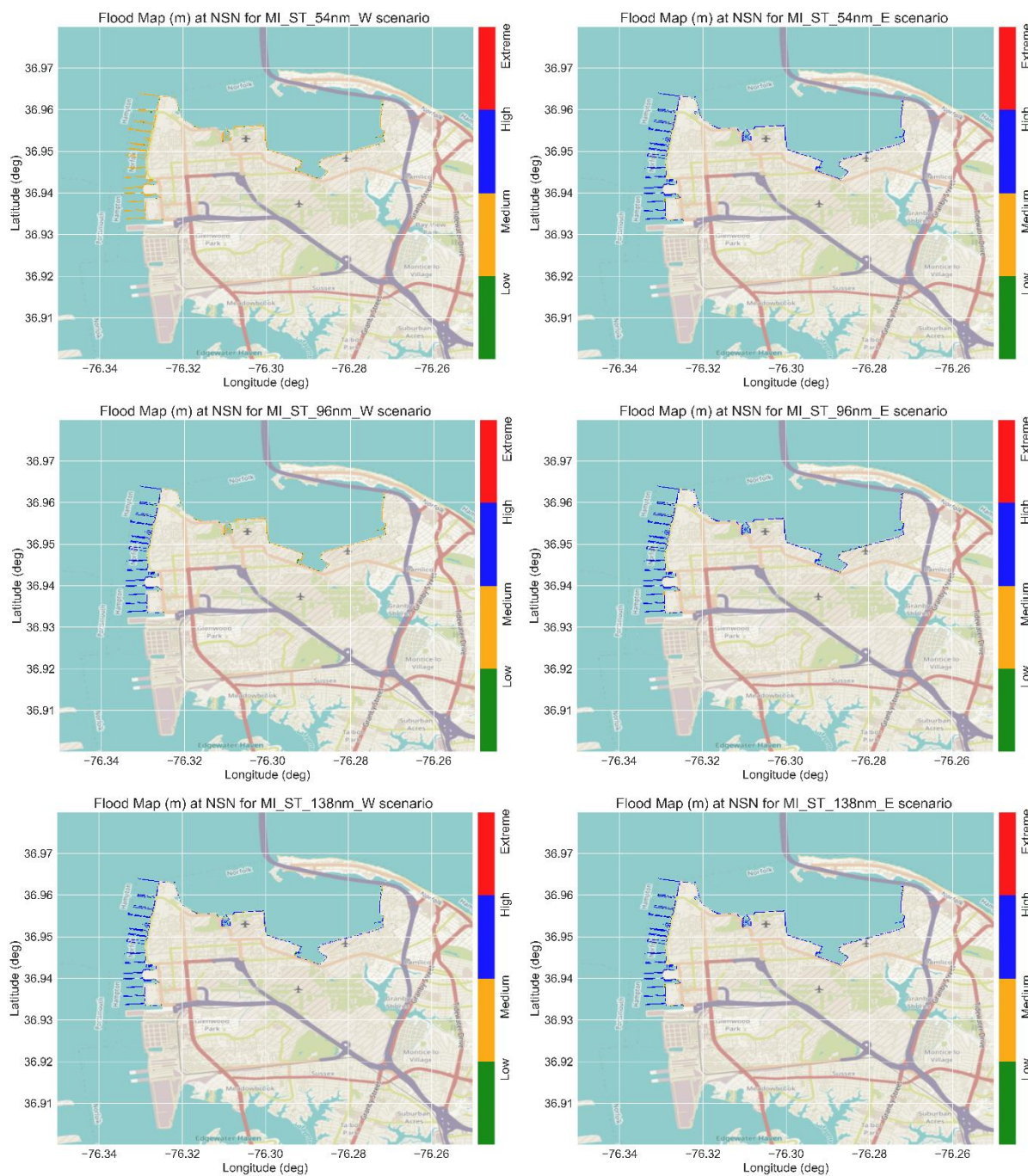


Figure 215. Flood maps with the flood levels for Hurricane Michael during the peak surge for the storm track shift scenarios at NSN, the US. West shifts (left panels) and East shifts (right panels).

V. Bathymetry Accuracy

We will three scenarios for bathymetry accuracy for Hurricane Irene only by adding a Gaussian noise of 0.3 m (IR_Bathy_Acc_GN_0.3m), 0.5 m (IR_Bathy_Acc_GN_0.5m), and 1.0 m (IR_Bathy_Acc_GN_1.0m). The model performance will be evaluated in terms of peak surge and flood area characteristics.

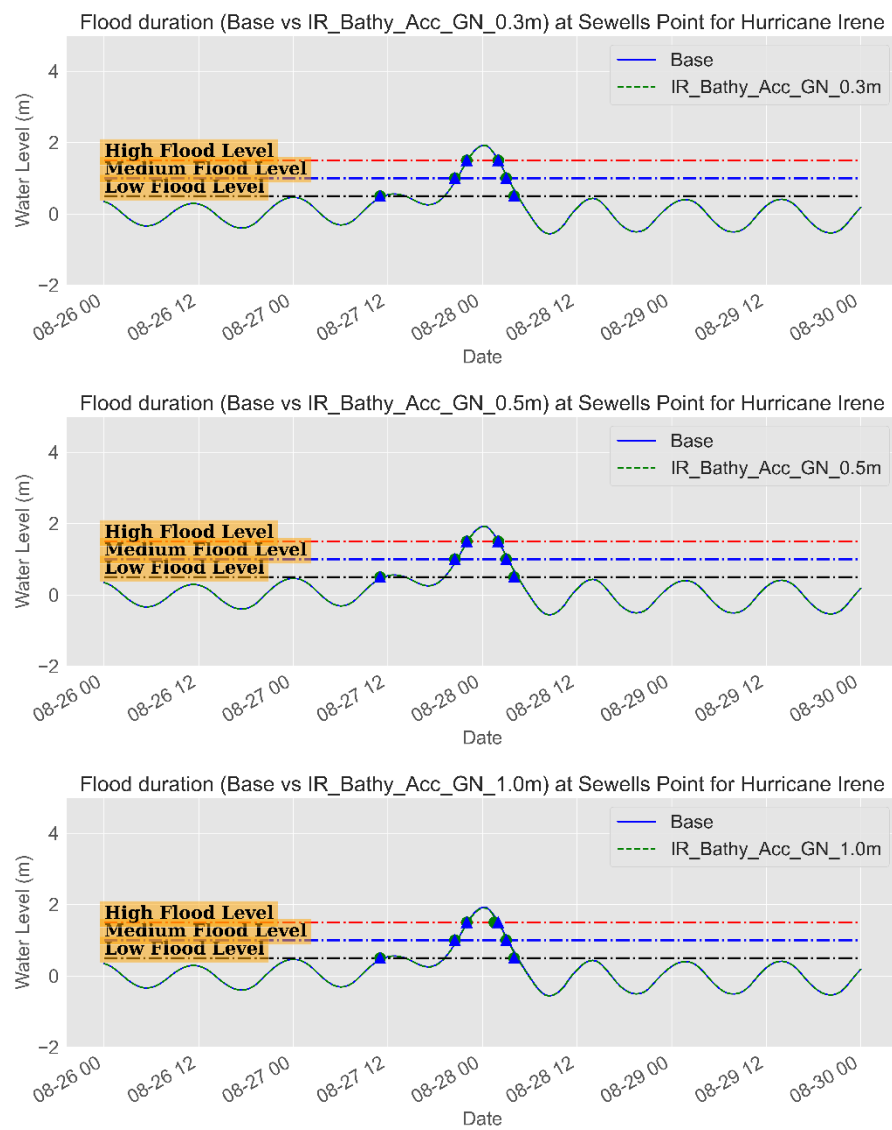


Figure 216. Water level time series (m) during Hurricane Irene showing the surge magnitude and duration for different surge levels for the base and Bathymetry Accuracy scenarios at Sewells Point, NSN, the US.

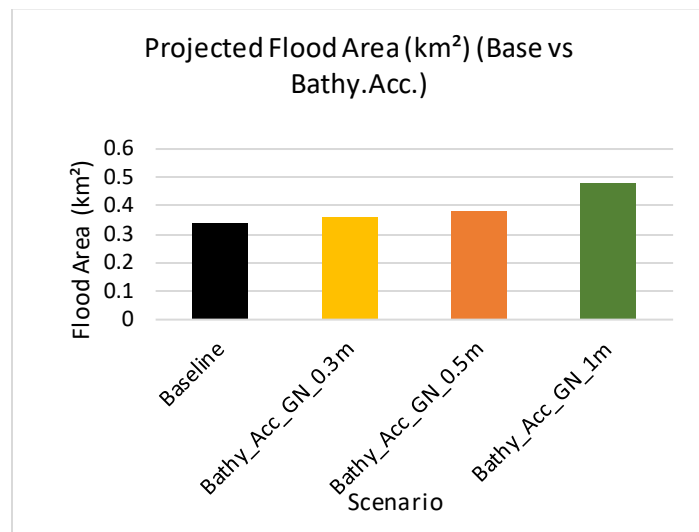


Figure 217. Flood area (km^2) of the Base and Bathymetry Accuracy scenarios at NSN, the US

Table 71. Flood area characteristics of the base and bathymetry accuracy scenarios at NSN, the US.

Group	Scenario	AFD (m)	MFD (m)	Flood area (km^2)	Flood (%)
Deg. Sc.	Base	1.31	1.94	0.34	2.47
	Bathy_Acc_GN_0.3m	1.27	1.94	0.36	2.6
	Bathy_Acc_GN_0.5m	1.23	1.94	0.38	2.8
	Bathy_Acc_GN_1m	1.1	1.93	0.48	3.5

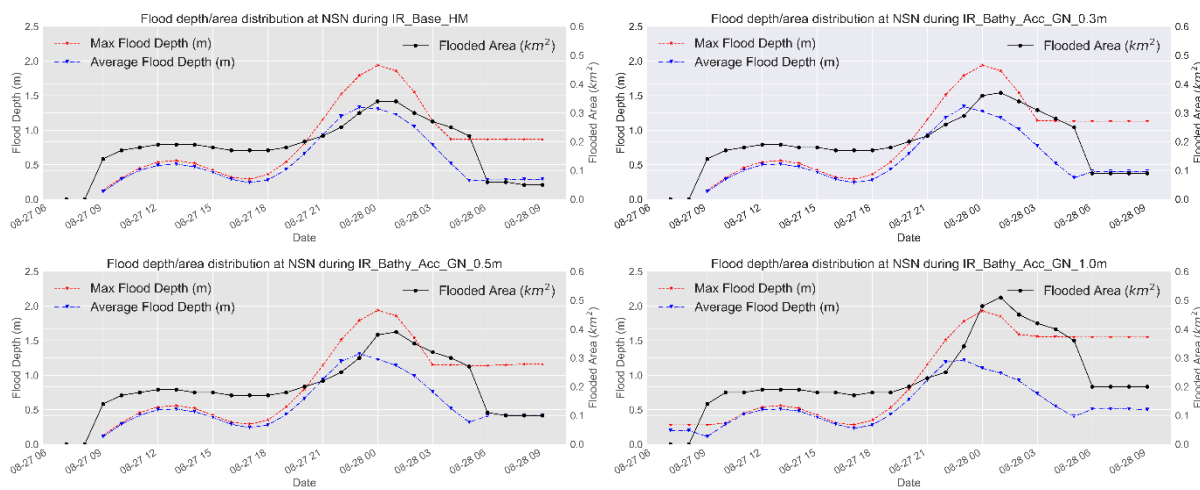


Figure 218. Time series of the projected average and maximum flood depth (left axis) and flood area (km^2 -right axis) for Hurricane Irene for the base and Bathymetry accuracy scenarios at NSN, the US.

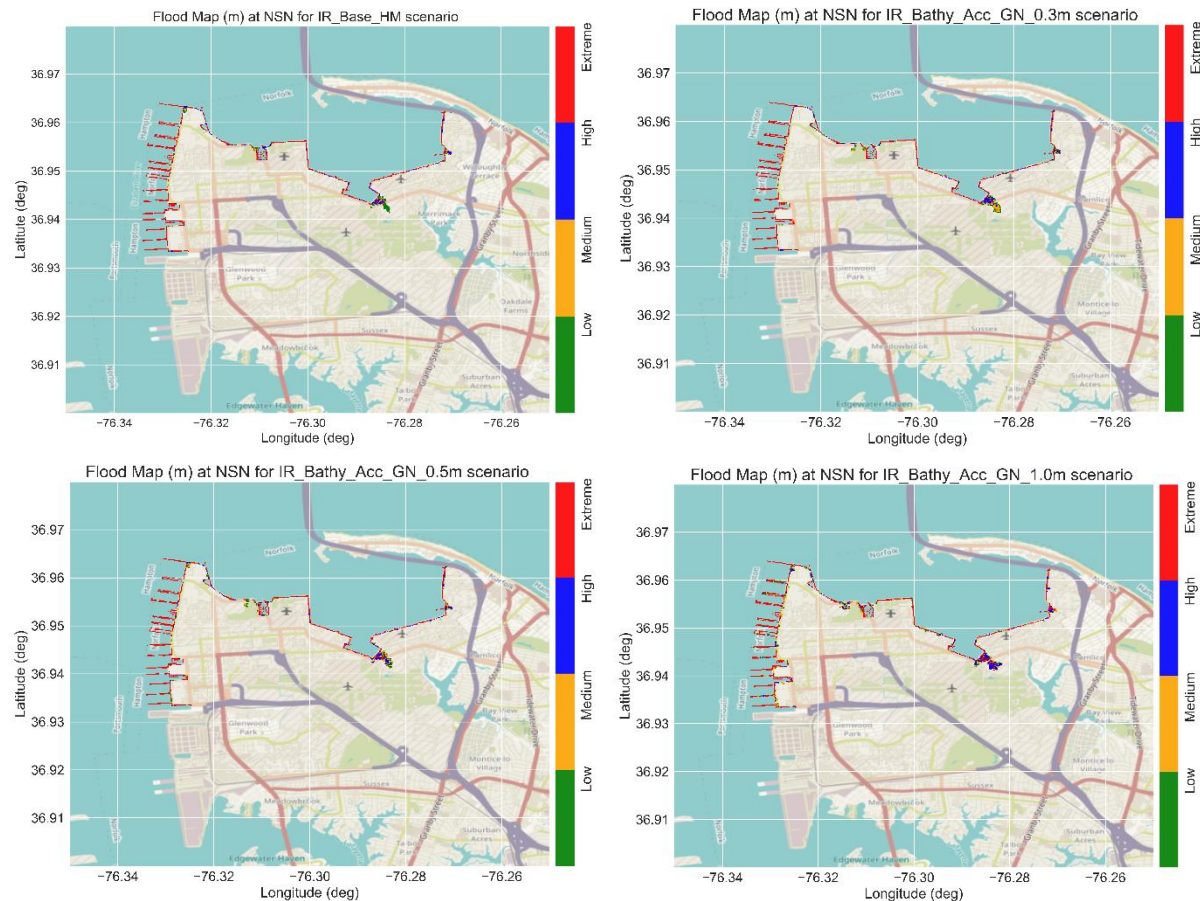


Figure 219. Flood maps with the flood levels for Hurricane Irene during the peak surge for the base and bathymetry accuracy scenarios at NSN, the US.

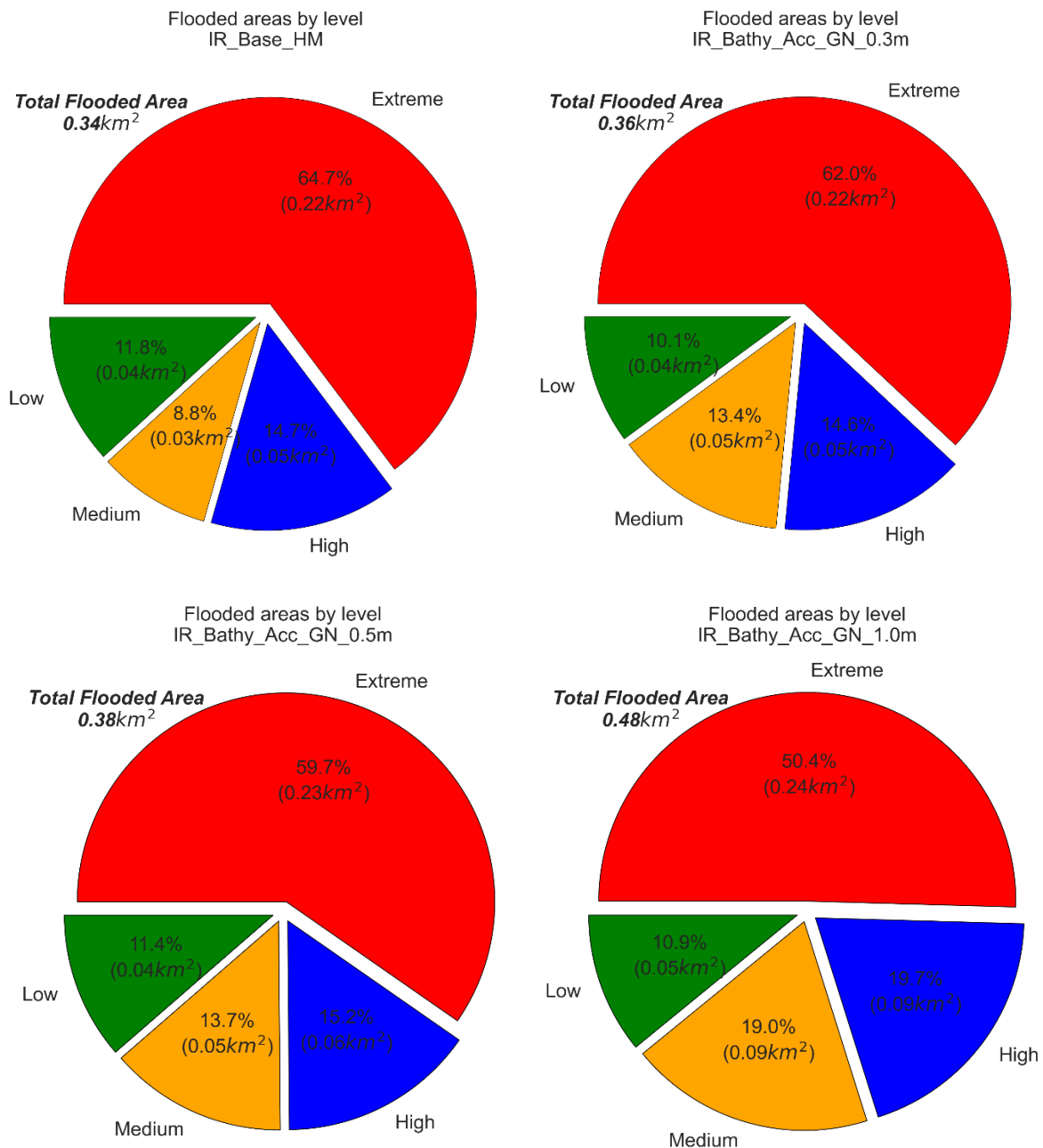


Figure 220. Pie chart of the flood areas, with percentages, of the different flood levels for the base and bathymetry accuracy scenario for Hurricane Irene-2011 at NSN, the US

VI. Bathymetry Resolution

We consider four scenarios for bathymetry/mesh resolution for Hurricane Irene only by decreasing the resolution of the baseline simulation by a factor of 5 (IR_Bathy_Res_F05), 16 (IR_Bathy_Res_F16), 33 (IR_Bathy_Res_F33), and 66 (IR_Bathy_Res_F66). The model performance will be evaluated regarding peak surge and flood area characteristics.

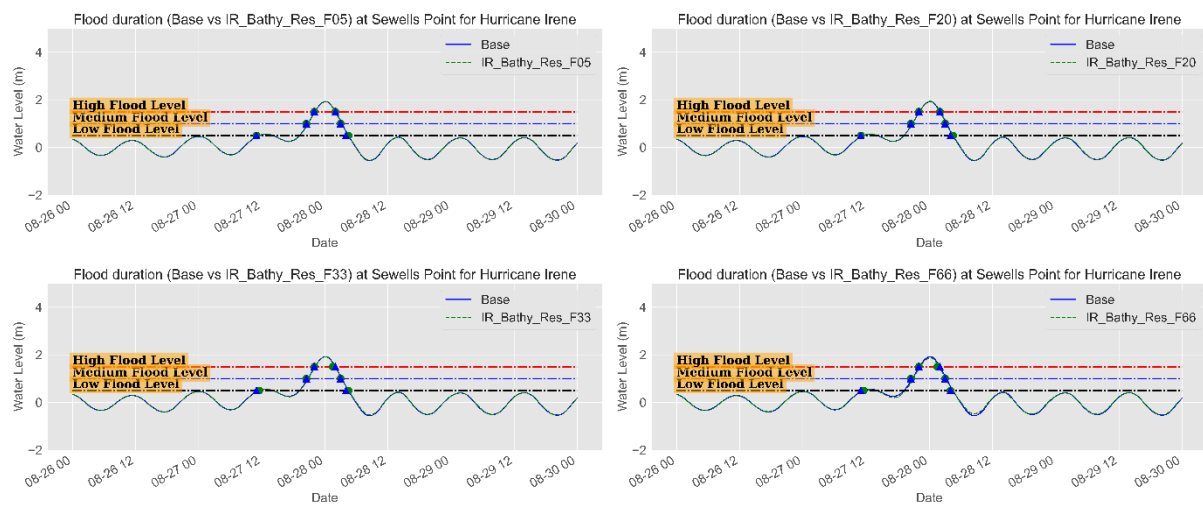


Figure 221. Water level time series (m) during Hurricane Irene showing the surge magnitude and duration for different surge levels for the base and Bathymetry Resolution scenarios at Sewells Point, NSN, the US.

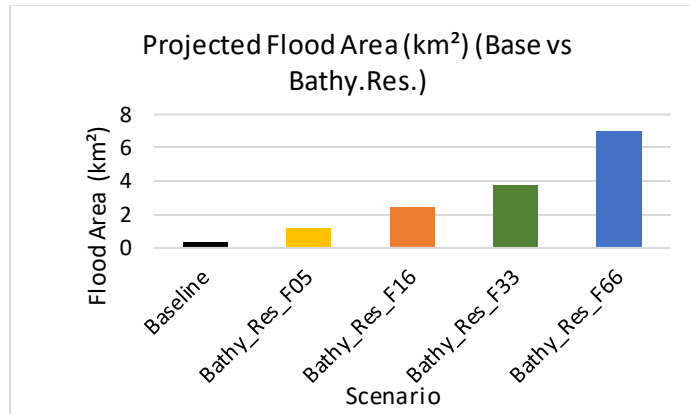


Figure 222. Flood area (km²) of the Base and Bathymetry Resolution scenarios at NSN, the US

Table 72. Flood area characteristics of the base and bathymetry Resolution scenarios at NSN, the US.

Group	Scenario	AFD (m)	MFD (m)	Flood area (km ²)	Flood (%)
Deg. Sc.	Base	1.31	1.94	0.34	2.47
	Bathy_Res_F05	1.23	1.96	1.18	8.6
	Bathy_Res_F16	1.67	1.96	2.43	17.6
	Bathy_Res_F33	1.85	1.94	3.77	27.4
	Bathy_Res_F66	1.83	1.89	6.99	50.8

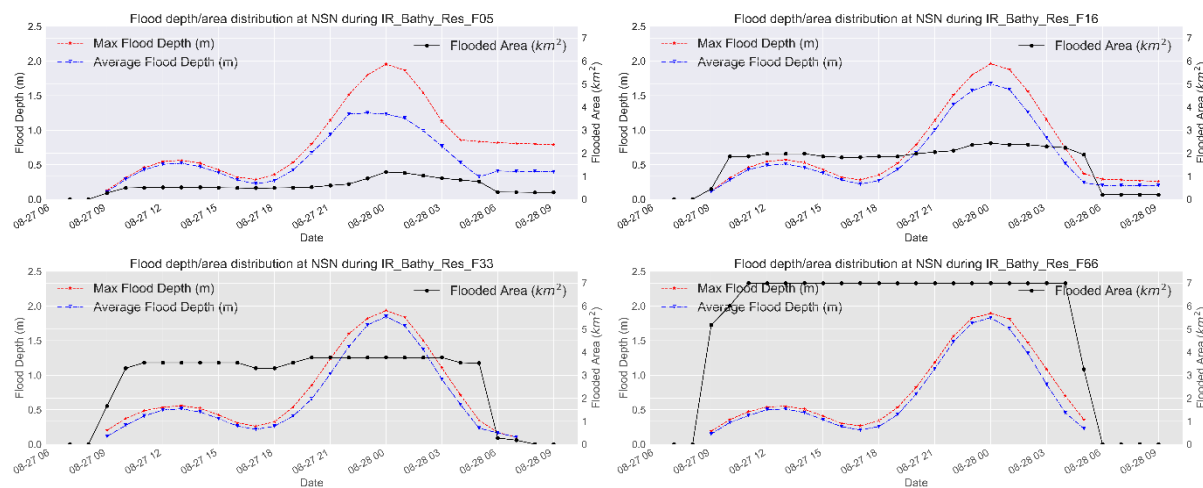


Figure 223. Time series of the projected average and maximum flood depth (left axis) and flood area (km²-right axis) for Hurricane Irene for the Bathymetry Resolution scenarios at NSN, the US.

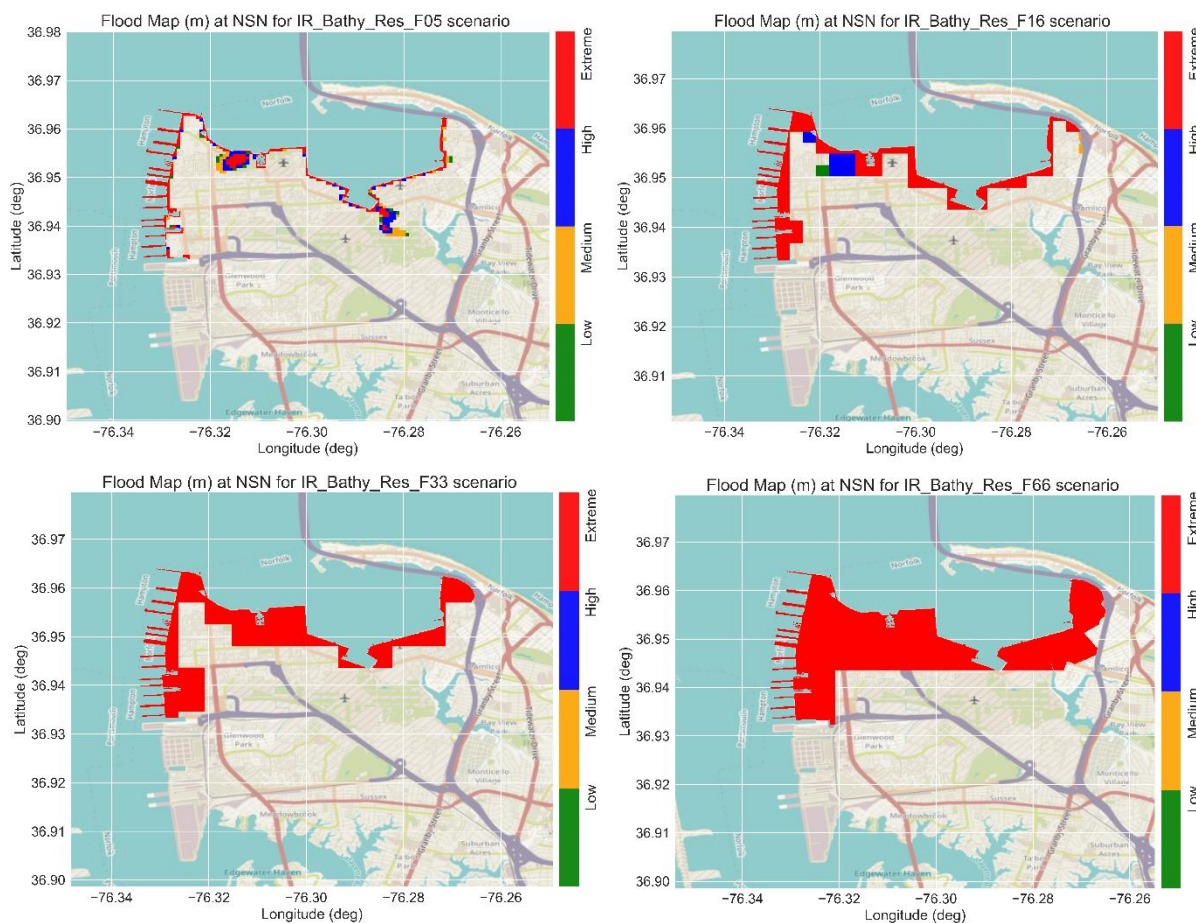


Figure 224. Flood maps with the flood levels for Hurricane Irene during the peak surge for the bathymetry Resolution scenarios at NSN, the US.

6.5. NearCoM

6.6. FUNWAVE

6.7. One-to-One Comparison (D-Flow FM – ADCIRC)

7. Summary and Conclusions

Brief background on the project and its objectives

Outline model setup and model characteristics

Calibration and Validation key results and conclusions

8. Recommendations and future developments

Limitations and low-performance behavior of the model and how to improve them in future versions of the model.

Improvements in network horizontal representation, and bathymetry, employ 3D version for better representation of water density changes and how they can affect the water level, open boundary forcing, Meteorological forcing, calibration, validation data, and procedure ... etc.

9. References

- Booij, N., Ris, R.C., Holthuijsen, L.H., 1999. A third-generation wave model for coastal regions 1. Model description and validation. *J Geophys Res Oceans* 104, 7649–7666. <https://doi.org/10.1029/98JC02622>
- Bunya, S., Dietrich, J.C., Westerink, J.J., Ebersole, B.A., Smith, J.M., Atkinson, J.H., Jensen, R., Resio, D.T., Luettich, R.A., Dawson, C., Cardone, V.J., Cox, A.T., Powell, M.D., Westerink, H.J., Roberts, H.J., 2010. A High-Resolution Coupled Riverine Flow, Tide, Wind, Wind Wave, and Storm Surge Model for Southern Louisiana and Mississippi. Part I: Model Development and Validation. *Mon Weather Rev* 138, 345–377. <https://doi.org/10.1175/2009MWR2906.1>
- Camelo, J., Mayo, T.L., Gutmann, E.D., 2020. Projected Climate Change Impacts on Hurricane Storm Surge Inundation in the Coastal United States. *Front Built Environ* 6. <https://doi.org/10.3389/fbuil.2020.588049>
- Campos, R.M., Gramcianinov, C.B., de Camargo, R., da Silva Dias, P.L., 2022. Assessment and Calibration of ERA5 Severe Winds in the Atlantic Ocean Using Satellite Data. *Remote Sens (Basel)* 14.

[https://doi.org/10.3390/rs1419
4918](https://doi.org/10.3390/rs14194918)

Deltires, 2023a. Delft3D fM Suite 1D2D Simulation software for safe, sustainable and future deltas User Manual D-Flow Flexible Mesh.

Deltires, 2023b. Delft3D FM Suite Simulation software for safe, sustainable and future deltas User Manual D-Flow Flexible Mesh.

Dietrich, J.C., Muhammad, A., Curcic, M., Fathi, A., Dawson, C.N., Chen, S.S., Luettich, R.A., 2018. Sensitivity of Storm Surge Predictions to Atmospheric Forcing during Hurricane Isaac. *J Waterw Port Coast Ocean Eng* 144.

[https://doi.org/10.1061/\(ASCE\)
WW.1943-5460.0000419](https://doi.org/10.1061/(ASCE)WW.1943-5460.0000419)

Dietrich, J.C., Zijlema, M., Westerink, J.J., Holthuijsen, L.H., Dawson, C., Luettich, R.A., Jensen, R.E., Smith, J.M., Stelling, G.S., Stone, G.W., 2011. Modeling hurricane waves and storm surge using integrally-coupled, scalable computations. *Coastal Engineering* 58, 45–65. <https://doi.org/10.1016/j.coastaleng.2010.08.001>

Egbert, G.D., Erofeeva, S.Y., 2002. Efficient Inverse Modeling of

Barotropic Ocean Tides. *J Atmos Ocean Technol* 19, 183–204.
[https://doi.org/10.1175/1520-0426\(2002\)019<0183:EIMOBO>2.0.CO;2](https://doi.org/10.1175/1520-0426(2002)019<0183:EIMOBO>2.0.CO;2)

Emanuel, K.A., 1987. The dependence of hurricane intensity on climate. *Nature* 326, 483–485.

Fleming, J.G., Fulcher, C.W., Luettich, R.A., Estrade, B.D., Allen, G.D., Winer, H.S., 2008. A Real Time Storm Surge Forecasting System Using ADCIRC, in: *Estuarine and Coastal Modeling* (2007). American Society of Civil Engineers, Reston, VA, pp. 893–912.
[https://doi.org/10.1061/40990\(324\)48](https://doi.org/10.1061/40990(324)48)

GAO, 2019. CLIMATE RESILIENCE: DOD Needs to Assess Risk and Provide Guidance on Use of Climate Projections in Installation Master Plans and Facilities Designs (Report to Congressional Requesters No. GAO-19-453). Washington D.C.

Gao, J., 2018. On the surface wind stress for storm surge modeling. University of North Carolina at Chapel Hill.

Hall, J.A., S. Gill, J. Obeysekera, W. Sweet, K. Knuuti, J. Marburger, 2016. Regional Sea Level Scenarios for Coastal Risk Management: Managing the Uncertainty of Future Sea Level

Change and Extreme Water Levels for Department of Defense Coastal Sites Worldwide.

Herold, N., 2014. NOAA's Coastal Change Analysis Program (C-CAP) land cover change data for the Continental and Coastal United States and Hawaii from 1975 to 2016 (NCEI Accession 0121254) [WWW Document]. NOAA National Centers for Environmental Information.

Holland, G., 2008. A revised hurricane pressure-wind model. Mon Weather Rev 136, 3432–3445.
<https://doi.org/10.1175/2008MWR2395.1>

Holland, G.J., 1980a. An analytic model of the wind and pressure profiles in hurricanes. Mon Weather Rev 108, 1212–1218.
[https://doi.org/10.1175/1520-0493\(1980\)108<1212:AAMOTW>2.0.CO;2](https://doi.org/10.1175/1520-0493(1980)108<1212:AAMOTW>2.0.CO;2)

Holland, G.J., 1980b. An analytic model of the wind and pressure profiles in hurricanes. Mon Weather Rev 108, 1212–1218.
[https://doi.org/10.1175/1520-0493\(1980\)108<1212:AAMOTW>2.0.CO;2](https://doi.org/10.1175/1520-0493(1980)108<1212:AAMOTW>2.0.CO;2)

Holland, G.J., Belanger, J.I., Fritz, A., 2010. A revised model for radial

profiles of hurricane winds. Mon Weather Rev 138, 4393–4401.

<https://doi.org/10.1175/2010MWR3317.1>

Hope, M.E., Westerink, J.J., Kennedy, A.B., Kerr, P.C., Dietrich, J.C., Dawson, C., Bender, C.J., Smith, J.M., Jensen, R.E., Zijlema, M., Holthuijsen, L.H., Luettich, R.A., Powell, M.D., Cardone, V.J., Cox, A.T., Pourtaheri, H., Roberts, H.J., Atkinson, J.H., Tanaka, S., Westerink, H.J., Westerink, L.G., 2013. Hindcast and validation of Hurricane Ike (2008) waves, forerunner, and storm surge. J Geophys Res Oceans 118, 4424–4460.

<https://doi.org/10.1002/jgrc.20314>

Kirby, J.T., Wei, G., Chen, Q., Kennedy, A.B., Dalrymple, R.A., 1998. FUNWAVE 1.0 Fully Nonlinear Boussinesq Wave Mode. Documentation and User's Manual.

Kumbier, K., Carvalho, R.C., Vafeidis, A.T., Woodroffe, C.D., 2018. Investigating compound flooding in an estuary using hydrodynamic modelling: A case study from the Shoalhaven River, Australia. Natural Hazards and Earth System Sciences 18, 463–477.

<https://doi.org/10.5194/nhess-18-463-2018>

Lesser, G.R., Roelvink, J.A., van Kester, J.A.T.M., Stelling, G.S., 2004. Development and validation of a three-dimensional morphological model. *Coastal Engineering* 51, 883–915.

<https://doi.org/10.1016/j.coastaleng.2004.07.014>

Luettich, R., Westerink, J., Scheffner, N., 1992. ADCIRC: An Advanced Three-Dimensional circulation model for shelves coasts and estuaries, report 1: Theory and methodology of ADCIRC-2DDI and ADCIRC-3DL.

Mousavi, M.E., Irish, J.L., Frey, A.E., Olivera, F., Edge, B.L., 2011. Global warming and hurricanes: The potential impact of hurricane intensification and sea level rise on coastal flooding. *Clim Change* 104, 575–597. <https://doi.org/10.1007/s10584-009-9790-0>

Muñoz, D.F., Moftakhar, H., Moradkhani, H., 2020. Compound Effects of Flood Drivers and Wetland Elevation Correction on Coastal Flood Hazard Assessment. *Water Resour Res* 56. <https://doi.org/10.1029/2020WR027544>

Muñoz, D.F., Yin, D., Bakhtyar, R., Moftakhar, H., Xue, Z., Mandli, K., Ferreira, C., 2022. Inter-Model Comparison of Delft3D-FM and 2D HEC-RAS for Total

Water Level Prediction in Coastal to Inland Transition Zones. *J Am Water Resour Assoc* 58, 34–49. <https://doi.org/10.1111/1752-1688.12952>

Nederhoff, K., Saleh, R., Tehranirad, B., Herdman, L., Erikson, L., Barnard, P.L., van der Wegen, M., 2021. Drivers of extreme water levels in a large, urban, high-energy coastal estuary – A case study of the San Francisco Bay. *Coastal Engineering* 170. <https://doi.org/10.1016/j.coastaleng.2021.103984>

Pringle, W.J., Wirasaet, D., Roberts, K.J., Westerink, J.J., 2021. Global storm tide modeling with ADCIRC v55: unstructured mesh design and performance. *Geosci Model Dev* 14, 1125–1145. <https://doi.org/10.5194/gmd-14-1125-2021>

Riverside Technology, AECOM, 2015. Mesh Development, Tidal Validation, and Hindcast Skill Assessment of an ADCIRC Model for the Hurricane Storm Surge Operational Forecast System on the US Gulf-Atlantic Coast.

Roberts, K.J., Pringle, W.J., Westerink, J.J., 2019. OceanMesh2D 1.0: MATLAB-based software for two-

dimensional unstructured mesh generation in coastal ocean modeling. *Geosci Model Dev* 12, 1847–1868.
<https://doi.org/10.5194/gmd-12-1847-2019>

Russo, E.P., 1998. ESTIMATING HURRICANE STORM SURGE AMPLITUDES FOR THE GULF OF MEXICO AND ATLANTIC COASTLINES OF THE UNITED STATES, in: Presented at the OCEANS'98, IEEE Oceanic Engineering Society. Nice, pp. 1301–1305.

Salehi, M., 2018. Storm surge and wave impact of low-probability hurricanes on the lower Delaware Bay-Calibration and application. *J Mar Sci Eng* 6, 1–28.
<https://doi.org/10.3390/jmse6020054>

Shi, F., Kirby, J.T., Harris, J.C., Geiman, J.D., Grilli, S.T., 2012. A high-order adaptive time-stepping TVD solver for Boussinesq modeling of breaking waves and coastal inundation. *Ocean Model (Oxf)* 43–44, 36–51.
<https://doi.org/10.1016/j.ocemod.2011.12.004>

Stockdon, H.F., Holman, R.A., Howd, P.A., Sallenger, A.H., 2006. Empirical parameterization of setup, swash, and runup. *Coastal Engineering* 53, 573–588.
<https://doi.org/10.1016/j.coastaleng.2005.12.005>

Sweet, W.V., B.D. Hamlington, R.E. Kopp, C.P. Weaver, P.L. Barnard, D. Bekaert, W. Brooks, M. Craghan, G. Dusek, T. Frederikse, G. Garner, A.S. Genz, J.P. Krasting, E. Larour, D. Marcy, J.J. Marra, J. Obeysekera, M. Osler, M. Pendleton, D. Roman, L. Schmied, W. Veatch, K.D. White, C. Zuzak, 2022. Global and Regional Sea Level Rise Scenarios for the United States.

Tanaka, S., Bunya, S., Westerink, J.J., Dawson, C., Luettich, R.A., 2011. Scalability of an Unstructured Grid Continuous Galerkin Based Hurricane Storm Surge Model. *J Sci Comput* 46, 329–358. <https://doi.org/10.1007/s10915-010-9402-1>

UOCS, 2016. The US Military on the Front Lines of Rising Seas (EXECUTIVE SUMMARY).

van der Westhuysen, A.J., Zijlema, M., Battjes, J.A., 2007. Nonlinear saturation-based whitecapping dissipation in SWAN for deep and shallow water. *Coastal Engineering* 54, 151–170. <https://doi.org/10.1016/j.coastaleng.2006.08.006>

Wei, Ge., Kirby, J., Grilli, S.T., Subramanya, R., 1995. A Fully Nonlinear Boussinesq Model for

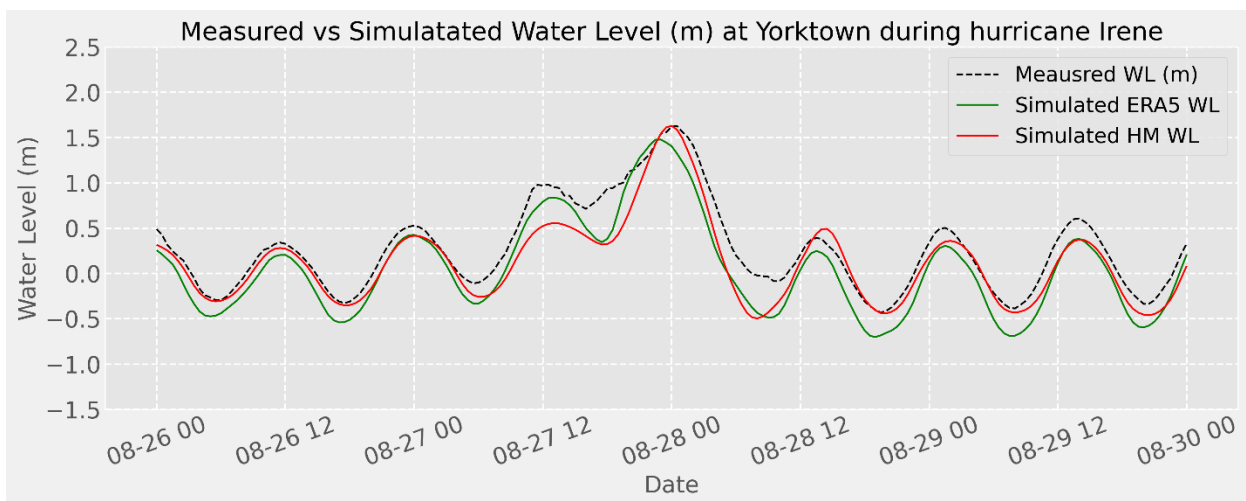
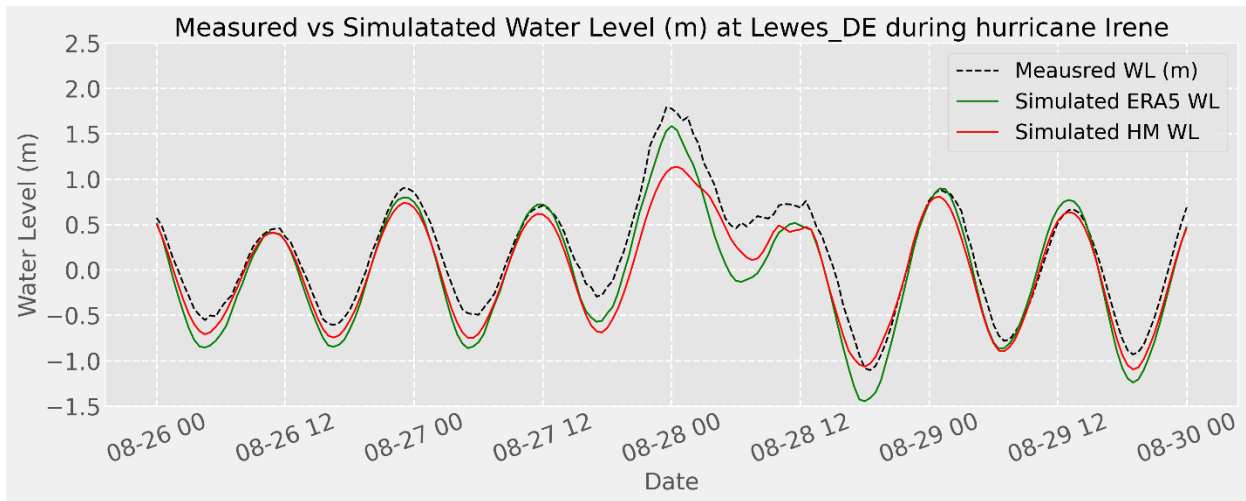
Surface Waves. Part 1. Highly Nonlinear Unsteady Waves. J Fluid Mech 294, 71–92.
<https://doi.org/10.1017/S0022112095002813>

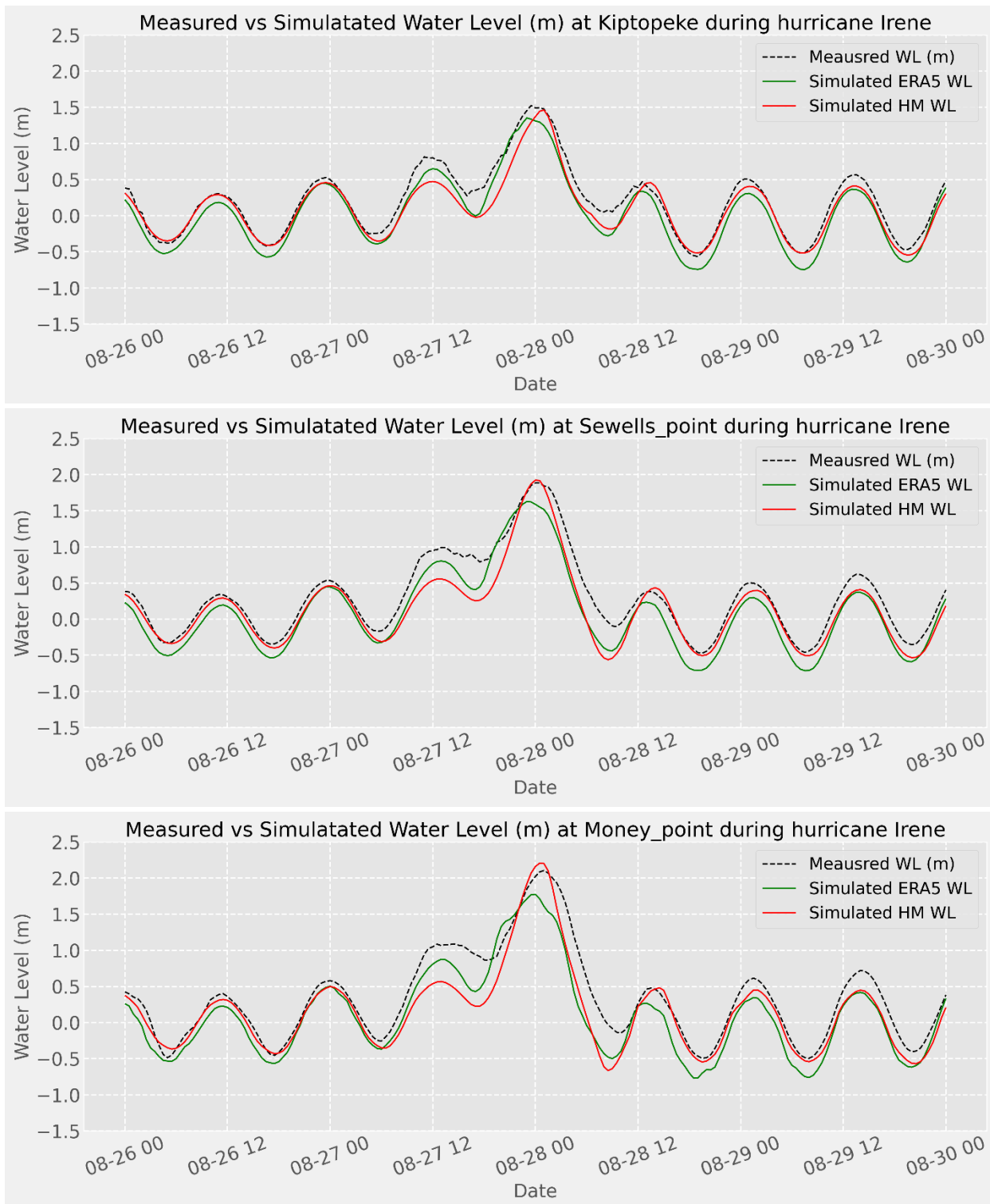
Westerink, J.J., Luettich, R.A., Feyen, J.C., Atkinson, J.H., Dawson, C., Roberts, H.J., Powell, M.D., Dunion, J.P., Kubatko, E.J., Pourtaheri, H., 2008. A Basin- to Channel-Scale Unstructured Grid Hurricane Storm Surge Model Applied to Southern Louisiana. Mon Weather Rev 136, 833–864.
<https://doi.org/10.1175/2007MWR1946.1>

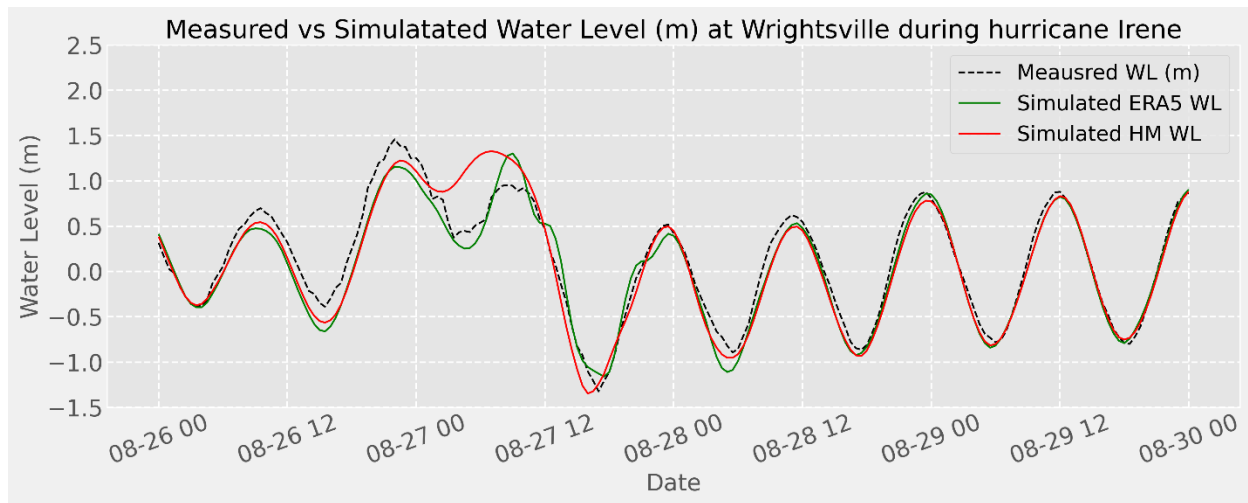
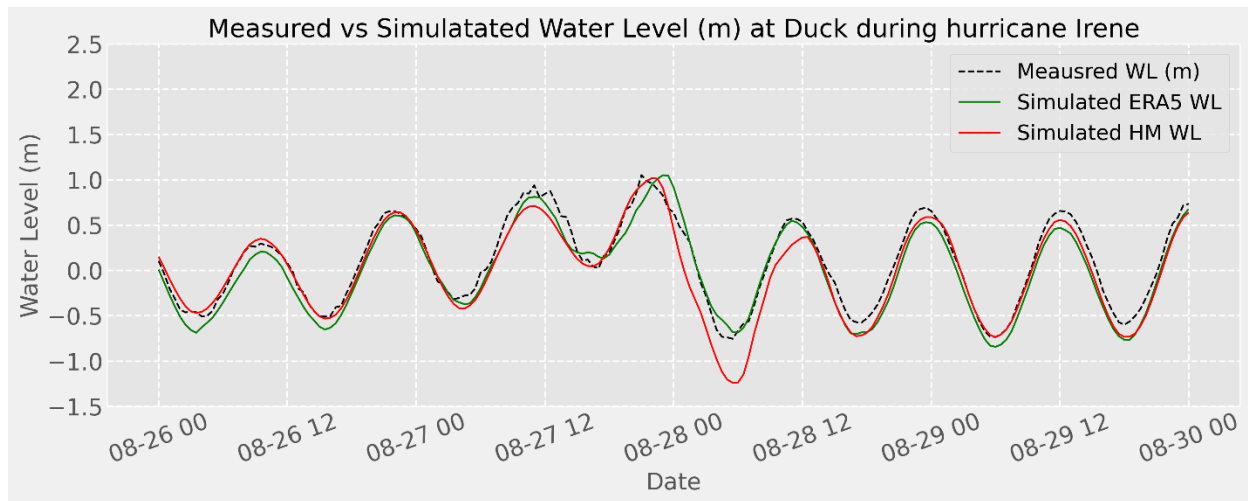
10. Appendix A (calibration figures)

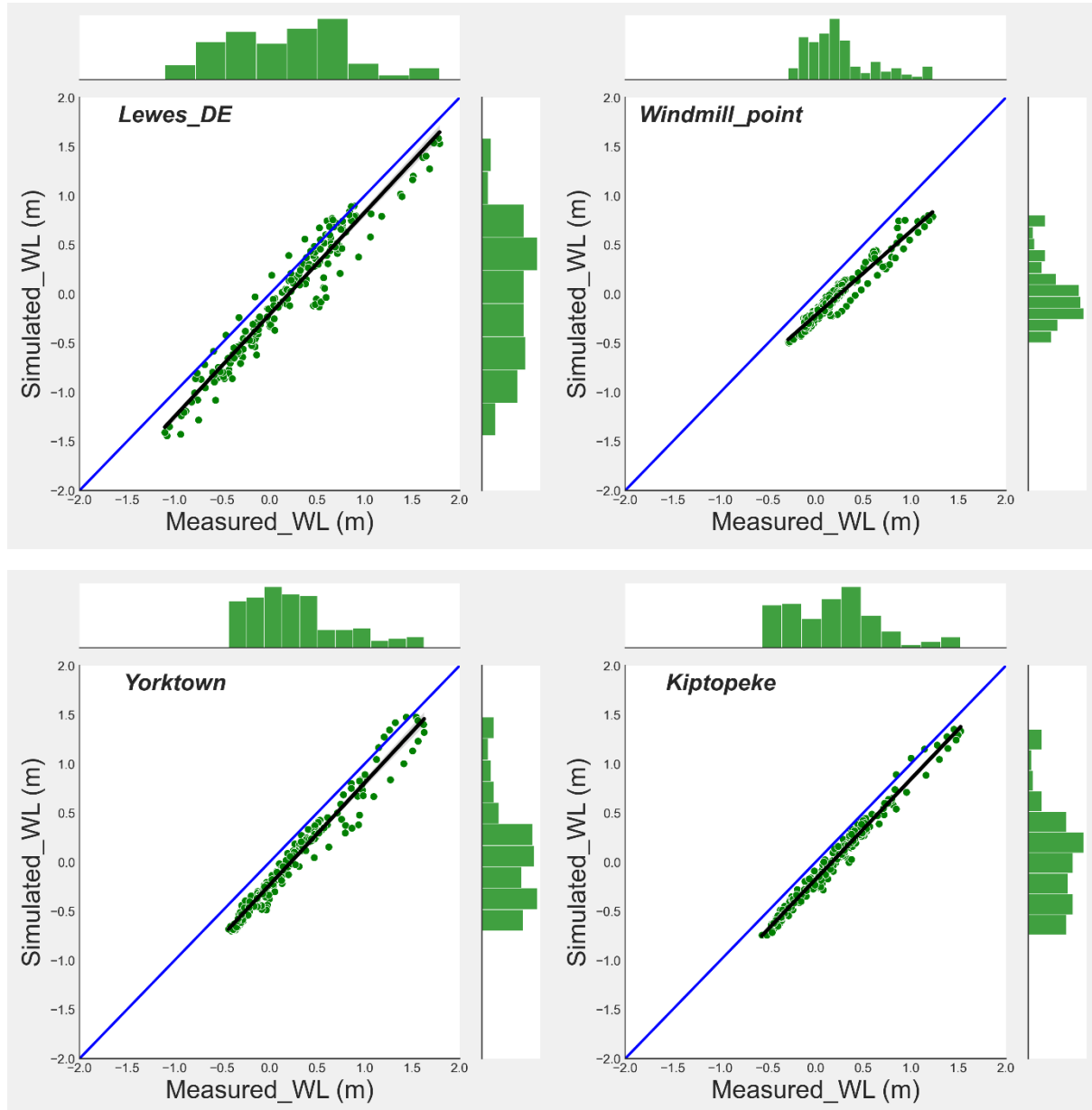
10.1. Hurricane Irene (2011)

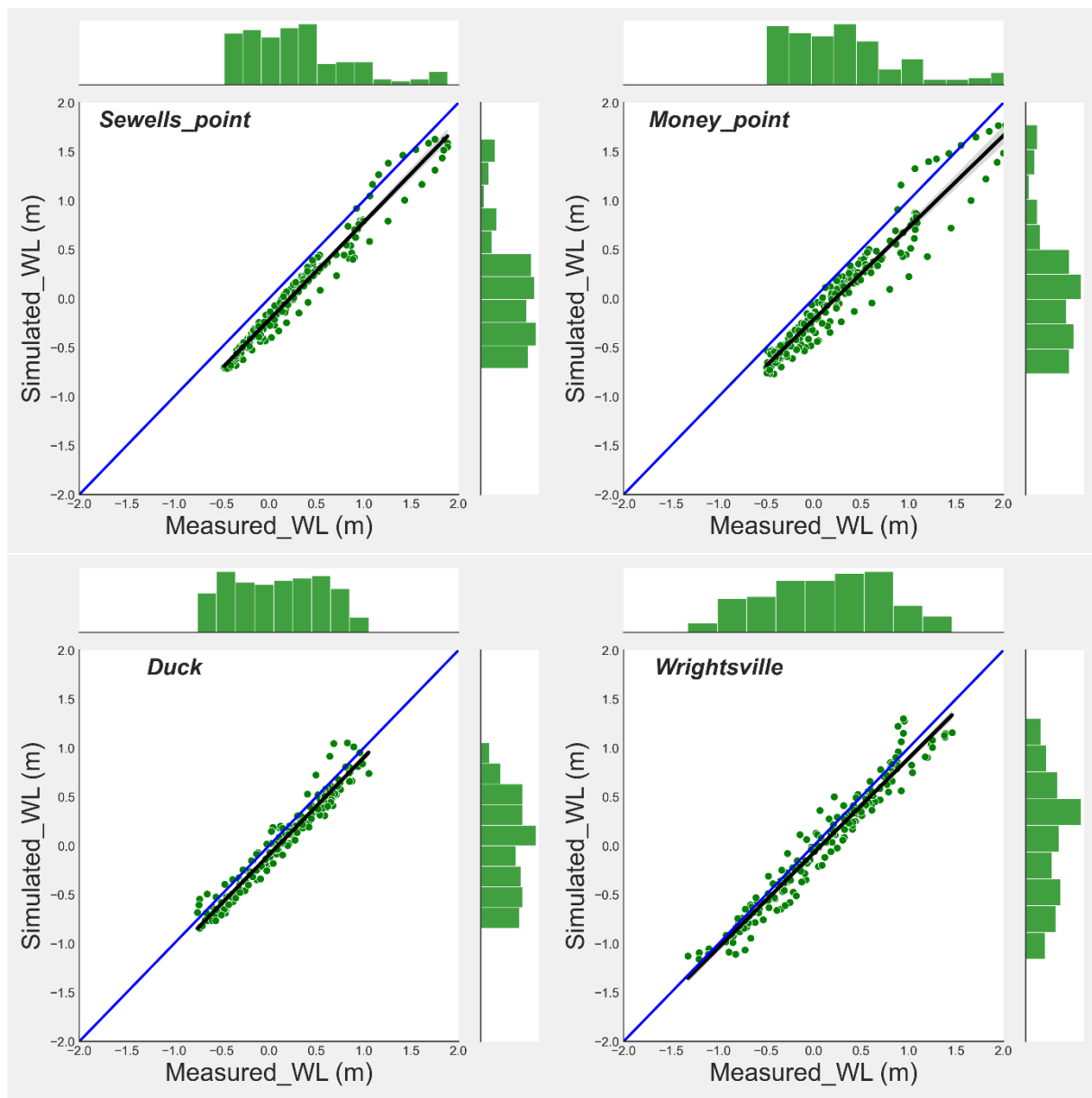
1. Time series plots of the measured and simulated water level in meters (ERA5 and HM)



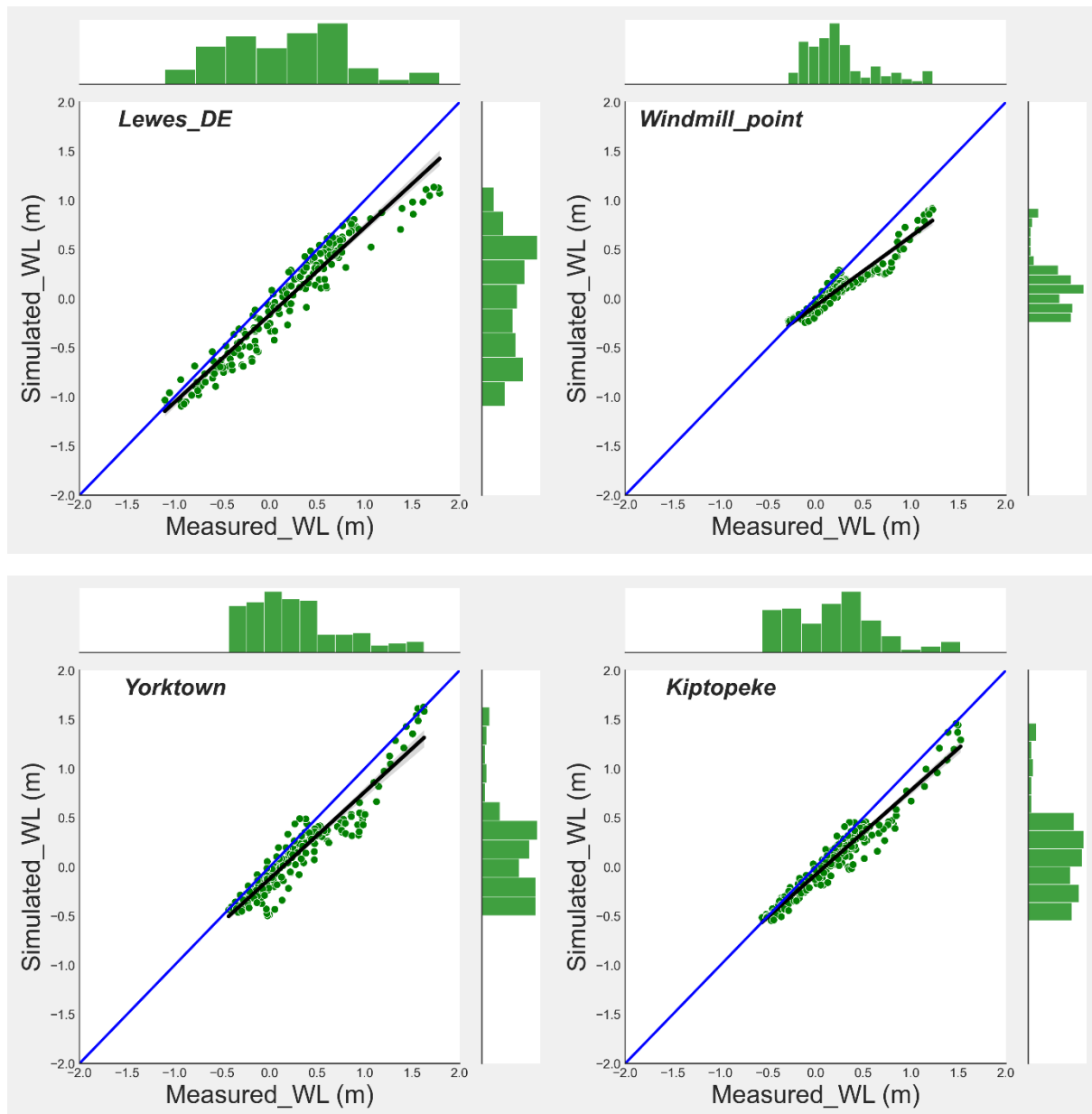


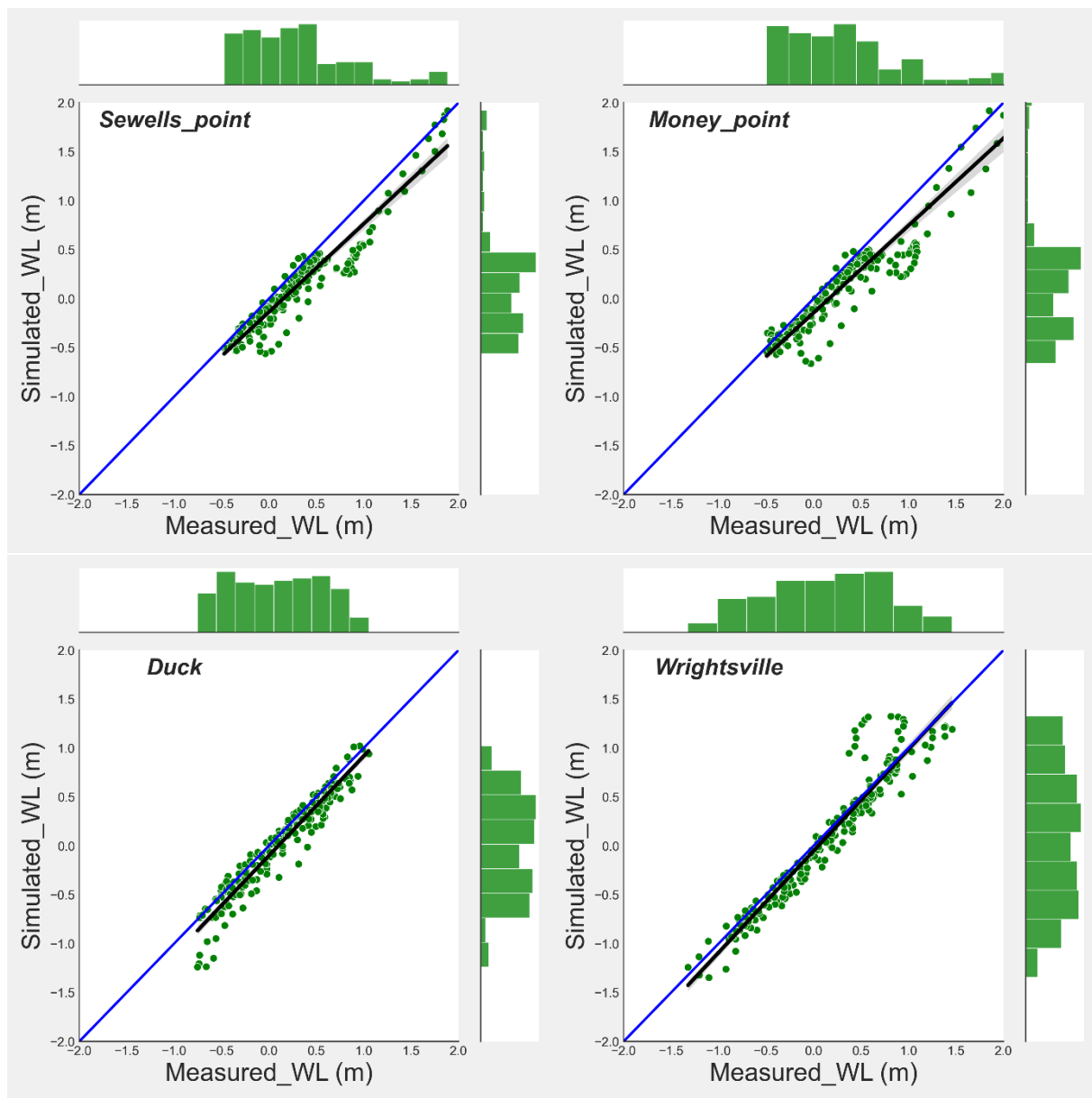


I. Scatter plots of the measured and simulated water level in meters using ERA5 wind forces

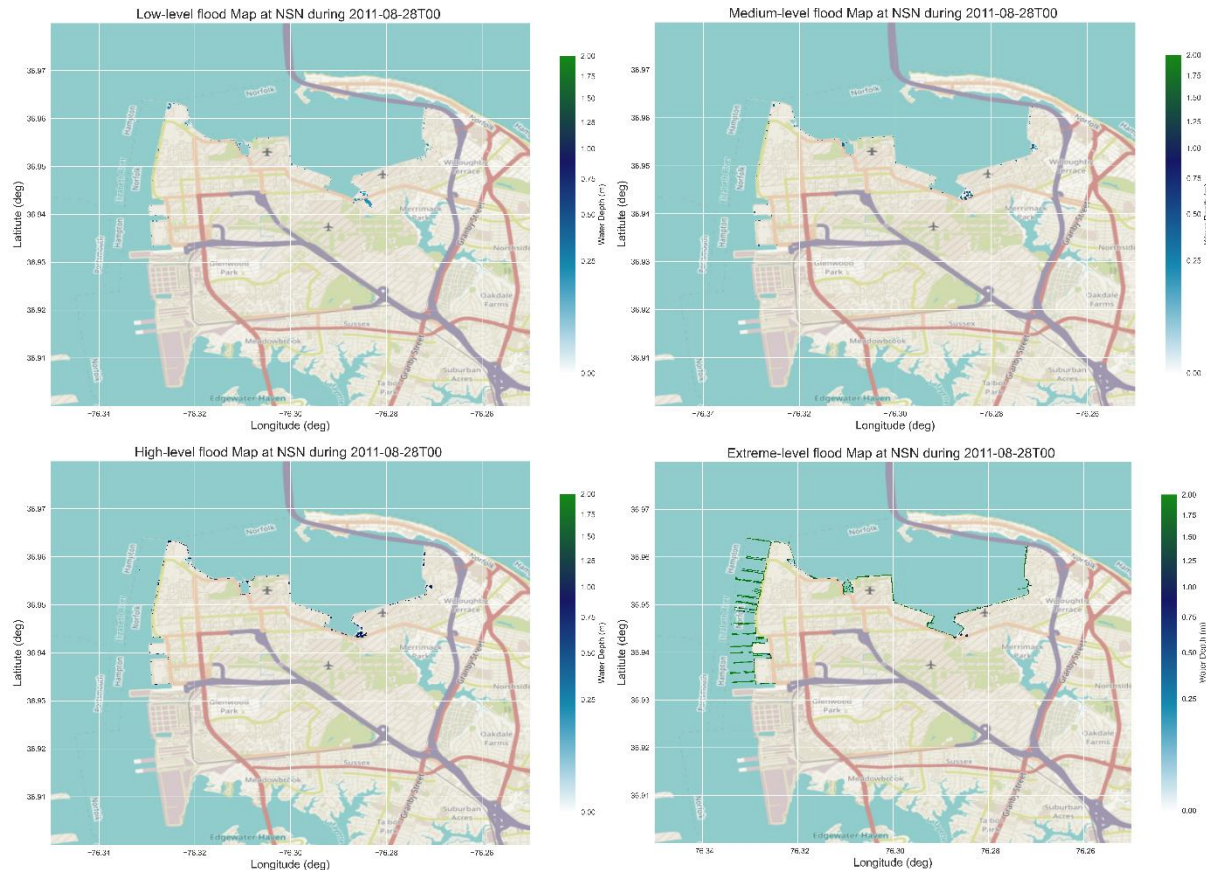


II. Scatter plots of the measured and simulated water level in meters using Holland Model (HM) wind forces



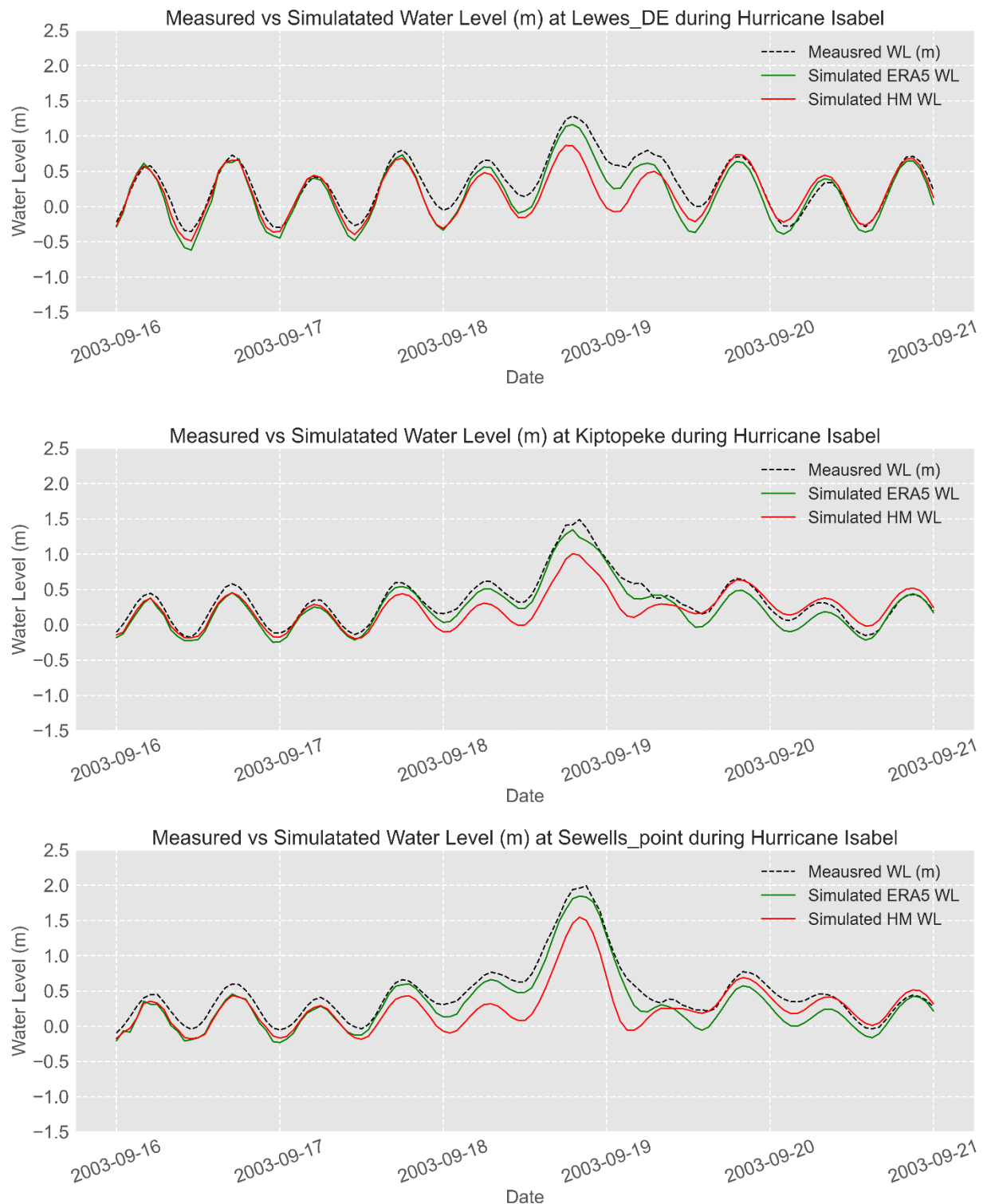


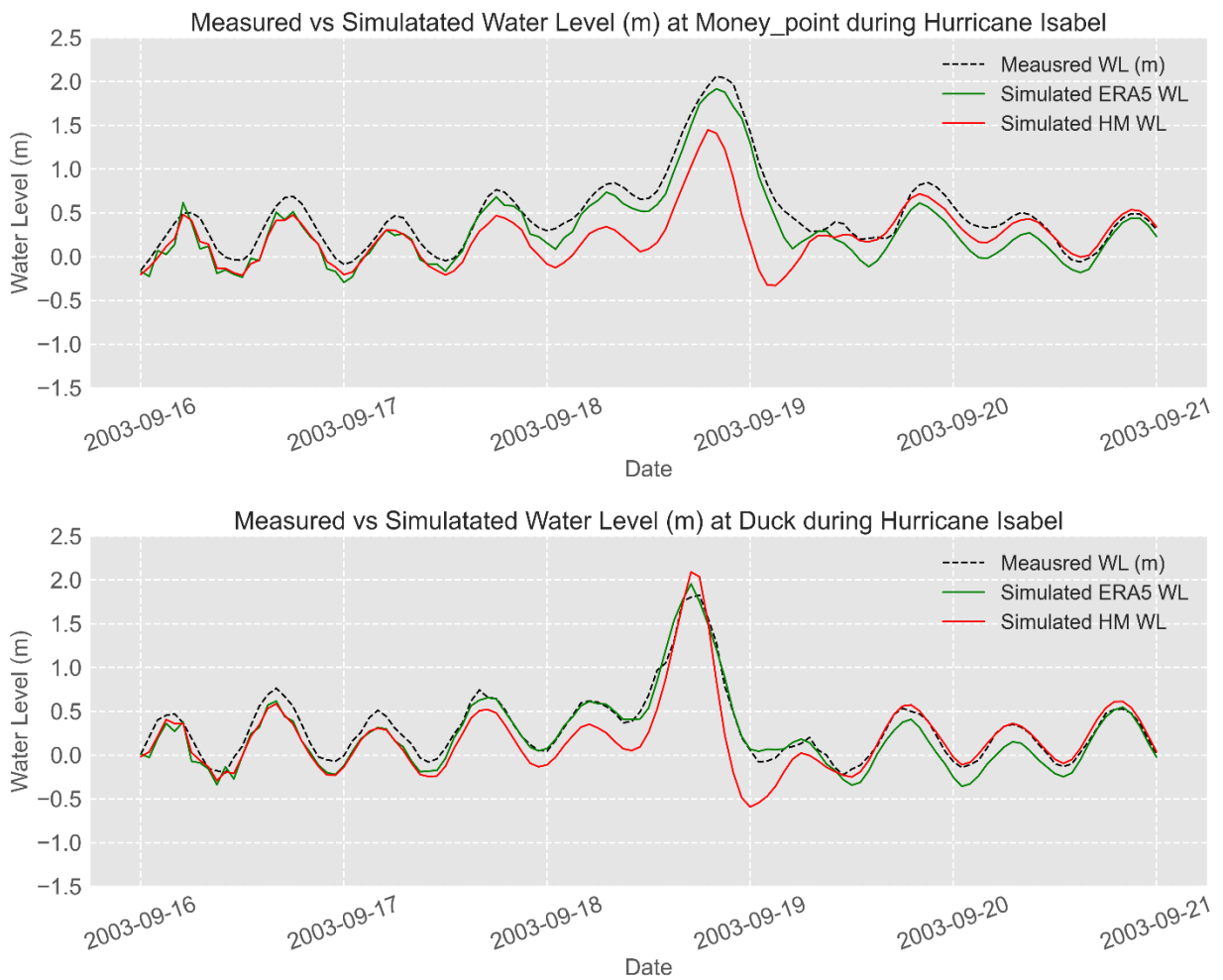
III. Flood maps of each flood level using HM wind forces.

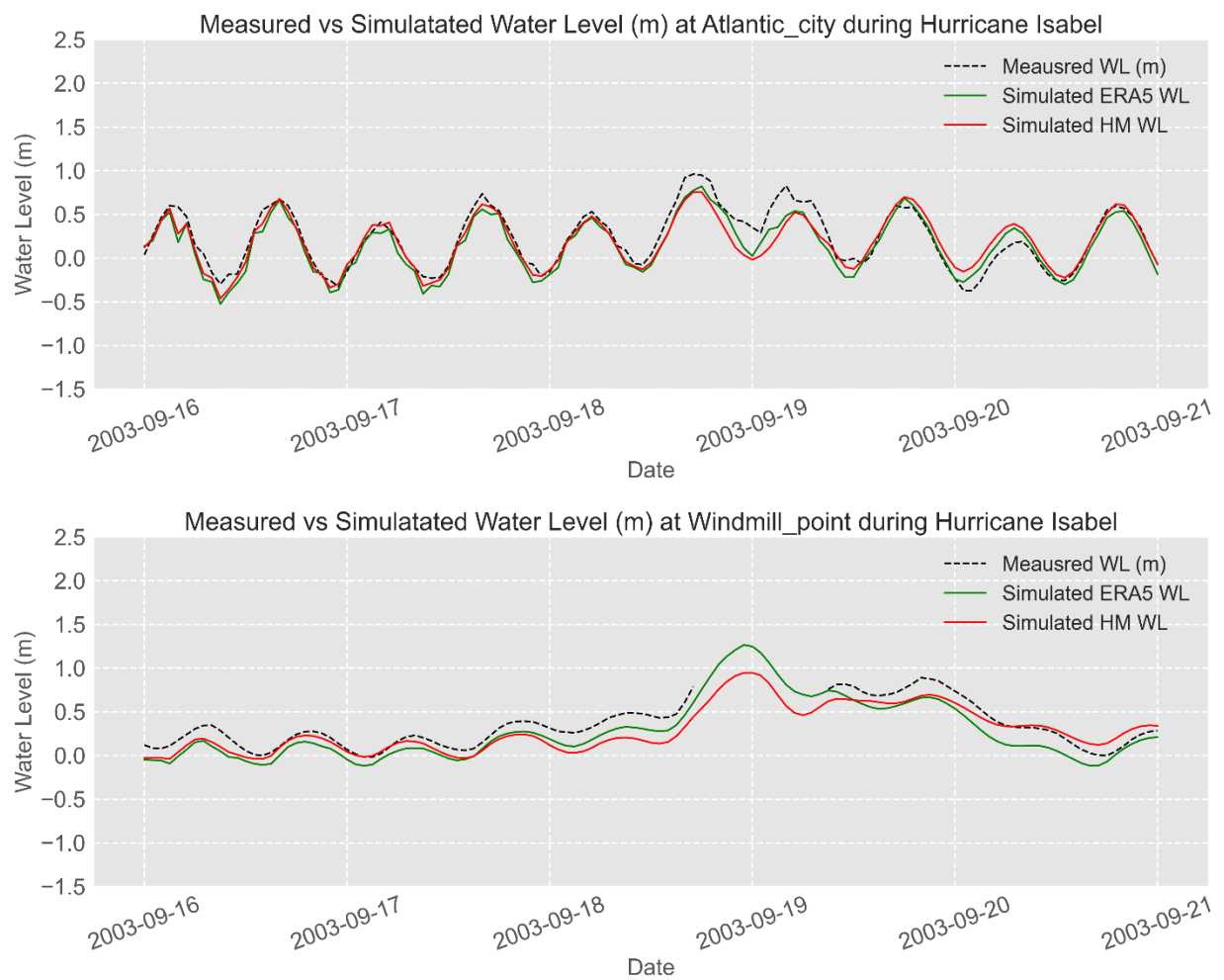


10.2. Hurricane Isabel (2003)

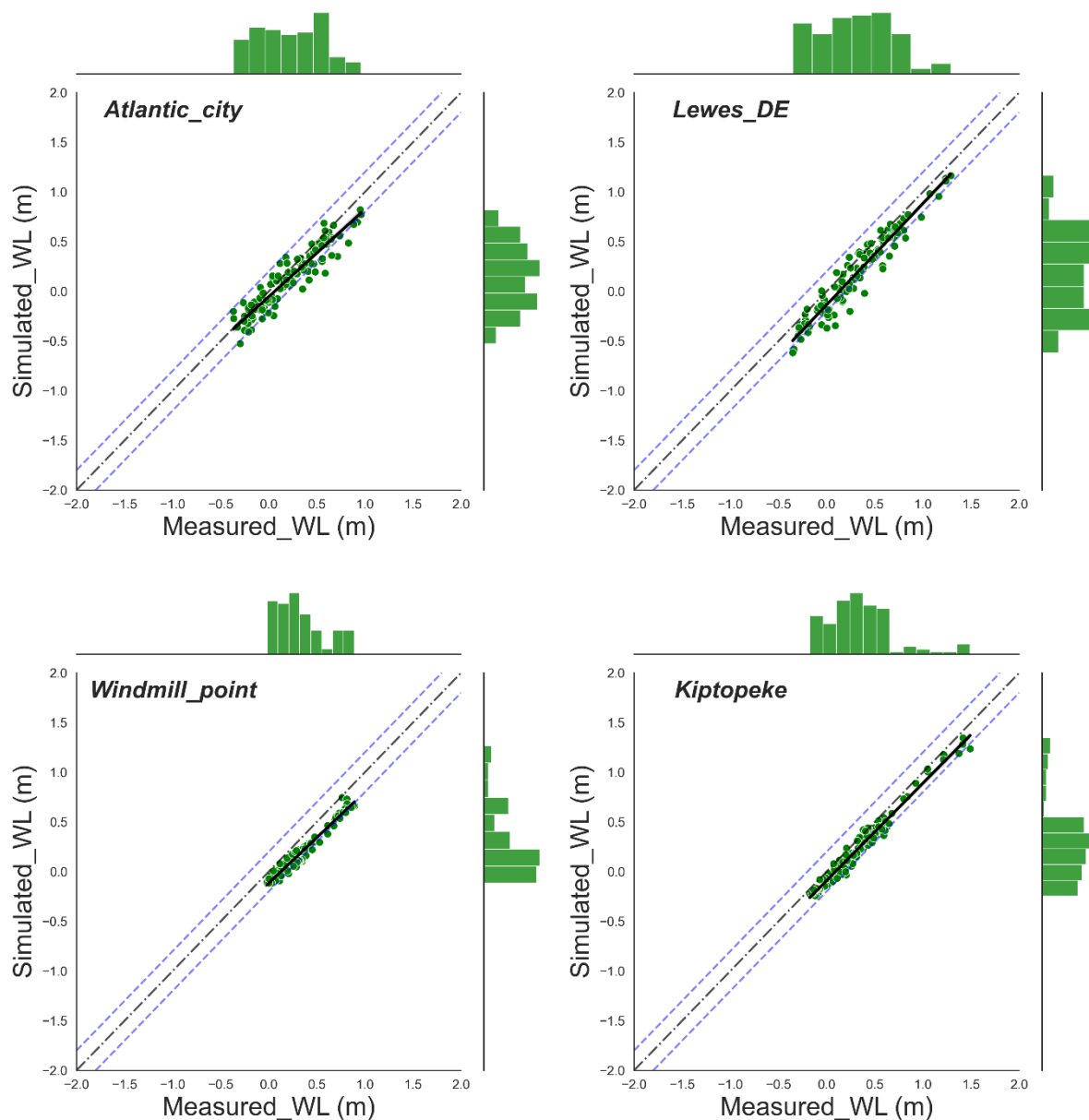
1. Time series plots of the measured and simulated water level in meters (ERA5 and HM)

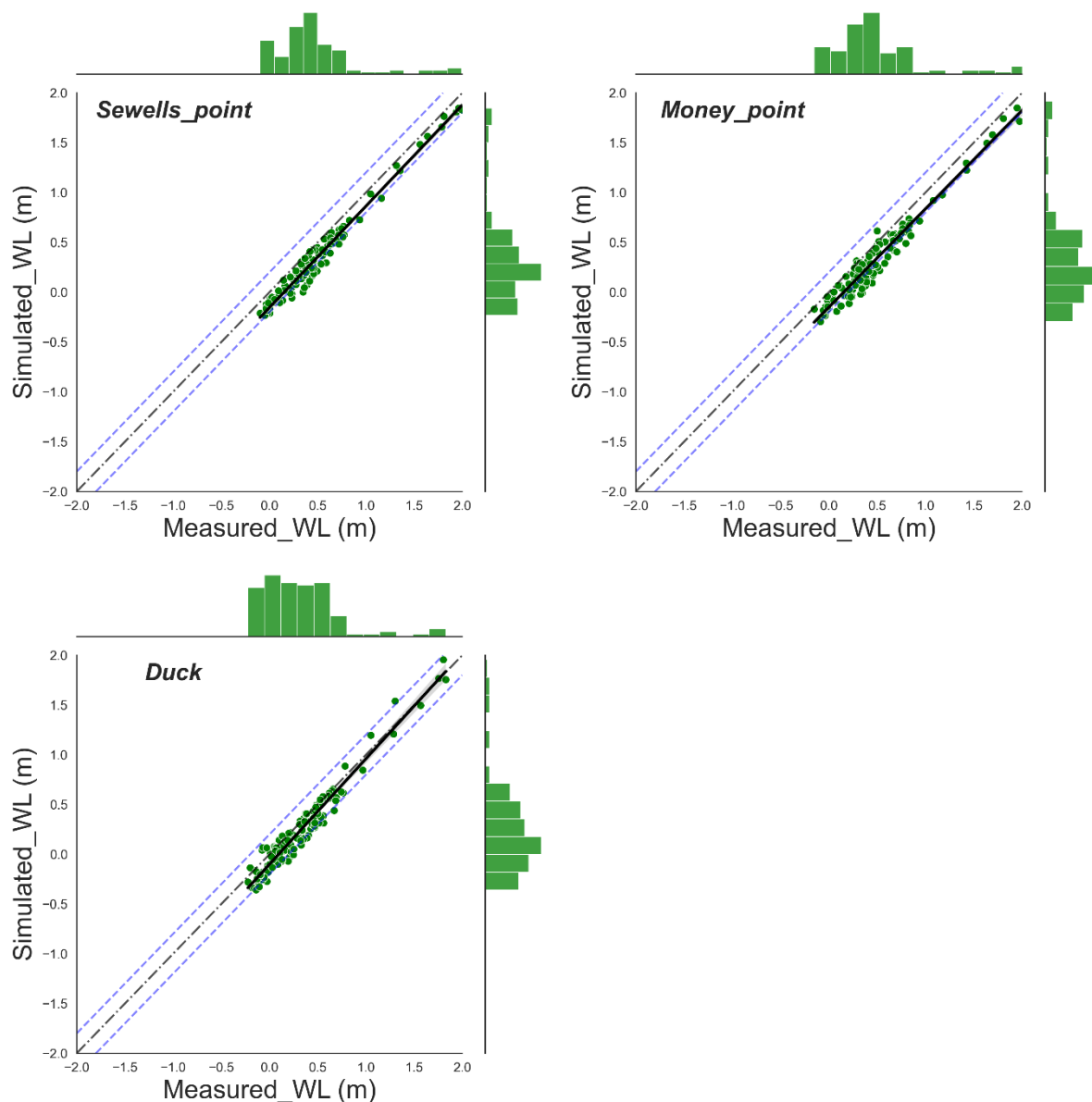




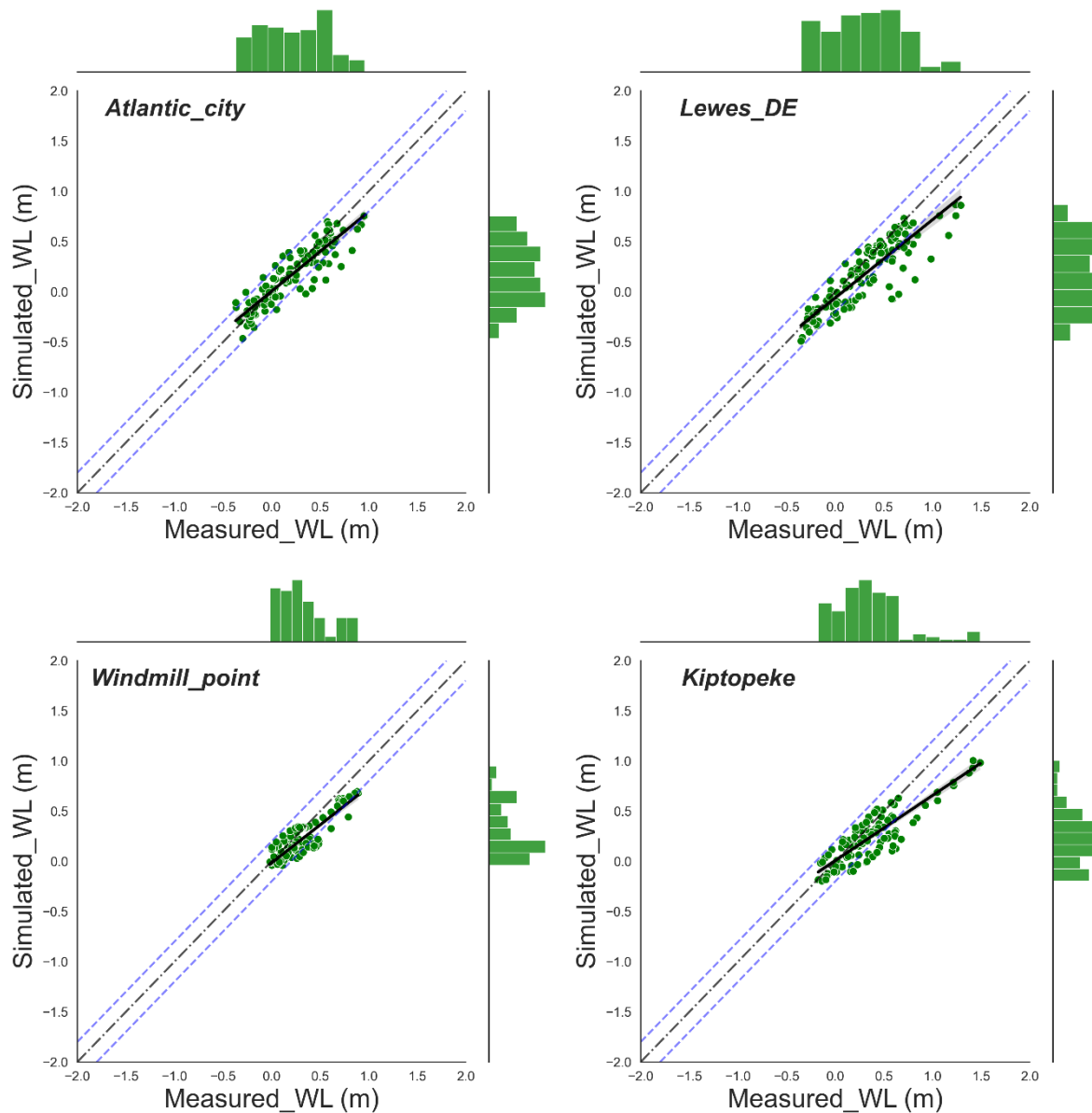


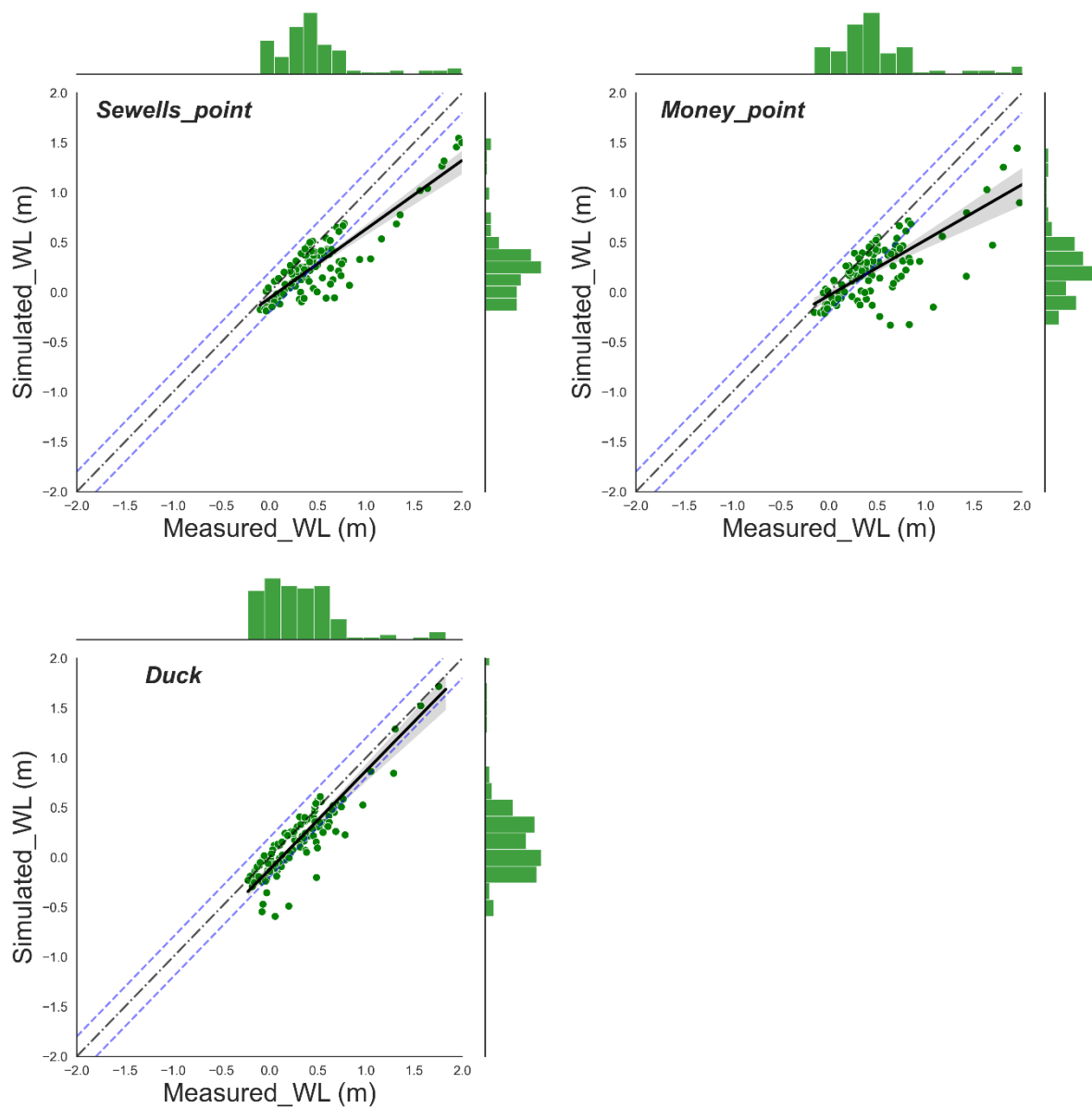
2. Scatter plots of the measured and simulated water level in meters using ERA5 wind forces



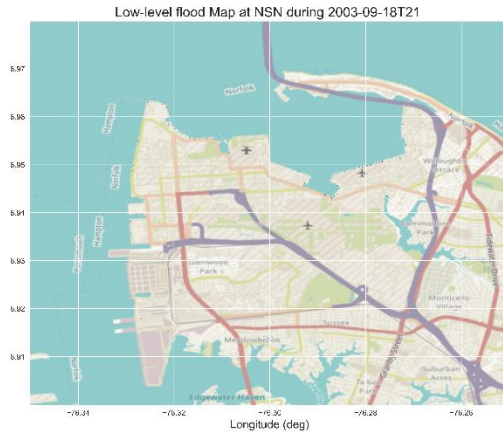


3. Scatter plots of the measured and simulated water level in meters using Holland Model (HM) wind forces



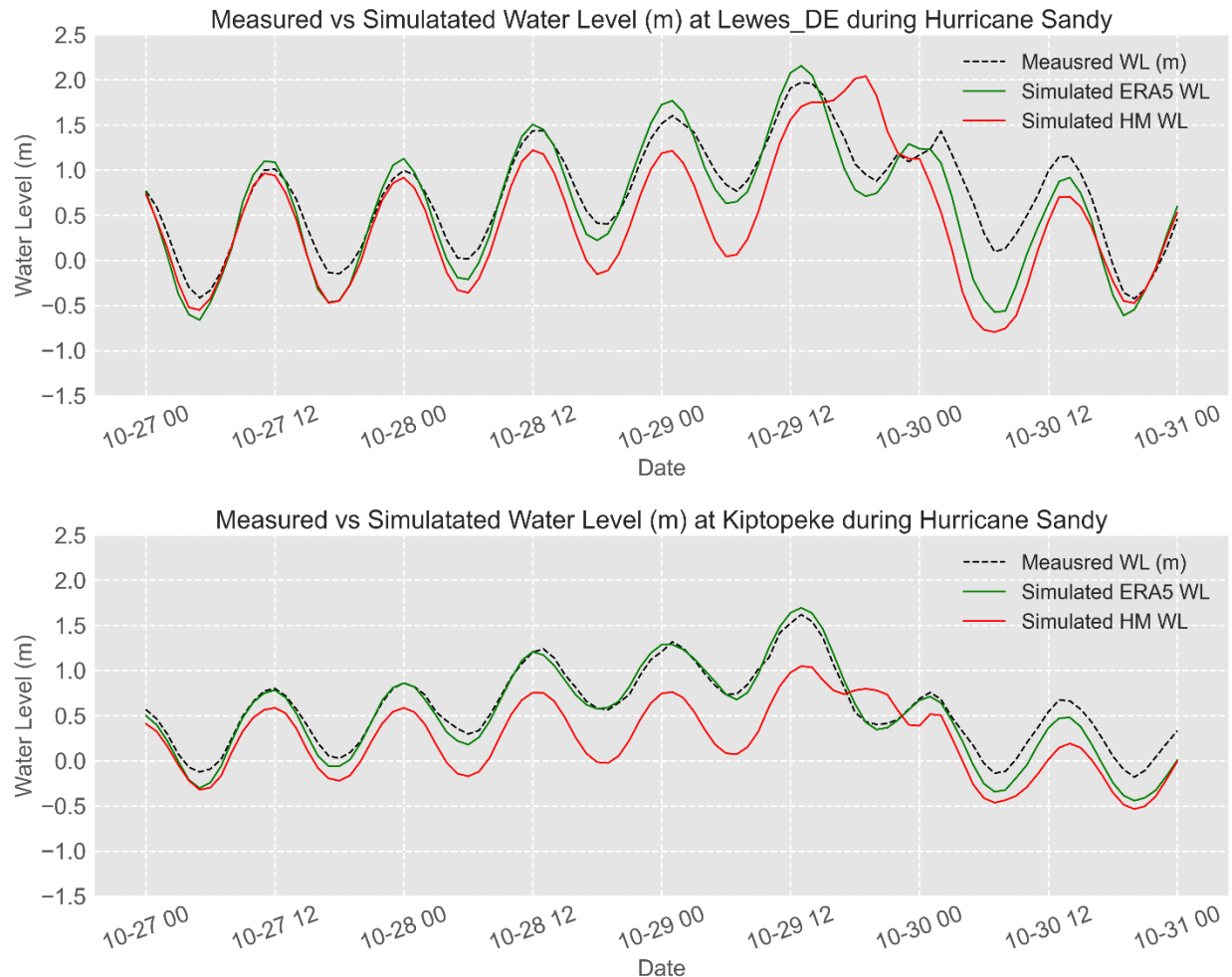


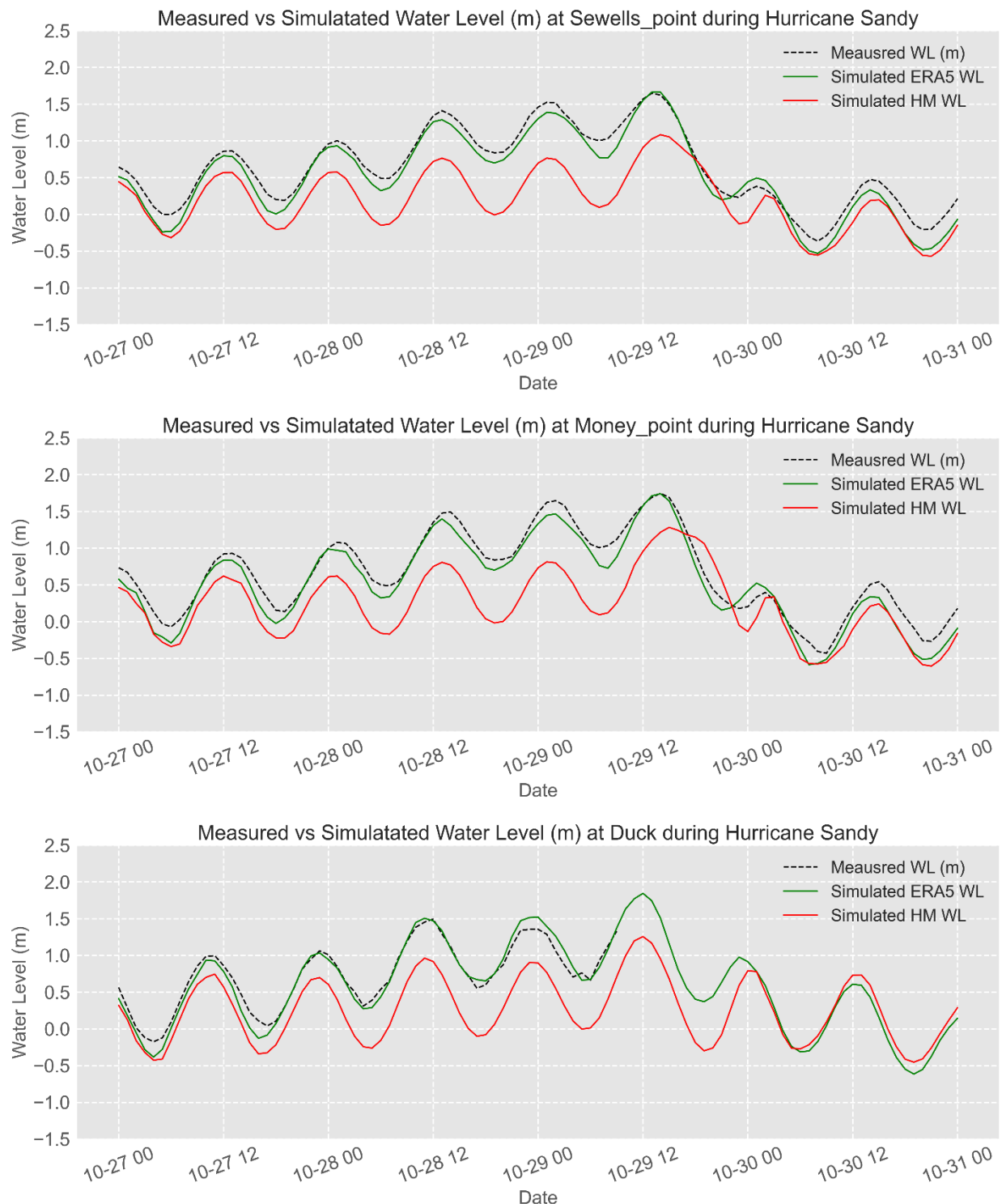
4. Flood maps of each flood level using HM wind forces.

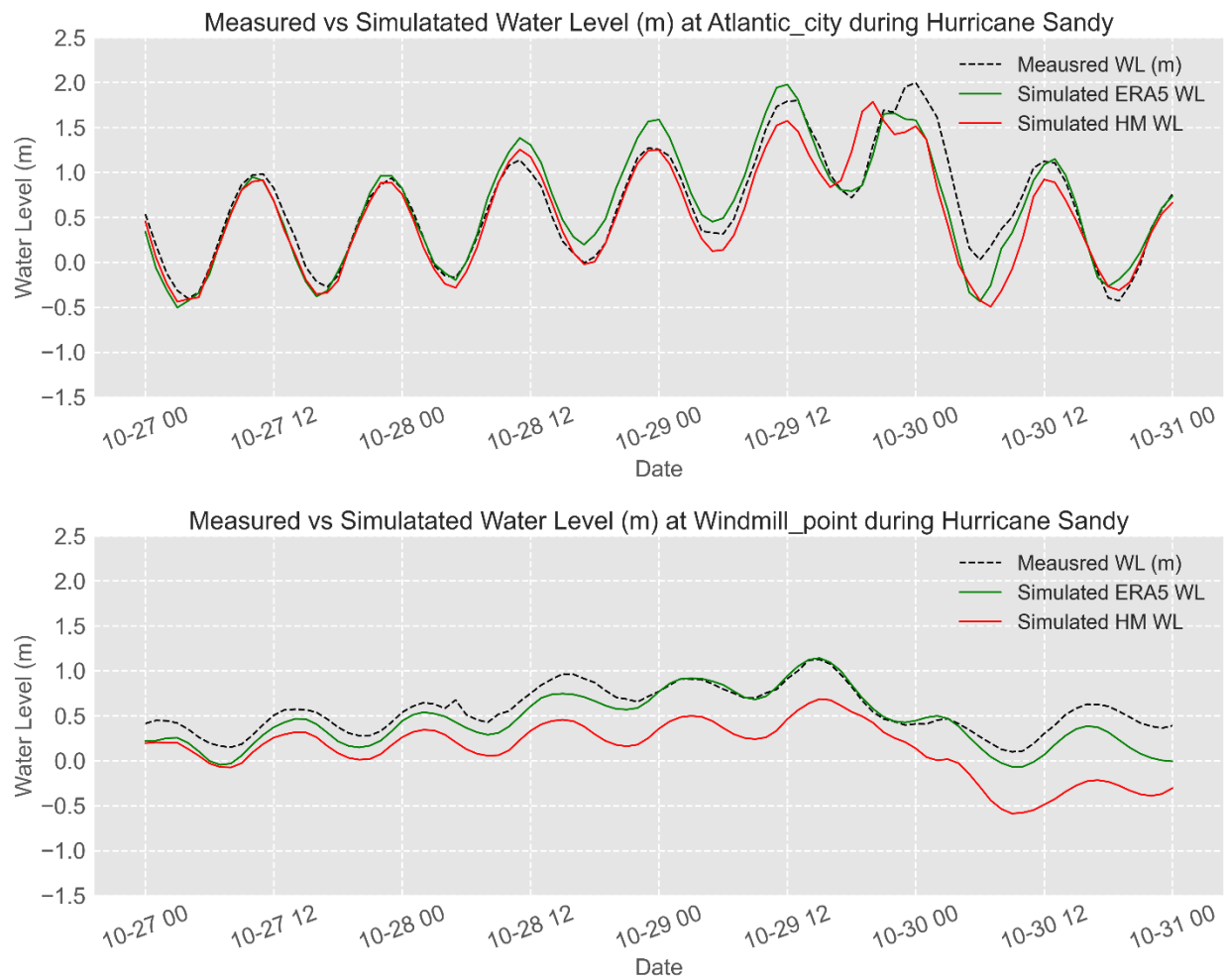


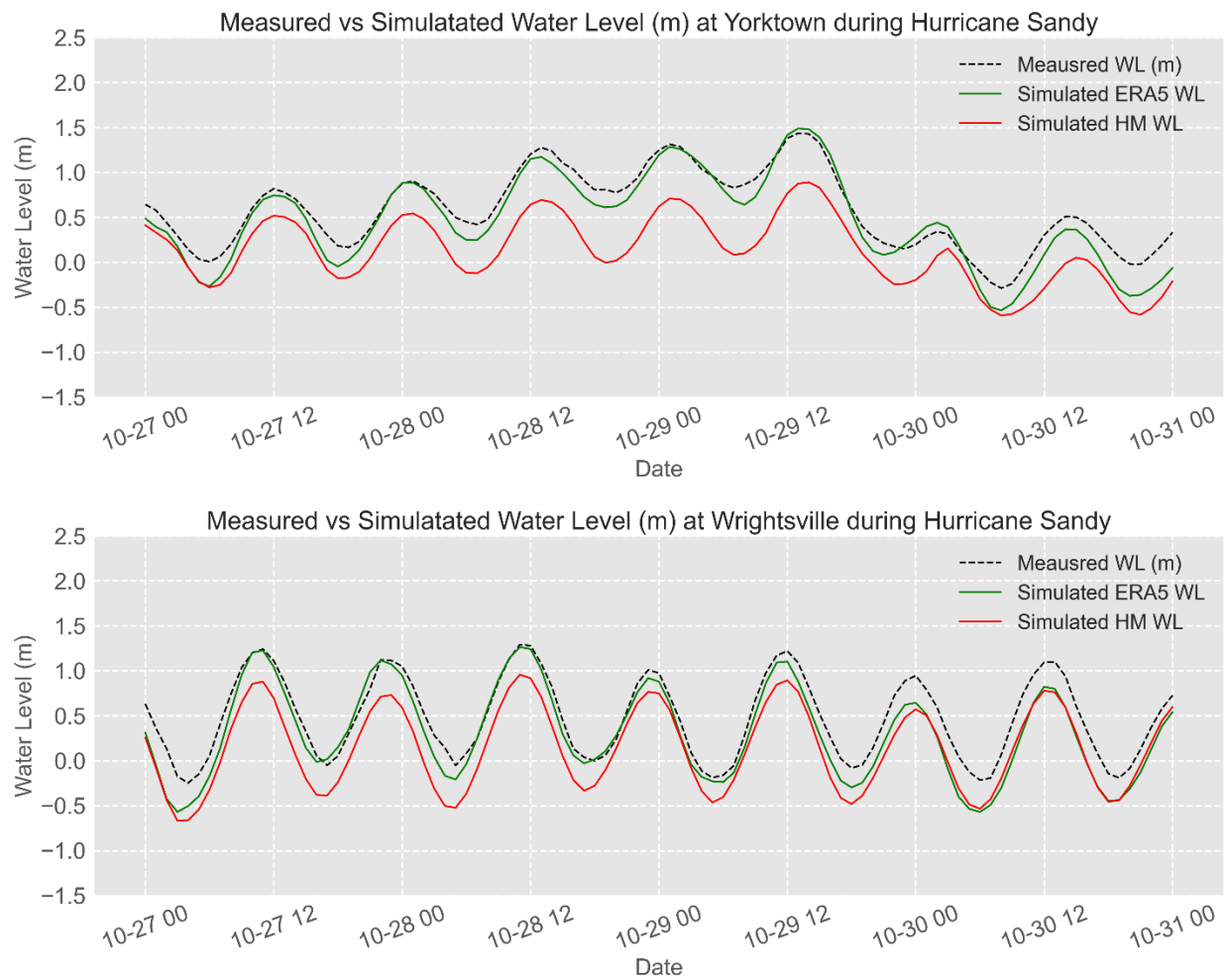
10.3. Hurricane Sandy (2012)

I. Time series plots of the measured and simulated water level in meters (ERA5 and HM)

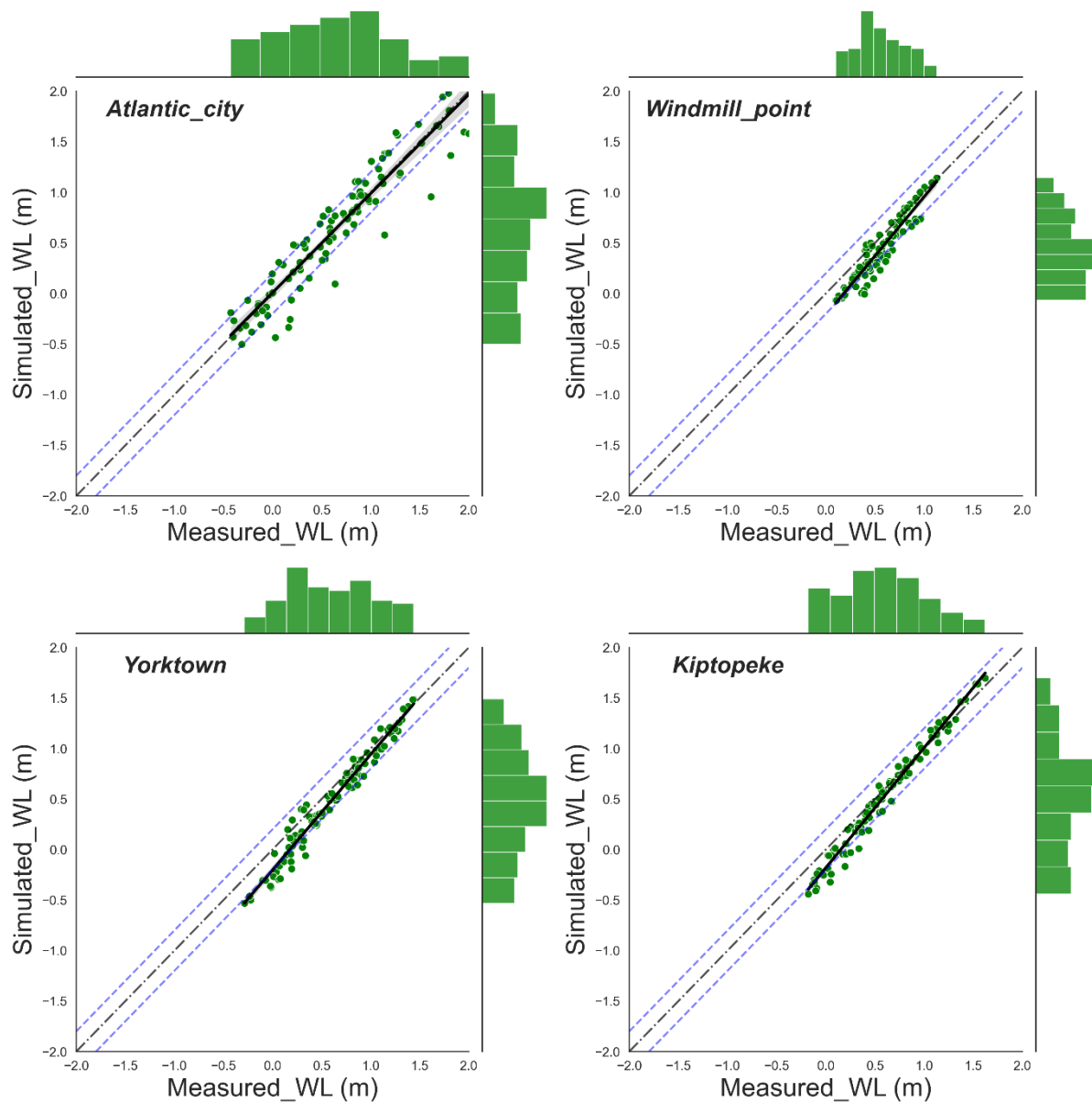


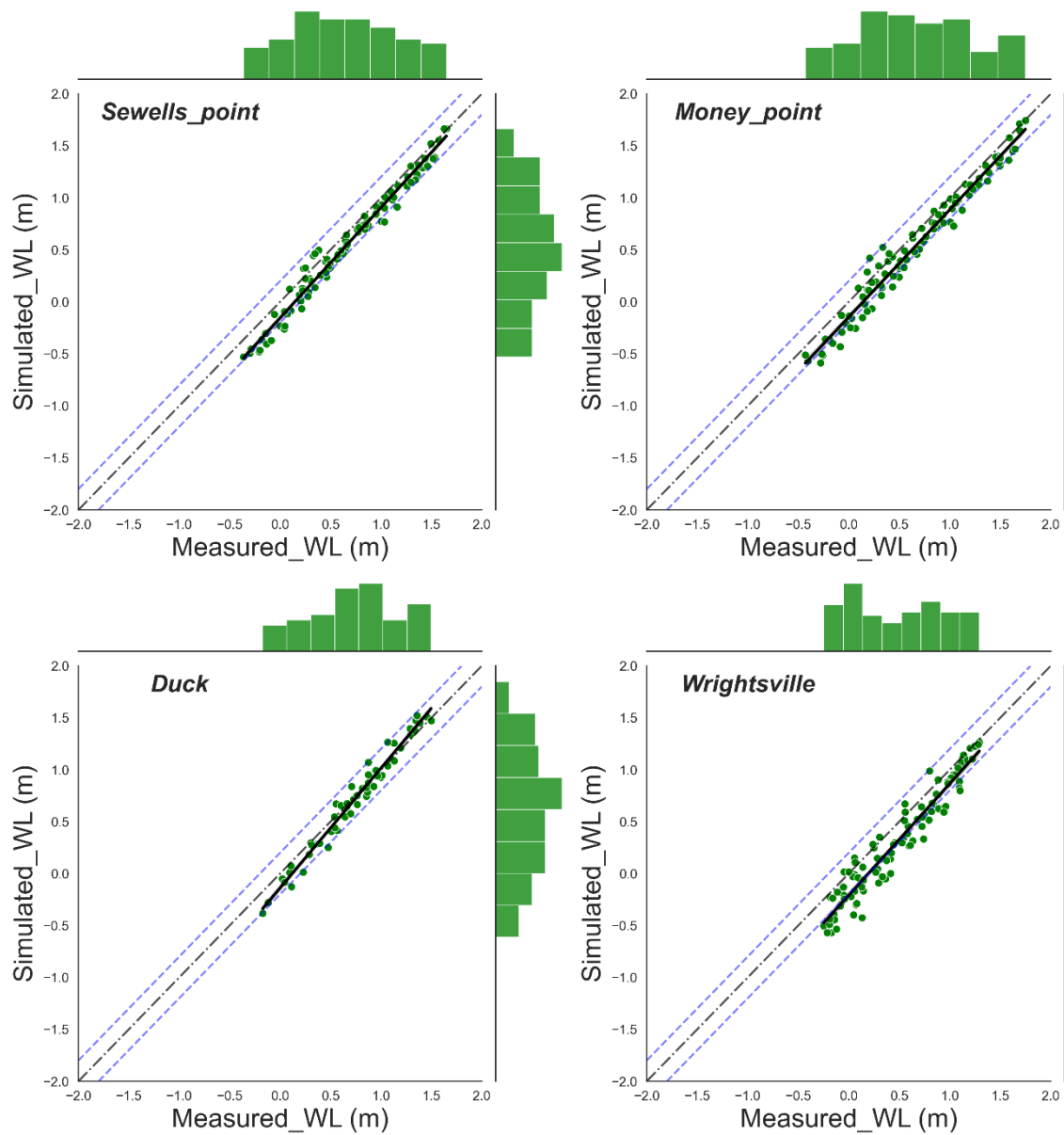


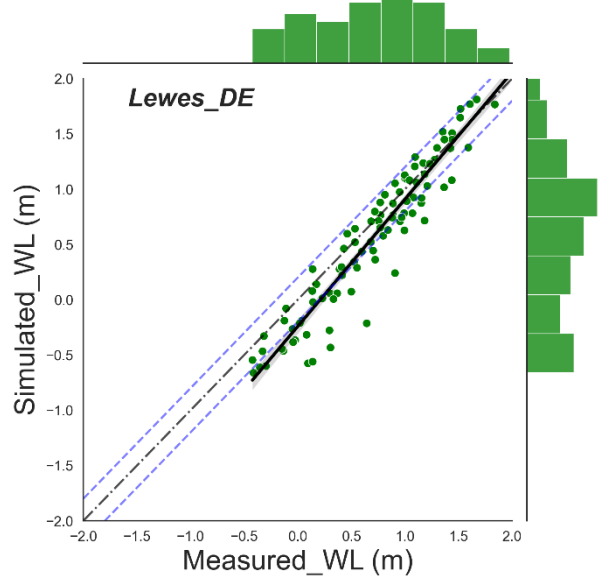




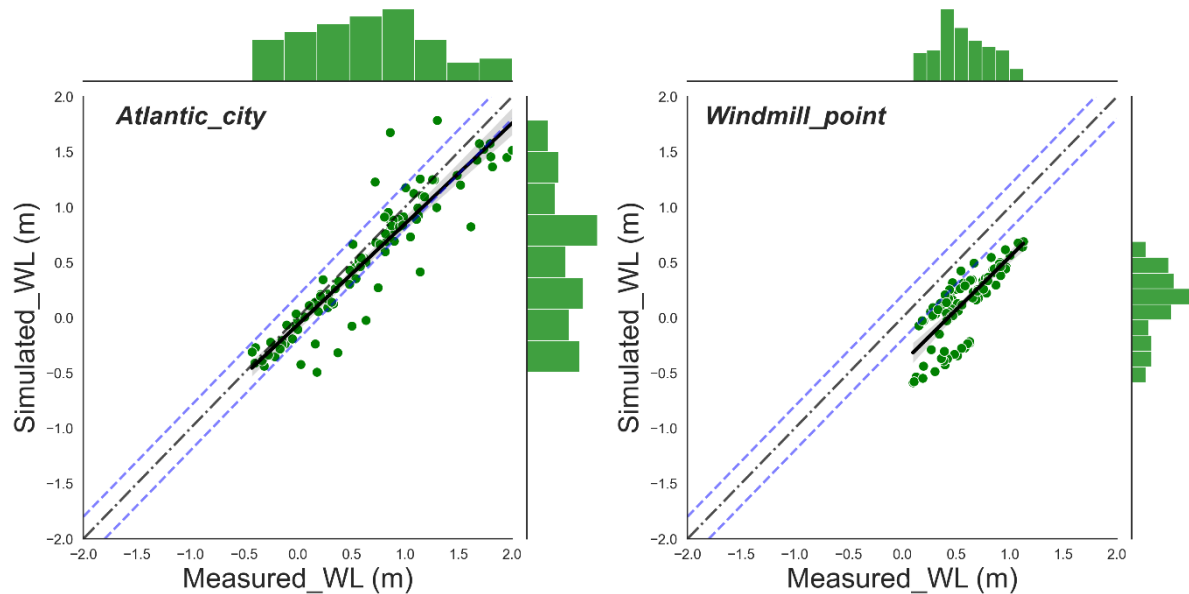
II. Scatter plots of the measured and simulated water level in meters using ERA5 wind forces

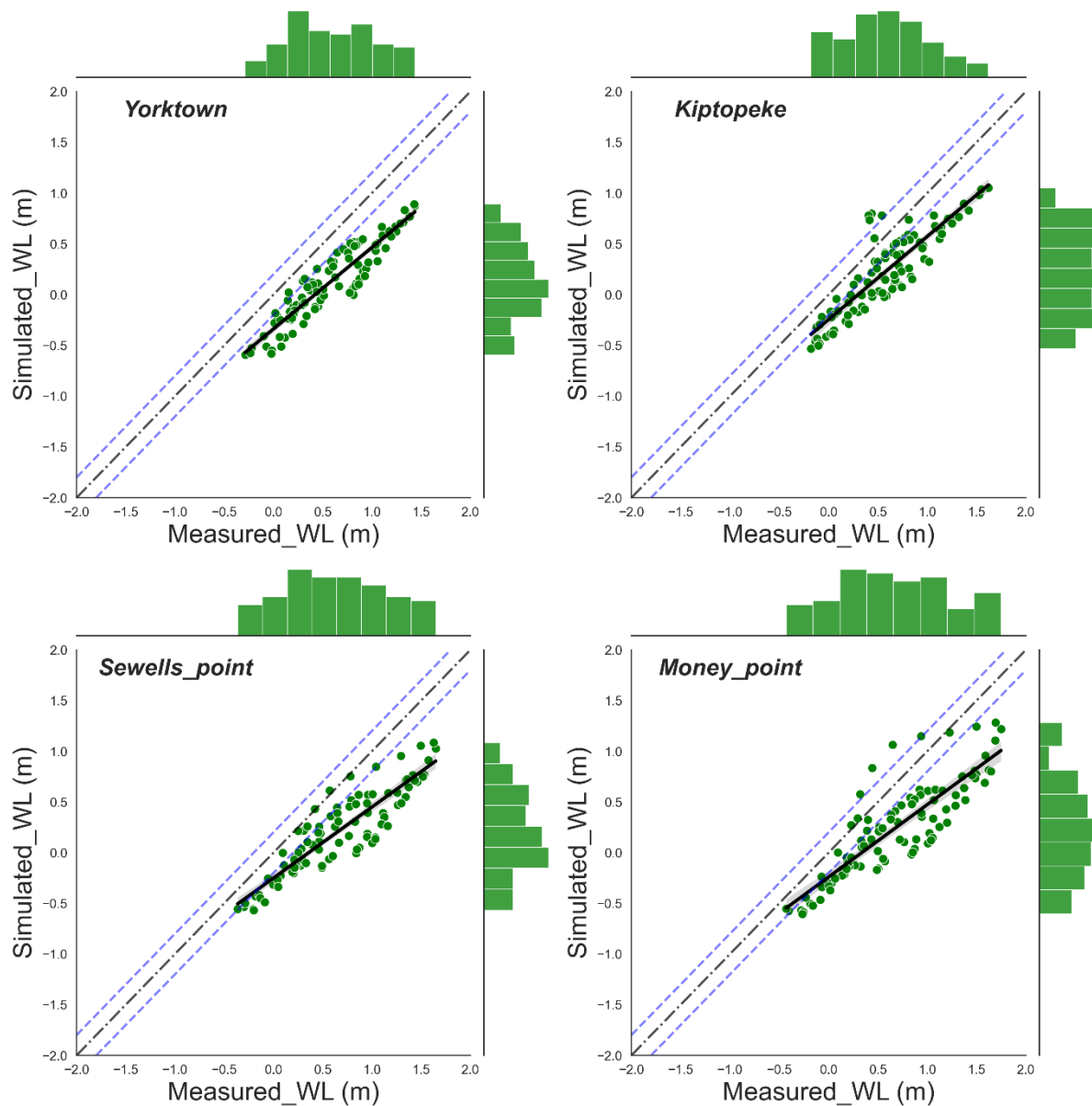


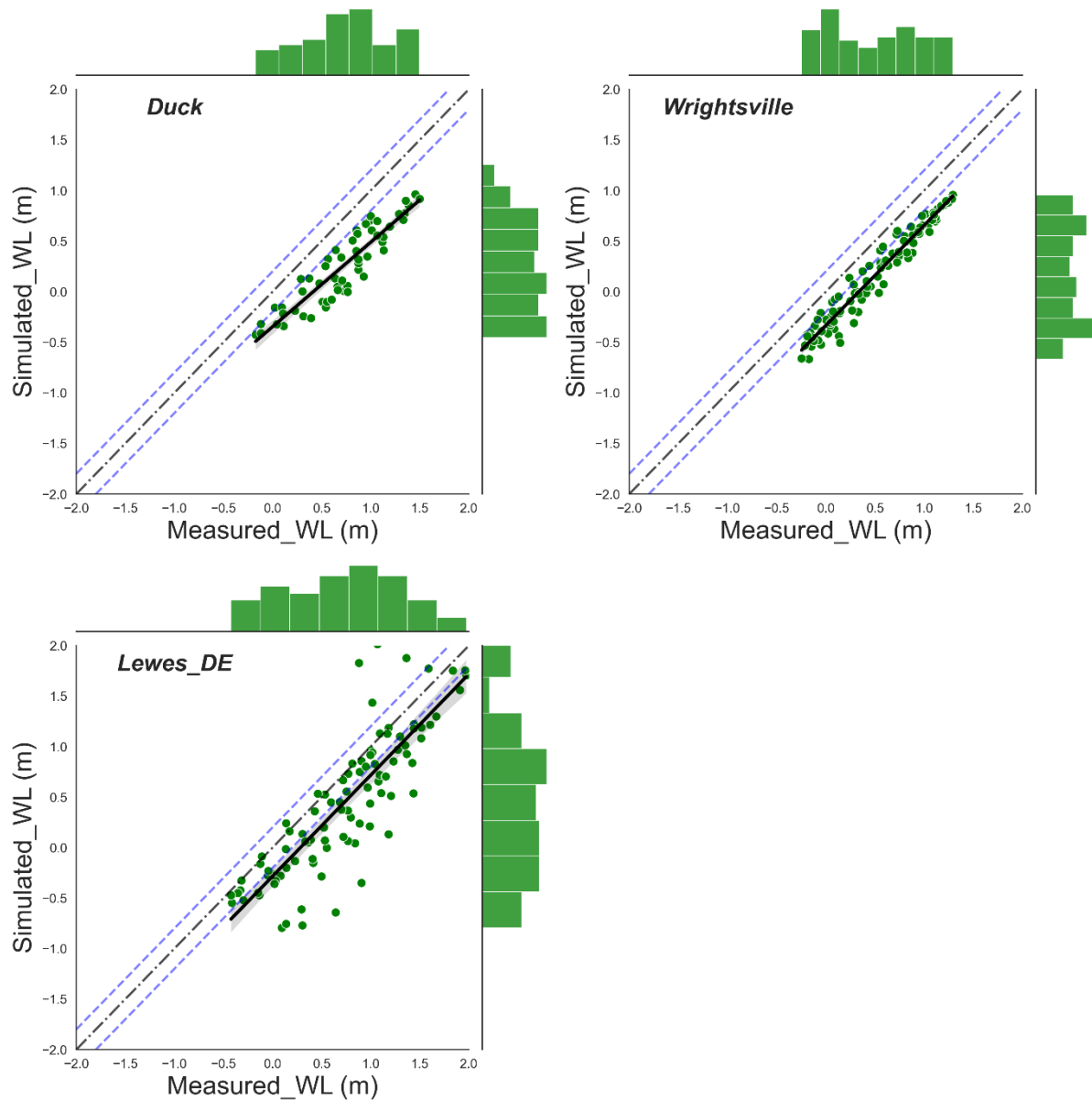




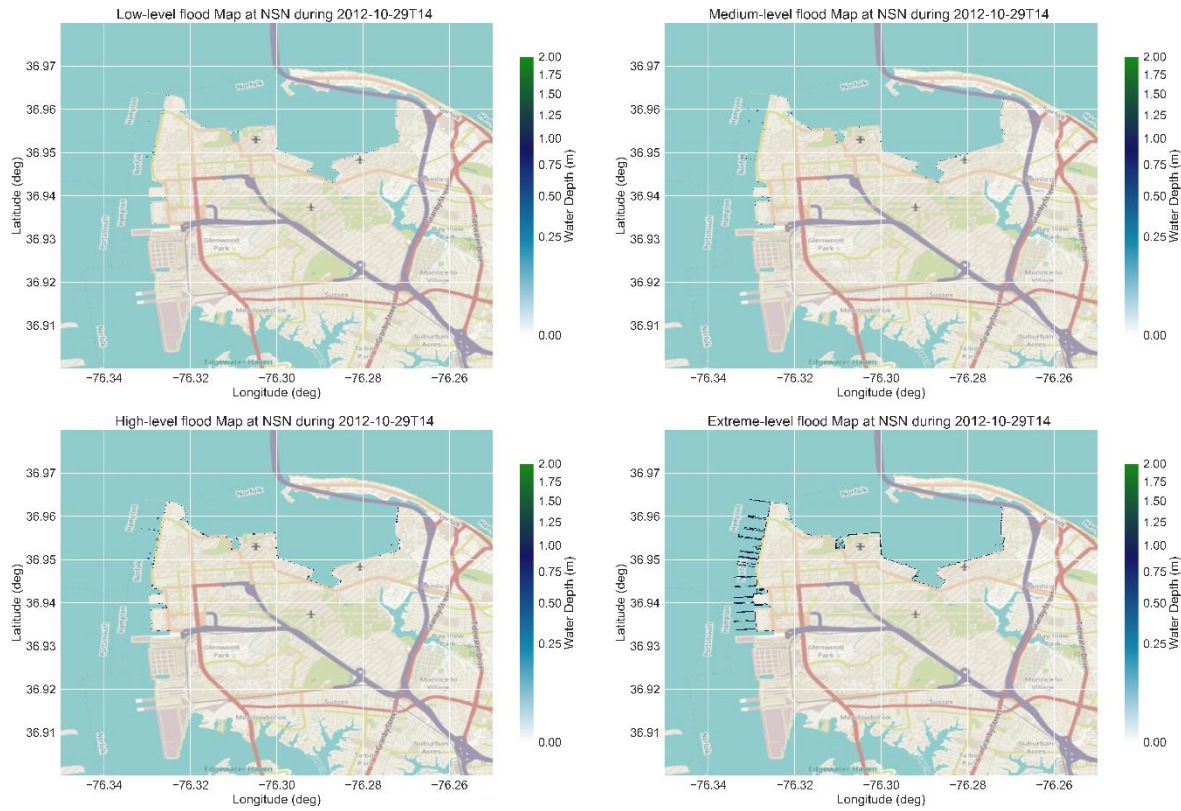
III. Scatter plots of the measured and simulated water level in meters using HM wind forces





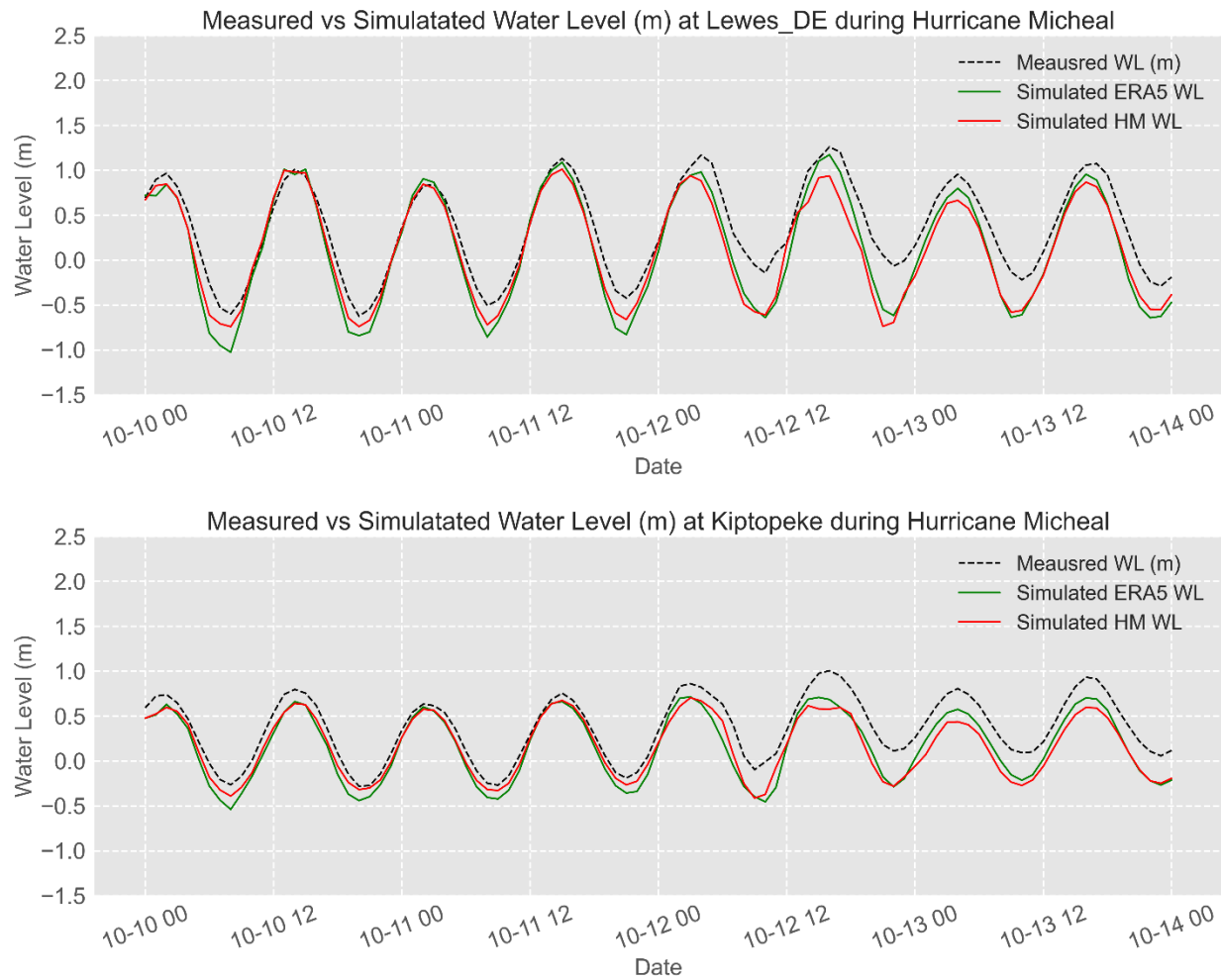


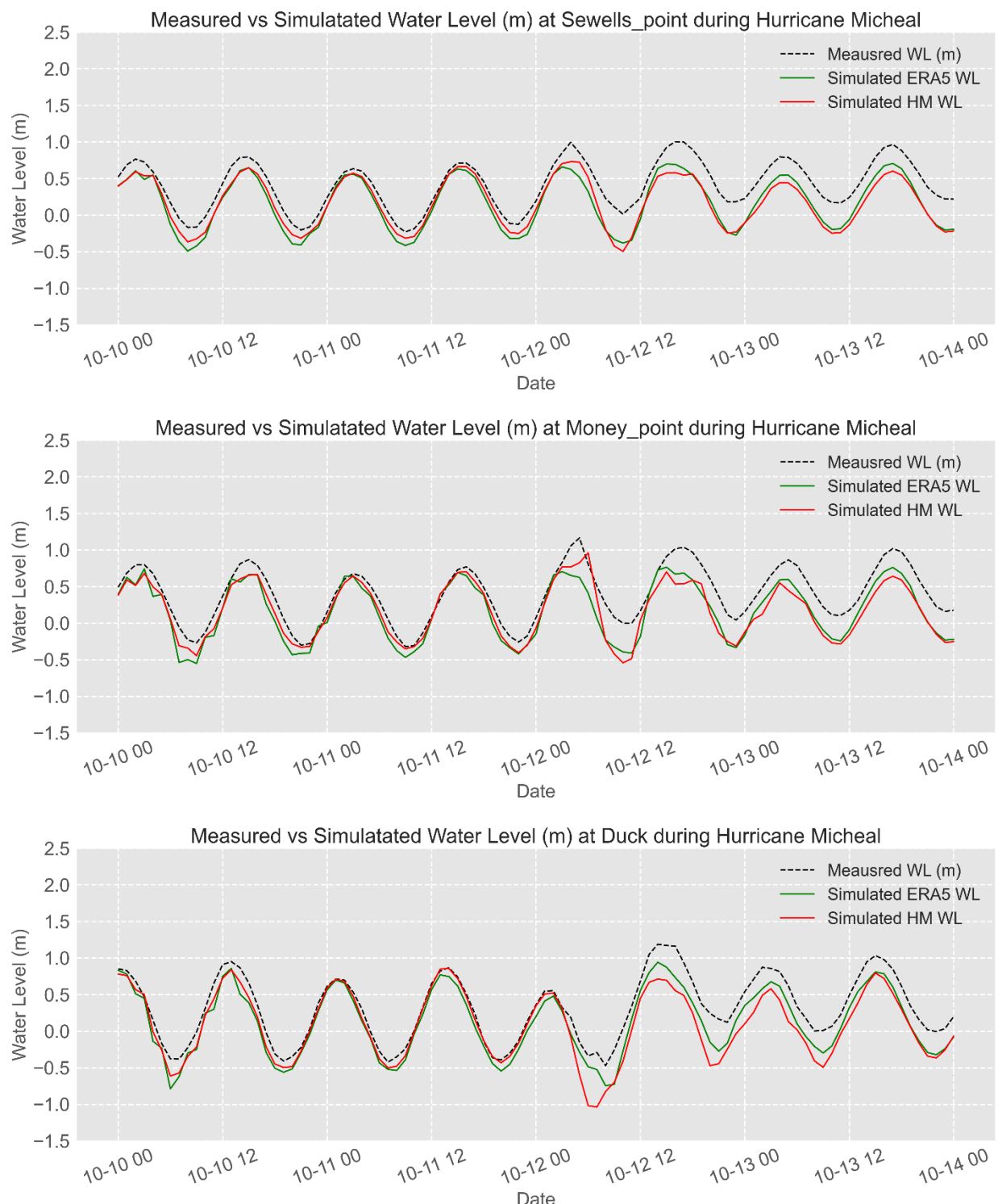
IV. Flood maps of each flood level using HM wind forces.

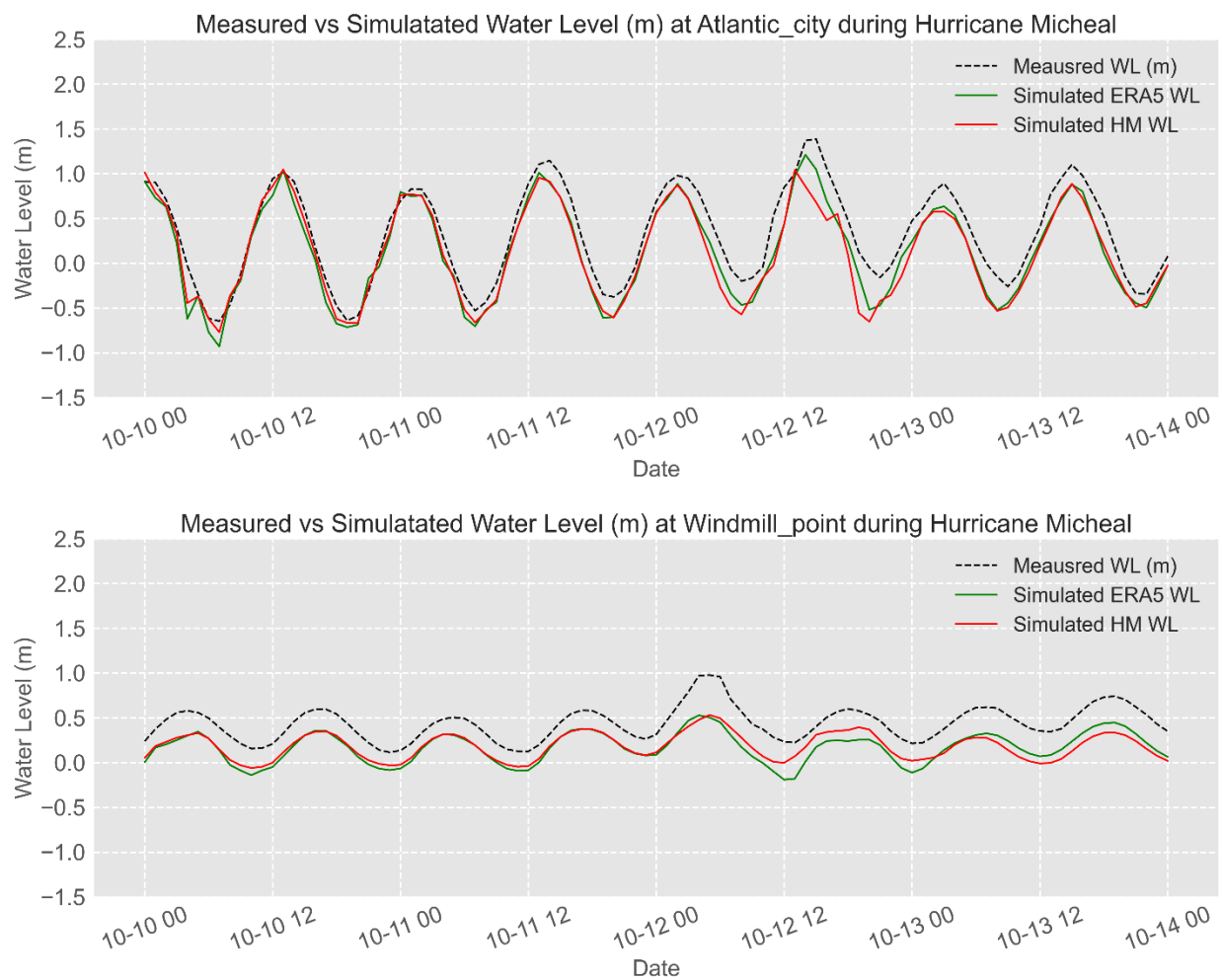


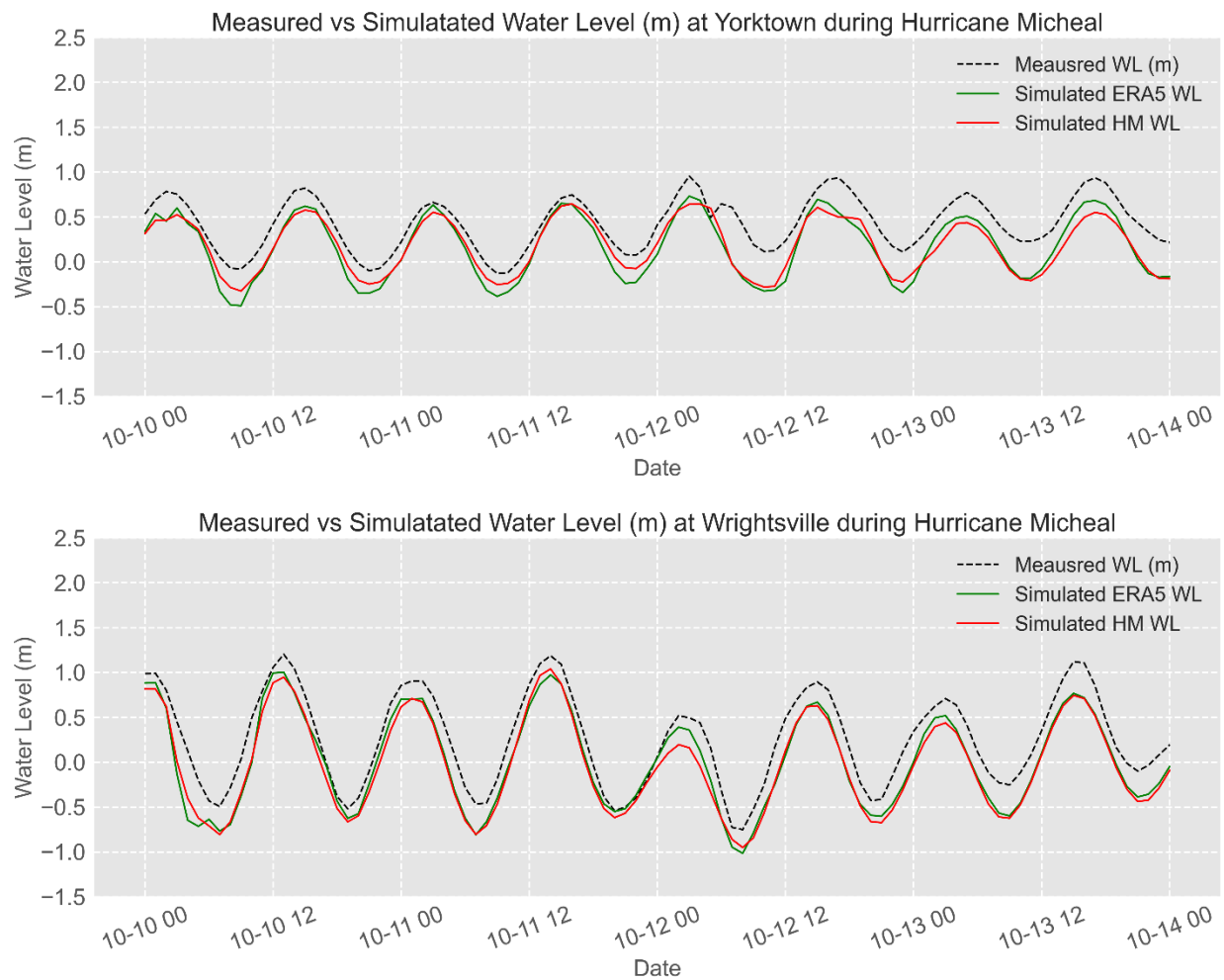
10.4. Hurricane Michael (2018)

I. Time series plots of the measured and simulated water level in meters (ERA5 and HM)

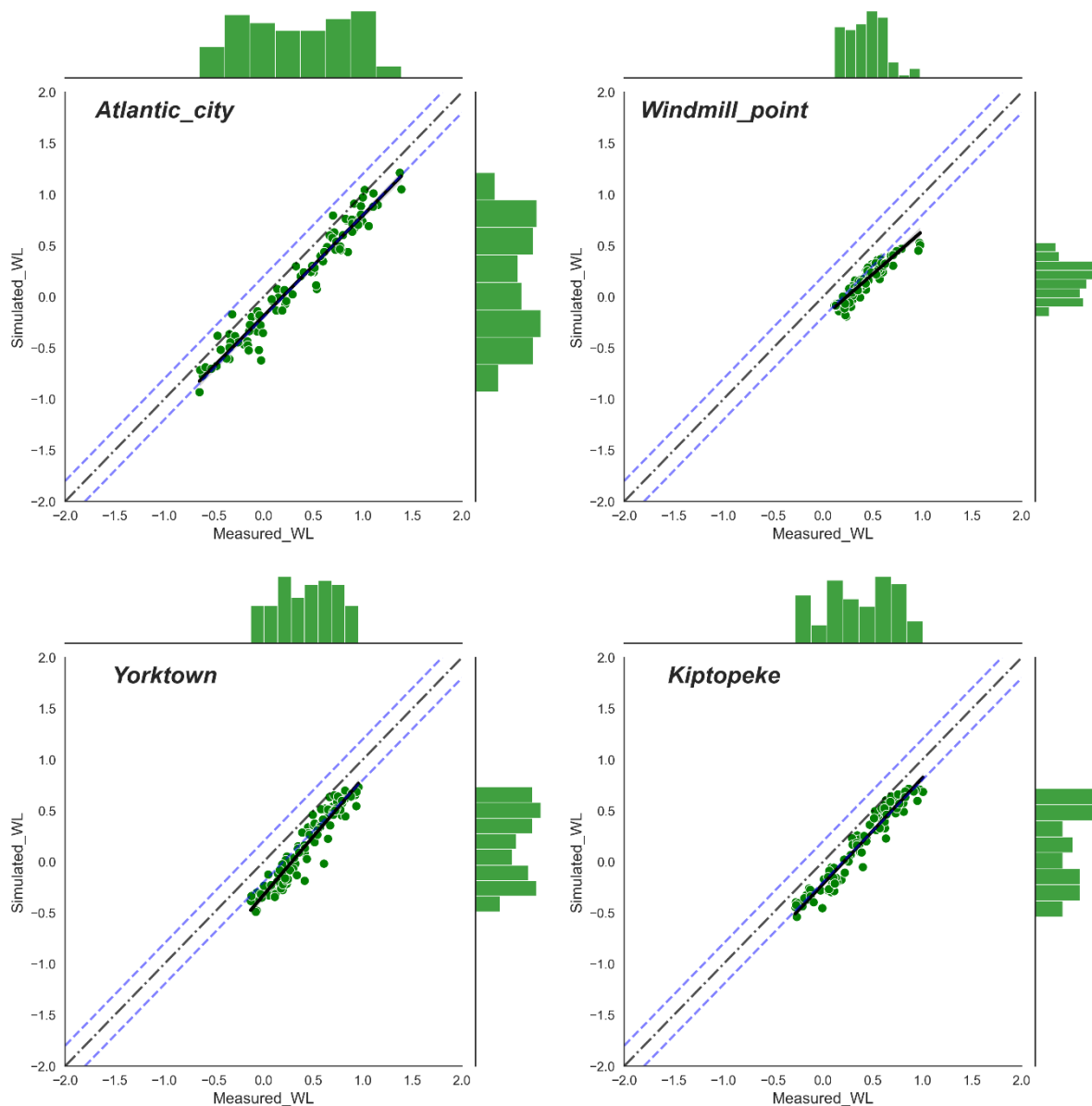


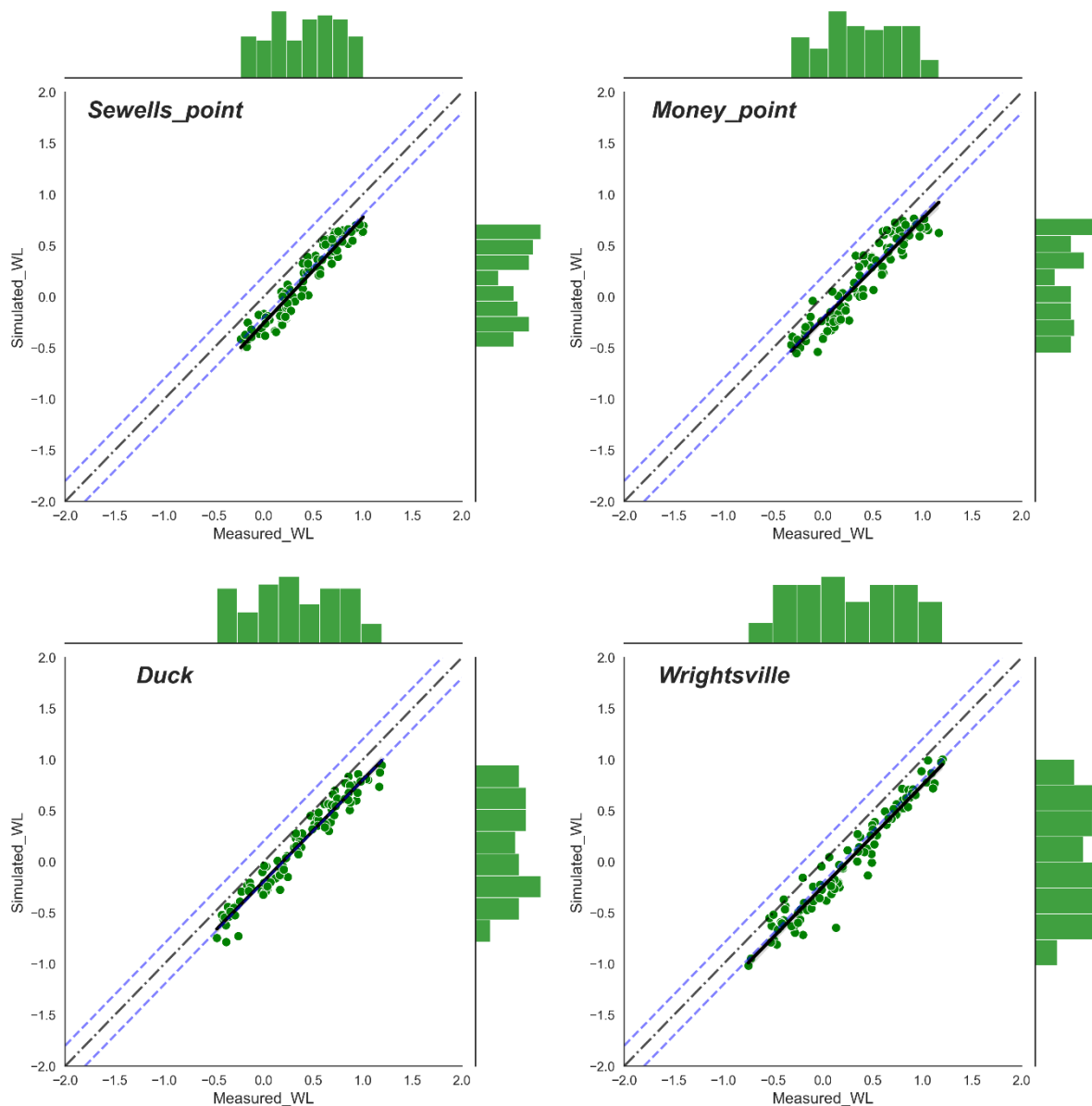


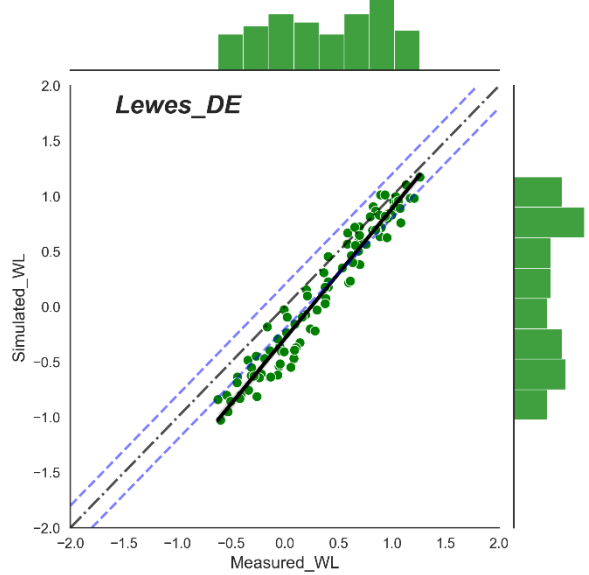




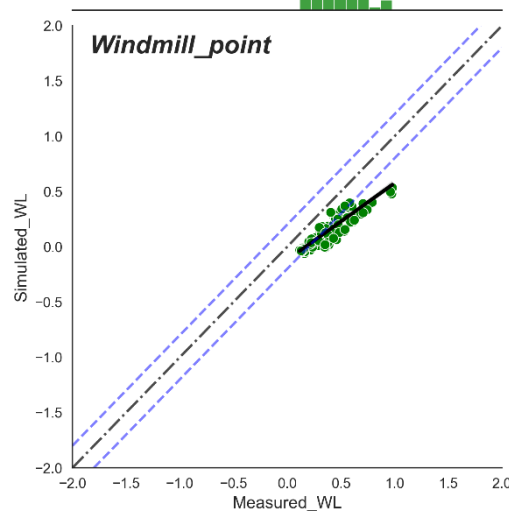
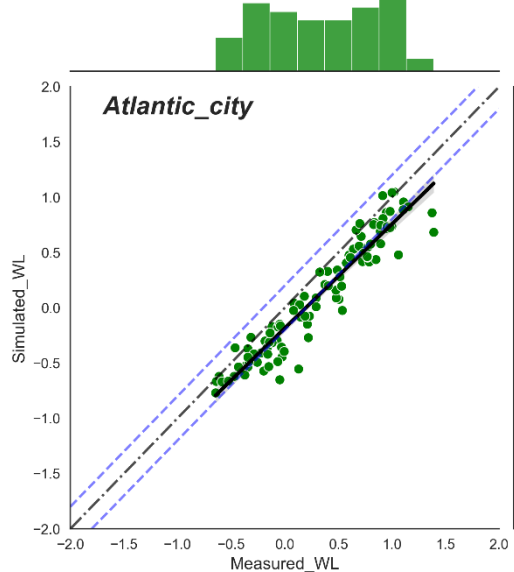
II. Scatter plots of the measured and simulated water level in meters using ERA5 wind forces

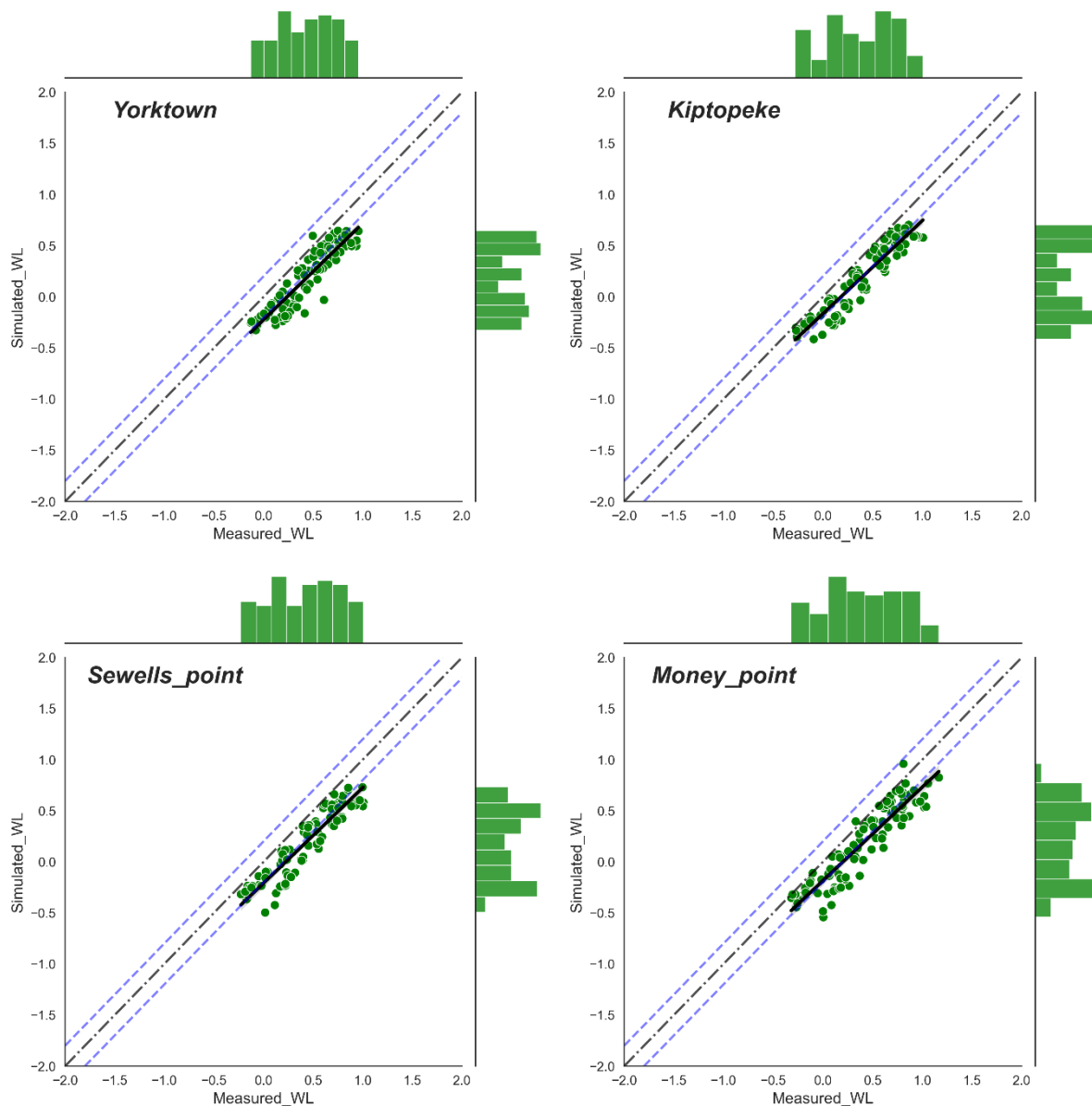


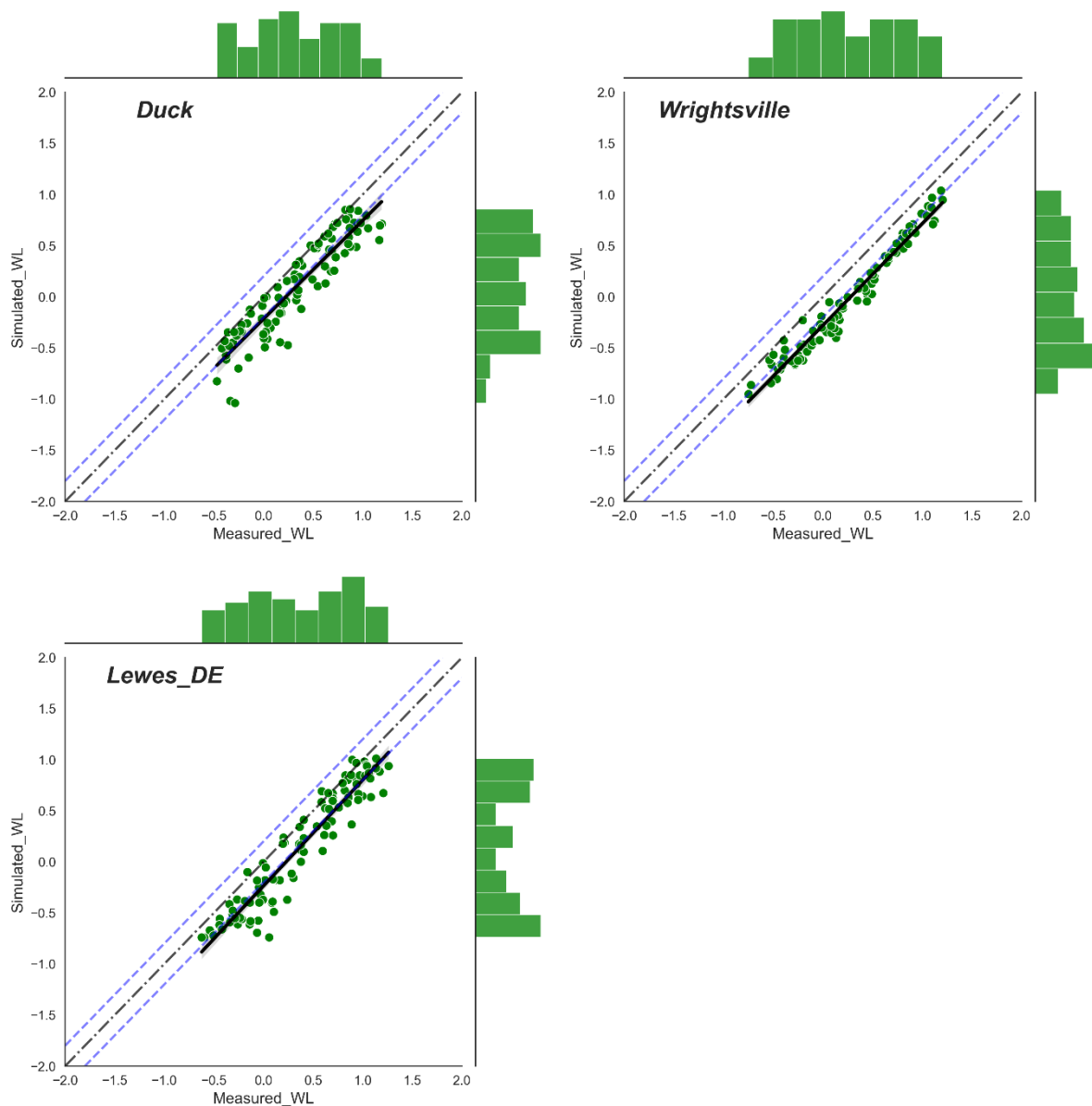




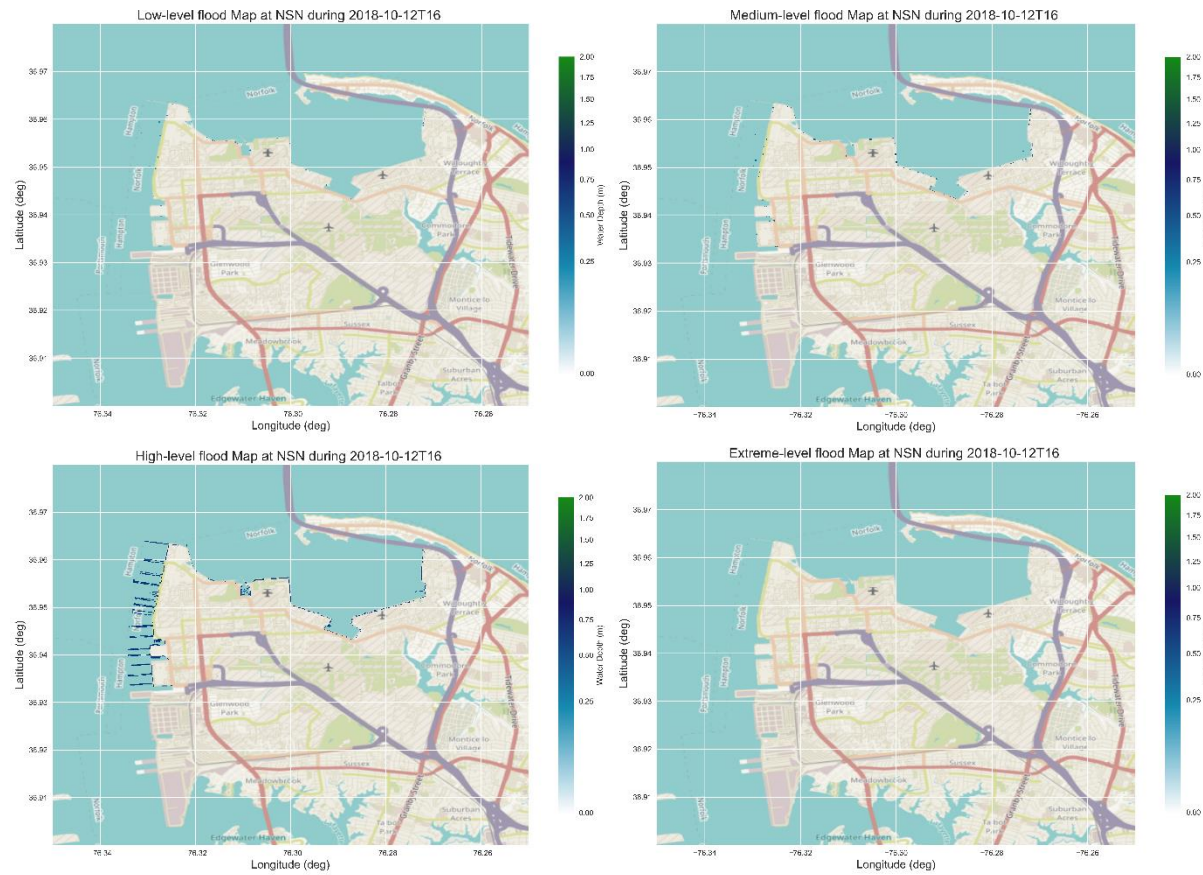
III. Scatter plots of the measured and simulated water level in meters using HM wind forces







IV. Flood maps of each flood level using HM wind forces.



11. Appendix B (Tables)

Table 73. Projected flood area statistics at the peak flood during Hurricane Irene-2011 for the base-HM scenario at NSN, the US

Flood_Level	Average_FD_(m)*	Max_FD_(m)**	Flooded_Area_(km)	Flood %
Low	0.18	0.25	0.02	0.11
Medium	0.36	0.50	0.02	0.18
High	0.73	1.00	0.05	0.33
Extreme	1.45	1.65	0.19	1.39
No Flood	0.00	0.00	13.50	97.97

* Average Flood depth in meters

**Maximum Flood depth in meters

Table 74. Projected flood area statistics at the peak flood during Hurricane Isabel-2003 for the base-HM scenario at NSN, the US

Flood_Level	Average_FD_(m)*	Max_FD_(m)**	Flooded_Area_(km)	Flood %
Low	0.17	0.25	0.01	0.07
Medium	0.37	0.49	0.01	0.10
High	0.77	1.00	0.03	0.23
Extreme	1.41	1.52	0.18	1.31
No Flood	0.00	0.00	13.54	98.26

Table 75. Projected flood area statistics at the peak flood during Hurricane Sandy-2012 for the base-HM scenario at NSN, the US

Flood_Level	Average_FD_(m)*	Max_FD_(m)**	Flooded_Area_(km)	Flood %
Low	0.18	0.25	0.01	0.09
Medium	0.37	0.50	0.02	0.12
High	0.76	1.00	0.03	0.21
Extreme	1.09	1.14	0.17	1.22
No Flood	0.00	0.00	13.55	98.33

Table 76. Projected flood area statistics at the peak flood during Hurricane Michael-2018 for the base-HM scenario at NSN, the US

Flood_Level	Average_FD_(m)*	Max_FD_(m)**	Flooded_Area_(km)	Flood %
Low	0.18	0.24	0.01	0.06
Medium	0.37	0.50	0.02	0.11
High	0.58	0.58	0.17	1.20
Extreme	0.00	0.00	0.00	0.00
No Flood	0.00	0.00	13.59	98.62

12. Appendix C (Model Results)

12.1. Impacts of Meteorological Forcing

12.1.1. Pressure Drop

a. PD_F0.64 Scenario

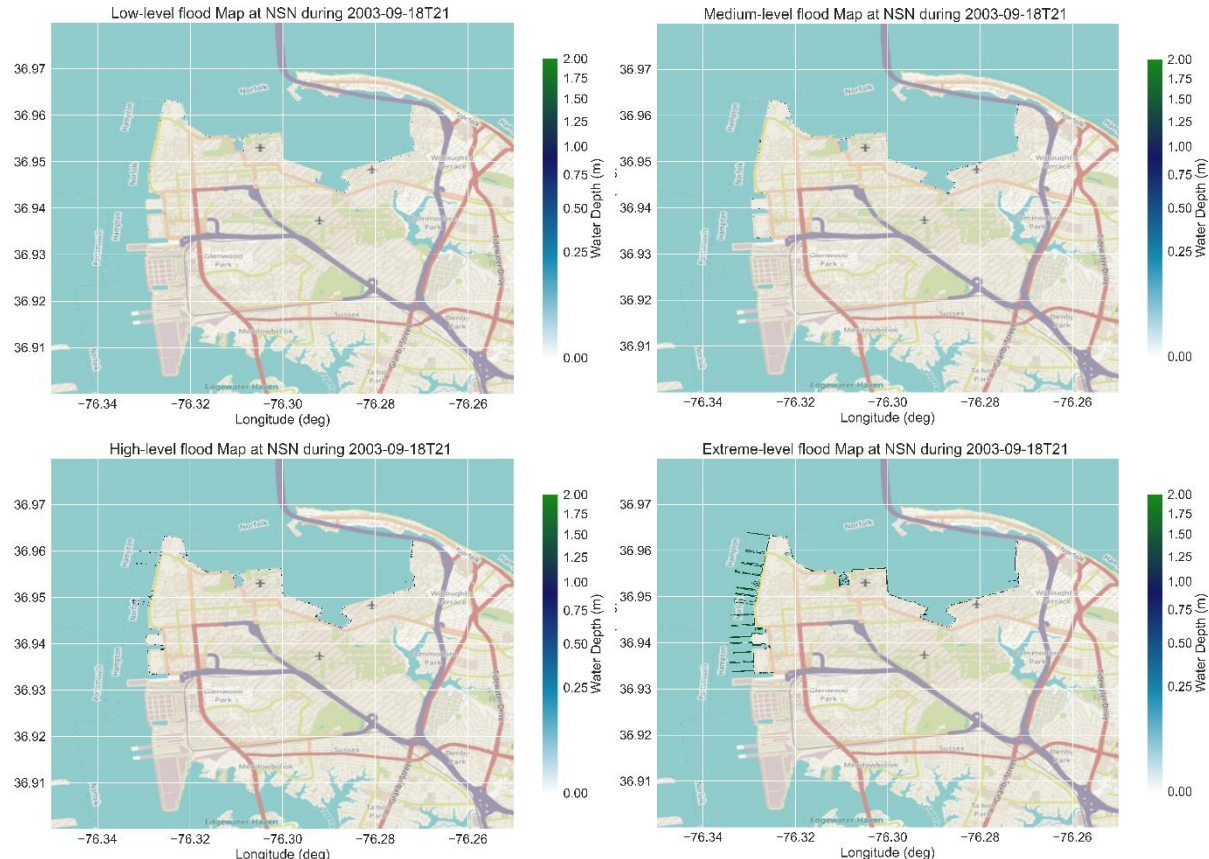


Figure 225. Flood area classification (Low, Medium, High, and Extreme) in meters of the PD_F0.64 scenarios during hurricane Isabel-2003 at NSN base, the US.

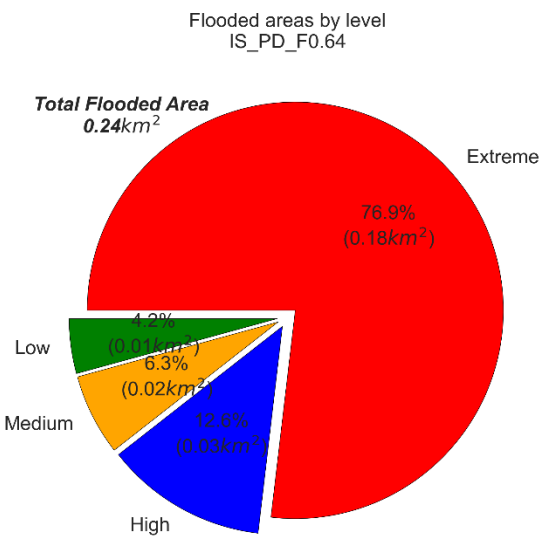


Figure 226. Pie chart of the flood areas, with percentages, of the different flood levels for PD_F0.64 scenario for Hurricane Isabel-2003 at NSN, the US.

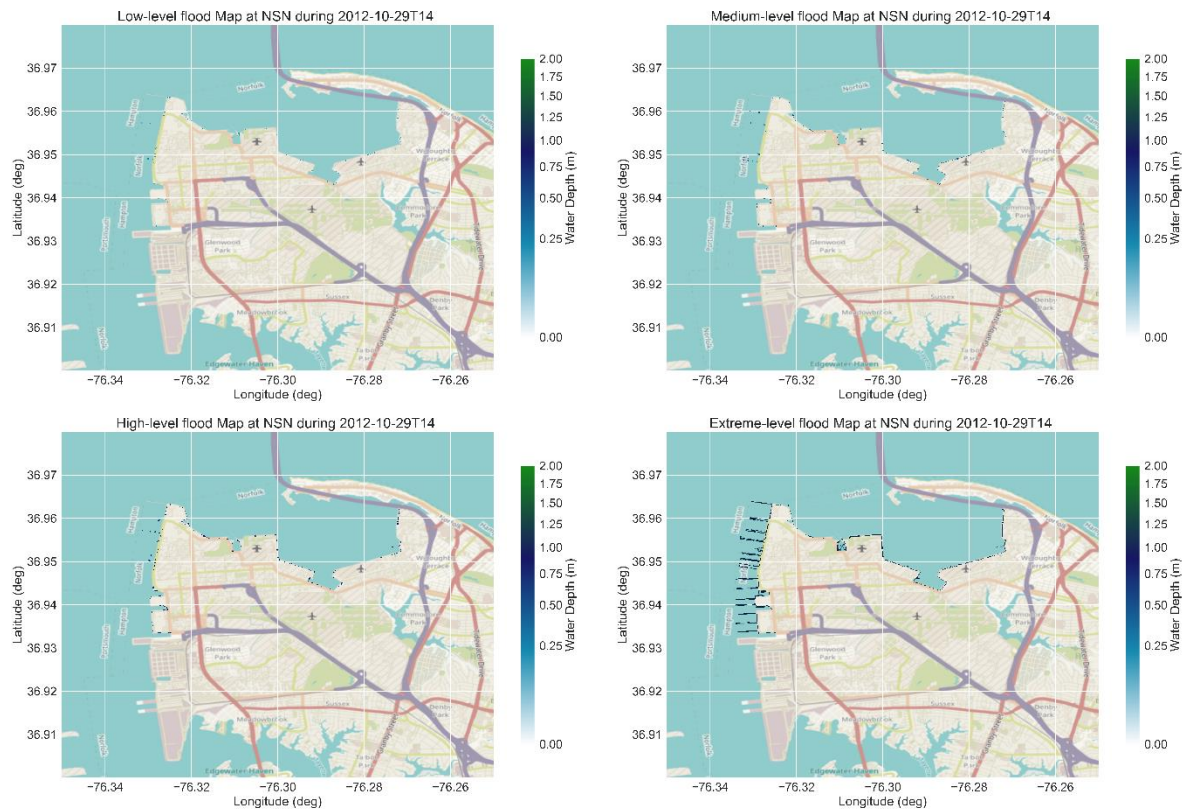


Figure 227. Flood area classification (Low, Medium, High, and Extreme) in meters of the PD_F0.64 scenarios during hurricane Sandy-2012 at NSN base, the US.

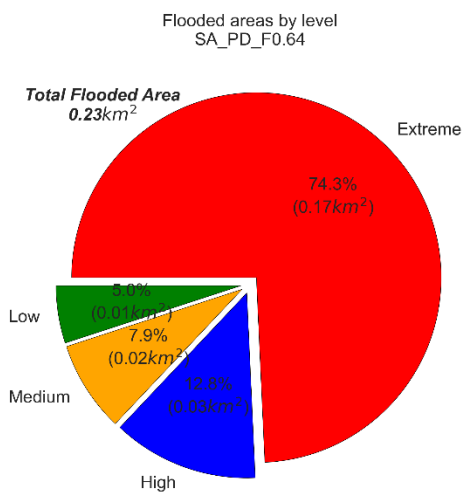


Figure 228. Pie chart of the flood areas, with percentages, of the different flood levels for PD_F0.64 scenario for Hurricane Sandy-2012 at NSN, the US.

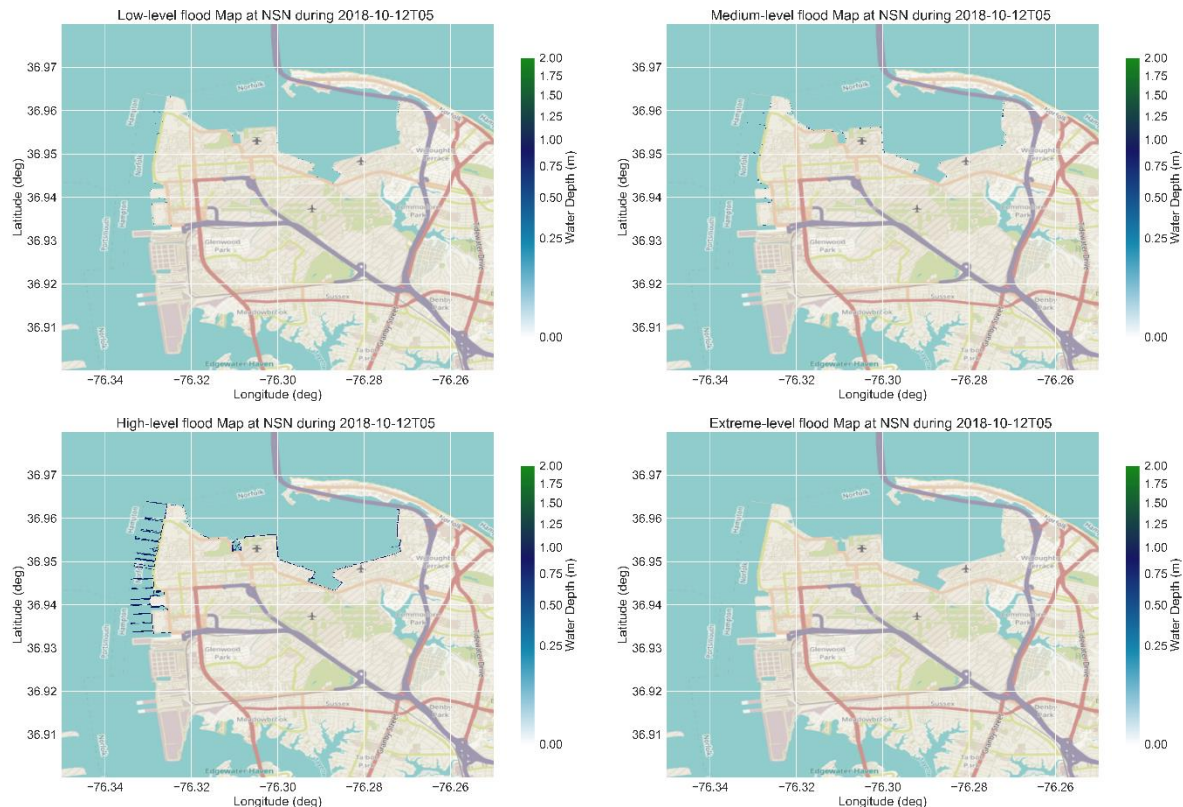


Figure 229. Flood area classification (Low, Medium, High, and Extreme) in meters of the PD_F0.64 scenario during hurricane Michael-2018 at NSN base, the US.

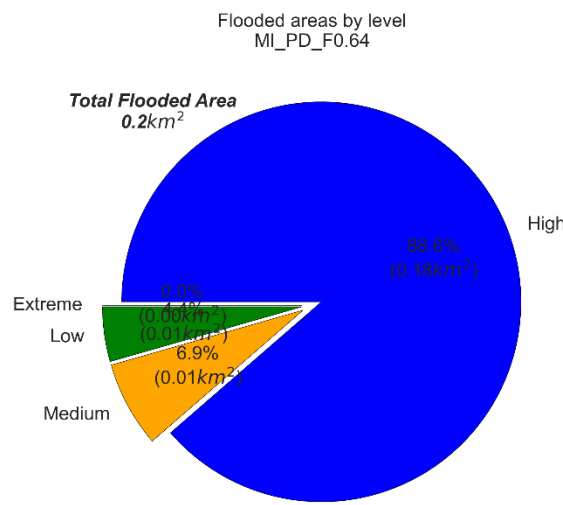


Figure 230. Pie chart of the flood areas, with percentages, of the different flood levels for PD_F0.64 scenario for Hurricane Michael-2018 at NSN, the US.

b. PD.76 Scenario

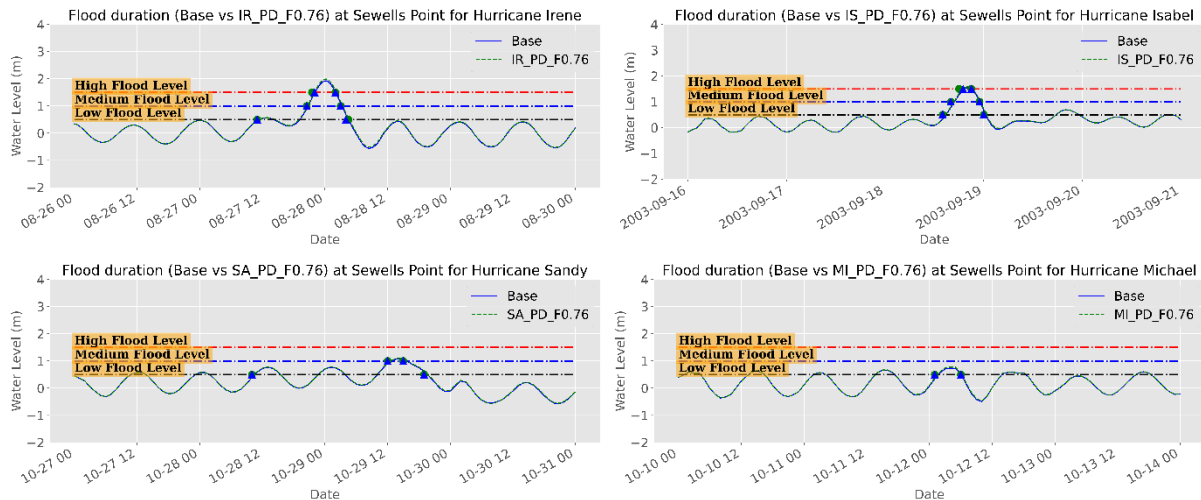


Figure 231. Water level time series (m) during the different hurricanes showing the surge magnitude and duration for different surge levels for the base and PD_F0.76 scenarios at Sewells Point, NSN, the US.

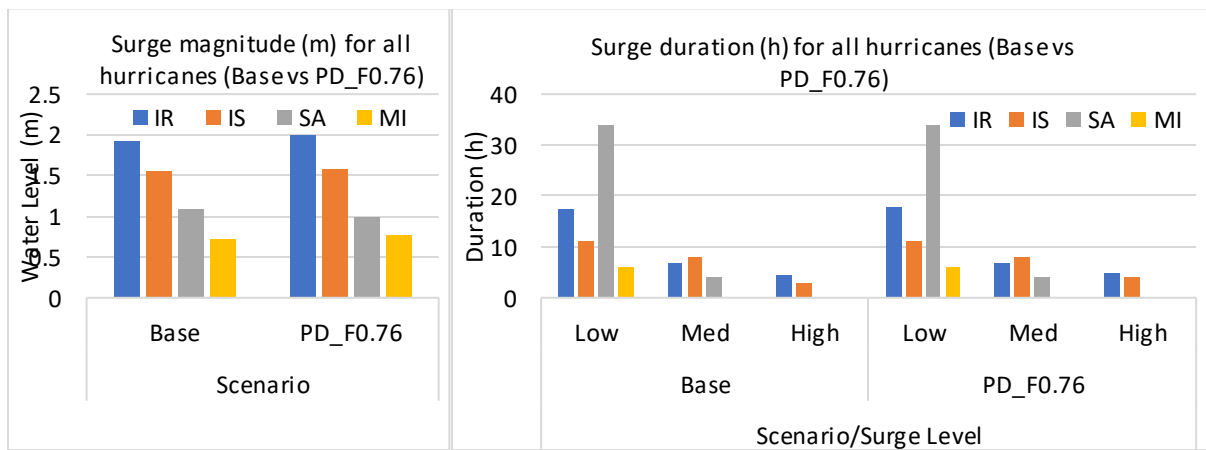


Figure 232. Peak surge (m) (left panel) and surge duration (h) of the different surge levels (right panel) for the base and PD_F0.76 scenario for all hurricanes, NSN, the US.

Table 77. Peak surge characteristics (Maximum and Duration) the base and the PD_0.76 scenarios for all Hurricanes at Sewells Point, NSN, the US.

Group	Hurricane ID	Max. Surge (m)		Duration (h)					
		Base	PD_F0.76	Base			PD_F0.76		
				Low	Med	High	Low	Med	High
Meteo. Forcing	IR	1.92	1.99	17.5	7	4.5	18	7	5
	IS	1.55	1.59	11	8	3	11	8	4
	SA	1.08	1	34	4	0	34	4	0
	MI	0.73	0.77	6	0	0	6	0	0

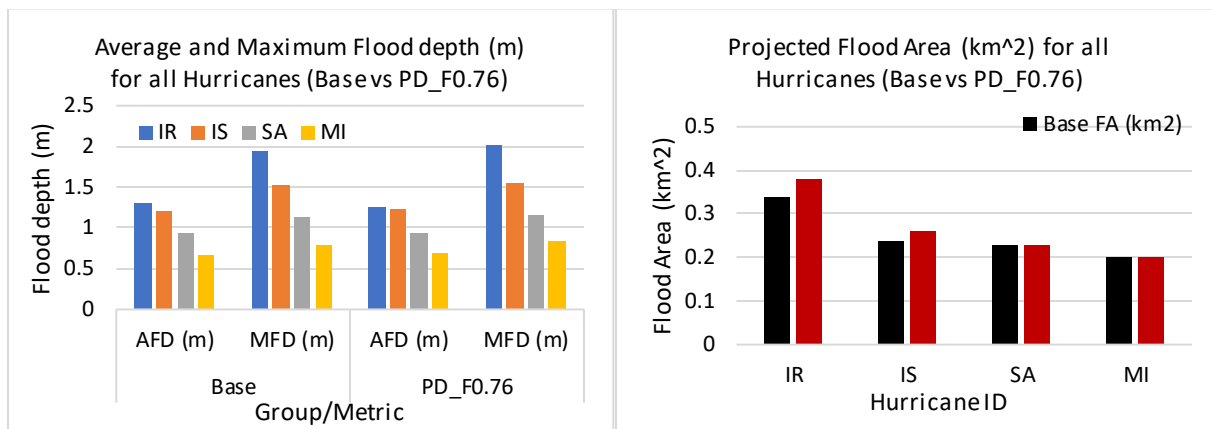


Figure 233. Average Flood Depth (AFD) & Maximum Flood Depth (MFD) in meters (left panel) and Flood area (km^2) (right panel) of all hurricanes for the Base and PD_F0.64 scenarios, NSN, the US.

Table 78. Flood area characteristics of the base and the PD_F0.76 for all hurricanes at NSN, the US.

Group	Hurricane ID	Base				PD_F0.76			
		Average FD (m)	Max FD (m)	Flood area (km^2)	%	Average FD (m)	Max FD (m)	Flood area (km^2)	%
Meteo. Forcing	IR	1.31	1.94	0.34	2.47	1.26	2.01	0.38	2.8
	IS	1.21	1.52	0.24	1.72	1.23	1.55	0.26	1.9
	SA	0.94	1.14	0.23	1.6	0.95	1.15	0.23	1.7
	MI	0.66	0.79	0.2	1.45	0.7	0.83	0.2	1.5

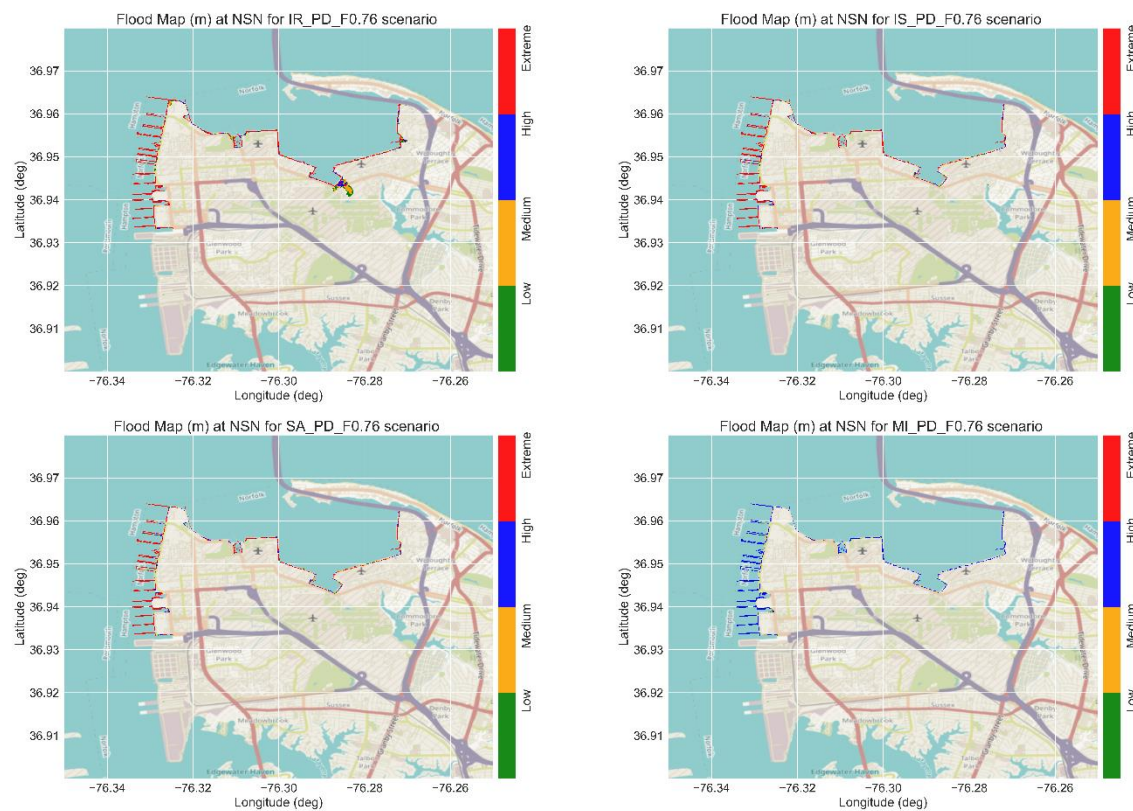


Figure 234. Flood maps with the flood levels for the different hurricanes during the peak surge for the PD_F0.76 scenario at NSN, the US.

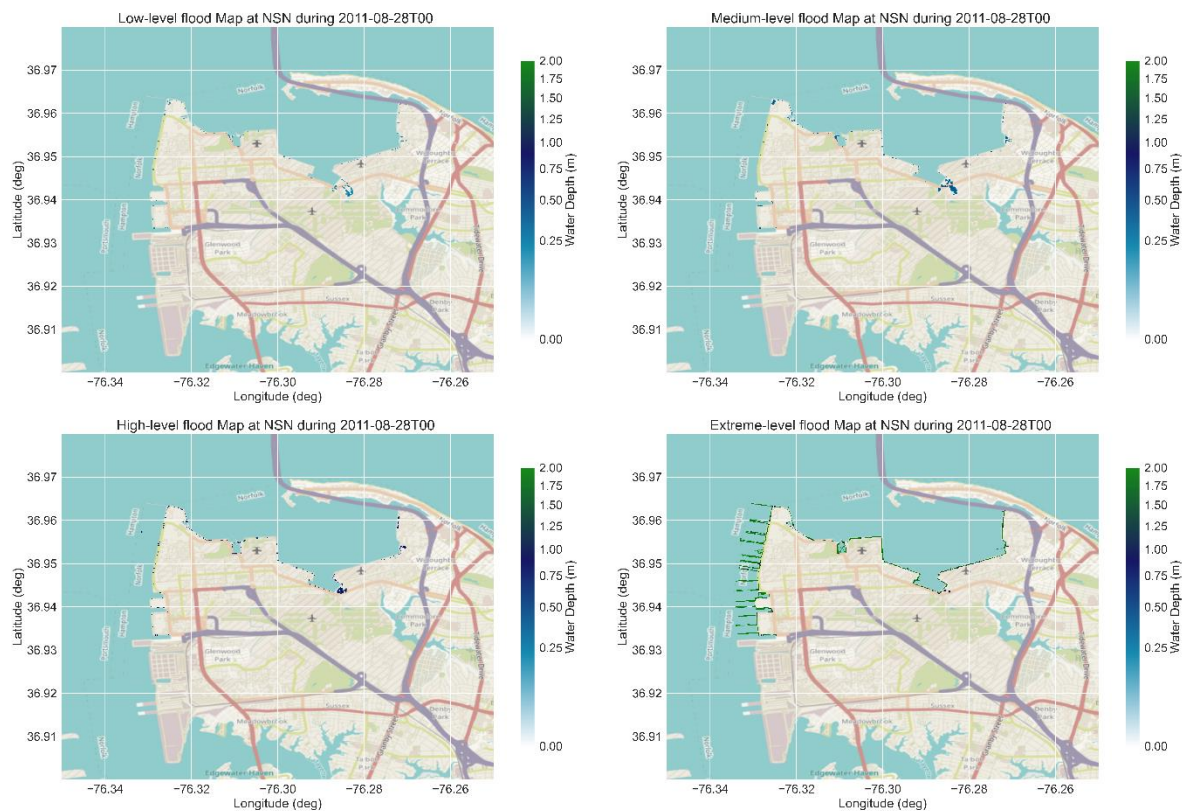


Figure 235. Flood area classification (Low, Medium, High, and Extreme) in meters of the PD_F0.76 scenarios during hurricane Irene-2011 at NSN base, the US.

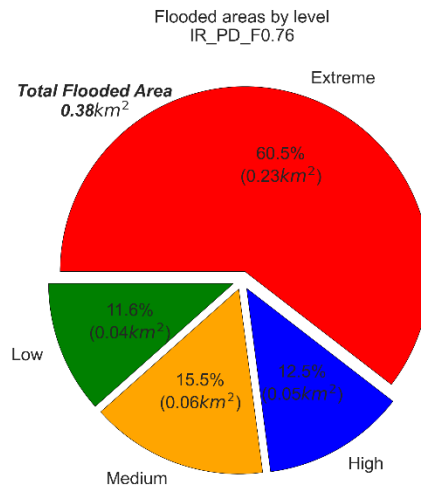


Figure 236. Pie chart of the flood areas, with percentages, of the different flood levels for PD_F0.76 scenario for Hurricane Irene-2011 at NSN, the US.

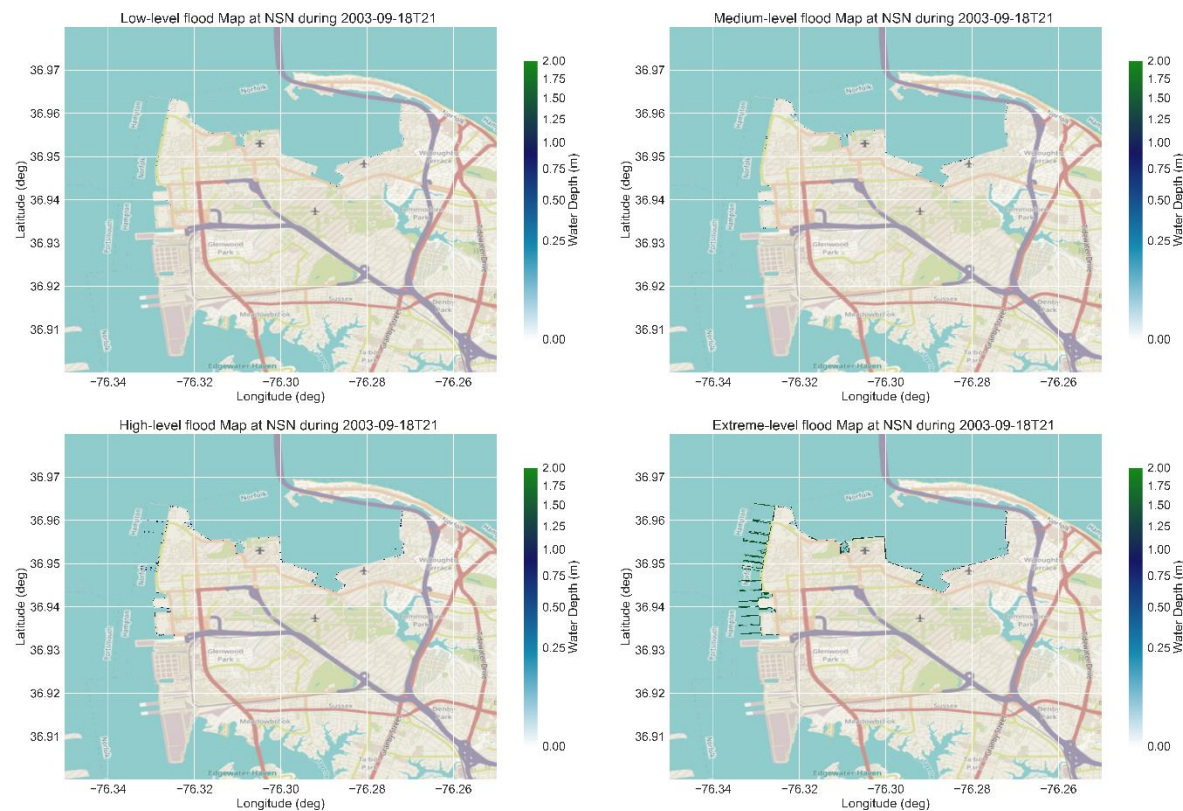


Figure 237. Flood area classification (Low, Medium, High, and Extreme) in meters of the PD_F0.76 scenarios during hurricane Isabel-2003 at NSN base, the US.

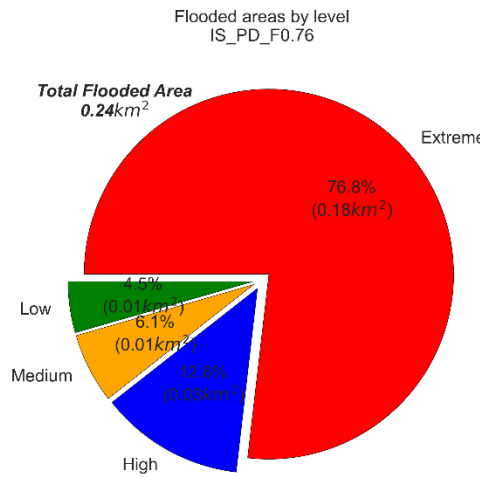


Figure 238. Pie chart of the flood areas, with percentages, of the different flood levels for PD_F0.76 scenario for Hurricane Isabel-2003 at NSN, the US.

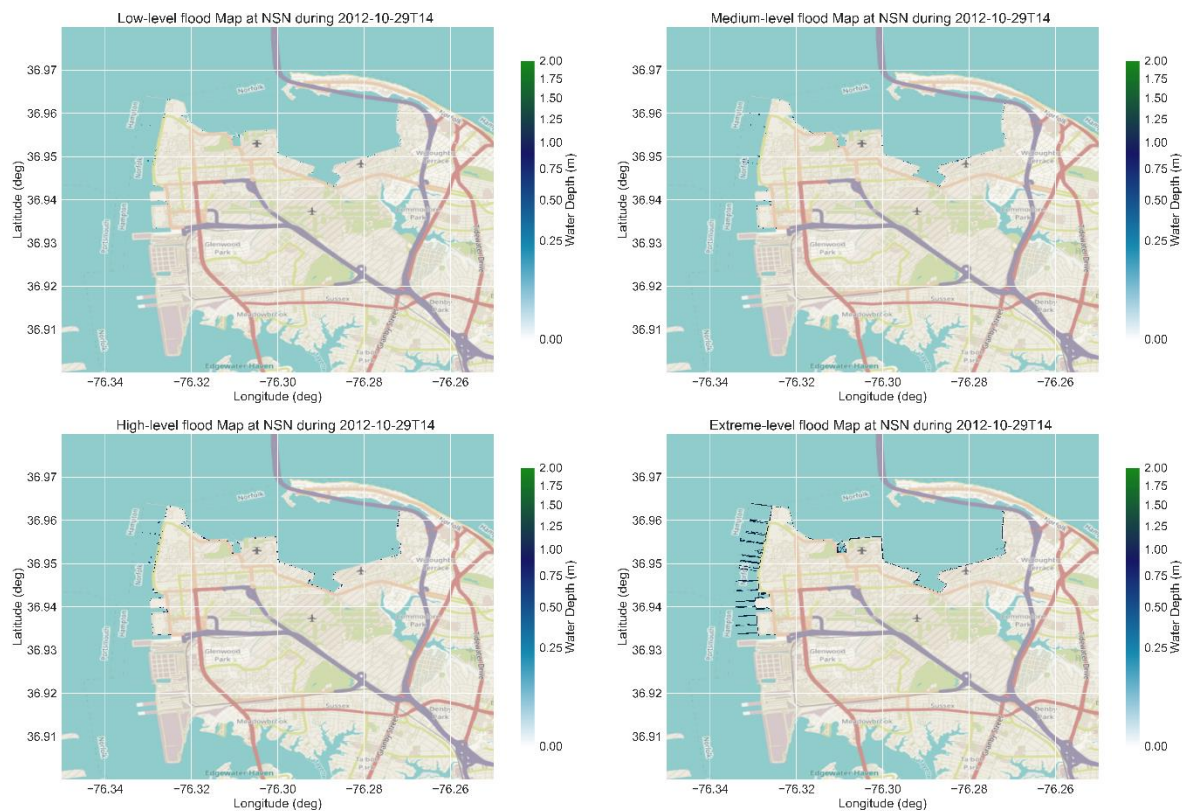


Figure 239. Flood area classification (Low, Medium, High, and Extreme) in meters of the PD_F0.76 scenarios during hurricane Sandy-2012 at NSN base, the US.

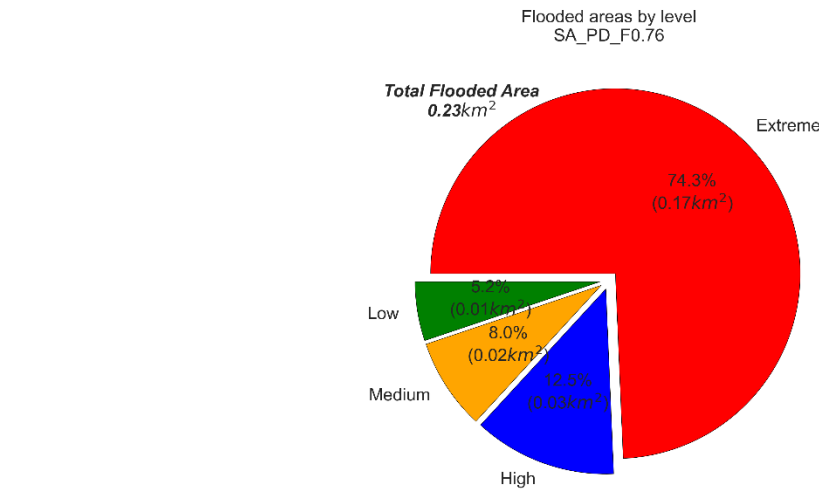


Figure 240. Pie chart of the flood areas, with percentages, of the different flood levels for PD_F0.76 scenario for Hurricane Sandy-2012 at NSN, the US.

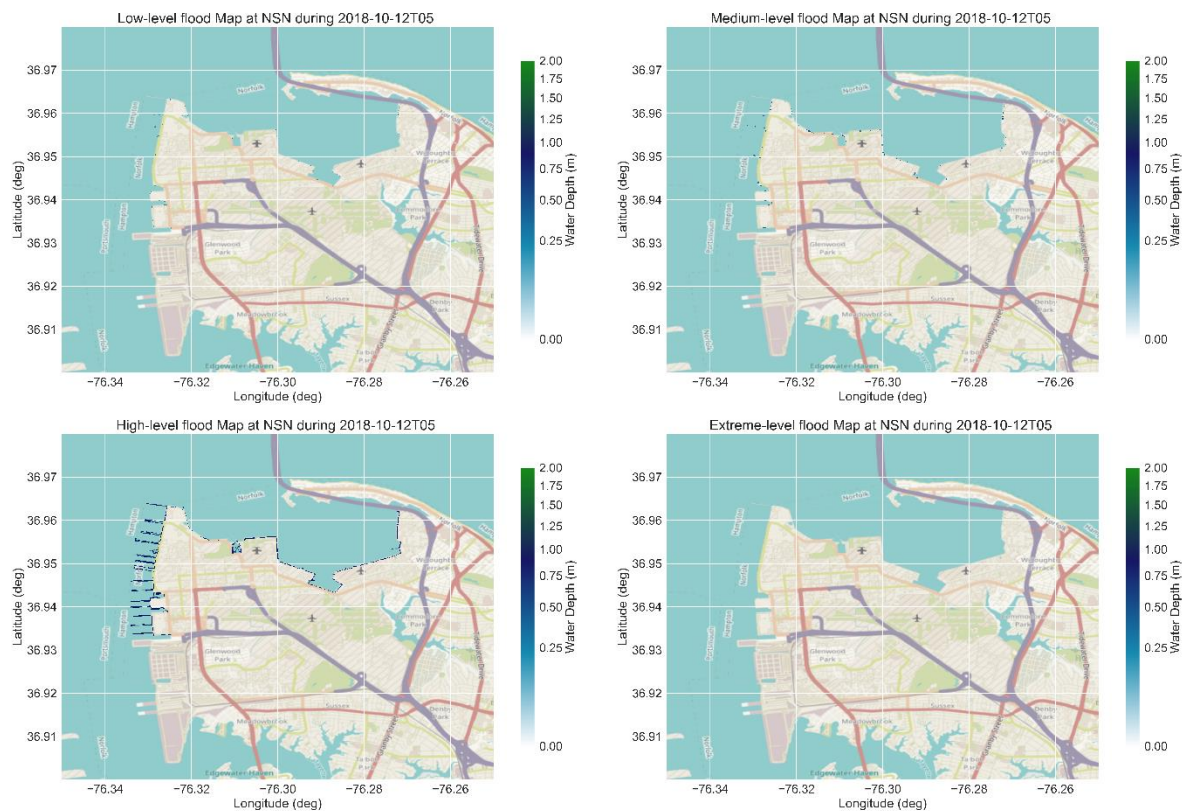


Figure 241. Flood area classification (Low, Medium, High, and Extreme) in meters of the PD_F0.76 scenarios during hurricane Michael-2018 at NSN base, the US.

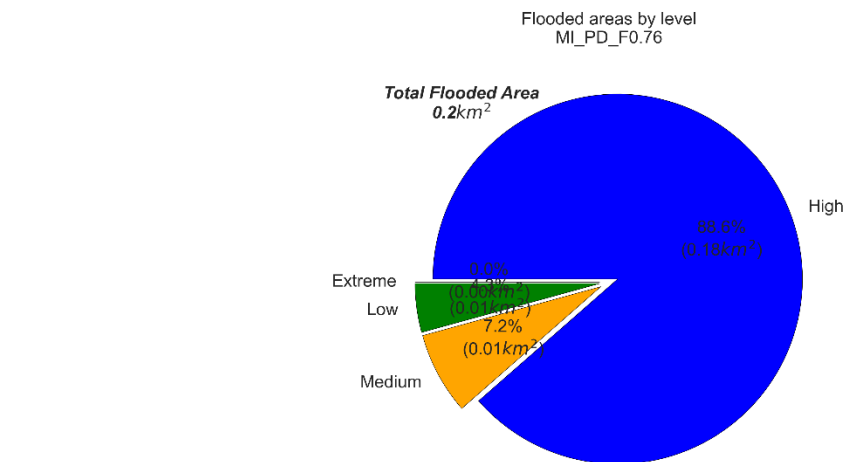


Figure 242. Pie chart of the flood areas, with percentages, of the different flood levels for PD_F0.76 scenario for Hurricane Michael-2018 at NSN, the US.

c. PD.88 Scenario

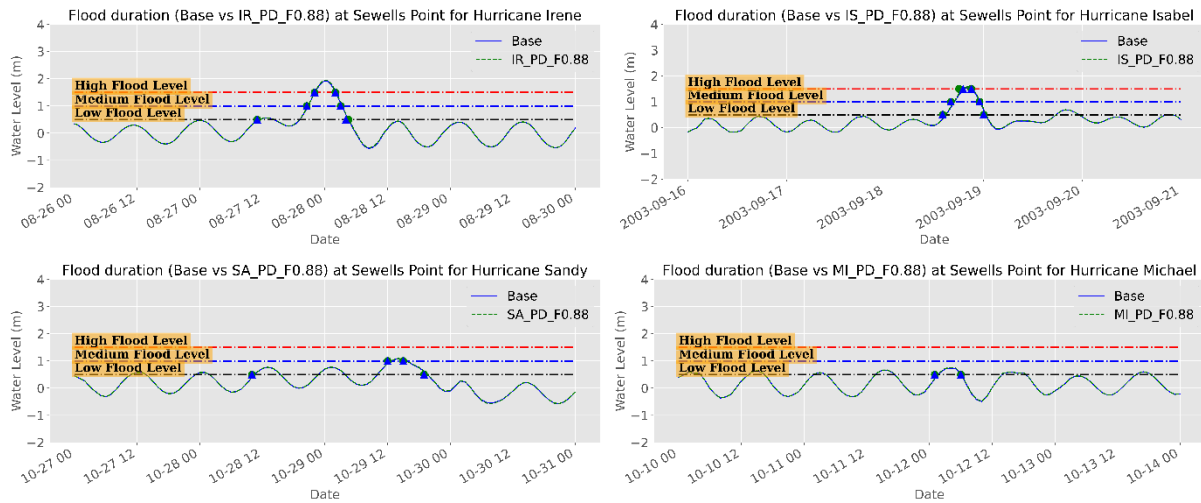


Figure 243. Water level time series (m) during the different hurricanes showing the surge magnitude and duration for different surge levels for the base and PD_F0.88 scenarios at Sewells Point, NSN, the US.

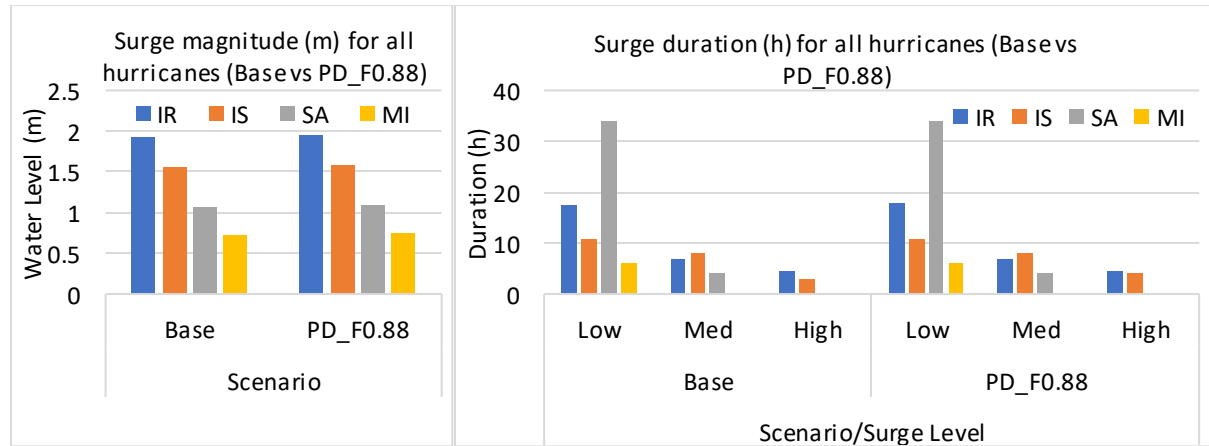


Figure 244. Peak surge (m) (left panel) and surge duration (h) of the different surge levels (right panel) for the base and PD_F0.88 scenario for all hurricanes, NSN, the US.

Table 79. Peak surge characteristics (Maximum and Duration) of the worst-case pressure drop scenario (PD_F0.88) and base scenarios for all Hurricanes at Sewells Point, NSN, the US.

Group	Hurricane ID	Max. Surge (m)		Duration (h)					
		Base	PD_F0.88	Base			PD_F0.88		
				Low	Med	High	Low	Med	High
Meteo. Forcing	IR	1.92	1.95	17.5	7	4.5	18	7	4.5
	IS	1.55	1.58	11	8	3	11	8	4
	SA	1.08	1.09	34	4	0	34	4	0
	MI	0.73	0.75	6	0	0	6	0	0

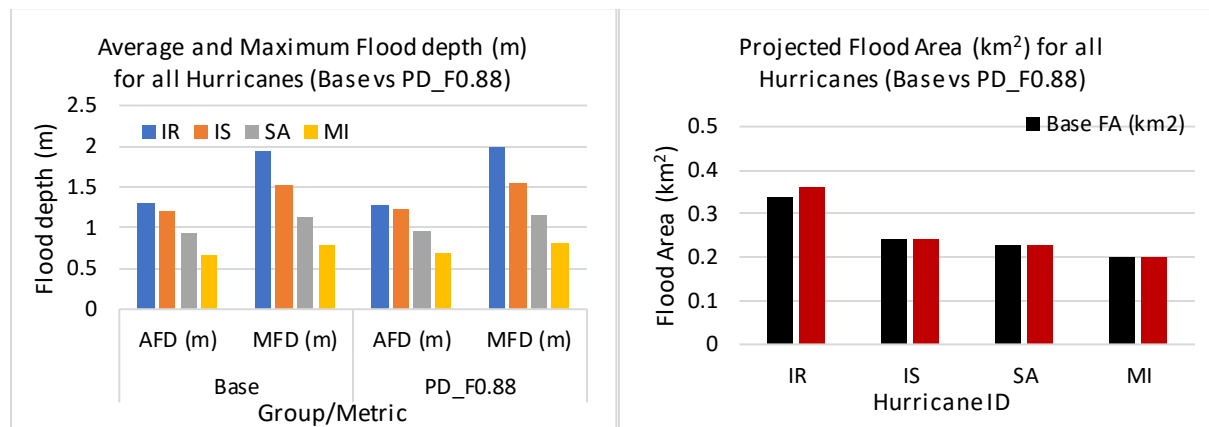


Figure 245. Average Flood Depth (AFD) & Maximum Flood Depth (MFD) in meters (left panel) and Flood area (km²) (right panel) of all hurricanes for the Base and PD_F0.88 scenarios, NSN, the US.

Table 80. Flood area characteristics of the worst-case pressure drop scenario (PD_F0.88) for all hurricanes at NSN, the US.

Group	Hurricane ID	Base				PD_F0.88			
		Average FD (m)	Max FD (m)	Flood area (km ²)	%	Average FD (m)	Max FD (m)	Flood area (km ²)	%
Meteo. Forcing	IR	1.31	1.94	0.34	2.47	1.29	1.98	0.36	2.6
	IS	1.21	1.52	0.24	1.72	1.23	1.55	0.24	1.7
	SA	0.94	1.14	0.23	1.6	0.95	1.15	0.23	1.7
	MI	0.66	0.79	0.2	1.45	0.68	0.81	0.2	1.5

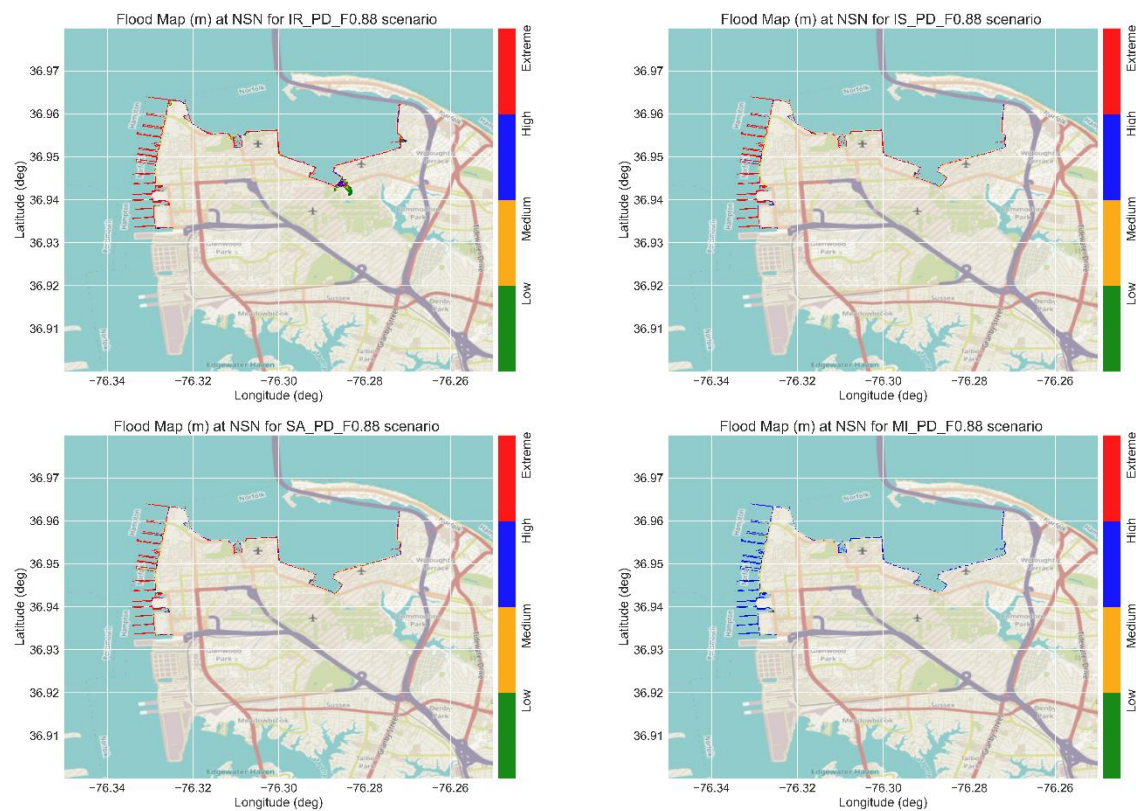


Figure 246. Flood maps with the flood levels for the different hurricanes during the peak surge for the PD_F0.88 scenario at NSN, the US.

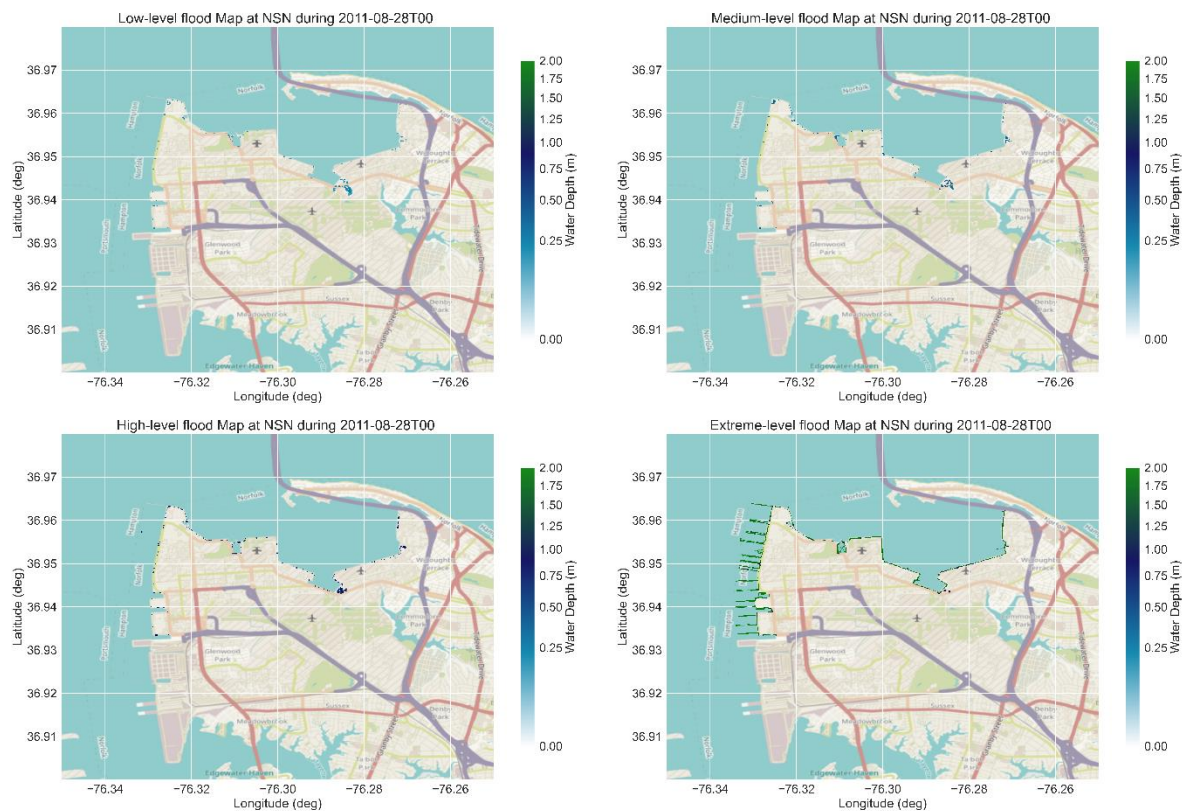


Figure 247. Flood area classification (Low, Medium, High, and Extreme) in meters of the PD_F0.88 scenarios during hurricane Irene-2011 at NSN base, the US.

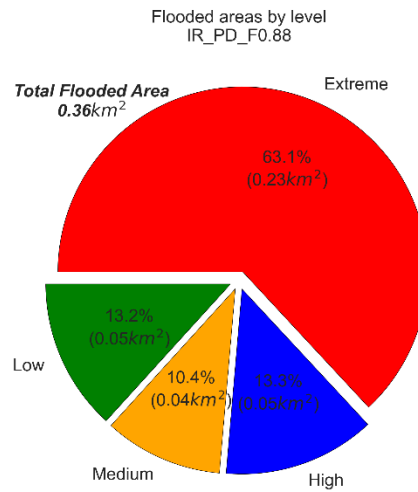


Figure 248. Pie chart of the flood areas, with percentages, of the different flood levels for PD_F0.88 scenario for Hurricane Irene-2011 at NSN, the US.

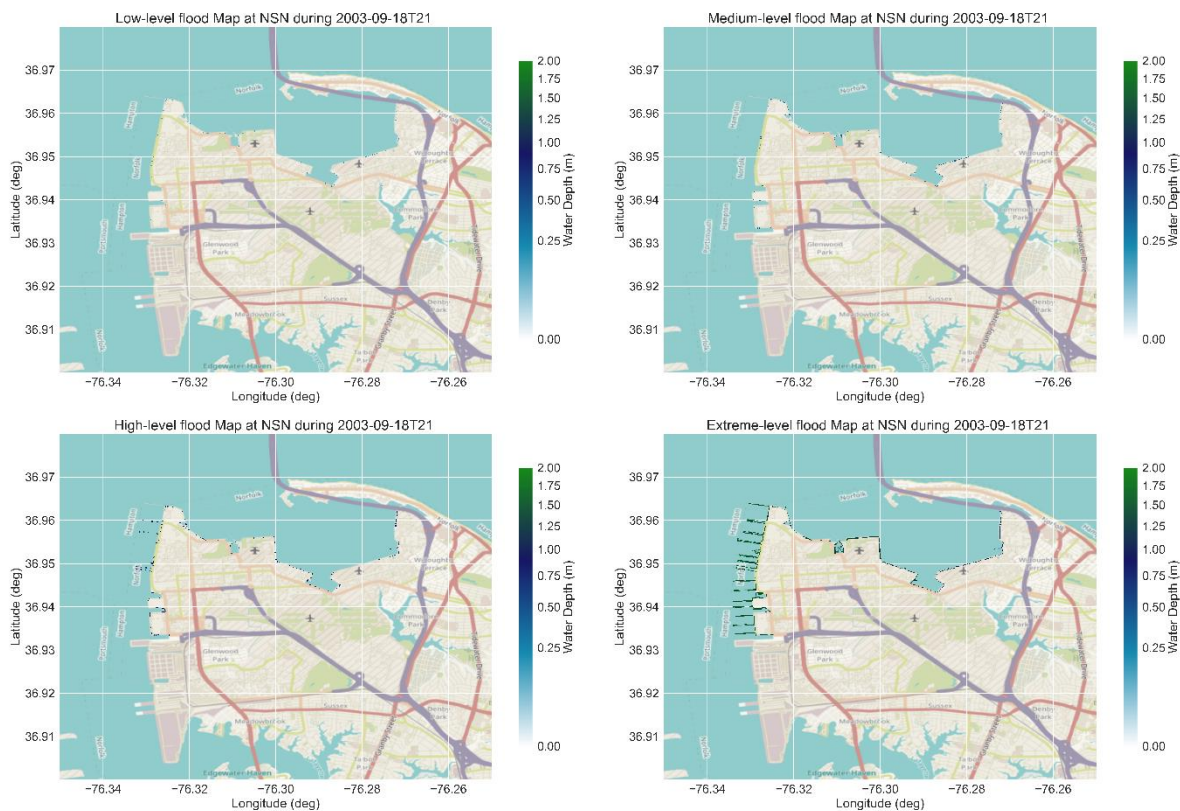


Figure 249. Flood area classification (Low, Medium, High, and Extreme) in meters of the PD_F0.88 scenarios during hurricane Isabel-2003 at NSN base, the US.

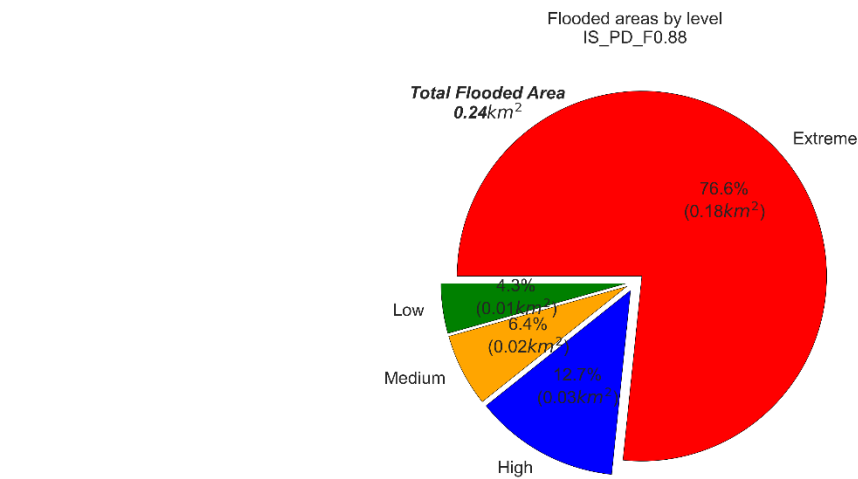


Figure 250. Pie chart of the flood areas, with percentages, of the different flood levels for PD_F0.88 scenario for Hurricane Isabel-2003 at NSN, the US.

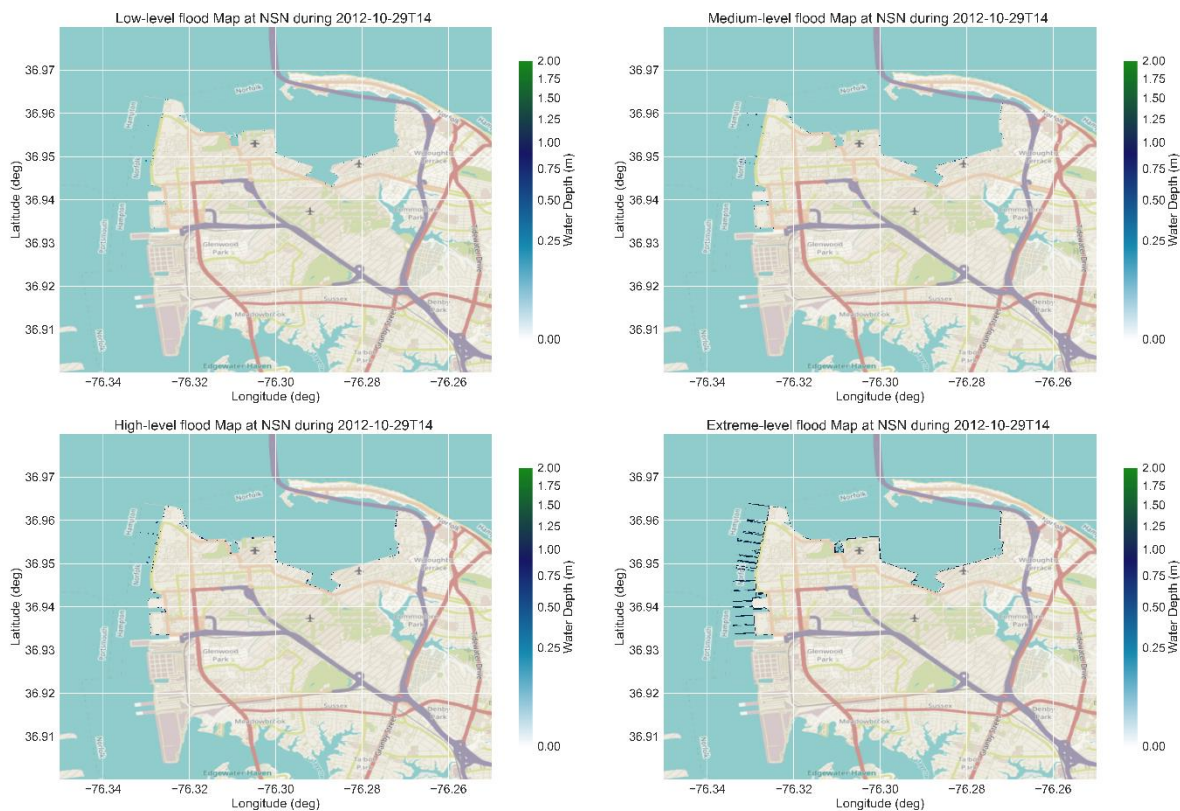


Figure 251. Flood area classification (Low, Medium, High, and Extreme) in meters of the PD_F0.88 scenarios during hurricane Sandy-2012 at NSN base, the US.

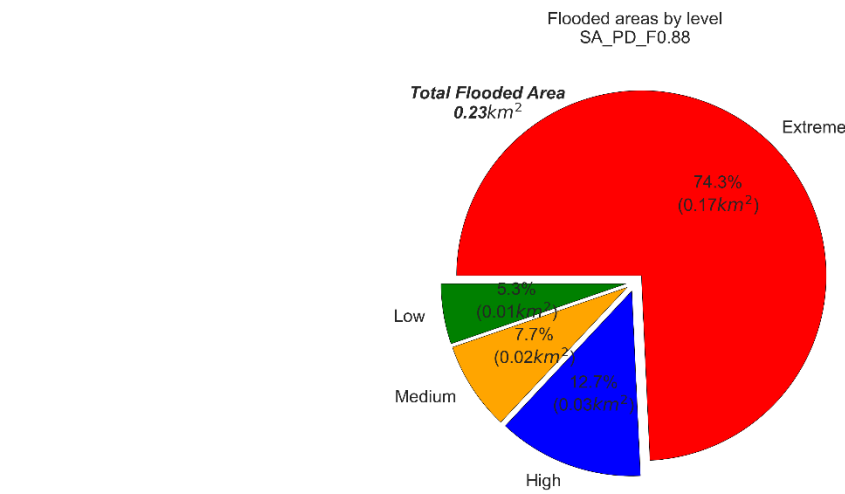


Figure 252. Pie chart of the flood areas, with percentages, of the different flood levels for PD_F0.88 scenario for Hurricane Sandy-2012 at NSN, the US.

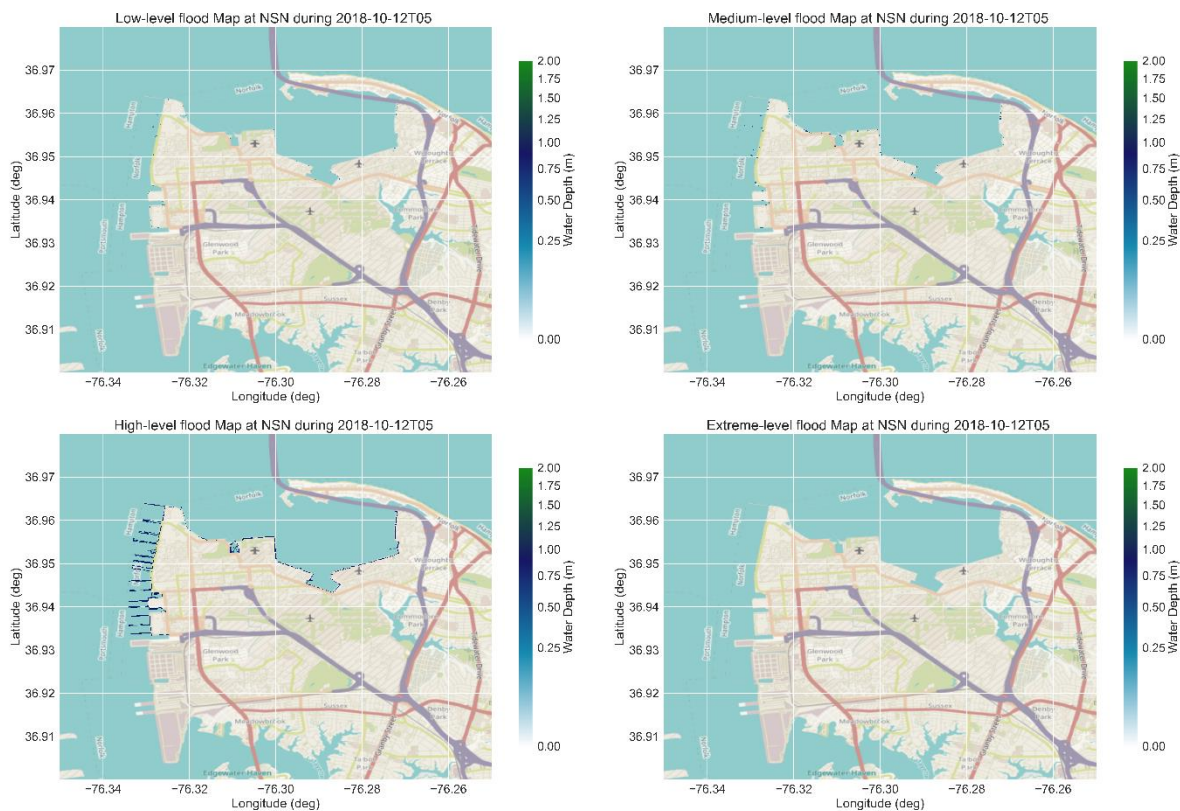


Figure 253. Flood area classification (Low, Medium, High, and Extreme) in meters of the PD_F0.64 scenarios during hurricane Michael-2018 at NSN base, the US.

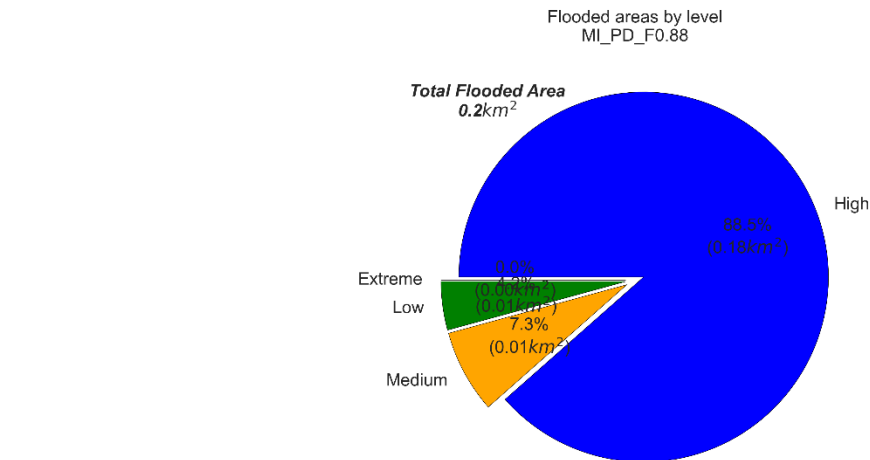


Figure 254. Pie chart of the flood areas, with percentages, of the different flood levels for PD_F0.88 scenario for Hurricane Michael-2018 at NSN, the US.

12.1.2. Radius of Maximum Wind

a. RMW_F0.9 Scenario

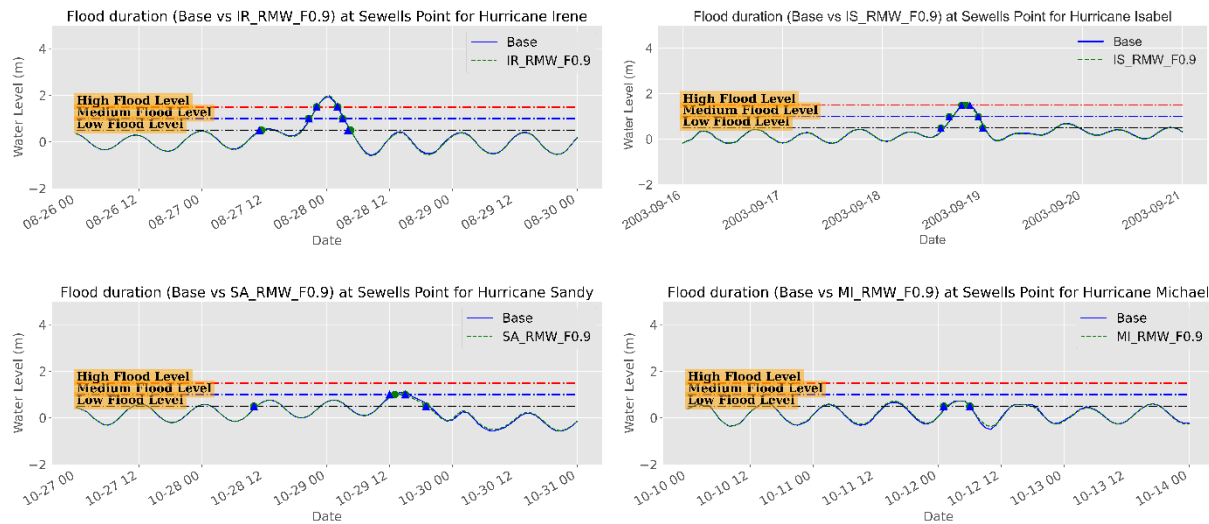


Figure 255. Water level time series (m) during the different hurricanes showing the surge magnitude and duration for different surge levels for the base and RMW_F0.9 scenarios at Sewells Point, NSN, the US.

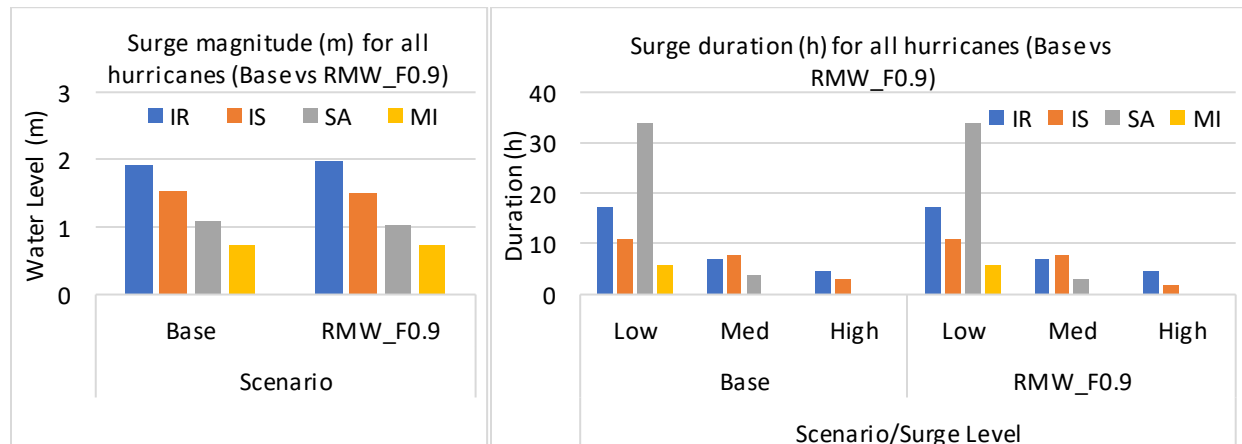


Figure 256. Peak surge (m) (left panel) and surge duration (h) of the different surge levels (right panel) for the base and RMW_F0.9 scenario for all hurricanes, NSN, the US.

Table 81. Peak surge characteristics (Maximum and Duration) for the base and the RMW_F0.9 scenarios for all Hurricanes at Sewells Point, NSN, the US.

Group	Hurricane ID	Scenario		Scenario/Surge Level					
		Base	RMW_F0.9	Base			RMW_F0.9		
				Low	Med	High	Low	Med	High
Meteo. Forcing	IR	1.92	1.98	17.5	7	4.5	17.5	7	4.5
	IS	1.55	1.52	11	8	3	11	8	2
	SA	1.08	1.04	34	4	0	34	3	0
	MI	0.73	0.72	6	0	0	6	0	0

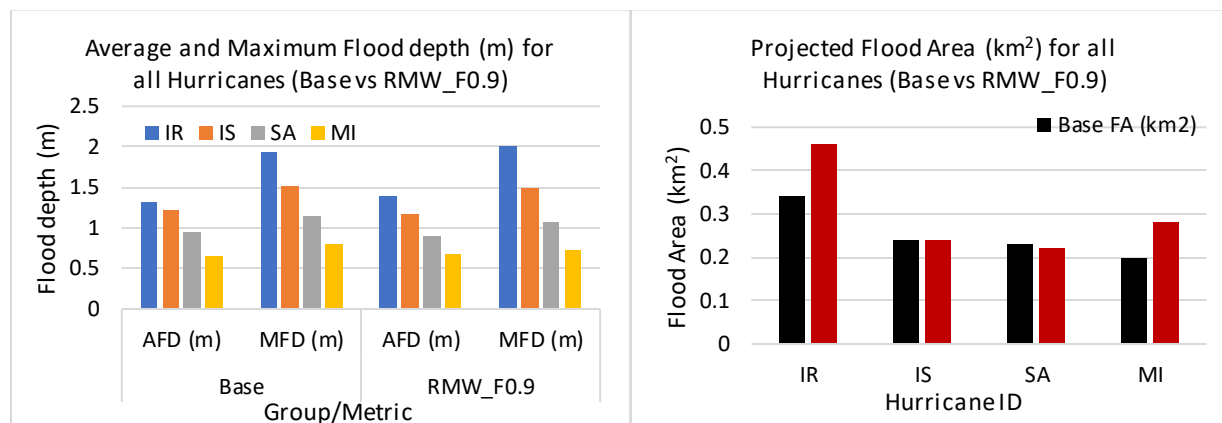


Figure 257. Average Flood Depth (AFD) & Maximum Flood Depth (MFD) in meters (left panel) and Flood area (km^2) (right panel) of all hurricanes for the Base and RMW_F0.9 scenarios, NSN, the US.

Table 82. Flood area characteristics of the base and the RMW_F0.9 scenarios for all hurricanes at NSN, the US.

Group	Hurricane ID	Base				RMW_F0.9			
		Average FD (m)	Max FD (m)	Flood area (km^2)	%	Average FD (m)	Max FD (m)	Flood area (km^2)	%
Meteo. Forcing	IR	1.31	1.94	0.34	2.47	1.4	2	0.46	3.3
	IS	1.21	1.52	0.24	1.72	1.18	1.5	0.24	1.7
	SA	0.94	1.14	0.23	1.6	0.9	1.08	0.22	1.6

	MI	0.66	0.79	0.2	1.45	0.68	0.73	0.28	2.0
--	-----------	------	------	-----	------	------	------	------	-----

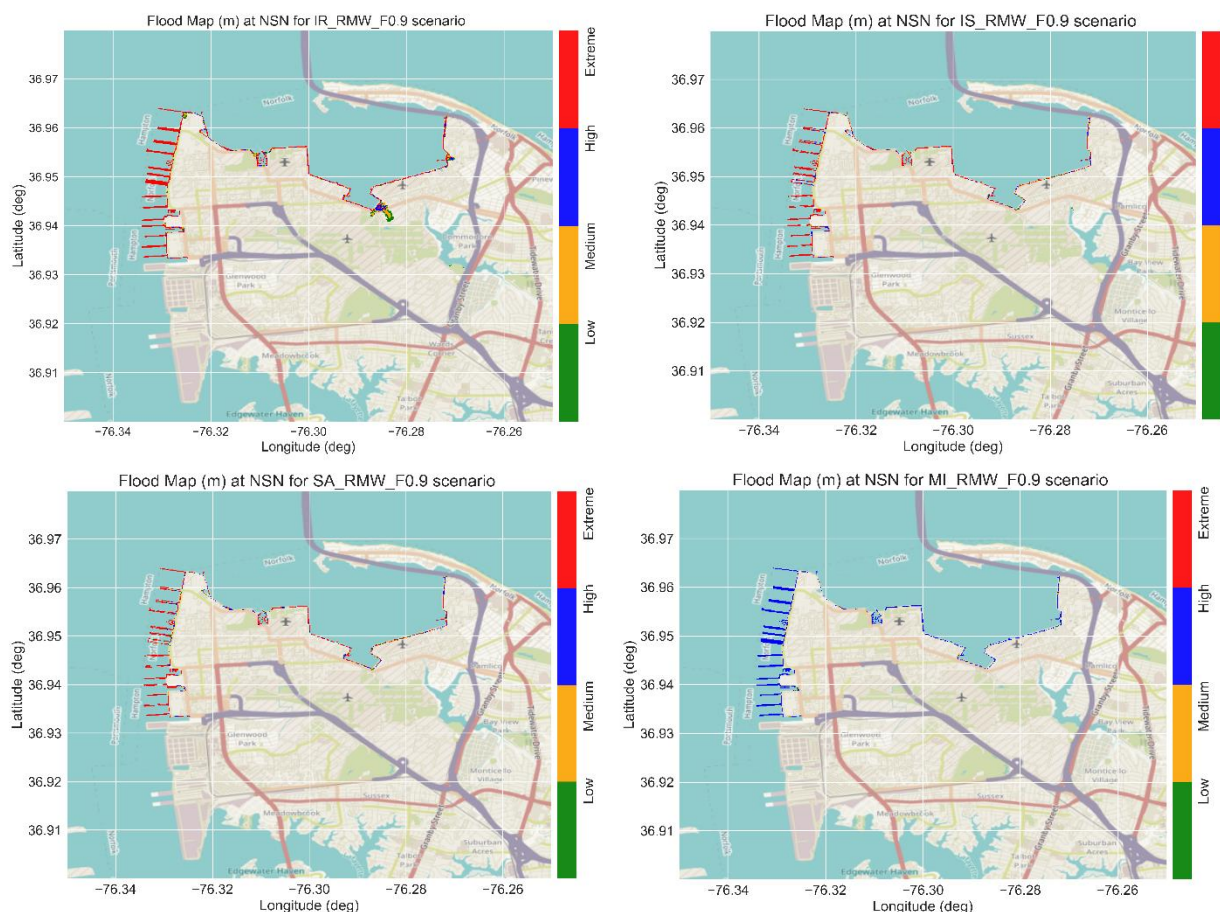


Figure 258. Flood maps with the flood levels for the different hurricanes during the peak surge for the RMW_F0.9 scenario at NSN, the US.

b. RMW_F1.1 Scenario

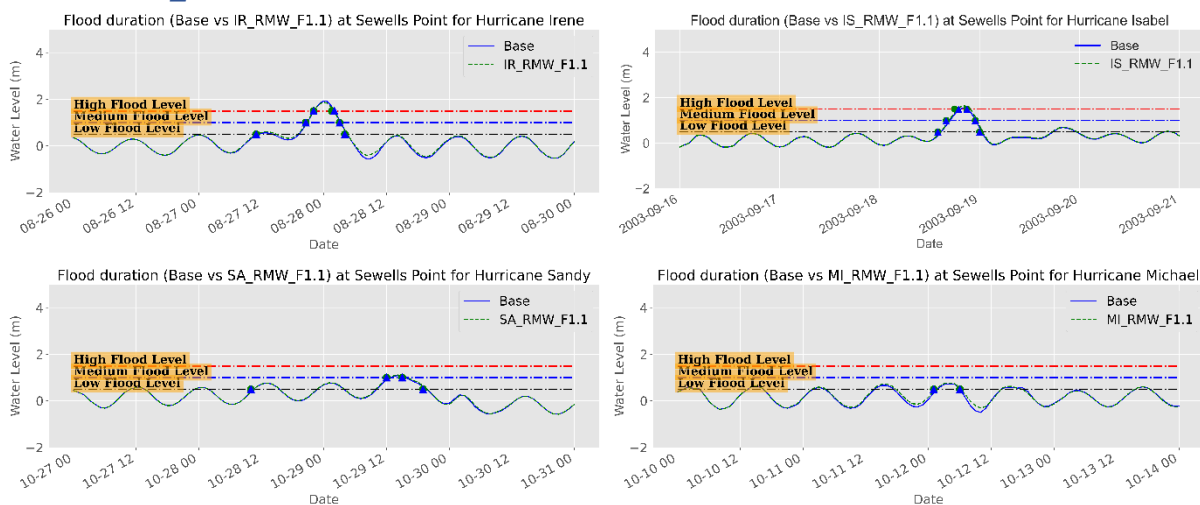


Figure 259. Water level time series (m) during the different hurricanes showing the surge magnitude and duration for different surge levels for the base and RMW_F1.1 scenarios at Sewells Point, NSN, the US.

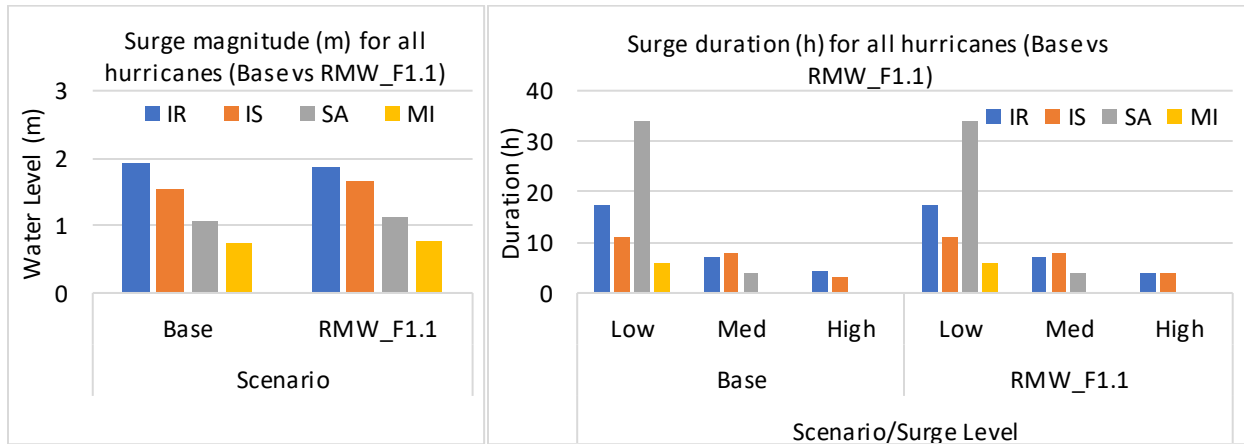


Figure 260. Peak surge (m) (left panel) and surge duration (h) of the different surge levels (right panel) for the base and RMW_F1.1 scenario for all hurricanes, NSN, the US.

Table 83. Peak surge characteristics (Maximum and Duration) the base and the RMW_F1.1 scenarios for all Hurricanes at Sewells Point, NSN, the US.

Group	Hurricane ID	Max. Surge (m)		Duration (h)					
		Base	RMW_F1.1	Base			RMW_F1.1		
Meteo. Forcing	IR	1.92	1.87	17.5	7	4.5	17.5	7	4
	IS	1.55	1.65	11	8	3	11	8	4
	SA	1.08	1.12	34	4	0	34	4	0
	MI	0.73	0.76	6	0	0	6	0	0

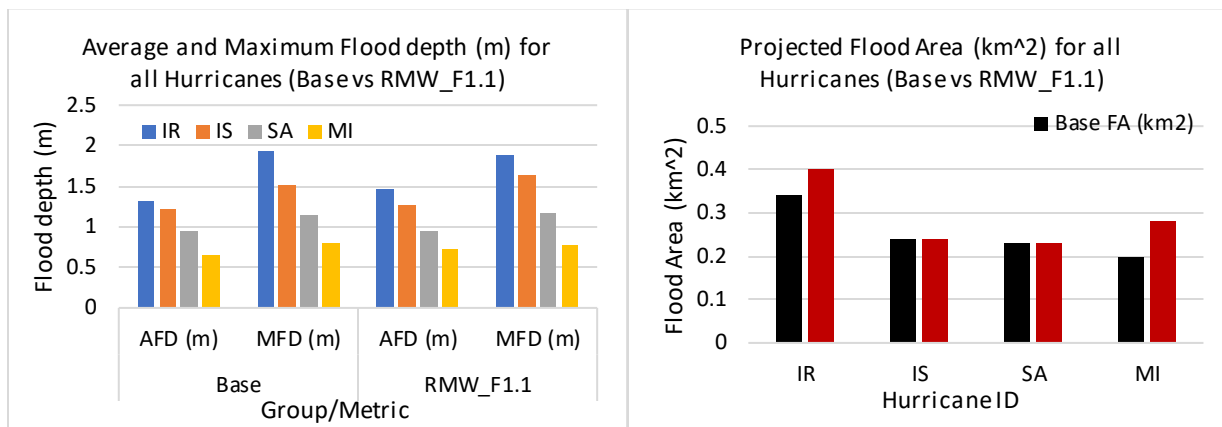


Figure 261. Average Flood Depth (AFD) & Maximum Flood Depth (MFD) in meters (left panel) and Flood area (km^2) (right panel) of all hurricanes for the Base and RMW_F1.1 scenarios, NSN, the US.

Table 84. Flood area characteristics of the base and the RMW_F1.1 for all hurricanes at NSN, the US.

Group	Hurricane ID	Base				RMW_F1.1			
		Average FD (m)	Max FD (m)	Flood area (km^2)	%	Average FD (m)	Max FD (m)	Flood area (km^2)	%
Meteo. Forcing	IR	1.31	1.94	0.34	2.47	1.47	1.89	0.4	2.9
	IS	1.21	1.52	0.24	1.72	1.28	1.64	0.24	1.7
	SA	0.94	1.14	0.23	1.6	0.96	1.18	0.23	1.7
	MI	0.66	0.79	0.2	1.45	0.72	0.77	0.28	2.0

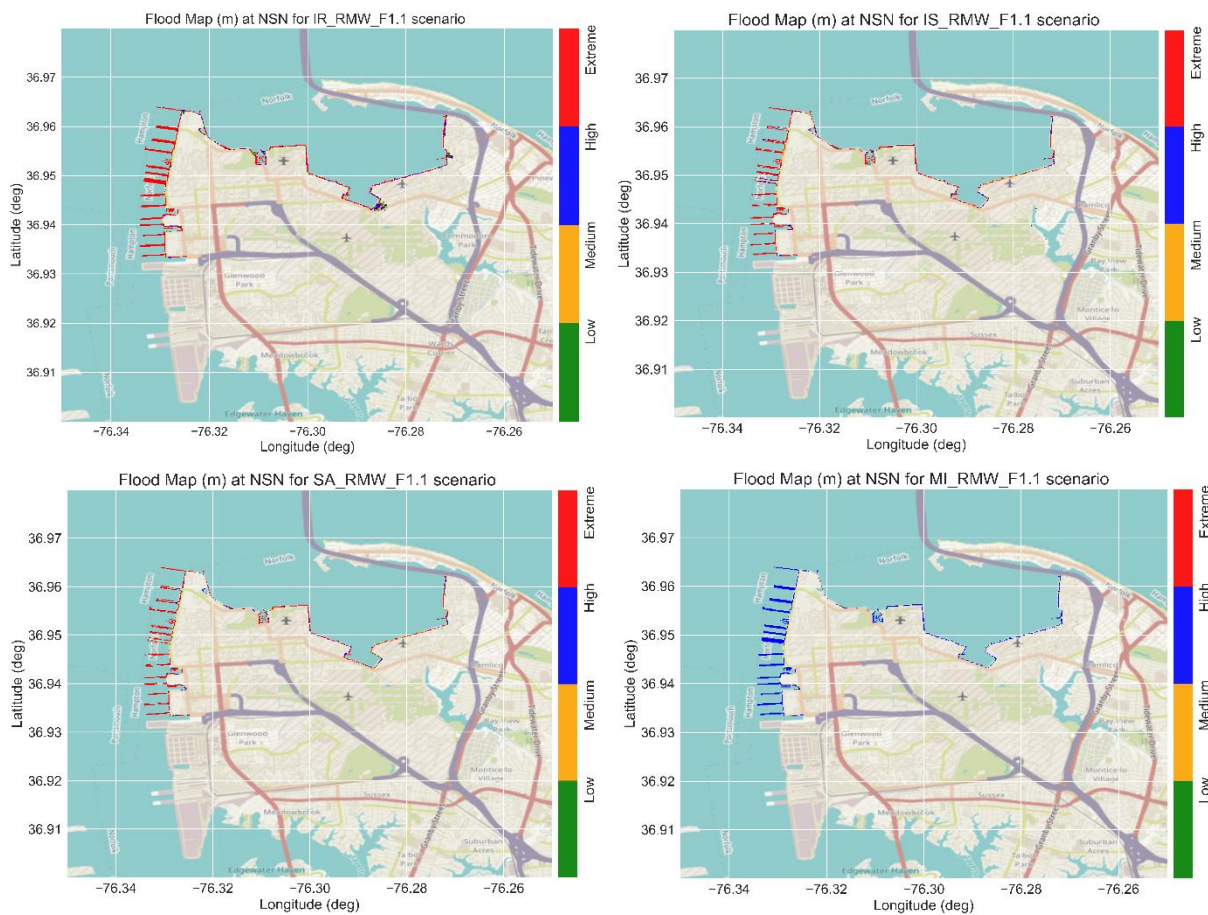


Figure 262. Flood maps with the flood levels for the different hurricanes during the peak surge for the RMW_F1.1 scenario at NSN, the US.

12.2. Impacts of Climate Change

12.2.1. Sea Level Rise

a. SLR_0.4M Scenario

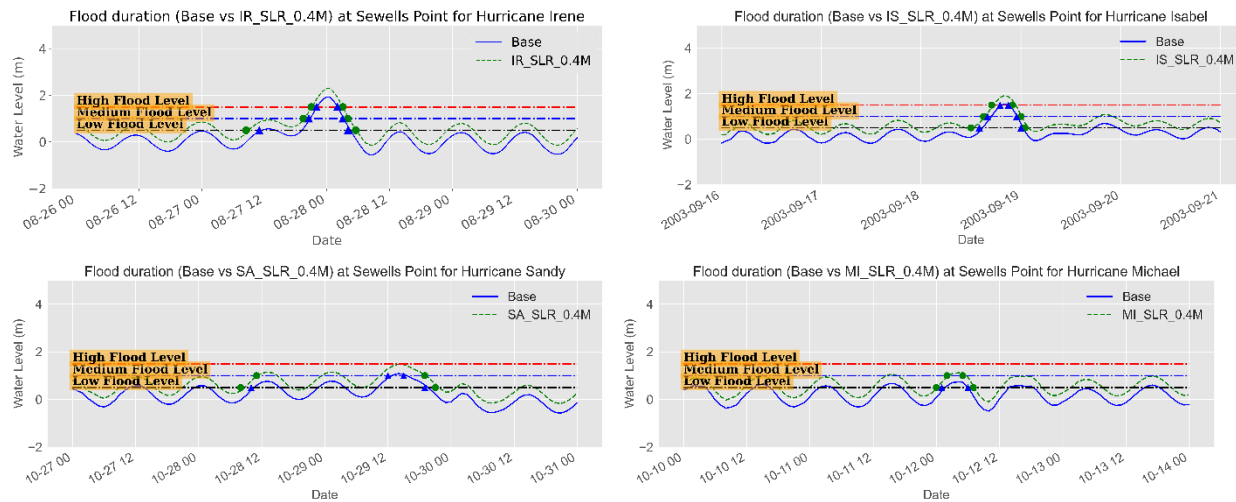


Figure 263. Water level time series (m) during the different hurricanes showing the surge magnitude and duration for different surge levels for the base and SLR_0.4M scenarios at Sewells Point, NSN, the US.

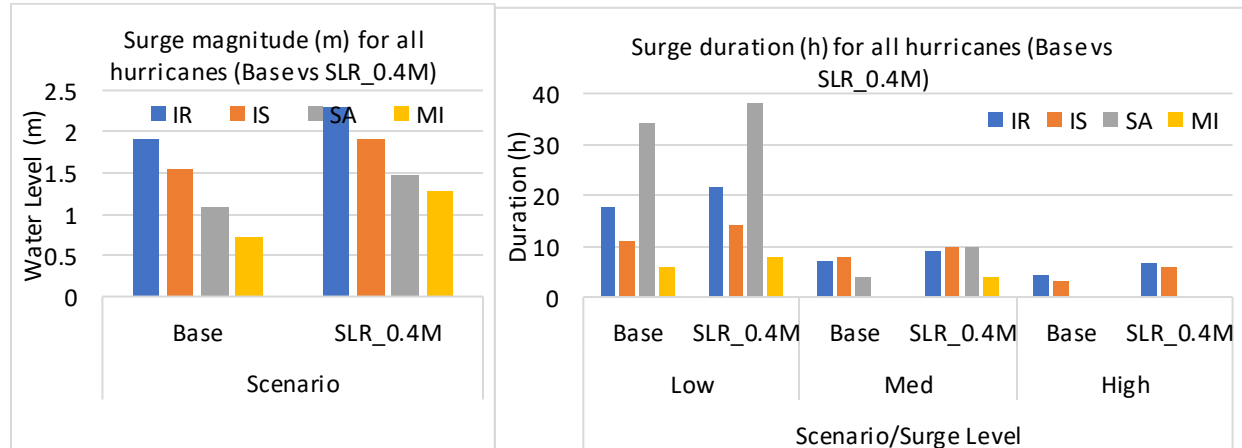


Figure 264. Peak surge (m) (left panel) and surge duration (h) of the different surge levels (right panel) for the base and SLR_0.4M scenario for all hurricanes, NSN, the US.

Table 85. Peak surge characteristics (Maximum and Duration) of the base and SLR_0.4M scenarios for all Hurricanes at Sewells Point, NSN, the US.

Group	Hurricane ID	Max. Surge(m)		Duration (h)					
		Base	SLR_0.4M	Low		Med		High	
				Base	SLR_0.4M	Base	SLR_0.4M	Base	SLR_0.4M
CC*	IR	1.92	2.29	17.5	21.5	7	9	4.5	6.5
	IS	1.55	1.91	11	14	8	10	3	6
	SA	1.08	1.48	34	38	4	10	0	0
	MI	0.73	1.27	6	8	0	4	0	0

*Climate Change

--the water level is above this level

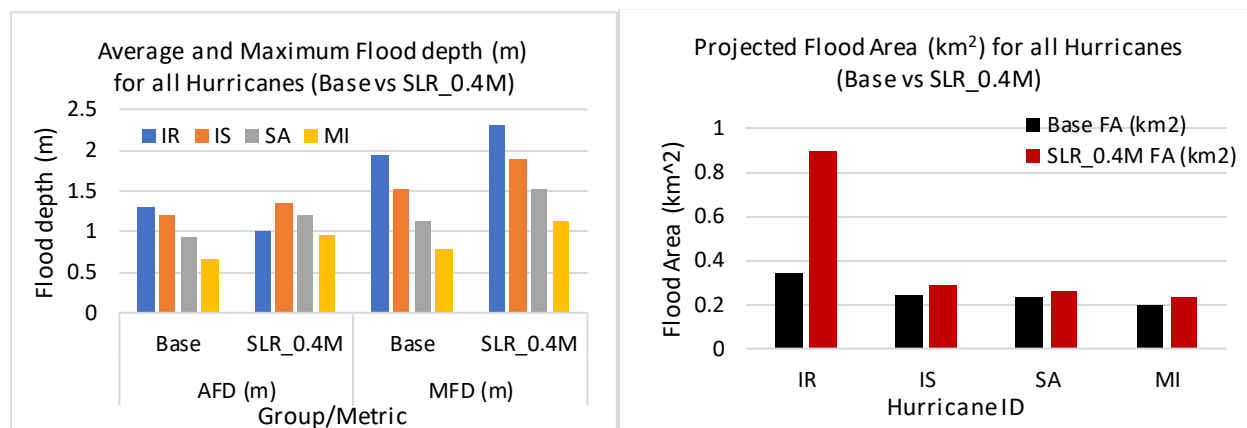


Figure 265. Average Flood Depth (AFD) & Maximum Flood Depth (MFD) in meters (left panel) and Flood area (km^2) (right panel) of all hurricanes for the Base and SLR_0.4M scenarios at NSN, the US.

Table 86. Flood area characteristics of the base and SLR_0.4M scenarios for all hurricanes at NSN, the US.

Group	Hurricane ID	Base				SLR_0.4M			
		Average FD (m)	Max FD (m)	Flood area (km^2)	%	Average FD (m)	Max FD (m)	Flood area (km^2)	%
CC	IR	1.31	1.94	0.34	2.47	1.01	2.31	0.9	6.5
	IS	1.21	1.52	0.24	1.72	1.36	1.89	0.29	2.1
	SA	0.94	1.14	0.23	1.6	1.2	1.53	0.26	1.9

MI	0.66	0.79	0.2	1.45	0.95	1.12	0.23	1.7
----	------	------	-----	------	------	------	------	-----

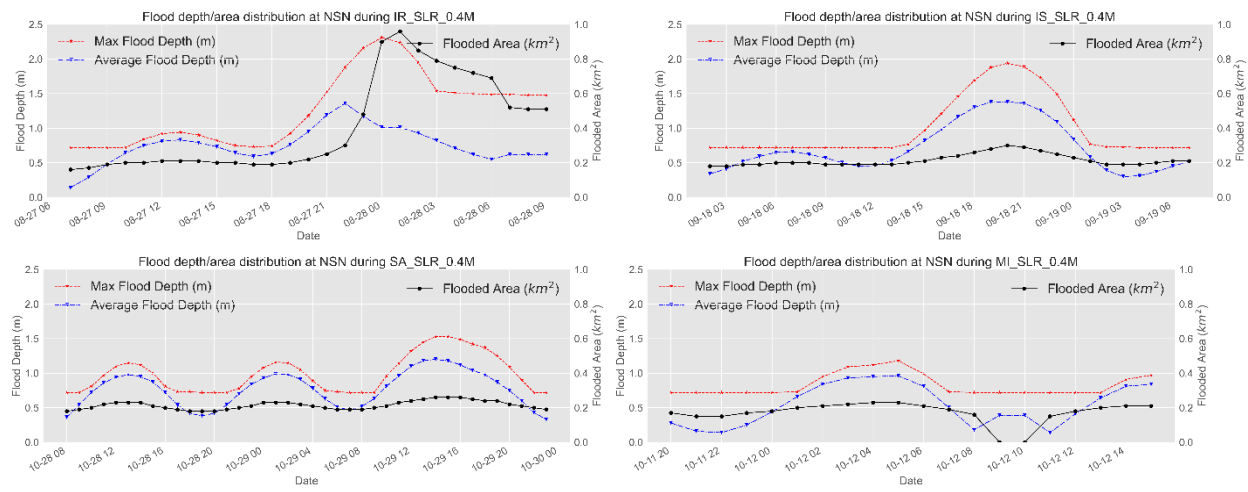


Figure 266. Timeseries of the projected average and maximum flood depth (left axis) and flood area (km²-right axis) for all hurricanes for SLR_0.4M scenario at NSN, the US.

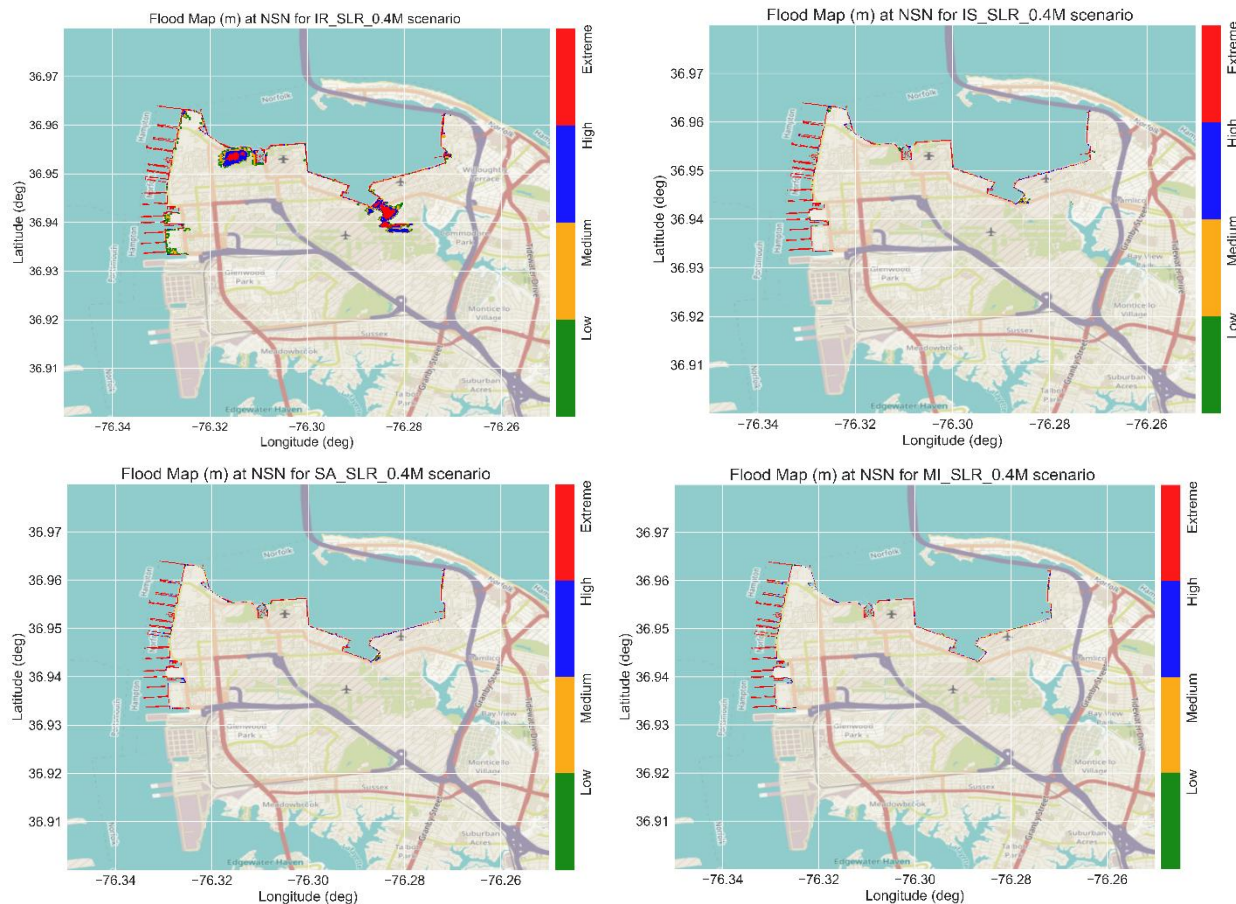


Figure 267. Flood maps with the flood levels for the different hurricanes during the peak surge for the SLR_0.4M scenario at NSN, the US.

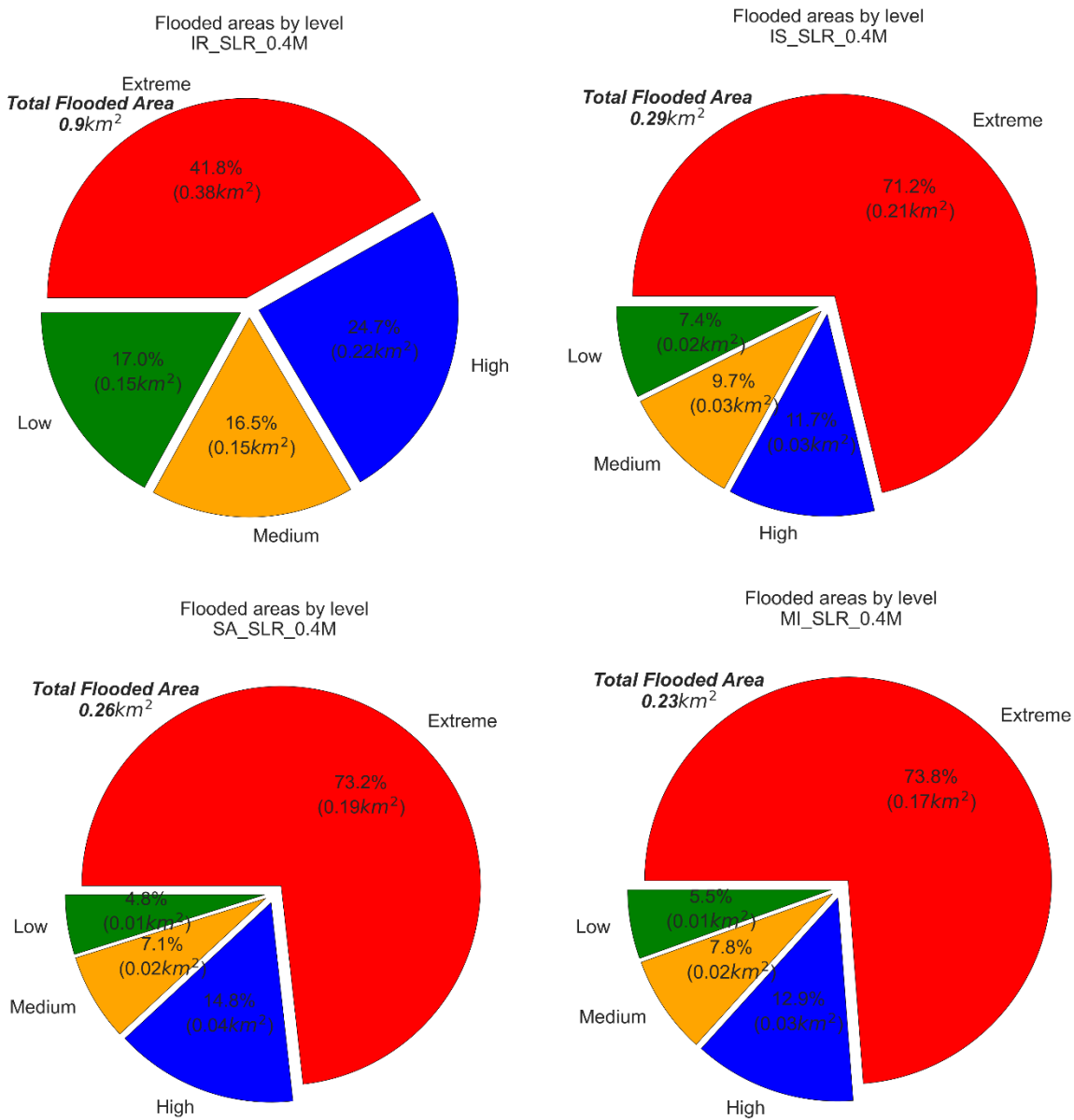


Figure 268. Pie chart of the flood areas, with percentages, of the different flood levels for SLR_0.4M scenarios for all hurricanes at NSN, the US.

b. SLR_0.8M Scenario

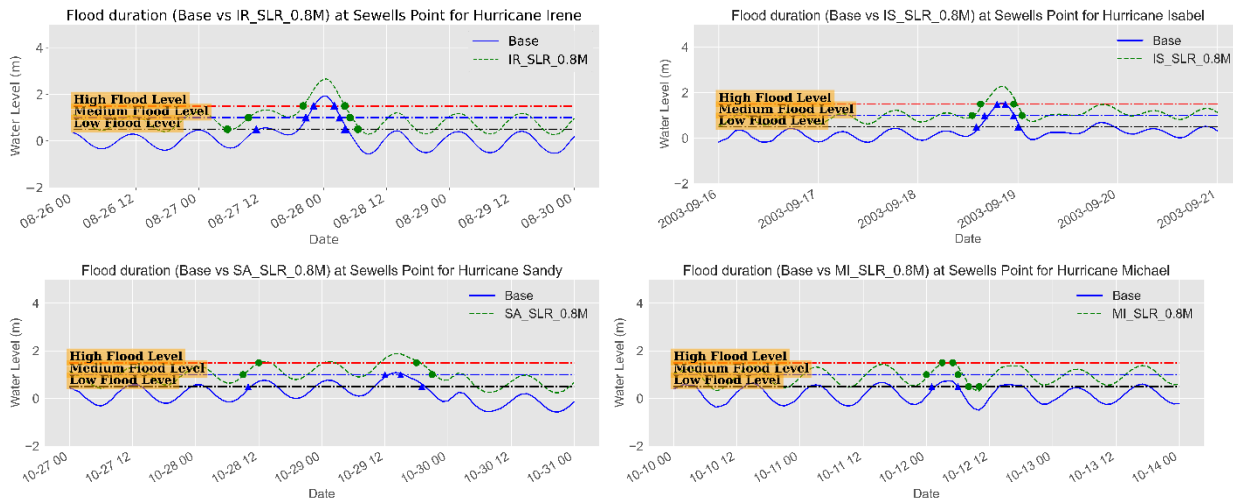


Figure 269. Water level time series (m) during the different hurricanes showing the surge magnitude and duration for different surge levels for the base and SLR_0.8M scenarios at Sewells Point, NSN, the US.

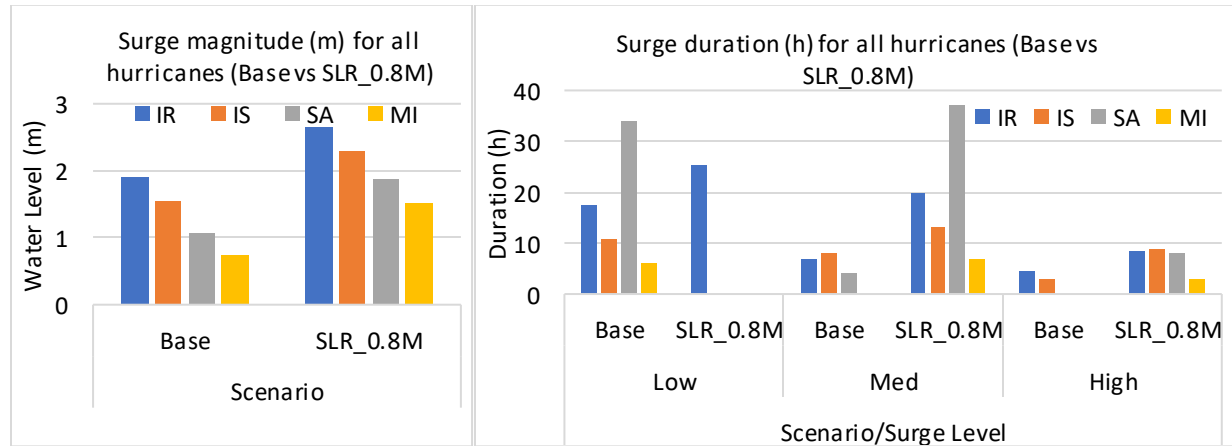


Figure 270. Peak surge (m) (left panel) and surge duration (h) of the different surge levels (right panel) for the base and SLR_0.8M scenario for all hurricanes, NSN, the US.

Table 87. Peak surge characteristics (Maximum and Duration) of the base and SLR_0.8M scenarios for all Hurricanes at Sewells Point, NSN, the US.

Group	Hurricane ID	Max. Surge (m)		Duration (h)					
		Base	SLR_0.8M	Low		Med		High	
				Base	SLR_0.8M	Base	SLR_0.8M	Base	SLR_0.8M
CC*	IR	1.92	2.66	17.5	25.5	7	20	4.5	8.5
	IS	1.55	2.28	11	--	8	13	3	9
	SA	1.08	1.88	34	--	4	37	0	8
	MI	0.73	1.53	6	--	0	7	0	3

*Climate Change

--the water level is above this level

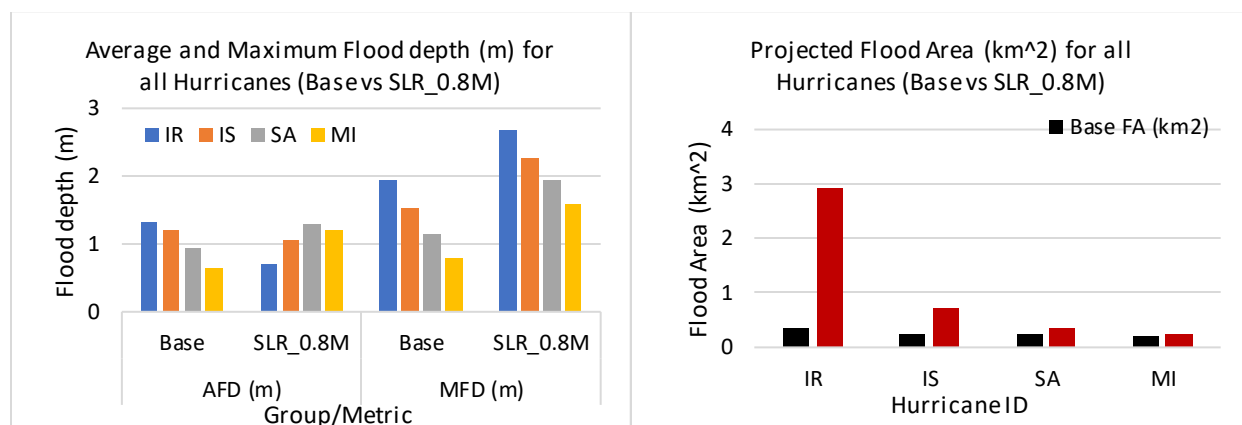


Figure 271. Average Flood Depth (AFD) & Maximum Flood Depth (MFD) in meters (left panel) and Flood area (km^2) (right panel) of all hurricanes for the Base and SLR_0.8M scenarios at NSN, the US.

Table 88. Flood area characteristics of the base and SLR_0.8M scenarios for all hurricanes at NSN, the US.

Group	Hurricane ID	Base				SLR_0.8M			
		Average FD (m)	Max FD (m)	Flood area (km^2)	%	Average FD (m)	Max FD (m)	Flood area (km^2)	%
CC	IR	1.31	1.94	0.34	2.47	0.71	2.67	2.94	21.4
	IS	1.21	1.52	0.24	1.72	1.06	2.26	0.72	5.2
	SA	0.94	1.14	0.23	1.6	1.29	1.93	0.34	2.5

	MI	0.66	0.79	0.2	1.45	1.22	1.58	0.26	1.9
--	----	------	------	-----	------	------	------	------	-----

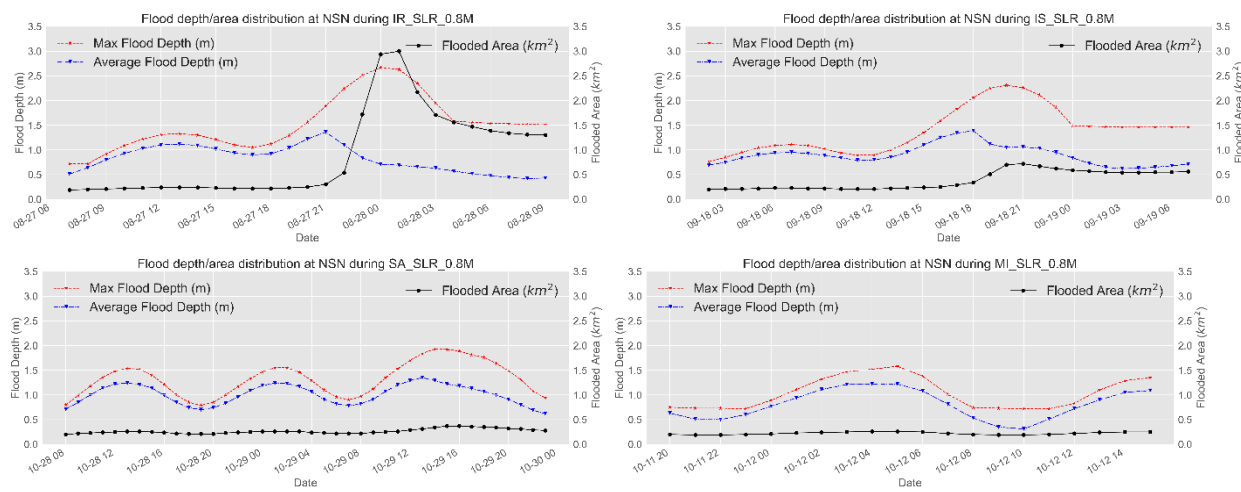


Figure 272. Timeseries of the projected average and maximum flood depth (left axis) and flood area (km^2 -right axis) for all hurricanes for SLR_0.8M scenario at NSN, the US.

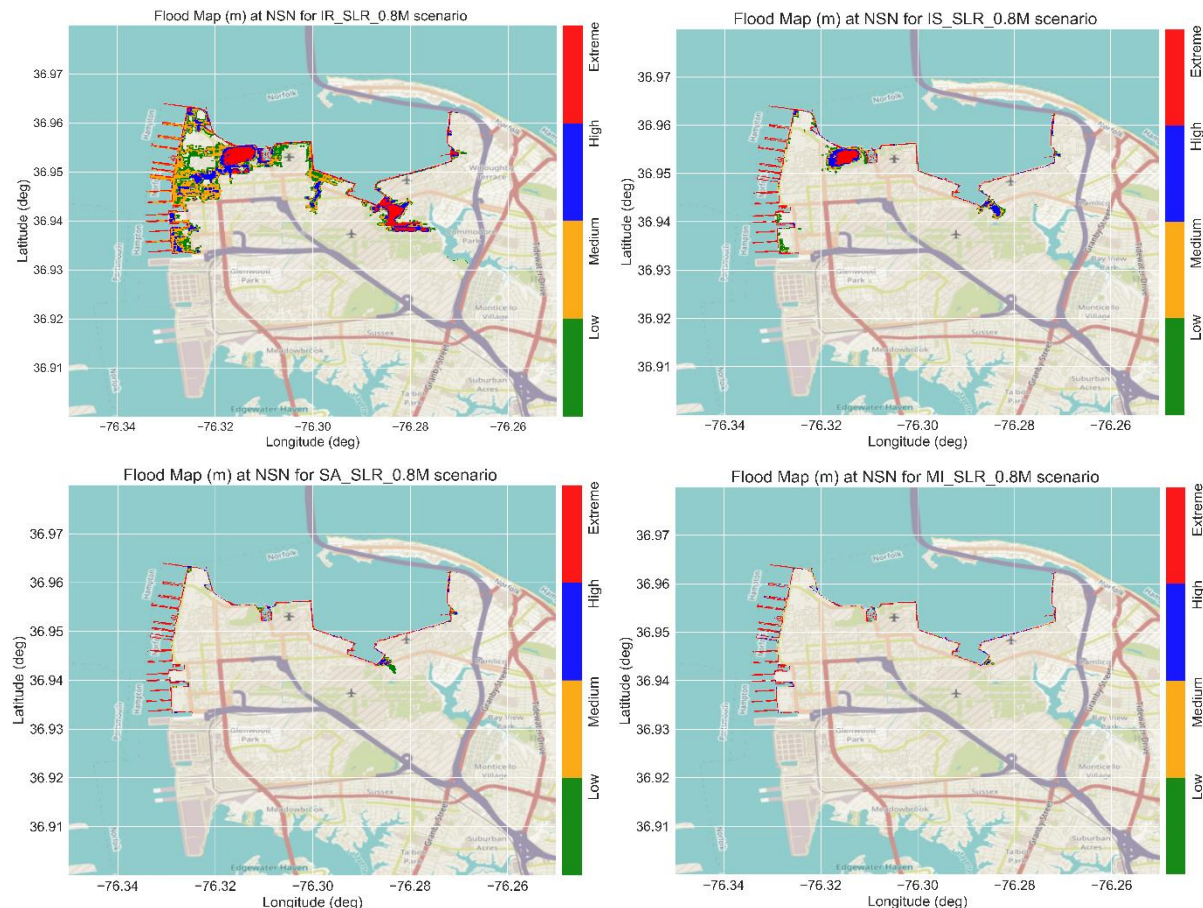


Figure 273. Flood maps with the flood levels for the different hurricanes during the peak surge for the SLR_0.8M scenario at NSN, the US.

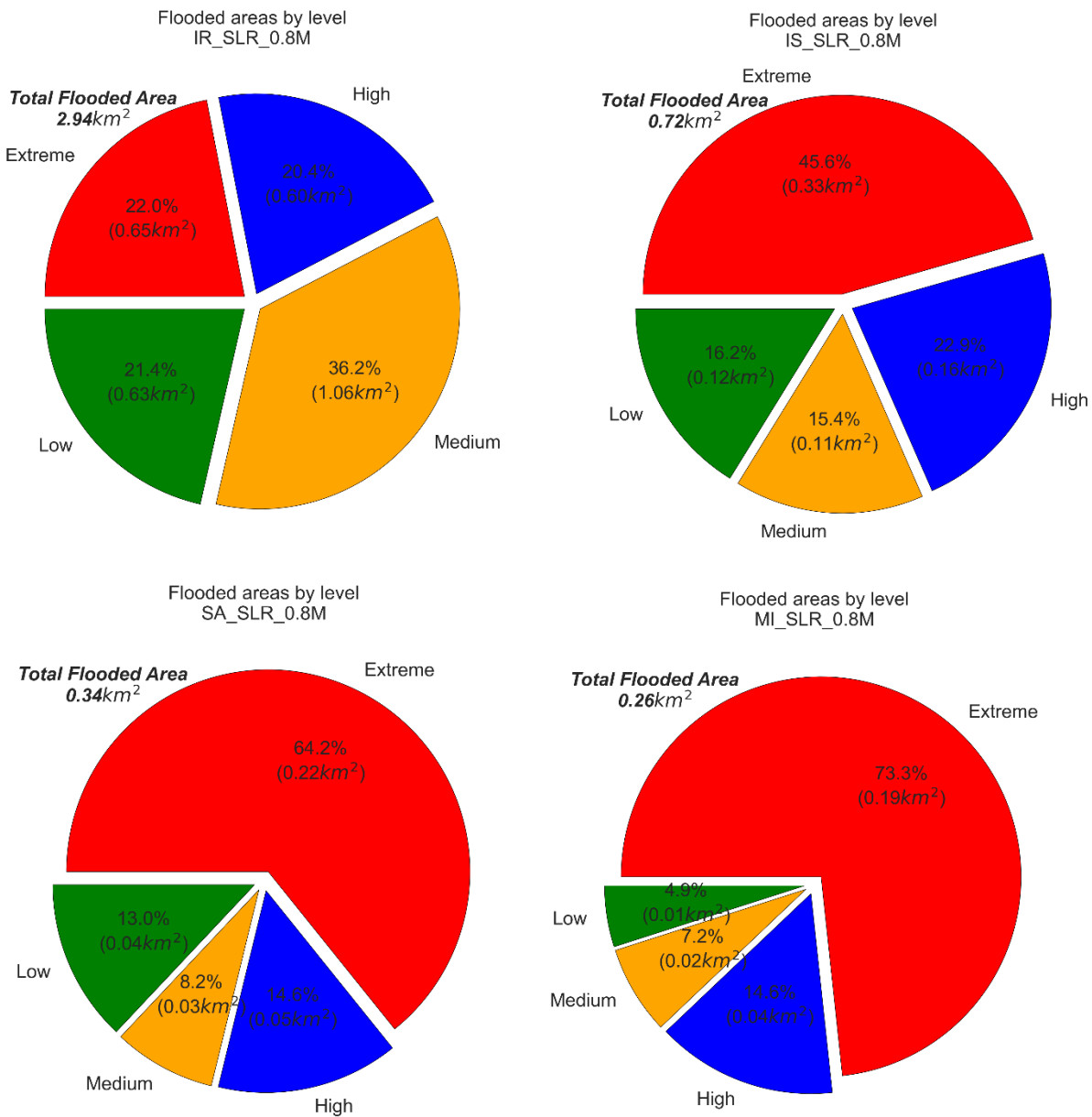


Figure 274. Pie chart of the flood areas, with percentages, of the different flood levels for SLR_0.8M scenarios for all hurricanes at NSN, the US.

12.2.2. Increasing Wind Speed

a. WSF_0.925 Scenario

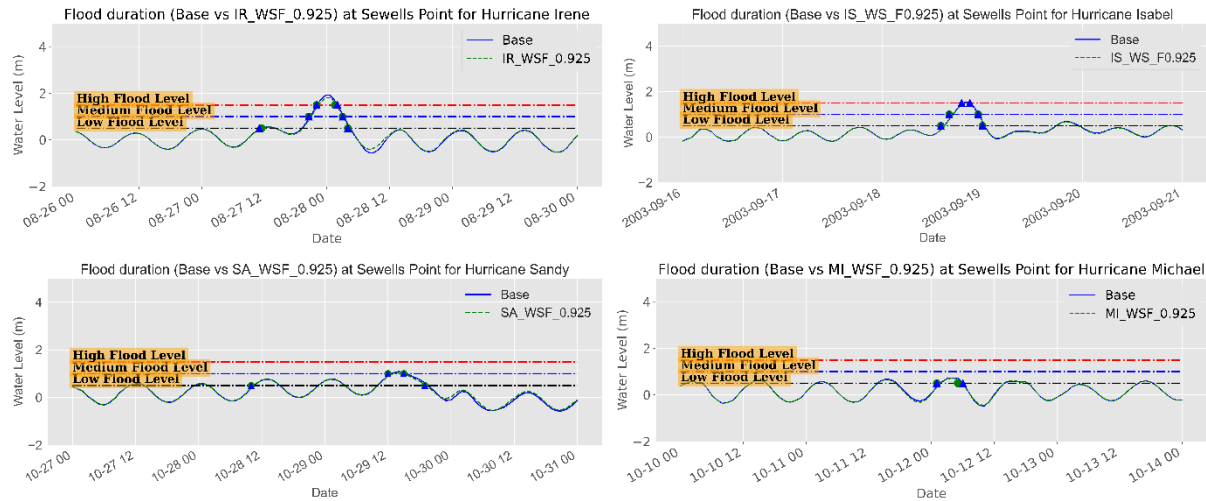


Figure 275. Water level time series (m) during the different hurricanes showing the surge magnitude and duration for different surge levels for the base and WSF_0.925 scenarios at Sewells Point, NSN, the US.

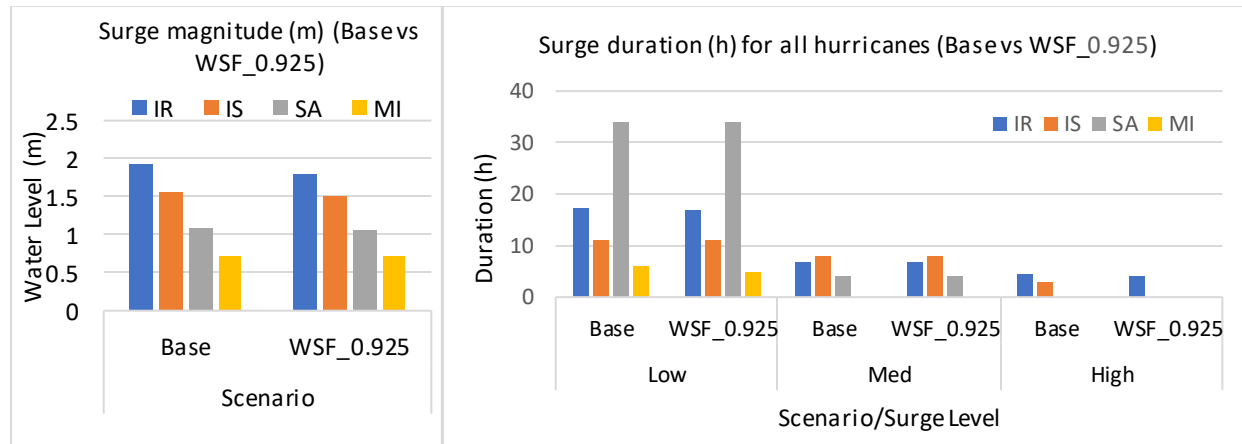


Figure 276. Peak surge (m) (left panel) and surge duration (h) of the different surge levels (right panel) for the base and WSF_0.925 scenario for all hurricanes, NSN, the US.

Table 89. Peak surge characteristics (Maximum and Duration) of the base and WSF_0.925 scenarios for all Hurricanes at Sewells Point, NSN, the US.

Group	Hurricane ID	Max. Surge (m)		Duration (h)					
		Base	WSF_0.925	Base			WSF_0.925		
				Low	Med	High	Low	Med	High
CC*	IR	1.92	1.81	17.5	7	4.5	17	7	4
	IS	1.55	1.5	11	8	3	11	8	--
	SA	1.08	1.05	34	4	0	34	4	--
	MI	0.73	0.71	6	0	0	5	--	--

*Climate Change

--the water level is above this level

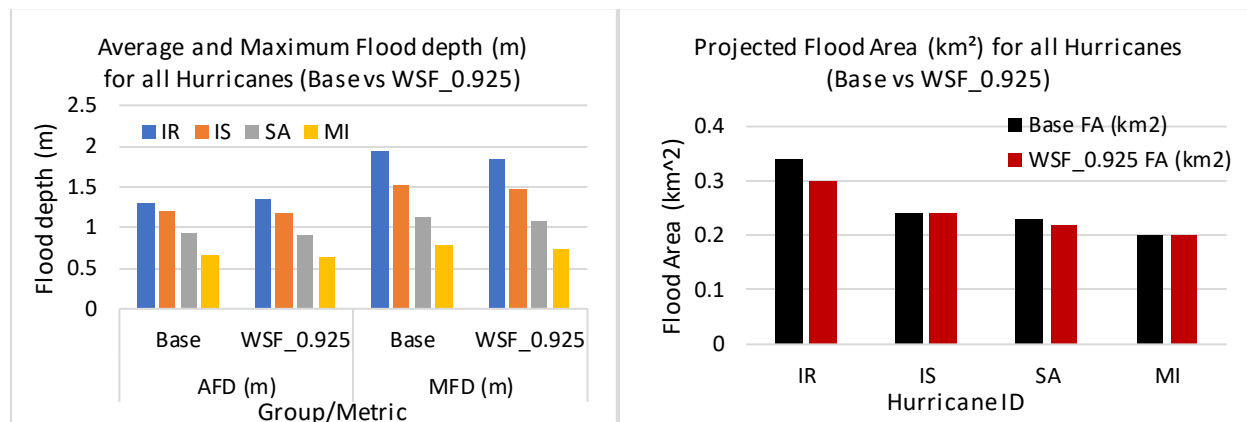


Figure 277. Average Flood Depth (AFD) & Maximum Flood Depth (MFD) in meters (left panel) and Flood area (km^2) (right panel) of all hurricanes for the Base and WSF_0.925 scenarios at NSN, the US.

Table 90. Flood area characteristics of the base and WSF_0.925 scenarios for all hurricanes at NSN, the US

Group	Hurricane ID	Base				WSF_0.925			
		Average FD (m)	Max FD (m)	Flood area (km^2)	%	Average FD (m)	Max FD (m)	Flood area (km^2)	%
CC	IR	1.31	1.94	0.34	2.47	1.34	1.83	0.3	2.2
	IS	1.21	1.52	0.24	1.72	1.17	1.46	0.24	1.7
	SA	0.94	1.14	0.23	1.6	0.91	1.09	0.22	1.6

	MI	0.66	0.79	0.2	1.45	0.63	0.74	0.2	1.5
--	----	------	------	-----	------	------	------	-----	-----

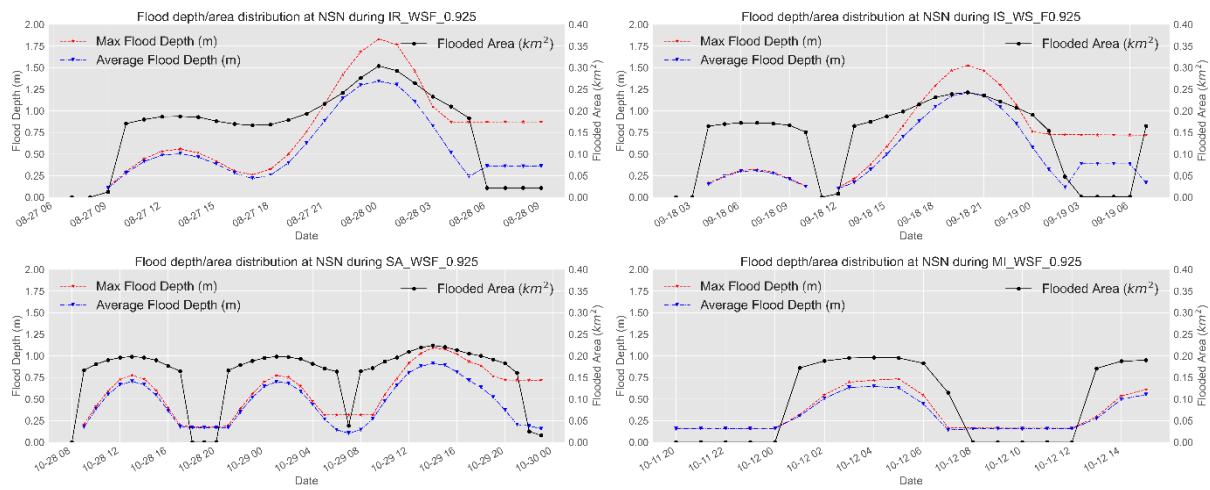


Figure 278. Timeseries of the projected average and maximum flood depth (left axis) and flood area (km^2 -right axis) for all hurricanes for WSF_0.925 scenario at NSN, the US.

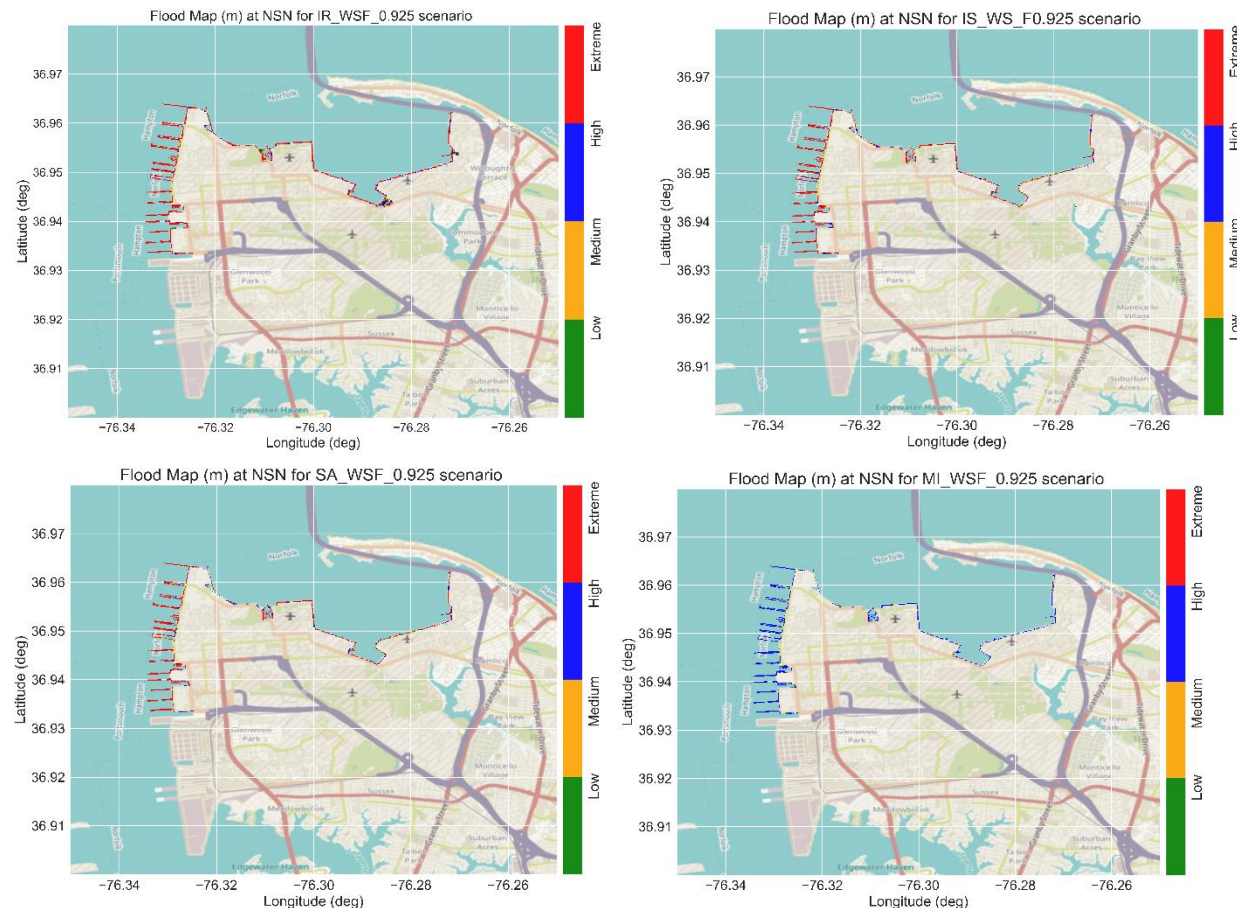


Figure 279. Flood maps with the flood levels for the different hurricanes during the peak surge for the WSF_0.925 scenario at NSN, the US.

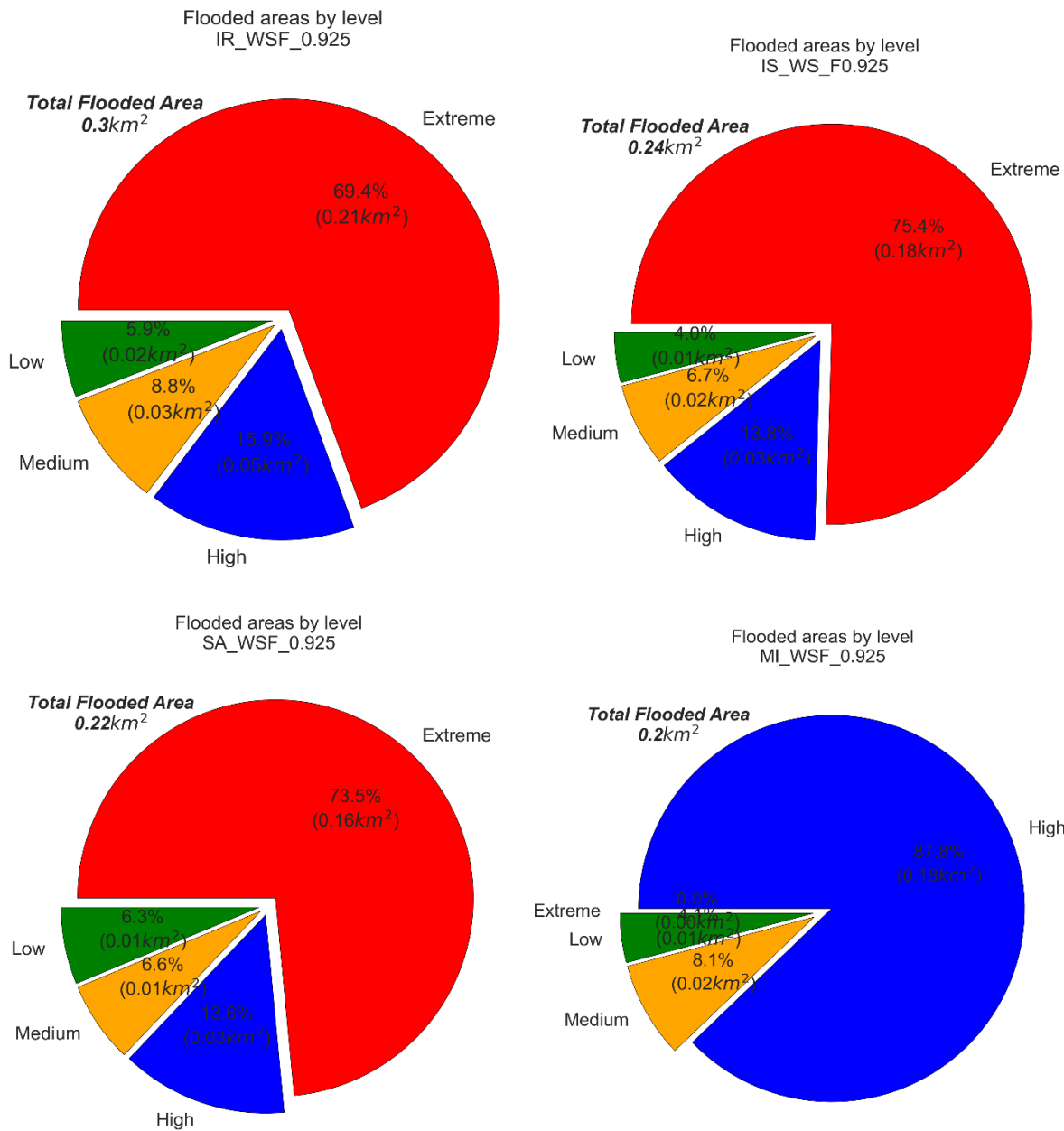


Figure 280. Pie chart of the flood areas, with percentages, of the different flood levels for WSF_0.925 scenarios for all hurricanes at NSN, the US.

b. WSF_1.075 Scenario

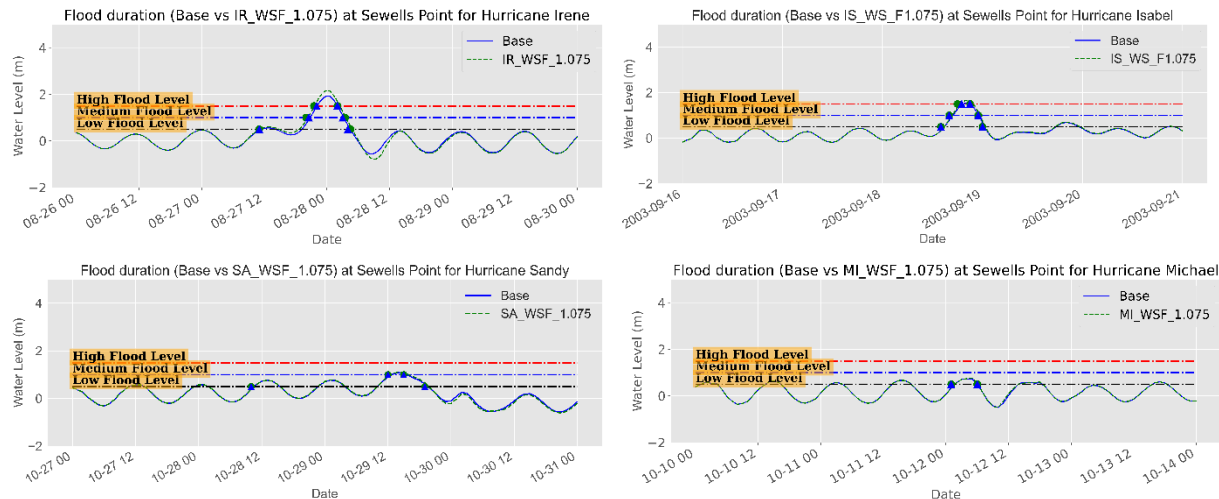


Figure 281. Water level time series (m) during the different hurricanes showing the surge magnitude and duration for different surge levels for the base and WSF_1.075 scenarios at Sewells Point, NSN, the US.

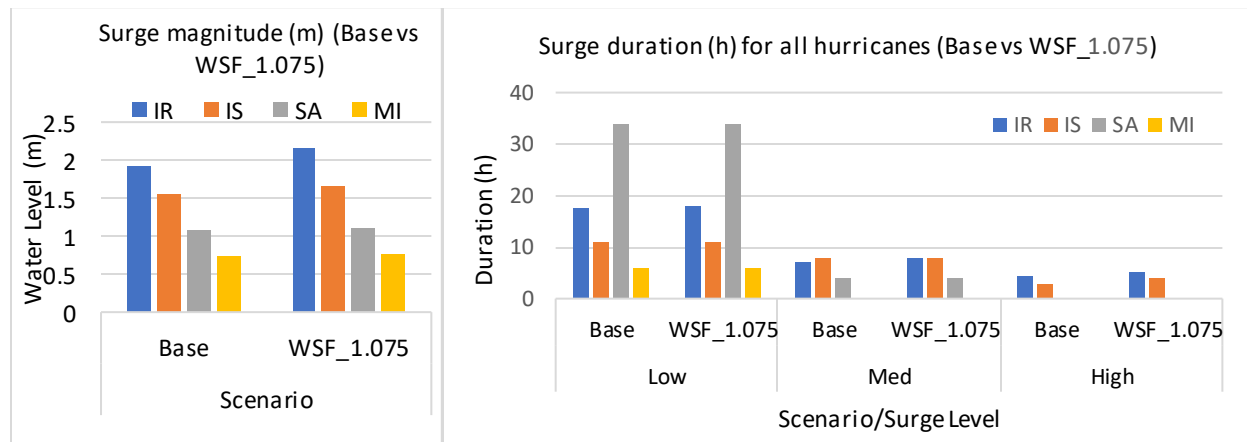


Figure 282. Peak surge (m) (left panel) and surge duration (h) of the different surge levels (right panel) for the base and WSF_1.075 scenario for all hurricanes, NSN, the US.

Table 91. Peak surge characteristics (Maximum and Duration) of the base and WSF_1.075 scenarios for all Hurricanes at Sewells Point, NSN, the US.

Group	Hurricane ID	Scenario		Scenario/Surge Level					
		Base	WSF_1.075	Base			WSF_1.075		
				Low	Med	High	Low	Med	High
CC*	IR	1.92	2.17	17.5	7	4.5	18	8	5
	IS	1.55	1.66	11	8	3	11	8	4
	SA	1.08	1.11	34	4	0	34	4	--
	MI	0.73	0.76	6	0	0	6	0	0

*Climate Change

--the water level is above this level

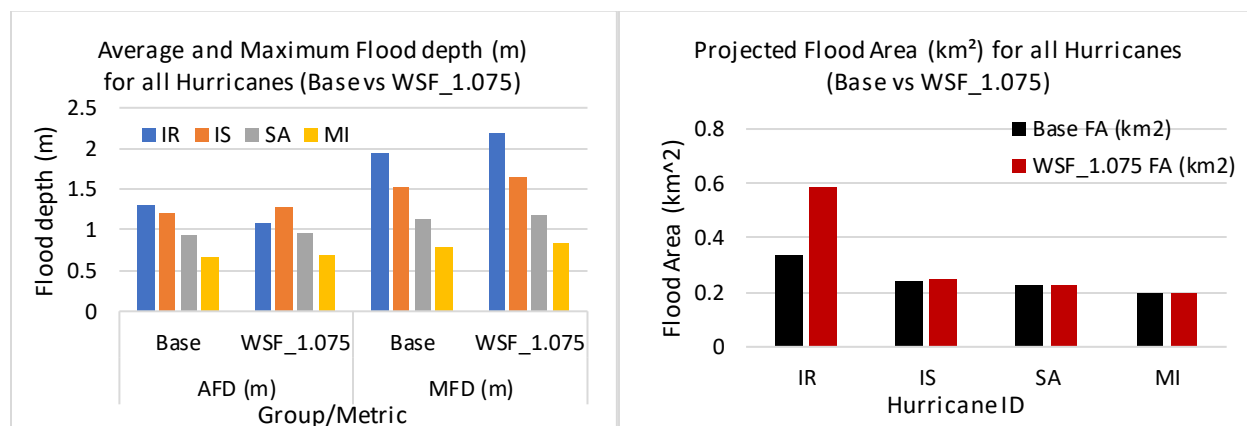


Figure 283. Average Flood Depth (AFD) & Maximum Flood Depth (MFD) in meters (left panel) and Flood area (km^2) (right panel) of all hurricanes for the Base and WSF_1.075 scenarios at NSN, the US.

Table 92. Flood area characteristics of the base and WSF_1.075 scenarios for all hurricanes at NSN, the US.

Group	Base	WSF_1.075
-------	------	-----------

Hurricane ID		Average FD (m)	Max FD (m)	Flood area (km ²)	%	Average FD (m)	Max FD (m)	Flood area (km ²)	%
CC	IR	1.31	1.94	0.34	2.47	1.09	2.19	0.59	4.3
	IS	1.21	1.52	0.24	1.72	1.28	1.65	0.25	1.8
	SA	0.94	1.14	0.23	1.6	0.96	1.18	0.23	1.7
	MI	0.66	0.79	0.2	1.45	0.69	0.84	0.2	1.5

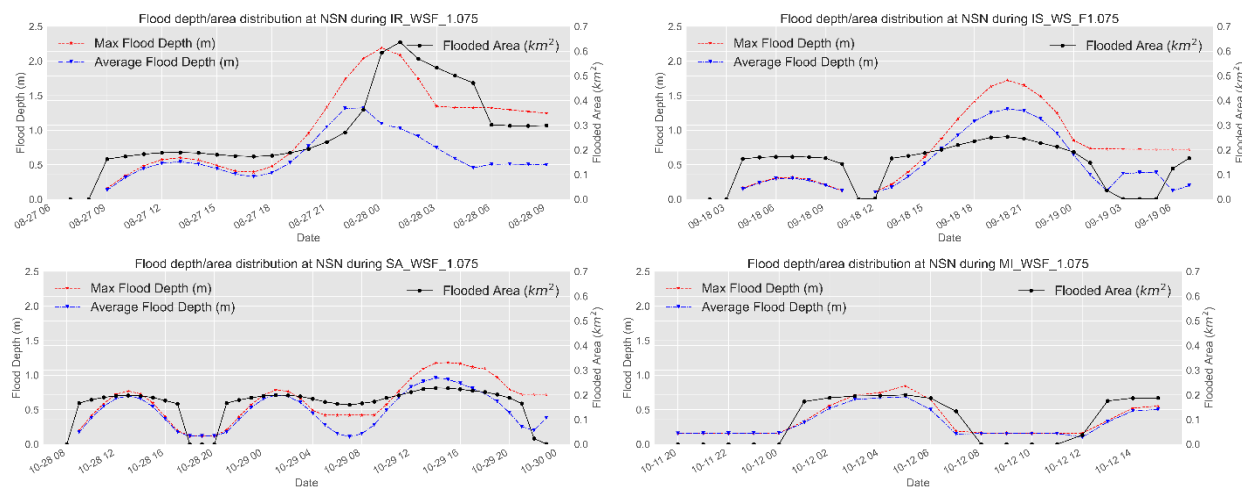


Figure 284. Timeseries of the projected average and maximum flood depth (left axis) and flood area (km^2 -right axis) for all hurricanes for WSF_1.075 scenario at NSN, the US.

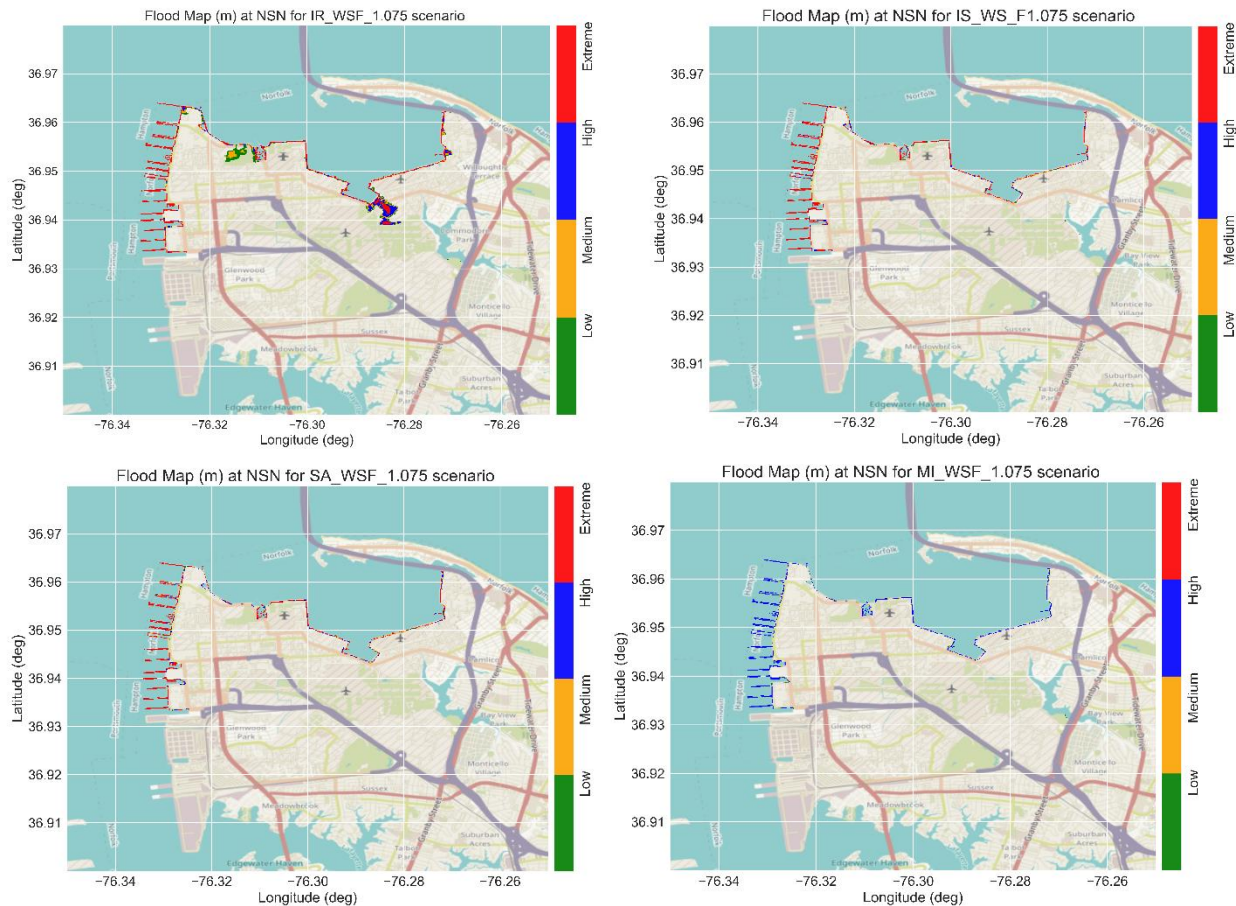


Figure 285. Flood maps with the flood levels for the different hurricanes during the peak surge for the WSF_1.075 scenario at NSN, the US.

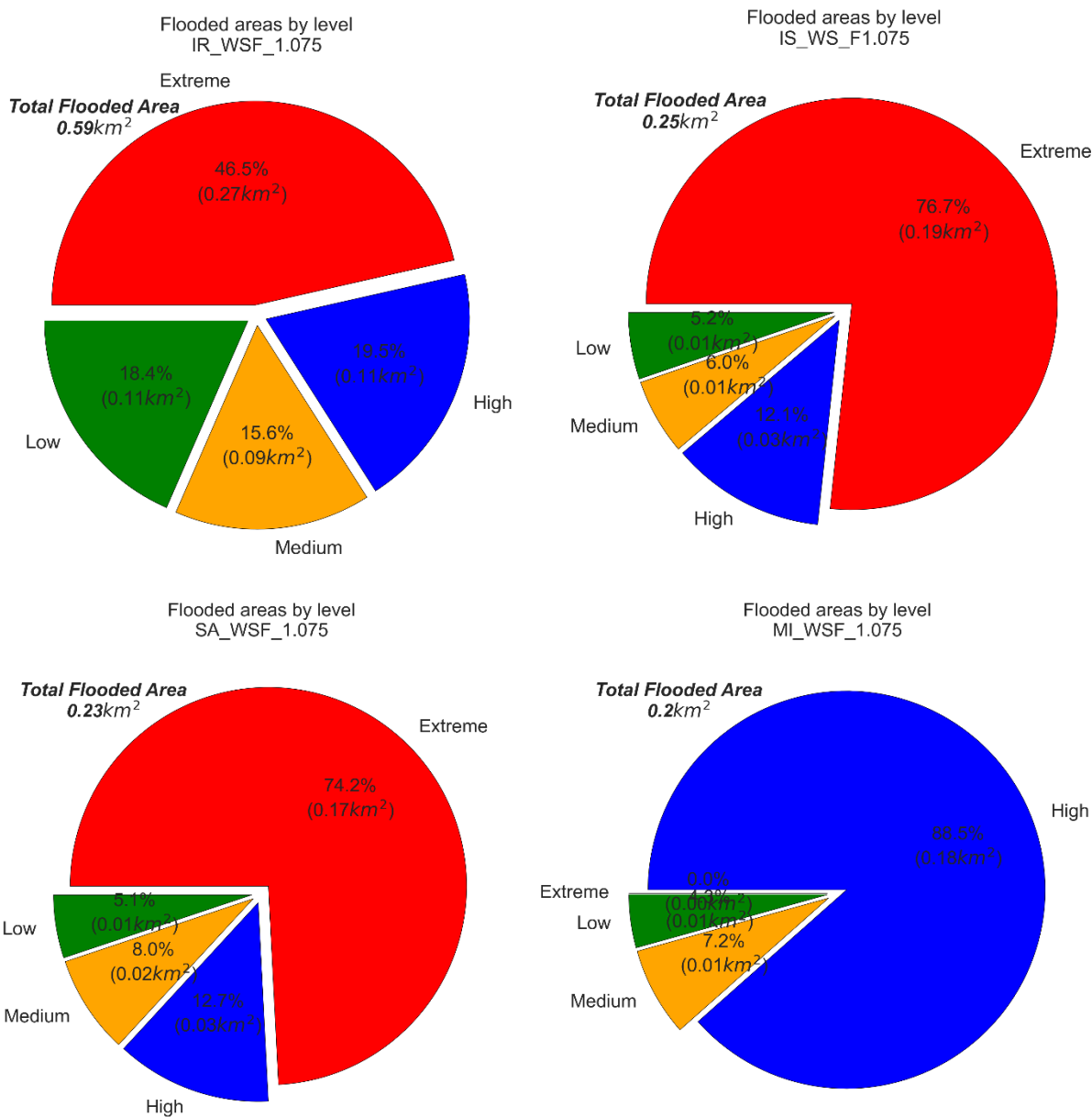


Figure 286. Pie chart of the flood areas, with percentages, of the different flood levels for WSF_1.075 scenarios for all hurricanes at NSN, the US.

12.3. Impacts of Lack of Data (Degradation scenarios)

- 12.3.1. Strom Track Shift (Error in Storm Track Prediction)
- 12.3.2. Bathymetry Accuracy
- 12.3.3. Bathymetry Resolution